

# Risk Analysis for Tunneling Projects

by

**Rita L. Sousa**

Licenciatura, Engenharia Civil , Universidade Técnica de Lisboa – Instituto Superior Técnico  
(1998)  
Master of Science in Civil Engineering, Ecole Nationale des Ponts et Chaussées (2000)

Submitted to the Department of Civil and Environmental Engineering  
in Partial Fulfillment of the Requirements for the Degree of

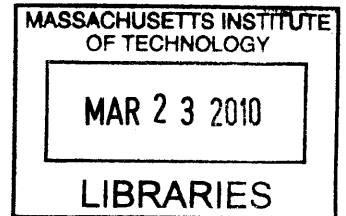
Doctor of Philosophy  
in the Field of Geotechnical and Geoenvironmental Engineering

at the

Massachusetts Institute of Technology

February 2010

**ARCHIVES**



© 2010 Massachusetts Institute of Technology  
All rights reserved

Signature of Author .....

Department of Civil and Environmental Engineering

January 8, 2010

Certified by .....

Herbert H. Einstein

Professor of Civil and Environmental Engineering

Thesis Supervisor

Certified by .....

Daniele Veneziano

Professor of Civil and Environmental Engineering

Thesis Supervisor

Accepted by .....

Daniele Veneziano

Chairman, Departmental Committee for Graduate Students





# **Risk Analysis for Tunneling Projects**

by

**Rita Leal e Sousa**

Submitted to the Department of Civil Engineering  
on January 8, 2010 in Partial Fulfillment of the  
Requirements for the Degree of Doctor of Philosophy in  
in the Field of Geotechnical and Geoenvironmental Engineering

## **ABSTRACT**

Tunnel construction is increasing world wide. Although the majority of tunnel construction projects have been completed safely, there have been several incidents that have resulted in delays, cost overruns, and sometimes more significant consequences such as injury and loss of life. To help eliminate these accidents, it is necessary to systematically assess and manage the risks associated with tunnel construction.

In order to better understand the conditions under which accidents occur, a database of 204 tunnel construction accidents was assembled. This is the most comprehensive database known to date. The database was analyzed to better understand the causes of accidents. Influence diagrams were constructed containing the main factors, and the interactions between them. These served as the basis of the risk assessment methodology presented in this work.

The risk assessment methodology consists of combining a geologic prediction model that allows one to predict geology ahead of the tunnel construction, with a decision support model that allows one to choose amongst different construction strategies the one that leads to minimum risk. The geologic prediction model is based on Bayesian networks because of their ability to combine domain knowledge with data, encode dependencies among variables, and their ability to learn causal relationships.

The combined geologic prediction – decision support model was then applied to the Porto Metro, in Portugal. The results of the geologic prediction model were in good agreement with the observed geology, and the results of the decision support model were in good agreement with the construction methods used. More significant, however, is the ability of the model to predict changes in geology and consequently changes in construction strategy. This was shown in two zones of the tunnel where accidents occurred, where the model predicted an abrupt change in geology, and the construction method should have been changed but was not. Using the model could have possibly avoiding the accidents.

This risk assessment methodology provides a powerful tool with which planners and engineers can systematically assess and mitigate the inherent risks associated with tunnel construction.

Thesis Supervisor: Herbert Einstein

Title: Professor of Civil and Environmental Engineering

Thesis Supervisor: Daniele Veneziano

Title: Professor of Civil and Environmental Engineering

## ACKNOWLEDGMENTS

I would like to thank a number of people for their support and for making this work possible. My advisor, Professor Herbert Einstein, for his unconditional support and guidance, and for being a father figure throughout this process. It has been an honor working with him. Professor Daniele Veneziano, for his encouragement, stimulation and insights into various aspects of this work. My committee members; Professor Jerome Connor for his enthusiasm towards the subject of this work; Professor António Gomes Correia for his help despite being based in Portugal.

The Fundação para a Ciência e Tecnologia (FCT) for the funding it has provided through a research fellowship. The MIT-Portugal Program for partially funding this work. The Porto Metro Authorities for generously allowing us to use data from the construction of the Porto metro, without which this work would not have been possible. To all the tunneling experts and entities who collaborated in this research, and were kind enough to provide data, especially Professor António Silva Cardoso from the University of Porto.

To all my friends on the other side of the Atlantic especially Rita Santiago, for being so caring and for personally making sure I would come to Boston; Madalena Trindade, for her kindness and great sense of humor; Carla e Pedro Freitas, for being always so adventurous and going all the way to Muscat for my “wedding”, Joaquim Manso, who I consider to be a bother, Nana Rebelo, for the “zen” moments, Sónia Machado for being always so ironic, Catarina Tomé, for great lunches, café com natas and incursions to Baixa; José Ramos for great advice; Sandra Galvão for making sure my wedding did not take place somewhere in the middle of Monsanto; Patricia e Joana Mantas, my eternal childhood friends; Miguel Nazareth for the great jokes; Ana Inácio, my Parisian friend; André Vicente for the skype “concerts”. Thank you all for being such wonderful friends!

To all my friends on this side of the Atlantic: Maria Nikolinakou who has been my closest friend in Boston and my adventure partner! Thanks for always being there for me; Rania and Jean-Claude for being such wonderful friends; Ralph Aucella for helping me find my home and Cynthia Aguilar for great Margaritas and Guacamole; the Portuguese crowd who never let me feel homesick, especially Filipa Sá, Pedro Pinto, Marcus Dahlem and Jorge Oliveira; Bruno Silva, my good friend and office mate, for Gatos Fedorentos and Co. and for making my last year at MIT so much more fun; Catarina Ferreira for the checking on me daily during the final stretch; Sherif Akl for being such a great friend and always up for a good meal; Anna Agarwal, my yoga partner, for being such a kind person; Ray Janeiro for Quim Barreiros, Vira, bacalhau a Gomes de Sá...; Yvonne Moret for making the office a great place to be; Irene Manzella for amazing times, my geotechnical friends: Gonzalo, Jay, Julia, Antonios, Naeem, Louie, Pong, Ba, Isabel...

To Carolyn and Alise for always taking such good care of me and making my life so much enjoyable at MIT.

To the Karams for all their encouragement and support, especially Marianne and Kika, for being my little sisters here in Boston!

To my cousin Tiago Sousa, who is one of the kindest people I have ever met, and who made the trip to Boston just to watch my defense.

This thesis is dedicated to my father, Luis, and my brother, Manuel, who have always been the source of love, encouragement, support and inspiration throughout my life. Thanks for believing in me!

Lastly, I would also like to dedicate this thesis to my husband, Karim, for his unconditional love and support, and with whom I have lived the best years of my life. I could not have done it without you!

# TABLE OF CONTENTS

ABSTRACT .....	3
ACKNOWLEDGMENTS .....	5
TABLE OF CONTENTS.....	7
LIST OF FIGURES .....	10
LIST OF TABLES.....	21
CHAPTER 1 Introduction.....	25
1.1 Problem definition .....	25
1.2 Research objectives.....	26
1.3 Thesis Outline .....	27
CHAPTER 2 Tunnel Construction .....	29
2.1 The origin and evolution of tunnel construction.....	29
2.2 Construction methods .....	40
2.2.1 NATM / Sequential Excavation Methods.....	41
2.2.2 Excavation Machines .....	45
2.3 Tunnel construction monitoring.....	59
2.4 References.....	66
CHAPTER 3 Accidents during Tunnel Construction .....	71
3.1 Accidents in tunnels.....	71
3.2 Accident Database .....	73
3.2.1 Data Collection .....	73
3.2.2 Database Structure .....	76
3.2.3 Type of Events .....	81
3.2.4 Database event classification .....	104
3.3 Data Analysis .....	107
3.4 Reported causes and consequences.....	114
3.4.1 Most commonly reported causes .....	114
3.4.2 Most commonly reported consequences.....	132
3.5 Remedial and Mitigation Measures .....	136
3.6 Important factors in tunneling.....	153
3.6.1 Ground parameters.....	153
3.6.2 Construction parameters .....	155
3.6.3 Observable parameters.....	156
3.6.4 Influence diagrams.....	158
3.7 Lessons learned / Conclusions / Contributions.....	178
3.8 References.....	180
3.9 Appendix A - MIT Tunnel Research Questionnaire.....	187
3.10 Appendix B – List of Experts .....	195
3.11 Appendix C – Database Records Example .....	196
3.12 Appendix D – List of Accident cases .....	200

CHAPTER 4	Knowledge Representation and Decision Making.....	209
4.1	Introduction.....	209
4.2	Rule Based Systems.....	210
4.3	Fuzzy – rule approach.....	212
4.4	Artificial Neural Networks .....	217
4.5	Classical Decision Analysis.....	218
4.5.1	Fault trees.....	218
4.5.2	Event Trees .....	222
4.5.3	Decision Trees .....	223
4.6	Bayesian Networks .....	225
4.6.1	Background and Probability Theory.....	225
4.6.2	Definition of Bayesian Network .....	228
4.6.3	Inference .....	229
4.6.4	Development of a Bayesian Network .....	232
4.6.5	Determination of the Probabilities.....	238
4.7	Influence Diagrams.....	265
4.7.1	Typical types of Influence diagrams.....	268
4.7.2	Inference for Influence diagrams.....	271
4.8	Conclusions.....	271
4.9	References.....	273
4.10	Appendix E - Example (adapted from Jensen, F. 1996).....	277
4.11	Appendix F - Derivation of the ML estimator for a multinomial distribution.....	284
CHAPTER 5	Risk Assessment and Mitigation.....	287
5.1	Risk Management .....	288
5.1.1	Definitions.....	288
5.1.2	“Classic” Risk Analysis techniques.....	295
5.1.3	Bayesian Networks and Influence Diagrams.....	316
5.2	Proposed Methodology for Decision Making during Design Phase and Construction Phase.....	321
5.2.1	Design Phase.....	321
5.2.2	Tunnel construction Phase .....	326
5.2.3	Application Results.....	331
5.3	Conclusions.....	350
5.4	References.....	352
5.5	Appendix G - Multiattribute utility functions.....	354
CHAPTER 6	Porto Metro Case study.....	365
6.1	The Project.....	365
6.1.1	The geology .....	367
6.1.2	Construction method.....	373
6.1.3	The accidents .....	375
6.1.4	Reported possible causes of Accident 3.....	380
6.1.5	Supplementary measures .....	394
6.2	Application of Risk Analysis Methodology .....	398
6.2.1	Design Phase.....	399

6.2.2	Construction Phase – Bayesian Prediction Model .....	417
6.2.3	Combined Risk Assessment Model .....	484
6.3	Summary and Conclusions of Porto Metro Case Study.....	507
6.4	References.....	514
6.5	Appendix H – Training Data set A and B.....	517
6.6	Appendix I – Geological Prediction Model Results for Rings 336 to 1611 ...	547
6.7	Appendix J – Machine Parameters Plots (Section 1 and 2).....	556
CHAPTER 7 Conclusions and Recommendations .....		563
7.1	Conclusions.....	563
7.2	Recommendations for future work .....	571
REFERENCES .....		574

## LIST OF FIGURES

Figure 2.1 a) Illustration of Samos tunnel in Greece; b) picture taken inside the tunnel. In cross section the floor is more or less horizontal but the roof slopes along the rock strata (Apostol, 2004)	30
Figure 2.2 Illustration of the construction process of the Tronquoy tunnel (Sandström, 1963).....	31
Figure 2.3 Timber support for the south ramp of the Lötschberg tunnel (1908.1913) .....	33
Figure 2.4 Central Artery Project Layout (Massachusetts Turnpike Authority, url: <a href="http://www.masspike.com/">http://www.masspike.com/</a> ).....	34
Figure 2.5 Construction of the eight.to.ten.lane underground expressway directly beneath the existing road, 1998 (Sousa, 2006). .....	35
Figure 2.6 Photographs depicting the “before” and “after” of the Central Artery/Tunnel Project (photo by David Pal).....	35
Figure 2.7 Two of the TBMs used in the construction of the Nanboku Line. a) TBM used in the construction the Shiroganedai station; (b) sketch of the station; (c) Double concentric TBM used in part of the line; d) simplified scheme of the TBM advance (Assis, 2001).....	36
Figure 2.8 a) Location of the trans.bay tube in San Francisco; b) launching of a pre.fabricated element of the trans.bay tube (ASME International, 1997) .....	38
Figure 2.9 a) Layout of the Marmarray Project; b) Schematic of the docking process between TBM and immersed tube (Horgan and Madsen, 2008). .....	38
Figure 2.10 . Different concepts for submerged floating tunnels. a) hanging from pontoons (concept developed by Kværner Rosenberg); b) held down by tension cables (concept developed by Aker Norwegian Contractors) (Moe, 1997).....	39
Figure 2.11 Illustration of the a proposal for transatlantic tunnel (Discovery Channel) ..	40
Figure 2.12 The basic principles of NATM (adapted from Müller and Fecker, 1978) ....	42
Figure 2.13 Typical cross section proposed by Rabecewicz (1965).....	43
Figure 2.14 Tunnel excavated in 3 partial faces (HSE, 1996).....	44
Figure 2.15 Tunnel excavated in 6 partial faces (HSE, 1996).....	44
Figure 2.16 Full face excavation of a tunnel under the protection of a forepole umbrella (Hoek, 2007).....	45
Figure 2.17. Classification of Tunnel Excavation Machines (AFTES, 2000).....	47
Figure 2.18 Photo of a roadheader .....	48
Figure 2.19 Main Beam TBM scheme (AFTES, 2000).....	48
Figure 2.20 Tunnel reaming machine (AFTES, 2000) .....	49
Figure 2.21 Gripper TBM (Wittke, 2007) .....	50
Figure 2.22 Single Shield TBM (Herrenknecht, url: <a href="http://www.herrenknecht.com">www.herrenknecht.com</a> ).....	51
Figure 2.23 Double Shield TBM (Herrenknecht, url: <a href="http://www.herrenknecht.com">www.herrenknecht.com</a> ).....	52
Figure 2.24 Double Shield TBM used in Guadarrama tunnels in Spain (Herrenknecht, url: <a href="http://www.herrenknecht.com">www.herrenknecht.com</a> ) .....	52
Figure 2.25 Mechanical.support TBM (AFTES, 2000).....	53
Figure 2.26 Compressed air TBM (AFTES, 2000).....	54
Figure 2.27 Slurry Shield Machine sketch (International Tunnelling Association, 2000)55	55
Figure 2.28 Slurry Shield Machine principles (Wittke, 2007) .....	55



Figure 2.29 Photograph of the cutterhead of a Slurry type tunneling machine for the underground metropolitan railway in Mühlheim, Germany (Wittke et al., 2007)....	55
Figure 2.30 EPB Machine (Herrenknecht, url: www.herrenknecht.com) .....	56
Figure 2.31 EPB Machine principles (Wittke et al., 2007).....	57
Figure 2.32 EPBM Operation modes (Barbenderede et al., 2005).....	58
Figure 2.33 Elb 4th tunnel Mixshield TBM, Hamburg $\phi$ 14.2 m (Toan, 2006) .....	59
Figure 2.34 Most frequently monitored physical quantities (Kovári and Ramoni, 2006)	61
Figure 2.35 Face mapping for Porto Metro Line C (Transmetro, 2001) .....	63
Figure 2.36 Typical convergence measurement cross section for crown and heading (Wittke et al., 2002).....	64
Figure 2.37 Typical extensometer and inclinometer measurement cross section for crown and heading (adapted from Wittke et al., 2002).....	64
Figure 2.38 Typical instrumented cross section for crown and heading (Sousa, 2002) ...	65
Figure 2.39 Measurement devices for face support pressure (Barbenderede et al. 2004)	66
Figure 3.1 Methodology followed during the creation and analysis of the database on accidents .....	73
Figure 3.2 Extract of the questionnaire – General Information section (Lausanne M2 metro line) .....	75
Figure 3.3 Relationship between the Project and Accident tables.....	77
Figure 3.4 Extract of section 2.2 of the questionnaire (Lausanne M2 metro line) .....	79
Figure 3.5 Geographical distribution of the tunnel cases .....	80
Figure 3.6 Distribution of the type of use of the tunnels in the database .....	80
Figure 3.7 Distribution of the tunnel cases by construction method .....	80
Figure 3.8 Undesirable event distribution.....	82
Figure 3.9 Event location.....	83
Figure 3.10 Photo of the collapsed area (Rocha, 1977).....	84
Figure 3.11 Accident schematic (Sousa, 2006) .....	84
Figure 3.12 loosening of rock wedges during gripper shield excavation (Wittke, W. et al., 2007).....	84
Figure 3.13 Covão tunnel, Socorridos Hydroelectric scheme, Madeira, Portugal (Cafopo, 2006).....	85
Figure 3.14 Overexcavation due to instable rock wedges, Gotthard base tunnel, Bodio section (Wittke, W. et al., 2007) .....	86
Figure 3.15 Collapse at the face of the TBM, Evino Mornos, Greece (Grandori et al., 1995).....	87
Figure 3.16 Partial collapse at Gotthard Base tunnel, Faido section (Einstein, 2007) .....	87
Figure 3.17 Collapse progression at Wienerwald tunnel (Seidenfuß, T., 2006).....	88
Figure 3.18 Crater caused by a collapse of the subway tunnel in Munich, Germany, 1994 (Wannick, H., 2006).....	89
Figure 3.19 Collapse that occurred in Pinheiros Station, São Paulo, Brazil, 2007 (Barton, 2008).....	90
Figure 3.20 Collapse that occurred in Olivais Station, Lisbon, Portugal (Appleton, 1998) .....	90
Figure 3.21 Demolition of buildings after the tunnel collapse in Metro Line No. 4 in Shanghai (Munich Re Group, 2004) .....	91

Figure 3.22 Collapse of a tunnel in Taegu in South Korea that led to the collapse of whole sections of the street (Knights, 2006).....	92
Figure 3.23 Crater caused by a collapse that occurred in the Aescher tunnel, Switzerland (Kovari, and Descoedres, 2001).....	92
Figure 3.24 Collapse of Porto Metro line C in January 2001 (Forrest, 2006).....	93
Figure 3.25 Aspect of the front after collapse (ingress of soil and water), Lausanne, Switzerland (Stallmann, 2005).....	94
Figure 3.26 Water burst resulting in flooding, China (private correspondence).....	95
Figure 3.27 Rockburst at the crown in a in a waterway tunnel in Korea (Lee et al., 2004).....	96
Figure 3.28 Example of rock-bursting in an exploratory tunnel for the Ortfjell open pit (Broch and Nilsen, 1977).....	97
Figure 3.29 Picture of deformed primary lining due to swelling clays, Naples, Italy (Wallis, 1991).....	98
Figure 3.30 Heave in the Bolu tunnel (Elmalık right tube) at km 54 + 135 (Dalgıç, 2002). .....	100
Figure 3.31 Failure of the support in the Bolu tunnel (Elmalık right tube) at km 54 + 135 (Dalgıç, 2002).....	100
Figure 3.32 Invert squeezing in the Bolu tunnel (Elmalık left tube) at km 64 + 260 (Dalgıç, 2002).....	100
Figure 3.33 Accident in the Munich metro construction (Weber, J., 1987).....	101
Figure 3.34 Collapse at Hull transfer tunnel project a) cross section at the collapse zone; b) aerial photo of the collapsed area. (Grose and Benton, 2005).....	102
Figure 3.35 Cave in of the South portal slope in the Haivan tunnel, Vietnam (Fukushima, H., 2002).....	103
Figure 3.36 Illustration of the collapse in a high speed train railway line in Germany (Leichnitz, 1990). .....	104
Figure 3.37 Classification method used in the database.....	105
Figure 3.38 Distribution of the accidents according to their location.....	108
Figure 3.39 Distribution of the event location according to the construction method ...	108
Figure 3.40 Distribution of the location for the different types of events.....	110
Figure 3.41 Volume involved in events (Collapse, Daylight collapse and rock fall) for different construction methods.....	111
Figure 3.42 Volume involved in collapses for both conventional and mechanized construction methods.....	112
Figure 3.43 Volume involved in daylight collapse for both conventional and mechanized construction methods.....	112
Figure 3.44 Volume involved in rock falls for both conventional and mechanized construction methods.....	112
Figure 3.45 Volume involved in daylight collapses in urban environments for all construction methods.....	112
Figure 3.46 Data available on volume of collapse versus H/D for tunnels in Rock formations.....	113
Figure 3.47 Data available on volume of collapse versus H/D for tunnels in Soil formations.....	113

Figure 3.48 Data available on volume of collapse versus H/D for tunnels in Mixed conditions .....	114
Figure 3.49 Main causes for accidents during construction .....	115
Figure 3.50 Ground conditions in the final design documents (Seidenfuss, 2006) .....	116
Figure 3.51 Actual ground conditions after collapse (Seidenfuss, 2006) .....	117
Figure 3.52 Two examples of fault-zone problems experienced at the Pont Ventoux HEP project in N. Italy (Barton, 2004) .....	118
Figure 3.53 Continuous collapses due to the ‘fault shaft’, assisted by water and/or water pressure. These sketches are super-imposed on one sheet, from the geologist’s daily logs. TBM was stuck for 6 months in this location (Barton, 2006) .....	119
Figure 3.54 Simplified geology, and the location (ch. 1,215) of the blow-out of water, sand and rounded quartzite pebbles .....	120
Figure 3.55 Man made water mines in Porto, Portugal (Forrest, 2006) .....	121
Figure 3.56 Longitudinal section through the collapse area showing geology and position of surface structures, Istanbul metro (Ayaydin, 2001) .....	122
Figure 3.57 Collapsed zone at surface, Istanbul metro (Ayaydin, 2001) .....	122
Figure 3.58 Approximate location of the tunnel collapses (Ghasemi, 2000) .....	123
Figure 3.59 Collapses at the Bolu tunnel in Turkey (Ghasemi, 2000) .....	124
Figure 3.60 Damaged concrete lining after the 1994 Great Belt fire, Denmark (Khoury, 2003) .....	125
Figure 3.61 Barcelona Metro Line 5 collapse illustration .....	127
Figure 3.62 Exhumed sections of invert and joint (HSE, 2000) .....	129
Figure 3.63 Photo at the surface at the site of the collapse at Shanghai metro line 4 (Wannick, 2006) .....	130
Figure 3.64 Photo at the surface at the site of the collapse of Heathrow (Clayton, 2008) .....	131
Figure 3.65 Most commonly reported consequences of undesirable events during tunnel construction. ....	133
Figure 3.66 Distribution of the delays (in months) caused by accidents during construction .....	136
Figure 3.67 Repair strategies for both Montemor tunnels (Wallis, 1995) .....	139
Figure 3.68 Phase 3 of remedial and mitigation measures at Lausanne metro (Seidenfuss, T., 2006) .....	140
Figure 3.69 plan view of the area affected by the remedial/ mitigation works (Seidenfuss, T., 2006) .....	140
Figure 3.70 Construction sequence for the recovery of the collapsed zone (Brown, 2004) .....	142
Figure 3.71 Cross section of ice structure with monitoring devices (T & TI, October 2000) .....	142
Figure 3.72 - Example of the ground reinforcing techniques using lateral drifts for the stop at the Chainage 39k+079 in the Hsuehshan Tunnel (Pelizza and Peila, 2005) .....	143
Figure 3.73 Geological conditions at the thrust zone (Barla G. and Pelizza S., 2000) .....	144
Figure 3.74 The stabilization measures adopted to free the TBM head (Barla G. and Pelizza S., 2000) .....	144
Figure 3.75 Access chamber completed with the TBM in the background (Barla and Pelizza., 2000) .....	145

Figure 3.76 collapse at tm 2720 in the Gotthard Base (AlpTransit-Tagung, 2004). .....	146
Figure 3.77 Grouting drilling patterns (Yoshimitsu and Takashi , 1986).....	148
Figure 3.78 Bypass tunnel for the 4 <sup>th</sup> flooding accident with execution of grouting around fault zone (Hashimoto, and Tanabe, 1986) .....	149
Figure 3.79 Cross section of a tunnel with compression slots applied in squeezing ground conditions (Schubert , 1996) .....	150
Figure 3.80 Invert heave at Chienberg tunnel (Chienbergtunnel, N2 Umfahrung Sissach, private correspondance) .....	151
Figure 3.81 Deformable invert at Chienberg tunnel (Private correspondence).....	151
Figure 3.82 Non-shielded TBM with expanded pre-cast concrete ring segments used in the tunnel from Rotarelle and San Vittore part of the Naples Aqueduct project (Wallis, 1991).....	152
Figure 3.83 Influence Diagram for Rock Fall.....	161
Figure 3.84 Influence Diagram for Rockburst.....	164
Figure 3.85 Influence Diagram for Excessive water inflow / Flooding .....	167
Figure 3.86 Case studies of tunnels with squeezing sections (Kovari, 1996).....	168
Figure 3.87 Influence Diagram for Excessive Deformation (inside tunnel).....	171
Figure 3.88 Probing methods.....	174
Figure 3.89 Exploratory adit located inside the final tunnel cross section .....	175
Figure 3.90 Exploratory adit located outside the final tunnel cross section .....	175
Figure 3.91 Influence Diagram for Collapse and Daylight collapse .....	177
Figure 4.1 Fuzzy membership function (for low pressure).....	213
Figure 4.2 Factors in deciding whether a liquid is potable or not.....	214
Figure 4.3 Membership function for Toxicity .....	214
Figure 4.4 Membership function for Alcohol content .....	215
Figure 4.5 Neural network with one hidden layer .....	217
Figure 4.6 Example of a fault tree for evaluation of failure on sub-sea tunnel project (Eskesen, 2004) .....	219
Figure 4.7 Symbols commonly used for events in fault tree .....	219
Figure 4.8 Typical event tree (Faber, 2005) .....	222
Figure 4.9 Combination of a fault tree and an event tree.....	223
Figure 4.10 Typical decision tree (Faber, 2005).....	224
Figure 4.11 Bayesian Network example.....	229
Figure 4.12 Variable Elimination illustration .....	232
Figure 4.13 Mediating variable example .....	233
Figure 4.14 Chain graph .....	234
Figure 4.15 Undirected relationship method applied to example in Figure 4.14 .....	234
Figure 4.16 Illustration of the “divorcing” method technique.....	236
Figure 4.17 Cold or Angina model (Jensen, 2001).....	240
Figure 4.18 Thumbtack.....	243
Figure 4.19 BN for thumbtack flipping .....	244
Figure 4.20 Bayesian Network with two binary nodes.....	246
Figure 4.21 Two different configurations for BN with variables A, B, C.....	249
Figure 4.22 Beta distribution .....	253
Figure 4.23 Bayesian Network model for estimating the parameter $\theta$ given the observed data .....	254

Figure 4.24 Example of overfitting.....	260
Figure 4.25 Bayesian Network describing the independence between data points given the structure and the parameters (G = BN structure; $\theta$ = conditional probability table parameters) .....	262
Figure 4.26 Typical transition operators (add, delete, reverse in blue) .....	264
Figure 4.27 Local maximum versus global maximum .....	265
Figure 4.28 Influence Diagram .....	267
Figure 4.29 Influence Diagram connections.....	267
Figure 4.30 Value Influence .....	268
Figure 4.31 Simple one stage, non-strategic decision.....	268
Figure 4.32 Simple one stage decision, plus value of perfect information.....	269
Figure 4.33 Simple one stage decision, plus value of imperfect information.....	270
Figure 4.34 Event probabilities depend on the decision .....	270
Figure 4.35 Two stage decision .....	271
Figure 4.36 Bayesian Network for Grass wet example .....	277
Figure 5.1 Marginal Utility function for different decision maker risk preference. ....	293
Figure 5.2 Exponential utility function.....	294
Figure 5.3 Utility function for money ( $U(X) = -e^{-3X}$ ) .....	295
Figure 5.4 Topography and Tunnel Alignment (from Karam, 2005) .....	296
Figure 5.5 Description of Construction Strategies (Min et al., 2003).....	298
Figure 5.6 Probabilistic Model (Decision Tree) for Section 1.....	299
Figure 5.7 Sensitivity analysis – varying the cost of Construction Strategy CS1 .....	301
Figure 5.8 Sensitivity analysis – varying the Consequences of Failure using construction strategy CS2 in geology G1 .....	301
Figure 5.9 Sensitivity analysis – varying the Probability of failure in geological state G1 with Construction Strategy CS2.....	301
Figure 5.10 Sensitivity analysis – varying the (prior) Probability of geological state G1 .....	301
Figure 5.11 Sensitivity analysis – relative change of cost variables and their effect on the max of Expected Utility given the construction strategy (Equation 5.11).....	304
Figure 5.12 Sensitivity analysis – relative change of probabilities and their effect on the max of Expected Utility given the construction strategy (Equation 5.11).....	305
Figure 5.13 Sensitivity analysis – effect of varying cost of CS1 and CS2 on the max of the expected utility given construction strategy .....	306
Figure 5.14 Sensitivity analysis – effect of varying cost of CS1 and CS2 on the “optimal” construction strategy .....	306
Figure 5.15 Illustration of Most Cost Effective Construction Strategies in Different Tunnel Sections.....	307
Figure 5.16 Information Decision Model for Section 1.....	311
Figure 5.17 Information Sub-Model for Section 1 – Imperfect information.....	311
Figure 5.18 Effect of P (G1) on the expected value of sample information (EVSI) .....	316
Figure 5.19 Bayesian Network for tunnel problem on Figure 5.4 .....	317
Figure 5.20 Results for influence diagram of Figure 5.19.....	318
Figure 5.21 Information model.....	319
Figure 5.22 Information model results.....	321

Figure 5.23 Influence diagram for Design phase.....	323
Figure 5.24 Influence diagrams used determined the max expected utility for each section .....	324
Figure 5.25 Optimal construction strategy for construction of tunnel presented in Figure 5.4.....	324
Figure 5.26 Optimal construction strategy for construction of tunnel presented in Figure 5.4, with (option 1) and without (option 2) considering switchover costs for the $C_{switch}$ =-.83 in option 1 both options have the same total expected utility). ....	326
Figure 5.27 Division of Section 1 into subsections. ....	327
Figure 5.28 Subdivision of Section 1 of tunnel in Figure 5.4.....	330
Figure 5.29 Probability of geological state for Section 1, 2 and 3.....	333
Figure 5.30 Expected utility for Sections 1, 2 and 3.....	334
Figure 5.31 Probability of Failure for Sections 1, 2 and 3.....	334
Figure 5.32 Updated Probability of geological state for Section 1, after excavation of subsection 1 .....	335
Figure 5.33 Updated Expected utility for Section 1, after excavation of subsection 1...	336
Figure 5.34 “Optimal” construction strategies for Section 1, after excavation of subsection 1 .....	336
Figure 5.35 Updated Probability of Failure for Section 1, after excavation of subsection 1 .....	337
Figure 5.36 Updated Probability of geological state for Section 1, after excavation of subsection 2 .....	338
Figure 5.37 Updated Expected utility for Section 1, after excavation of subsection 2...	338
Figure 5.38 “Optimal” construction strategies for Section 1, after excavation of subsection 2 .....	339
Figure 5.39 Updated Probability of Failure for Section 1, after excavation of subsection 2 .....	339
Figure 5.40 Updated Probability of geological state for Section 1, after excavation of subsection 3 .....	340
Figure 5.41 Updated Expected utility for Section 1, after excavation of subsection 3...	341
Figure 5.42 “Optimal” construction strategies for Section 1, after excavation of subsection 3 .....	341
Figure 5.43 Updated Probability of Failure for Section 1, after excavation of subsection 3 .....	342
Figure 5.44 Geological states after excavation of subsections 1 and 2 (dotted lines are the design values).....	345
Figure 5.45 Geological states after excavation of subsections 1, 2 and 3 .....	346
Figure 5.46 Updated Expected utility for Section 1, after excavation of subsection 3...	347
Figure 5.47 Utility function plot .....	349
Figure 5.48 Expected Utility given Construction Strategy .....	349
Figure 5.49 Updated Expected utility for Section 1, after excavation of subsection 3, with utility function presented in Figure 5.47 .....	350
Figure 5.50 Marginal Utility function for different decision maker risk preference. ....	355
Figure 5.51 Exponential utility function plot (risk prone).....	356
Figure 5.52 Exponential utility function plot (risk averse).....	357
Figure 5.53 Determination of weight $k_c$ for cost .....	358

Figure 5.54 Determination of weight $k_T$ for cost .....	358
Figure 5.55 Utility Functions for decision makers with different risk preferences .....	360
Figure 5.56 Multiattribute utility function .....	362
Figure 5.57 risk neutral conditional utility function .....	363
Figure 5.58 Utility Functions for decision makers with different risk preferences (Attribute dominance utility).....	364
Figure 6.1 Porto Metro Network. The tunnels are Line C from Campanhã to Trindade (green) and Line S from Salgueiros to São Bento (purple).....	366
Figure 6.2 Distribution of the Granite formation within the city of Porto.....	368
Figure 6.3 Appearance of the different degrees of weathering of the granite formation in a core recovered from a site investigation borehole in the Line C tunnel alignment. ....	368
Figure 6.4 Idealized weathered profiles based on classification by Geological Society of London, 1995, and the recommendations of ISRM .....	370
Figure 6.5 Line C Tunnel layout.....	371
Figure 6.6 Longitudinal Campanhã to Trindade section .....	372
Figure 6.7 EPBM machine scheme.....	373
Figure 6.8 EPBM Operation modes (Babendererde et al., 2005) .....	374
Figure 6.9 Line C and location of the accidents .....	377
Figure 6.10 Zone of Accident 1 (building 44) .....	378
Figure 6.11 Location of the 2 <sup>nd</sup> incident and 3 <sup>rd</sup> accident.....	379
Figure 6.12 Monitoring results (vertical deformations at surface) for buildings 181, 182, 183. The warning value is 28mm. ....	380
Figure 6.13 Location of investigation points and chronology their installation .....	385
Figure 6.14 Typical old well (Geodata, 2001).....	386
Figure 6.15 Failure mechanism – hypothesis 1 (adapted from Geodata, 2001) .....	387
Figure 6.16 Failure mechanism – hypothesis 2 (adapted from Geodata, 2001) .....	389
Figure 6.17 Geological scenario for Hypothesis 3 (adapted from Geodata, 2001) .....	390
Figure 6.18 Failure mechanism – hypothesis 3a (adapted from Geodata, 2001) .....	391
Figure 6.19 Failure mechanism – hypothesis 3b (adapted from Geodata, 2001) .....	392
Figure 6.20 Location of boreholes where leached granite samples were obtained (Geodata, 2001).....	393
Figure 6.21 Additional Face Support System (Barbendererde, 2005).....	396
Figure 6.22 Illustration of Active Support System for overcoming the support pressure deficiency in mixed face conditions for Porto Metro (Barbendererde, 2004) .....	396
Figure 6.23 TBM follow up team organizational chart (T&TI, 2003) .....	397
Figure 6.24 decision support framework for the design and construction phase.....	399
Figure 6.25 Influence diagram for Porto Metro Line C tunnel.....	402
Figure 6.26 Geological ground class .....	405
Figure 6.27 Decision Model for Line C tunnel.....	406
Figure 6.28 Geological longitudinal profile for Line C tunnel (from PK 298 to PK 624) .....	410
Figure 6.29 Design Results – Optimal Construction strategy.....	416
Figure 6.30 TBM machine scheme .....	419
Figure 6.31 Relative Frequency of Cutting Wheel Force in Ground conditions G1, G2, G3 .....	422

Figure 6.32 Relative Frequency of the discretized variable Cutting Wheel Force showing the contribution of ground conditions G1, G2, G3 .....	423
Figure 6.33 Relative Frequency of Penetration rate in ground conditions G1, G2, G3..	425
Figure 6.34 Relative Frequency of discretized variable Penetration rate showing contribution of ground conditions G1, G2, G3 .....	426
Figure 6.35 Relative Frequency of Torque of the Cutting Wheel in ground conditions G1, G2, G3 .....	428
Figure 6.36 Relative Frequency of discretized variable Torque of Cutting Wheel showing contribution of ground conditions G1, G2, G3 .....	429
Figure 6.37 Relative Frequency of Torque/Force of the Cutting Wheel in ground conditions G1, G2, G3.....	431
Figure 6.38 Relative Frequency of discretized variable TOC showing contribution of ground conditions G1, G2, G3 .....	432
Figure 6.39 Relative Frequency Total Thrust Force in ground conditions G1, G2, G3.	434
Figure 6.40 Relative Frequency Cutting Wheel Force / Total Thrust in ground conditions G1, G2, G3 .....	436
Figure 6.41 Relative Frequency of discretized variable COTT showing contribution of ground conditions G1, G2, G3 .....	437
Figure 6.42 Penetration rate (P) versus Cutting Wheel Force (CF), in G1, G2, G3 .....	438
Figure 6.43 Joint relative frequency of penetration rate (P) and cutting wheel force (CF) for all ground conditions (G1, G2 and G3) .....	439
Figure 6.44 Joint relative frequency of penetration rate (P) and cutting wheel force (CF), in G1 (soil) .....	440
Figure 6.45 Joint relative frequency of penetration rate (P) and cutting wheel force (CF), in G2 (mixed) .....	440
Figure 6.46 Joint relative frequency of penetration rate(P) and Cutting wheel force (CF), in G3 (rock) .....	441
Figure 6.47 Penetration rate (P) versus Torque of the Cutting Wheel (TO), in G1, G2, G3 .....	442
Figure 6.48 Joint relative frequency of penetration (P) and torque of the cutting wheel (TO) for all ground conditions (G1, G2 and G3) .....	444
Figure 6.49 Joint relative frequency of penetration (P) and torque of the cutting wheel (TO), in G1 .....	444
Figure 6.50 Joint relative frequency of penetration (P) and torque of the cutting wheel (TO), in G2 (mixed) .....	445
Figure 6.51 Joint relative frequency of penetration (P) and torque of the cutting wheel (TO), in G3 (rock) .....	445
Figure 6.52 Cutting Wheel Force (CF) versus Torque of the Cutting Wheel (TO), in G1, G2, G3 .....	446
Figure 6.53 Joint relative frequency of cutting wheel force (CF) and torque of the cutting wheel (TO) for all ground conditions (G1, G2 and G3) .....	448
Figure 6.54 Joint relative frequency of cutting wheel force (CF) and torque of the cutting wheel (TO), in G1 (soil).....	449
Figure 6.55 Joint relative frequency of cutting wheel force (CF) and torque of the cutting wheel (TO), in G2 (mixed).....	449



Figure 6.56 Joint relative frequency of cutting wheel force (CF) and torque of the cutting wheel (TO), in G3 (rock).....	450
Figure 6.57 Torque / Cutting Wheel Force (TOC) versus Penetration (P), in G1, G2, G3 .....	451
Figure 6.58 Cutting Wheel Force / Torque (COT) versus Penetration (P), in G1, G2, G3 .....	452
Figure 6.59 Joint relative frequency of penetration (P) and torque of the cutting wheel / cutting wheel force (TOC) for all ground conditions (G1, G2 and G3) .....	453
Figure 6.60 Joint relative frequency of penetration (P) and torque of the cutting wheel / cutting wheel force (TOC) in G1 (soil).....	454
Figure 6.61 Joint relative frequency of penetration (P) and torque of the cutting wheel / cutting wheel force (TOC) in G2 (mixed).....	454
Figure 6.62 Joint relative frequency of penetration (P) and torque of the cutting wheel / cutting wheel force (TOC) in G3 (rock).....	455
Figure 6.63 Penetration (P) versus Cutting Wheel Force / Total Thrust Force (COTT), in G1, G2, G3 .....	456
Figure 6.64 Joint relative frequency of cutting wheel force/ total thrust (COTT) and penetration rate (P) for all ground conditions (G1, G2 and G3) .....	457
Figure 6.65 Joint relative frequency of cutting wheel force/ total thrust (COTT) and penetration (P), in G1 (Soil).....	458
Figure 6.66 Joint relative frequency of cutting wheel force/ total thrust (COTT) and penetration (P), in G2 (mixed) .....	458
Figure 6.67 Joint relative frequency of cutting wheel force/ total thrust (COTT) and penetration (P), in G3 (rock) .....	459
Figure 6.68 Scatter plot of CF, TO and P of the data .....	460
Figure 6.69 General configuration for the geological prediction Bayesian model.....	463
Figure 6.70 Hierarchical discretization algorithm .....	466
Figure 6.71 Illustration of the application of the geological prediction model (** if GC is known, it is not necessary to enter evidence on the machine parameters to update geological conditions ahead of the face, since the model assumes that geological condition at ring 3 only depends on the geology at ring 2).....	469
Figure 6.72 best structure for geological prediction model .....	477
Figure 6.73 Geological prediction Bayesian model (same model as the one of Figure 6.69, with structure 22) .....	485
Figure 6.74 Bayesian decision model .....	485
Figure 6.75 illustration of step 1 and 2 for tunnel at ring 1 .....	486
Figure 6.76 Bayesian decision model (nodes in red are the updated geological states obtained from Figure 6.75, in green is the updated “optimal” decision) .....	487
Figure 6.77 Geological longitudinal profile for Line C tunnel (from PK 298 to PK 624) .....	488
Figure 6.78 Geology updating after excavating ring 292 (accident zone 3).....	489
Figure 6.79 Geology updating after excavating ring 293 (accident zone 3).....	489
Figure 6.80 Geology updating after excavating ring 296 (accident zone 3).....	490
Figure 6.81 Geology updating after excavating ring 298 (accident zone 3).....	490
Figure 6.82 Expected utility updating after excavating ring 292 (accident zone 3) .....	491
Figure 6.83 Expected utility updating after excavating ring 293 (accident zone 3).....	492

Figure 6.84 Expected utility updating after excavating ring 296 (accident zone 3) .....	492
Figure 6.85 Expected utility updating after excavating ring 298 (accident zone 3) .....	493
Figure 6.86 Probability failure updating after excavating ring 293 (accident zone 3) ...	494
Figure 6.87 Probability failure updating after excavating ring 296 (accident zone 3) ...	494
Figure 6.88 Probability failure updating after excavating ring 298 (accident zone 3) ...	495
Figure 6.89 Prediction of geological conditions along section 1 (using model 22). Note that for this section there is no detailed information regarding the encountered geology except at face survey points.....	502
Figure 6.90 Prediction of geological conditions along section 2 (using model 22). Note that for this section there is no detailed information regarding the encountered geology except at face survey points.....	503
Figure 6.91 Post accident survey results and predicted geology .....	504
Figure 6.92 Alarm criteria for extracted weight limits and rate (section 1) .....	505
Figure 6.93 Alarm criteria for extracted weight limits and rate (section 2) .....	506
Figure 6.94 decision support framework for the design and construction phase.....	508
Figure 6.95 Section 1: a) design geological longitudinal profile ; b)Extracted weight (measured by the EPBM scales) per ring .....	557
Figure 6.96 Section 1 a) Injected grout per ring in Section 1; b) Total thrust and cutting wheel force per ring.....	558
Figure 6.97 Section 1: a) torque of the cutting wheel; b) penetration and advance rate	559
Figure 6.98 Section 2: a) design geological longitudinal profile ; b)Extracted weight (measured by the EPBM scales) per ring .....	560
Figure 6.99 Section 2: a) Injected grout per ring in Section 1; b) Total thrust and cutting wheel force per ring.....	561
Figure 6.100 Section : a) torque of the cutting wheel; b) penetration and advance rate	562

## LIST OF TABLES

Table 3.1 List of variables for each record .....	78
Table 3.2 Undesirable event list.....	81
Table 3.3 Events related to the use of conventional methods.....	107
Table 3.4 Major losses since 1994.....	135
Table 3.5 List of ground parameters and their influence .....	155
Table 3.6 List of construction parameters and their influence.....	157
Table 3.7 List of observable parameters and their influence .....	158
Table 3.8 Comparison between geophysical methods (adapted from Galera and Pescador, 2005).....	176
Table 4.1 Conditional probability table for $P(D=\text{yes}   a, b, c)$ .....	235
Table 4.2 $P(B=b   a_1, a_2, a_3, a_4)$ .....	236
Table 4.3 $P(B=b   c_1, c_2)$ .....	237
Table 4.4 $P(S = \text{yes}   c, a)$ for the Cold and Angina model. ....	241
Table 4.5 Data set .....	249
Table 4.6 Probability of variable A in BN a).....	250
Table 4.7 Conditional Probability associated with variable B in BN a).....	250
Table 4.8 Conditional Probability associated with variable A in BN b) .....	251
Table 4.9 $P(B A)$ .....	257
Table 4.10 Conditional probabilities of the example. $P(J R)$ .....	278
Table 4.11 Conditional probabilities of the example. $P(M R, S)$ .....	278
Table 4.12 Prior probability table for $P(J, R)$ .....	279
Table 4.13 Prior probability table for $P(M, R, S)$ .....	279
Table 4.14 Calculation of $P^*(M, R, S) = P(M, R, S   M=y)$ .....	280
Table 4.15 Calculation of $P^*(J, R)$ .....	280
Table 4.16 Calculation of $P^{**}(J, R) = P(J, R   J = \text{yes}, M = \text{yes})$ .....	281
Table 4.17 Calculation of $P^{***}(M, R, S) = P(M, R, S   M=\text{yes}, J = \text{yes}) = P(M, R, S   M=\text{yes})$ .....	281
Table 5.1 Prior geological states for section 1 .....	296
Table 5.2 Construction Strategies Costs .....	296
Table 5.3 Probability of Failure given construction strategy and geological state (vulnerability).....	297
Table 5.4 Consequences of Failure (Utilities) .....	297
Table 5.5 Information Phase in Decision Analysis for Tunnel Exploration (after Einstein et al., 1978).....	309
Table 5.6 Exploration Reliability Matrix.....	310
Table 5.7 Geological state prior probability for each section.....	323
Table 5.8 Construction costs for each section (in utilities).....	323
Table 5.9 Transition model for section 1 of the tunnel in Figure 5.4 .....	329
Table 5.10 Transition matrix (second order Markov model).....	344
Table 6.1 Geomechanical groups and associated conditions.....	369

Table 6.2 Mode of Operation of the Porto Metro EPBM Machine along Line C tunnel (from Transmetro, 2000).....	375
Table 6.3 Ground Classes .....	405
Table 6.4 Prior Probability of Ground Condition at tunnel face (Section 1).....	411
Table 6.5 Prior Probability of Ground Condition at tunnel face (Section 2).....	411
Table 6.6 Prior Probability of piezometric level (Section 1 and Section2) .....	411
Table 6.7 Probability of GC (Section 1 and Section2) .....	412
Table 6.8 Probability of Failure given CGC and construction strategy (Section 1 and Section 2).....	413
Table 6.9 Probability of Damage Level given SO and Failure, (Section 1 and Section 2) .....	413
Table 6.10 Construction costs (Section 1 and Section 2) .....	414
Table 6.11 Failure “costs” (Section 1 and Section 2) .....	415
Table 6.12 Mean Value (in kN), Standard Deviation (in kN) and Coefficient of Variation for Cutting Wheel Force.....	421
Table 6.13 Discretization of the variable Cutting Wheel Force (CF).....	422
Table 6.14 Mean Value (in mm/rev), Standard Deviation (in mm/rev) and Coefficient of Variation for Penetration rate (P) .....	424
Table 6.15 Discretization of the variable Penetration rate (P).....	425
Table 6.16 Mean Value (in MNm), Standard Deviation (in MNm) and Coefficient of Variation for Torque of the Cutting Wheel (TO).....	427
Table 6.17 Discretization of the variable Torque of the Cutting Wheel (TO).....	428
Table 6.18 Mean Value (in m), Standard Deviation (in m) and Coefficient of Variation for Torque / Cutting Wheel Force (TOC) .....	430
Table 6.19 Discretization of the variable Torque / Cutting Wheel Force (TOC).....	431
Table 6.20 Mean Value (in kN), Standard Deviation (in kN) and Coefficient of Variation for Total Thrust Force (TT).....	433
Table 6.21 Mean Value, Standard Deviation and Coefficient of Variation for Cutting Wheel Force / Total Thrust Force (COTT) .....	435
Table 6.22 Discretization of the variable Cutting Wheel Force/Total Thrust (COTT) ..	436
Table 6.23 Correlation coefficient between Penetration rate and Cutting Wheel Force in G1, G2 and G3 .....	439
Table 6.24 Correlation coefficient between P and TO in G1, G2 and G3 .....	442
Table 6.25 Correlation coefficient between cutting wheel force (CF) and Torque of the cutting wheel (TO) in G1, G2 and G3.....	447
Table 6.26 Correlation coefficient between Torque / Cutting Wheel Force (TOC) and Penetration (P), in G1, G2 and G3 .....	452
Table 6.27 Correlation coefficient between Penetration (P) and Cutting Wheel Force/ Total Thrust (COTT) in G1, G2 and G3 .....	456
Table 6.28 Geological transition matrix .....	463
Table 6.29 Discretization of the machine parameter variables.....	465
Table 6.30 Discretization of the machine parameter variables (uniform width) .....	466
Table 6.31 Model structure results.....	471
Table 6.32 Five best overall models – Set A. ....	477
Table 6.33 Best models in predicting G1 (Soil) – Set A .....	478
Table 6.34 Best models in predicting G3 (Rock) – Set A .....	478

Table 6.35 Five best overall models – Set B .....	479
Table 6.36 Best models in predicting G1 (soil) – Set B .....	479
Table 6.37 Best models in predicting G3 (rock) – Set B .....	480
Table 6.38 Confusion matrix for model 22 (training set A) .....	480
Table 6.39 Confusion matrix for model 22 (training set B) .....	481
Table 6.40 Transition matrices used in sensitivity analysis for model 22 .....	483
Table 6.41 Results of sensitivity analysis (for the effect of geological transition matrices) on model 22, data set B. ....	483
Table 6.42 Reference unit weight values (kN/m <sup>3</sup> ).....	498
Table 6.43 total weight values per ring (ton).....	500



# CHAPTER 1 Introduction

## 1.1 Problem definition

Tunnel construction has been increasing world wide. The majority of tunnel construction projects have been completed safely. There is, however, an intrinsic risk associated with tunnel construction, since it involves the subsurface, which is largely unknown. There have been several incidents in various tunneling projects that have resulted in delays, cost overruns, and in a few cases more significant consequences such as injury and loss of life. As is common with problems in construction projects these have been widely publicized, and pressure has been mounting from the society to eradicate these problems. There is, therefore, an increasing urgency to assess and manage the risks associated with tunnel construction.

Tunneling is characterized by high degrees of uncertainty, which arise from two major factors. The first one involves the geologic conditions, which can never be known exactly. Problematic geologic conditions include, for example, rock bursts or faults, squeezing and swelling ground, hard and abrasive rock. The second factor is the construction process itself. Even if geologic conditions are known, there is still considerable uncertainty about the construction process, since this depends on the performance of the equipment as well as the skills of the workers.

Various commercial and research software for risk analysis during tunnel construction have been developed over the years, the most important of which is the DAT (Decision Aids for Tunneling), developed at MIT in collaboration with EPFL (Ecole Polytechnique Fédérale de Lausanne). The DAT are based on an interactive program that uses probabilistic modeling of the construction process to analyze the effects of geotechnical uncertainties and construction uncertainties on construction costs and time. (Dudt et al, 2000; Einstein, 2002b).

The majority of existing risk analysis systems deal only with the effects of random (“common”) geological and construction uncertainties on time and cost of construction. There are, however, other sources of risks, not considered in these systems, which are related to specific geotechnical scenarios that can have substantial consequences on the tunnel process, even if their probability of occurrence is low. Good examples of such situations are the construction of Porto Metro, in Portugal, the Barcelona Metro in Spain and the Pinheiros Metro Station, in Brazil, where collapses with catastrophic consequences occurred. Not considering specific geotechnical risk explicitly is an issue that can have substantial consequences on project delivery.

## **1.2 Research objectives**

This study attempts to address the issue of specific geotechnical risk by first developing a methodology that allows one to identify major sources of geotechnical risks, even those with low probability, in the context of a particular project and then performing quantitative risk analysis to identify the “optimal” construction strategies, where “optimal” refers to minimum risk. In order to achieve this, a database of accidents that occurred during tunnel construction was assembled and analyzed. The analyses of the database led to a better understanding of the main causes and consequences of accidents. The important parameters, whether ground related, construction related, or monitoring related were then used to develop the risk assessment methodology that is presented in this work. Thus the specific objectives of this research are as follow:

- The creation of a database of tunnel construction accidents. This database contains information regarding the incident(s), the possible causes and failure mechanisms, consequences and remedial measures. The database will be made available to designers, contractors, owners and experts in the tunneling domain, and is considered to be the most comprehensive tunnel accident database available.



- The development of a decision support framework for determining the “optimal” (minimum risk) construction method for a given tunnel alignment. The system should be usable both during the design phase and during the construction phase. The decision support system consists of two models: a geologic prediction model, and a construction strategy decision model. Both models are based on the Bayesian Network technique, and when combined allow one to determine the ‘optimal’ tunnel construction strategies. The decision model contains an updating component, by including information from the excavated tunnel sections.
- The implementation of the decision support system in a real case tunnel project, namely the Porto Metro in Portugal.

### **1.3 Thesis Outline**

This thesis is organized as follows:

In Chapter 2, a historical overview of tunnel construction is presented. This includes basic terminology and developments of tunnel construction, focusing on mechanized and conventional excavation methods.

In Chapter 3, a database of accidents that occurred during tunnel construction worldwide is presented. The process of data collection and the structure of the database are explained. Different types of accidents are identified, and their causes and consequences are presented.. We believe that the creation of the database and its analysis is of great use to decision makers (owners, designers, contractors), leading to better knowledge on accidents during tunnel construction, and allowing one to identify different types of accidents, their causes, the chain of events and their consequences. The database is then analyzed to identify common and important parameters that are related to ground, construction, and monitoring. The parameters’ importance and interrelationships are analyzed and general influence diagrams are built for each type of tunnel accident during construction. The results of this study can be used as starting points for risk assessment for tunnel projects.

In Chapter 4, several models for data analysis and representation are described, and common techniques for risk assessment are presented. The fundamentals of Bayesian Networks and Influence diagrams are introduced, since these will be used in following chapters. A comparison is made between classic decision analysis, and BN's, and the advantages, and disadvantages of each are stated.

In Chapter 5, a risk assessment and mitigation methodology is proposed. This is done based on the results of the database analysis in Chapter 3. The proposed methodology allows one to determine the “optimal” construction method(s) for a given alignment, using Bayesian networks and influence diagrams. A simple example is used to illustrate the methodology.

In Chapter 6, a general description of the Porto Metro project, including geological conditions, tunnel alignment, and construction methods is provided. Details on the three accidents that occurred during the first 320 m of construction of the tunnel of Line C are presented. Emphasis is placed on the circumstances which led to the accidents, and their possible causes. The risk assessment methodology presented in Chapter 5 is then applied to the real case of the Porto Metro. The methodology combines two steps, geological prediction and decision on the construction strategy. The geology prediction is based, during construction, on the automatically recorded machine performance parameters, such as penetration, torque and cutting wheel force. It is shown that the geological predictions of the model are close to reality, that the model is able to predict changes in geology and, therefore, allows one to adapt the construction strategy to the encountered ground conditions.

Chapter 7 summarizes the results of the research and provides recommendations for future work.

## **CHAPTER 2 Tunnel Construction**

### **2.1 The origin and evolution of tunnel construction**

Tunnel construction originated from the need of overcoming major natural barriers, such as mountains, and bodies of water or from the need of crossing highly built up urban areas. The principal uses of tunnels are, among others, fresh water supply, road, railroad, mining, sewage, hydropower schemes.

The historical origin of the tunnel is uncertain; Archeologists believe that the earliest underwater tunnel was built by the Babylonians under the Euphrates River between 2180 and 2160 B.C. in what is now Iraq. They used what is now called the cut and cover method. 5000 years ago the Egyptians have constructed tunnels to access tombs. They developed techniques to cut soft rocks with copper saws and hollow reed drills, both surrounded by an abrasive (Sandström, 1963)

The ancient Greeks and the Romans built several tunnels for carrying water and for mining, some of which are still in use. The tunnel of Samos, excavated on the Greek Island of Samos in the sixth century B.C. is an example of one of the great engineering achievements of ancient times (Figure 2.1). It was a water tunnel of 1036 m length dug through solid limestone by two separate teams advancing from both ends (Apostol, 2004)

Tunneling in the Middle Ages was limited and mainly used for mining and military purposes. The next major advances occurred in Europe due to its growing transportation needs. The first of several major canal tunnels was on the canal du Midi in France, part of the first canal linking the Atlantic and the Mediterranean. It was built in 1666-81 with a length of 515 feet and a cross section of 22 by 27 feet. One of the first tunnels with a considerable length (about 2 mi) was part of the Grand Trunk Canal in Great Britain and was completed in 1777 (Stack, 1982).

According to Kovári (2001), the start of tunnel engineering occurred with the construction of the Tronquoy Tunnel on the canal of St. Quentin in France, 1803-1810. The tunnel had a really large width, for that time (8 m) and was driven through a sandy squeezing rock. An arch was constructed from bottom to top, through several individual adits. The excavation of the core was then done under the protection under the protection of the arch (Figure 2.2)

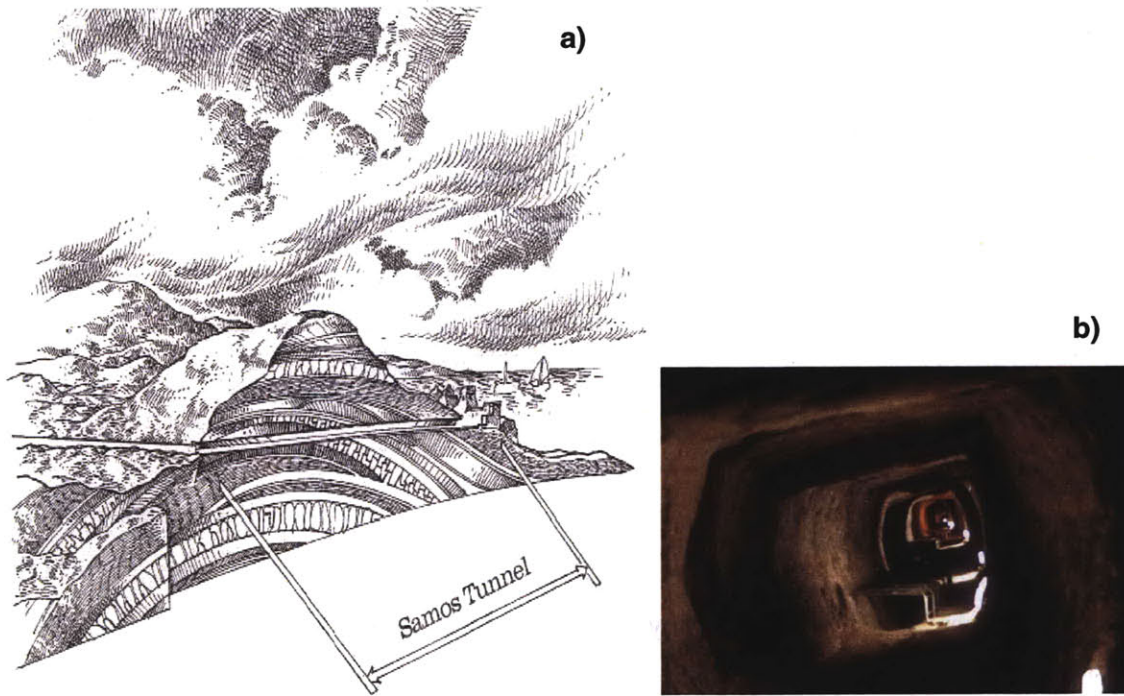


Figure 2.1 a) Illustration of Samos tunnel in Greece; b) picture taken inside the tunnel. In cross section the floor is more or less horizontal but the roof slopes along the rock strata (Apostol, 2004)

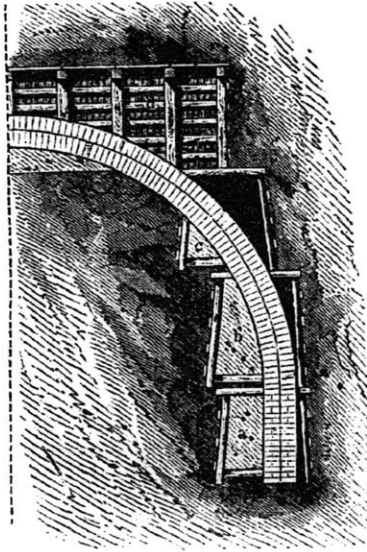


Figure 2.2 Illustration of the construction process of the Tronquoy tunnel (Sandström, 1963)

Many other canal tunnels were built in Europe and North America during the 18th and the early 19th centuries. At the beginning of the 19th century these tunnels were built with temporary supports made of timber and applying different sequential excavation methods, such as the system used in the Tronquoy tunnel on the St. Quentin Canal by the French engineers.

Tunnelling under rivers was finally possible when the shield technique was invented by M. I. Brunel who was the first to use it in 1825 tunneling under the Thames River in London, with a rectangularly shaped shield. The cylindrical form of the shield was first patented by Peter Barlow. This method was then improved considerably by the supervising engineer James Henry Greathead who joined Barlow for the design of the Tower Hill tunnel under the Thames (Kovari, 2001)

In 1830 with the introduction of railways, tunneling increased immensely. Most of the developments in this area occurred in England. In the United States the first important tunnel was the Hoosac railroad tunnel in Massachusetts. It was 4.5 miles long with a cross section of 24 by 22 feet. Although the initial estimation for completion was 3 years it took 21 years to finish construction in part due the fact that the rock was too hard for the drilling tools available at the time. It was finally finished in 1876. Despite the time it took to be completed it contributed to the advances in tunneling technology by being one of

the first times that dynamite was used and the first time electric firing of explosives was used and power drills were introduced.

Spectacular tunnels were built in Alps, after the introduction of railways. The first was Mont Cenis, an 8.5mi tunnel that took 14 years to be built and was completed in 1871. It was followed by the Saint Gotthard (1872-82), about 13 km long (9 mi), the Simplon tunnel, consisting of two parallel single-track tunnels (both 12.3 mi/19.8 km) and completed in 1906 and 1919 respectively, which was for many years the longest railway tunnel in the world, and the Lötschberg tunnel (1906-11) with a length of 13 km (9 mi), where a major accident occurred in 1908 when a heading collapsed.

During the second half of the 20<sup>th</sup> century and early 21<sup>st</sup> century there was an increase in demand for tunnels and other underground structures, due to the need for constructing longer and deeper railway tunnels such as those in the Alps (Mt Cenis, Gotthard, etc), for hydroelectric power stations as well as tunnels for motorways. This provided the right environment for new inventions, philosophies and associated techniques. The growth of the mining activities since the 19<sup>th</sup> century had also a decisive effect on tunnel engineering triggering new developments mainly regarding more economical rock supports. Conventional tunneling world wide was dominated by timber up to the 50's (Figure 2.3); gradually it was replaced by steel, then shotcrete, anchors and finally a combination of these supports.

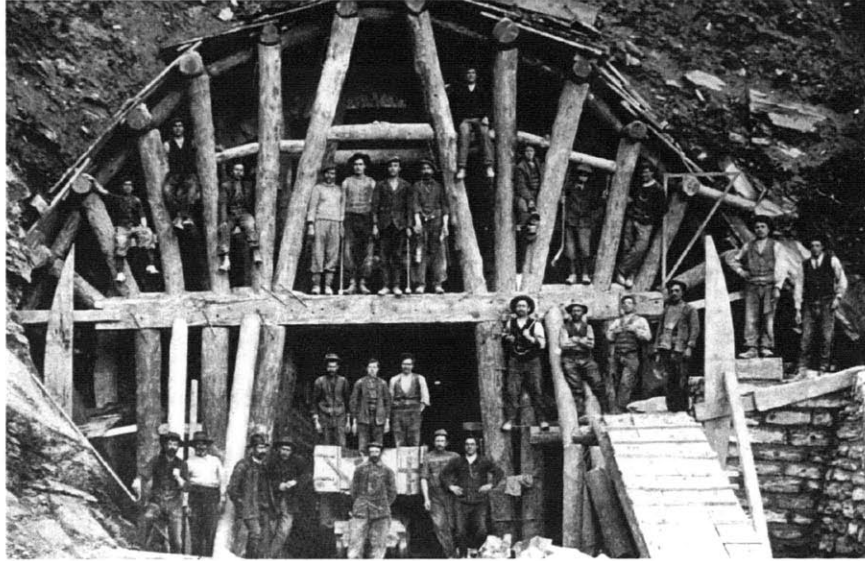


Figure 2.3 Timber support for the south ramp of the Lötschberg tunnel (1908-1913)  
(Kovári, 2001)

The use of tunnels for metro systems started in London, England in 1863. Since then many large and densely populated cities have constructed metro systems. Metro lines are normally part of larger urban underground projects. During the last four decades, due to the rapid increase in urbanization in the world, which brought many problems (congestion, air pollution, loss of surface area for transport infrastructures, etc), there has been a growing awareness to solve these problems and reconstitute life quality to the urban areas by using underground space. In developing countries one of the main obstacles to underground construction is that its cost is much higher than an alternative on the surface. However, in developed countries there is increased use of the underground, especially because of (Longo, 2006): i) public pressure for a better quality of life in the cities; ii) technological advances and iii) the increasing cost of surface area in the cities and the impact of construction at the surface.

There are several recent examples of major uses of the underground in Boston, Stuttgart and Tokyo, which will now be briefly described.

The Central Artery in Boston, the Big Dig, is the most costly highway project ever done in the US. It was initiated due to the chronic congestion of the Central Artery (I-93), an elevated six-lane highway passing through the center of downtown Boston, and cutting



off Boston's North End and Waterfront neighborhoods from downtown, making it difficult for these areas' to participate in the city's economic life. In 2001 the traffic was of 190000 vehicles per day with stop and go traffic jams of 10 hours per day (McNichol, 2000). The solution to these problems was the so called Central Artery/Tunnel Project (CA/T), which consisted of two major components (Massachusetts Turnpike Authority, url: <http://www.masspike.com/>):

- i) The replacement of the six-lane elevated highway with an eight-to-ten-lane underground expressway directly beneath the existing road (Figure 2.5)
- ii) The extension of I-90 (the Massachusetts Turnpike) from its former terminus south of downtown Boston through a tunnel beneath South Boston and Boston Harbor to Logan Airport

The project contains 7.8 miles of highway, 161 lanes miles in all, about half of which are in tunnels (Figure 2.4).



Figure 2.4 Central Artery Project Layout (Massachusetts Turnpike Authority, url: <http://www.masspike.com/>)



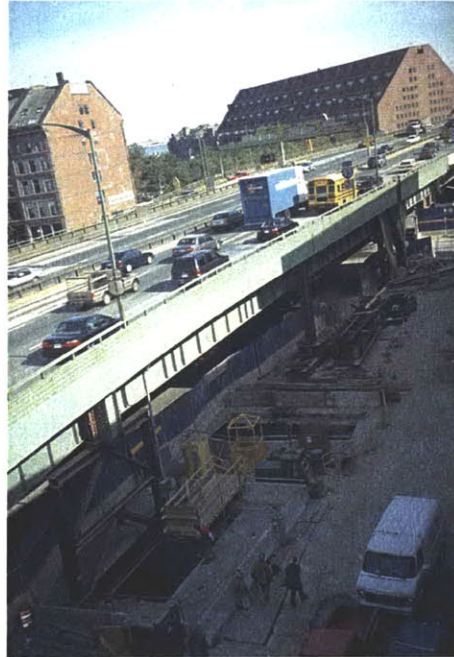


Figure 2.5 Construction of the eight-to-ten-lane underground expressway directly beneath the existing road, 1998 (Sousa, 2006).

The completion of this project brought considerable improvements to the city's traffic congestion problems, to the air quality of the city and quality of life (Figure 2.6)



Figure 2.6 Photographs depicting the “before” and “after” of the Central Artery/Tunnel Project (photo by David Pal).

Another important project is Stuttgart 21, which is one of Deutsche Bahn's largest projects consisting mainly of a comprehensive redesign of Stuttgart's dead-end central station, the Feuerbach-Wendlingen south rail connection as part of the Stuttgart-Ulm high speed line and a new railway station connecting the airport. In the North the center of the city will also be connected to the high speed line to Mannheim (Stuttgart21, url: <http://www.stuttgart21.de>).

The total length of the new routes is 56.9 km, of which 32.8 km are tunnels. The construction is expected to start in 2010 and to be completed in 2020.

In Tokyo the scarceness of surface area, coupled with the better behavior of underground structures in earthquakes has contributed to the development of new technologies in tunnel construction. Japan invests strongly in the design of TBMs. A good example of the use of these new generation TBMs are the ones conceived specially for the construction of the Nanboku line of the Tokyo underground. In the construction of a station, a TBM resulting from the union of three TBMs was used (Figure 2.7a and b). In this line a TBM composed of two concentric TBMs (Figure 2.7c and d) was also used (Assis, 2001)

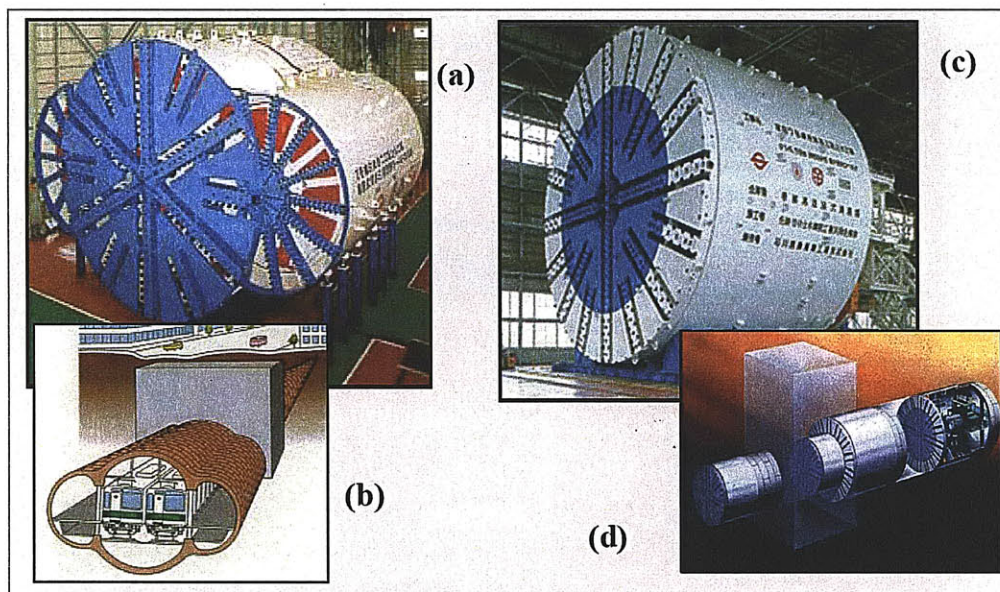


Figure 2.7 Two of the TBMs used in the construction of the Nanboku Line. a) TBM used in the construction the Shiroganedai station; (b) sketch of the station; (c) Double concentric TBM used in part of the line; d) simplified scheme of the TBM advance (Assis, 2001).

Immersed and floating tunnels are alternatives for crossing water and can be alternatives to bored tunnels. Immersed tunnels consist of concrete or steel tunnel elements, pre-fabricated on shipways, in dry docks, or in improvised floodable basins (Saveur & Grantz, 1993; Schultz & Kochen, 2005). The history of Immersed Tunnels started in 1893 with the construction of three 6 feet diameter sewage lines in the port of Boston, the Shirley Gut Siphon, the Nut Island Outfall and the Deer Island Outlet (Grantz, 1997). The first immersed tunnel that was constructed for transportation purposes was a railroad tunnel under the Detroit river between the US and Canada, in 1910. The most common solution used in the United States is steel tunnel segments. In the Europe the most common are concrete elements (Saveur & Grantz, 1993)

The North American experience, especially in the United States, is of great relevance. The immersed tunnel of the Bart (Bay Area Rapid Transit) in San Francisco is the longest in the world. The Trans-Bay tube consists of 57 mixed steel-concrete elements with a total length of approximately 6.1km. This system started to be planned in 1946 and construction of an immersed rail tunnel near the existing bridge (Figure 2.8a) was considered. This way the environmental impact on the Bay would be minimized. The construction of BART started officially in July 19, 1964. The first section was placed in the Bay in November of 1966 (Figure 2.8b)

The Marmaray Project, in Turkey, comprises 76 km of triple track, 13.6 km of which are underground. Two of the tracks will be upgraded from existing ones on both sides of the Bosphorus, connected to each other through a two track railway tunnel under Istanbul and the Bosphorus. The third track (only on land) will be totally new and will be used for inter-city and freight. The tunnels comprise 1.4 km of immersed tube tunnel across the Bosphorus Straits in Istanbul up to 58m deep, 9.8km twin bored tunnel and 2.4km of cut & cover tunnel. There are three large underground stations and 37 surface stations. All tunnels and stations are designed to remain operational after an earthquake of 7.5 magnitude. (Ingerslev, 2005; Lykke and Belkaya, 2005). The immersed tube has a cross-



section of 15.3m wide by 8.75m deep within which are two cells for single rail. The first section of the tube was placed in the summer of 2007 (Horgan and Madsen, 2008.)

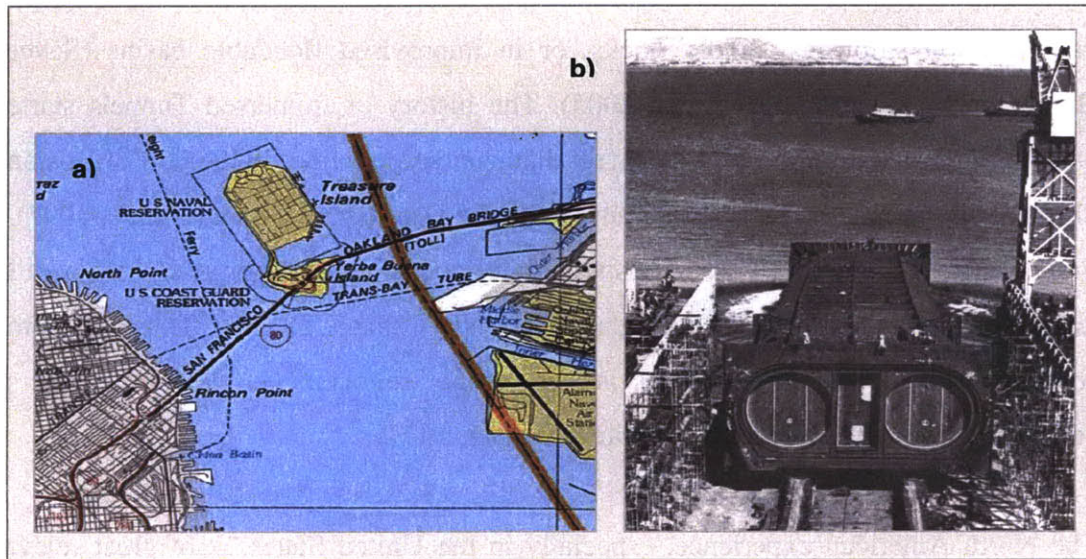


Figure 2.8 a) Location of the trans-bay tube in San Francisco; b) launching of a pre-fabricated element of the trans-bay tube (ASME International, 1997)

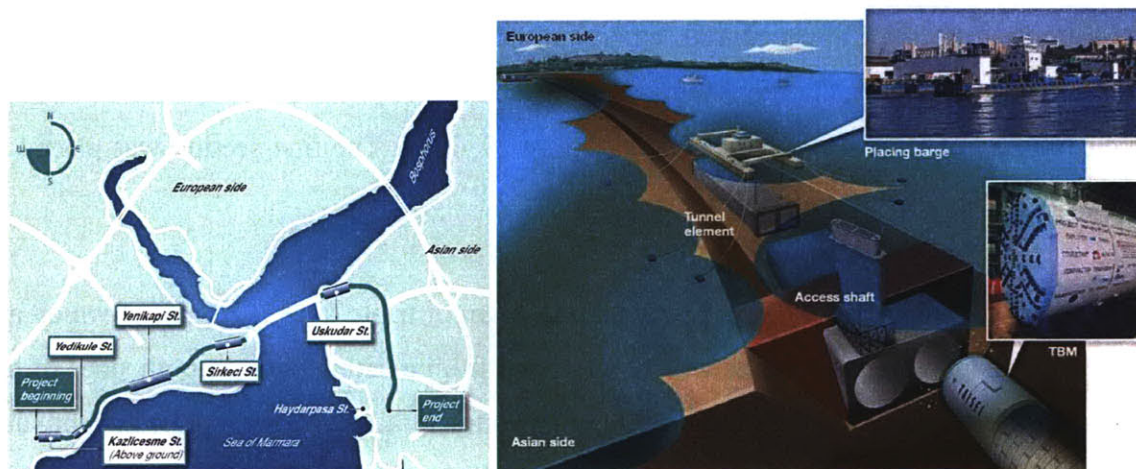


Figure 2.9 a) Layout of the Marmaray Project; b) Schematic of the docking process between TBM and immersed tube (Horgan and Madsen, 2008).

Submerged floating tunnels (SFT) are immersed tunnels supported within the water column above the sea bed. They can be supported like an underwater bridge on piers, be hung from pontoons, may span from side to side (no support in the middle), or if buoyant, could be held down using tension legs similar to oil platforms (Figure 2.10a and b).

SFT's are a viable and useful concept for crossing deep bodies of water, or water bodies where bridges would be undesirable due to their environmental impact or difficulty of construction. Although no SFT has yet been built, considerable efforts have been invested in research and development. Examples of projects that were or are under study are: Høgsfjord in Norway, which was stopped due to regional changes. A tunnel in the Strait of Messina connecting Calabria to Sicily, that was first proposed in 1969. Later on in 1984 several extended structural analyses were performed, but it was considered not the most viable solution due to the risk of being hit by sinking ships. A thirty-kilometer long link, crossing the Funka Bay at Hokkaido, in Japan. A tunnel crossing Lake Washington in Seattle USA. (Ingerslev, 2003; Norwegian public road administration, 2006). A consortium between the Chinese Academy of Sciences and Ponte di Archimede S.p.A., financed by the Italian Ministry of Foreign Affairs, the Chinese Ministry of Science and Technology and the Institute of Mechanics of the Chinese Academy of Sciences, has started to build a 100m demonstration floating tunnel in Qiandao Lake in the eastern Chinese province of Zhejiang. Inside it, two levels of one-way motorways will run through in the middle, with two railway tracks on the sides. The Qiandao Lake prototype will serve to help plan for the project of a 3,300-meter submerged floating tunnel in the Jintang Strait, in the Zhoushan archipelago, also situated in Zhejiang (Ponte di Archimede International S.p.A. ;People's Daily Online, 2007)

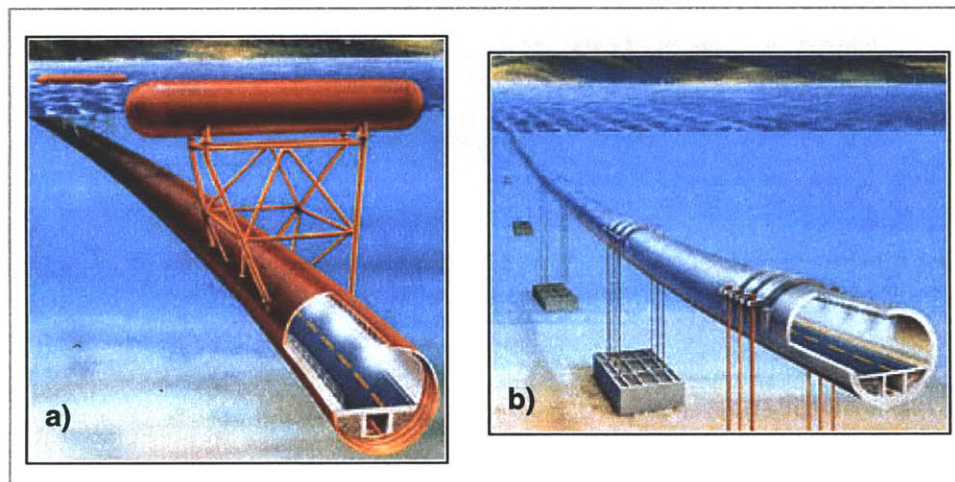


Figure 2.10 Different concepts for submerged floating tunnels. a) hanging from pontoons (concept developed by Kværner Rosenberg); b) held down by tension cables (concept developed by Aker Norwegian Contractors) (Moe, 1997)



With the advances of high speed trains and associated technologies, such as magnetic levitation, projects such as the transatlantic tunnel have been proposed. Plans for such a tunnel have not progressed beyond the conceptual stage, however. The main barriers to constructing such a tunnel are cost and the limits of current materials science. Figure 2.11 illustrates a proposal for a 3,100-mile (5,000-km) long near-vacuum tunnel with vactrains, a theoretical type of maglev train that could travel at speeds up to 5,000 mph (8,000 km/h). SFT was considered the most viable alternative to build the Transatlantic tunnel Most concepts for this tunnel envision it between the New York City and London. The travel time at these speeds would be of less of an hour between the two cities.

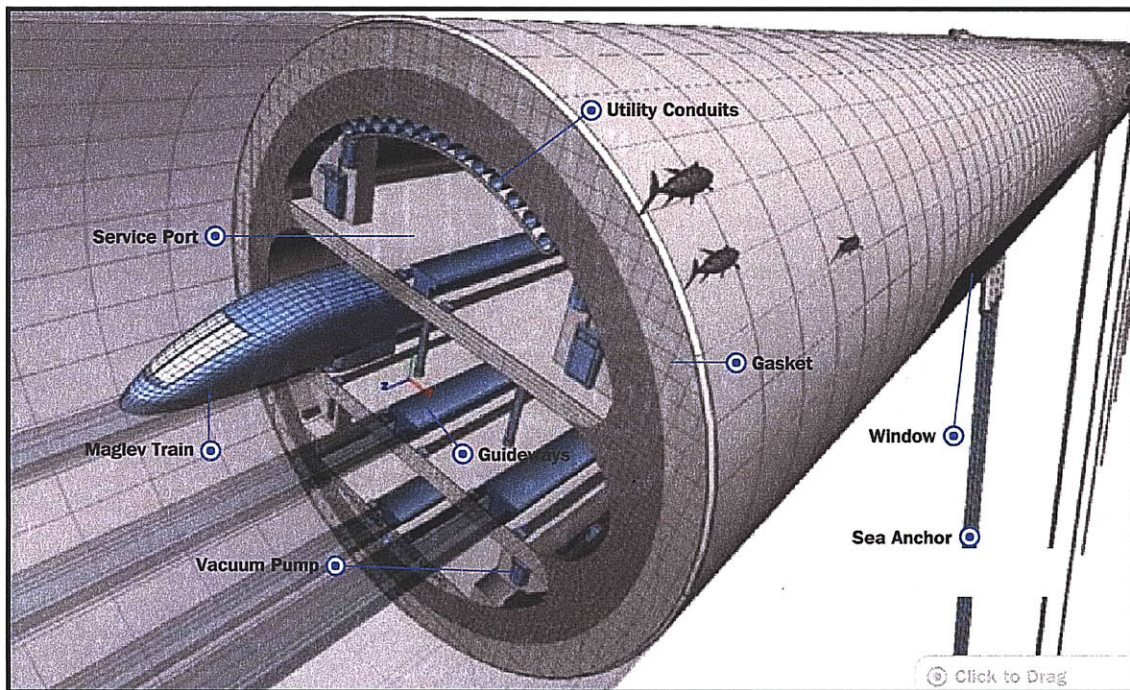


Figure 2.11 Illustration of the a proposal for transatlantic tunnel (Discovery Channel)

## 2.2 Construction methods

Since the origin of tunneling many types of construction methods have been developed. In this section, two main groups will be described: Conventional Excavation methods and

Excavation by machines. In the conventional excavation methods section only NATM or sequential excavation methods will be described.

## **2.2.1 NATM / Sequential Excavation Methods**

### **2.2.1.1 Historical Background**

The New Austrian Tunneling Method (NATM) was originally developed during the 1950's when shotcrete started to be used systematically. At the time it was called shotcrete method, the term NATM originated during a lecture by professor Rabcewicz at the Thirteenth Geomechanics Colloquium in 1962 in Salzburg. NATM expressed the advantage of allowing the ground to deform before placing the final lining so that the loads on this are reduced. This concept of dual lining supports (initial and final support) had been introduced by Rabcewicz in 1948.

The name NATM, however, is still a controversial matter amongst the experts in the field. Other designations used are Sequential Excavation Method (SEM) and Sprayed Concrete Lining (SCL). Also when talking about NATM some tunneling engineers and experts define NATM as a technique and others as a design philosophy (or both).

### **2.2.1.2 Principal features**

The key features of the NATM design philosophy and construction method are as follows:

- the strength of the ground is mobilized deliberately to its maximum extent, which is achieved by allowing controlled deformation of the ground

The initial support system must have stress – deformation characteristics suitable for the ground conditions and its installation must be timed with respect to the

deformations of the ground. Figure 2.12 shows a schematic of ground-support interaction curves (stress- deformation). If a stiffer support (c) is used it will carry more load than a more flexible one (d) because the ground won't be able to deform as much until the equilibrium is reached. As important as the rigidity of the support is the time when it is applied. If the same support is applied after some deformation occurs it will reach the equilibrium with a lower load on the support. Therefore the support should not be too stiff (c) nor too flexible (d) and it should not be applied too early (a), in order to take advantage of the reduction in load in the support, nor too late (b) in order not to increase the deformations drastically.

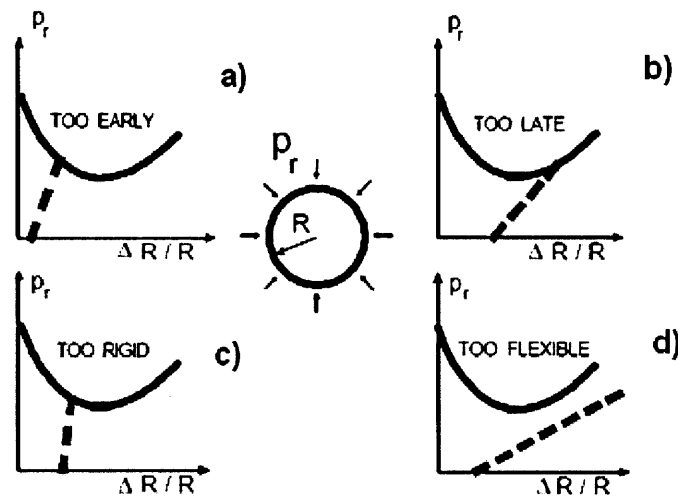


Figure 2.12 The basic principles of NATM (adapted from Müller and Fecker, 1978)

- Observation of the excavation is essential to monitor the performance of the excavation, i.e. the deformations of the ground and of the initial support, as well as to verify the initial support design and change it if necessary.
- The construction of the tunnel is often done by sequentially excavating and supporting the tunnel. The sequence depends mainly on the response of the ground. Typically the tunnel cross section is divided into a number of smaller faces. Normally the tunnel face is divided into two or three sections (crown-heading and invert or crown-heading, bench and invert, respectively), but this



number can be increased in case of very large cross sections and/or poor ground conditions. If the ground conditions and/or geometry of the cross section permit the tunnel can also be excavated in full. Figure 2.14 and Figure 2.15 show examples of a tunnel excavated in three partial faces and in six partial faces, respectively.

- The primary support normally consists of shotcrete reinforced with fiber or steel mesh in combination with steel sets, rock bolts or forepoling (Figure 2.16)
- The permanent support normally consists of a cast in place concrete.

Figure 2.13 shows a typical cross section for a NATM tunnel proposed by Rabecewicz (1965)

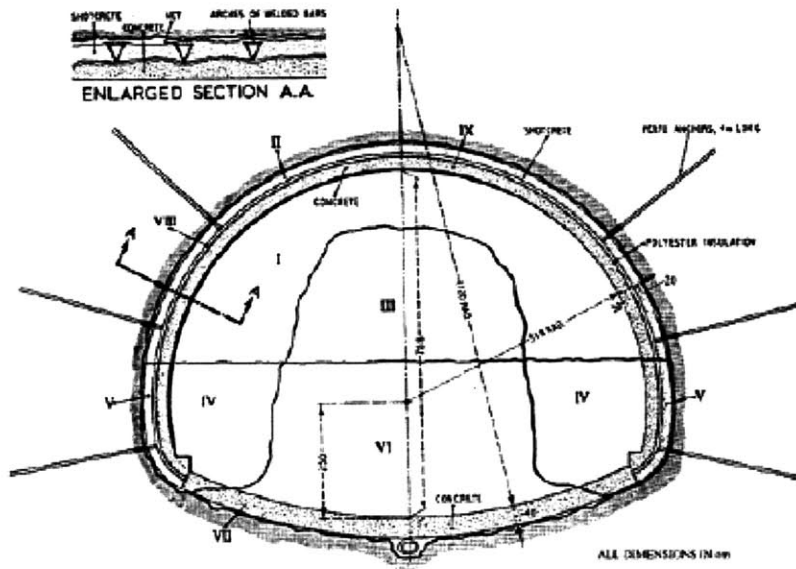


Figure 2.13 Typical cross section proposed by Rabecewicz (1965)

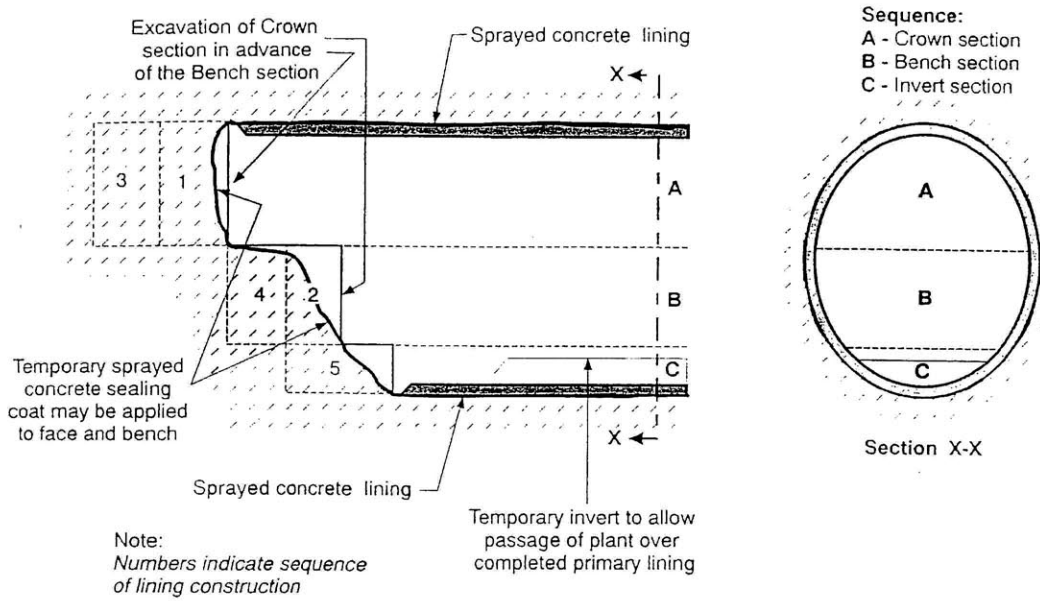


Figure 2.14 Tunnel excavated in 3 partial faces (HSE, 1996)

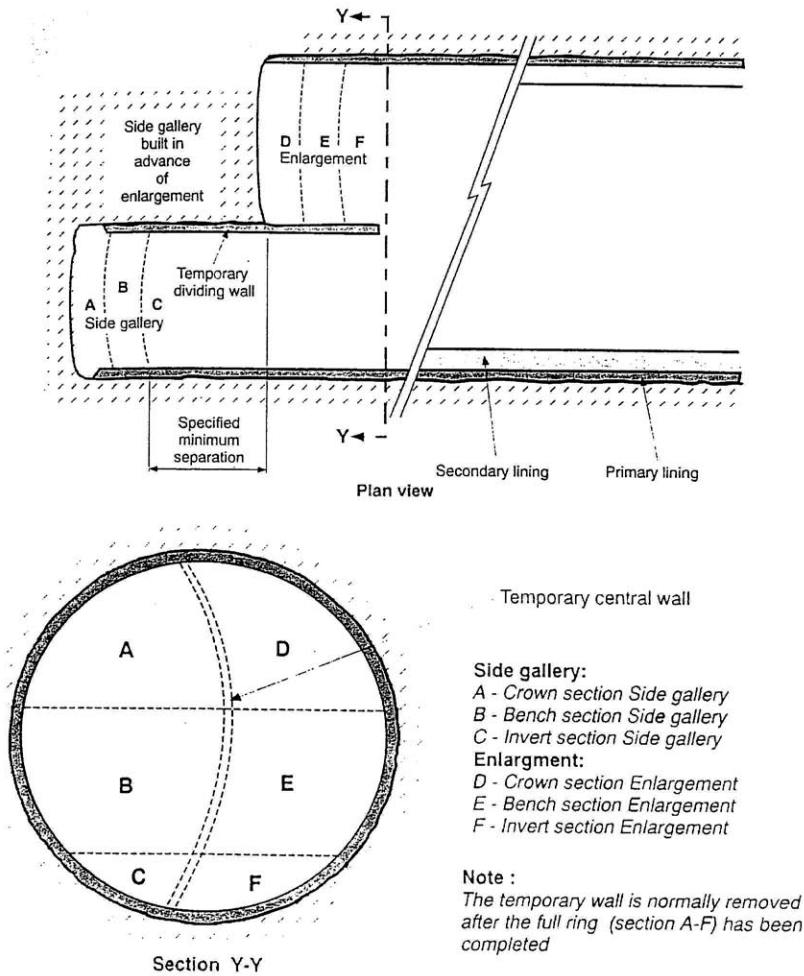
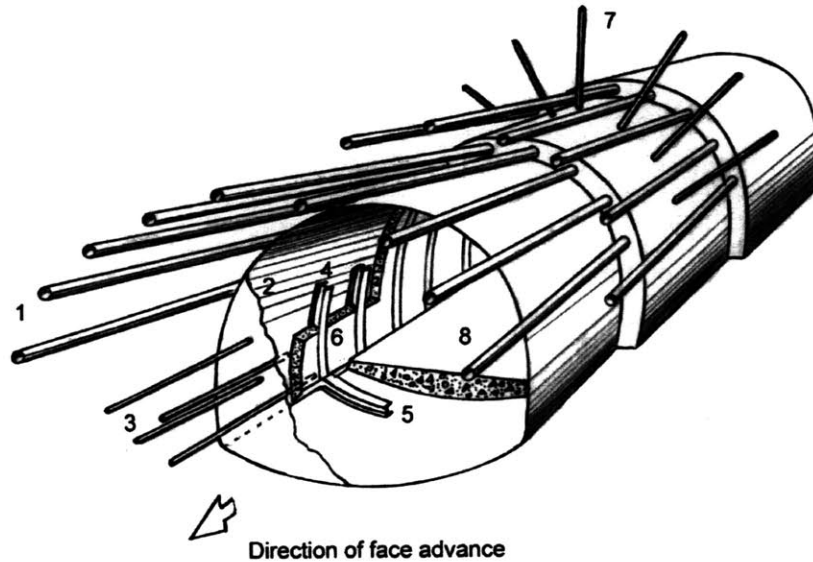


Figure 2.15 Tunnel excavated in 6 partial faces (HSE, 1996)



- 1- Forepoles; 2- shotcrete (at the face); 3- Grouted fiberglass dowels (at the face); 4- Steel sets;  
 5 - Shotcrete reinforced with fiber or wire mesh; 6 – Rockbolts; 7- invert lining;  
 Note: the final lining is not represented.

Figure 2.16 Full face excavation of a tunnel under the protection of a forepole umbrella  
 (Hoek, 2007)

## 2.2.2 Excavation Machines

### 2.2.2.1 Historical Background

As previously mentioned the shield was developed in England by Marc Brunel and first used in 1825 to dig under the Thames River. The development of the TBMs paralleled the development of the long railroad tunnels of the first half of the 19<sup>th</sup> century. In Europe the first big obstacle to overcome in building a railway network was the crossing of the Alps. The first tunnel through the Alps was the Mont Cenis, also known as the Frejus tunnel, built between 1857 and 1871. For this tunnel a Belgian engineer named Henry Maus, built and tried out the first rock-tunneling machine. The machine was never actually used for the construction of the tunnel (Pelizza, 1999a).

During the period 1846-1930, close to 100 rock or hard-ground tunnelling machines of various types were designed and patented, but many of those were never actually built. The Beaumont machine patented in 1875 and the Beaumont/English machine patented in 1880 are examples that were in fact built and used. Considered to be the first successful soft rock tunneling machine, the Beaumont machine was actually used in the first attempt to construct the channel tunnel, boring over a mile of tunnel in 1882; construction stopped in 1883 due to a strong Military opposition in England (Kirkland, 1986). By the end of the 1920s, after many unsuccessful attempts, the interest in the development of tunneling machines faded. Finally during the period of 1952-53 the American company, James S. Robbins and Associates, designed and manufactured the “Mittry Mole” (7.8m diameter, 149kW), the first mechanical rotary excavator which was the pioneer of modern rock TBMs (Stack, 1982). Rapid developments in the technology led to broaden their application range into harder and harder rock.

#### **2.2.2.2 Types of TBMs**

Nowadays there are several types of tunnel excavation machines and different classifications have been adopted. This chapter will follow the classification adopted by AFTES (2000), “new recommendations on choosing mechanized tunneling techniques”, presented in Figure 2.17.

The machines are classified according to the type of support they provide to the excavation: None, Peripheral and Peripheral and Frontal.

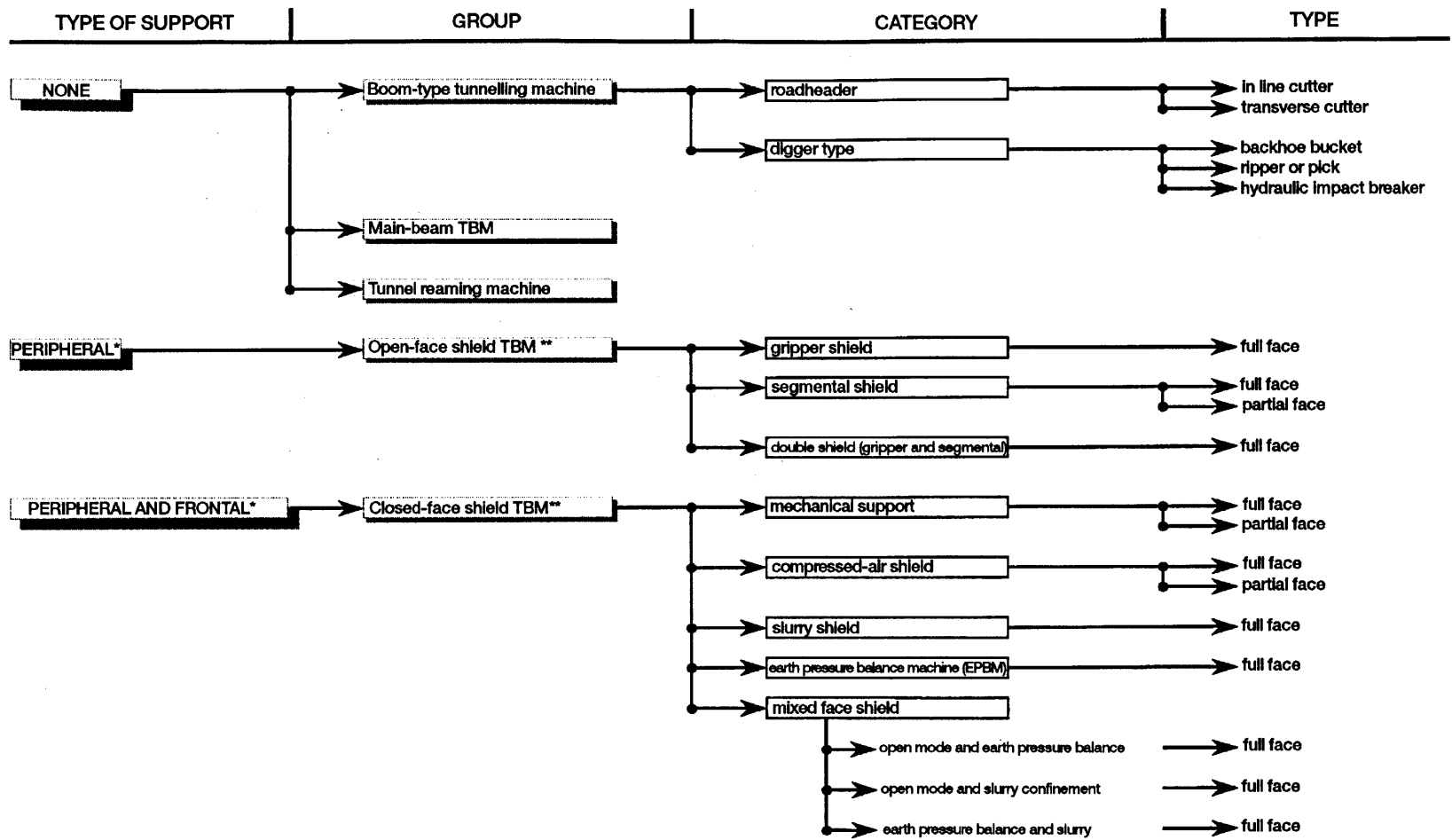


Figure 2.17 Classification of Tunnel Excavation Machines (AFTES, 2000)

### ***A. Machines providing no support***

These types of machines are used in ground conditions that do not require immediate and continuous excavation support. They are classified in three groups:

- *Boom type tunneling machines.* These are machines with an arm with an excavating tool at the end. In these cases the excavation of the face is partial. A common example is the roadheader (Figure 2.18)
- *Main beam TBM.* This is a TBM that has cutterhead that excavates the full face at once. However the cutterhead does not provide immediate peripheral support for the excavation. The machine advances by means of grippers that push radially against the rock. Figure 2.19 shows a scheme of a main beam TBM.
- *Tunnel reaming machine.* It has the same principles of the main beam TBM. However the excavation of the face in this case progresses from a pilot bore. The machine is pulled forward by grippers located at the pilot bore unit (
- Figure 2.20)



Figure 2.18 Photo of a roadheader

(Anshan Power Heavy Industry CO, LTD, url: [www.anshanhongqi.com](http://www.anshanhongqi.com) )

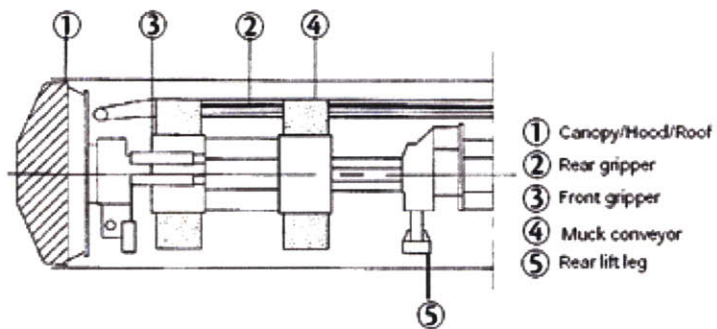


Figure 2.19 Main Beam TBM scheme (AFTES, 2000)

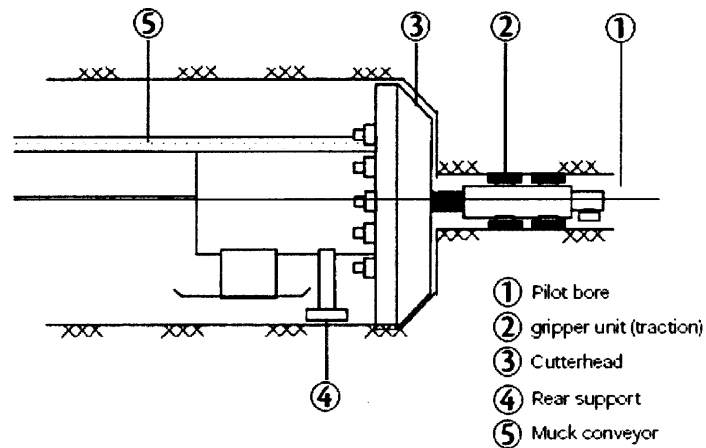


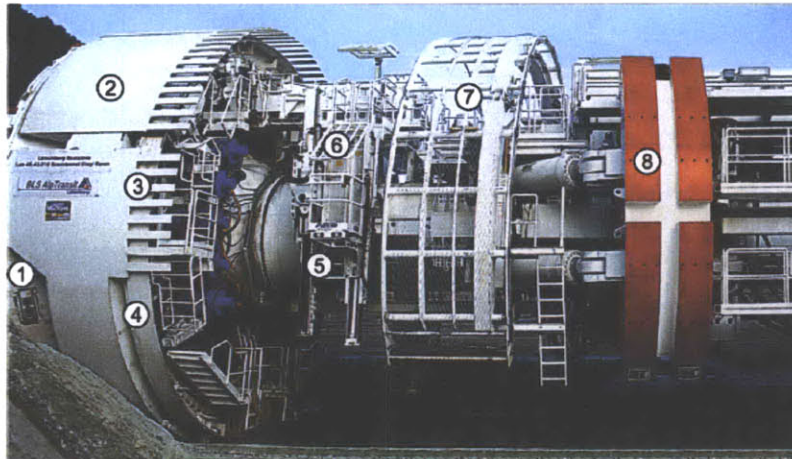
Figure 2.20 Tunnel reaming machine (AFTES, 2000)

### ***B. Open Face TBM***

Open Face TBM's provide only peripheral support. They can be composed of one shield or two shields connected by an articulation. The main difference between the different types of open face tunneling machines is the mechanism they use to advance.

#### **Gripper Shield TBM**

It is composed of a cutterhead, thrust cylinders and gripper plates. The advance is achieved by means of grippers reacting against the rock mass. A gripper TBM is suitable for tunnels in rock, in which the support needs are minimal or can be achieved by rockbolts, steel sets and / or shotcrete applied locally to the tunnel. Figure 2.21 shows a Gripper Shield machine and its main components.



- |                  |                              |
|------------------|------------------------------|
| ① cutterhead     | ⑤ anchor drill               |
| ② gripper shield | ⑥ work cage with safety roof |
| ③ finger shield  | ⑦ wire mesh erector          |
| ④ ring erector   | ⑧ gripper plates             |

Figure 2.21 Gripper TBM (Wittke, 2007)

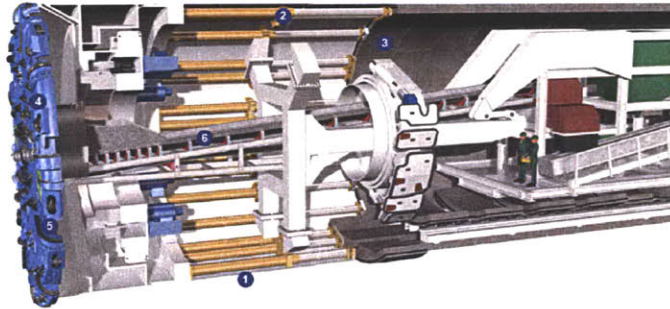
### Segmental-shield (or single shield TBM)

Single shield machines are fitted with an open shield for peripheral support (1). They do not provide counterpressure at the face (Figure 2.22).

They are normally used in ground where the strength is too low to transmit the gripper reaction forces. These machines move forward by means of thrust cylinders (2) reacting against the last placed ring of the final lining (3). The cutting wheel (4) is fitted with hard rock disks. Muck bucket lips (5), which are positioned at some distance behind the disks, remove the excavated rock behind the cutting wheel. The excavated material is carried away by conveyers (6).

The cutterhead (or cutting wheel) diameter is normally slightly larger than that of the shield, in order to avoid the shield getting stuck during the drive. The void between the shield and the excavated rock is called the steering gap. The void between the lining and the excavation contour is called the annular gap and is normally grouted through the use of grouting lines installed in the tail –skin (tail of the shield).



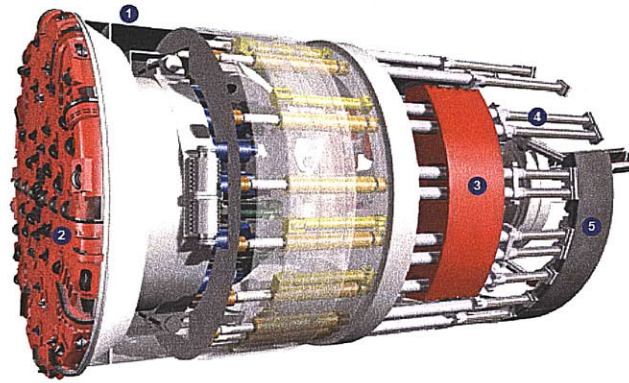


- |                     |                  |             |
|---------------------|------------------|-------------|
| 1- Shield           | 3- Lining        | lips        |
| 2- Thrust cylinders | 4- Cutting wheel | 6- Conveyer |
|                     | 5- Muck bucket   |             |

Figure 2.22 Single Shield TBM (Herrenknecht, url: [www.herrenknecht.com](http://www.herrenknecht.com))

### Double-shield TBM

A double shield TBM is a combination of the gripper shield TBM and a shielded TBM. This type of machine can easily adapt to different geologies along a tunnel route. It is particularly suitable for tunnels in hard rock where fault or weak zones occur. It is composed of an extendable front shield that can move over the full face cutterhead, grippers located in the middle section of the TBM and auxiliary thrust cylinders. The rear part of the machine does not move during the excavation process and forces are transmitted to the rock through the extended grippers installed in the middle of the machine. For this reason the lining segments can be installed during the excavation process. This continuous excavation process can only be carried out in undisturbed zones, since the grippers require good rock for reaction. When the double shield reaches a fault zone, the telescopic front shield is pulled back. The machine is then moved forward only by the auxiliary thrust cylinders, which react on the tunnel lining. This process is similar to the one of the single shield TBM.



- |                             |                      |
|-----------------------------|----------------------|
| 1 - Extendable front shield | 3 - Grippers         |
| 2 - Cutterhead              | 4 - Thrust cylinders |
|                             | 5 - Lining segments  |

Figure 2.23 Double Shield TBM (Herrenknecht, url: [www.herrenknecht.com](http://www.herrenknecht.com))



Figure 2.24 Double Shield TBM used in Guadarrama tunnels in Spain (Herrenknecht, url: [www.herrenknecht.com](http://www.herrenknecht.com))

### ***C. Closed Face TBM***

Closed Face TBMs, provide simultaneous peripheral and face support. Except for the mechanical support TBMs, they all have a cutterhead chamber in front of the machine that is isolated from the rest of the machine by a bulkhead. In this chamber a confinement pressure is maintained in order to provide an active support on the face. The main difference between the types of closed face TBMs, is how this support is achieved.

## Mechanical-support TBM

A mechanical support TBM is composed of a cutterhead that provides face support by continuously pushing against the excavated material. The muck is extracted by openings located in the cutterhead that is equipped with gates controlled in real time. The difference between these machines and the open face segmental shield is the type of cutterhead. The mechanical support TBM's contain opening with adjustable gates and a peripheral seal between the cutterhead and the shield that allow the face support to be achieved by holding excavated material ahead of the cutterhead. It provides a passive support, clearly different from the other types of closed face machines.

These types of machines are suitable for soft rock and consolidated ground with little to no water pressure. Figure 2.25 shows a photo of a mechanical support TBM as well as a schematic showing its principal components.

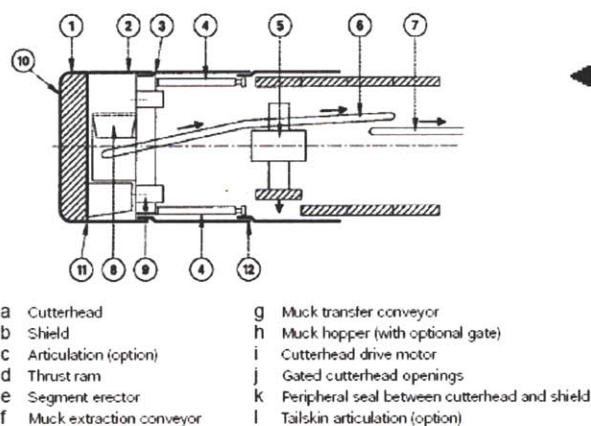


Figure 2.25 Mechanical-support TBM (AFTES, 2000)

## Compressed air TBM

The compressed air TBM achieves face support through pressurized air inside the cutting chamber. This type of machine can have a full cutterhead or an excavating arm as shown in Figure 2.26.

The compressed air method is the oldest one of the active counter pressure methods, but it is not very common anymore due to the difficult working conditions it imposes.



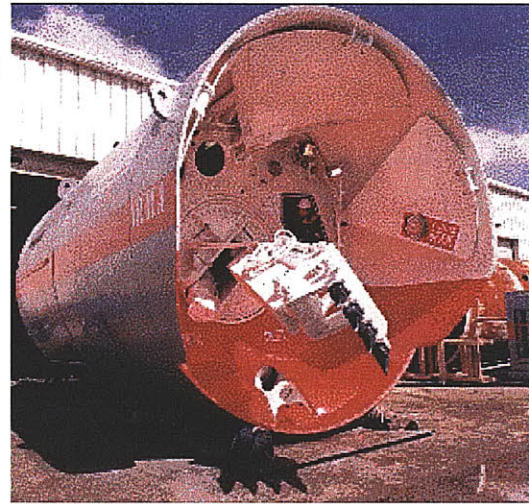
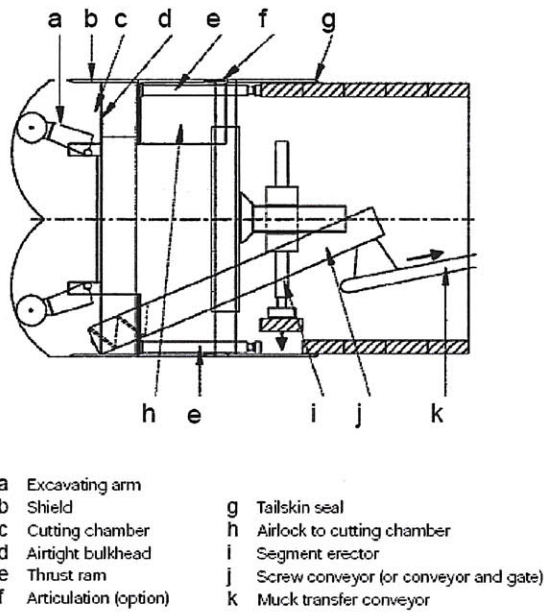


Figure 2.26 Compressed air TBM (AFTES, 2000)

### Slurry shield

In slurry type tunneling machines the cutterhead excavates the ground, and support of the face is achieved by slurry pressure, such as a suspension of bentonite or a clay and water mix. The main components are a cutterhead that excavates ground, a slurry mixer, slurry pumps to feed and discharge, circulate and pressurize the slurry mix and finally a slurry treatment plant to separate the bentonite from the excavation material allowing it to be recycled. Figure 2.27 is a schematic of such a machine.

Figure 2.28 shows the face support principles of a slurry tunneling machine. The support pressure at the face  $p_s$  has to balance at least the ground horizontal pressure  $p_h$  and water pressure  $p_w$ .

This type of machine is used in ground with limited self-supporting capacity, such as sands and gravels with silts, with the presence of groundwater. Using disc cutters permits the machine to also excavate in rock (Figure 2.29).

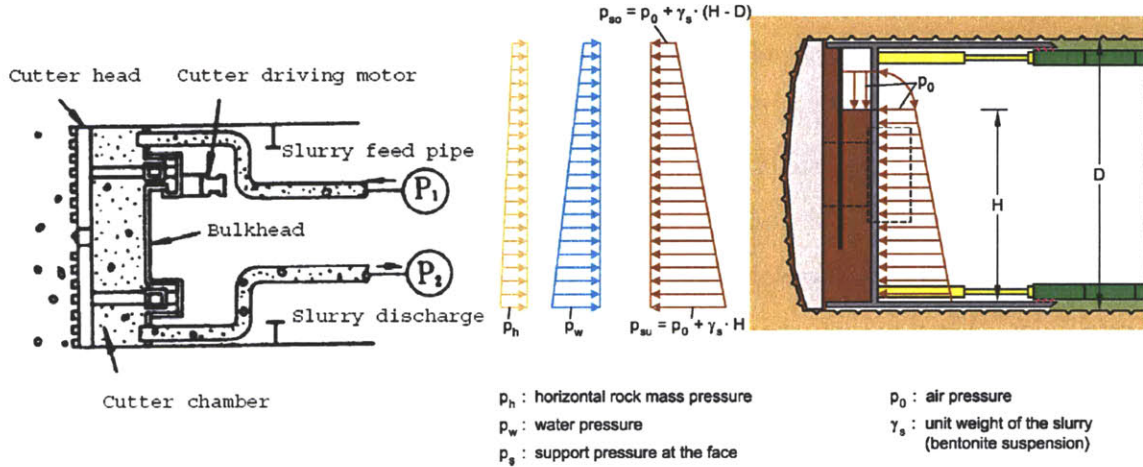


Figure 2.27 Slurry Shield Machine sketch (International Tunnelling Association, 2000)

Figure 2.28 Slurry Shield Machine principles (Wittke, 2007)



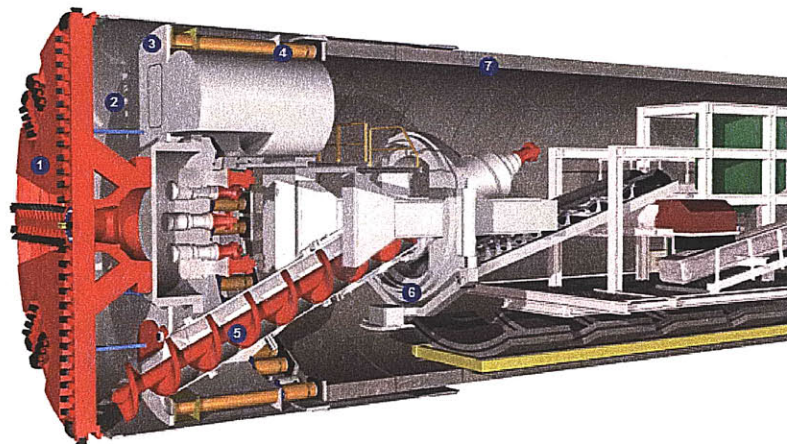
Figure 2.29 Photograph of the cutterhead of a Slurry type tunneling machine for the underground metropolitan railway in Mühlheim, Germany (Wittke et al., 2007)

### EPB Machine

In an Earth Pressure Balance Machine (EPBM), presented in Figure 2.30, the stability of

the face is achieved by pressurizing the excavated material in the cutterhead chamber (2), which is separated from the section of the shield under atmospheric pressure by the pressure bulkhead (3). The excavated material is removed by an auger conveyer (5). The amount of material removed is controlled by the speed of the auger. The tunnels are normally lined with steel reinforced concrete lining segments (7), which are positioned by means of erectors (6) in the area of the shield behind the pressure bulkhead and then temporarily bolted in place. Grout is continuously forced into the remaining gap between the segments' outer side and the ground through injection openings in the tailskin or openings directly in the segments. Figure 2.31 shows a schematic with the EPBM principles. When operating in closed mode, the supporting pressure  $p_s$  has to balance at least the horizontal ground pressure  $p_h$  and the water pressure  $p_w$ .

These types of machines are particularly suitable for soils that are likely to have a consistency capable of transmitting the pressure to the cutterhead (clayey soil, fine clayey sand, marl, etc). In some cases the classical application could be broadened to tunnels that cross more cohesive soil conditions and tunnels that cross both rock and soil, i.e. mixed face conditions, through the use of additives (Herrenknecht and Rehm, 2003). In hard abrasive ground it is normally necessary to use additives or install hard face wear plates.



- |                       |                      |                   |
|-----------------------|----------------------|-------------------|
| 1- Cutterhead         | 3- pressure bulkhead | 5- Auger conveyer |
| 2- Excavation chamber | 4- Thrust cylinders  | 6- Erector        |
|                       |                      | 7- Lining         |

Figure 2.30 EPB Machine (Herrenknecht, url: [www.herrenknecht.com](http://www.herrenknecht.com))



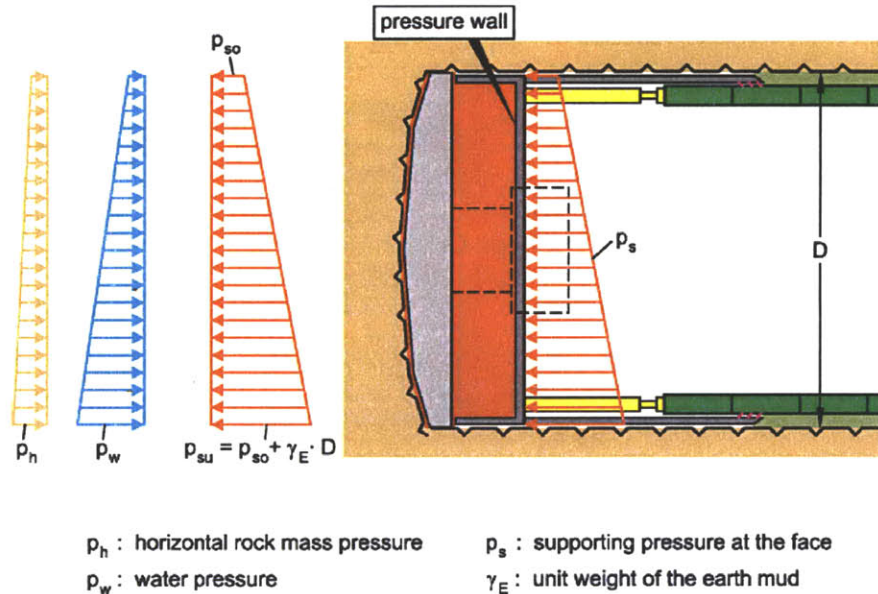


Figure 2.31 EPB Machine principles (Wittke et al., 2007)

The EPB TBM can operate in different modes (Babendererde et al., 2005):

- i) **Open mode** if there no active support of the face, only the passive support from the cutterhead.
- ii) **Semi-closed mode** if the excavation chamber is not completely filled with earth. Compressed air in the empty part of the chamber provides moderate support against face instabilities. This mode is normally used in more stable ground with sufficient cohesion. It produces a higher rate of advance, less tool wear and savings in the conditioning additives, when compared with the closed mode.
- iii) **Closed mode** if the excavation chamber is completely filled with pressurized earth. In this case the pressure level is controlled by the rotation of the cutterhead and the rotation of the auger conveyer (or screw conveyer), which are manually controlled by the machine operator.

Note that only in mode iii) the earth pressure is balanced. Figure 2.32 shows a summary of the modes described above.

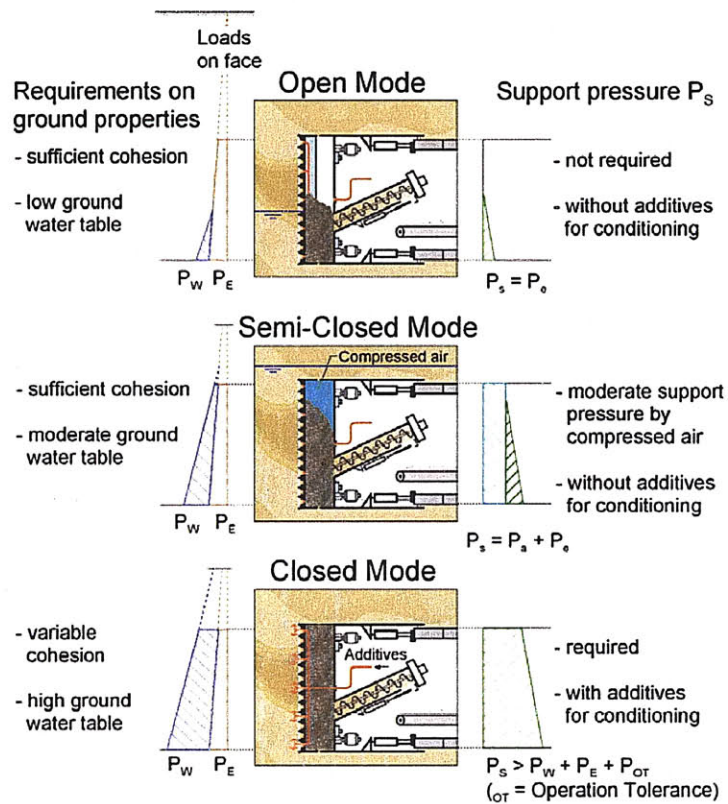


Figure 2.32 EPBM Operation modes (Barbarderede et al., 2005)

Note:  $P_E$  is the horizontal ground pressure equivalent to  $P_h$  in Figure 2.31

## Mixed Face shield TBM

Mixed Face shield TBM can work both in closed or open mode and with different confinement techniques (slurry, earth pressure). The main types of mixed face shields are (AFTES, 2000):

- Machines that can work in open mode and can change to closed mode with face support provided by earth pressure;
- Machines that can work in open mode and can change to closed mode with face support provided by slurry pressure;
- Machines that can work in closed mode capable of providing face support provided by both earth pressure balance and slurry confinement.



In Germany, in the 1980s, companies Wayss & Freytag and Herrenknecht developed the MixShield TBM that combines both air pressure and slurry pressure. In this machine the pressure in the excavation chamber is not controlled directly by the suspension pressure but by a compressible air cushion, which keeps the suspension at the exact target pressure value through a compressed-air control system. This way the irregularities in the bentonite feeding circuit can be compensated much more effectively, and therefore the risks of settlements in urban areas can be reduced (Herrenknecht and Rehm, 2003b). Figure 2.33 shows a picture of the 12.40m diameter MixShield TBM used in the Elb 4<sup>th</sup> tube in Hamburg, Germany.



Figure 2.33 Elb 4th tunnel Mixshield TBM, Hamburg  $\phi$  14.2 m (Toan, 2006)

## 2.3 Tunnel construction monitoring

Tunneling carries greater risk than most of other civil construction due to its complexity and the uncertainties associated with the ground. An essential element of managing and controlling those risks is Monitoring and Observation during all stages of tunnel construction.

Monitoring allows one to control the stability of the tunnel and of adjacent structures by registering deformations in the ground and displacements on the surface, and comparing them with those predicted in the design. This makes it possible to quickly identify unpredicted behavior and implement countermeasures. This is the basis for adapting the

support to the local ground conditions. Finally the information collected during monitoring/observation should be used to verify and optimize the design of the supports through the reduction of the uncertainties associated with the assumed geomechanical parameters.

Monitoring is especially important when construction is crossing an urban environment. The excavation of the tunnel causes deformations around the cavity that propagate to the surface. In these cases the deformations at the surface are the most important and it is fundamental to make sure that these deformations remain within the allowable limits.

For tunnels in an urban environment monitoring is done in different phases of the project (Longo, 2006):

- Before construction: to determine a reference point in the area of construction.
- During construction: to measure convergences, states of stress and deformation of the ground and the water levels. This will allow one to verify the stability of the excavation as well as admissible deformations at the surface and inside the tunnel.
- After construction: to control the behavior of the tunnel lining with time and identify phenomena of deterioration. In this stage, monitoring will include scheduled visual inspections of the tunnels as well as systems of permanent monitoring that may be installed during the previous stage.

The type of measurements and instrument location should be adapted to the existing geology, environmental conditions and construction methods. The most commonly monitored quantities are displacements at the surface, inside the tunnel and inside the ground; water table levels and pressures and inclination of structures, as shown in Figure 2.34.

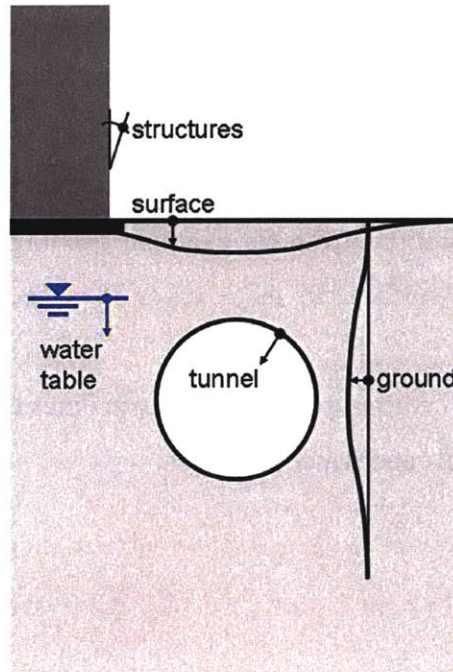


Figure 2.34 Most frequently monitored physical quantities (Kovári and Ramoni, 2006)

The main components of geotechnical monitoring and observation during construction are, among others:

- **Face Mapping:** geotechnical mapping of the tunnel face which can include comprehensive information on the ground formation (intact rock, degree of weathering, discontinuities) and on the ground water. This can only be carried out when the excavation is stopped, and the details of the information recorded depends on the time available (Figure 2.35)
- **Positional surveying**
- **Convergence measurements,** record the changes in distance of points on the tunnel contour. Figure 2.36 shows typical cross section with convergence measurement points.
- **Extensometer measurements and inclinometer measurements,** both record displacements and relative displacements in the ground. Figure 2.37 shows a typical cross with extensometers and inclinometers for shallow tunnels. Figure 2.38 shows a typical measurement cross section for deep tunnels.

- **Stress measurements** are carried out normally to assess the load in the initial and final liner. (Figure 2.38 shows the typical arrangement of a stress (pressure) cell in a shotcrete shell)
- **Vibration measurements.** Some of the main causes of damages to structures at the surface are vibrations from for example blasting that are transmitted through the ground to the surface. In these cases it is necessary to measure vibration waves.
- **Water level and water pressure measurements.** Piezometers are used to measure water levels and water pressures.



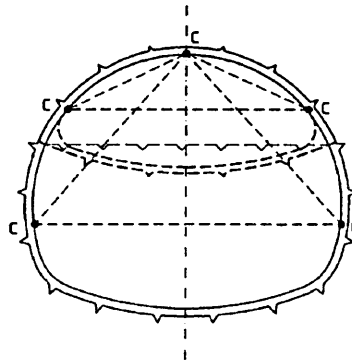


Figure 2.36 Typical convergence measurement cross section for crown and heading (Wittke et al., 2002)

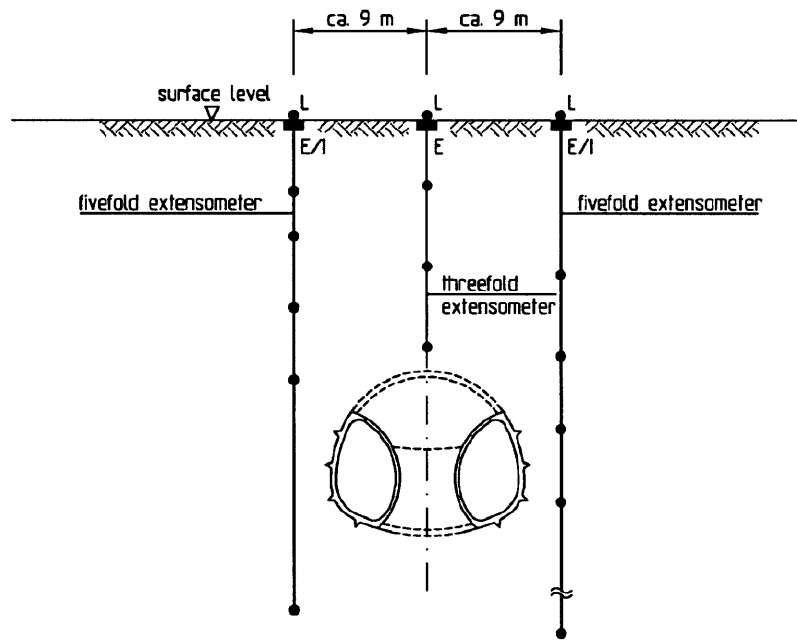
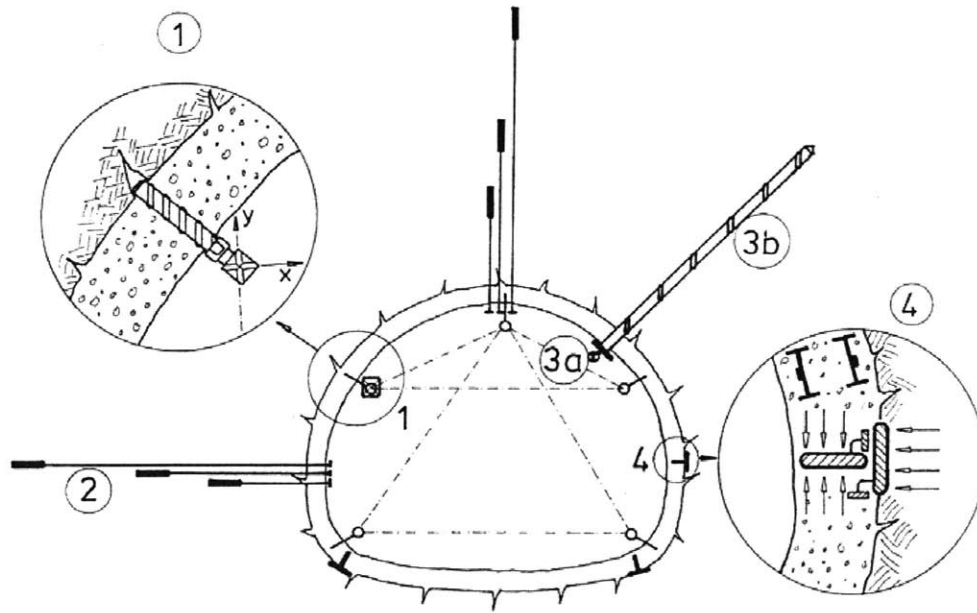


Figure 2.37 Typical extensometer and inclinometer measurement cross section for crown and heading (adapted from Wittke et al., 2002)



Legend	Measuring objective	Instrument
1	Deformation of the excavated tunnel surface	Convergence tape Surveying marks
2	Deformation of the ground surrounding the tunnel	Extensometer
3	Monitoring of ground support element 'anchor'	Total anchor force
4	Monitoring of ground support element 'shotcrete shell'	Pressure cells Embedments gauge

Figure 2.38 Typical instrumented cross section for crown and heading (Sousa, 2002)

When the construction method used is a shield there are some additional measurements that should be performed (Japan Society of Civil Engineers, 1996):

- i) For a closed-face type shield: Earth pressure in the cutter chamber, slurry pressure at the face, characteristics of the slurry. Figure 2.39 shows the pressure cells location for measuring of earth pressure in an EPB Machine.



- ii) Hydraulic pressure of the jacks, torque of the cutter, meandering and balance of the shield machine, control of the volume and pressure of backfill grout, control of the volume of excavated soil discharge
- iii) Deformation of the shield tunnel and deviation of the centerline from then designed alignment

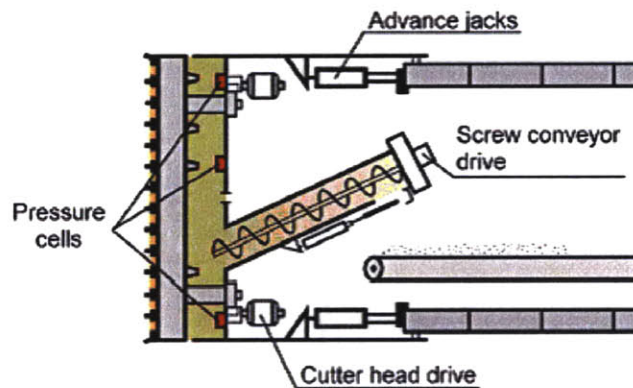


Figure 2.39 Measurement devices for face support pressure (Barbendererde et al. 2004)

## 2.4 References

- AFTES (2000). “New recommendations on Choosing mechanized tunneling techniques”. French Tunnelling and Underground Engineering Association.
- American Society of Mechanical Engineers International (1997). “National Historic Mechanical Engineering Landmark – San Francisco Bay Area Rapid Transit System”.
- Apostol, T. (2004). “The Tunnel of Samos”. Engineering & Science No.1 2004
- Assis, A. (2001). “Métodos construtivos aplicados a túneis urbanos” (In Portuguese). Curso sobre Túneis em Meios Urbanos, SPG, Coimbra.
- Babendererde, S.; Hoek, E.; Marinos, P.; Silva Cardoso, A. (2005). “EPB-TBM Face Support in the Metro do Porto Project, Portugal”. Proceedings 2005 Rapid Excavation & Tunneling Conference, Seattle.



Babendererde, S.; Hoek, E.; Marinos, P.; Silva Cardoso, A. (2004). "Geological risk in the use of TBMs in heterogeneous rock masses - The case of "Metro do Porto" and the measures adopted". Presented at the Course on Geotechnical Risks in Rock Tunnels, University of Aveiro, Portugal, 16-17 April, 2004.

Discovery Channel (2003), "Extreme Engineering": Transatlantic Tunnel. DVD.

Grantz, W (1997). "Steel-Shell Immersed tunnels - Forty years of experience". *Tunnelling and Underground Space Technology*, Vol. 12, No. 1, pp. 23-31, 1997.

Health Safety of New Austrian (1996), "Tunnelling Method (NATM) tunnels". A review of sprayed concrete lined tunnels with particular reference to London Clay. HSE Books, 1996.

Herrenknecht, M., Rehm, U. (2003a). "Earth Pressure Balanced Shield Technology". Soft Ground and Hard Rock Mechanical Tunneling Technology Seminar, held on March 28, 2003 at Colorado School of Mines campus.

Herrenknecht, M., Rehm, U. (2003b). "Mixshield Technology". Soft Ground and Hard Rock Mechanical Tunneling Technology Seminar, held on March 28, 2003 at Colorado School of Mines campus.

Hoek, E. (2007). "Practical rock engineering. Graduate courses notes in rock engineering at the University of Toronto".

(url: [http://www.roscience.com/hoek/pdf/Practical\\_Rock\\_Engineering.pdf](http://www.roscience.com/hoek/pdf/Practical_Rock_Engineering.pdf))

Horgan, D.; Madsen, D. (2008). "Crossing the Bosphorus and beyond". BTS meeting report.

Ingerslev, L. (2005). "Considerations and strategies behind the design and construction requirements of the Istanbul Strait immersed tunnel". *Tunnelling and Underground Space Technology*, 20, pp. 604–608.

Ingerslev, L. (2004). "Immersed and floating tunnels across Lake Zurich". *Tunnelling and Underground Space Technology*, 19, pp. 477–478

International Tunnelling Association (2000). "Recommendations and Guidelines for Tunnel Boring Machines (TBMs)" Working Group N°14 - Mechanized Tunnelling -. Tribune Hors Série Mai 2001 - ISSN1267-8422. 34 pages.

Japan Society of Civil Engineers (1996). "Japanese standard for shield tunneling". The third edition.

Kirkland, C. J. (1986). "The proposed design of the English Channel tunnel". Tunnelling and Underground Space Technology, Vol. 1, No. 3/4, pp. 271-282.

Kovári (2001). "The Control of Ground Response - Milestones up to the 1960s". AITES - ITA 2001 World Tunnel Congress, Milano. 26 pp.

Kovári, K. & Ramoni, M. (2006): "Urban tunnelling in soft ground using TBMs"; Tunnelling and trenchless technology in the 21st century; International conference and exhibition on tunnelling and trenchless technology, Subang Jaya – Selangor Darul Ehsan; 17-31; The Institution of Engineers, Malaysia.

Longo, S. (2006). "Análise e Gestão do Risco Geotécnico de Tuneis" (In Portuguese). 309 pp. Instituto Superior Técnico da Universidade Técnica de Lisboa. PhD Thesis.

Lovat, R. (2006). "TBM Design Considerations: Selection of Earth Pressure Balance or Slurry Pressure Balance Tunnel Boring Machines". International Symposium on Utilization of Underground Space In Urban Areas. Sharm El Sheikh, Egypt, November 2006

Lykke, S.; Belkaya, H. (2005). "Marmaray project: The project and its management". Tunnelling and Underground Space Technology, Vol. 1, No. 20, pp. 600-603.

McNichol, Dan. (2000) "The Big Dig". Silver Lining Books, Inc. pp. 239

Moe, G. (1997). "Design philosophy of floating bridges with emphasis on ways to ensure long life". Journal of Marine Science and Technology, 2:182-189.

Müller, L., Fecker, E. (1978). Grundgedanken und Grundsätze der "Neuen Österreichischen Tunnelbauweise", Felsmechanik Kolloquium Karlsruhe, Trans Tech

Publ., Claustal.

Pelizza, S. (1999a). “Scavo Meccanizzato delle Gallerie” (in Italian). *Gallerie e Grandi Opere Sotterranee*. 59: 48.

Pelizza, S. (1999b). “TBM Bored Long Rock Tunnels”. *ITA 25th Anniversary Commemorative Book*, ITA 60pp.

Rabcewicz L. (1965). “The New Austrian Tunnelling Method”, Part one, Part Three, *Water Power*, January 1965, 19-24.

Saveur, J.; Grantz, W. (1993). “Structural design of immersed tunnels”. *Tunnelling and Underground Space Technology*, Vol. 8, No. 2, pp. 123-139.

Schultz, C.; Kochen, R. (2005). “Túneis imersos para travessias subaquáticas” (in Portuguese). *Principais aspectos geotécnicos e construtivos*. *Revista Engenharia*, 569, pp. 95-98.

Sousa, L.R. (2006). “Big Dig the major road project in USA” (in Portuguese). *Journal Engenharia e Vida*, no. 26 July/August, Lisbon.

Sousa, L.R. (2002). “Innovative aspects in the design and construction of underground structures” (in Portuguese). *7th Portuguese Geotechnical Congress*, Porto, pp. 1313-1373.

Stack, B. (1982). “Handbook of Mining and Tunnelling Machinery”. John Wiley and Sons Ltd, 772 pp.

Toan, Nguyen Duc (2006). “TBM and Lining Essential Interfaces”. Postgraduate master course in Tunnelling and Tunnel Boring Machines, V Edition 2005-06, Politecnico di Torino, Italia.

Transmetro (2001). “Face mapping for Line C of the Porto Metro”.

United States Department of Transportation (1993). “Charles River Crossing - Central Artery / tunnel project, Boston, Massachusetts Supplemental environmental impact statement” report by US Department of Transportation, Federal Highway Administration and Massachusetts Highway Department.

Wittke, W. et al. (2007). "Stability Analysis and Design for Mechanized Tunneling". Geotechnical Engineering in Research and Practice WBI Print 6. Editor WBI Professor Dr.-Ing. W. Wittke, Beratende Ingenieure für Grundbau Und Felsbau GmbH, Aachen,Germany, 563 pages.

Wittke, W. et al. (2002). "New Austrian Tunnelling Method (NATM), Stability Analysis and Design". Geotechnical Engineering in Research and Practice WBI Print 6. Editor WBI Professor Dr.-Ing. W. Wittke, Beratende Ingenieure für Grundbau Und Felsbau GmbH, Aachen,Germany, 424 pages.

### **Internet references**

Herrenknecht url :[www.herrenknecht.com](http://www.herrenknecht.com)

<http://www.stuttgart21.de> (in german)

Norwegian Public Roads Administration (2006) <http://www.vegvesen.no>

"Archimedes Bridge". Ponte di Archimede International S.p.A.

"First Archimedes bridge prototype to be realized in southern China". People's Daily Online (April 18, 2007).

## **CHAPTER 3 Accidents during Tunnel Construction**

### **3.1 Accidents in tunnels**

Construction of tunnels has been increasing world-wide. The majority has been completed safely. However there are a number of events that happened all around the world that have raised concerns regarding the risk of tunneling.

There are not enough and reliable data regarding the risks that tunnels face during construction. Efforts have been made by some institutions and researchers to collect data on problems occurring during construction as will be briefly discussed later. However, there is no centralized world wide database on tunnel failures.

In 1994, following the collapse of three tunnels of the Heathrow Express in the United Kingdom, HSE (Health and Safety Executive) collected cases of failures during the construction of NATM tunnels (39 cases). In 2001 a book by Vlasov, S. was published regarding accidents in transportation and subway tunnels, during construction and operation. The book contains data on several accidents in Russia and around the world occurring during construction and operation. It also presents preliminary recommendations on accident forecast and prevention based on the analyzed data. In 2006, HSE issued a research report entitled “the risk to third parties from bored tunneling in soft ground” that contains a list of NATM events (66 cases) and a list of non-NATM Emergency events (42 cases) during construction and operation. The list does not provide many details regarding the actual events (apart from the type of event, reported causes and references). Stallman (2005) contains a collection of 33 cases of failures during construction with details on the geological and hydrological conditions of the accident, the causes, consequences and type of collapse. Seidenfuß (2006) compiled 110 cases of problems that occurred during construction and operation, categorizing them, describing their causes and mechanisms.

In addition to these above listed reports and thesis, 71 incidents have been reported in 65 tunnels constructed in Japan between 1978 and 1991 at unspecified locations. These ground collapses ranged from the “quite small” through volumes of between 50 – 500 m<sup>3</sup> of ground (15 Incidents.) to volumes of over 1000 m<sup>3</sup> of ground (3 Incidents.) (Inokuma, 1994)

This chapter describes the process of data collection on accidents that occurred during tunnel construction worldwide. The definition of accidents in this thesis is the one given by the The Mining Encyclopedia (in Vlasov et al., 2001) that states the following:

“An accident is a sudden complete or partial breakdown of equipment, mining workings, structures or any kind of devices device that is accompanied by a prolonged interruption (typically more than one shift of work) of the operational process, the work of an organization or sector of the construction as a whole. Accidents are always accompanied by financial losses, in some cases cause injury or death”

The data on accidents were collected from the technical literature, newspapers and correspondence with experts in the tunneling domain. The data were stored in a database and analyzed, and the accidents were classified into different categories, their causes and their consequences were evaluated. The structure of the database will be explained and the identification of the different types of accidents, their causes, the chain of events and their consequences will be presented. The main goal of this chapter is to determine the major undesirable events that may occur during tunnel construction, their causes and consequences and ultimately present mitigation measures to avoid accidents on tunnels during construction. Figure 3.1 shows the methodology used in creating the database.

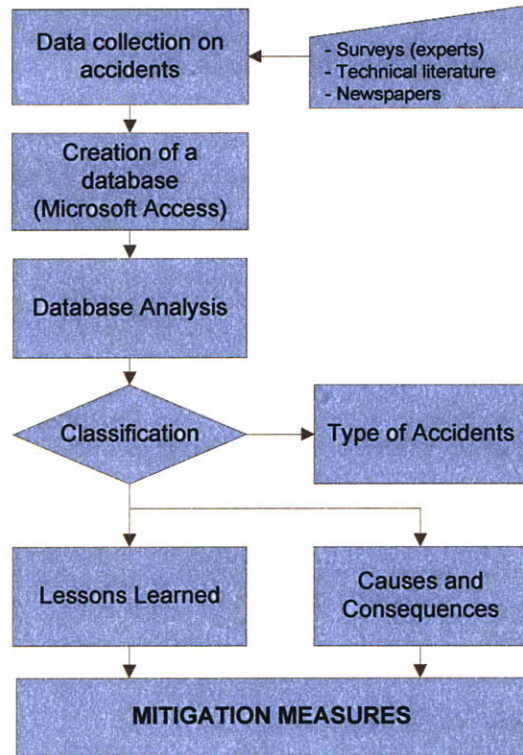


Figure 3.1 Methodology followed during the creation and analysis of the database on accidents

## 3.2 Accident Database

### 3.2.1 Data Collection

In order to assess and understand what type of undesirable events may occur during tunnel construction, data on “major problems” occurring during construction were collected and stored in the database. This permits one to improve the knowledge on accidents during tunnel construction, and allows one to identify different types of accidents, their causes, the chain of events and their consequences.

A type survey was created in order to facilitate the interaction with the experts. The survey consists of two sections: Project Information and Accident Information.



The **Project Information** section asks for information related to the project, where the accident occurred and comprises five subsections:

- 1.1. *General information.* Contains general information on the project such as its location, the client, the contractor, the start and end of construction and the type of tunnel among others. Figure 3.2 contains an extract of a filled in questionnaire concerning the Lausanne M2 metro line (case 002).
- 1.2. *Tunnel dimensions.* Contains information on the length of the tunnel, as well as information on the shape and dimensions of the cross section.
- 1.3. *Geological and geotechnical information:* Includes a description on the ground type that the tunnel crosses, the groundwater condition, and maximum, minimum and predominant overburden.
- 1.4. *Construction method.* Reserved for information on the type construction methods used in the project and its details.
- 1.5. *Other relevant information / Comments.* Includes any other information or comments that one considers relevant to the case.

The **Accident Information** section is most important and collects information that is specific to the accident itself. It comprises two subsections:

- 2.1. *General Information.* Contains information regarding the date of occurrence, as well as the geomechanical characterization and construction sequence of the collapsed zone.
- 2.2. *Description of the occurrence.* This is the most relevant sub-section. Here the accident is described as well as the conditions, in which it occurred. Information such as the type of occurrence, the location of the occurrence (heading, lining, etc), the time of occurrence, consequences and possible causes are some of the information registered in this sub section. An extract of this section is presented in Figure 3.4.

## MIT Tunnel Research Questionnaire

H. Einstein – R. Sousa

### 1. PROJECT INFORMATION

#### 1.1 General information

Project Name:	Lausanne Metro M2
Client:	Metro Lausanne-Ouchy SA
Designer :	Several Designers (table attached)
Contractor:	Several contractors (table attached)
Location:	Lausanne / Switzerland
Start of construction:	Spring 2004
End of construction:	Fall 2008
Type of environment <sup>(1)</sup> :	Urban
Type of tunnel	Metro tunnel

Maps, Figures:



Layout of the Lausanne M2 Metro Line



Saint-Laurent tunnel's passage under the 19th Century masonry bridge



Line M2 in construction on the stretch of the former Metro-Ouchy

Figure 3.2 Extract of the questionnaire – General Information section (Lausanne M2 metro line)

The completed questionnaire, regarding the accident that occurred in the construction of the metro in Lausanne, Switzerland, in 2005, is presented in Appendix A.

A total of 113 questionnaires with the type survey were sent out to experts in the field, resulting in total of 204 cases which were registered into the database. Each record in the database is based on the interpretation of both the questionnaires filled and private correspondence with experts and technical and newspaper articles

Appendix B contains a list of the experts who collaborated in this research and were so kind to provide information on accidents. Each respective case is also listed. For the remaining cases the respective questionnaires were filled in based on technical literature and newspapers.

### **3.2.2 Database Structure**

The database is a collection of information from accidents/major problems that have occurred in different areas of the world and covers almost all types of tunnels: railway, road, subway, hydraulic and sewage.

The process of data collection and the structuring of the database was iterative. It started as a simple structure, where data on the project and on the respective accident/problem were recorded, and as more data were collected it evolved into a more complex data structure. It now consists of records of different projects in a database created with Microsoft Access. Each record contains general information about the project. Linked to each project record there are one or more accident records, which contain detailed information on the accident/problem(s) that occurred during the construction of the tunnel. For each case different qualitative and quantitative information was recorded. The most important variables recorded are presented in Table 3.1. Figure 3.3 shows the relationship between the Project record and the Accident record. They are linked by the ProjectID, i.e. if an accident occurred in a certain project then its record will have the same ProjectID as the project record.

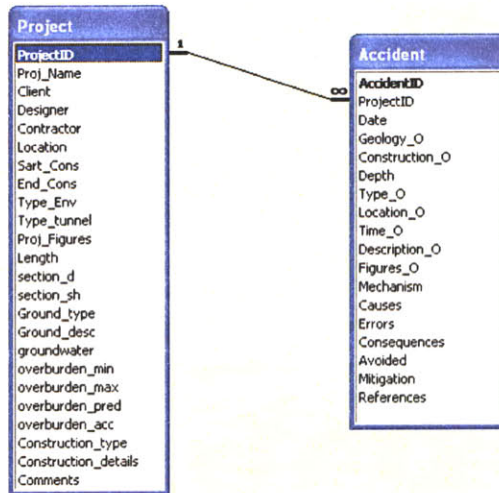


Figure 3.3 Relationship between the Project and Accident tables

In addition to these variables other information was also registered, such as the Client, Designer, Contractor, date of start and end of construction, average, maximum and minimum overburden along the tunnel, general geological and groundwater conditions.

Appendix C shows an example of a project record and its associated accident record from the database. The example shown is the Hull wastewater flow transfer tunnel (Project ID 26), part of the Hull wastewater treatment directive, located in the United Kingdom. The tunnel, driven by an Earth Pressure Balance Machine, suffered a collapse on November, 16, 1999. No one was injured but the remedial works took over a year to be complete and cost several tens of millions of pounds.

The database contains information on 204 cases of major problems that occurred in tunneling projects during construction. Figure 3.5 shows the distribution of the locations of these tunnels. Figure 3.6 shows the distribution of the use of these tunnels.

Table 3.1 List of variables for each record

<i>Number</i>	<i>Variables</i>
1	Title
2	Location
3	Type of tunnel
4	Length
5	Number of accidents registered
6	Type of environment <sup>(1)</sup>
7	Cross section shape
8	Cross section dimensions
9	Ground Mass Type
10	Construction Method
11	Type of occurrence
12	Year of occurrence
13	Local of occurrence <sup>(2)</sup>
14	Time of occurrence <sup>(3)</sup>
15	Description of occurrence
16	Overburden
17	Geomechanical characterization of the collapsed zone
18	Errors / Possible Causes
19	Consequences
20	Mitigation Measures <sup>(4)</sup>
21	Source of information
22	Photos

- (1) Type of environment where the tunnel was constructed: urban, mountainous, rural or other
- (2) Location of the occurrence: heading, lining, shaft, portal, other...
- (3) Time of occurrence: when in the constructive process did the failure occur? : During excavation of the section heading? During the excavation of section invert? After excavation?
- (4) What measures were taken after the occurrence in order to ensure the successful completion of the construction? Were they effective?



## 2.2 Description of the occurrence

Type of the occurrence :	Daylight collapse	
Location of the occurrence :	Heading <input checked="" type="checkbox"/>	Invert <input type="checkbox"/>
	Lining <input type="checkbox"/>	Other: <input type="checkbox"/>
Time of occurrence <sup>(5)</sup> :	The cave-in occurred on Tuesday at six o'clock in the evening. At the time of the incident investigation works were said to be underway following an earlier inrush.	
Description of the occurrence:	A tunnel collapse on Lot 1200 consisting of the 306 m-long Saint-Laurent tunnel between Flon and Riponne stations and the 272 m-long Viret tunnel between Riponne and Bessières stations displaced a huge amount of material – soil + water (1400m <sup>3</sup> ) into the tunnel and caused extensive damage as it cratered towards the surface in the busy St. Laurent's commercial district.	

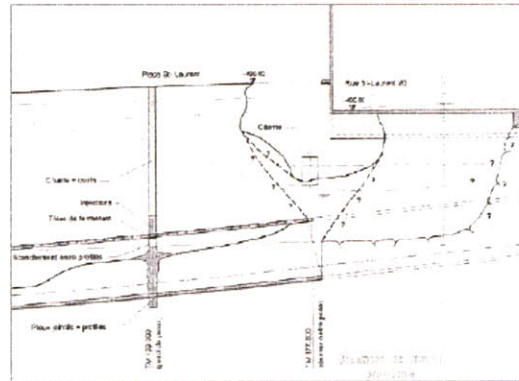
Possible mechanisms (sketches or figures):



Collapsed area at the surface



Aspect of the front after collapse  
(ingress of soil and water)



Drawing of the collapse

Figure 3.4 Extract of section 2.2 of the questionnaire (Lausanne M2 metro line)

The collection of data focused on tunnels excavated by the NATM / sequential excavation method, standard drill and blast, and TBM or Shields. More than 50% of the



cases collected are from tunnels excavated by conventional means (i.e. NATM / Sequential Excavation and/or Drill and Blast). There is a small percentage (7%) of the cases where the information is limited regarding the construction method used. It is important to relate the construction method and type of ground with the events since different construction methods will most likely imply different risks during construction.

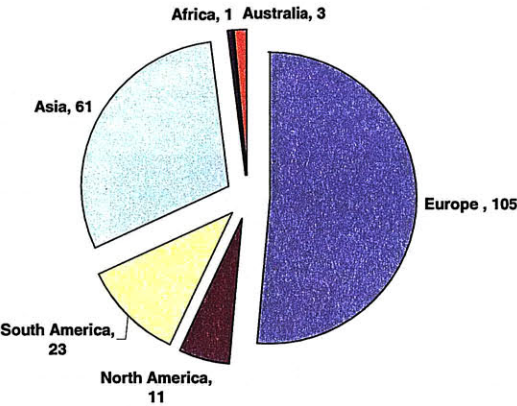


Figure 3.5 Geographical distribution of the tunnel cases

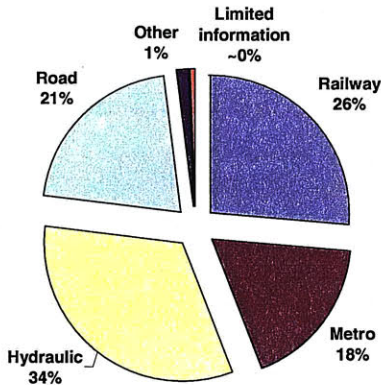


Figure 3.6 Distribution of the type of use of the tunnels in the database

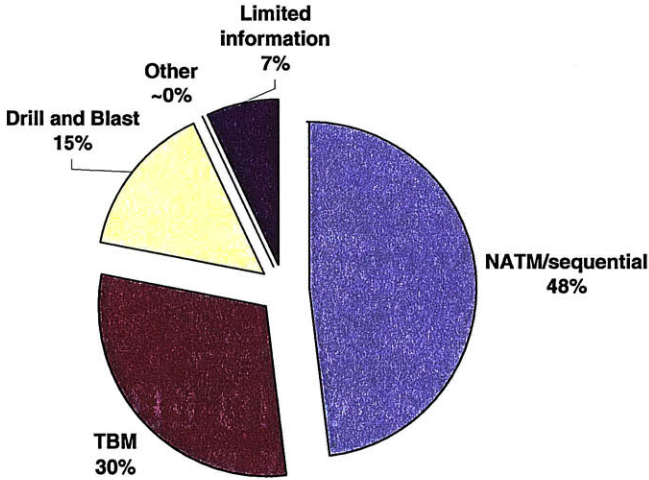


Figure 3.7 Distribution of the tunnel cases by construction method

### 3.2.3 Type of Events

It is necessary to identify and classify the types of events that can occur during tunnel construction. Based on the data collected the main observed accidents are presented in Table 3.2. Fire and Explosions are probably the most common type of accidents during the operation of tunnels. They can also occur during construction but are less frequent. They can cause loss of live, equipment damage and damage to the tunnel structure that may lead to a collapse. Since they do not occur frequently in tunnel under construction and although one case was collected will not be considered in detail.

Table 3.2 Undesirable event list

<i>Undesirable events</i>	<i>Description</i>
Rock Fall	Fall of rock blocks of major dimensions. The different mechanisms involved are wedge or planar failure..
Collapse	Heading collapse / failure of the heading / lining failure .
Daylight Collapse	Heading collapse / lining failure of the heading that reaches the surface creating a crater.
Excessive Deformation	Excessive deformations inside the tunnel or at the surface. This can occur for example due to deficient design, construction defects and/or due to particular type of terrains such as swelling and squeezing ground, which had not been predicted.
Flooding	Comprises cases where the tunnel was invaded by large quantities of underground water.
Rock Burst/ Spalling	Overstressing of massive or intact brittle rock, i.e. the stresses developed in the ground exceed the local strength of the material. It can cause spalling or in the worst cases sudden and violent failure of the rock mass
Portal failure	Particular locations of a tunnel, where there is a lower resistance of ground mass and/ or concentration of stresses.
Shaft failure	
Other	Other types of collapse that include slope failures, etc

Figure 3.8 shows the distribution undesirable events in the database. The great majority of events reported are *Collapses* and *Daylight Collapses* (36% and 28%). This does not mean that these are the great majority of events that occur during tunnelling construction. They are however the most frequently reported in the literature and by the experts because most likely they are the ones with more severe consequences on the construction process, the safety of the workers and people and structures at the surface.

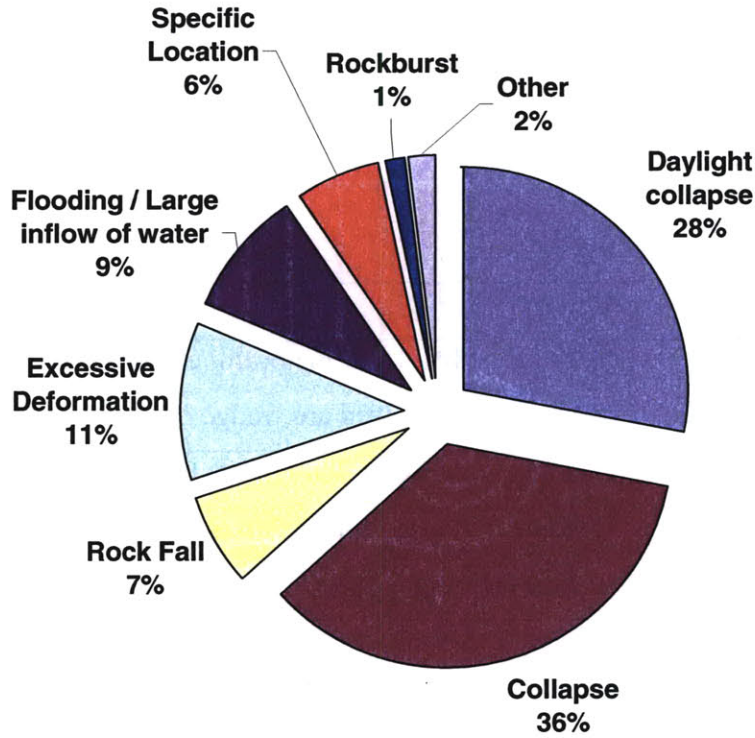


Figure 3.8 Undesirable event distribution

Each event can occur at different places in the tunnel, namely at the face and behind the face. Figure 3.9 shows the event location for NATM / Convention excavation and for TBM.

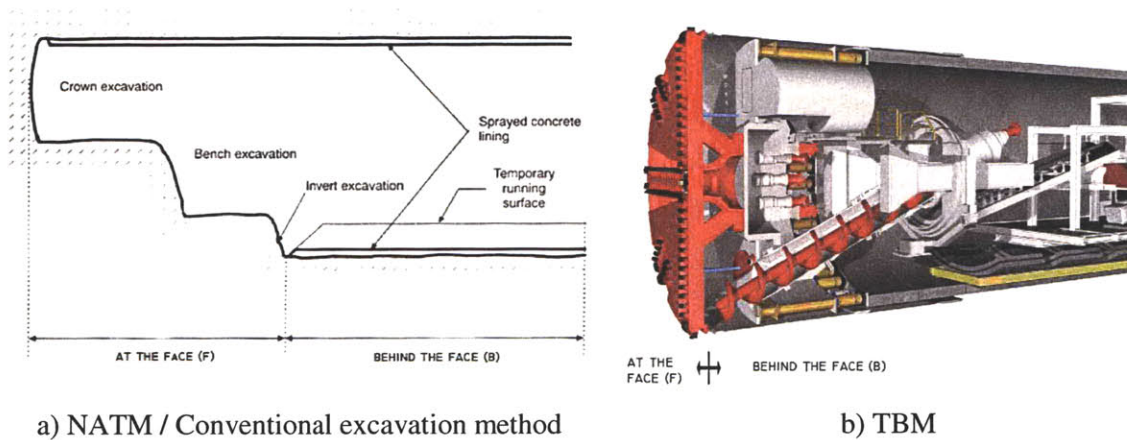


Figure 3.9 Event location

Details on the different types of undisarable events are now provided:

### Rock Fall

A rock fall consists of a block that detaches by sliding or falling. The different mechanisms involved are wedge or planar failure. Unfavorable geology is the principal cause for the mechanisms of rock fall. This includes discontinuities within the rock mass, weathered and weak zones in the rock.

An example of a large rock fall (about 2000m<sup>3</sup> block) is the accident that occurred during the construction of one of the surge chambers part of the Cahora-Bassa hydroelectric system (project ID 50). The rock fall was due to a wedge failure that took place along the intersection line of the two inclined discontinuity planes belonging to the family of discontinuities and bounded on top by a lamprophiric dyke (Figure 3.10 and Figure 3.11)



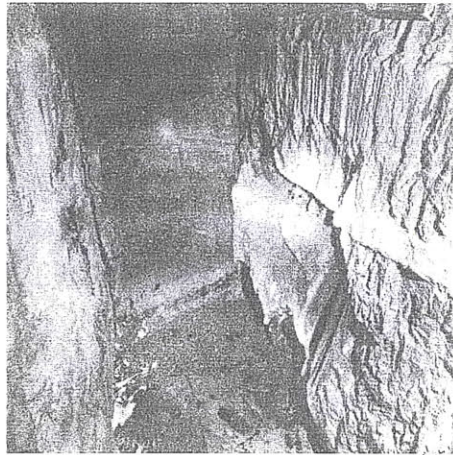


Figure 3.10 Photo of the collapsed area (Rocha, 1977)

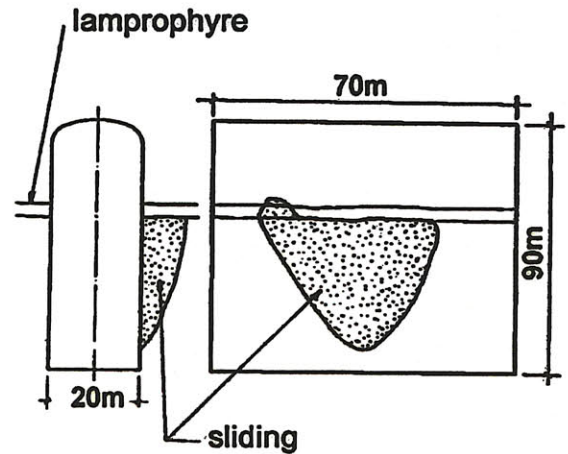


Figure 3.11 Accident schematic (Sousa, 2006)

The strength of the intact rock and the shear strength along the discontinuities are of great importance for the stability of the tunnel. Existing discontinuities may form wedges that may fall into the tunnel. Figure 3.12 shows a schematic of loosening of rock wedges during gripper shield excavation.

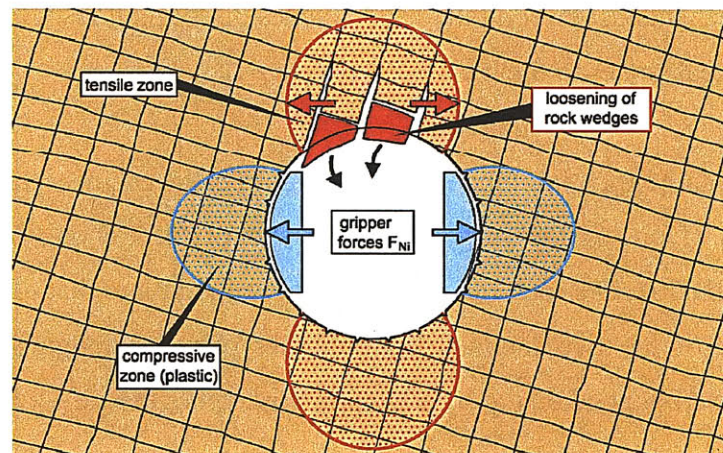
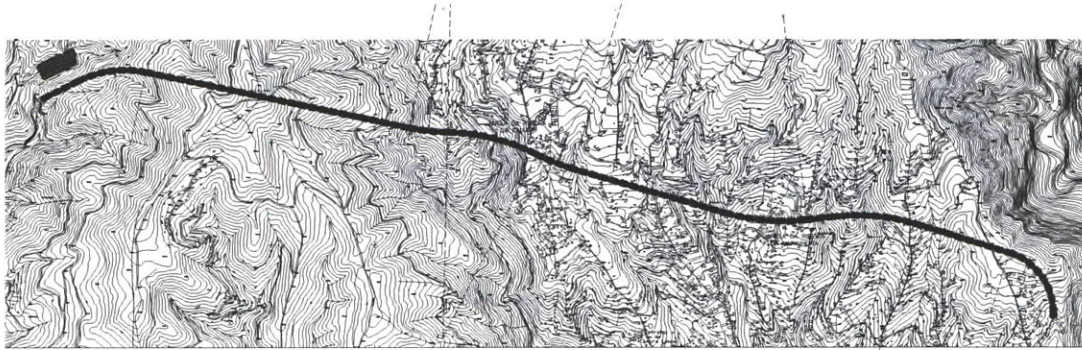


Figure 3.12 loosening of rock wedges during gripper shield excavation (Wittke, W. et al., 2007)

An example where blocks fell down into the tunnel blocking the TBM is the Covão tunnel (Project ID 122) which is the upper reservoir of a hydroelectric power scheme in Madeira Island, Portugal (Cafofo, 2006). The tunnel, 5244 m long, was designed in a complex topography region, in the volcanic formation (basalts, breccias and tuffs),

predominantly basaltic. This type of volcanic formation is heterogeneous and prone to block falls during the excavation process. Figure 3.13 a shows the plan view of the tunnel. The first 100 m were excavated by drill and blast and the remainder was excavated by an open TBM with a diameter of 3.016 m (Figure 3.13 b). A rock fall that occurred during excavation is presented in Figure 3.13 c.



a) Plan view



b) TBM used in the excavation



c) rock fall in volcano formations

Figure 3.13 Covão tunnel, Socorridos Hydroelectric scheme, Madeira, Portugal (Cafoto, 2006)

The rock wedges can either fall down in the area of the face or immediately behind the shield / face. Figure 3.14 shows over excavation due to unstable rock wedges that occurred during the excavation of the Gotthard base tunnel, Bodio section (Project ID 98). In this case the wedge has fallen immediately behind the head of the machine.



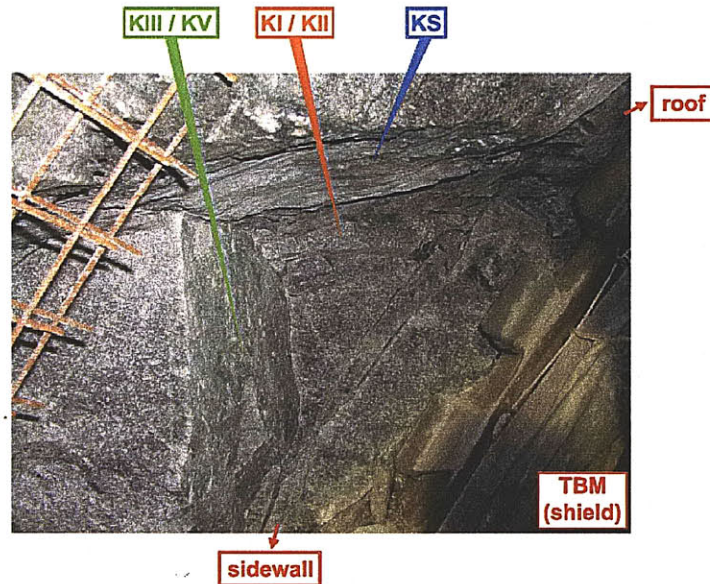


Figure 3.14 Overexcavation due to instable rock wedges, Gotthard base tunnel, Bodio section (Wittke, W. et al., 2007)

## Collapse

These are collapses which occur in tunnels under construction but do not reach the surface. The majority occurs in the heading (face and or roof) area of the tunnel. Others occur behind the face.

Figure 3.15 is an illustration of an event that occurred, in Evino-Mornos, a 30 km long hydraulic tunnel in Greece (Project ID 49). The large collapse occurred in front of the face and stopped the cutter head rotation, creating a cavern more than 10 m high over the TBM. This was an example of a full collapse of the face.

A collapse can also be partial like the one that occurred on 11 April 2002 in the Fadio zone, at the Gotthard base tunnel (Project ID 97) in Switzerland, leaving a cavity of about 8m (Figure 3.16). In this case the accident was caused by squeezing ground that led to excessive deformation that ultimately led to the partial collapse of the lining. This is a good example that shows that an accident is normal a result of a chain of events and has at its origin more than one cause or error.

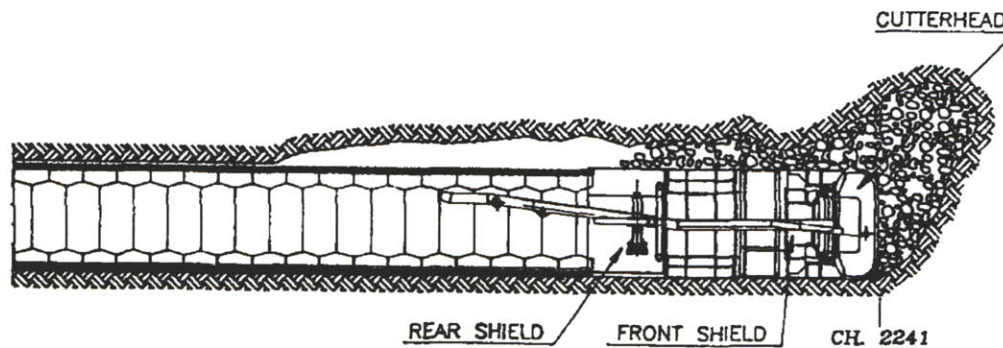


Figure 3.15 Collapse at the face of the TBM, Evino Mornos, Greece (Grandori et al., 1995)

The most common location of the collapses is the face and roof as shown in Figure 3.15. Other locations include the side walls (near the face) or in the lining behind the face. Figure 3.17 shows the progression of significant deformations and water ingress that resulted in the collapse of the side wall in the Wienerwald tunnel (Project ID 97) in Austria. In this case, ground water led to de-compaction and bulking of the sandstone, which caused the shear strength to decrease. From this it follows that the strength of rock was very low and ground pressure loaded the temporary shotcrete shell, which was not designed for that kind of high loading. Therefore the shotcrete shell spalled off and the lattice girder was deformed.



Figure 3.16 Partial collapse at Gotthard Base tunnel, Faido section (Einstein, 2007)



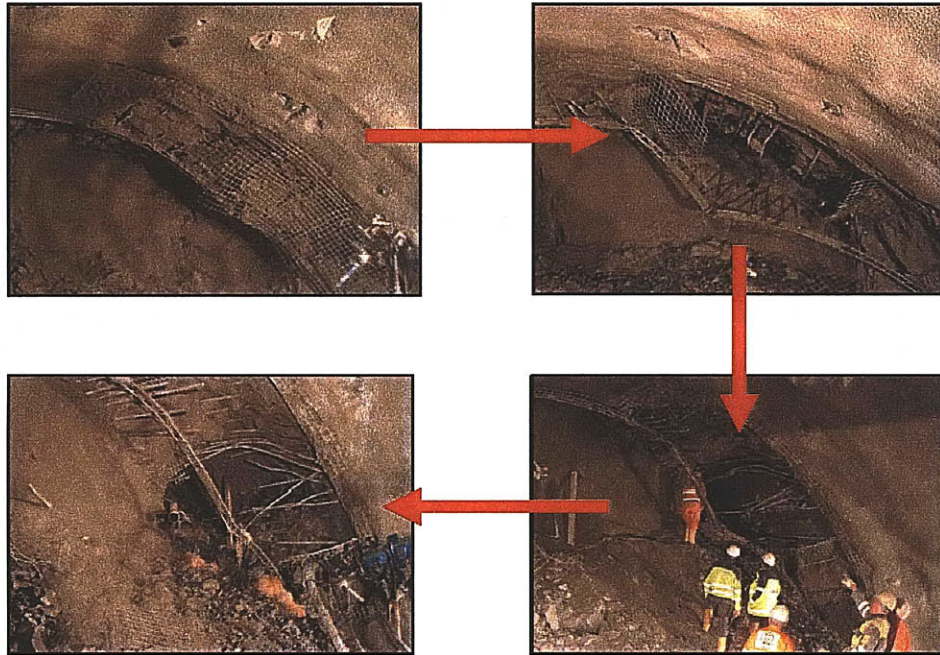


Figure 3.17 Collapse progression at Wienerwald tunnel (Seidenfuß, T., 2006)

### Daylight Collapse

These are collapses that reach the surface creating a crater. They are the most sensational types of events and frequently the ones that cause the most serious consequences, specifically if they occur in urban areas. The propagation of the collapse to the surface can be quick and without warning as happened in the Munich Metro in 1994 (Project ID 121) where a bus passing by was trapped in the sinkhole (Friedrichsen G.,1998) or more recently in the Pinheiros Station in São Paulo, in 2007 (Project ID 93), which dragged pedestrians and a passing minibus into the crater, causing seven victims (Figure 3.18 and Figure 3.19).

On December 12, 1996, 6.00 am, a collapse reaching the surface occurred at Olivais Station (Project ID 10), in Lisbon, Portugal, as a consequence of a previous collapse. The volume of this collapse was 2500 m<sup>3</sup>. Despite the volume involved and although it occurred in an urban area in Lisbon, there were no deaths and the consequences were not as severe as other cases in similar circumstances (Figure 3.20).

When a daylight collapse occurs in an urban area it can produce serious consequences such as the ones in an accident that occurred in the Shanghai metro in 2003 (Project ID 33), shown in Figure 3.21. The accident occurred in a cross passage between the two parallel tunnel tubes that had already been driven using earth-pressure-balance TBMs. Shortly before the cross passage broke through, at a depth of about 35 m, massive inrushes of material and water occurred, which the tunnel crew was not able to bring under control and which resulted in a large scale subsidence at the surface that seriously affected neighboring buildings and other structures. A number of high-rise office blocks suffered serious damage, collapsed, or had to be demolished because the risk of collapse was too great.



Figure 3.18 Crater caused by a collapse of the subway tunnel in Munich, Germany, 1994  
(Wannick, H., 2006)





Figure 3.19 Collapse that occurred in Pinheiros Station, São Paulo, Brazil, 2007 (Barton, 2008)

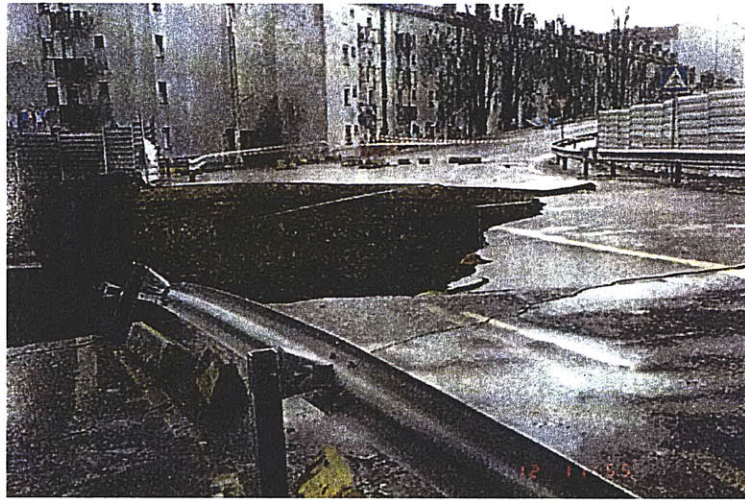


Figure 3.20 Collapse that occurred in Olivais Station, Lisbon, Portugal (Appleton, 1998)



Figure 3.21 Demolition of buildings after the tunnel collapse in Metro Line No. 4 in Shanghai  
(Munich Re Group, 2004)

Another example of a failure with considerable consequences at the surface is the accident that occurred during the construction of an underground line in the South Korean city of Taegu on 22 January 2000<sup>1</sup> following the failure of a diaphragm wall. Part of a station excavation pit caved in, burying a bus under the debris. Three passengers were killed and the driver of the bus was seriously injured. Neighboring buildings also suffered considerable damage (Figure 3.22).

---

<sup>1</sup> Not in the database.



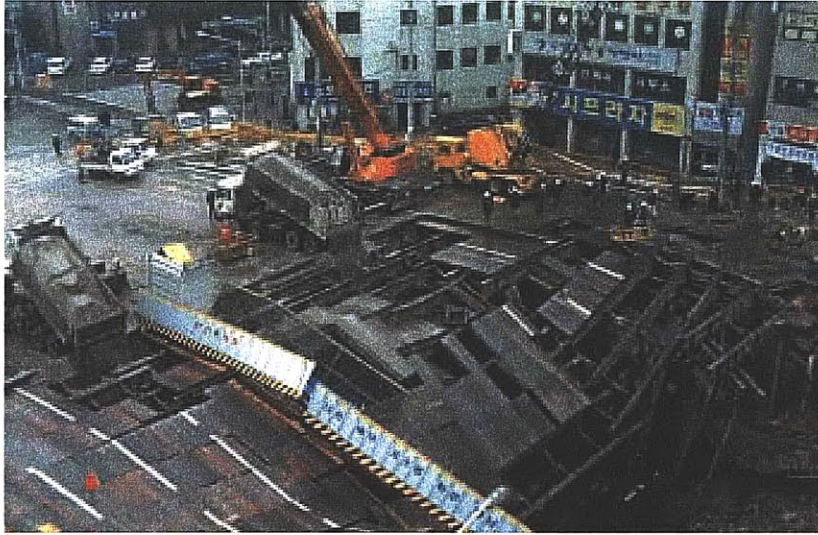


Figure 3.22 Collapse of a tunnel in Taegu in South Korea that led to the collapse of whole sections of the street (Knights, 2006)

In rural areas the consequences of daylight collapses are far less catastrophic. Figure 3.23 shows the crater caused by the collapse of a highway tunnel in Switzerland (Project ID 101), in a rural area.



Figure 3.23 Crater caused by a collapse that occurred in the Aescher tunnel, Switzerland (Kovari, and Descoedres, 2001)

As mentioned before the majority of events occur in the heading (face and or roof) area of the tunnel, but some behind the face. This is the case of the Porto Metro accident (Project ID 9). On the 12th of January 2001 the foundation underneath a building



collapsed suddenly in just a few minutes, resulting in the death of one person located inside the building and causing a crater on the surface with a net volume of around 250 m<sup>3</sup> (Figure 3.24). The TBM had passed under building between 16 and 18<sup>th</sup> of December and it was stopped 50 m ahead since 28<sup>th</sup> of December 2000. This case will be described and analyzed in more detail in Chapter 6.

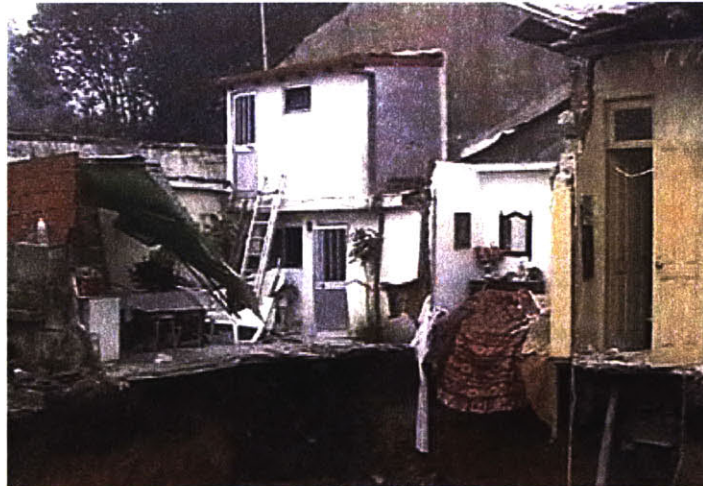


Figure 3.24 Collapse of Porto Metro line C in January 2001 (Forrest, 2006)

### **Flooding / Large water inflow**

There are cases where the tunnel was invaded by large quantities of underground water, causing flooding. It is during the construction of underwater tunnels that largest scale floodings have occurred. The ground under rivers, channels and bays is normally weak and under high water pressure and therefore extreme safety measures and efficient protection against water inflow are normally required.

The Seikan tunnel is a 53.85 km long railway tunnel in Japan with 23.3 km long underwater tunnel portion, embedded underneath the Tsugaru strait, with an overburden of 100 m and 240 m below the water surface. A great majority of the tunnel crosses heavily fissured rock (9 large shear zones). The sea and underground water penetrate into these zones and the maximum water pressure is about 25 MPa. In order to minimize the risk of water inflows and rock failures cementation and chemical stabilization was carried

out along the main tunnel. Despite these measures 4 large flooding accidents (Project ID 88) occurred between 1969 and 1976, with severe consequences on tunnel construction and resulting in 34 casualties. The fourth accident, which took place in May 1979 while driving the service tunnel, was the most severe. The water inflow was of  $70 \text{ m}^3/\text{min}$  under a maximum pressure of 2.8 MPa, causing the flooding of 3015 m of service tunnel and 1493 m of the main tunnel with  $120\,000 \text{ m}^3$  of water, in the first three days.

Groundwater inflow compromises the construction process of the tunnel, its stability. The consequences of groundwater inflow can vary from delays in the construction process to actual collapse or daylight collapse.

Many collapses (or daylight collapse) occur with water inflow or may lead to flooding. An example of a daylight collapse with water inflow is the one that occurred in Switzerland in the Lausanne metro construction (Project ID 2). A huge amount of soil and water ( $1400\text{m}^3$ ) displaced into the tunnel and caused extensive damage as it cratered towards the surface in the busy St. Laurent's commercial district (Figure 3.25).



Figure 3.25 Aspect of the front after collapse (ingress of soil and water), Lausanne, Switzerland  
(Stallmann, 2005)

A particular case is water burst which consists of water inflow under pressure in the tunnel. Figure 3.26 shows water bursts that occurred in a tunnel in China (case 174).



Figure 3.26 Water burst resulting in flooding, China (private correspondence)

### **Rockburst/ Spalling**

This type of event is caused by the overstressing of massive or intact brittle rock, i.e. the stresses developed in the ground exceed the local strength of the material. It can cause spalling or in the worst cases sudden and violent failure of the rock mass. Rockbursts are violent and sudden ruptures of bedrock and can cause serious, and often fatal, injuries. They are mainly dependent on the stress exerted on the rock, which increases with depth. Figure 3.27 shows a tunnel crown after a rock a burst (project ID 123).





Figure 3.27 Rockburst at the crown in a in a waterway tunnel in Korea (Lee et al., 2004)

Norwegian tunneling experience includes a significant number of tunnels with high rock stresses. The majority of the problems are associated with spalling due to anisotropic stresses below steep valleys. This is found normally in road tunnels along or between the fjords under high overburden. An example is the 24.5km Laerdal tunnel (Project ID 61) where moderately intense spalling and slabbing was encountered most of the time. In some areas heavy rock bursts caused violent ejection of sharp edged rock plates, crushed rock 'popped' out or moved steadily into the tunnel from the roof, the walls or the tunnel face itself. Heavy spalling often occurred near the boundaries between the stiffer and the softer rock types (T&TI, 1999; Grimstad, E. and Bhasin, R.,1999; T&TI, 2003)

Another example of rock burst is presented in Figure 3.28. It occurred in an exploratory tunnel for the Ortfjell open pit in Norway (Project ID 124). In the worst parts of the tunnel, such as shown in the picture, it was necessary to install up to 10 rock bolts per meter of the tunnel. All together 13.000 rock bolts were used in the 4.000 m long tunnel (Broch and Nilsen, 1977).

The experiences from deep level mining have contributed significantly to the understanding of the rock mechanics involved in the phenomenon of rock burst. Methods for prediction of rock stress problems that cause spalling and rock burst have been developed based on experience (Vlasov, 2001).

Intensive spalling and rock burst can cause significant delays to tunneling and the latter represents also a significant threat to the workers. The term rock burst has been often used to refer to a variety of sudden and violent dislocations of rock slabs, usually from the wall and roof of tunnels (mines), although potentially they can occur from the floor. The rocks affected by rock burst are normally hard and brittle



Figure 3.28 Example of rock-bursting in an exploratory tunnel for the Ortfjell open pit (Broch and Nilsen, 1977)

### **Excessive Deformation**

These are cases where excessive deformations occur inside the tunnel or at the surface but an actual total collapse does not happen. This can occur for example due to deficient design, construction defects and/or due to particular type of terrains such as swelling and squeezing ground, which had not been predicted.

Some minerals exhibit the property of increasing their volume when absorbing water (swelling). If this volume increase is prevented (for example by a tunnel invert) then a corresponding pressure is exerted against the element preventing the movement. In tunnel construction swelling can cause a long-term heave of the tunnel floor, which can impair

the serviceability of the structure, or result in partial failure of the lining (Kolymbas, 2005, Einstein, 2000)

An example of excessive deformation due to swelling is what occurred in a tunnel from Rotarelle to San Vittore, part of the Naples Aqueduct, in Italy (Project ID 22). After 650m of excavation, enormous ground pressures caused cracking of the shotcrete, buckling of the steel arches after a few hours, and deformations of 200 mm in 24h and 400 mm after 12 days (Figure 3.29). The deformations were caused by swelling clay filling of the rock.



Figure 3.29 Picture of deformed primary lining due to swelling clays, Naples, Italy (Wallis, 1991)

Einstein (2000) presents several tunnel case studies of tunnels excavated through Opalinus Clayshale and gypsum (Keuper) in the Swiss Jura Mountains, which show how problematic swelling can be during construction and also during operation, if the invert is not strong enough and if water reaches into the shale.

Another frequent cause for excessive deformation is squeezing. Squeezing is characterized large time-dependent convergence during tunnel excavation. Many authors refer to squeezing ground behavior whenever large convergences appear, whether they happen during construction or with time delay. This occurrence of large pressure may lead to failure of the lining and / or result in great difficulties for completing underground works, with major delays in construction schedules and cost overruns. (Barla, 2001; Kovari, K. and Staus, J. 1996).

An example of a case where squeezing ground led to failures of the lining and subsequent partial collapse is the Gotthard Base tunnel (Project ID 97) presented in Figure 3.16.

The Bolu (Turkey) two tube tunnels (Project ID 58) were subject to considerable deformation which resulted in some serious geotechnical problems. The problems occurred when the tunnel drive reached the Asarsuyu thrust fault, after 700m of tunneling in good rock conditions. In the Asarsuyu thrust fault area large movements up to 1 m were measured at the crown that caused construction problems such as twisted steel supports and breaking of the shotcrete. Due to excessive displacements, tunnel construction was stopped on 14 December 1994 and new design construction procedures were applied. After this deformations in both tunnels were 20 cm at the crown. These lower deformations are believed to be due to the better quality of the rock mass and not because of the flexible system adopted.

In the area where the Elmalık low-angle thrust zone occurs between the granite and the flysch contact in the right and left tube of the Bolu tunnel (km 54 + 137 to km 54 + 076, right tube; km 64 + 170 and km 64 + 210, left tube), deformations significantly increased, therefore, a section of approximately 60 m in length was back filled with gravel and grouted in order to prevent tunnel failure in the right tube (km 54 + 137 and km 54 + 076) (Figure 3.30 and Figure 3.31). Heaving in the invert reached 60–80 cm (Figure 3.32), in both tubes.





Figure 3.30 Heave in the Bolu tunnel (Elmalık right tube) at km 54 + 135 (Dalgıç, 2002).



Figure 3.31 Failure of the support in the Bolu tunnel (Elmalık right tube) at km 54 + 135 (Dalgıç, 2002).



Figure 3.32 Invert squeezing in the Bolu tunnel (Elmalık left tube) at km 64 + 260 (Dalgıç, 2002).

The problems that occurred in the Bolu twin tubes were mainly due to squeezing ground and inadequate support for such ground conditions.

### **Collapses in specific locations**

These are collapses that occur in particular locations of a tunnel, where there is a lower resistance of the ground and/ or concentration of stresses, such as portals and connections to shafts.

Collapses at connection zones between shafts and tunnel are often associated with weak ground, concentration of stresses and / or water on the outside of the shaft construction.

A tunnel collapse and flooding of a shaft during Metro construction occurred in Munich Germany (Project ID 121). The competent rock cover just outside the shaft was not the predicted 1.5 m but around half that value. A full collapse involving 450 m<sup>3</sup> of ground occurred (Figure 3.33)

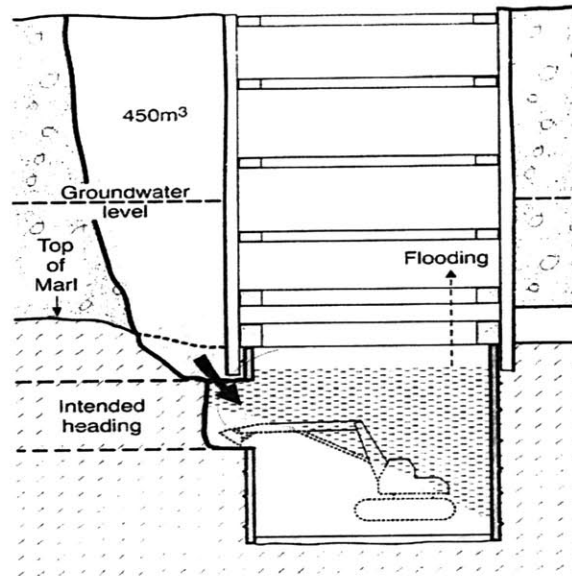
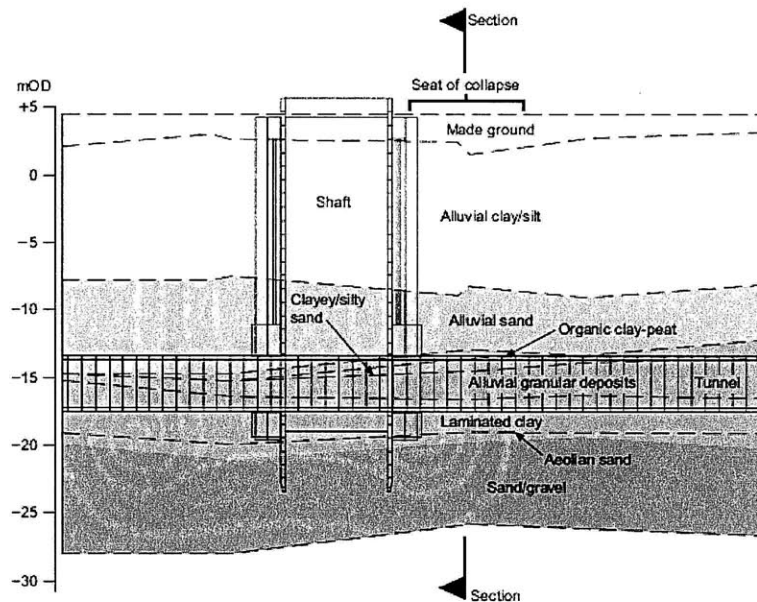


Figure 3.33 Accident in the Munich metro construction (Weber, J., 1987)

During the construction of a the Hull wastewater flow transfer tunnel (Project ID 26), which is part of the Hull Urban Wastewater Treatment Directive, a collapse of 100 m of tunnel occurred near to one of the shafts. The TBM had passed through the previously constructed 7.5 m diameter access shaft T3, two weeks prior to the incident. The center of the collapse was within a few meters of the shaft, which was at that time about 200 m behind the face (Figure 3.34) Approximately 2000 m<sup>3</sup> of soil and water entered the tunnel. No one was injured, but the remedial works took over a year to complete, and cost several tens of millions of dollars.

In the portal area, it is often the more weathered rock, the a lack of confinement (loose rock or ground) and low overburden that makes it a location prone to accidents. During the excavation of the Haivan tunnel in Vietnam (Project ID 62), when it had only progressed approximately 30 m from the southern portal in the soft ground section of the

main tunnel a major collapse occurred, in September 2001. From the initial breakout at the portal until the 30 m point was reached, the ground water encountered in the tunnel face had increased considerably. This led initially to a small loss of ground above the tunnel face that rapidly progressed upwards, with a large quantity of sand and boulders filling the excavation, to form a crater in the portal slope (Figure 3.35). The volume collapsed was 300 m<sup>3</sup>.



a)



b)

Figure 3.34 Collapse at Hull transfer tunnel project a) cross section at the collapse zone; b) aerial photo of the collapsed area. (Grose and Benton, 2005).



Figure 3.35 Cave in of the South portal slope in the Haivan tunnel, Vietnam (Fukushima, H., 2002).

The lack of temporary invert in a zone of very weathered granite was the main cause for the collapse.

In Germany in a tunnel part a high speed railway line (Project ID 116), a collapse occurred after 10 m of driving of top heading, from the portal. At first minor rock falls occurred. In order to prevent further rock falls shotcrete was applied to the collapse area. This failed and six hours later about 120 to 150 m<sup>3</sup> of rock collapsed. Due to the low cover of 6 m the collapse reached the surface (Figure 3.36). It was reported that the clearing out of the collapse site showed that the collapse was caused by the geological conditions. The collapse zone was at the interface of a known fault and an unexpected large size fissure where the rock was loosened and fractured to a degree that even the spilling (grouted steel bars) was not able to prevent breaking of fractured material.

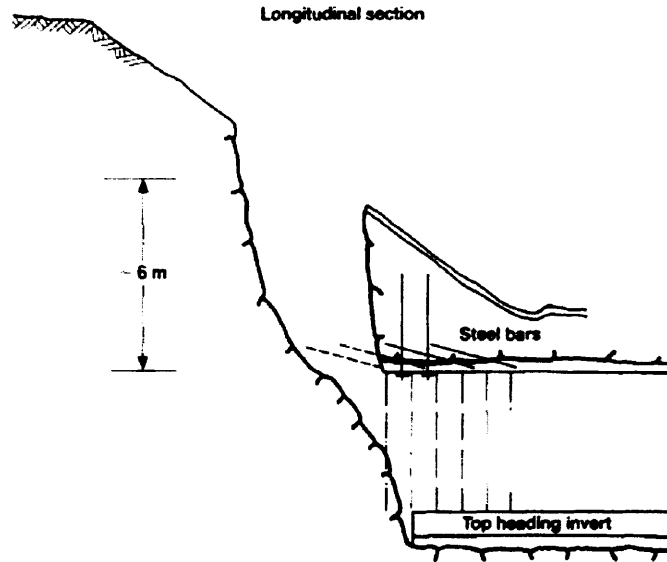


Figure 3.36 Illustration of the collapse in a high speed train railway line in Germany (Leichnitz, 1990).

### 3.2.4 Database event classification

In order to better classify the events registered in the database a range of symbols and abbreviations were adopted in the categorization of the events. The method used to classify the events stored in the database is presented in Figure 3.37. The classification consists of three symbols, which represent the construction method, the location where the event occurred and the type of event.

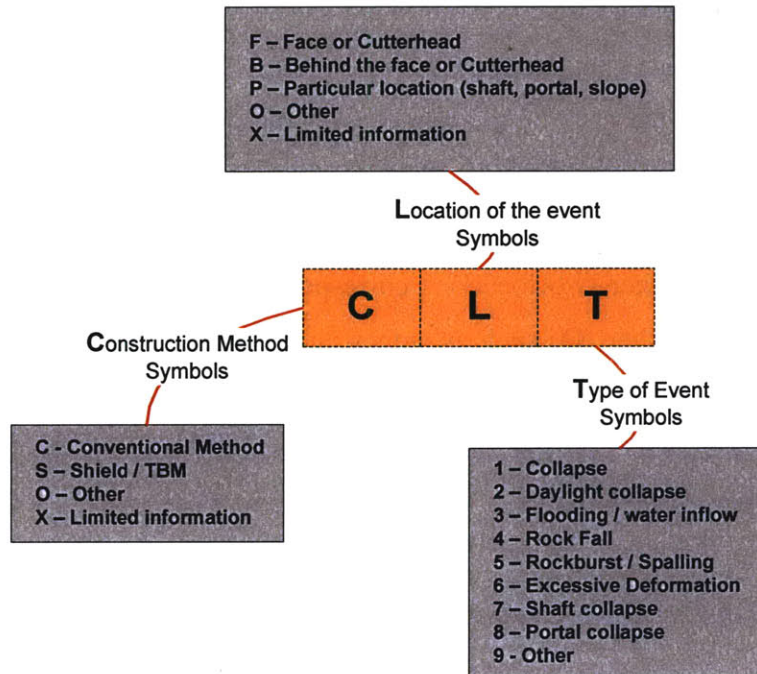


Figure 3.37 Classification method used in the database

*Note: Methods that do not provide face and peripheral support, such as roadheaders are considered conventional methods. The reason is that they use similar support systems as the NATM and drill and blast.*

The first symbol, the construction method, represents the type of construction method used. It is important to distinguish between construction methods since for each different type there are different risks. The construction methods considered in the database are the NATM/ sequential excavation (C) and Shield / TBM (S). There were also some cases, such as cut and cover, which due to their magnitude were also included. The symbol used for other types of construction methods is (O). When the excavation method is not known an (X) will appear.

The second symbol, location of the event, describes the location where the accident occurs. It can be at the face, behind the face, at a particular location such as the portals and shafts or other locations. In the Conventional Method (NATM/Sequential Excavation and/ or Drill and Blast) the events at the face (F), correspond to events that occurred in the area of the tunnel heading between the excavated face and the first completed ring of



support (definition used by HSE, 1994). In the shield / TBM construction (**F**) correspond to events that occurred at the cutterhead. The symbol behind the face (**B**) corresponds to events that occur in the area of the tunnel with the completed primary lining (for the conventional excavation methods). In TBM driven tunnels (**B**) corresponds to events that occur behind the cutterhead, either immediately behind it in the shield area or in the primary lining. The other two locations correspond to specific locations such as shafts and portals (**P**), and other (**O**) such as slopes and retaining walls. Once again when the information is limited the symbol (**X**) will be used. The sketches of Figure 3.9 present the location of the events, at the face (**F**) and behind the face (**B**) for the two types of construction methods considered. .

The types of events are the ones described in previous section, summarized in Table 3.2.

The combination of the type of event (Table 3.2), the construction method used and the location where the event occurred (Figure 3.37) is the basis for the classification system. Presented in Table 3.3 are the most common events related with the use of conventional excavation methods and the ones related with the use of a shield or TBM. Each case stored in the database was classified according to this system, i.e. according to the construction method, location and type of event. The list of cases is presented in Appendix D.

Table 3.3 Events related to the use of conventional methods

Location of the event	Symbols	Description of the event
At the face	CF1	Heading collapse
	CF2	Heading collapse (daylight)
	CF3	Water inflow
	CF2+3	Heading collapse with water inflow
	CF4	Rock fall at the face
Behind the face / Perimeter	CB1	Collapse/Failure of the lining
	CB6	Excessive deformation
At a particular location	CP7	Collapse at a shaft
	CP8	Collapse at the portal

### 3.3 Data Analysis

The analysis of the data shows that:

- More than half (56%) of the accidents occur near the face, while a smaller percentage occurred behind face and at particular locations (Figure 3.38). This is expected because the largest perturbation to the ground occurs naturally at the face, either in terms of deformations or modification of the stress state
- Figure 3.39a and Figure 3.39b show the distribution of the different types of events, considering the influence of the construction method, divided into conventional and mechanized methods,. It is interesting to compare the two methods and it is possible to observe that: daylight collapse normally associated with larger volumes and larger consequences are greater (reported) in the conventional type of construction (NATM and Drill and Blast), than in Shield/TBM cases. Although this collection is not complete and exhaustive this is already an important conclusion. It is also possible to observe that excessive

deformations and rock falls have occurred more frequently in the conventional type of construction (NATM / Drill and Blast). Flooding and water inflow have occurred more in mechanized methods, which can be explained by the fact that more catastrophic flooding have occurred in long underwater tunnels or long mountain tunnels with high overburden and water pressures that are normally driven by TBMs. For the other events (specific location and rockburst) the construction method is not so relevant, since it looks that they occur approximately equally (%) for both methods.

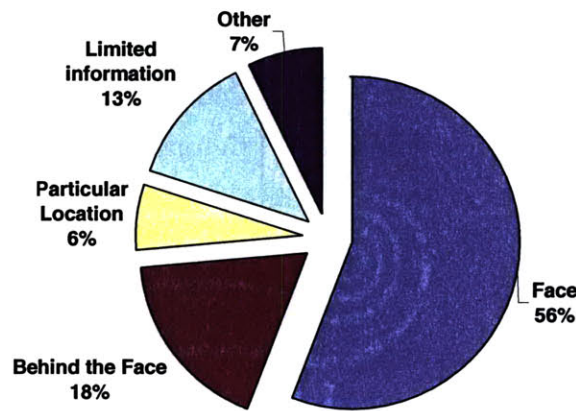
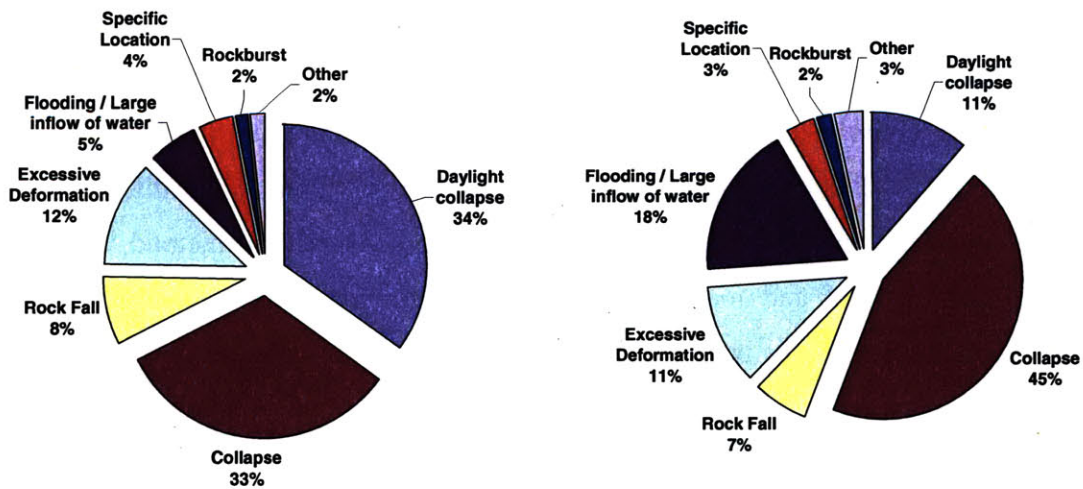


Figure 3.38 Distribution of the accidents according to their location



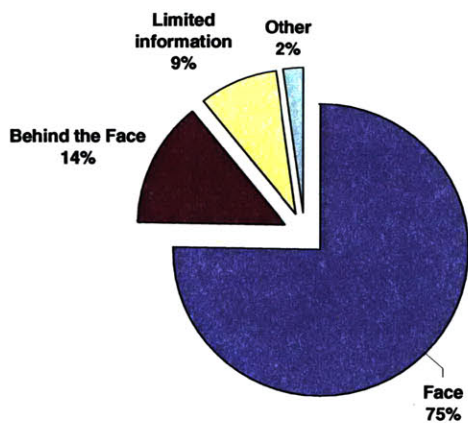
a) Conventional construction method

b) Shield machines and TBMs

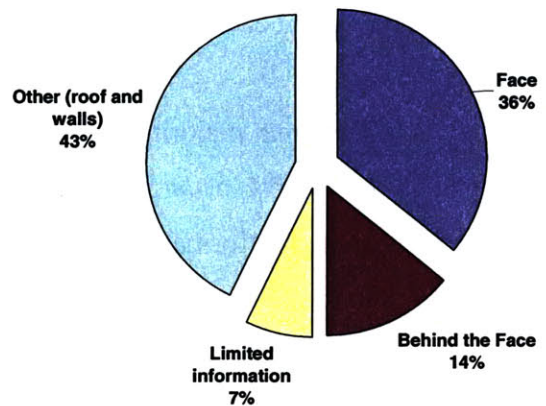
Figure 3.39 Distribution of the event location according to the construction method

The analysis of each event separately shows that (Figure 3.40):

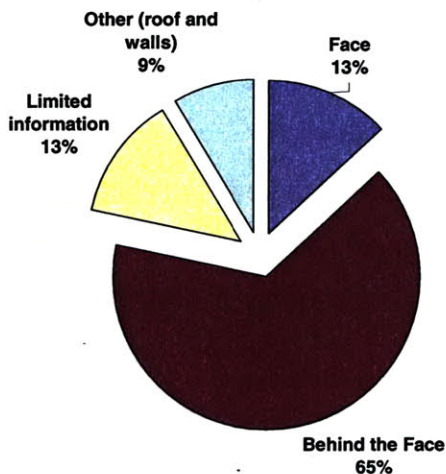
- The great majority (75%) of collapses and daylight collapses occurred at the face. Only 10% occurred behind the face and in almost 15% of the cases there is not enough information regarding the location of the collapse.
- In the case of the rock falls, the majority occurred at the roof or walls (54%), with no clear indication whether they occurred at or behind the face, and at the face of the excavation (31%)
- In the excessive deformation 45% of the events occurred after the face had passed, ranging from days and in some cases reaching up to a year, mainly due to swelling or squeezing ground. In almost one third (30%) of the cases there is not enough information regarding the exact location of the event. One fifth (20%) of the events occurred at the face of the excavation.
- In half of the cases of flooding and water inflow there is not enough information regarding where the water entered the tunnel. In 35% of the cases the inflow occurred at the face and in 14% of the cases it occurred from both the face and behind the face.
- All rockburst and spalling events occurred at different places: roof, walls and floor, at the face and behind the face.



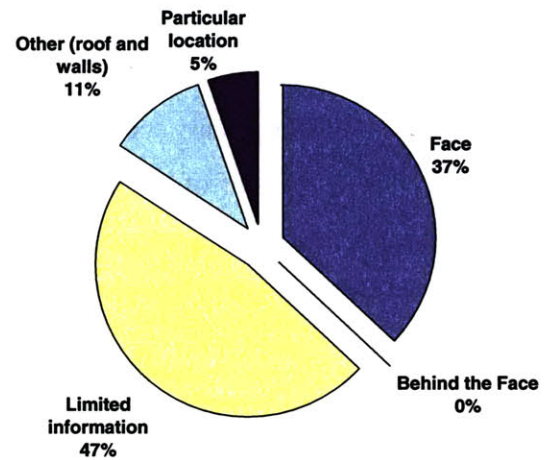
a) Collapse and Daylight collapse



b) Rock Fall



c) Excessive Deformation



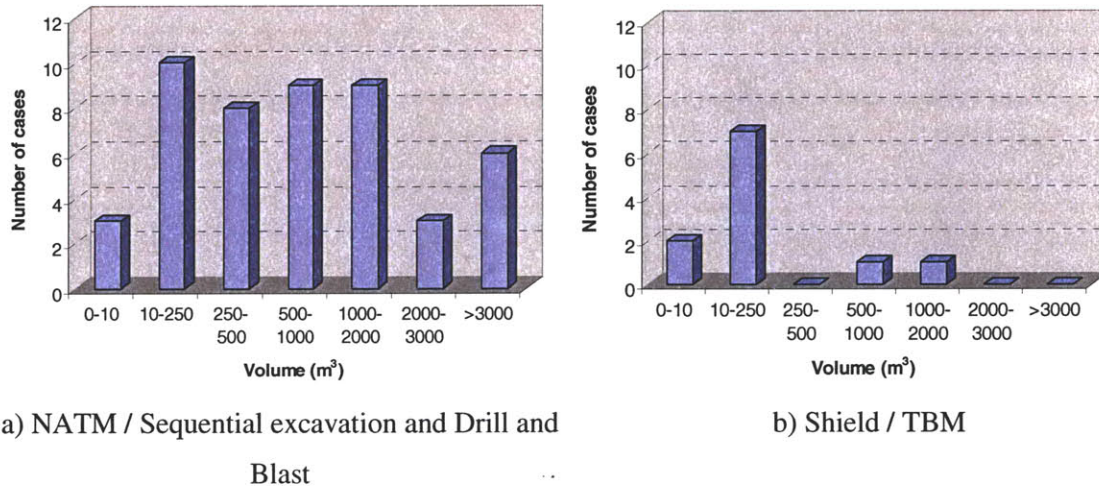
d) Flooding / Water inflow

Figure 3.40 Distribution of the location for the different types of events

The impact of an event, such as collapses, daylight collapses or rock falls, is related in some way to the volumes of ground involved and whether or not the tunnel is in urban environment. Figure 3.41a show the volumes associated with conventional type of construction (NATM and Drill and Blast) events. Figure 3.41b shows the volumes of collapses associated with TBM events. Although the number of cases for which there is information regarding the volume involved in the collapse is about 5 times larger for the conventional excavation methods than for mechanized methods, it is possible to observe that the volumes associated with TBM construction are normally in the range 0-250 m<sup>3</sup>,



while the volumes associated with NATM and, Drill and Blast collapses tend to be larger in volume and have also a larger range from 10 and 2000 m<sup>3</sup>. Some cases involve large volumes, with one of 14 000m<sup>3</sup>.



a) NATM / Sequential excavation and Drill and Blast  
 b) Shield / TBM

Figure 3.41 Volume involved in events (Collapse, Daylight collapse and rock fall) for different construction methods

Analyzing the different events, taking into account all the construction methods, one can observe the following:

- The volumes involved on collapses are mainly in the range of 10-250 m<sup>3</sup>, although some very large volumes can occur (Figure 3.42). The volume can be probably associated with the dimensions of the tunnel.
- The volume involved in daylight collapses is normally associated with the crater that reaches the surface, and therefore with the overburden and characteristic dimensions of the tunnel. The volumes are more or less uniformly distributed between 10 and 3000m<sup>3</sup> as can be seen in Figure 3.43.
- Finally the volumes involved in rock falls are generally much smaller, in the range of 0-250m<sup>3</sup>. There are however two cases, the Cahora Bassa hydroelectric scheme (Sousa, 2006) and the Laerdal road tunnel (T&TI, 2003) where a large volumes of rock fell. In the case of Cahora Bassa this rock slide was associated with unfavorable low strength surfaces (Figure 3.44)

Figure 3.45 presents the distribution of volumes corresponding to daylight collapses in urban areas. They follow the same pattern of Figure 3.43.

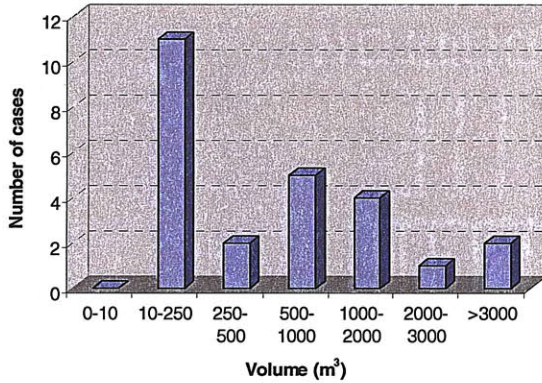


Figure 3.42 Volume involved in collapses for both conventional and mechanized construction methods

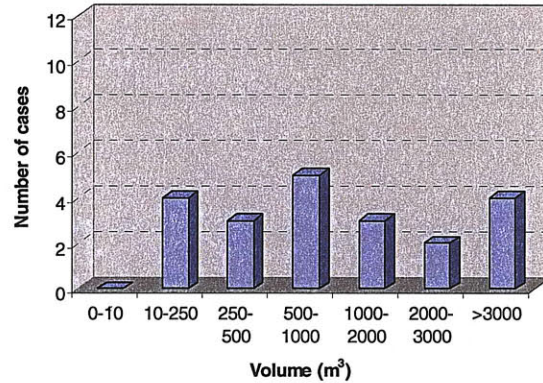


Figure 3.43 Volume involved in daylight collapse for both conventional and mechanized construction methods

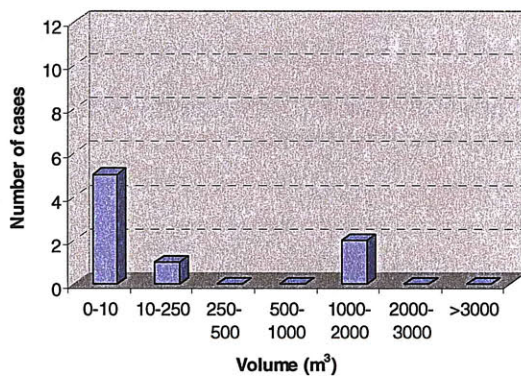


Figure 3.44 Volume involved in rock falls for both conventional and mechanized construction methods

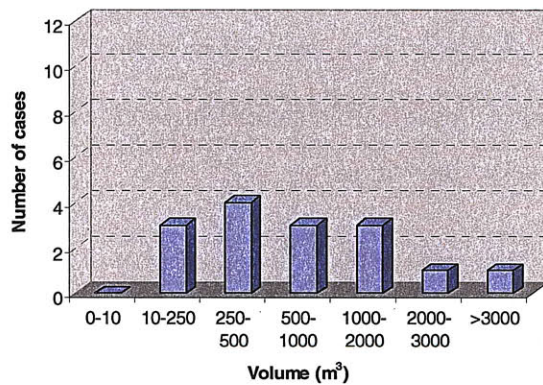


Figure 3.45 Volume involved in daylight collapses in urban environments for all construction methods

In the next figures (Figure 3.46 to Figure 3.48) are shown volume of collapse versus H/D, the relation between overburden (H) and equivalent diameter of the tunnel (D). The Figures have been divided by ground type (Rock, Soil and Mixed). Within each ground type a division between construction method (NATM, Drill and Blast or TBM) was also made. It is possible to observe that daylight collapses occur generally for H/D up to 5



(normally  $H/D < 3$ ), i.e. for overburden up to 5 times greater than the diameter of the excavation. This is an expected observation since for a collapse to reach the surface the excavation should somewhat close to the surface. Also tunnels in rock present a broader range of  $H/D$ . This is also expected since deeper tunnels are normally in rock. Unfortunately, based on the available data it is not possible to observe a clear trend related the volume of the collapse with  $H/D$ . This could be a result of not enough data available as well as a not enough detailed description of the ground type, again due to lack of information.

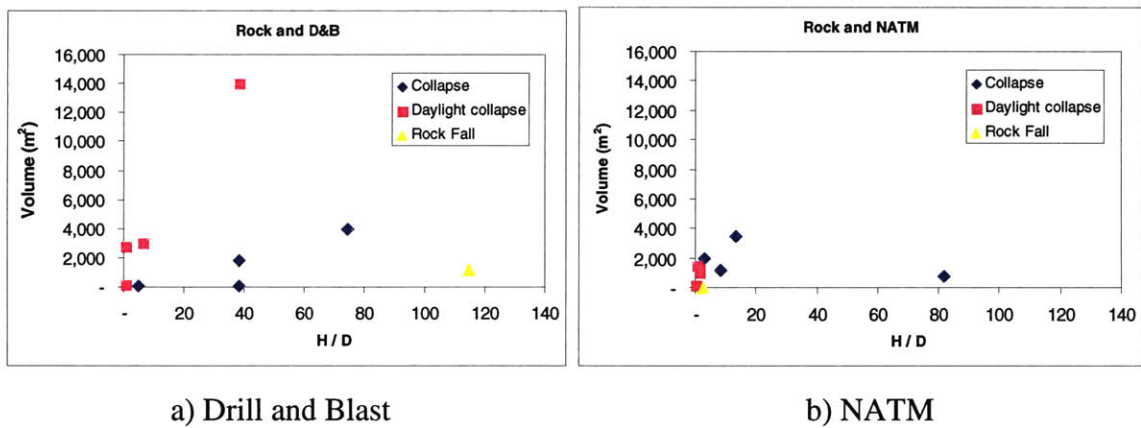


Figure 3.46 Data available on volume of collapse versus  $H/D$  for tunnels in Rock formations

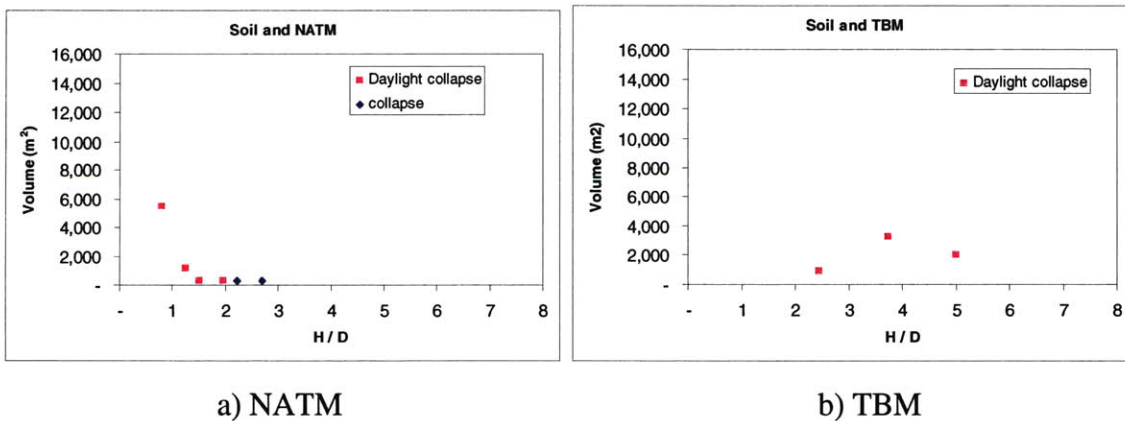


Figure 3.47 Data available on volume of collapse versus  $H/D$  for tunnels in Soil formations

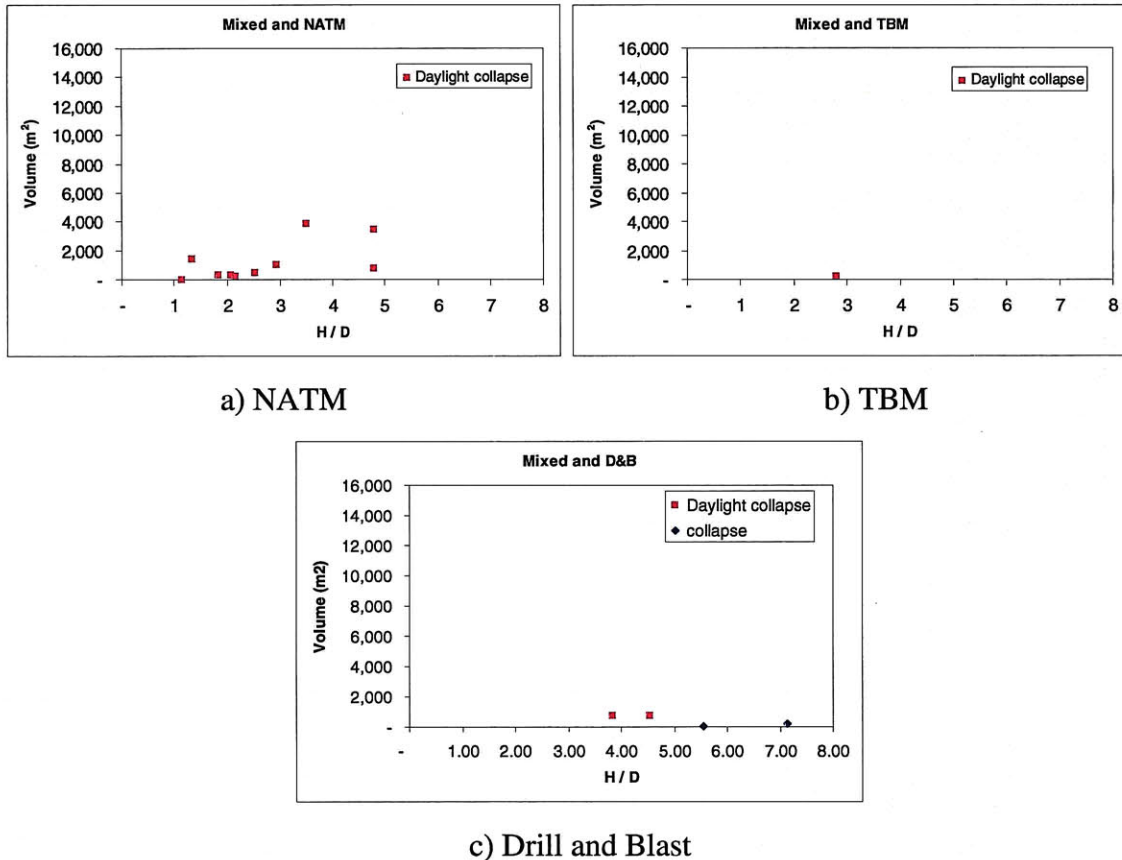


Figure 3.48 Data available on volume of collapse versus H/D for tunnels in Mixed conditions

### 3.4 Reported causes and consequences

#### 3.4.1 Most commonly reported causes

The causes for accidents in tunnels under construction do not depend exclusively on the behavior on the ground but also human errors and environmental external factors, such as earthquakes or changes in the water level due intense and persistent precipitation.

The causes for accidents in tunnels can be divided in internal and external (Vlasov, 2001; Longo, 2006). Internal causes are related to the design and planning of the tunnel as well as basic construction and management errors during tunnel construction. The external causes are related to hydrological and geological conditions, as well as earthquakes and fires.

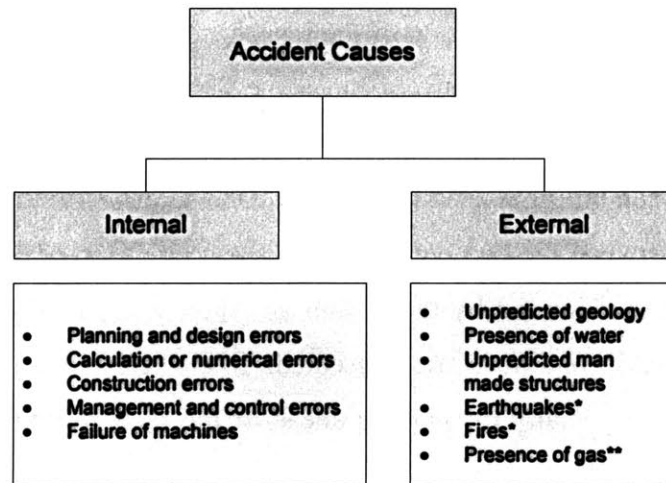


Figure 3.49 Main causes for accidents during construction

(\* - very low probability but if occurring can have severe consequences

\*\* - very important in the case of tunnels for mines, such as coal mines among others)

Earthquakes and Fires are causes for collapses and damages that are mostly associated with tunnels during the operation phase, due to the low likelihood that they occur during the construction of the tunnel. However they may occur and the consequences can be significant for the construction process.

There is normally more than one cause associated to an accident. Most of the times, several errors and causes led to a chain of events that result into an event. In the next section the most commonly reported causes and errors will be detailed.

### 3.4.1.1 External Causes

#### Unpredicted geology

The main reported cause of failure in tunnels during construction is attributed to unpredicted ground conditions.



The most commonly reported unpredicted features in soils are lenses of water bearing sand or gravel that cause the reduction of the resistance of the ground. This was the case of collapse that occurred in the metro of Lausanne (Project ID 2), mentioned previously in section 3.2.3. It was assumed in the design that there was a constant gradient of the molasse layer between boring no. A21 and A22 (50 m apart). Unfortunately there was no constant gradient between the two boreholes. This can be observed in Figure 3.50 where the ground conditions assumed by the design are shown and in Figure 3.51 where the ground actual ground conditions are presented. It is therefore important to continue ground exploration, especially by probing ahead of the face, during the construction of the tunnel.

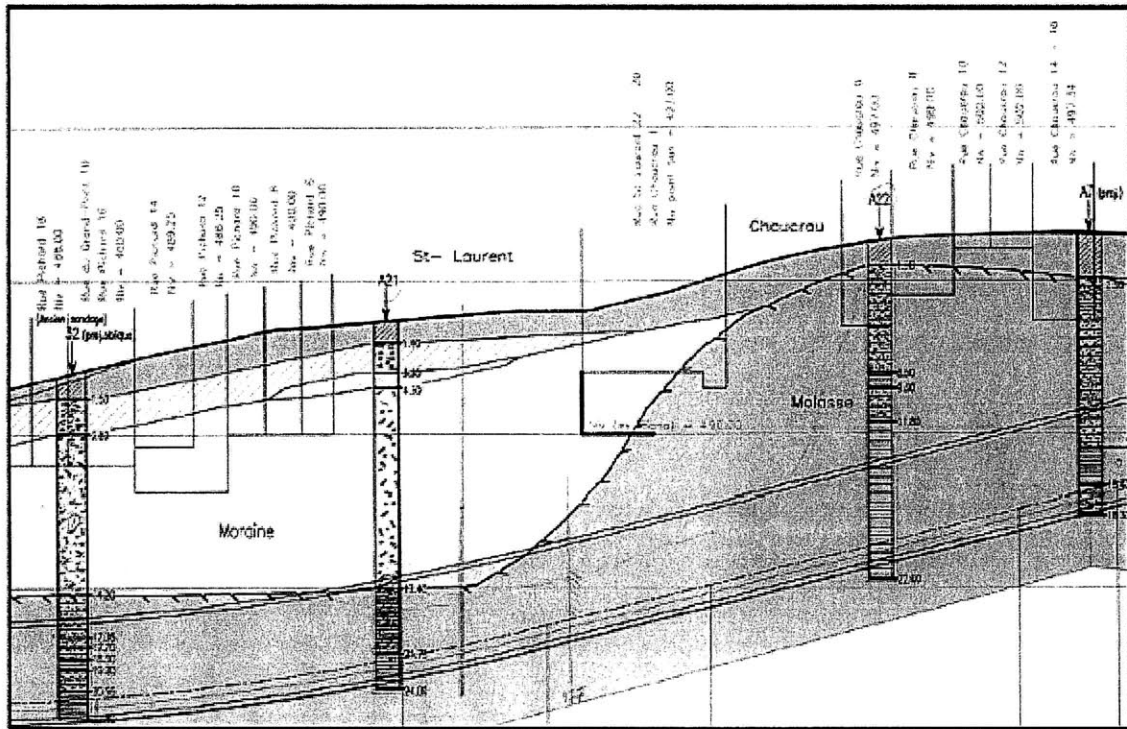


Figure 3.50 Ground conditions in the final design documents (Seidenfuss, 2006)

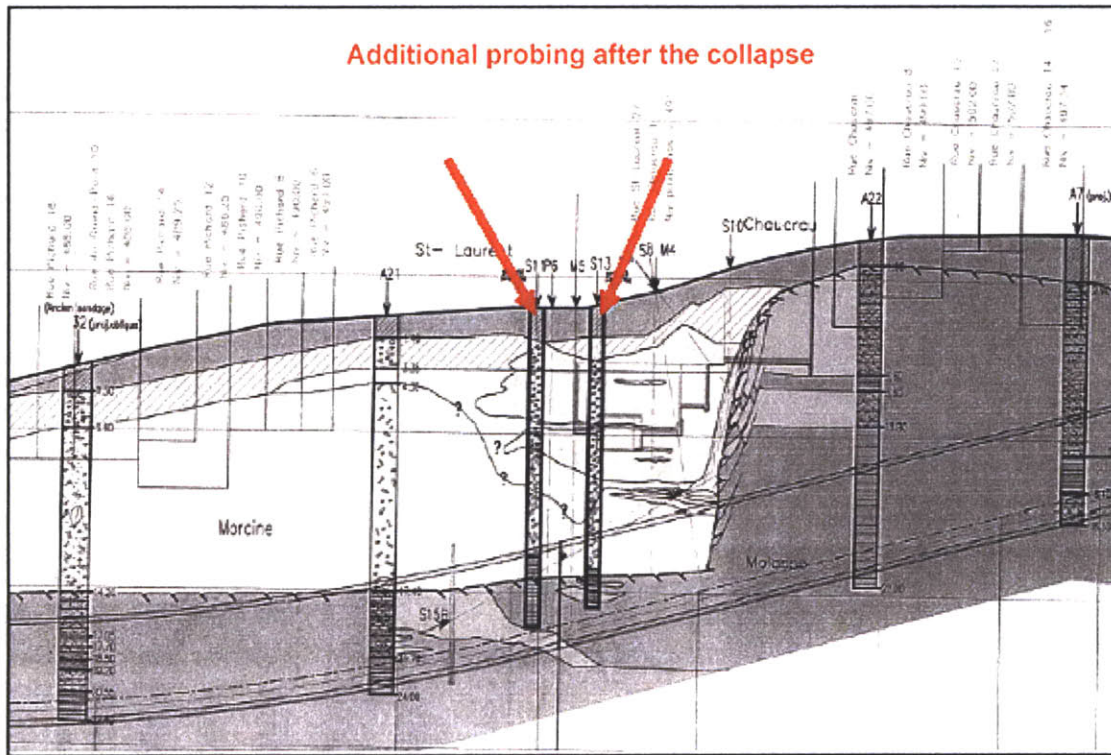


Figure 3.51 Actual ground conditions after collapse (Seidenfuss, 2006)

For tunnels in rock one of the most common features are weak zones, fault zones and/or low strength surfaces. Fault zones are particularly adverse in the cases of tunnels driven by TBMs where a collapse may bury the TBM causing it to get stuck, which may require excavation of bypass tunnels in order to rescue it or may even lead to abandon the TBM, in extremely severe cases (Barton, 2006).

The case of Evinos-Mornos Tunnel (Project ID 49) in Greece (Figure 3.15) is an example where several (Grandori et al. 1995) problems, ranging from small continuous collapse of the face, squeezing ground and some larger collapses where caused by faults. In some of these situations when the TBM cutterhead is pulled back for ground treatment after the collapse, loosening happens creating a larger collapse dome (Grandori, 1995)

A fault zone can have an adverse effect on the tangential stress arch, and tunnel stability problems often occur as a result. An example is the Italian Pont Ventoux HEP headrace tunnel (Project ID 69), which was tangent to numerous faults, resulting in collapses or in

the cutterhead getting stuck (Figure 3.52). In the Pont Ventoux case, it was the combination of the tangential fault zones and adverse water problems that were the main cause for the problems during the construction, causing the TBM to be stuck 6 months in one case due to continuous collapses with water or water pressure as shown in Figure 3.53 (Barton, 2006)

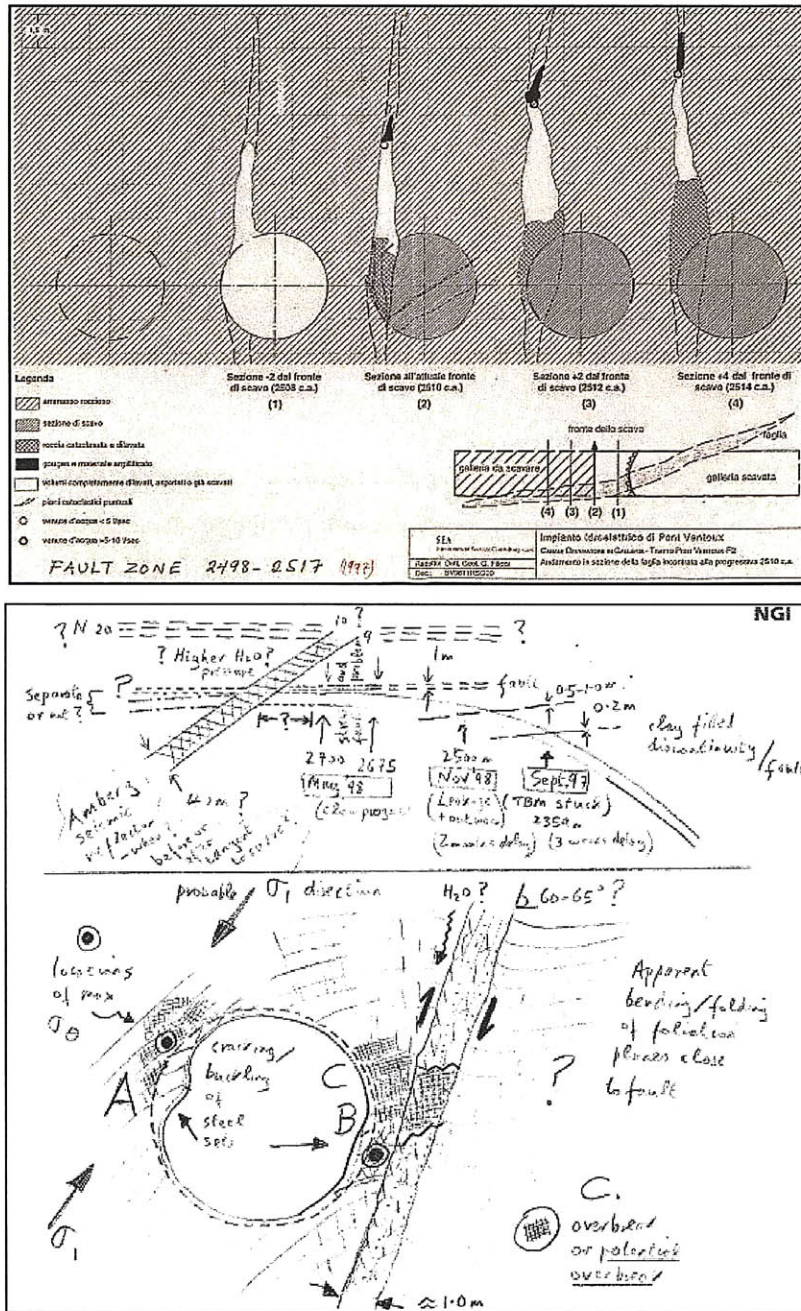


Figure 3.52 Two examples of fault-zone problems experienced at the Pont Ventoux HEP project in N. Italy (Barton, 2004)



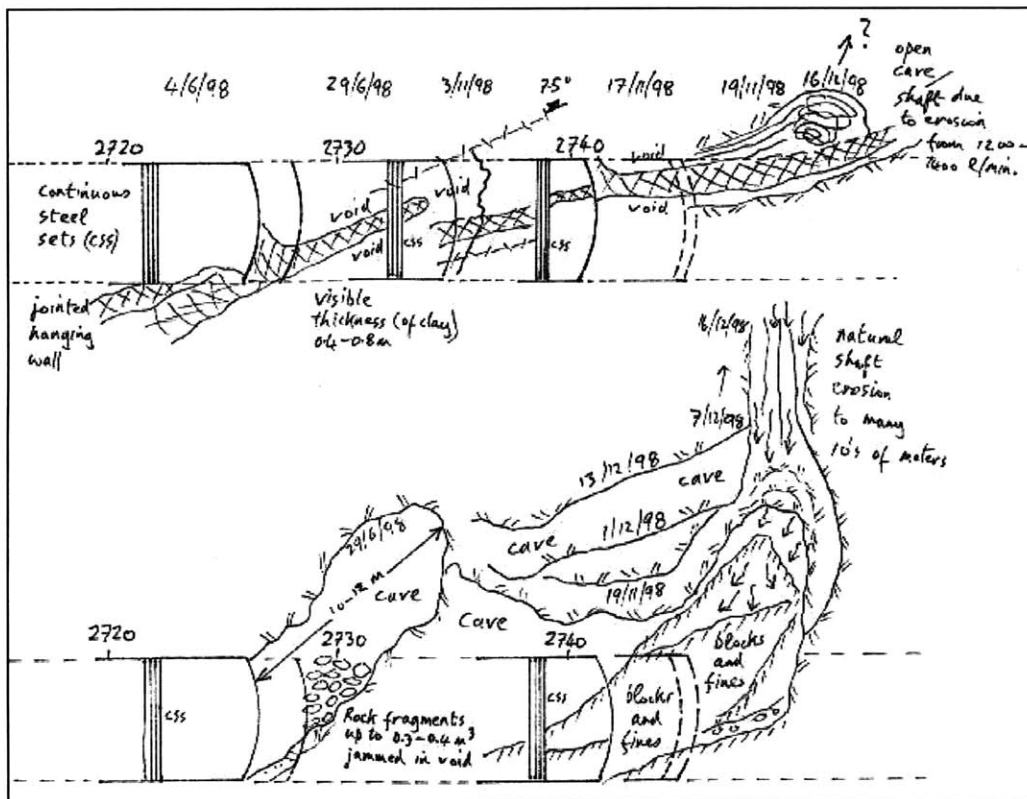


Figure 3.53 Continuous collapses due to the 'fault shaft', assisted by water and/or water pressure. These sketches are super-imposed on one sheet, from the geologist's daily logs. TBM was stuck for 6 months in this location (Barton, 2006)

### Presence of water

The presence of water and especially high water pressures, can be very adverse to tunnel stability during construction and may lead to collapse or / and flooding.

The Pont Ventoux continuous collapses presented in Figure 3.53 is a good example where adverse water pressure was the most important cause with respect to the cutter-head getting stuck in the various fault zones. In this tunnel, the high (non-vertical)  $\sigma_1$  stress, and very high water inflows, were very adverse to stability in fault zones full of clay, silt, sand and crushed rock.

Another case where high water pressures caused problems to tunnel construction is the Dul Hasti HEP (Project ID 64). During the construction an extreme water and pebble/sand blow-out, plus stand-up time problems in inter-bedded phyllites occurred.

The blow-out consisted of about 4,000 m<sup>3</sup> of sand and quartzite pebbles, and an initial 60m<sup>3</sup>/min water inrush which buried the TBM. The blow out originated in the invert and was therefore not detectable by 'conventional' forward-and-upward probe drilling, which nevertheless was absent. The overburden in the zone was of about 750 m (Figure 3.54)

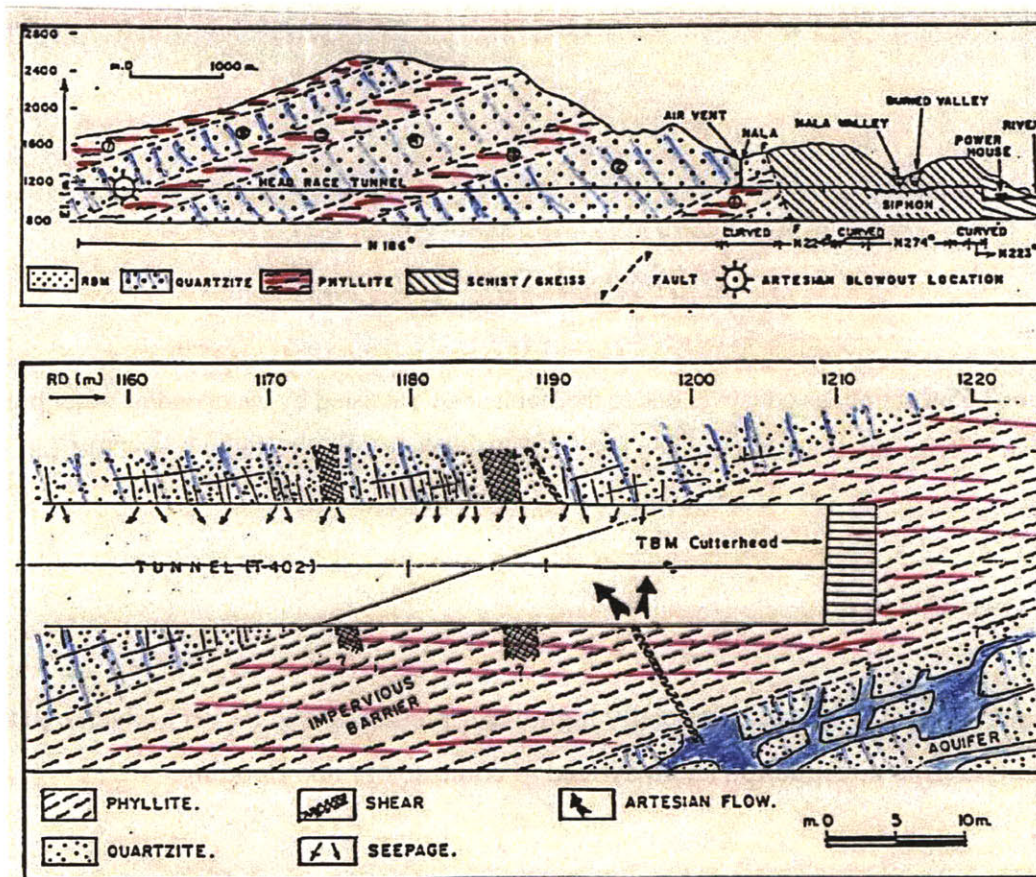


Figure 3.54 Simplified geology, and the location (ch. 1,215) of the blow-out of water, sand and rounded quartzite pebbles



## Unpredicted man made structures

Man made structures, such as wells, old galleries or old boreholes, can affect the stability of a tunnel while being excavated and may be the cause for a collapse. Some features when in large number can also alter the hydro-geological characteristics of the ground. This was the case in the Porto Metro (Project ID 9), in Portugal, where a large number of old wells and “minas” (old and small handmade water tunnels) were present in the area and uncharted due to their ancient nature. They modified the hydro-geological characteristics of the ground, such that the groundwater moved not only in the porous medium and fractures, but also along the preferential channels represented by the “minas”, which strongly influence the underground water circulation (Grasso et al., 2003). Figure 3.55 shows a Man-made water mine beneath the city of Porto.



Figure 3.55 Man made water mines in Porto, Portugal (Forrest, 2006)

In September 2001, a tunnel under construction for the Istanbul metro (Project ID 14) in Turkey collapsed due to an unidentified well. At the time of the occurrence the top heading was being excavated, under a hotel. The collapse occurred when the section was being expanded to 100 m<sup>2</sup> to accommodate a switch tunnel area for the single track system (Ayaydin, 2001). The cause of the collapse was an unidentified well 1.5 m above the switch tunnel crown (Figure 3.56). It is assumed from the reconstruction of the

situation that this well was almost exactly above the place where the liquefied mud had flowed into the tunnel. It was assumed that there was only about 1.5-2.0 m between the well bottom and the tunnel crown and that the saturated clay and well water flowed into the tunnel, causing the well walls and surrounding clay to collapse. This allowed the fine-grained sand layer to drain into the resulting cavity. This undermining of the foundation slabs and supporting walls of the buildings above led to their collapse. Three buildings collapsed at the surface, causing 5 deaths (Figure 3.57).

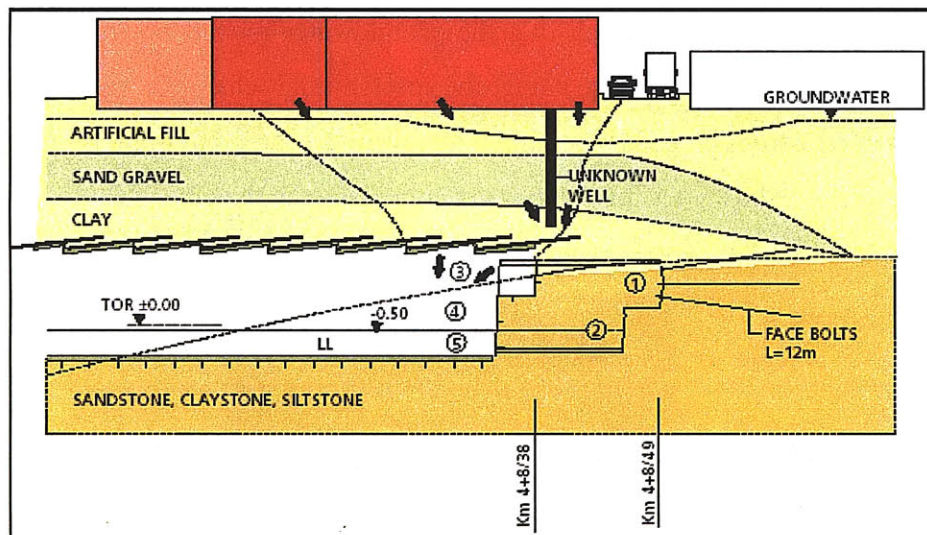


Figure 3.56 Longitudinal section through the collapse area showing geology and position of surface structures, Istanbul metro (Ayaydin, 2001)



Figure 3.57 Collapsed zone at surface, Istanbul metro (Ayaydin, 2001)

## Earthquakes

Although Earthquake associated collapses during construction are extremely rare, such a case occurred in Bolu tunnels in Turkey (Project ID 65). In 12 November 1999 an earthquake and the following aftershocks caused the failure of both Bolu tunnels, Turkey, 300 m from the Elmalık portal. At the time of the earthquake, a 700 m section had been excavated from the Elmalık Portal, and a 300 m section of reinforced concrete lining had been completed. The collapse took place in the clay gouge material in the unlined section of the tunnel. The investigation indicated that the tunnel collapsed or the primary lining completely deformed over an approximately 400-m long section, due to strong ground shaking and not because of fault displacement. The collapse was progressive. Two sinkholes appeared at the surface. One of them occurred immediately after the major earthquake of 12 November 1999 and the other one occurred 2 months later (Ghasemi, 2000, Dalgıç, 2002).

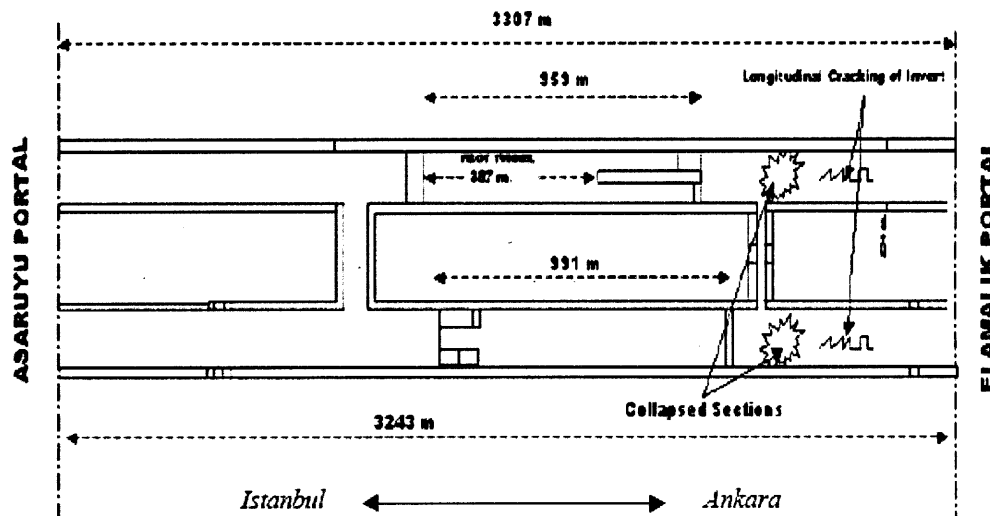


Figure 3.58 Approximate location of the tunnel collapses (Ghasemi, 2000)





a) view looking at the westbound tunnel  
(Asarsuyu portal)

b) view looking at the eastbound tunnel  
(Elmalik portal)

Figure 3.59 Collapses at the Bolu tunnel in Turkey (Ghasemi, 2000)

## Fires

The great majority of the fires in tunnels during construction are associated with mines. Nevertheless in the history of tunneling there several cases of fire during excavation, generally associated with the use of timber for temporary supports, blasting with high explosives, tunnel driving under compressed air with elevated oxygen content among others. The main causes are normally faults in electric equipment or short circuits in power lines.

In June 1994 a TBM fire occurred in the Great Belt (Project ID 125), when oil from the TBM spilled and ignited during construction. The fire that lasted for several hours produced temperatures of about 800° C and damaged up to two-thirds of the concrete lining (Figure 3.60). The reported costs associated to this accident were of about US\$ 33 millions (Vlasov, 2001; Khoury, 2003)

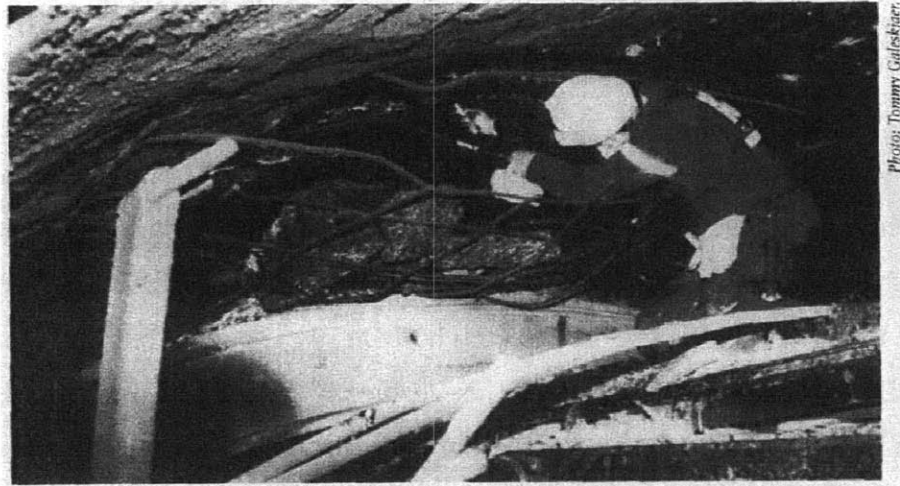


Photo: Tommy Gårdskjær

Figure 3.60 Damaged concrete lining after the 1994 Great Belt fire, Denmark (Khoury, 2003)

### **Presence of gas**

The excessive presence of gas in the air during construction may lead to emergency situations. Accidents that occur are normally mainly due to an inadequate ventilation system. The gas can result from several sources, such as construction procedures like blasting and soil freezing, or as a result of the geological composition of the rock being excavated. Although normally associated with tunnels for mines, there have been such cases in the construction of metros in the city of Baku, in 1983 and 1987, Moscow, in 1982 and Nizhny Novgorod, in 1981 (Vlasov, 2001). In all of these cases the source of elevated concentrations of saturated hydrocarbons in the air was because of petroleum products that had seeped into the tunnel works from the surrounding ground. In the case of Baku and Moscow the excavation through these rocks was accompanied by flames. Most of the tunnels that were affected by this problem were in places where oil storage and oil pipes were previously situated.

An emergency situation that dealt with presence of gas while performing artificial soil freezing, occurred also in the Moscow metro in 1989 (case 179). Soil freezing was done by using liquid nitrogen. A 1.5 m deep trench was made for the purpose. The access to the trench was prohibit while nitrogen was being discharged and for a period of 40 min afterwards. The nitrogen that evaporated during the procedure was withdrawn with the



help of a fan. A worker died and another was rescued alive, because they were inside the trench carrying out works while the nitrogen was being discharged (Vlasov, 2001).

During the construction of the Los Angeles subway (case 180) through sandstones and limestones containing hydrocarbons characteristics of the California oil bearing field, problems related to the presence of gas occurred. Analysis of the data on the gases and soils and the location of active gas bearing horizons were carried out, in order to specify the ventilation requirements as well as technical procedures for the detection of hazardous gas concentrations. Ventilation was the principal means to prevent gas explosions (ENR, June 1989)

### **3.4.1.2 Internal Causes**

#### **Planning and Design errors**

Tunnel collapses have occurred due to errors and mistakes that occurred during planning or design. Among others they include (HSE, 1996; Vlasov, 2001):

- Lack of surveying and geotechnical studies and/or inadequate evaluation of the geotechnical information available.
- Inadequate competent ground cover
- Inadequate excavation process and / or support system for the ground
- Inadequate or faulty ground classification system leading to inappropriate support
- Wrong choice of construction method
- Inadequate planning for emergency measures
- Inadequate specification for lining repair procedures

An important case related to insufficient geotechnical studies was the collapse that occurred in 2005 in the Barcelona Metro line 5 (Project ID 29). According to the parliamentary investigation conducted after the accident, the lack of geological studies

prevented the presence of a fault to be known. The original alignment of the tunnel did not go through the Carmel neighborhood (where the collapse occurred). This decision was made 9 months before the collapse, and the necessary geological studies were not made (Figure 3.61).

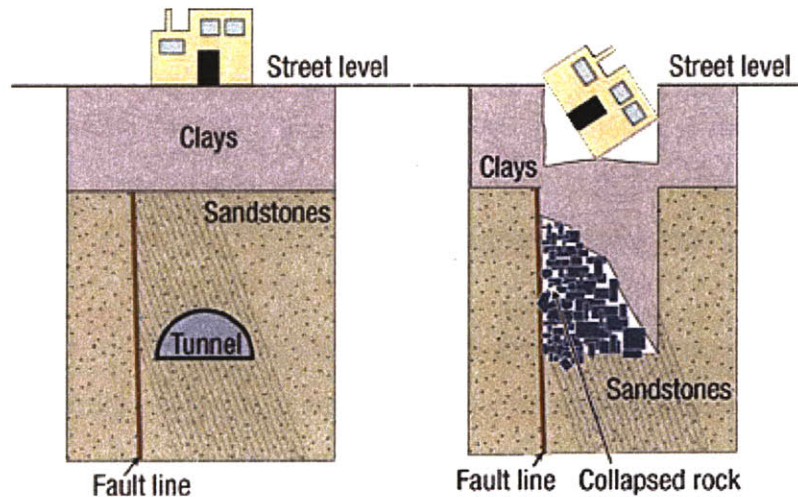


Figure 3.61 Barcelona Metro Line 5 collapse illustration

### Calculation and numerical errors

Calculation and numerical errors can occur both during the design phase and the construction phase. Most of the calculation and numerical errors that occur during construction are related to the monitoring data, whether it is in their collection or in their processing. The most reported causes are:

- The adoption of incorrect geomechanical design parameters.
- Use of inappropriate models; no considering the effect of water; no considering the 3D effects such as existing tunnels.
- Errors in the collection of monitoring data
- Errors in the processing and not fast enough delivery of monitoring data.

Adoption of incorrect geomechanical design parameters and use of inappropriate models were some of the errors, that occurred in the case of Olivais metro (Project ID 10) in Lisbon (Figure 3.20), where the geomechanical parameters used in the design numerical calculations were overestimated (Appleton, 1998).

### **Construction errors**

There are numerous reported construction errors and they are normally related to use of poor quality materials or not following the design specification requirements. More specifically some of the reported errors are:

- Lining not constructed with the specified thickness.
- Wrong installation of rock anchors, bolts and (lattice) steel arches.
- Errors in the installation of ground freezing pipes
- Poor profiling of the invert and badly executed lining repairs.
- Faulty dewatering system

In the case of the Heathrow collapse (Project ID 24), in London, an inspection made during construction revealed construction defects, such as an inadequate thickness of the shotcrete. Remedial work which consisted on repairing the lining was done. Unfortunately the repairs were also badly executed. Besides these errors, other construction errors were later pointed out by an HSE investigation such as the failure to produce correct wall profiles; defective invert construction, due to shotcrete rebound; defective joint construction, due to poor design detail (Figure 3.62) and an over-flat invert. The accumulation of all this errors along with management and design errors led to a major collapse of the three NATM tunnels in October 1994 (HSE, 2000)

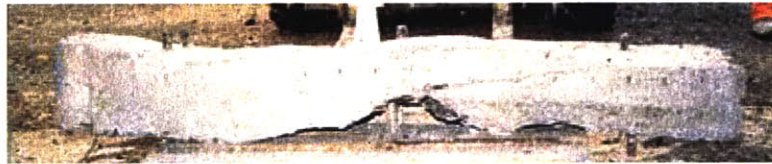


Figure 3.62 Exhumed sections of invert and joint (HSE, 2000)

Another example where construction errors played an important role in major collapse were the Montemor tunnels (Project ID 11) in Portugal. The observation data indicates systematic errors when installing the Swellex bolts used in the primary support. The correct sequence of installation of each Swellex bolt is: i) Drill the hole in the rock ; ii) Insert the Swellex bolt in the hole, not expanded; iii) Expand Swellex bolt with the hydraulic pump (reaching 30MPa); iv) Remove the pump, keeping the bolt pressurized. However the adopted sequence was (at least in several occasions): i) Drill the hole in the rock; ii) Expand the Swellex bolt on the floor of the tunnel; iii) Remove the pump, keeping the bolt pressurized; iv) Insert the Swellex bolt in the hole. This process instead of reinforcing and strengthen the rock mass as was intended by the design ended up probably damaging the ground surrounding the crown of the excavation, due to the wrong installation of the Swellex bolts.

### **Management errors**

In many cases, among other causes, management and control errors are reported as one of the causes for the accident:

- Failure to act on monitoring data and early signs of danger;



- Improper management and inadequate emergency response measures;
- Inexperienced site management;
- Poor supervision of construction work
- Allowing the wrong sequence of tunnel construction (especially in multi-tunnel situations)

The Shanghai Metro line 4 collapse (Project ID 33), which occurred in July 2003 was found to be by an accident investigation due to improper management and inadequate emergency response measures (Figure 3.63). The parties involved are accused of failing to take timely emergency measures to deal with danger signs when technical problems were detected in the equipment used in the tunnel construction. When the cooling equipment used to freeze the ground before digging under the river broke down on June 28, two days before the collapse, no one reported the early signs of the impending cave-in to the project's management and engineering supervision officials. The officials were found to be have been absent from the site in the days before the accident while reporting everything was "normal" on their daily logs. Instead of halting the excavation and taking effective emergency measures, digging continued and the water pressure built up, resulting in the cave in (T&TI July 2003, August 2003).



Figure 3.63 Photo at the surface at the site of the collapse at Shanghai metro line 4 (Wannick, 2006)



Following the Heathrow collapse (Project ID 24) the Health and Safety Executive (HSE) published a report identifying the errors that occurred during the tunnel construction and causes for the accident (Figure 3.64). According to HSE the direct cause for the accident was a chain of events, from substandard construction in an initial length of the concourse tunnel, to damage from grout jacking done to correct settlement in a building above, ending in the fact that this damage was inadequately repaired (T&TI, August 2000). Among the errors identified by HSE were poor design and planning, lack of quality, a lack of engineering control and a lack of safety management. The construction management errors identified by the investigation included (Clayton, 2008):

- Insufficient specialist staffing
- Poor communication between different companies
- Poor sequence of tunnel construction
- Bad timing of invert repairs
- No integration in planning construction activities
- Compensation grouting over tunnel
- Lack of awareness of instrumentation data warning of impending failure
- Allowing the construction of a parallel tunnel



Figure 3.64 Photo at the surface at the site of the collapse of Heathrow (Clayton, 2008)

## **Failure of machines**

Failures of TBM machines or some of their components such as the earth pressure control system of an EPBM or the slurry injection system of a slurry machine may contribute to accidents of tunnels during construction.

### **3.4.2 Most commonly reported consequences**

The consequences of the undesirable events can be:

- In the tunnel (structure, people and equipment)
- At the surface (structures, people) or other structures (utilities etc)

Figure 3.65 contains the list of most commonly reported consequences (apart from costs and delays) in the tunnel and, on the surface and on other structures.

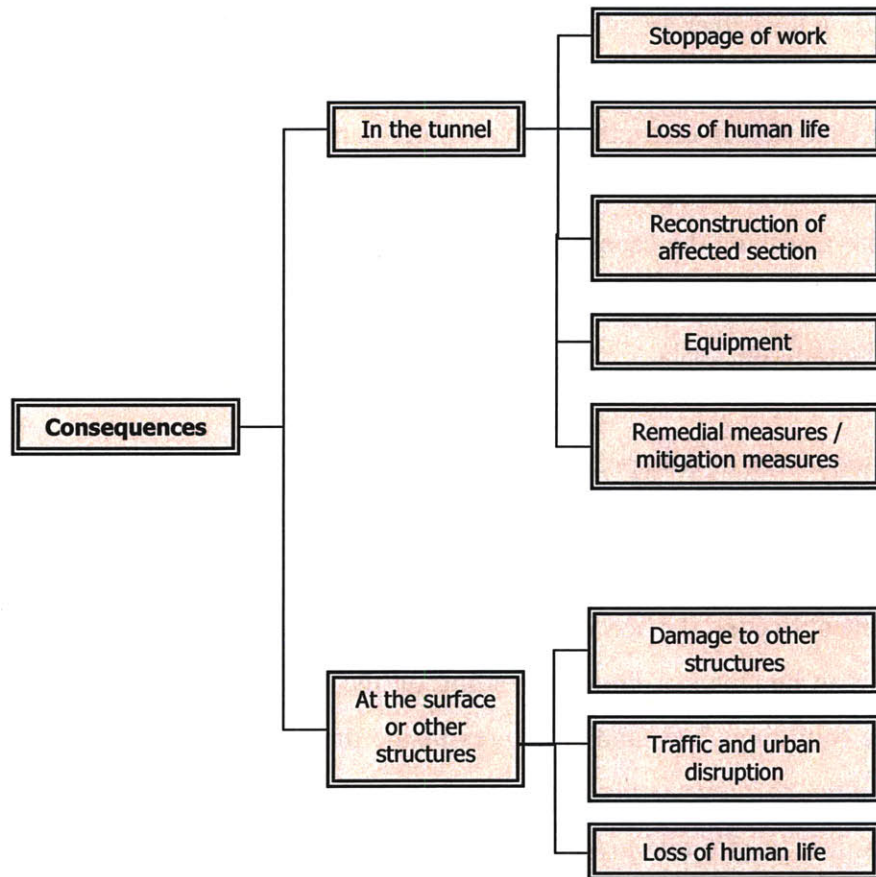


Figure 3.65 Most commonly reported consequences of undesirable events during tunnel construction.

When an event occurs, depending on its magnitude the work will have to stop (*stoppage of works*). Before the work re-starts it is necessary to be sure that all measures are taken to ensure safety. Additional investigation may be required. In some cases deaths (*loss of human life*) and injuries occur. The loss of human life is the one consequence that is extremely difficult to quantify. In the majority of cases when an event occurs there is the need of reconstruct the affected section of the tunnel (*reconstruction of the affected section*), which is reflected in an additional cost to the project. Equipment can be affected by the incident as well. It can be buried and damaged for example due to face / roof collapse. It can also be damaged due flooding. In the case of a TBM, the cutterhead maybe be damaged due to collapse of blocks or unexpected boulders in the ground, or in the most severe cases, cause the TBM to be stuck in the ground (*equipment*). *Remedial*

*and mitigation measures* are often needed, the first in order to overcome the accident and the latter in order to ensure the safe completion of the tunnel excavation. When a collapse occurs the first step is normally to prevent the damage to extend to the surface. This is normally accomplished by pouring material into the crater. This mitigation measures are taken before assessing the causes of the accident. After investigation and determining the cause the remedial methods are normally decided. These measures are translated in delays and additional costs.

Other consequences of collapses in some cases were the change of the alignment (Project ID 80) or abandonment of the tunnel (Project ID 94).

When an event occurs, it often induces movement at the ground around its location. This movement can be small or large depending on the event itself. Damage to structures on the surface (buildings, etc) and structures inside the ground (utilities, other tunnels) can occur (*damage to other structures*). Daylight collapses when occurring in urban areas usually result in *traffic and urban disruption*, such as evacuation of residents from their homes, power and water supply cuts and traffic detours, and ultimately they can cause death of people at surface (loss of life).

Since the 1990s there have been a number of great losses involving tunnels in urban areas. In some cases, repairs costed up to US\$ 100m. In the last decade CAR (contractors all risks) insurers have suffered losses totaling up to more than 750 million dollars in property damage only (Landrin et al, 2006). Table 3.4 shows some of the major losses, as well as respective delays, that occurred in tunnel construction since 1994.

Table 3.4 Major losses since 1994

Year	Project	Method	Loss (\$m)	Delay (months)
1994	Great Belt Link, Denmark	TBM	33	?
1994	Munich Metro, Germany	NATM	4	10
1994	Heathrow Express Link, UK	NATM	141	14
1994	Taipei Metro, Taiwan	TBM	12	12
1995	Los Angeles Metro, USA	TBM	9	15
1995	Taipei Metro, Taiwan	TBM	12	18
1999	Hull Yorkshire, UK	TBM	55	26
1999	Anatolian Motorway (Bolu), Turkey		115	36
2000	Taegu Metro, Korea	Cut and Cover	13	9
2002	Taiwan High Speed Railway	NATM	11	0
2003	Shanghai Metro	Freezing	60	47*

Note: \* estimate

Source of data is Landrin et al, 2006 and Munich Re Group, 2004.

Figure 3.66 shows a histogram of delays, in months, caused by accidents during tunnel construction. This represents the data available in the database (64 cases for which data on delays is available). It is possible to observe the majority of the delays varied between 0 and 7 months, being the average of delays around 6 months.



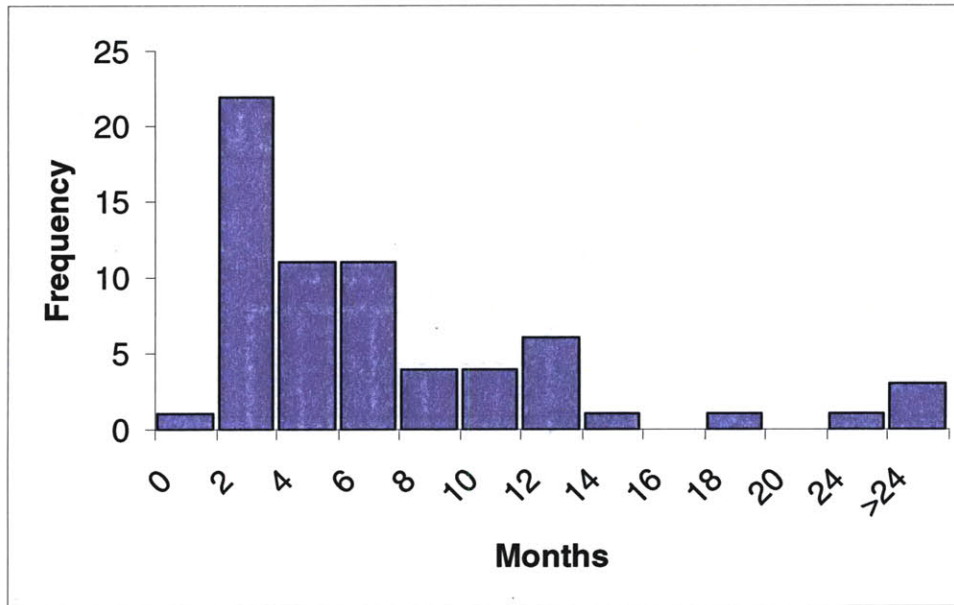


Figure 3.66 Distribution of the delays (in months) caused by accidents during construction

### 3.5 Remedial and Mitigation Measures

The remedial methods are very specific to each situation. There are however some methods that are common in many of these situations. The next table shows the most common mitigation measures per event.

Event	Mitigation measures
Collapse	<ul style="list-style-type: none"> <li>• Fill tunnel with materials (concrete, rock, sand bags and even water) for immediate stabilization and prevent further propagation of the collapse (used in most of the collapse/ daylight collapse cases)</li> <li>• Collapse hole bulkheaded and backfilled with concrete or / and materials (such as collapsed rock) and then remove.</li> <li>• Stabilization of the tunnel face and crown with shotcrete</li> <li>• Reinforcement of the ground in advance (bolts, forepoling, fiberglass bolts, pre-stressed anchors, etc). Normally applied in combination with preceding measure.</li> <li>• Drainage in advance and / or from the surface (when collapse occurs with or due to water inflow)</li> <li>• Modification of excavation sequence (multiple headings, pilot tunnel) and support</li> <li>• Grouting (in advance or /and from the surface) for consolidation.</li> </ul>

	<ul style="list-style-type: none"> <li>• Injection of resins of stabilization</li> <li>• Ground freezing</li> <li>• Bypass tunnel (used also in combination with grouting from inside the bypass tunnel)</li> <li>• Change of alignment / abandon</li> <li>• Change of construction method (drastic change of construction method, such as change from TBM construction to Drill and Blast)</li> <li>• Modification of TBM ( for example : cutterhead and cutterwheel or introduction in a EPBM of an automatic system that pumps bentonite slurry into the excavation chamber whenever the pressure drops below a preset level)</li> <li>• Hand mining of the material accumulated against the cutterhead together with applying a maximum torque + posterior grouting</li> </ul>
Daylight collapse	<p>All the above and :</p> <ul style="list-style-type: none"> <li>• Circular cofferdam isolating the collapse area (for major collapses - Heathrow case) for posterior excavation from the surface.</li> <li>• Filling in of the cavity at the surface with concrete or other material.</li> <li>• Tieback walls used to isolate collapse and allow open excavation</li> </ul>
Rock fall	<ul style="list-style-type: none"> <li>• Rock bolts</li> <li>• Shotcrete</li> <li>• Fill the cavity with concrete + wire mesh</li> <li>• Reinforcement with concrete buttresses supported at the wall by anchors ( extremely large block fall)</li> </ul>
Flooding / Water inflow	<ul style="list-style-type: none"> <li>• Drainage (in advance and from the surface; use of pumping systems).</li> <li>• Grouting</li> <li>• By pass tunnel</li> </ul>
Rockburst	<ul style="list-style-type: none"> <li>• Special bolts</li> <li>• Destress blasting</li> </ul>
Excessive deformation	<ul style="list-style-type: none"> <li>• Remine or reprofile the deformed section</li> <li>• Use of yielding elements</li> <li>• Modification of the shape / dimensions of cross section</li> <li>• Modification and reinforcement of the invert lining, such as reinforced invert or a deformable invert (in swelling cases)</li> <li>• Special rock bolt of yielding type</li> </ul>
Events in particular locations	<ul style="list-style-type: none"> <li>• Similar to collapse / heading collapse</li> <li>• Slope protection and support, like tiebacks (portal areas)</li> <li>• Slope cut back to stable geometry (portal areas)</li> </ul>

## **Collapse / Daylight collapse**

The methods used in collapses and daylight collapses are normally very similar. The major different is that in the latest the consequences at the surface must be addressed. Also daylight collapses are normally the largest and most catastrophic, so sometimes specific measures must be taken to isolate the collapse zone at the surface, such as a cofferdam or tieback walls, in order to safely access the collapse zone from the surface and clean the debris.

When a collapse occurs the first step is normally to take measures that will prevent it to progress further (to the surface for example). For that purpose the tunnel is normally filled with materials such as rock, sand bags, concrete or even water for immediate stabilization.

In most of the collapse/ daylight collapse cases that did not involve large volumes the measures consisted in bulkheading and backfilling the collapse hole with concrete or / and other materials (such as collapsed rock) and then remine. In some cases remining was done with the reinforcement of the ground ahead with elements such as forepoling, fiberglass bolts among others.

When a collapse occurs with or due to water inflow, drainage is normally used, in combination with the preceding methods, in advance or from the surface.

Figure 3.67 shows the repair strategy used in both daylight collapses of the Montemor tunnel (Project ID 11) in Portugal. Drainage was used in all sections where seepage was evident, as well as reinforcing measures were added to the already installed support measures. At the actual collapse zones the first step was to shotcrete the walls of the collapse, and arches were placed to reinforce the standing tunnel on each side of the hole (Wallis, 1995). On the surface a 2 m meter thick concrete slab was cast at the bottom of the crater, which was then backfilled with soil. An umbrella of Jet grouting columns was used to protect the excavation through the collapsed area.

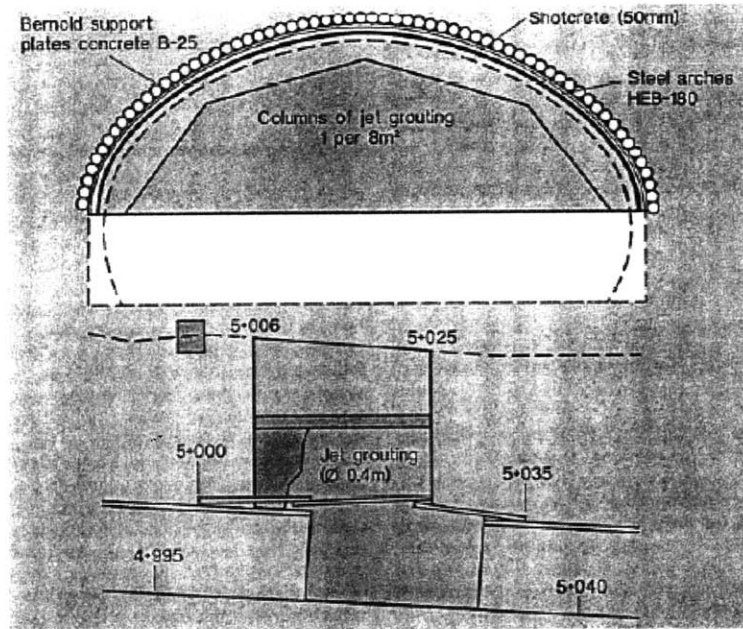


Figure 3.67 Repair strategies for both Montemor tunnels (Wallis, 1995)

Grouting is often used to consolidate and reinforce the collapse zone. This was the method used in the Lausanne metro collapse (Project ID 2). A curtain of eleven piles was drilled and concreted ahead of the collapsed face to consolidate the ground and limit the possible flow of further material into the tunnel, in conjunction with grouting.

The different phases of the remedial measures were as follow (Seidenfuss, T., 2006):

Phase 1 – Drilling of pile curtain and injection of concrete in order to limit collapsed area and possible flow.

Phase 2 – Partial backfilling of the crater (up the foundation level of the building) with crushed glass.

Phase 3 – Vertical grouting from the surface to consolidate ground (Figure 3.68)

Phase 4 – Excavation of the collapsed zone under the protection of an umbrella of steel pipes and steel arches.

Figure 3.69 is a plan of the area affected by the remedial/ mitigation works. For more details see case 002 record.

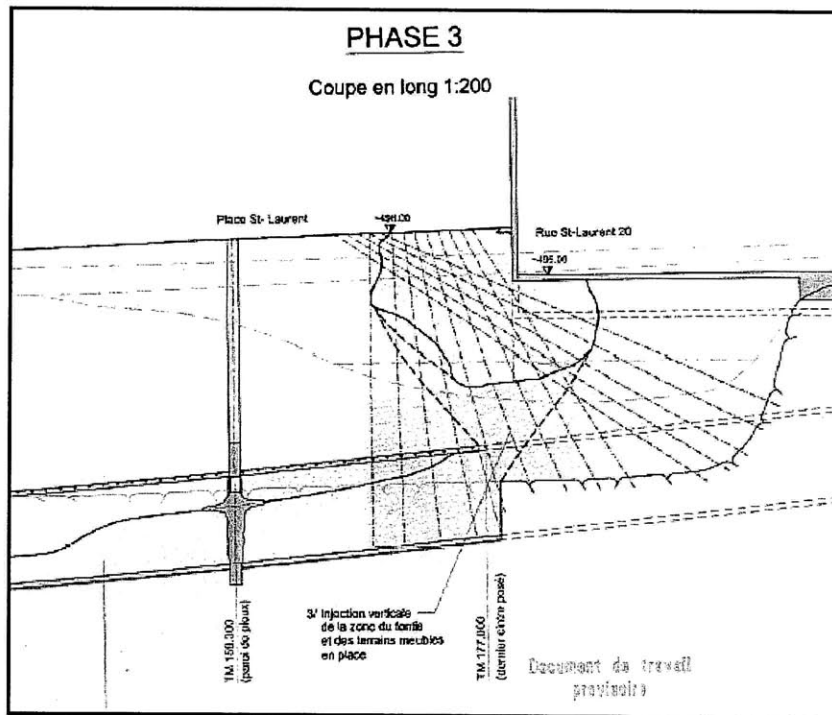


Figure 3.68 Phase 3 of remedial and mitigation measures at Lausanne metro (Seidenfuss, T., 2006)

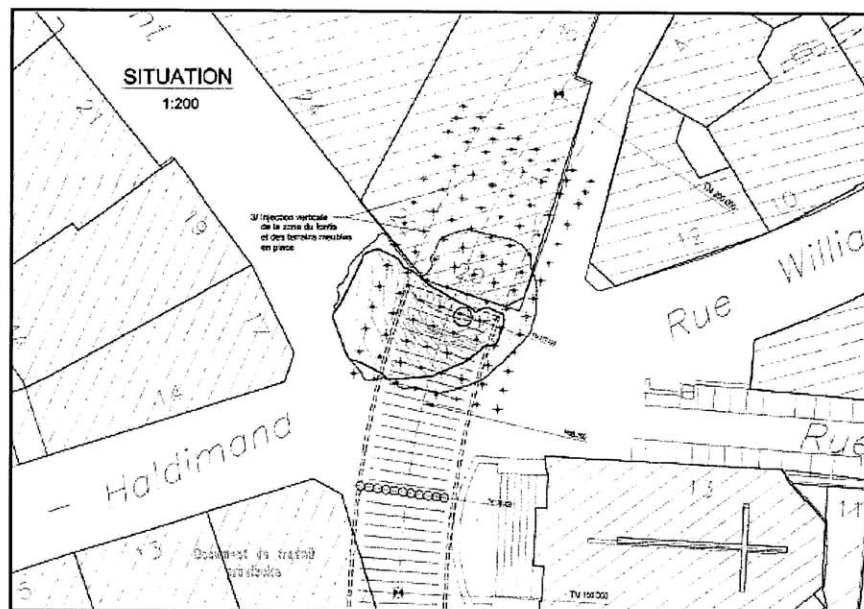


Figure 3.69 plan view of the area affected by the remedial/ mitigation works (Seidenfuss, T., 2006)



Following the collapse at Saint-Laurent, it was decided to drive the Viret tunnel 3.5m deeper in the molasse preventing endangerment of the historic buildings of the old part of town.

Freezing was also used in some cases in order to overcome the collapsed zone. An example is the Hull wastewater flow transfer tunnel collapse (Project ID 26). The immediate measure in this daylight collapse (in a shaft) was to stabilize the tunnel using compressed air. Air-lock doors that had been installed in the tunnel to allow compressed air access for cutter-head maintenance were used for this purpose. For the reconstruction of the tunnel, a supporting system by Artificial Ground Freezing (AGF) and NATM tunneling was considered the best solution considering the local ground conditions, safety, program, constructability and cost. Liquid Nitrogen (LIN) was chosen as the freeze medium.

The freeze system used at Hull was an open system, with LIN, which exists at approximately  $-196^{\circ}\text{C}$ , being pumped into a series of freeze tubes. The reconstruction of the collapsed section of tunnel was conducted in five stages, with two to the west, and three to the east of Shaft T3. The five construction stages were referred to as West 1 (W1), West 2 (W2), East 1 (E1), East 2 (E2), and East 3 (E3), each approximately 20-25 m in length. . The principal reason for this had to do with the capability to drill horizontally with the required accuracy. The tunnel axis was at a depth of 15m below ground level. The construction sequence is illustrated on Figure 3.70. Each construction stage was supported and closed to the surrounding ground and ground water horizontally with a circular ice wall and vertically with a frozen bulkhead. Each horizontal zone consisted of a vertical ice bulkhead consisting of typically 23 freeze pipes and a horizontal 'cone' of typically 33 freeze pipes. Figure 3.71 shows the cross section of the ice structure.

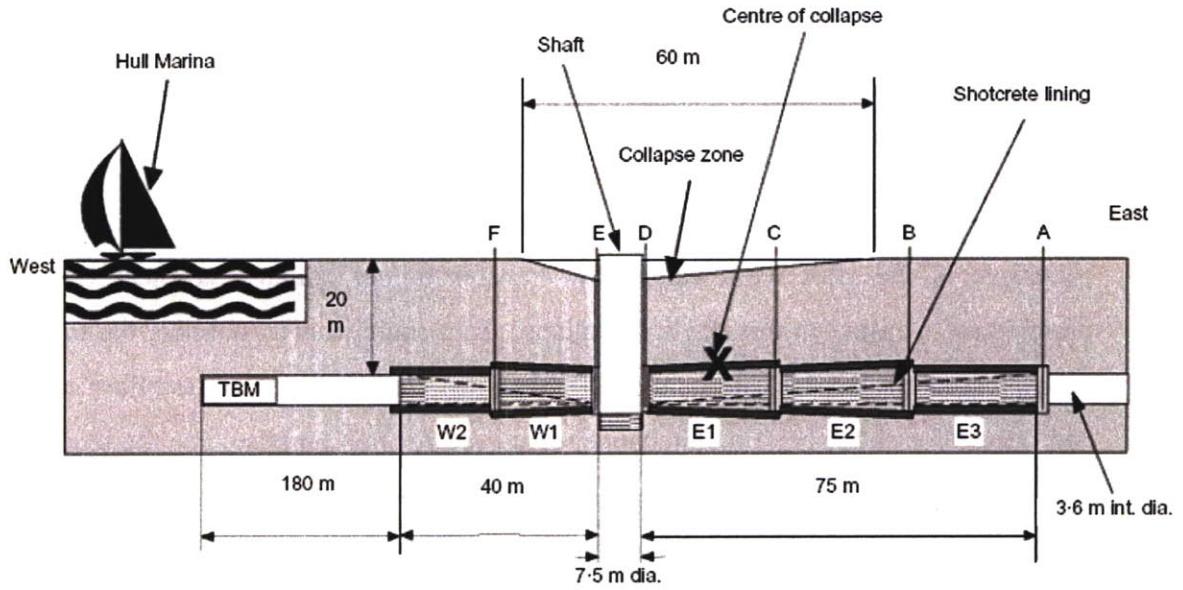


Figure 3.70 Construction sequence for the recovery of the collapsed zone (Brown, 2004)

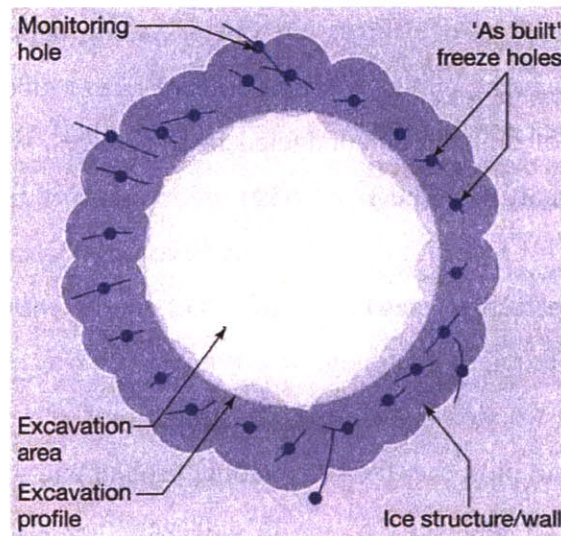


Figure 3.71 Cross section of ice structure with monitoring devices (T & TI, October 2000)

In the cases where severe cave-ins are accompanied with water inflow and this resulted in the jamming of the TBM, excavation of bypass tunnels from the side walls of the main tunnel behind the TBM may be necessary in order to rescue the machine and apply ground treatment measures, such as grouting or freezing. Commonly these by pass tunnels are excavated to the front of the cutter head and extending the overmining until working clearances were obtained. A top drift to explore the geological conditions or to

perform ground improvement ahead can be performed. The determination of the location of entrance for the bypass tunnel is dependent on many factors (such as the length of bypass, processing time etc).

During the excavation of the Hsuehshan tunnel (Project ID 30), in Taiwan the three TBMs were stopped several times (28 major stoppages in total). One of the most serious was the 10<sup>th</sup> stoppage due to a collapse at the TBM in the pilot tunnel. It was caused mainly by a sudden high-pressure groundwater ingress. In order to rescue the TBM, a detour tunnel parallel to the pilot tunnel was excavated which provided a passage for further excavation by Drill and Blast in front of the TBM (Figure 3.72). The ground was improved by grouting.

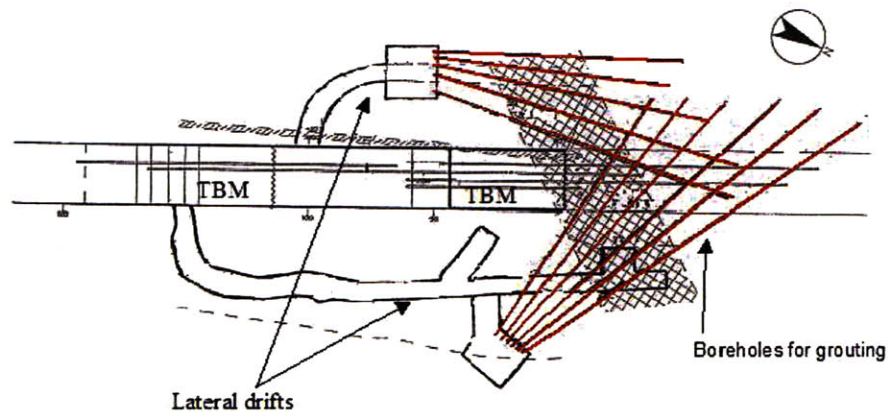


Figure 3.72 - Example of the ground reinforcing techniques using lateral drifts for the stop at the Chainage 39k+079 in the Hsuehshan Tunnel (Pelizza and Peila, 2005)

In another case, where the TBM was buried and blocked due to a collapse was the Frasdanello TBM tunnel in Italy (Project ID 95), which required complex stabilization measures to be adopted in order to resume the excavation.

Based on preliminary studies and pilot tunnel mapping, in conjunction with drilling of a number of exploratory holes following the machine blockage, the geological conditions in the thrust zone could be defined in detail as illustrated in the cross section of Figure 3.73.

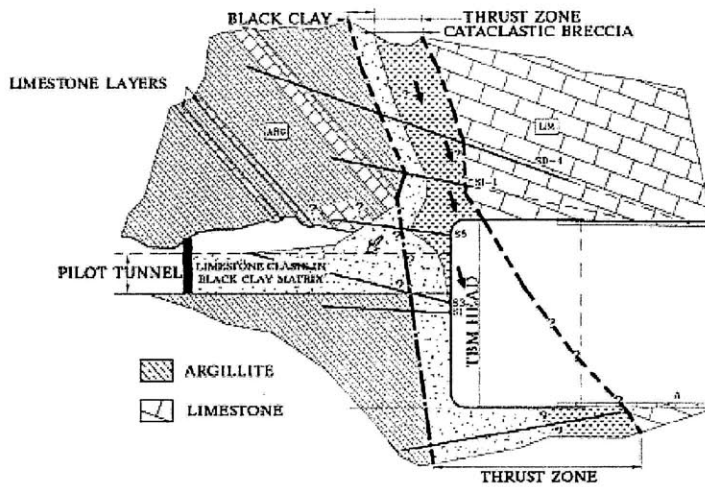


Figure 3.73 Geological conditions at the thrust zone (Barla G. and Pelizza S., 2000)

In this case the TBM was stuck by the ground above, making it impossible to continue with face advance, independent of the many attempts made to free the TBM ahead. It was decided that ground freezing was the most reliable measure to be carried out from the pilot tunnel, previously excavated (Figure 3.74)

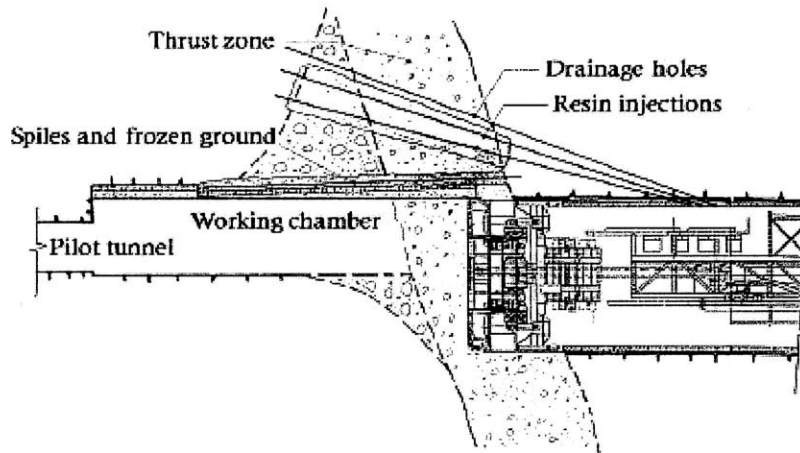


Figure 3.74 The stabilization measures adopted to free the TBM head (Barla G. and Pelizza S., 2000)



As shown in Figure 3.75, a working access chamber was created, starting from the pilot tunnel, with the intent to reach the TBM head. The main working stages were:

- i) Creation of a consolidated arch around the tunnel perimeter, performed from the back of the TBM, just behind the shield.
- ii) Creation of a working access chamber starting from the pilot tunnel, in order to allow for the launching of pipe spiles (length 22 m) ahead.
- iii) Ground freezing by using liquid nitrogen: a frozen vault was formed having a minimum thickness of 80 cm at the crown and 100 cm at the footwall;
- iv) Excavation of the access chamber to full length, to reach the TBM head (Figure 3.75 shows the chamber completed)
- v) Driving of the TBM through the thrust zone and placement of the precast reinforced concrete segments, followed by filling the gap with pea-gravel.



Figure 3.75 Access chamber completed with the TBM in the background (Barla and Pelizza., 2000).



## Rock Fall

The mitigation and remedial measures taken in rock fall events depend of the magnitude of the rock fall. Most events of smaller dimensions shotcrete and rock bolts is normally used. In other cases the cavity was filled with concrete and wire mesh.

In the Gotthard Base tunnel in Switzerland (Project ID 98) an unexpected horizontal fault zone which was penetrated during the start-up phase of the eastern TBM led to substantial hold ups for both drives (Bodio zone). On Feb 19th 2003 a kakaritic cataclastic fault was encountered after roughly 200m had been driven in the eastern tube which varied in thickness from a few decimeters to some meters. The fault zone accompanied the eastern drive over a distance of about 516m adopting an undulated form. The TBM moved out of it on August 31st 2003. In the western tube the fault was penetrated on June 9th 2003, and wandered through the profile for about 68m. Several overbreaks and a collapse (large overbreak) at tm 2720 occurred (Figure 3.76). For the overbreaks: shotcreting and shotcreting behind steel sets was used as remedial measure. For the collapse steel sets were used after hand-enlargement of the tunnel (AlpTransit-Tagung, 2004).

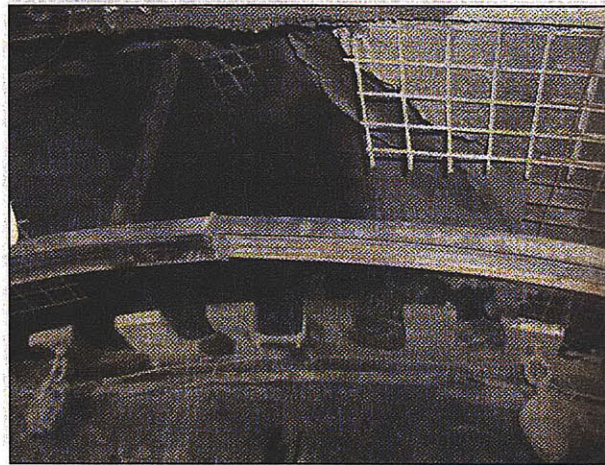


Figure 3.76 collapse at tm 2720 in the Gotthard Base (AlpTransit-Tagung, 2004).

In really large events such as the Cahora Bassa case discussed previously (Figure 3.10), reinforcement with concrete buttresses supported at the wall by anchors was used.

### **Water inflow / Flooding**

In order to seal the tunnel from water surrounding, and prevent major water inflow and possible flooding, pre-ground treatment with grouting or/ and draining is used in many situations. There were some cases where ground freezing was also used.

Grouting is not only to control water inflow but since it reinforces the ground, it is also used to control instability of the face and walls of the tunnel during excavation.

Drainage ahead of the face is used very often in association with grouting in order to reduce water pressure and cross water bearing zones. This allows lowering the ground water around the tunnel face and, in combination with grouting, preventing a strong inflow of water through the tunnel, increasing the performing of the heading face, by improving its stability (Pelizza, 2005). Drainage deep wells from the surface can be also used to lower the groundwater level

In Seikan tunnel, in Japan (Project ID 88) four major water inflows occurred. In one case the tunnel works were restored by draining and performing grouting to stop the seepage of water (Figure 3.77)

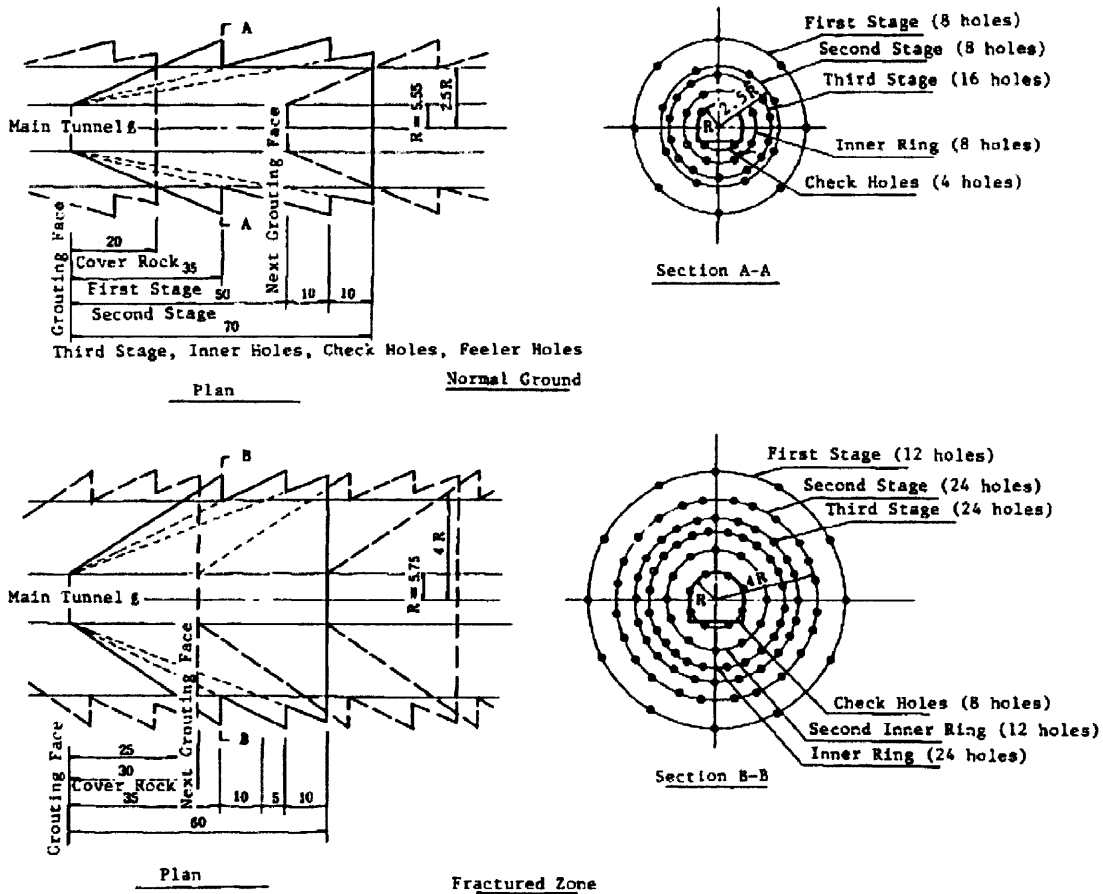


Figure 3.77 Grouting drilling patterns (Yoshimitsu and Takashi , 1986).

In the last major flooding event (May 1976) grouting was carried out in order to fill the void left by the collapse, which extended 75 m from the face. It was decided to construct a bypass tunnel 60m from the original route, on the opposite side of the main tunnel. By October 15, 1976, the bypass tunnel had reached a point beside the point of the water inflow; and, on January 31, 1977, the bypass tunnel rejoined the original route of the service tunnel at a point 148m ahead of the water inrushing point (Hashimoto, and Tanabe, 1986). Figure 3.78 shows the by-pass tunnel executed around the 4th flooding accident in the Seikan tunnel.



Along with remining or reprofiling of the section, modification of the support system is common. When the cause was squeezing ground yielding elements and compression slots can be used, as shown in Figure 3.79. The design consists normally of a slotted shotcrete membrane and yielding anchors that allow for radial displacements. After the displacements necessary to allow the formation of an arch in the ground the slots in the shotcrete will be closed and the anchors will be tied in. The remaining loads can be then taken by the support without failure.

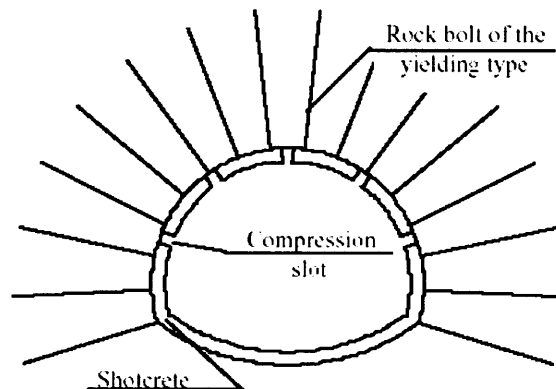


Figure 3.79 Cross section of a tunnel with compression slots applied in squeezing ground conditions (Schubert , 1996)

Swelling is another possible cause for excessive deformation. During the construction of the Bypass Sissach, N2 Chienberg tunnel (Project ID 71), when construction was stopped due to a collapse, the invert was left open. After 4 weeks a heave of 1.5m was observed in the invert near (behind) the zone of the collapse. The fact that the ground consisted of swelling rock and the lining was not closed and therefore there was not counteraction to the heave, plus the direct access to surface water that could enter the tunnel through the crater caused by the collapse, caused the excessive deformation (heave) of the invert (Figure 3.80). The mitigation measures consisted on the construction of a deformable invert, shown in Figure 3.81 (SchweizerBauJournal, 2004; private correspondence).



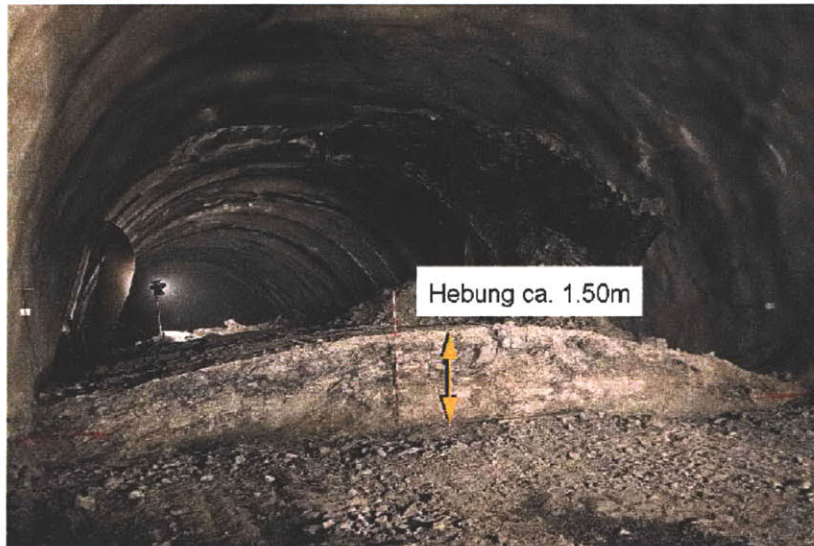


Figure 3.80 Invert heave at Chienberg tunnel (Chienbergtunnel, N2 Umfahrung Sissach, private correspondence)

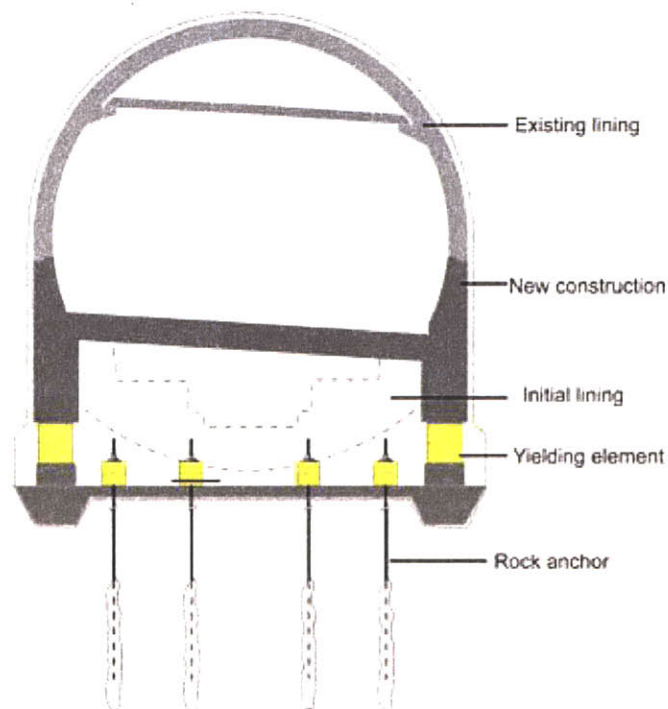


Figure 3.81 Deformable invert at Chienberg tunnel (Private correspondence)

Another swelling case is the Naples Aqueduct (Project ID 22), tunnel from Rotarelle to San Vittore, in Italy, presented in Section 3.2.3 (Figure 3.29). In order to complete the tunnel safely the the construction method was changed from sequential excavation with

roadheaders to a non shielded TBM with expanded precast segmental concrete lining. A Shielded TBM would not be suitable due to the risk of the TBM become trapped by the swelling ground.

The German firm Bade & Theelen was commissioned to develop the machine. The result was a 34 m long open face, non-shield TBM with a blade type ripping and loading shovel erector boom (Figure 3.82). The lining comprises 6 precast concrete segments (50 cm wide x 50 cm thick). The TBM was launched from the opposite end of the failed roadheader excavation.

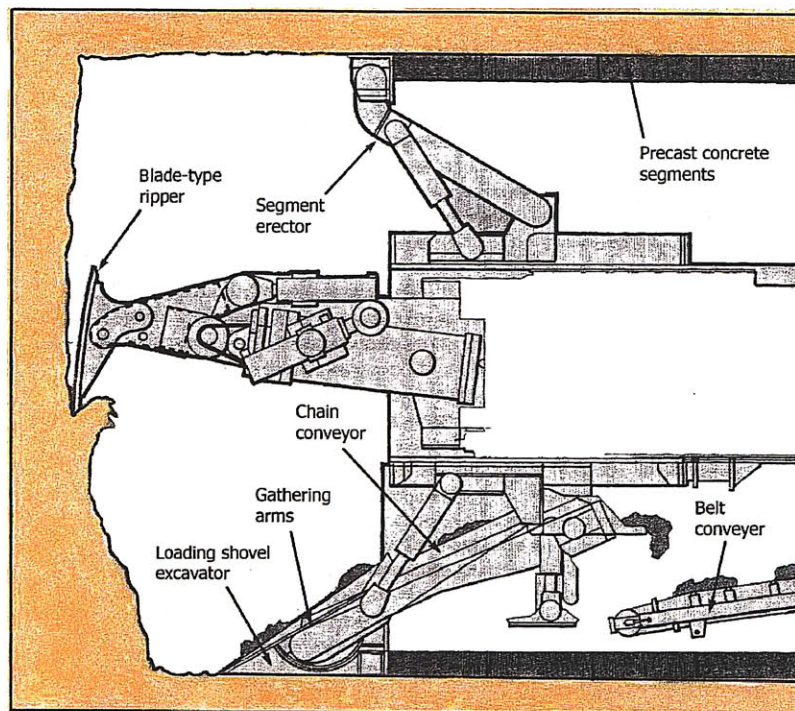


Figure 3.82 Non-shielded TBM with expanded pre-cast concrete ring segments used in the tunnel from Rotarelle and San Vittore part of the Naples Aqueduct project (Wallis, 1991)

### Particular Locations

The mitigation and remedial measures applied in collapses in particular locations are similar to the ones discussed in the *Collapse / Heading collapse* section. The case of the

Hull wastewater flow transfer tunnel collapse (Project ID 26), described previously is in fact a shaft collapse.

There are however certain cases namely portal collapses that are due to slope failure. In such circumstances the measures taken consist of slope protection and support, like tiebacks or to cut back the slope to a stable geometry.

### **3.6 Important factors in tunneling**

The analysis of the Database cases allowed one to compile a list of main factors that interact and influence the behavior of tunnel construction. The next sections will present lists of ground parameters, construction parameters as well as variables that are observable during construction and that can give valuable information on the construction behavior. Later, influence diagrams relating these variables to each other and to the different undesirable events are presented.

#### **3.6.1 Ground parameters**

Table 3.5 shows a list of the ground parameters that most influence excavation and their relative relevance for the different type of events. The relation among them as well as how they influence each type of undesirable event is detailed in Section 3.6.4.

The type of ground is obviously important, since depending if it is soil, rock, mixed or even a more specific type of ground, such as one with tendency to swell or squeeze different events should be taken into consideration when designing and constructing a tunnel.

The existence of groundwater can seriously affect the stability of a tunnel, so it is, of course, a variable to consider, in the form of pore pressure (including seepage pressures). Not only the presence of groundwater but also the permeability or fracture conductivity

are important variables, essential to characterize the hydrology (water flow patterns, preferred channels, etc) of the tunnel construction site.

When tunneling through rock, fracture characterization is essential (spacing, orientation, persistence as well as their filling) especially when considering the occurrence of unstable blocks.

Weathering is also extremely relevant. Not only it is necessary to characterize the degree of weathering, since this will govern parameters such as strength and permeability, but also its distribution at the face and along the tunnel alignment, will be of great importance regarding stability, deformability and to characterize the hydrogeology of the site, especially when driving the tunnel with EPBM machines in mixed conditions.

Crossing Fault zones are one of the major causes for collapses and delays. They are identified and characterized by their thickness, orientation in relation to the tunnel and filling material. Many times the fault zones are composed of materials of lower quality than the surrounding ground, other times of less permeable material, acting as a dam to ground water, so when the tunnel hits the fault it may be invaded by large quantities of material and water under pressure, causing flooding or collapse of the tunnel.

The presence of underground man-made structures is another cause of collapses. It is necessary to try to detect and chart old wells and other man made underground structures the best possible and proceed to treat the area surrounding them if necessary in order to avoid running into them and destabilizing the excavation resulting in a possible collapse.

The parameters listed in Table 3.5 and their influence, and role in each of the defined undesirable events will further detailed in Section 3.6.4.

Table 3.5 List of ground parameters and their influence

Ground parameters	Rock Fall	Collapse	Daylight collapse	Rockburst	Flooding / Water inflow	Excessive deformation
Type of ground	++	++	++	++	++	++
Water pressure	++	++	++	-	++	?
Overburden or H/D	-	-	++	++	-	++
Permeability / fracture conductivity	+	+	+	-	++	+
Weathering						
Degree	-	+	+	-	-	-
Distribution at face	-	++	++	-	-	-
Fractures						
Spacing	++	++	++	++	++	-
Orientation	++	+	+	-	-	?
Filling type	++	++	++	-	+	?
Persistence	++	+	+	+	?	?
Faults						
Thickness	-	+	+	-	+	+
Orientation	-	++	++	-	+	+
Material	-	++	++	-	+	++
Compressive strength of rock	-	-	-	++	-	-
Presence of underground man-made structures	-	+	+	-	+	-
Stress conditions (due to geological structures)	+	+	+	++	-	++
Mineral composition	-	-	-	-	+	++

++: high; + some; - low

### 3.6.2 Construction parameters

Table 3.6 shows the same information as the previous table but now regarding construction parameters, i.e. variables that are related to the construction process. Extremely important to understand the type of events that one can be facing during construction is to know the type of construction that will be used. Different construction



methods (combined with other ground parameters) will be susceptible to different risks. When excavating with conventional methods, parameters related to construction sequence and support system, such as round length, reinforcement measures, existence of pre-support, must be taken into consideration. Also whether or not drainage, and what type will be used before and during construction, as well as other methods to deal with ground water and water pressure such as grouting is important. When excavating with shield / TBM it is important to know the type of machine, i.e. which type of support does the machine provide, (none, peripheral or peripheral and face). Finally the dimensions and geometry of the tunnel, as well as its relation with the overburden, are important parameters when studying almost all the undesirable events.

Note that it is extremely difficult to enumerate all the parameters that influence the construction process. However Table 3.6 presents a list of what are considered to be the most relevant ones. Each project is unique and these listings should be adapted according to the project specificities.

### **3.6.3 Observable parameters**

Observable parameters are parameters that are often measured or monitored during construction. They give information on the ground crossed and, most importantly, on the behavior of the excavation. Table 3.7 shows a list of observable parameters, which are considered to be the most relevant ones. Each project is unique and these listings should be adapted according to its specificities.

Table 3.6 List of construction parameters and their influence

Construction parameters	Rock Fall	Collapse	Daylight collapse	Rockburst	Flooding / Water inflow	Excessive deformation
For NATM / Drill and Blast:						
<ul style="list-style-type: none"> <li>• Round length</li> <li>• Full face excavation / partial excavation</li> </ul>	- -	++ ++	++ ++	++ -	- -	
For TBM:						
Type of machine (EPB, slurry, etc)	++ N/A	++ ++	++ ++	+ ?	+ ++	+ ++
• Operation mode						
For all Construction methods:						
Pre- support measures (such forepoling, glass fiber bolts, etc)	+	++	++	++	+	++
Drainage (from the surface, at the face, etc)	+	++	++	-	++	+
Support measures	++	++	++	++	-	++
Geometry and Dimensions	+	+	+	++	-	+

++: high; + some; - low

Table 3.7 List of observable parameters and their influence

Observable parameters	Rock Fall	Collapse	Daylight collapse	Rockburst	Flooding / Water inflow	Excessive deformation
TBM:						
Earth / slurry pressure	-	++	++	-	++	+
Penetration rate	-	+	+	+	-	+
Torque	-	-	-	-	-	-
Injected grout	-	+	+	-	+	-
Weight of excavated material	-	+	+	-	-	-
All excavation methods:						
Convergences	-	+	+	-	-	++
Deformations at surface	-	+	++	-	+	+
Piezometric level	-	+	+	-	++	-
Geology (face mapping)	++	++	++	++	+	+

++: high; + some; - low

### 3.6.4 Influence diagrams

When designing a tunnel it is essential to consider the different possible undesirable events that may occur during its construction. For that it is crucial to be aware of the conditions in which they may occur. The study of the different cases of the database made it possible to identify different scenarios, in which these events are most likely to occur. Influence diagrams, containing the parameters listed before, were built as a result of that.

## **Rock Fall**

Given the existence of a block there can be three kinematic possibilities: 1) block fall; 2) block slides and 3) block is stable. The block falls when it detaches from the roof without sliding due to gravity. Although the database shows no such case, they are in fact not that uncommon and responsible for fatalities during tunnel construction due to the unexpected nature of this event. There are two mechanisms for rock slide: 1a) the block slides on a discontinuity plane, i.e. planar failure. This is what happened during the construction of Holjebro hydroelectric power plant in Sweden, (Project ID 52), where a planar failure occurred on the sidewall along 35m length of the tunnel. The area where the failure occurred had been pre-supported but the support proved not to be sufficient. 1b). The block slides along a line of intersection, i.e. wedge failure. This is the case of the extension of the Harsprånget hydroelectric power plant in Norway (Project ID 51) during 1974-1982, through the execution of a new unlined tailrace tunnel, where while excavating the upper bench a rock slide occurred along 60 m of the tunnel.

Block falls and slides are normally caused by discontinuities in the ground such as fractures and faults. The orientation (between the discontinuities and the tunnel and between discontinuities themselves), the spacing, the persistence, as well as the thickness of the discontinuity and the filling material, and shear strength of the discontinuities, are extremely important factors in the determination of potential unstable wedges or blocks. The shape and dimensions of the tunnel itself will have some influence on the dimension and volume of the potential unstable blocks.

The stress state is also an important factor to consider in the evaluation of potential unstable rock blocks. The weight of the wedges is one of the main destabilizing forces. The presence of water and its pressure is normally an instability factor, as well, and it must be taken into consideration in the calculation of potential unstable blocks. The dashed arrows in Figure 3.83 show how the factors related to the rock structure (discontinuities), stress state, water flow and construction method relate to each other. The presence of the discontinuities influences the local stress field around it (principal

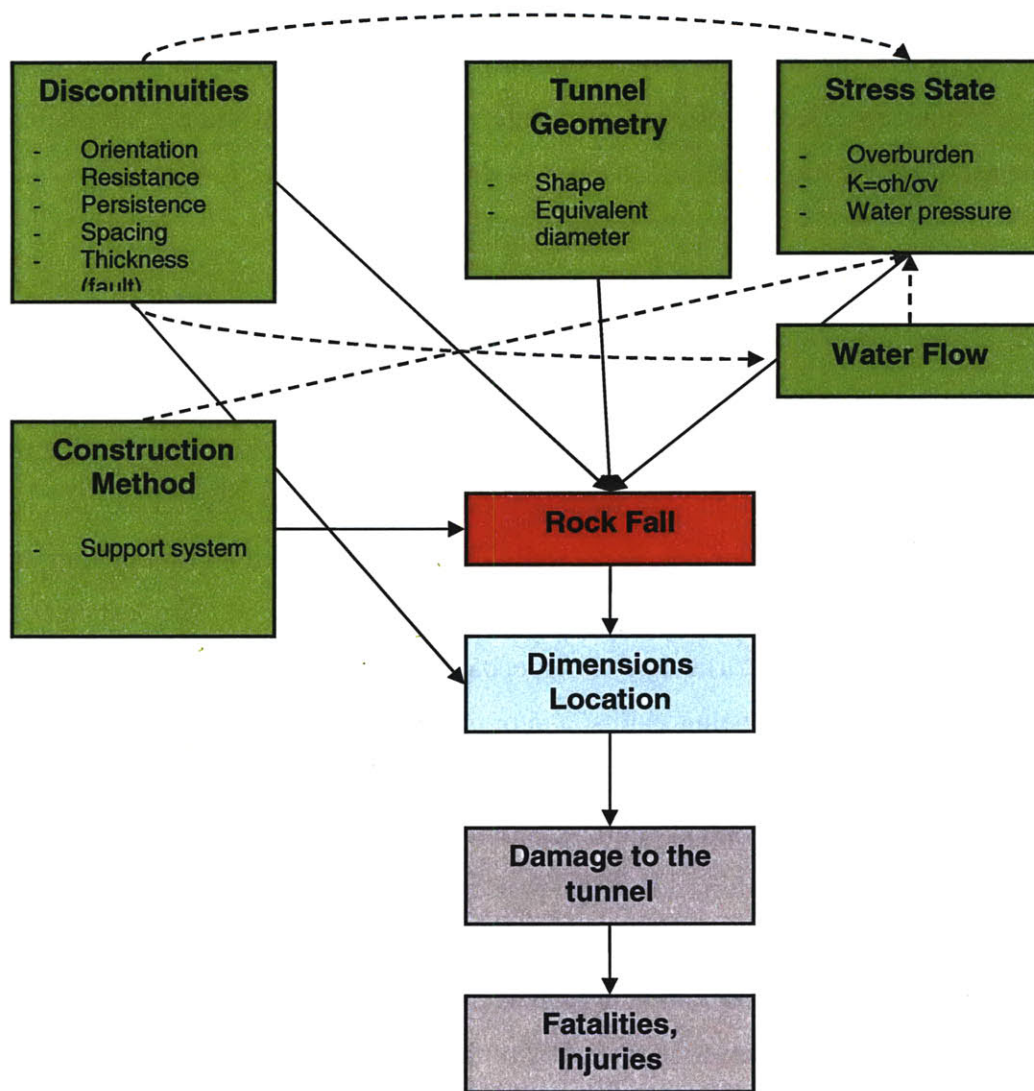
stresses and magnitude). The discontinuities affect the water flow, since they will dictate the permeability during construction. Also the presence of water / water flow will affect the effective stress state. Finally the support system used is extremely important. The existence of an adequate support system will prevent an unstable wedge to slide and cause damage to the tunnel and machinery, as well as injuries to the workers. If the construction method is drill and blasting, it will affect the rock stress around the excavation and lead fractures to open which may cause water flow to increase.

The combination of all the factors, previously described, will determine whether or not the rock fall will occur, as well as its volume and location regarding the tunnel. It can range from 0.5-1m<sup>3</sup> (Cross City tunnel (project ID 5) and M5 East Motorway (project ID 6), both in Australia) to 2000m<sup>3</sup> in a very extreme case such as the Cahora Bassa power scheme in Mozambique (project ID 50), where a wedge failure took place along the intersection line of the two inclined discontinuity planes and an upper boundary consisting of lamprophiric dyke.

Rock falls are difficult to predict with monitoring instrumentation such as convergence measurements, inclinometers, among others, since they are normally localized incidents. The best way to try to predict is in fact, careful mapping of the tunnel roof face and wall during construction. These comprises mapping of significant structural features in the roof, walls and face of the tunnel provide valuable information for estimating potential unstable wedges or blocks, that can form at the roof or walls of the tunnel. Potential unstable wedges or blocks should be stabilized by means of rockbolts and shotcrete/wire mesh. At each step of the excavation these evaluations of potential unstable wedges must be reassessed as new information becomes available. In the case of particularly large wedges detailed calculations of the factor of safety and support requirements must be carried out. To assess the risk, the potential unstable wedges, should be mapped out along with information on their weight, their possible failure mode(s) and factor of safety.

Figure 3.83 shows the influence diagram containing the factors that affect the likelihood of a rockfall as well as its consequences.





**Recommendations:**

**Design:** characterization of possible wedges

**Construction:** Face mapping; exploration ahead of the face.

**Monitoring:** Difficult to predict with monitoring instrumentation, such as convergence measuring, inclinometers, extensometers, etc.

Figure 3.83 Influence Diagram for Rock Fall

## **Rockburst**

Rockbursts are the result of brittle fracturing of the rock. They not only disrupt the construction process, they are as well a safety hazard to the workers, due mainly to the violence of the ejection of blocks, as well as their sharp shapes.

There are several mechanisms by which the rock fails, originating the rockburst. The main source mechanisms are according to Ortlepp and Stacey, 1994: strain bursting, buckling, face crushing, virgin shear in the rock mass and reactivated shear on existing faults and/or shear rupture on existing discontinuities. For the first three mechanisms, the source and damage locations are normally coincident--i.e., where the source occurs is normally where the damage occurs as well. These mechanisms, strain bursting, buckling and face crushing, are strongly influenced by stress concentration / stress state and by the shape of the excavation. The last two mechanisms, virgin shear in the rock mass and reactivated shear on existing faults and/or shear rupture on existing discontinuities, correspond to shear failure on a plane and can extend for several meters. They normally can occur in large scale mining operations. In civil works the most common phenomenon is strain bursting, although buckling and face crushing may also occur.

The most typical type of rockburst in tunnels is due to strain bursting (Ortlepp, 2001), the resulting fragments of rock consist usually of thin plates with sharp edges, that are violently ejected locally from the rock surface.

The location where the rockburst (ejection of fragments of rock) occurs normally depends on the in-situ stress and the geometry of the tunnel. In some cases (for example in Norway) the in-situ stress field is essentially related to the topography of the site. This is for example the case of the Laerdal tunnel in Norway (Project ID 61), where the vertical stress was high due to overburden reaching a maximum of 1450 m, but where the horizontal stress was also high, caused by the tectonics of the area. The rockburst can occur at the face of the tunnel or behind the face (i.e. once the face has passed) on the side walls and roof. A case of rockbursts occurring at the roof of the tunnel was a water

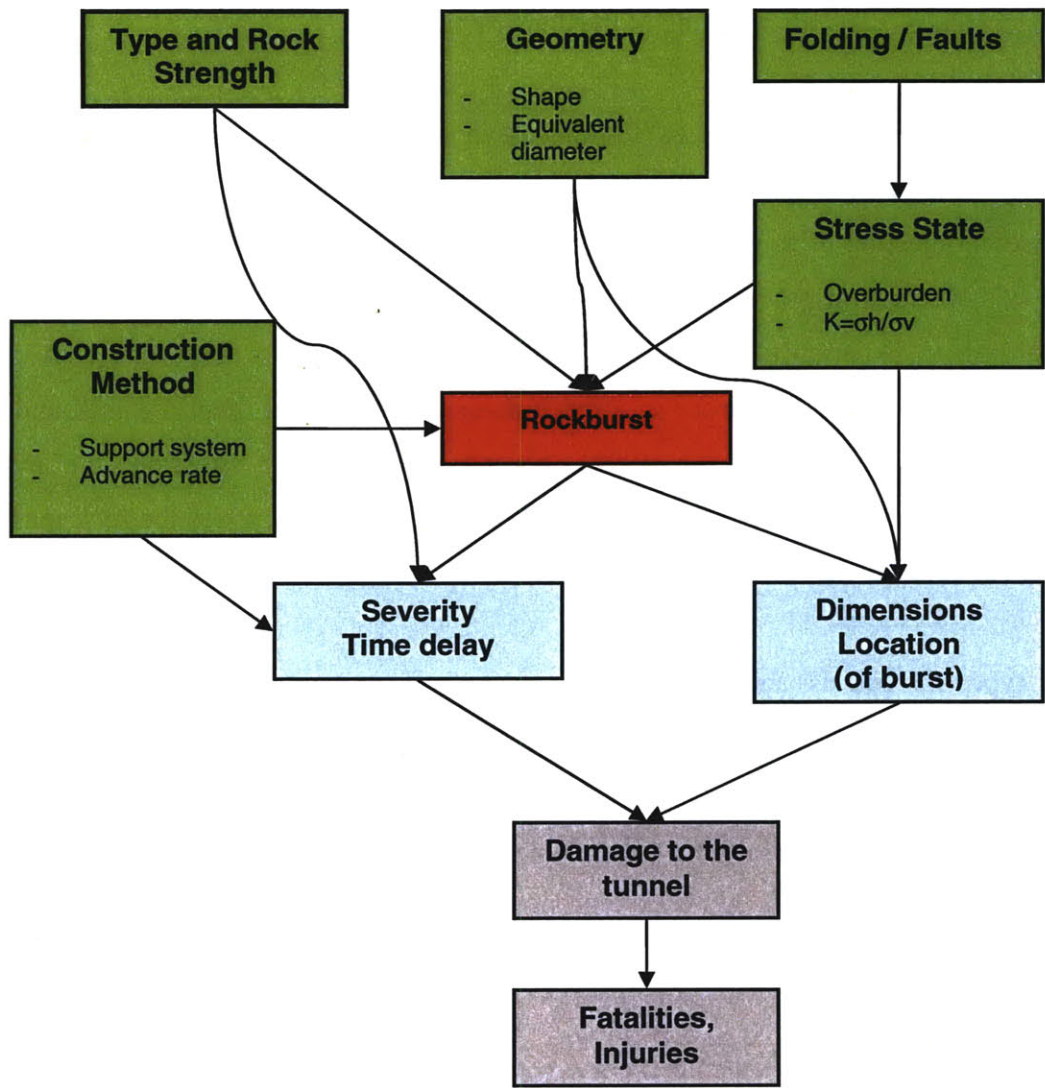
tunnel in Korea, project ID 123). A parameter that seems to influence the time delay of the occurrence is the advance rate of the construction.

The construction method seems to also have an influence on the behavior of the excavation in regards to rockburst. Not only the existence of a support system that stops the violent ejection of fragments of rock is essential to guarantee the safety, but also the type of construction process seems to have an effect on the severity of the rockburst. According to experience, for the same type of conditions, for the same rock, strain bursting is more likely to occur in a machine-excavated tunnel than in a drill-and-blast tunnel (Stacey and Thompson 1991), because in the latter situation, the induced fracturing in the rock around the tunnel caused by blasting, destresses the rock mass and creates conditions that are less prone to rockburst by strain bursting

The type of rock is another important factor affecting rockburst and its severity. Rockburst occurs more likely and with greater severity in brittle rocks.

Rock bursts are not easy to predict. Investigations using acoustic emission monitoring are sometimes recommended. Acoustic emissions allow one to monitor the accumulation of cracking and evaluate the tendency for the rock to suffer rockburst.

There are studies where seismic energy release data, geotectural data and in-situ stress measurements are collected and were then used with the goal of detect and reduce rockbursts. The goal is to use data to develop a methodology to actively map and forecast potentially hazardous stress concentrations and thus improve mining and tunneling operations and safety (INEEL, url: <http://www.inl.gov/factsheets/industrial/rockburst-modeling.pdf>).



**Recommendations:**

**Construction:** Face mapping; characterization of rock mass; destress blasting and special bolts.

**Monitoring:** Acoustic emissions (to establish risk index, map hazardous zones)

Figure 3.84 Influence Diagram for Rockburst

## **Water Inflow / Flooding**

The impact of ground water on tunnel construction can be considerable. It will influence the design, the choice of construction methods and the construction process itself. In addition to this, excessive water inflow can lead and has led to serious problems during construction, requiring substantial changes in design and causing considerable delays, as well as financial loss.

It was during the construction of underwater tunnels that the largest floodings have occurred (Seikan tunnel, cases 116-119). The ground under rivers, channels and bays is normally weak and under high water pressure (and constant supply of water) and therefore extreme safety measures and efficient protection against water inflow are normally required. Whether or not the tunnel is below a body of water and the magnitude of the water pressure are an important factor since the accessibility of water, as well as its pressure on the tunnel face and walls will determine what is the risk that water inflow can occur during construction.

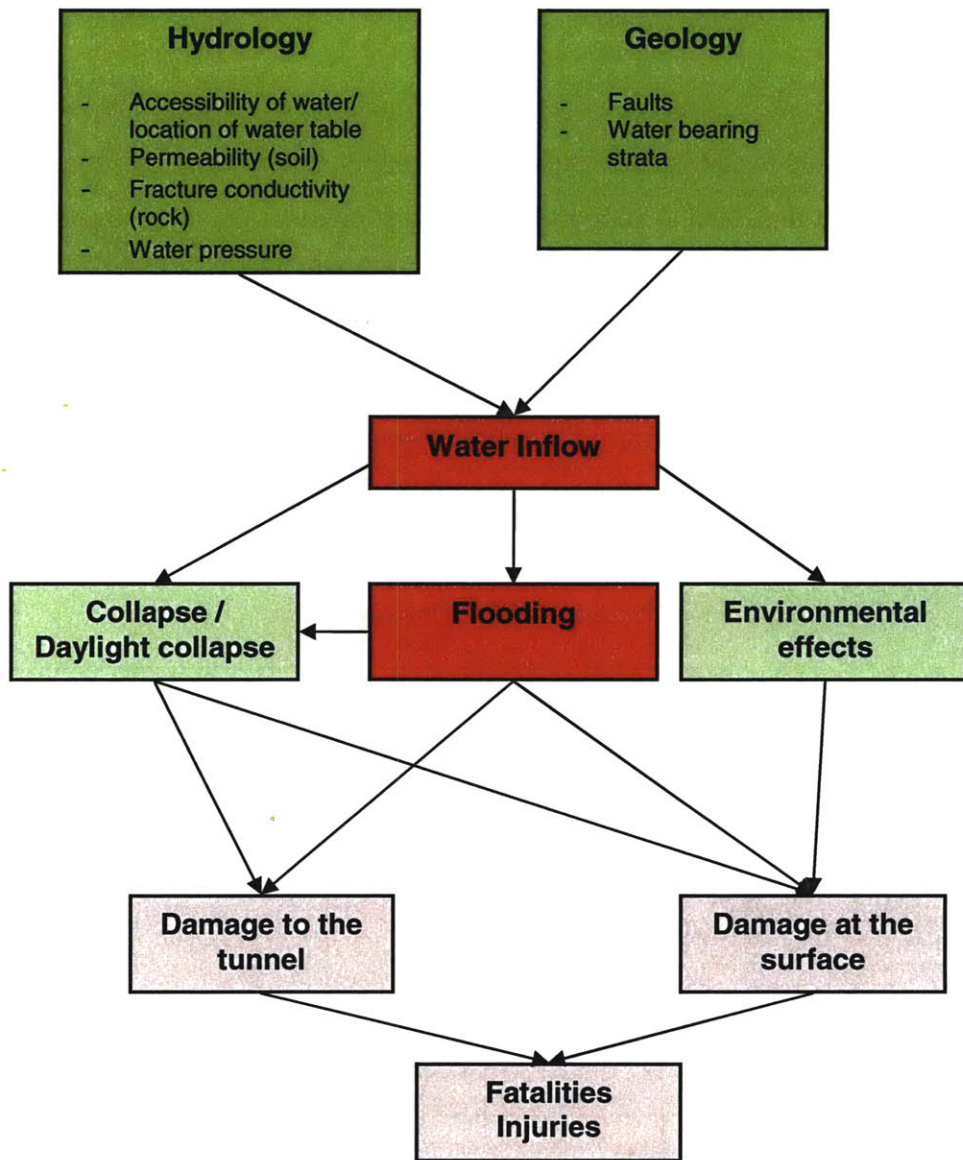
Gradual inflow of water is detrimental to the construction process, while the sudden inrush of water is a source of great danger, and many accidents have been caused by it. The sources of a sudden water inflow into the tunnels are faults, water bearing strata, caverns in karst formations. Therefore the hydrology and geology along the tunnel alignment, such as the presence of faults or water bearing strata, as well as the knowledge of the permeability (soil) and fracture conductivity (rock) are extremely important when studying the problem of water inflow, in order to design and choose construction and mitigation measures that are adequate for the encountered conditions.

Water inflow and presence of water during construction can lead to flooding of the tunnel, can cause instability and eventually collapse or daylight collapse of the tunnel and / or have adverse effects on the environment, due to lowering of the water table. An example where collapses occurred with flooding of the tunnel is the case of the Pinglin tunnels, in Taiwan (project ID 30). Several incidents occurred due to a combination of



fracture shear zone and highly pressurized water inflow. The collapses were larger due to the fact that the water washed the fine grained material into the excavation, burying the TBM. The 10th stoppage was the worst incident of the pilot tunnel, and caused the TBM to be totally buried requiring the construction of a bypass tunnel (see Figure 3.72)

Finally, water inflow is difficult to predict based on monitoring instrumentation results. However, exploration ahead of the face can be of great use in the identification of faults and water bearing strata. The most common mitigation measure for the problem of water inflow is to pre-treat the ground with grouting or/ and drainage. There were some cases where ground freezing was also used (see Section 3.5 for more details on mitigation measures for water inflow).



**Recommendations:**

**Construction:** exploration ahead of the face; ground treatment with grout or/and drainage.

**Monitoring:** Difficult to predict with monitoring

Figure 3.85 Influence Diagram for Excessive water inflow / Flooding

## Excessive Deformation

One of the main causes of excessive deformation is crossing fault zones composed of squeezing and weak strata. Squeezing ground is characterized by excessive ground pressure that may lead to support failure and sometimes even cause collapse. It generally occurs around the whole cross section frequently involving the invert as well. The development of both rock pressure and rock deformations is time dependent. Empirical data suggest that low strength, high deformability and the presence of water pressure facilitate squeezing (Kovari, K. 1996). Figure 3.86 shows the type of rock prone to develop this type of behavior as well as the range of overburden conditions. As one can see squeezing behavior occurred mostly in high overburden.

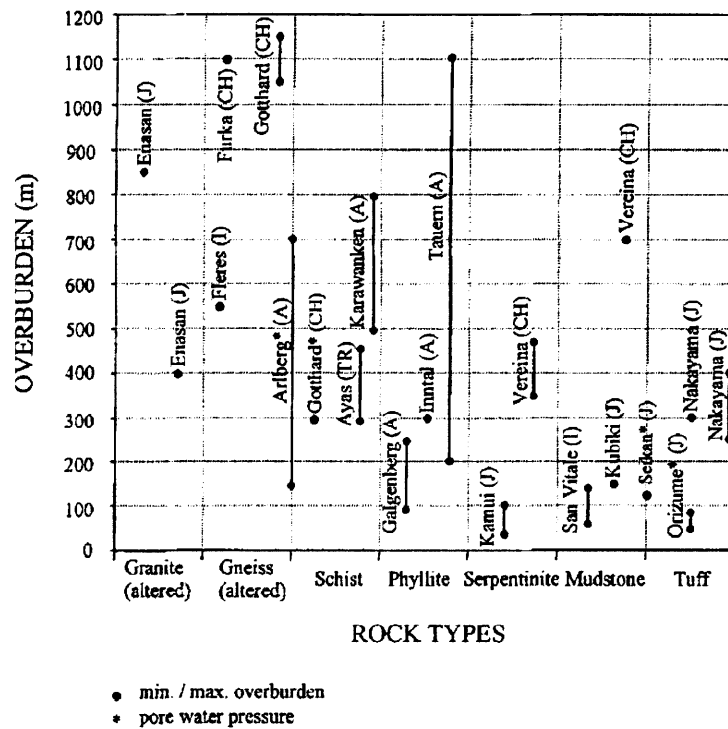


Figure 3.86 Case studies of tunnels with squeezing sections (Kovari, 1996)

During construction one strategy can be probing ahead of the face. If for example a fault (composed of squeezing ground) is anticipated and an adequate strategy is developed, normally the squeezing problems can usually be overcome (Hoek, 2001).

Depending on the construction method used the consequences of excessive deformation will be different as well as the mitigation measures that can be used to address this situation. If the tunnel is excavated by conventional means the excessive excavation will usually cause failure and damage to the primary support, requiring re-excavation to the original tunnel profile (due to the reduction in cross-section) and replacement of the support in the affected section. The support options for tunnel in squeezing ground go from rock bolts (minor squeezing) to shotcrete with longitudinal slots (severe squeezing).

In the case of mechanized tunneling with a shield or TBM, a possible consequence is for the machine to get trapped during the drive, which in the worst case can lead to abandonment of the TBM.

Another possible cause to excessive deformation is swelling. This phenomenon in tunnels is described as a time dependent volume increase of the ground, leading to inward movement of the tunnel perimeter. Three types of mechanisms have been identified (Einstein, 1996):

- i) 'Mechanical' swelling, which is what occurs in most clays, silty clays, clayey silts and corresponding rocks, caused by the dissipation of negative excess pore pressure.
- ii) 'Osmotic' swelling which occurs in clays or clayey (argillaceous) rocks. It is related to the double layer effect.
- iii) 'Intra crystalline' swelling/hydration which occurs in occurs in smectite and mixed layer clays, in anhydrite and in pyrite and marcasite. The mechanisms involved depend on the type of material. For more details see Einstein, 1996,

Common to all three mechanisms is the important role of pore pressure in the phenomena of swelling. In order to predict the behavior of a tunnel on swelling or squeezing ground, it is necessary to know the natural stress state, stress changes, ground water conditions and material properties. In order to be able to make adequate predictions regarding this type of behavior, the engineer should perform several tests that will allow him to identify

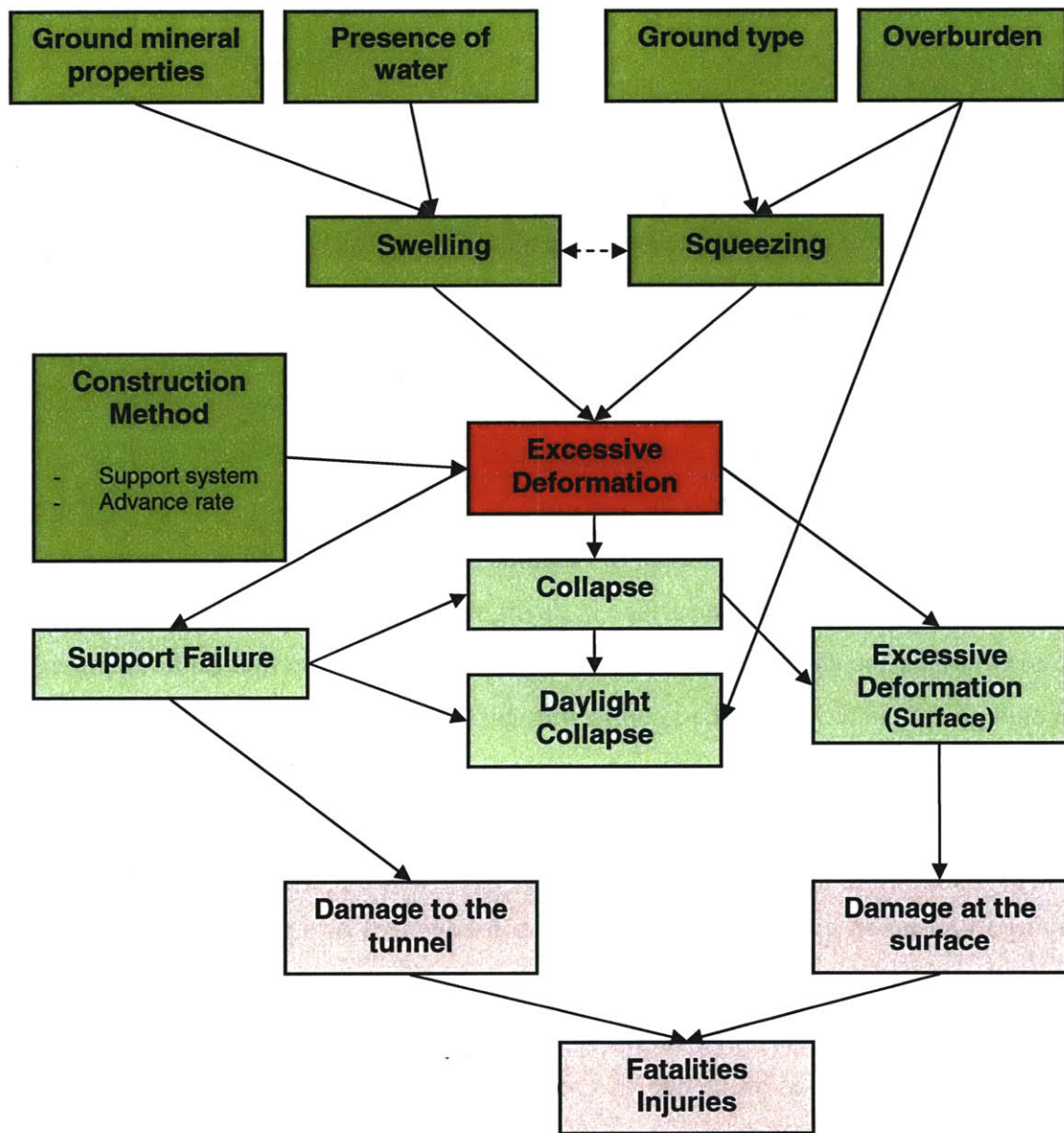
and quantify the swelling properties of the ground (see Einstein, 1996; Barla, 2008). However, due to interaction of different mechanisms, it is not always very easy to predict the amount of swelling that may occur. Swelling occurs mostly in the tunnel invert, and can develop more or less rapidly depending on the access of water to the excavation. A case of swelling that occurred during tunnel construction is the one of the Chienberg tunnel in Switzerland (project ID 71), where during the time that the tunnel construction was stopped due to a previous collapse, the invert was left open. After 4 weeks a heave of 1.5m was observed in the invert near (behind) the zone of the collapse.

The support systems available for this type of situation (swelling ground) range from the use of yielding support (yielding principle) allowing controlled amount of deformation to reinforced concrete with or anchoring system (resisting principle), designed to resist the load created by the swelling. In a case in Italy for a tunnel for the Naples Aqueduct (case 024), a non shielded TBM with expanded precast segmental concrete lining was used in order to deal with the swelling properties of the ground.

Squeezing and Swelling can often occur in combination. The effects of swelling and/ or squeezing can be monitored by means of leveling and convergence measurements, as well as other instruments used to measure ground deformation, such as implementers and extensometers. In order to access the stress or loading in the tunnel lining, load cells or strain gauges, among others can be used.

Finally a more extreme consequence of excessive deformation in tunnels is the partial or total collapse of a tunnel, which was the case in the Gotthard base tunnel (Project ID 97) in Switzerland, where a partial collapse occurred due to squeezing.





**Recommendations:**

**Construction:** yielding support, lining with longitudinal slots to allow excessive deformation, among others. Also rigid support in some cases

**Monitoring:** Convergences, Inclometers, Extensometers, strain gages, load cells etc.

Figure 3.87 Influence Diagram for Excessive Deformation (inside tunnel)

## **Collapse / Daylight Collapse**

The main “reported” cause of collapse and daylight collapses is unpredicted geology, i.e. geology that has not been predicted during the design phase. In most of the cases this corresponded to weak zones and fault zones, or karstic features. They can also be a consequence of excessive deformation and excessive water inflow.

The construction method used is of great importance. Different construction methods lead to different consequences and thus risk. According to the results of the database collapses/ daylight collapses in tunnels excavated by conventional means tend to involve on average greater volumes than the ones driven by shield or TBM. Obviously there are also other factors that will determine the volume of ground involved in collapses, as well as the shape of the crater at the surface in daylight collapses, such as the type of ground , the overburden, the shape and dimensions of the tunnel cross section (although there are not enough data in the database to confirming this).

The overburden is a very important parameter. The lower the overburden the more likely is that the collapse reaches the surface. This is extremely important especially when driving in an urban environment, where the consequences of a daylight collapse can be extremely severe.

Many cases of collapses were due to crossing of faults or weak zones, as mentioned before, examples are the collapses that occurred in Kurtkullagi irrigation tunnel in Turkey (project ID 12) , where 4 collapses (2 of them reaching the surface) occurred when the tunnel crossed an oversaturated clayey fault zone. Other examples are the Pinglin tunnels (project ID 30), mentioned previously, the Evino-Morno tunnel in Greece (project ID 49) where a collapse occurred when the TBM ran into a very disturbed flisch zone or the Shisanling pumped storage power station in China (project ID 54) where 3 large scale collapses occurred when the penstock tunnel was crossing a fault zones. Sometimes, hitting a water bearing layer that was not predicted during the design phase will cause a collapse, such as what occurred during the construction of the Lausanne metro (project

ID 2), when the tunnel excavation ran into a pocket in the glacial moraine filled with water. In the Wienerwald Railway tunnel – Eastern section (project ID 7), deformations and water pressure behind the lining resulted in the collapse of the side wall. In the Karawanken tunnel (project ID 28), a combination of running into a fault and water ingress that destabilized the ground caused a huge collapse of the crown at the face .

The presence of other man made structures is an important factor to take into consideration in the design phase. In case of old wells and galleries it is important to have them charted as best as possible, in order to avoid running into them and possible destabilizing the excavation, causing a collapse. This is what happened in the first collapse that occurred in the Porto metro (project ID 9) construction when the TBM hit a old well causing a collapse. Another collapse caused by man made structures is the Istanbul metro (project ID 14), which involved an uncharted well. (1.5m diameter to about 12 m deep), located almost exactly above the place where the liquefied mud had flowed into the tunnel. It can be assumed that there was only about 1.5-2.0m between the well bottom and the tunnel crown and that the saturated clay and well water flowed into the tunnel, causing the well walls and surrounding clay to collapse. This allowed a fine-grained sand layer to drain into the resulting cavity. In the case other structures already built in the ground, it is necessary to consider their effect on the excavation of the new structure and vice versa. In the case of the Olivais station of the Lisbon metro (project ID 10), Portugal, a daylight collapse occurred in December 1996; one of the errors during construction that ultimately contributed to the daylight collapse was that a pre existing large technical tunnel located near the metro tunnel was not considered.

In some of the cases described (project ID 7, project ID 97) previously, excessive deformation among other causes led to a total or partial collapse of the tunnel lining. Excessive deformation of the lining can reach certain values that will result in the failure of the lining and eventually led to a partial or total collapse.

In order to avoid these incidents it is extremely important to characterize any possible occurrence of faults, weak zones, water bearing pockets, karst zones, during the design

phase through careful survey plans. During construction it is crucial to monitor the behavior of the excavation, compare it with the one predicted in the design phase and adjust the construction if the behavior of the excavation is different from what was predicted. Surveying the face, walls and crown should be done in order to anticipate any adverse geological feature. The encountered geology should be compared with the predicted one and the support system and construction method should be changed to adapt to encountered ground conditions.

The most common probing method for TBMs and conventional excavation methods are presented in Figure 3.88. They can be classified into two main groups: Direct and Indirect exploration. Direct explorations are normally made by advance borings, which can be done with or without core recovery to investigate the ground mass quality, the position of a weak or critical zone, the presence of groundwater, boundaries between formations, location and extent of fault zones, etc. Advance boring can be combined with geophysical methods in order to obtain more comprehensive results. Core borings are more expensive and take considerable more time than borings without core recovery, although they provide more information. The length of the borings is normally around 100 m, however this depends on the geological situation. Exploratory adits are a more reliable source of information than the boreholes however they are more expensive and take considerably more time. The location of the adit varies with each particular case. It can be located inside or outside the cross-section of the final tunnel cross section (Figure 3.89 and Figure 3.90).

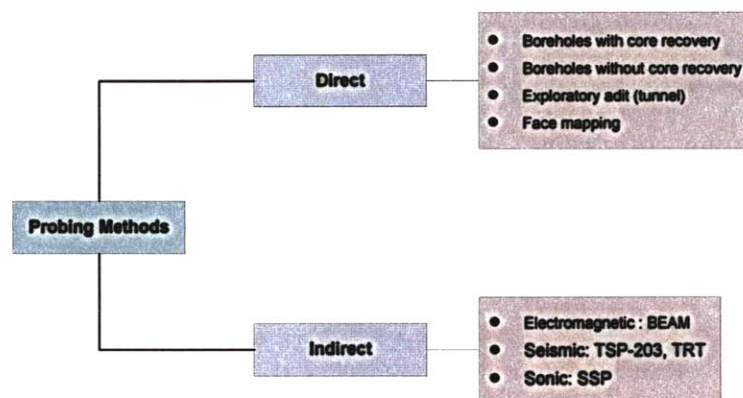


Figure 3.88 Probing methods



Indirect probing consists on using geophysical methods which, can be divided into three main groups: Electromagnetic, Seismic and Sonic. The most common electromagnetic method is the BEAM (Bore-Tunnelling Electrical Ahead Monitoring). This is a system based on the induced polarization measurements using the TBM head as an electrode. Currents of a defined frequency are induced that generate a high density current zone ahead of the TBM. The percentage frequency effect (PFE) and resistivity (R) are the base for the geological and hydrological of the BEAM predictions. The PFE characterizes the ability of the ground to store electrical energy and can be correlated to the effective porosity. The resistivity gives information on fracture and cavity fillings. This method allows one to explore the ground conditions, about 3 diameters ahead of the face while the tunnel is being driven (Galera & Pescador, 2005).

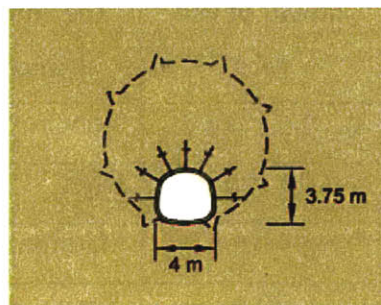


Figure 3.89 Exploratory adit located inside the final tunnel cross section

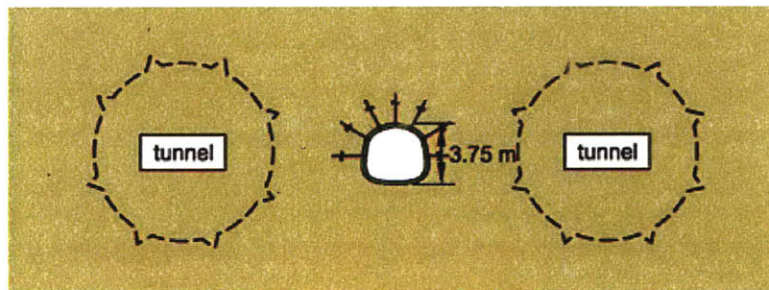


Figure 3.90 Exploratory adit located outside the final tunnel cross section

TSP 203 (Tunnel Seismic Prediction) and TRT (Tunnel Reflection Tomography) are the most frequently used seismic methods. Similar to the BEAM system the TSP 203 allows one to detect boundaries between formations, faults and cavities ahead of the tunnel. The system does not require access to the tunnel face but it requires a period of 1h-1h30 to acquire the data. TRT provides a 3D image of elastic wave velocities which differs

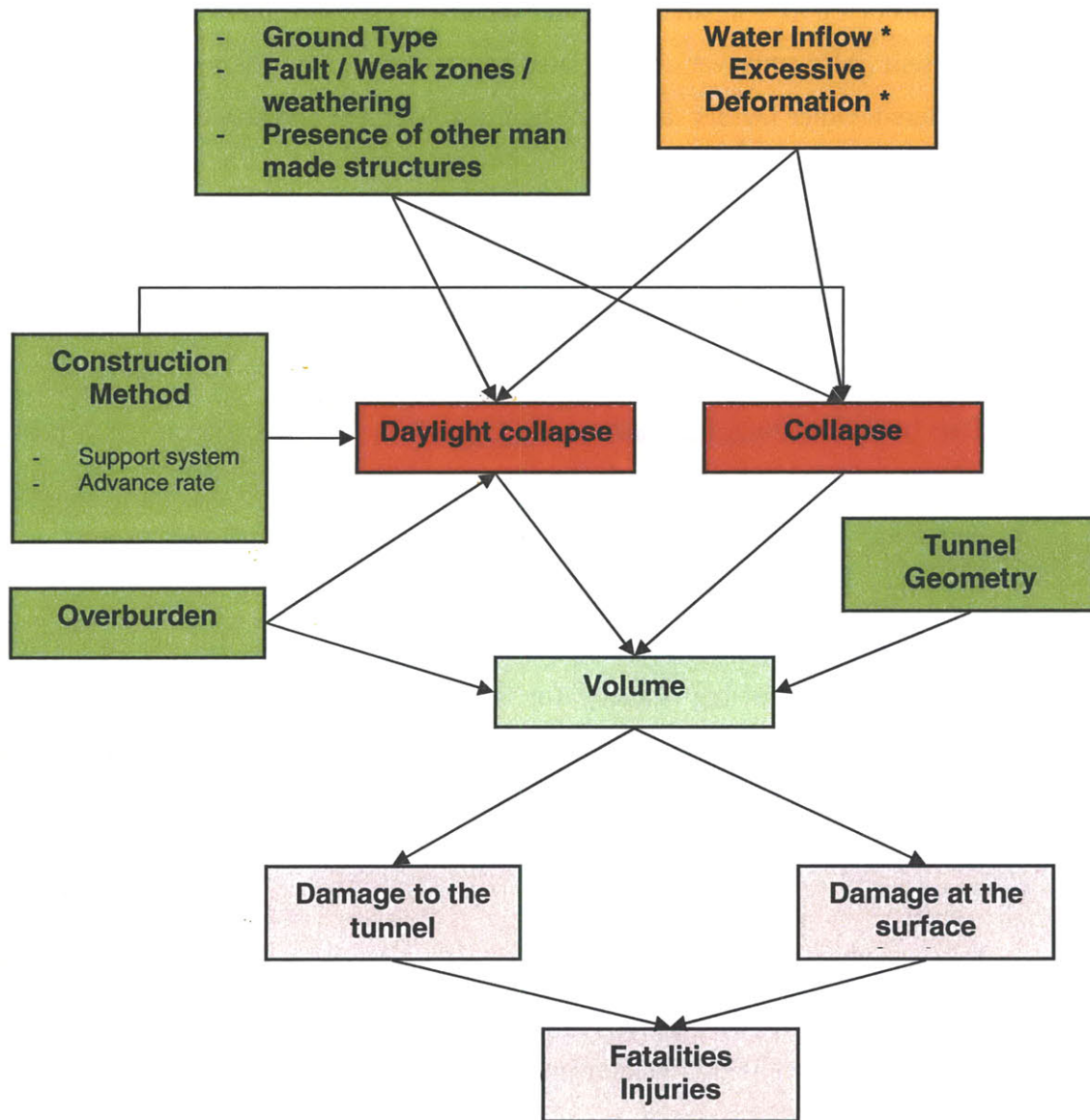


depending on presence of discontinuities and voids. This method requires the construction to be stopped for 20 minutes. Both methods require relatively long time for data processing.

The Sonic Softground Probing (SSP) detects changes in the density of the ground based on acoustic waves generated by geophones installed on the cutterhead. The velocity of the wave depends on the density of the medium through which it propagates, and it is therefore possible to detect variations in density due to faults, cavities, boulders, etc. It does not interfere with the advance of the TBM.

Table 3.8 Comparison between geophysical methods (adapted from Galera and Pescador, 2005)

<b>Method</b>	<b>Principle</b>	<b>Penetration ahead of the face</b>	<b>Interference with the construction procedure</b>	<b>Data Evaluation and Interpretation</b>
BEM	Electromagnetic	2.5 – 4 $\phi$	None	Medium
TSP-203	Seismic	10 – 20 $\phi$	High	Complex
TRT	Seismic	5 – 15 $\phi$	Medium	Complex
SSP	Sonic	30 $\phi$	None	Complex



\* These events are shown here as possible causes for Collapse/ Daylight collapse. For more details see their own influence diagrams, which are not shown in this figure for reasons of space.

Figure 3.91 Influence Diagram for Collapse and Daylight collapse

The influence diagrams (Figure 3.83 to Figure 3.91) intended to show which parameters in general influence the behavior of the excavation and the probability of a certain event. Note that this is not an exhaustive list of all the parameters and relations, since they are

mainly based on the information collected in the database. Each new tunnel project should be considered as a separate case and specific conditions, that were not listed here, may be present. Also only variables related to the ground and the type of construction were considered. Other factors such as design, management and construction errors were not included.

### **3.7 Lessons learned / Conclusions / Contributions**

- **Database:** Creation of a database of accidents (description of occurrence, possible causes and mechanisms, consequences and remedial measures) during construction available for designers, contractors, owners and experts in the tunneling domain.

Note: the database can be made available on the internet, for example through international tunneling society (or similar society), for members, with the possibility of addition of new cases and complementing of already existing. This should probably be done under the supervision of a moderator, to avoid false and erroneous entries.

- **Events:** The majority of events reported in the literature and by experts are collapses and daylight collapses, not because they are the most likely but because they are the ones with a greater impact on the construction process, the safety of the workers and people and structures at the surface. Daylight collapses in NATM are the events that involved a greater volume.
- **Causes:** There is not one single probable cause for an accident. They are normally the result of a chain of events and of multiple causes and errors. It was however possible to point out “typical” causes common to all events. They were divided into Internal and External causes. Common to many accidents described in the previous sections was the fact that the main reported causes were unpredicted geotechnical conditions (external cause), whether they consisted of faults zones

(and their extent), weak zones or groundwater presence. Thus, exploration during construction is important and necessary to explore ahead of the face, and sometimes also to the sides. Several techniques are available for probing and advancing exploration. The question is when and where to applied them.

- **Consequences:** Undesirable events have always consequences on the tunneling process, but many times they can also have consequences on the surface (people, traffic) and on other structures (other existing tunnels, utilities). These consequences can be catastrophic, especially in the case of daylight collapses in urban areas and in the most unfortunate cases can result in deaths.

In the past decade there have been a number of great losses involving tunnels in urban areas, which in some cases up to US\$ 100m. The delays associated with accidents were in average 6 months. Only in 7 cases the delays reported were over 12 months.

- **Mitigation and Remedial Measures:** The remedial methods used to overcome an accident and the mitigation measures used to ensure safe completion of tunnel excavation are very specific to each situation, however one was able to identify some methods that were commonly used, per event, in many of these situations.

- Accidents are still occurring and the losses associated have been in some cases been catastrophic, examples are the recent cases of the Sao Paulo Metro (Pinheiros Station) in Brazil and the Barcelona metro in Spain. There is still not a systematic way of considering these specific risks. This issue will be address in the next chapter with the introduction of a new methodology.

### 3.8 References

AlpTransit-Tagung (2004). "Fauchtagung für Untertagbau". D 0202. Band 3. 17 Juni 2004 in Interlaken.

Appleton, J. (1998) "Acidente nas Obras da Estação Olivais Sul do Metropolitano de Lisboa" (in Portuguese). Parecer n.º 241/PI. Conselho Superior das Obras Públicas.

Ayaydin, N., (2001) "Istanbul Metro collapse investigations", World Tunnelling.

Barla, M. (2008). "Numerical Simulation of the swelling behaviour around tunnels based on triaxial tests". Tunnelling and Underground 23 (2008) 508-521.

Barla G. (2000). "Lessons learnt from the excavation of a large diameter TBM tunnel in complex hydrogeological conditions". GeoEng 2000, International Conference on Geotechnical & Geological Engineering, Melbourne, Australia, 19-24 November 2000.

Barla G. and Pelizza S. (2000), "TBM tunneling in difficult ground conditions", GeoEng 2000, International Conference on Geotechnical & Geological Engineering, Melbourne, Australia, 19-24 November 2000.

Barton, N. (2008). "Summary of the main factors that caused the uniquely sudden collapse at Pinheiros". Presentation.

Barton, N. (2006). "Fault Zones and TBM. Geotechnical risk in rock tunnels", ed. Matos; Sousa; Kleberger and Pinto, Taylor and Francis, pp. 75-118

Broch, E. And Nilsen, B. (1977) "Comparison of Calculated, Measured and Observed Stresses at the Ortfjell Open Pit (Norway)". Norwegian Hard Rock Tunneling. Norway Tunneling Society. url: <http://www.tunnel.no/article.php?id=113&p=>

Brown, D.A. (2004). Hull wastewater flow transfer tunnel: recovery of tunnel collapse by ground freezing. Geotechnical Engineering 157 Issue GE2. April 2004. pp. 77-83



Chienbergtunnel (N2 Umfahrung Sissach). 9 pages , private correspondence.

Clayton, C. (2008). “The Heathrow Tunnel Collapse”. Advanced Course on Risk Management in Civil Engineering LNEC Lisbon November 17-22 2008.

Dalgıç, S (2002). “Tunneling in squeezing rock, the Bolu tunnel, Anatolian Motorway, Turkey”. Engineering Geology 67 (2002) 73–96.

Einstein, H.H. (2007). “Transalpine Tunnels in Switzerland“. MIT MEng Presentation.

Einstein, H.H. (2000). “Tunnels in, Opalinus Clayshale“. A Review of Case Histories and

Einstein, H. H. (1996). “Tunnelling in Difficult Ground - Swelling Behaviour and Identification of Swelling Rocks”. Rock Mech. Rock Engineering. (1996) 29 (3), 113-124

Engineering News Record (1989). “L.A. tunnelers overcome gassy soil”. ENR 1989 222 (23), pg. 38-43

Forrest, M. (2006). “Porto pressure”. Materials World July 2006 pp 31-33.

Friedrichsen G (1998). “Wos für ein Einbruch“. Der Spiegel Nr 19, Spiegel-Verlag, Hamburg.

Fukushima, H. (2002). “Examples of the tunnel portal collapse excavated in highly weathered granite”.

Galera J.M. and Pescador S. (2005), “Métodos geofísicos no destructivos para predecir el terreno por delante de las tuneladoras”, IV UN-ITA Workshop on “Gibraltar Strait crossing”, Madrid (in Spanish).

Ghasemi, H.; Cooper, J.; Imbsen, R.; Piskin, H, Imal, F. and Tiras, A. (2000). “The November 1999 Duzce Earthquake: Post Earthquake Investigation of the Structures on the TEM (Trans-European Motorway)”. Publication No. FHWA-RD 00-146. 26 pages

Gradori, R. et al. (1995). "Evinos-Mornos tunnel – Greece construction of a 30 km long hydraulic tunnel in less than three years under the most adverse geological conditions". 1995 RETC Proceedings.

Grasso et al. (2003) "Experience on Porto – EPB follow up". Tunnel and Tunnelling International, Dec 2003.

Grimstad, E. and Bhasin, R. (1999) "Rock support in hard rock tunnels under high stress". Norwegian Geotechnical Institute.

Grose, J. W. and Benton, L. (2005). "Hull wastewater flow transfer tunnel: tunnel collapse and causation investigation. Geotechnical Engineering 158 Issue GE4". October 2005. pp. 179-185.

Hashimoto, K. and Tanabe, Y. (1986). "Construction of the Seikan Undersea Tunnel--II. Execution of the Most Difficult Sections". Tunnelling and Underground Space Technology, Vol. 1, No. 3/4, pp. 373-379, 1986.

Health Safety of New Austrian (2006). "The risk to third parties from bored tunnelling in soft ground". HSE Books, 78 pages.

Health & Safety Executive (2000). "The collapse of NATM tunnels at Heathrow Airport – a report on the investigation", by the Health & Safety Executive, Sudbury, Suffolk, HSE Books.

Health Safety of New Austrian (1996). "Tunnelling Method (NATM) tunnels". A review of sprayed concrete lined tunnels with particular reference to London Clay. HSE Books, 1996.

Hoek, E. (2001). "Big Tunnels in Bad Rock". ASCE Journal of Geotechnical and Geoenvironmental Engineering Vol. 127, No. 9. September 2001, pages 726-740.

Inokuma, A. et al. (1994). "Studies on the present state and the mechanism of trouble occurrence in tunnel in Japan 1994". ITA Conference (Cairo) Tunnelling Ground Conditions pages 283-246, Balkema.

Japan Society of Civil Engineers (1996). "Japanese standard for shield tunneling". The third edition.

Kaiser, P. (1999). "Lessons learned for deep tunnelling from rockburts in Mining". GEAT'99 Switzerland.

Khoury, G. (2003). "Passive fire protection in tunnels". Concrete: Feb 2003. Vol. 37, Iss. 2; pg. 31, 6 pgs

Knights, M. (2006). "Are we managing the risks in tunnelling?". International Seminar on Tunnels and Underground Works. Lisbon 2006.

Kolymbas, D. (2005). "Tunnelling and Tunnel Mechanics". A Rational Approach to Tunnelling. Ed. Springer. 437 pages.

Kovari, K. and Descoedres, F. (2001). "Tunnelling Switzerland". Swiss Tunnelling Society, Bertelsmann Fachzeitschriften GmbH, Gütersloh/Germany.

Kovari, K. and Staus, J. (1996). "Basic Considerations on Tunnelling in Squeezing". Ground. Rock Mechanics and Rock Engineering, 29 (4), pp. 203-210.

Landrin et al. (2006). "ALOP/DSU coverage for tunneling risks?". The international Association of Engineering Insurers. 39<sup>th</sup> Annual Conference, Boston, 2006.

Lee, S.M., Park B.S., Lee, S.W. (2004). "Analysis of Rockbursts that have occurred in a waterway Tunnel in Korea". Int. J. Rock Mech. Min. Sci. Vol. 41, No. 3, SINOROCK 2004 Symposium.

Lechnitz, W. (1990). "Analysis of Collapses on Tunnel Construction Sites on the New Lines of the German Federal Railway". Tunnelling and Underground Space Technology,

Vol. 5, No. 3, pp. 199-203

Longo, S. (2006). "Análise e Gestão do Risco Geotécnico de Tuneis". 309 pp. Instituto Superior Técnico da Universidade Técnica de Lisboa. PhD Thesis.

Munich Re Group (2004). "Underground transportation systems. Chances and risks from the reinsurer's point of view". 69pp.

Ortlepp, W. D. (2001). "The behaviour of tunnels at great depth under large static and dynamic pressures". *Tunnelling and Underground Space Technology* 16 - 2001. pp 41-48

Ortlepp, W. D. and Stacey, T. R. (1994) "Rockburst Mechanisms in Tunnels and Shafts". *Tunnelling and Underground Space Technology*, Vol. 9, No. 1, pp. 59-65, 1994

Pelizza, S. and Peila, D. (2005). "TBM Tunnelling In Rock: Ground Probing and Treatments". *World Long Tunnels*, 2005.

Rocha, M. (1977). "Some Problems related to the rock mechanics of low strength material" (in Portuguese). *Journal Geotecnia*, no.18, pp. 3-27.

*SchweizerBauJournal. Tunnelbau.* 3/2004.

Seidenfuss, T. (2006). "Collapses in Tunnelling". Master Thesis, University of Stuttgart, EPFL and ITA.

Sousa, L.R. (2006). "Learning with accidents and damage associated to underground works". *Geotechnical Risk in Rock Tunnels*. Ed(s) Campos e Matos, A; Sousa, L.R.; Kleberger, J. Pinto, P., Francis & Taylor, 199p.

Stallmann, M. (2005) "Verbrüche im Tunnelbau Ursachen und Sanierung". *Diplomarbeit.Fachhochschule Hochschule Für Stuttgart Technik Stuttgart University Of Applied Sciences*. 122 pages.

*Tunnels and Tunnelling International*, October 2003. "Learning from the Laerdal tunnel".

Tunnels and Tunnelling International, August 2003

Tunnels and Tunnelling International, July 2003.

Tunnels and Tunnelling International. August 2000. "Heathrow collapse was organizational".

Tunnels and Tunnelling International. October 2000. "When Hull freezes over". pp. 16-17.

Tunnels and Tunnelling International, September 1999. "Laerdal collapse halts progress".

Tunnels and Tunnelling International, September 1999. "The world's longest road tunnel".

Tunnelling and Underground Space Technology, Vol. 15, No. 1, pp. 13-29, 2000. "New Developments".

Vlasov, S.N. et al. (2001). "Accidents in Transportation and Subway Tunnels. Construction to Operation". Russian Tunnelling Association. Elex-KM Publ. Ltd. Pagg.200. ISBN 5-93815-002-7.

Yoshimitsu Maru and Takashi Maeda (1986). "Construction of the Seikan General Scheme of Execution Undersea Tunnel—I". Tunnelling and Underground Space Technology, Vol. 1, No. 3/4, pp. 357-371, 1986.

Wallis, S. (1995). "NATM challenge at Montemor tunnel". Tunnels and Tunnelling International, Dec 1995, pp. 32-34.

Wallis, S. (1991) "Non-shielded TBM holds squeezing clay in check". Tunnels and Tunnelling International. January 1991. pp. 50-52

Wannick, H.(2006). "The Code of Practice for Risk Management of Tunnel Works Future Tunnelling Insurance from the Insurers" Point of View (Presentation). ITA Conference Seoul, April 25, 2006



Wittke, W. et al. (2007), "Stability Analysis and Design for Mechanized Tunneling". Geotechnical Engineering in Research and Practice WBI Print 6. Editor WBI Professor Dr.-Ing. W. Wittke, Beratende Ingenieure für Grundbau Und Felsbau GmbH, Aachen,Germany, 563 pages.

Wittke, W. et al. (2002) New Austrian Tunnelling Method (NATM), "Stability Analysis and Design". Geotechnical Engineering in Research and Practice WBI Print 6. Editor WBI Professor Dr.-Ing. W. Wittke, Beratende Ingenieure für Grundbau Und Felsbau GmbH, Aachen,Germany, 424 pages.

Weber, J. (1987). "Limits of shotcrete construction methods in urban railway tunneling". Tunnel 3/87. pp. 116-124.

### 3.9 Appendix A - MIT Tunnel Research Questionnaire

#### MIT Tunnel Research Questionnaire

H. Einstein – R. Sousa

#### 1. PROJECT INFORMATION

##### *1.1 General information*

Project Name:	Lausanne Metro M2
Client:	Metro Lausanne-Ouchy SA
Designer :	Several Designers (table attached)
Contractor:	Several contractors (table attached)
Location:	Lausanne / Switzerland
Start of construction:	Spring 2004
End of construction:	Fall 2008
Type of environment <sup>(1)</sup> :	Urban
Type of tunnel	Metro tunnel
Maps, Figures:	



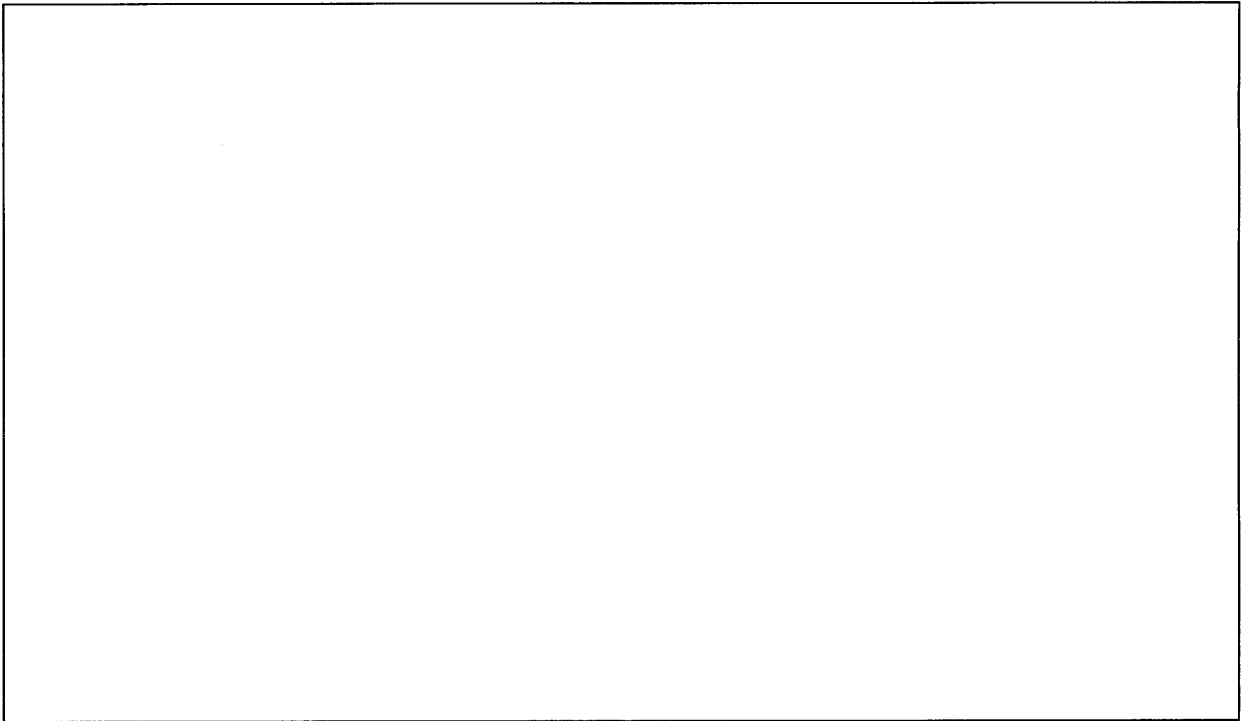
### 1.3 Geological and geotechnical information

Ground type :	Loose ground: Molasse, marls and sandstone
<p>Ground Description <sup>(2)</sup> :</p> <p>For rock mass:</p> <ul style="list-style-type: none"> <li>- Rock type</li> <li>- Discontinuities: pattern, spacing, persistence, orientation</li> <li>- Weathering</li> <li>- Strength</li> </ul> <p>For soil:</p> <ul style="list-style-type: none"> <li>- Soil classification (USCS)</li> <li>- Soil density</li> <li>- Geomechanical properties</li> <li>- ...</li> </ul>	
<p>Groundwater condition:</p> <ul style="list-style-type: none"> <li>- water pressure / level</li> <li>- “permeability”</li> <li>- freezing and thawing</li> </ul>	Ground is generally dry but sometimes saturated with water.
<p>Overburden:</p> <ul style="list-style-type: none"> <li>- maximum</li> <li>- minimum</li> <li>- predominant</li> </ul>	12 m on the area of the collapse.

### 1.4 Construction method

<p>Construction method type <sup>(3)</sup></p> <p>NATM / sequential excavation</p> <p>Drill and Blast</p> <ul style="list-style-type: none"> <li>- single heading</li> <li>- multiple headings</li> </ul> <p>Open face TBM</p> <ul style="list-style-type: none"> <li>- with gripper</li> <li>- with shield (single or double)</li> <li>- with shield and segments</li> </ul> <p>Closed face TBM</p> <ul style="list-style-type: none"> <li>- EPBS</li> <li>- Slurry shield</li> <li>- Compressed air</li> </ul> <p>Excavation with mechanical assistance</p>	<p>The section Flon-Croisettes consists of 2,884 metres of tunnels driven by underground means and 260 metres of cut-and-cover tunnels.</p> <p>The tunnelling method has required a fleet of two small roadheaders for tunnelling in top heading and bench sequence and five big roadheaders for full section tunnelling. Using top heading the crown is excavated before the bench.</p> <p>Almost all of the stations have been built with cut-and-cover method, except the Place de l'Ours and Bessières stations, which have been constructed in top heading and bench sequence. The Fourmi station quite close to the motorway A9 has been built from a shaft in a cavern excavated in divided sequence horizontally.</p> <p>All the spoil is mucked away by loaders and dumpers, and is reused in La Sallaz for landscaping purpose and stored at a dump site between Vennes and Croisettes. The support consists of 15-20 cm of steel fibre-reinforced shotcrete, HEB steel arches, lattice girders, Swellex and other bolts.</p>
<p>Construction method details <sup>(4)</sup>:</p> <ul style="list-style-type: none"> <li>- pre-support</li> <li>- face reinforcement</li> <li>- water inflow control</li> <li>- temporary invert</li> <li>- ground reinforcement</li> <li>- other relevant details</li> </ul>	

***1.5 Other relevant information / Comments***





## 2. ACCIDENT INFORMATION

### 2.1 General information

Date of the occurrence:	22 February 2005
Geomechanical characterization of the collapsed zone:	Section consisted of glacial moraine and molasse
Construction sequence in the collapsed zone:	<i>Subdivision of excavation:</i> Top heading/ bench or full section. <i>Primary support:</i> 15-20cm of steel reinforced concrete, HEB steel arches, lattice girders and Swellex.

### 2.2 Description of the occurrence

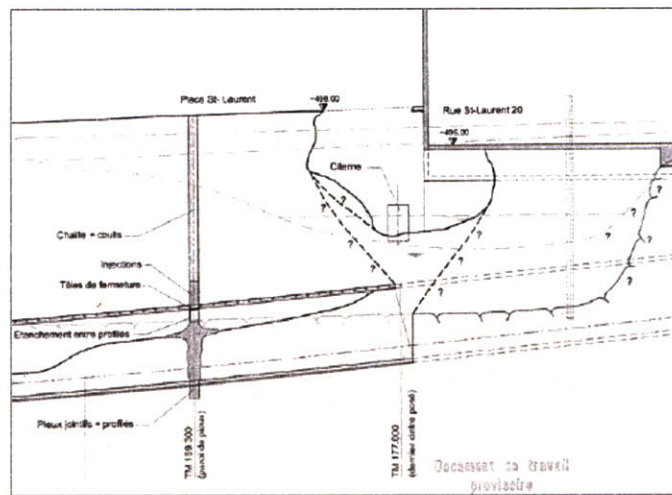
Type of the occurrence :	Daylight collapse		
Location of the occurrence :	Heading <input checked="" type="checkbox"/>	Invert <input type="checkbox"/>	
	Lining <input type="checkbox"/>	Other:	
Time of occurrence <sup>(5)</sup> :	The cave-in occurred on Tuesday at six o'clock in the evening. No work was being carried out in the tunnel. Investigation works were being carried out at the time of this incident. This work was underway following a previous inrush of groundwater from a pocket of glacial moraine.		
Description of the occurrence:	A tunnel collapse on Lot 1200 consisting of the 306 m-long Saint-Laurent tunnel between Flon and Riponne stations and the 272 m-long Viret tunnel between Riponne and Bessières stations displaced a huge amount of material – soil + water (1400m <sup>3</sup> ) into the tunnel and caused extensive damage as it cratered towards the surface in the busy St. Laurent's commercial district.		
Possible mechanisms (sketches or figures):			



Collapsed area at the surface



Aspect of the front after collapse  
(Ingress of soil and water)



Drawing of the collapse

Possible causes or errors:	The collapse was triggered by a pocket in the glacial moraine filled with water, that had not been predicted and therefore the support measures were adequate
Consequences :	Extensive damage at the surface. Delays (almost a year – 9 months) Urban disruption.
Could the occurrence have been avoided? If yes how?	
Mitigation measures <sup>(6)</sup> :	A curtain of eleven piles was drilled and concreted ahead of the collapsed face to consolidate the ground and limit the possible flow of further material into the tunnel, in conjunction with grouting. Roughly 800 m <sup>3</sup> of glass-sand

	were required to backfill up to the damaged buildings
References:	<p>Private correspondence with Dr. Zhao.</p> <p>Seidenfuß, T. (2006). "Collapses in Tunnelling". Master Thesis, 194 pp.</p> <p>Stallmann, M. (2005), "Verbrüche im Tunnelbau Ursachen und Sanierung " Master Thesis, Stuttgart University of Applied Sciences, 122 pp.</p>

- (1) Type of environment where the tunnel was constructed: urban, mountainous, rural or other
- (2) Provide information, when possible, on the following items.
- (3) Choose the construction method from the list. If the construction method used is not on the list please describe.
- (4) Provide details on the following items, if relevant.
- (5) Time of occurrence: when in the constructive process did the failure occur? : During excavation of the section heading? During the excavation of section invert? After excavation?
- (6) What measures were taken after the occurrence in order to ensure the successful completion of the project? Were they effective?

### 3.10 Appendix B – List of Experts

<b>Country</b>	<b>Name</b>
Austria	M John
Austria	R Pöttler
Austria	W Schubert
Austria	F Starjakob
Austria	H Wagner
Brazil	F Asis
Canada	P Kaiser
China	X T Feng
Germany	P Arz
Germany	M Stallmann
Portugal	C Dinis da Gama
Portugal	A Silva Cardoso
Portugal	L Ribeiro e Sousa
Russia	S Yufin
Switzerland	G. Anagnostou
Switzerland	Nutal Bischoff
Switzerland	Flavio Chiaverio
Switzerland	D.Hartmann
Switzerland	Zhao Jian
Switzerland	Walter Steiner
The Netherlands	Robert Hack
USA	Charles W. Daugherty
USA	Allen W. Hatheway
USA	Christopher Laughton
USA	Edward S. Plotkin
USA	Gerhard Sauer

### 3.11 Appendix C – Database Records Example

#### Example of a project record from the Database (Hull wastewater flow transfer tunnel)

1.1 General Information	
Project ID	26
Project Name	Hull wastewater flow transfer tunnel
Client	Yorkshire Water
Designer	Miller Civil Engineering (MCEL), now Morgan EST with design ARUP as project manager
Contractor	Miller Civil Engineering (MCEL), now Morgan EST
Location	United Kingdom
Start of construction	
End of construction	
Environment	Urban
Type of tunnel	Hydraulic
1.2 Dimensions	
Length	10500 m
Shape	Circular
Section dimensions	diameter 3.6m
1.3 Geological and geotechnical information	
Ground type	Soft Soil
Ground Description	<p>The majority of the tunnel was in glacial soils. The collapse, however, occurred in a relatively short length of tunnel in alluvium.</p> <p>Shaft T3 (where the accident occurred) was located in a channel formed by the former alignment of the River Hull indented in the glacial deposits. The channel had been filled with alluvial sand and gravel. Due to several phenomena the geology around the collapse was complex, layered with soils with highly variable permeability, strength and stand up time (Figure 2).</p>
Groundwater	
Overburden	
Minimum	
Maximum	
Predominant	
1.4. Construction method	
Type of construction	Closed face TBM
Construction details	<p>TBM EPBM</p> <p>The tunnel ring comprised six trapezoidal concrete segments, 250 mm thick. The rings were assembled with temporary bolts, which were removed once there was access beyond the rear of the 70 m long TBM train. At the location of the collapse the bolts had been removed four days prior to the collapse.</p> <p>Shaft T3 has a diameter of 7.5m and is composed of rings with twelve, 250mm thick precast concrete segments. The shaft was sunk as a caisson and the excavation was carried out under water. The soil at the connection shaft / tunnel was treated with jet-grouted columns and with continuous flight auger piles in order</p>



## Example of a project record from the Database (cont')

**1.5. Other Relevant Information / Comments**

**Comments**

The Hull wastewater flow transfer tunnel is part of the Hull Urban Wastewater Treatment Directive (UWWTD) Flow Transfer Works Contract. The scheme required the construction of a 10.5 km of 3.6 m internal diameter segmental tunnel alongside the north bank of the Humber estuary between West Hull Pumping Station and a new outfall at Saltend to the east of the city (Figure 1)

**Project Photos**

ImageID	ProjectID	txtImageName
▶ 59	26	E:\DatabaseNew\Images\26\fig1.jpg
60	26	E:\DatabaseNew\Images\26\fig2.jpg
* (AutoNumber)	26	

Record: 1 of 2

**Accidents**

Accident ID	Project ID	Date
▶ 28	26	16 Nov 1999
* 0	26	

One accident occurred during the construction of the Hull wastewater flow transfer tunnel (red circle in the picture above). The Project record stores the number of accidents that occurred during construction. The button *Accident(s) details* (in blue) links the user to the respective accident(s) records. The accident record of the Hull wastewater flow transfer tunnel is presented below.



# Accident record

1.1. General information	
Accident ID:	<input type="text" value="28"/>
Date	<input type="text" value="16 Nov 1999"/>
Geological conditions at the accident zone	<input style="width: 100%;" type="text" value="Alluvium. The overburden was 7.8 m."/>
Depth	<input type="text" value="Medium (2 &lt; H/D &lt;=50)"/>
Construction sequence at the accident zone	<input style="width: 100%;" type="text"/>
1.2. Description of the occurrence	
Type of occurrence	<input type="text" value="Daylight collapse"/>
Location	<input type="text" value="Shaft"/> Time: <input type="text" value="after heading passed the access"/>
Description	<p>During excavation between shaft T3 on the east side of Hul Marina and shaft T2, about 1145 m to the west, on the opposite side of the marina, a 100 m sector of the new tunnel collapsed (Figure 1).</p> <p>About two weeks earlier the tunnel boring machine (TBM) heading west had passed through the previously constructed 7.5 m diameter access shaft T3, having stopped in the shaft for about a week for essential maintenance to the cutter head. The centre of the collapse was within a few metres of the shaft, which was at that time about 203 m behind the face (Figure 2).</p>
Causes	<p>Extensive layers of uniform fine sand under considerable water pressure beneath the tunnel, and a leak large enough to admit sand particles.</p> <p>The leak was most likely caused by differential movement between the tunnel and an access shaft immediately adjacent to the seat of the collapse, a consequence of relatively compressible peat at the crown of the tunnel that was probably adversely affected by the stress relief of boring the tunnel.</p>
Errors	<input style="width: 100%;" type="text"/>
Possible Mechanism	<input style="width: 100%;" type="text"/>
Consequences	<p>No one was injured, but the remedial works took over a year to complete, and cost several tens of millions of pounds. A water main burst due to the collapse.</p> <p>Fortunately the area around the shaft was being used as a surface car park, so no major damage to structures occurred (see Figure 4). There were some vacant storage buildings to the south, but they suffered relatively little damage, limited to some cracking. Door openings were braced to protect against potential further settlement. Figure 5 shows the contours of settlement at the ground surface.</p>
Could it have been avoided? If yes, how?	<input style="width: 100%;" type="text"/>
Mitigation measures	<p>Within 24 h of the start of the collapse it was possible to stabilize the tunnel using compressed air. Air-lock doors that had been installed in the tunnel to allow compressed air access for cutter-head maintenance were used for this purpose. Twelve hours later the inflow of water had ceased. Later the compressed air was</p>

Photos

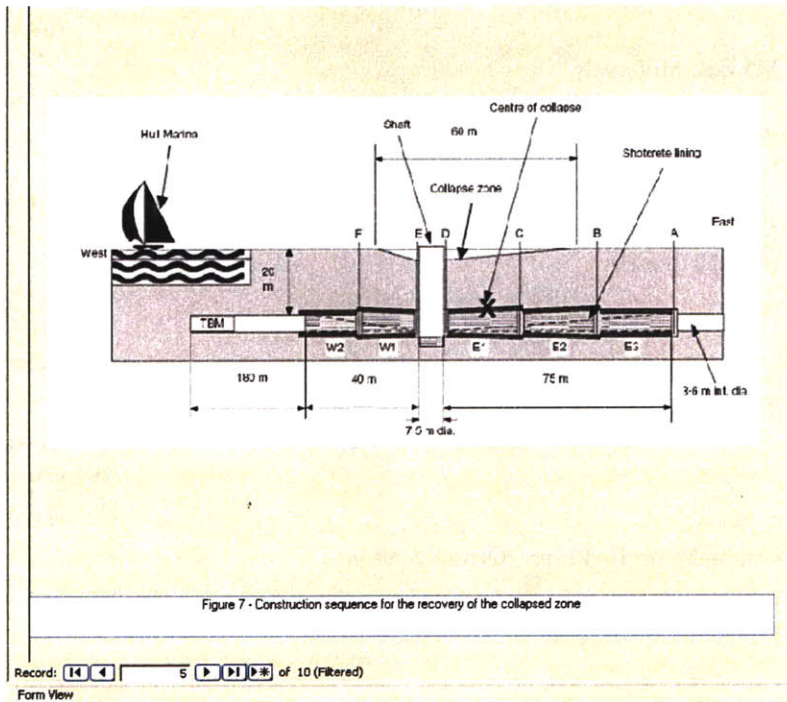
ImageID	AccidentI	txtImageName
57	26	E:\DatabaseNew\Images\26\fig3.jpg
58	26	E:\DatabaseNew\Images\26\fig4.bmp
59	26	E:\DatabaseNew\Images\26\fig5.jpg
60	26	E:\DatabaseNew\Images\26\fig6.jpg

Record: 14 of 10

References

[1] J.W. Grose and L. Benton. Hull wastewater flow transfer tunnel tunnel collapse and causation investigation. Geotechnical Engineering 158 Issue GE4, October 2005. pp. 179-185

The button Photos (circled in green) gives access to the photos related to the accident. Below is presented one of photos.



### 3.12 Appendix D – List of Accident cases

<b>ProjectID</b>	<b>Project Name</b>	<b>AccidentID</b>	<b>Type of Accident</b>
1	Goegglsbuch tunnel	1	Daylight collapse
2	Lausanne Metro Line M2	2	Daylight collapse
3	Tunnel Schulwald	3	Daylight collapse
4	NYC Water tunnel - Stage 1	4	Rock Fall
5	Cross City tunnel	5	Rock Fall
6	M5 East Motorway	6	Rock Fall
7	Wienerwald Railway Tunnel, section LT26/WT2/TF3 - Eastern Section	7	Side wall collapse
8	New Nuremberg-Ingolstadt Railway Line (Irlahüll tunnel)	130 8	Daylight collapse Excessive Deformation
9	Porto Metro (Line C)	9 10 11	Daylight collapse Collapse Daylight collapse
10	Lisbon Metro Red Line - Olivais Station	19	Daylight collapse
11	Montemor road tunnel	202 203	Daylight collapse Daylight collapse
12	Kurtkulagi irrigation tunnel	12 13 15 14	Daylight collapse Collapse Daylight collapse Collapse
13	High Voltage cable tunnel	201	Daylight collapse
14	Istanbul Metro - Phase 2	204	Daylight collapse
15	Playas Hydroelectric Scheme	125	Collapse

16	Wienerwald Railway Tunnel, section LT26/WT2/TF3 - Western Section	190	Flooding
17	Juktan hydro power plant	17	Rock Fall
18	Aalensund Fjord tunnels	16	Collapse
19	Galgenberg tunnel	18	Collapse
21	Maria Maluf road tunnel	20	Large inflow of water
22	Naples Aqueduct - tunnel from Rotarelle and San Vittore	21	Collapse
24	Heathrow Express	22	Collapse
25	Portsmouth and Havant Wastewater Flow Transfer Tunnel	25	Daylight collapse
26	Hull wastewater flow transfer tunnel	24	Excessive Deformation
27	Liyama tunnel	26	Daylight collapse
28	Karawanken tunnel	27	Excessive Deformation
29	Barcelona line 5	28	Daylight collapse
30	Pinglin (Hsuehshan) tunnels	29	Collapse
31	Athens Metro (Line 2 - tunnel B)	62	Collapse
32	Hokou tunnel - THSRL - contract C215	30	Daylight collapse
33	Shanghai Metro Line 4	31	Collapse
34	CTRL (Channel Tunnel Rail Link) - contract 240	32	Collapse
		33	Collapse
		34	Collapse
		35	Daylight collapse
		100	Excessive Deformation
		36	Daylight collapse

35	Tunnel in urban environment (unknown name)	37	Daylight collapse
36	São Paulo Metro Line 2 Jaciporã	38	Daylight collapse
37	Unknown Railway tunnel in Brazil	39	Rock Fall
		40	Collapse
38	Unknown roadway tunnel in Brazil	98	Collapse
39	Tribunal de Justica Road Tunnel (Road Tunnel at Avienda Santo Amaro)	47	Daylight collapse
40	Sao Paulo Metro 3 - Cristovao Burgos Shaft	43	Collapse
41	Sao Paulo Metro - Line 2 Cardoso Almeida / Sorocaba	44	Collapse
42	Sao Paulo Metro Line 3 Itaquera tunnel	45	Collapse
43	São Paulo Sewer (SANEGRAN)	46	Daylight collapse
44	Frei Caneca Tunnel (or Tunnel Martim de Sa)	102	Excessive Deformation
45	São Paulo Metro Line 1 Extensao Norte Tunnel	41	Collapse
		42	Excessive Deformation
46	North East Line	48	Collapse
47	Kaohsiung Metro	99	Daylight collapse
		189	Daylight collapse
48	Guangzhou Metro Line 1 and Line 3	49	Daylight collapse
		50	Daylight collapse
49	Evino Mornos Tunnel	152	Collapse
		52	Collapse
		51	Collapse
50	Cahora -Bassa hydroelectric system (surge chamber)	53	Rock Fall
51	Harspranget hydroelectric power plant (extension works)	54	Rock Fall

52	Holjebro hydroelectric	55	Rock Fall
53	Forsmark power station	56	Large inflow of water
54	Shisanling Pumped Storage Power Station	59	Collapse
		58	Collapse
		57	Collapse
55	Herzogberg Tunnel second tube	60	Rock Fall
		61	Collapse
56	Lane Cove tunnel	63	Daylight collapse
57	Tuzla tunnel	64	Collapse
58	Bolu tunnel	205	Daylight collapse
			Excessive
		65	Deformation
59	Los Angeles Metro (Red Line)	66	Daylight collapse
60	Dranaz tunnel	67	Collapse
61	Laerdal tunnel	68	Rockburst
		69	Collapse
62	Hai Van Pass tunnel	70	Daylight collapse
63	Jammu - Udhampur Link (tunnel 8)	71	Collapse
64	Dul Hasti HEP (head race tunnel)	73	Flooding
		23	Large inflow of water
		200	Collapse
		103	Large inflow of water
		72	Large inflow of water
65	Konkan railway	74	Collapse
		75	Collapse
66	Fuessen tunnel	76	Large inflow of water
67	Calcutta Metropolitan railway	77	Collapse
68	Dodoni tunnel		



		78 Daylight collapse
		192 Daylight collapse
69 Pont Ventoux Susa Hydropower System		
		79 Large inflow of water
		80 Rock Fall
		82 Large inflow of water
		83 Daylight collapse
		Excessive
		95 Deformation
		84 Collapse
		Excessive
		81 Deformation
		87 Daylight collapse
		86 Daylight collapse
		85 Daylight collapse
		91 Collapse
		Excessive
		92 Deformation
		Excessive
		93 Deformation
		94 Slope slide
		96 Slope slide
		97 Slope slide
		Excessive
		170 Deformation
		169 Collapse
		168 Collapse
		109 Blow out
		104 Daylight collapse
		105 Daylight collapse
		106 Daylight collapse
		108 Daylight collapse
		107 Daylight collapse
70 SSDS (Strategic Sewage Disposal Scheme) tunnel		
71 Bypass Sissach, N2 Chienbergtunnel		
72 Tymfristos		
73 Wilson tunnel		
74 Barcelona Metro line 9		
75 Lilla Tunnel		
76 Tauern tunnel		
77 Grizzly hydroelectric project		
78 Coyote outlet works		
79 Forks of the Butte		
80 Maneri - Uttarkashi		
81 Munich Metro		

82	Adler tunnel	171	Collapse
		158	Daylight collapse
		159	Daylight collapse
83	Egnatia Highway (Driskos tunnel)		Excessive
		90	Deformation
			Excessive
		101	Deformation
84	Egnatia Highway (Anthochori tunnel)		Excessive
		111	Deformation
85	Galindo El Parque wastewater and effluent tunnel		
		112	Collapse
		113	Collapse
86	Casecnan Multipurpose Project		
		114	Difficult ground
87	Landrucken tunnel		
		110	Collapse
88	Seikan tunnel		
		119	Flooding
		116	Flooding
		117	Flooding
		118	Flooding
89	Whabang tunnel		
		115	Collapse
90	Seoul metro Line 5		
		121	Daylight collapse
		122	Daylight collapse
		123	Daylight collapse
		124	Daylight collapse
		120	Daylight collapse
91	Buenavista tunnel		
		126	Collapse
92	Papallacta tunnel		
		127	Collapse
93	Sao Paulo Metro - estação Pinheiros (Pinheiros Station)		
		129	Daylight collapse
94	Khimti I hydropower project		
		132	Collapse
		131	Collapse
		133	Collapse
		134	Daylight collapse
95	Frasdanello and Antea tunnel		

		135	Collapse
96	Highway A1 between Sasso Marconi and Barberino del Mugello		
		136	Rock Fall
97	Gotthard Base Tunnel - Faido Multifunction section		
		137	Collapse
98	Gotthard Base Tunnel - Bodio section		
		138	Collapse
99	Gotthard Base Tunnel - Piora Zone (pilot tunnel)		
		139	Flooding
100	Grauholz tunnel		
		140	Daylight collapse
101	Aescher tunnel		
		141	Daylight collapse
102	Meteor Metro Line (Line 14)		
		142	Daylight collapse
103	Montelungo tunnel		
		143	Collapse
104	Pacheco Pumping Chamber and Shafts		
			Excessive
		144	Deformation
105	Kallidromo tunnel		
		145	Collapse
106	Trojane tunnel		
		146	Daylight collapse
107	Guadarrama tunnels		
		88	Collapse
		89	Collapse
108	Tunnel TO8 (THSRC)		
		147	Collapse
109	Pitan tunnel		
		148	Daylight collapse
		149	Collapse
110	Abdalajis Tunnel (tunnel East)		
		128	Collapse
111	Hurtieres tunnel		
		150	Daylight collapse
		151	Daylight collapse
112	Trasvase Guadiaro Majaceite Project		
		193	Collapse
		194	Collapse
		195	Flooding
113	Inter-Island tunnel (Boston harbor Project)		

		154	Collapse
		153	Flooding
114	Lotschberg Base tunnel		Excessive Deformation
		175	
115	Girokomeion Tunnel Patras by-pass		Daylight collapse
		155	
116	German Federal Railway Lines		Daylight collapse
		156	
		157	Daylight collapse
117	Umiray - Angat Transbasin Project		Flooding Excessive Deformation
		162	
		165	Excessive Deformation
		163	Deformation
		161	Collapse
		160	Collapse Excessive
		164	Deformation
118	St Petersburg metro (red Line)		Daylight collapse
		166	
		167	Collapse
119	Paramithia tunnels, Egnatia Motorway		Collapse
		172	
120	Yunnan tunnel		Collapse
		173	
121	Munich Metro (1994)		Daylight collapse
		174	
122	Covao Tunnel		Rock Fall
		184	
123	Waterway tunnel in Korea		Rockburst
		185	
124	Ortfjell open pit - exploration tunnel		Rockburst
		186	
125	Great Belt Link		Flooding
		181	
		187	Fire
126	Baikal - Amur line - No 2 Mysovy tunnel		Rock Fall
		180	
		179	Rock Fall
127	Baikal - Amur line -No1 by - pass route for the Severo-Muysky tunnel		Slope slide
		178	
128	Baikal - Amur line - Kodarsky tunnel		Collapse
		177	

129	Sewage tunnel (Bolshaya Dmitrovka street in Moscow)	176	Collapse
130	Walgau headrace tunnel	188	Daylight collapse
131	Iwate tunnel (Ichinoche Contract section)	182	Collapse
		191	Difficult ground
		196	Collapse
132	Yacambu-Quibor	183	Excessive Deformation
		197	Excessive Deformation
		198	Excessive Deformation
		199	Collapse

# **CHAPTER 4 Knowledge Representation and Decision Making**

## **4.1 Introduction**

Chapter 3 described a database of accidents in tunnels during construction. Through the analysis of the data, different events were identified. The circumstances in which each event could occur, the possible causes, the most important variables and the relationship among them, were then determined. The database was used to gather information on the conditions in which the events may occur. This information could then be used to support decision making during construction, with the aim of trying to avoid these events. For this it is necessary to identify which tools / models to use to represent this knowledge and perform a decision analysis.

There are a number of models available for data analysis and representation, including event trees, rule-based systems, fuzzy-rule based systems, artificial neural networks, and Bayesian networks. There are also several techniques for data analysis such as classification, density estimation, regression and clustering.

Knowledge representation systems (or knowledge based systems) and decision analysis techniques were both developed to facilitate and improve the decision making process. Knowledge representation systems use various computational techniques of AI (artificial intelligence) for representation of human knowledge and inference. Decision Analysis uses decision theory principles supplemented by judgment psychology (Henrion, 1991). Both emerged from research done in the 1940's regarding development of techniques for problem solving and decision making. John von Neumann and Oscar Morgenstern, who introduced game theory in "Games and Economic Behavior" (1944), had a tremendous impact on research in decision theory.



Although the two fields have common roots, since then they have taken different paths. More recently there has been a resurgence of interest by many AI researchers in the application of probability theory, decision theory and analysis to several problems in AI, resulting in the development of Bayesian Networks and Influence diagrams, an extension of Bayesian Networks designed to include decision variables and utilities.

There are several advantages that Bayesian Networks have over other methods. In this chapter some of the most common methods available for knowledge representation and decision making are briefly presented. Their main advantages and shortcomings are discussed. Finally the technique that was chosen to model the accident data, Bayesian Networks, is described in more detail.

## **4.2 Rule Based Systems**

Rule Based Systems are computer models of experts of a certain domain. The building blocks for modeling the experts are called production rules. A production rule is of the form:

If A then B

Where A (premise) is an assertion, and B (conclusion) can be either an action or another assertion. A rule based system consists of a library of such rules. These rules reflect essential relationships within the domain, or rather: they reflect ways to reason about the domain. When specific information about the domain comes in, the rules are used to draw conclusions and to point out appropriate actions.

A rule based system (or expert system) consists of a knowledge base and an inference engine. The knowledge base is the set of production rules and the inference engine combines rules and observations to come up with conclusions on the state of the world and on what actions to take.

One of the major problems of rule based systems is how to treat uncertainty. A way to incorporate uncertainty in rule based systems is to have production rules of this type:

If condition with certainty  $x$

then fact with certainty  $f(x)$

where  $f$  is a function.

There are many schemes for treating uncertainty in rule based systems. The most common are fuzzy logic, certainty factors and (adaptations of) Dempster - Shafer belief functions. Dempster - Shafer theory is a theory that computes the probability that the evidence supports the proposition, using a measure of belief often called a belief function (Dempster, 1968; Russell and Norvig, 2004). However, it is not easy to capture reasoning under uncertainty with inference rules for production rules. The reason for this is that in all the schemes for treating uncertainty, mentioned above, the uncertainty is treated locally. That is, the treatment is connected directly to each rule and the uncertainty of their elements. Therefore information on one variable does not easily propagate to the other variables. More specifically, it is difficult to combine (un)certainties from different rules, as is shown below:

Imagine the following two rules:

If  $a$  then  $b$  with certainty  $x$

If  $c$  then  $b$  with certainty  $y$

If  $a$  and  $c$  happen together, a rule for how to combine certainties is needed in this case, i.e. a function that combines certainty  $x$  and certainty  $y$  and returns another certainty. A similar situation occurs when trying to chain different rules:

If a then b with certainty x

If b then c with certainty y

When a is known, what is the certainty of c? A function for chaining is therefore also required.

Besides the problems related to the propagation of uncertainty from one variable to the others, rule based systems are difficult to debug and to update. When new information needs to be introduced in the system, the “programmer” needs to review the entire database of rules.

Despite their shortcomings, Rule Based Systems have been used in many applications in different domains, such as Medicine, for diagnosis and assisting in the selection of antibiotics (MYCIN, Stanford University, in 1976 see Shortliffe, 1976 and Melle et al., 1981); Banking, to detect fraud in use of credit cards (FRAUDWATCH, Touche Ross, UK, 1992); Aerospace Engineering for scheduling operations for the recycling Space Shuttle flights (GPSS, NASA, USA, 1993) and Civil Engineering for recommendation system in the maintenance and repairing of tunnels (MATUF, Silva, C, 2001) and a recommendation systems for repairing bridges (Sousa, R. 2000), among others (Darlington, 2000). More recently, these types of systems have been substituted by other techniques that allow one to better and more efficiently incorporate uncertainty. An example in Civil Engineering is the MATUF system that is currently being updated to Bayesian Networks (Sousa et al., 2007)

### **4.3 Fuzzy – rule approach**

Fuzzy logic is a way of introducing uncertainty into rule based systems. It is a superset of conventional logic that has been extended to handle the concept of “partial truth”, i.e. a value between (completely) true and (completely) false (Zadeh, 1965 and 1999). Based

on fuzzy logic, fuzzy rule expert systems were created. They use a collection of fuzzy membership functions (Figure 4.1) and rules drawn-out from the experts.

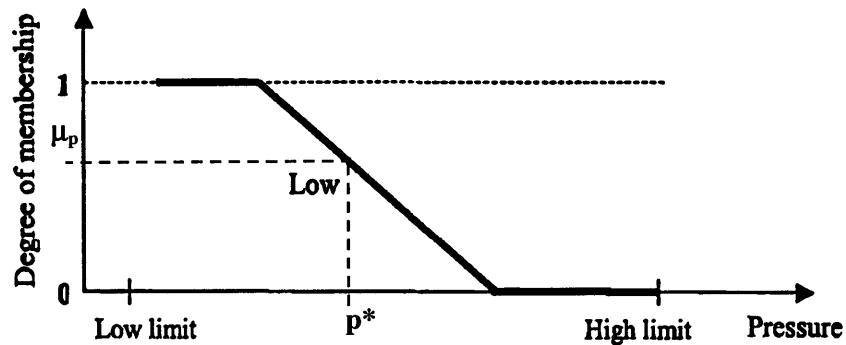


Figure 4.1 Fuzzy membership function (for low pressure)

In Figure 4.1, the degree of membership of  $p^*$  is  $\mu_p$ , which represents the degree of truth. The rules to evaluate the fuzzy “truth”  $T$  of a sentence are the following (Russel and Norvig, 2003):

$$T(A \wedge B) = \min(T(A), T(B))$$

$$T(A \vee B) = \max(T(A), T(B))$$

$$T(\neg A) = 1 - T(A)$$

Equation 4.1

where  $T$  is the fuzzy “truth” and  $A$  and  $B$  are variables or complex sentences. The AND ( $\wedge$ ), OR ( $\vee$ ), and NOT ( $\neg$ ) operators of Boolean logic exist in fuzzy logic; usually define the minimum, maximum, and complement. For example if  $A$  represents Low Pressure of the value  $p^*$  then  $T(A) = \mu_p$ . Imagine that  $B$  represents High Temperature, of the value  $t^*$  and  $T(B) = \mu_t$ . The result of Low Pressure ( $p^*$ ) and High Temperature ( $t^*$ ), i.e.  $T(A \wedge B)$  would be the  $\min(T(A), T(B)) = \min(\mu_p, \mu_t)$ . The way this process of fuzzification and defuzzification works will be demonstrated through an example, presented next:

Imagine the rule about deciding whether or not a liquid is potable. The factors to consider are toxicity, measured in parts per million, and the alcohol content, measured in percent (Figure 4.2).

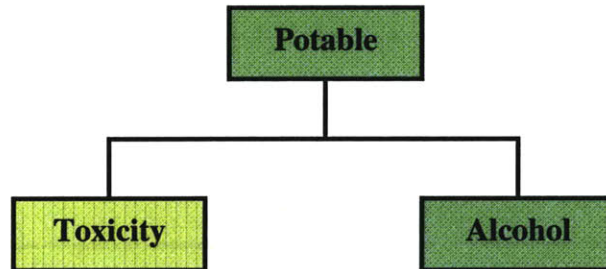


Figure 4.2 Factors in deciding whether a liquid is potable or not

The rule is

*IF* nontoxic  
*AND* low alcohol  
*THEN* potable

Equation 4.2

Imagine that we have a situation in which the toxicity of a liquid Z is equal to 210ppm and the fuzzy membership function is presented in Figure 4.3. The liquid Z is nontoxic with membership 0.6.

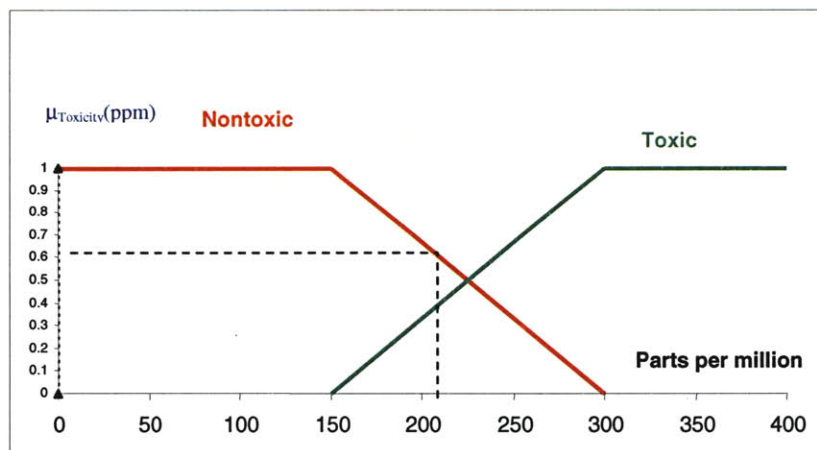


Figure 4.3 Membership function for Toxicity

The alcohol content of the liquid is 20%, resulting in low alcohol content with membership 0.75 (see Figure 4.4)

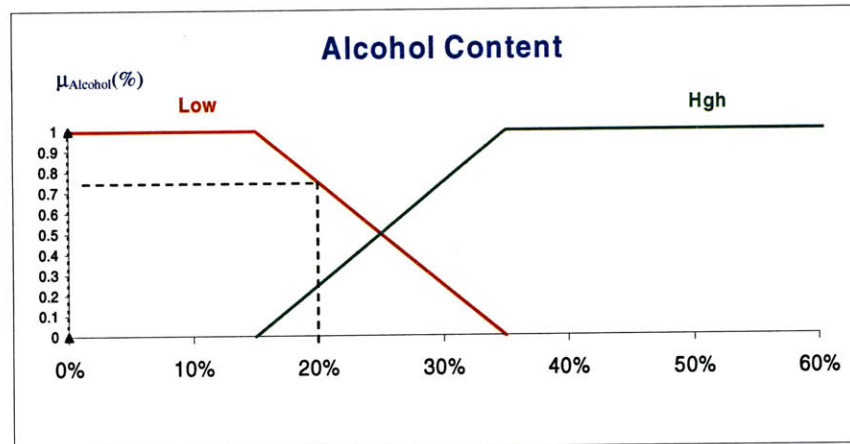


Figure 4.4 Membership function for Alcohol content

Applying the rule in Equation 4.2, one will obtain that the truth value of the sentence *liquid Z is potable* is 0.6 (Equation 4.3):

IF	nontoxic (Z)	(=0.6)
AND	low alcohol (Z)	(=0.75)
THEN	potable (Z)	
	$\text{Min}(0.6, 0.75) = 0.6$	

Equation 4.3

The inference mechanisms of these rules have some weaknesses; they have a weak theoretical foundation, inconsistency and sometimes oversimplification of the real world.

One inconsistency can be shown through a simple example (from Ruseel and Norvig, 2003). Imagine one would like to evaluate the sentence:

$$\text{Tall}(\text{John}) \wedge \text{Heavy}(\text{John})$$

Equation 4.4



Supposing that:

$$T(\text{Tall}(\text{John})) = 0.6$$

$$T(\text{Heavy}(\text{John})) = 0.4$$

Which means that the John is **Tall** with a membership of 0.6, and John is **Heavy** with a membership of 0.4

Then the truth value of Equation 4.4 will be  $T(\text{Tall}(\text{John}) \wedge \text{Heavy}(\text{John})) = 0.4$  which seems reasonable. However one will get the same result from evaluation the truth value of the sentence  $T(\text{Tall}(\text{John}) \wedge \neg \text{Tall}(\text{John})) = 0.4$ , i.e. the fuzzy truth of the sentence: John is **Tall** and John is **not Tall**, is 0.4, which does not make much sense. This is due to the fact that fuzzy logic approach does not allow one to take into account correlations between components of the sentences (or propositions).

Fuzzy logic is also controversial in some circles and is rejected by some engineers and by statisticians who hold that probability is the only rigorous mathematical description of uncertainty. Finally a way of incorporating the same type of idea of representing vague statements is to use conditional probabilities. For example, based on the membership for toxicity represented on Figure 4.3, one could define the event  $E = \text{parts per million} > 200$  and the complementary event  $\bar{E} = \text{parts per million} \leq 200$ . This way one could say the  $P(\text{Non toxic} | E) = 0.60$  and so forth.

Despite their shortcomings, fuzzy logic has been applied to several domains. In geotechnical engineering an application of fuzzy logic is use of Fuzzy set rules in rock mass characterization (Sonmez et al., 2003).

## 4.4 Artificial Neural Networks

An artificial neural network (ANN) or commonly just neural network (NN) is an interconnected group of artificial neurons (Figure 4.5), similar to the network of neurons in the human brain, that uses a mathematical model or computational model for information processing based on a connectionist approach to computation (Russell and Norvig, 2003; Mehrotra, K. et al.,1997).

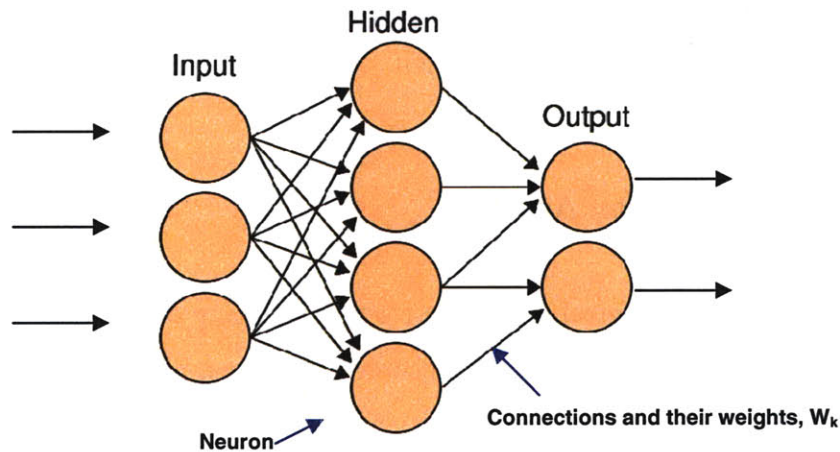


Figure 4.5 Neural network with one hidden layer

An ANN consists of multiple layers of single processing elements called neurons and of their connections. Each Neuron is linked to some of its neighbors with a varying coefficient of connectivity (weight) that represent the strength of these connections. This is stored as a weight value on each connection. The ANN learns new knowledge by adjusting these weights and the connections between neurons. Figure 4.5 shows an example of a neural network with one hidden layer.

The ANN rely on data to be trained, adjusting their weights and connections to optimize their behavior as pattern recognizers, decision makers, system controllers, predictors, etc. The strength of these models is their adaptiveness, without requiring a deep knowledge about the complex relationships of the domain of application. This adaptiveness allows the system to perform well even when the system that is being modeled, or controlled, changes over time.

The objective of using an ANN is to make predictions in the future. Although, an ANN network could provide almost perfect answers to the set of data with which it was trained, it may fail to produce an adequate answer when “new” data surfaces. This is a result of “overfitting” (Suwansawat, 2002; Suwansawat and Einstein, 2006). In order to perform adequately and produce good results, these systems require a large number of sample data in order to be trained. Also, since there is not a complete understanding of the learning process, the analysis of the results may be difficult. Thus, this is not the right approach in cases in which one needs to have a complete understanding of the problem domain and relationship among variables of the domain.

## **4.5 Classical Decision Analysis**

Decision Analysis is a logical procedure for the balancing of the factors that influence a decision. The procedure incorporates uncertainty, values, and preferences in a structure that models decision (Howard, 1966 and 1984). A classical tool used to model decisions and incorporate in a formal manner the relevant components of decision analysis is the decision tree. Prior to decision analysis, Fault trees and event trees can be used to model on one hand the different ways an event can occur (fault tree) and on the other hand, systematically identify the possible sequence of events and their consequences (event tree).

### **4.5.1 Fault trees**

Fault tree analysis is a technique used to analyze an undesirable event and the different ways that the undesirable event can be caused. A typical fault tree is composed of several different symbols, which will be described next.

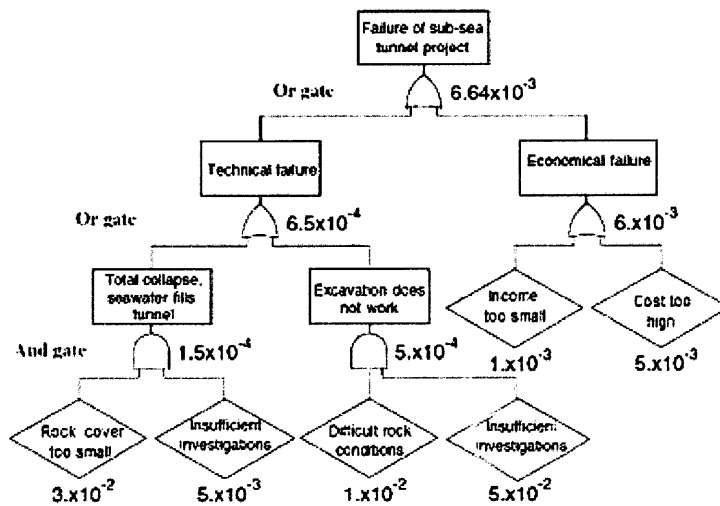


Figure 4.6 Example of a fault tree for evaluation of failure on sub-sea tunnel project (Eskesen, 2004)

### Events

The commonly used symbols for events are represented in Figure 4.7

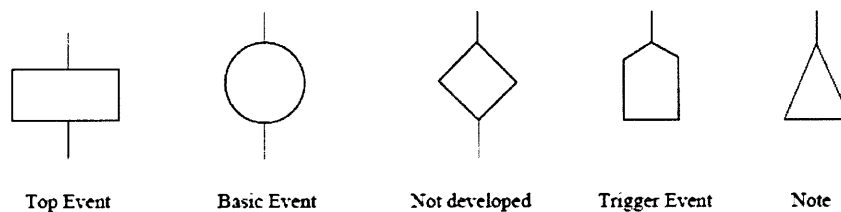


Figure 4.7 Symbols commonly used for events in fault tree

A top event (or also sometimes called intermediate event) is an event that occurs because of one or more antecedent causes.

A basic event is an initiating event requiring no further development.

An undeveloped event is an event that is not further developed either because of lack of information or because it is of little consequence.

A trigger event (also called external event) is an event that is expected to occur but is not itself a fault of the system, although it could trigger one.

## Gates

There are two basic types of fault tree gates, the OR-gate and the AND-gate. The symbols are shown in Figure 4.6.

The OR-gate is used to show that the output event occurs only if one or more of the input events occur. In the example the “*Failure of the sub-sea tunnel project*” can occur only if a “*technical failure*” or an “*economical failure*”, or both occur. Note that the inputs to an OR-gate are restatements of the output but are more specific as to what causes them, i.e. in the case of Figure 4.6 *Technical failure* is a restatement of “*failure of the sub-sea tunnel project*”, but it is more specific to what is the cause of failure. This is also true for “*economical failure*”.

The AND-gate is used when the output event occurs only if all the input events occur. Unlike the OR-gate, causes can be direct inputs of AND-gates. In the example of Figure 4.6a “*total collapse, seawater fills tunnel*” occurs only if the “*rock cover is too small*” AND “*investigations are insufficient*”.

A fault tree can be evaluated quantitatively and often is, but this is not necessary. Based on the rules of probability theory the probability of an AND gate is evaluated by

$$P = \prod_{i=1}^n p_i \quad \text{Equation 4.5}$$

And an OR-gate by

$$P = 1 - \prod_{i=1}^n (1 - p_i) \quad \text{Equation 4.6}$$

Where  $n$  is the number of ingoing events to the gate.  $p_i$  are the probabilities of failure of the ingoing events and it is assumed that the ingoing events are independent.

In Figure 4.6 the undesirable event being analyzed is the *Failure of a sub-sea tunnel*. According to the model failure can occur only if a *Technical Failure* OR an *Economical Failure* (or both) occur. A *Technical Failure* can occur if a *total collapse occurs* OR *excavation construction does not work* (or both). According to the model a total collapse can only occur if the *rock cover of the tunnel is insufficient* AND the *geotechnical investigations are insufficient*. On the other hand, the *Excavation may not work* if both *difficult rock conditions* are encountered AND *geotechnical investigations are insufficient*.

An *Economical Failure* occurs if the *income is too small* OR the *cost of the tunnel is too high*. The probability of an economical failure occurring can be evaluated as follows, (using Equation 4.6, and the numbers shown in Figure 4.6):

$$P_{\text{economical failure}} = 1 - [(1 - 1 \times 10^{-3})(1 - 5 \times 10^{-3})] = 6 \times 10^{-3}$$

The probability of “*total collapse*” occurring is evaluated using Equation 4.5 and the numbers shown in Figure 4.6, as follow:

$$P_{\text{total collapse}} = (3 \times 10^{-2})(5 \times 10^{-3}) = 1.5 \times 10^{-4}$$

The Probability of “*Failure of the tunnel*” can be evaluated as follow, using Equation 4.6 and the numbers shown in Figure 4.6 (assuming that all the other probabilities have already been evaluated)

$$P_{\text{tunnel failure}} = 1 - [(1 - 6.5 \times 10^{-4})(1 - 6 \times 10^{-3})] = 6.64 \times 10^{-3}$$

It is important to understand that a fault tree is not a representation of all possible undesirable events, but they are normally developed around an output event (in the example that event is “*Failure of sub-sea tunnel*” project), which corresponds to a



particular mode of failure of the system being analyzed. For further reading see Sturk (1998) and Ang and Tang (1984).

### 4.5.2 Event Trees

An event tree is a representation of the logical order of events leading to consequences. In contrast to the fault tree it starts from a basic initiating event and develops from there in time until all possible states with consequences (adverse or not) have been reached. A typical graphical representation of an event tree is shown in Figure 4.8. This is an example regarding the non-destructive testing of a reinforced concrete structure for corrosion. The inspection may or not detect the corrosion. The event  $CI$  denotes that corrosion is present, and the event  $I$  that the corrosion is found by the inspection. The bars over the events represent the complementary events. Based on this tree, one can evaluate the probability that corrosion is in fact present given that the inspection says so.

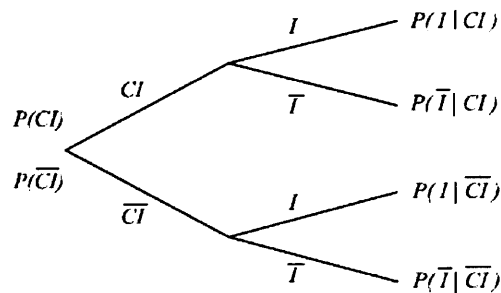


Figure 4.8 Typical event tree (Faber, 2005)

Event trees can become very complex to analyze rather quickly. For a tree with  $n$  two-state components the total number of paths is  $2^n$ . If each component has  $m$  states the total number of branches is  $m^n$ .

Fault trees and event trees (or decision trees) can be combined. The top event of a fault tree, in example of Figure 4.6, Failure of the tunnel, can be used as an initiating event for an event tree to assess the risk associated with that particular event. The combined fault tree and event tree is illustrated in Figure 4.9, which shows how fault trees can model an initiating event for the event tree. Note that the same fault tree can be combined with a

decision where one can assess whether or not it would be worth taking measures to avoid or mitigate damage.

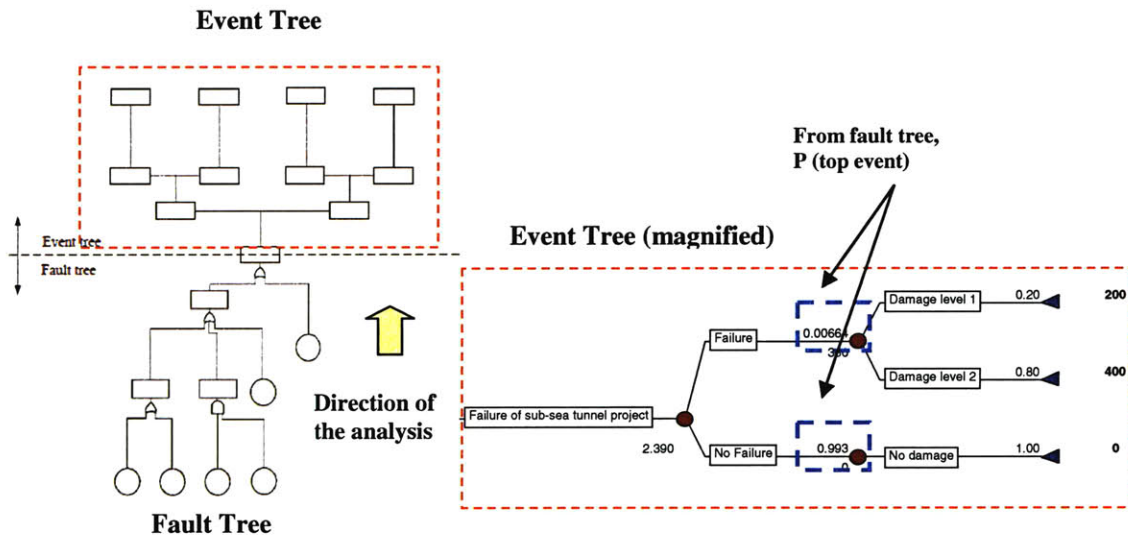


Figure 4.9 Combination of a fault tree and an event tree

### 4.5.3 Decision Trees

A decision tree is a formal representation of the various components of a decision problem. It consists of a sequence of decisions, namely a list of possible alternatives; the possible outcomes associated with each alternative; the corresponding probability assignments; monetary consequences and utilities (Ang and Tang, 1975). The typical configuration of a simple decision tree is shown in Figure 4.10. There are three types of nodes in a decision tree. The decision nodes, which are squared, represent different decisions or actions. The chance nodes, which are circular, are nodes that identify an event in a decision tree where a degree of uncertainty exists. The utility nodes, which are triangular, are nodes that terminate a branch path and represent the utilities associated with the path.

Figure 4.10 models a case where the decision maker is faced with two decisions / actions,  $a_1$  and  $a_2$ . The consequence of action  $a_1$  is with certainty B. However the consequence of decision  $a_2$  depends on the state of nature. Before the true state of nature is known the

optimal decision depends upon the likelihood of the various states of nature  $\theta_i$  and of the consequences  $A$ ,  $B$  and  $C$ .

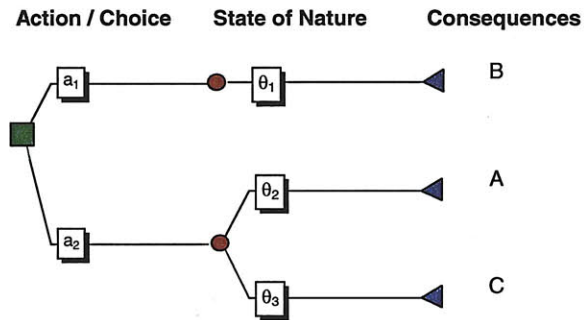


Figure 4.10 Typical decision tree (Faber, 2005)

The decision maker will choose action  $a_1$  over  $a_2$  if the expected utility associated with action  $a_1$  is greater than that of  $a_2$ .

$$E[u(a_1)] > E[u(a_2)]$$

$$u(B) > pu(A) + (1-p)u(C)$$

where

$u(A)$ ,  $u(B)$  – utility of consequence A and B, respectively

$p$  – probability of state  $\theta_2$

$(1-p)$  - probability of state  $\theta_3$

The valuation of an outcome, or the utility of an outcome, translates the relative preference of the decision maker towards different outcomes. The utilities are commonly based on monetary values, but they can also be based on other dimensions such as time or environmental effects. Multiattribute theory provides a way to combine all different measures of preference to come out with one single scalar utility to represent the relative preference of any outcome. The issue of utilities and utility functions is further detailed in Chapter 5.

## 4.6 Bayesian Networks

### 4.6.1 Background and Probability Theory

A Bayesian network, also known as belief network, is a graphical representation of knowledge for reasoning under uncertainty. Over the last decade, Bayesian networks have become a popular model for encoding uncertain expert knowledge in expert systems (Heckerman et al., 1995). Bayesian networks can be used at any stage of a risk analysis, and may substitute both fault trees and event trees in logical tree analysis. While common cause or more general dependency phenomena pose significant complications in classical fault tree analysis, this is not the case with Bayesian networks. They are in fact designed to facilitate the modeling of such dependencies. Because of what has been stated, Bayesian networks provide a good tool for decision analysis, including prior analysis, posterior analysis and pre-posterior analysis. Furthermore, they can be extended to influence diagrams, including decision and utility nodes in order to explicitly model a decision problem.

The concepts of Bayes' theorem, independence and conditional independence, as well as the chain rule, essential for Bayesian networks are presented in this section. For the basic concepts of probability theory (such as event, random variable, probability function, among others) necessary to understand the methodology of Bayesian networks, please refer to Ang & Tang, 1975.

#### Bayes' Theorem

$$P(A|B) = \frac{P(B|A)P(A)}{P(B)}$$

Equation 4.7

Where the  $P(B) = \sum_{i=1}^n P(A_i)P(B|A_i)$

Bayes Theorem has a many uses. Many times it is much easier to estimate the probabilities on the right side of Equation 4.7 than the one on the left side. A good

example is the case where one want to estimate the probability of the disease given a certain symptom,  $P(A|B)$ , being  $A = \text{disease}$  and  $B = \text{symptom}$ .

In order to estimate  $P(A|B)$  one would have to go through the population and then find people that had the symptom ( $B$ ) and from these find out how many of these had the disease ( $A$ ). Counting these cases maybe very hard especially if the disease is very rare; one may have to look at millions and millions of people. However, finding the probability of the symptom given the disease,  $P(B|A)$  is much easier. One just has to check hospital records and find people that had the disease and count how many of them had the symptom. Then one will also have to find the probability of the symptom and the probability of the disease, these also easier to get than  $P(A|B)$ .

For random variables the Bayes' theorem can be written as follows:

$$P_X(x|Y=y) = \frac{P_Y(y|X=x)P_X(x)}{P_Y(y)}, \text{ where } P_Y(y) = \sum_{x \in X} P_Y(y|X=x)P_X(x)$$

## Independence

The random variables  $A$  and  $B$  are independent if:

$$\begin{aligned} P(A \cap B) &= P(A) \times P(B) \\ &\equiv P(A|B) = P(A) \\ &\equiv P(B|A) = P(B) \end{aligned}$$

Equation 4.8

This means that the fact that one know  $B$  does not affect the probability of  $A$  and vice versa. For random variables Equation 4.8 is written as:

$$\begin{aligned} P_{X,Y}(x,y) &= P_X(x) \times P_Y(y) \\ &\equiv P_X(x|Y=y) = P_X(x) \\ &\equiv P_Y(y|X=x) = P_Y(y) \end{aligned}$$

Equation 4.9

## Conditional Independence

Random variable A and B are conditionally independent given C if

$$\begin{aligned}P(A \cap B | C) &= P(A | C) \times P(B | C) \\ &\equiv P(A | B, C) = P(A | C) \\ &\equiv P(B | A, C) = P(B | C)\end{aligned}$$

Equation 4.10

This is the generalization of independence but subject to a conditioning event, i.e. subject to knowing C. What these equations state is that once one knows the state of variable C, any information on the state of variable B won't give new information on variable A state and vice versa. For random variables Equation 4.10 is written as:

$$\begin{aligned}P_{x,y|z}(x, y | z) &= P_{x|z}(x | z) \times P_{y|z}(y | z) \\ &\equiv P_{x|y,z}(x | y, z) = P_{x|z}(x | z) \\ &\equiv P_{y|x,z}(y | x, z) = P_{y|z}(y | z)\end{aligned}$$

Equation 4.11

These Independence conditions are those that will be used to simplify the representation of joint distributions (in the form of Bayesian Networks).

## Chain rule

Writing the joint distribution of  $P(X_i = x_1, x_2, \dots, x_n)$  in terms of conditional probability will give:

$$P(X_i = x_1, x_2, \dots, x_n) = P(x_n | x_1, x_2, \dots, x_{n-1}) \times P(x_1, x_2, \dots, x_{n-1})$$

Repeating the process will yield:



$$\begin{aligned}
P(X_1 = x_1, x_2, \dots, x_n) &= \\
&= P(x_n | x_1, x_2, \dots, x_{n-1}) \times P(x_{n-1} | x_1, x_2, \dots, x_{n-2}) \times \dots \times P(x_2 | x_1) \times P(x_1) \\
&= \prod_i^n P(X_i | x_1, \dots, x_{i-1})
\end{aligned}$$

Equation 4.12

This is the so-called Chain rule. This rule computes joint probabilities from conditional probabilities, and it is very useful for Bayesian networks, which describe a joint probability distribution in terms in term of conditional probabilities.

#### 4.6.2 Definition of Bayesian Network

A Bayesian Network is a concise graphical representation of the joint probability of the domain that is being represented by the random variables, consisting of (Russell & Norvig, 1995):

- A set of random variables that make up the nodes of the network.
- A set of directed links between nodes. (These links reflect cause-effect relations within the domain.)
- Each variable has a finite set of mutually exclusive states.
- The variables together with the directed links form a directed acyclic graph (DAG).
- Attached to each random variable  $A$  with parents  $B_1, \dots, B_n$  there is a conditional probability table  $P(A = a | B_1 = b_1, \dots, B_n = b_n)$ , except for the variables in the root nodes. The root nodes have prior probabilities.

Figure 4.11 is an illustration of a simple Bayesian network. The arrows going from one variable to another reflect the relations between variables. In this example the arrow from  $C$  to  $B_2$  means that  $C$  has a direct influence on  $B_2$ .

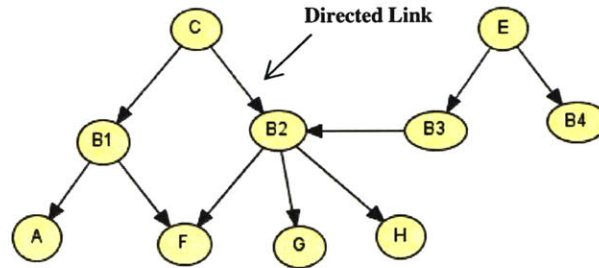


Figure 4.11 Bayesian Network example

A Bayesian Network (BN) is a graphical and concise representation of a joint probability distribution of all the variables, taking into account that some variables are conditionally independent. The simplest conditional independence relationship encoded in BN is that a node is independent of any ancestor<sup>1</sup> nodes given its parents, i.e. that a node only depends on its direct parents. Thus, the joint probability of a Bayesian network over the variables  $U = \{A_1, \dots, A_n\}$ , can be represented by the chain rule:

$$P(U) = \prod_i^n P(A_i = a_i | \text{parents}(A_i))$$

where “parents ( $A_i$ )” is the parent set of  $A_i$ .

Equation 4.13

The difference between Equation 4.12 (general chain rule) and Equation 4.13, chain rule applied to Bayesian networks is that in Bayesian Networks a variable is conditionally independent of their non-descendants, given the values of their parent variables, e.g. in the network of Figure 4.11 the variable A is conditionally independent of C given B1. It is this property that makes Bayesian Networks a very powerful tool for representing domains under uncertainty.

### 4.6.3 Inference

Since a Bayesian Network defines a model for variables in a domain and their relationships, it can be used to answer probabilistic queries about them. This is called inference.

---

<sup>1</sup> Ancestor nodes of a node are all nodes that come prior to that node in topologic order, e.g. the ancestors of A are B1 and C.

The most common types of queries are the following:

- *A priori* probability distribution of a variable.

$$P(\mathbf{A} = \mathbf{a}) = \sum_{x_1} \dots \sum_{x_k} P(x_1, \dots, x_k, \mathbf{A} = \mathbf{a})$$

Where  $A$  is the query-variable and  $X_1$  to  $X_k$  are the remaining variables of the network. This type of query can be used during the design phase of a tunnel for example to assess its probability of failure for the design conditions (geology, hydrology, etc).

- Posterior distribution of variables given evidence (observations). This query consists of updating the state of a variable (or subset of variables) given the observations (new information).

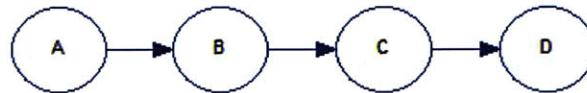
$$P(A = a | \mathbf{e}) = \frac{P(A = a, \mathbf{e})}{\sum_{x_1} \dots \sum_{x_k} \sum_A P(x_1, \dots, x_k, \mathbf{A} = \mathbf{a}, \mathbf{e})}$$

Where  $\mathbf{e}$  is the vector of all the evidence, and  $A$  is the query variable and  $X_1$  to  $X_k$  are the remaining variables of the network. This type of query is used to update the knowledge of the state of a variable (or variables) when other variables (the evidence variables) are observed. It could be used, for example, to update the probability of failure of a tunnel, after construction has started and new information regarding the geology crossed becomes known.

The most straightforward way to make inference in a Bayesian Network, if efficiency were not an issue, would be to use the equations above to compute the probability of every combination of values and then marginalize out the ones one needed to get a result. This is the simplest but the least efficient way to do inference. There are several algorithms for efficient inference in Bayesian Networks, and they can be grouped as follows: Exact inference methods and approximate inference methods. The most common

exact inference method is the *Variable Elimination* algorithm that consists of eliminating (by integration or summation) the non-query, non-observed variables one by one by summing over their product. This approach takes into account and exploits the independence relationships between variables of the network.

Figure 4.12 illustrates the Variable Elimination algorithm in Bayesian Networks. As illustrated instead of computing the product of  $P(d|c)P(c|b)P(b|a)$  and then eliminating A, B and C, to obtain  $P(D)$ , the Variable Elimination algorithm, eliminates each variable (marginalized out) one by one taking advantage that some conditional distributions do not depend on certain variables, minimizing the amount of computations. In this case A is eliminated first. Since  $P(d|c)$  and  $P(c|b)$  do not depend on A, this variable only needs to be eliminated from  $P(b|a)$ . The product of the result of this elimination and  $P(c|b)$  is a so called probability potential<sup>2</sup>,  $\phi(b,c)$ , which only depends on B and C. Then variable B is eliminated from  $\phi(b,c)$ , since  $P(d|c)$  does not depend on it. The product of this elimination and  $P(d|c)$  is a probability potential that only depends on C and D,  $\phi(c,d)$ . The final step is to eliminate C from  $\phi(c,d)$  in order to obtain  $P(D=d)$ .



$$\begin{aligned}
 P(D=d) &= \sum_{ABC} P(a,b,c,d) \\
 &= \sum_{ABC} P(d|c)P(c|b)P(b|a) \\
 &= \sum_C \sum_B \sum_A P(d|c)P(c|b)P(b|a) \\
 &= \sum_C P(d|c) \underbrace{\sum_B P(c|b) \sum_A P(b|a)}_{\phi(b,c)} \\
 &\quad \underbrace{\hspace{10em}}_{\phi(c,d)}
 \end{aligned}$$

<sup>2</sup> Probability potential is a non negative function defined over the product space over the domains of a set of variables (Finn, 2001). It is transformed into a probability distribution through a process called normalization.

Figure 4.12 Variable Elimination illustration

Approximate inference algorithms are used when exact inference may be computationally expensive, such as in temporal models, where the structure of the network is very repetitive, or in highly connected networks.

Appendix E provides a detailed description of the BN methodology, illustrated by an example.

## **4.6.4 Development of a Bayesian Network**

### **4.6.4.1 Organization of variables**

The purpose of the Bayesian model for decision support is to give estimates of certainties of events, which are not observable (or only observable at an unacceptable cost!). This can be for example the failure of a tunnel structure. Therefore, when organizing a model the initial task is to identify these events (“hypothesis” events). After identification, “hypothesis” events must be organized into a set of variables. A variable contains an exhaustive set of mutually exclusive events (or states), i.e. for each variable only one of these events (states) is true. The next task is to identify the types of achievable information which may reveal something about the “hypothesis” variables’ state. This is also done by establishing variables (information variables) such that a piece of information corresponds to a statement about the state of the variable, i.e. particular information will be a statement that the variable is in a certain state.

After identifying all variables, it is necessary to consider the causal structure between them. It is necessary to assess which variables have a direct impact on other variables. For example, with two variables, A and B that are correlated, in order to determine the direction of the arrow, one can imagine that an external agent fixes the state of A. If that does not change the belief of B then A is not a cause of B, and vice versa, but if one ends

up with arrows in both directions then one should check for another event which has a causal impact on both A and B and check whether A and B become independent given this new event. Sometimes it is necessary to introduce so-called mediating variables. These variables reflect the independence properties in the domain, and may facilitate the acquisition of conditional properties or/and may be used to reduce the number of conditional distributions that need to be acquired. The use of mediating variables is a common modeling technique used in BN, named Divorcing (see Section 4.6.4.2). Figure 4.13 illustrates a case where a mediating variable is introduced. In the model represented Figure 4.13a) the variable has four parents ('causes'), A1 to A4. In the model represented in Figure 4.13b) a mediating variable C was introduced. This variable may reflect the fact that A1 and A2 have similar effects on B and therefore can be grouped together, or it may be simply used in order to facilitate the probability distributions acquisition. This will be explained in more detail on Section 4.6.4.2.

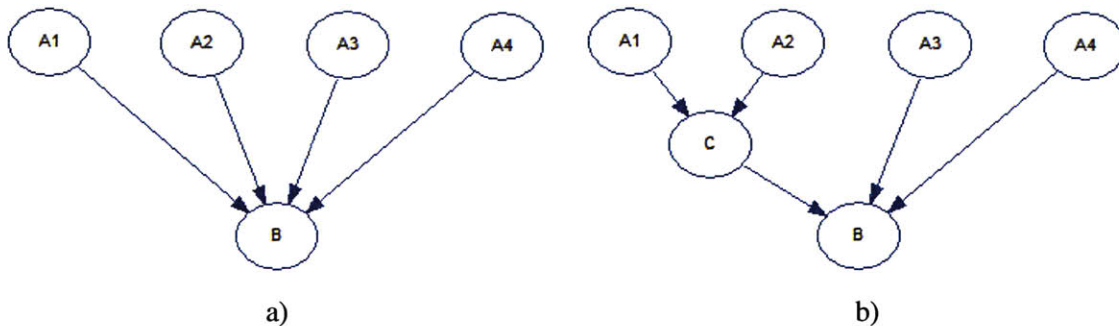


Figure 4.13 Mediating variable example

#### 4.6.4.2 Modeling Techniques

##### Undirected relationships

It is possible that a BN model must contain dependent relationships among variables, but it is not possible to determine the direction of the edges<sup>3</sup> as presented in Figure 4.14. One way to overcome this difficulty is by using undirected relationships (conditional

<sup>3</sup> Such models are called chain graphs. A chain graph is an “acyclic” graph with both directed and nondirected links, where acyclic means that all cycles consist of only nondirected links.



independence). So instead of the graph on Figure 4.14 one can use the model in Figure 4.15.

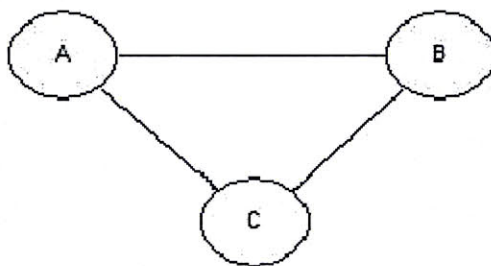


Figure 4.14 Chain graph

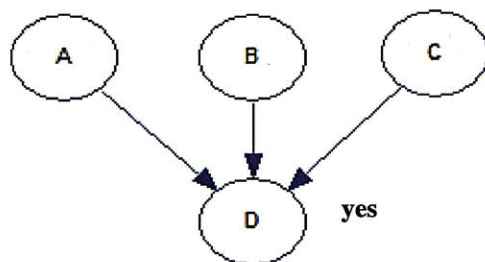


Figure 4.15 Undirected relationship method applied to example in Figure 4.14

In Figure 4.15 a new variable  $D$ , with states “yes” and “no”, is introduced into the network, as a common “child” of  $A$ ,  $B$  and  $C$ . If  $R(a, b, c)$  describes the relationship between variables  $A$ ,  $B$  and  $C$ , one should assign to  $D$  the deterministic probability table given as  $P(D = y | a, b, c) = R(a, b, c)$  (and  $P(d = n | a, b, c) = 1 - R(a, b, c)$ ) and enter the evidence  $D = \text{yes}$ . The variable  $D$  is called a constraint variable and by setting  $D = \text{yes}$  one is forcing the relationship between  $A$ ,  $B$  and  $C$  to hold. If  $A$ ,  $B$  and  $C$  have no parents, then  $R(a, b, c)$  can represent the joint probability distribution of these three variables.

If one would like to model that  $A$ ,  $B$  and  $C$  always have the same state, i.e. they are all equal to yes or they are all equal to no (and all the other possible combinations are impossible), the conditional probability  $P(D = \text{yes} | a, b, c)$  should be the one represented in Table 4.1.

Table 4.1 Conditional probability table for  $P(D=\text{yes} | a, b, c)$

A	B	C	P (D=d   a,b,c)
Yes	Yes	Yes	1
Yes	Yes	No	0
Yes	No	Yes	0
No	Yes	Yes	0
Yes	No	No	0
No	Yes	No	0
No	No	Yes	0
No	No	No	1

*Note: In this case  $R(a, b, c) = P(D=\text{yes} | a, b, c)$  is not a joint distribution. In order to be a joint distribution the table should add up to one.*

## Divorcing

A major inconvenience of BNs is the large number of conditional probabilities needed to define conditional probability tables (CPT). The number of conditional probabilities grows exponentially with the number of parent variables (the number of variables that have a causal relationship with another variable) and the number of states of each variable. In a situation of many parent variables, the “Divorcing” method can reduce the number of probabilities that one needs to acquire. Figure 4.16 illustrates this technique. Let  $A_1, A_2, A_3, A_4$  be variables, which are “causes” (or influence) of  $B$ . One needs to specify  $P(B=b | a_1, a_2, a_3, a_4)$  to describe the behavior of  $B$ . This might result in a large knowledge acquisition task. It may even be that no expert will be able to determine all these probabilities easily. To reduce this task one can use the modeling technique called Divorcing. This consists of introducing mediating variables that will separate  $B$  from its parents  $A_1, A_2 \dots A_n$ , reducing in this way the number of probabilities needed to define the BN.

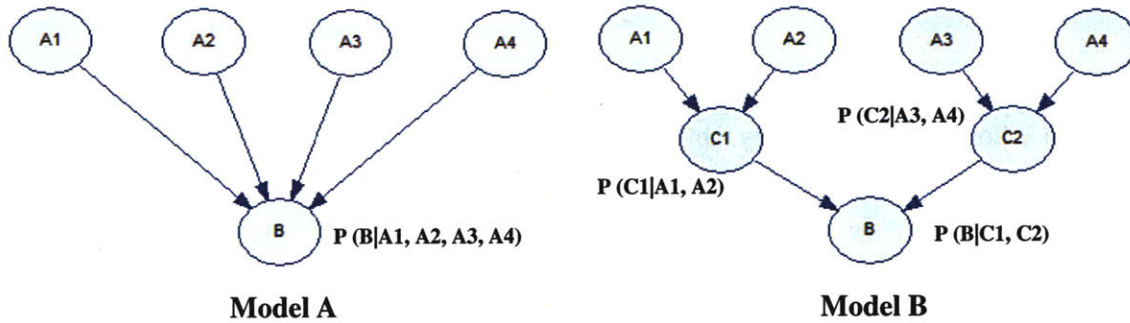


Figure 4.16 Illustration of the “divorcing” method technique

This technique reduces not only the number of probabilities that one has to acquire but the number of situations and combinations of variables, making the process of acquiring the probabilities easier.

Table 4.2 illustrates the probability conditional table of  $P(B=b|a_1, a_2, a_3, a_4)$ , for Model A illustrated in Figure 4.16, assuming that possible states for the variables  $A_1, A_2, A_3, A_4$  are (State 1, State 2, State 3) and the possible states for variable  $B$  are ( $b_1, b_2, b_3$ ). In this example, for model A, in order to specify  $P(B=b|a_1, a_2, a_3, a_4)$  one needs to acquire  $3^4 = 81$  distributions, if 3 is the number of states of each variable and the number of parents is 4.

Table 4.2  $P(B=b|a_1, a_2, a_3, a_4)^4$ .

				P(B=b A1,A2,A3,A4)						
				A1 =	A2 =	A3 =	A4 =	B = $b_1$	B = $b_2$	B = $b_3$
(N. of states) N of parents =81	{	State 1	State 1	State 1	State 1	.4	.4	.2		
		State 1	State 1	State 1	State 2	.1	.4	.5		
		State 1	State 1	State 2	State 2	.45	0	.55		
		...	...	...	....	....	...	...		
		...	...	...	....	....	...	...		
		State 3	State 3	State 3	State 3	.3	.3	.4		

In the case of Model B one only needs to acquire  $3^2+3^2+3^2 = 27$  distributions, which correspond to the conditional probability distributions  $P(B=b|c_1, c_2)$ ;  $P(C_1=c_1 | a_1, a_2)$  and  $P(C_2=c_2|a_3, a_4)$ . Table 4.3 represents  $P(B=b|c_1, c_2)$  for Model B, assuming that

<sup>4</sup> All numbers are arbitrary, for illustration purposes.

possible states for the variables C1, C2 are (State 1, State 2, State 3) and the possible states for variable B are (b<sub>1</sub>, b<sub>2</sub>, b<sub>3</sub>). The probability tables for P (C1=c1| a1, a2) and for P (C1=c1| a3, a4) are also tables with 9 distributions similar to Table 4.3.

Table 4.3 P (B=b|c1, c2)<sup>5</sup>

		C1	C2	P (B = b <sub>1</sub> )	P (B=b <sub>2</sub> )	P (B =b <sub>3</sub> )
(N. of states) N of parents=9	}	State 1	State 1	.4	.4	.2
		State 1	State 2	.1	.4	.5
		State 1	State 3	.45	0	.55
		State 2	State 1	...	....	...
		State 2	State 2	.1	.6	.3
		State 2	State 3	...	....	....
		State 3	State 1	....	...	...
		State 3	State 2	....	...	...
		State 3	State 3	.3	.3	.4

One can conclude that not only the number of probabilities needed is smaller in Model B but also that the task of obtaining them will be easier, since one will be asking experts to reason about situations where the number of variables is smaller. For example one (Model A in Figure 4.16) would be asking an expert what is the probability of a failure of a tunnel when a fault is at a certain inclination to the tunnel, the fault zone consists of a certain material, water is present, and the construction method is the NATM. It is better to use Model B (Figure 4.16) with two intermediate variables that represent, for example, the existence of adverse geotechnical conditions and a different type of construction.

The main problem with the divorcing technique is how to group the parent variables. One solution is to group the parents that have similar effects on the child variable. For example in the tunnel construction problem, there are several variables that can have an impact on a certain type of occurrence (heading failure). They can be geomechanical properties, existence of faults, hydrological properties, thickness of lining, type of lining, construction method type, and existence of reinforcement of the face, pre-support, etc. In this case, one can group the variables regarding the ground into a mediating factor

<sup>5</sup> All numbers are arbitrary, for illustration purposes.

describing the ground conditions. The same can be done for other variables such as construction method, type of environment etc.

#### **4.6.5 Determination of the Probabilities**

The last step of building a Bayesian Network model is to determine probabilities of events and conditional probabilities. These probabilities can be obtained from available data, from experts through subjective estimates or by combination of both. In the case of tunnel construction and failures some of the probabilities will have to be subjective estimates since there are normally not enough data to determine frequencies. When most of the probabilities come from subjective estimates and the number of probability distributions that need to be “known” is large for a reasonable estimation, simplifying assumptions can reduce this. The following sections will first describe a technique named “Noisy-or, which is used to reduce the number of distributions one needs to know. Then it will focus on methods to estimate probability density estimation. This is divided into two groups: 1) parameter estimation, which consists on estimating conditional probability tables from data (Parameter estimation); 2) structural learning, which consists on estimating both conditional probability tables and the structure Bayesian Network for data.

##### **4.6.5.1 Subjective Estimation (Noisy-Or Technique)**

###### **Degree of Belief**

Degree of belief is an expression of a person’s degree of belief in a proposition or in the occurrence of an event (Bayesian probability). The degree of belief can be objective, if there is some prior knowledge or subjective if no prior knowledge exists (Baecher, 1972)

This is in contrast with the frequentist approach in which the probability  $P(A)$  is the relative frequency of occurrence of the event  $A$  as observed in an experiment with  $n$

trials, i.e. the probability of an event A is defined as the number of times that the event A occurs divided by the number of experiments that is carried out (Venn limit)

The subjectivist generally starts with a prior belief, and will then update (using Bayes' rule) this belief as data become available. Eventually, the Bayesian probability will converge to the frequency as the data overwhelms the prior belief. However a key difference between these two approaches is that a subjectivist is willing to assign probabilities to non repeatable events such as the probability of a certain geology occurring in a zone of a tunnel, and the frequentist won't. This distinction is important in many engineering problems, particularly when data are not available, and expert knowledge (or opinion) must be used.

### Noisy-Or Technique

If the number of probability distributions that one has to assign is very large for reasonable estimation, then some simplifying assumptions can be made to reduce this number. A technique commonly used is called Noisy-or, and is defined as (Jensen, 2001):

Let B have parents  $A_1, \dots, A_n$  (all variables binary). Suppose  $A_i = y$  causes  $B=y$  unless it is inhibited by an inhibitor  $Q_i$  which is active with a probability  $q_i$ . Assume that the inhibitors are independent. Then

$$P(B = n|a_1, \dots, a_n) = \prod_{j \in Y} q_j, \text{ where } j \text{ belongs to } Y, \text{ the set of indices to states } y$$

To understand this technique refer to Figure 4.17 that presents a simple model for Cold (C) or Angina (A). The information variable is S (Sore Throat). The possible states for Sore Throat (S) are Yes and No, i.e. one either has a Sore Throat or not. The possible states for Cold (C) are also Yes and No, meaning one may have a cold or not. The possible states for Angina are No, Mild and Severe. If one knows which are the events



that can cause a sore throat and their respective probabilities it is possible to estimate the probability distributions of  $P(S=s | C=c, A=a)$ .

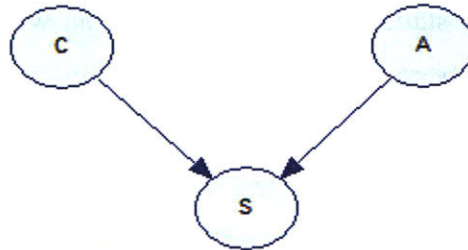


Figure 4.17 Cold or Angina model (Jensen, 2001)

The three events that can cause a sore throat are:

- *Cold*. Lets assume it causes a Sore Throat with probability 0.4, i.e.  $P(S=\text{yes} | \text{Cold} = \text{Yes}) = 0.4$
- *Angina*, which when is mild causes a Sore Throat with probability 0.7, i.e.  $P(S=\text{yes} | \text{Angina} = \text{mild}) = 0.7$ , and when it is severe will certainly cause a Sore Throat, i.e.  $(P(S=\text{yes}, \text{Angina}=\text{severe}) = 1$ .
- Some other unknown event. Let's assume its probability to be 0.05. This event is implicitly in the model. It portraits the situation where one does not have a cold or an Angina but that the throat is sore.  $P(S=\text{yes} | \text{Unknown event}) = 0.05$  or  $P(S=\text{yes} | \text{Cold} = \text{no}, \text{Angina} = \text{no})$

If any of the causes are present (Cold, Mild Angina or Unknown Event), then one will have a Sore Throat unless certain circumstances prevent it. These circumstances are called inhibitors.

For example the probability of a Sore Throat not happening given that one has Cold is 0.6, i.e.  $1 - P(S=s | \text{Cold} = \text{yes}) = 1 - 0.4$ . Similarly if one has a mild Angina, one will have a Sore Throat unless some inhibitor prevents it. The chances of that to happen are 0.3, i.e.,  $1 - P(S=s | \text{Angina} = \text{mild})$ . The unknown event is also prevented with probability of 0.95. Assume that the inhibitor for the unknown event is named  $q_1=0.95$ , the one for cold is named  $q_2=0.6$ , and the one for mild angina  $q_3=0.3$

Assuming these preventing factors are independent, then the probabilities for  $P(S = \text{yes} | c, a)$  can be calculated. The probabilities will equal one minus the joint probability of the respective inhibitors, and because of the assumption of independence, it will equal the product of the marginal probability of each inhibitor occurring (Table 4.4).

Table 4.4  $P(S = \text{yes} | c, a)$  for the Cold and Angina model.

Cold	Angina	P (Sore Throat = yes)
no	no	0.05 <sup>(1)</sup>
no	mild	1 - 0.95*0.3 <sup>(2)</sup>
no	severe	1 <sup>(3)</sup>
yes	no	1 - 0.95*0.6 <sup>(4)</sup>
yes	mild	1 - 0.95*0.3*0.6 <sup>(5)</sup>
yes	severe	1 <sup>(3)</sup>

- (1) This is the probability of the unknown event occurring
- (2)  $P(\text{Sore Throat} = \text{yes} | \text{Cold} = \text{no}, \text{Angina} = \text{mild}) = 1 - P(\text{Sore Throat} = \text{no} | \text{Cold} = \text{no}, \text{Angina} = \text{mild}) = 1 - q_1 \times q_3 = 1 - 0.95 \times 0.3 = 0.715$
- (3) This probability means that whenever one have a severe Angina case one will always have Sore Throat
- (4)  $P(\text{Sore Throat} = \text{yes} | \text{Cold} = \text{yes}, \text{Angina} = \text{no}) = 1 - P(\text{Sore Throat} = \text{no} | \text{Cold} = \text{yes}, \text{Angina} = \text{no}) = 1 - q_1 \times q_2 = 1 - 0.95 \times 0.6 = 0.43$
- (5)  $P(\text{Sore Throat} = \text{yes} | \text{Cold} = \text{yes}, \text{Angina} = \text{yes}) = 1 - P(\text{Sore Throat} = \text{no} | \text{Cold} = \text{yes}, \text{Angina} = \text{yes}) = 1 - q_1 \times q_2 \times q_3 = 1 - 0.95 \times 0.6 \times 0.3 = 0.829$

So, using the “Noisy-or” technique there is no need to compute probability values for combination of causes, which can reduce considerably the number of probabilities that need to be estimated.

#### 4.6.5.2 Learning Algorithms

Humans are normally better at providing structure than probabilities. Therefore, when possible, it is good to use data to obtain the conditional probability tables.

The structure is normally given by experts and the conditional probability tables can be estimated through available data. When there is a good amount of data available and not enough domain knowledge it is also possible to learn the network structure from data.

Learning is basically to search over a space of models to find the one that suits best. For this one has to define:

- The space of models
- Criteria or an objective function on models (i.e. What is the meaning of “a model that suits one better”)

One of the most common problems that one tries to solve in applying learning to BN is:

*Density estimation.* The idea is that the data were presumably generated according to some probability distribution  $P_X(x)$ . There is some process out in the world that is generating these data that are observed, and there is a joint probability distribution (of the data)  $P_X(x)$ . The goal is to estimate that probability distribution as well as one can,  $\hat{P}_X(x)$ , i.e. as close to the reality as possible.

There are different versions of the problem of density estimation, which have to do with what is given. This can be:

1. **Parameter estimation.** One is given the variables and the structure of the model. The only thing left to do is parameter estimation, i.e. what are the probabilities that go into the probability tables.
2. **Structure learning.** One is given the variables only. In this case one will have to search over the space of possible structures as well as estimate the parameters.

The next sections will discuss point 1) parameter estimation and point 2) structure learning, which are the one that interest for the application in this study. For more

information on the other subjects see Pearl, J.,1988; Jordan, M., 1998; Jensen, F. V, 2001 and Cowell., R. G. et al., 2003.

### ***A. Parameter estimation***

Parameter estimation in a Bayesian Network is the task of estimating the values of the parameters of the conditional distributions for each node  $X$ , given  $X$ 's parents, from a data set (Jensen, 2001). The methods of parameter estimation can be grouped into main groups: maximum likelihood and Bayesian estimation.

#### ***A.1 Maximum Likelihood***

Maximum likelihood estimation (MLE) is statistical method used for fitting a statistical model to data, and provide estimates for the model's parameters. The principle of MLE is to find parameter values that make the observed data most likely (Kjaerulff, 2008; Jensen, 2001).

In order to illustrate the method of Maximum Likelihood in Bayesian Networks, consider the simple experiment of flipping a thumbtack. The outcomes of the experiment are heads or tails (see Figure 4.18). Let's say that one is ignorant about what one will get when flipping a thumbtack.

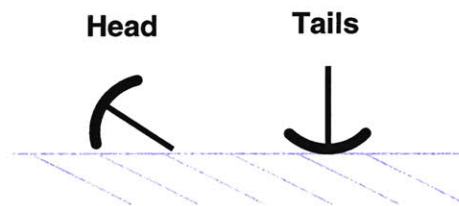


Figure 4.18 Thumbtack

The simplest Bayesian network possible to illustrate this situation corresponds to a binomial variable,  $X$  where the values are either heads or tails, presented in Figure 4.19.

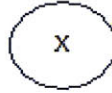


Figure 4.19 BN for thumbtack flipping

This BN has a probability table associated to it and it has only one parameter  $\theta$ , the  $P(\text{Heads})$ . What would be a good way to estimate parameter  $\theta$ , given some data  $D$  and some assumptions?

Imagine that the outcomes of the experiment are  $D = \{x[1]=H, x[2]=T, x[3]=H, x[4]=H, x[5]=T\}$ .

Assume that the elements of  $D$  are independent, i.e. that  $x[i]$  is independent of  $x[j]$  given  $\theta$ , and that  $\theta$  does not change over time.

Unscientifically looking at the data one would say that a good estimator for  $\theta$  could be as follows:

$$\hat{\theta} = 0.6 = \frac{\text{number of heads}}{\text{number of tails} + \text{number of heads}}$$

Equation 4.14

This intuition of what  $\hat{\theta}$  should be is correct and it is possible to prove it mathematically, as will be shown next.

As mentioned before, the learning process is about defining a space of answers (models) and then deciding what makes an answer good, i.e. apply a criterion in order to determine which answer (model) is best. So the hypothesis space in this case is  $\theta$ , a probability and therefore is going to be in the range  $[0, 1]$ . The criterion is to maximize the likelihood of the data given  $\theta$ , i.e. find the model ( $\theta$ ) which makes the data as likely as possible.

*Hypothesis space:*  $\theta \in [0, 1]$ .

*Criterion:* Maximize likelihood of  $D$ . This is called the maximum likelihood criterion.

The likelihood of the data is the probability of getting the data assuming a value of  $\theta$ .  $L(D : \theta) = P(D : \theta)$ <sup>6</sup>.

Now applying this to the data  $D = \{H T H H T\}$ , what is the probability of getting that particular set of data (or the likelihood of the data)? It will be:

$$P(D : \theta) = \theta^3 (1 - \theta)^2$$

More generally if  $M_h$  and  $M_t$  are the number of heads and the number of tails observed:

$$P(D : \theta) = \theta^{M_h} (1 - \theta)^{M_t}$$

Now what one needs to do is to find the  $\theta$  that maximizes the Likelihood function. It is easier to take the log of the function before maximizing it:

$$\text{Log}(P(D : \theta)) = l(D : \theta) = M_h \log \theta + M_t \log(1 - \theta)$$

The next step is to find the maximizing value of  $\theta$ , by taking the derivative of  $l(D : \theta)$  with respect to  $\theta$  and setting it equal to zero.

$$\begin{aligned} \frac{\partial l(D : \theta)}{\partial \theta} &= 0 \\ \Leftrightarrow \frac{M_h}{\theta} - \frac{M_t}{1 - \theta} &= 0 \\ \Leftrightarrow M_h(1 - \theta) - M_t \theta &= 0 \\ \Leftrightarrow M_h - M_h \theta - M_t \theta &= 0 \\ \Leftrightarrow \theta &= \frac{M_h}{M_h + M_t} \end{aligned}$$

Equation 4.15

The intuitive result of Equation 4.14 has been mathematically proved to be correct by Equation 4.15

The example considered is too simple with only one variable. In real problems, however, one is typically interested in looking for relationships among a large number of variables.

---

<sup>6</sup> The reason for having  $P(D : \theta)$  instead of  $P(D | \theta)$  is that  $\theta$  in this model is not a random variable but a parameter.



In order to illustrate how this method can be applied to a case of more than one variable, consider the BN with known structure and 2 nodes presented in Figure 4.20, and assume the following:

- The existence of a data set  $D = \{ \langle v_1^1, v_2^1 \rangle, \dots, \langle v_1^k, v_2^k \rangle \}$   

Value of nodes in sample 1
Value of nodes in sample k
- The elements of  $D$  are independent given Model (M), i.e.  $x[i]$  is independent of  $x[j]$  given  $\theta$  and that  $\theta$  does not change over time.

The goal is to find the model M (in this case Conditional Probability tables) that maximizes the  $P(D|M)$ , i.e. the probability of data occurring given the Model. This is known as the *maximum likelihood* model.

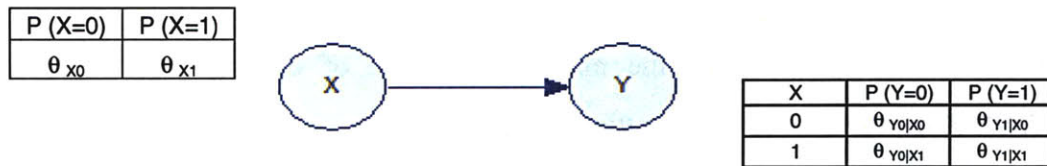


Figure 4.20 Bayesian Network with two binary nodes

The parameters that one wants to determine are the probabilities in the probability tables associated with each node (Figure 4.20). The vector of parameters is the following:

$$\theta = \langle \theta_{x1}, \theta_{x0}, \theta_{y0|x0}, \theta_{y1|x0}, \theta_{y0|x1}, \theta_{y1|x1} \rangle$$

Where,

$$\theta_{x1} = P(X=1)$$

$$\theta_{x0} = P(X=0)$$

$$\theta_{y0|x0} = P(Y=0 | X=0)$$

$$\theta_{y1|x0} = P(Y=1 | X=0)$$

$$\theta_{y0|x1} = P(Y=0 | X=1)$$

$$\theta_{y1|x1} = P(Y=1 | X=1)$$

The maximum likelihood function for these parameters given data set D is

$$L(D : \theta) = \prod_m P(X[m], Y[m] : \theta) = \prod_m P(X[m] : \theta) P(Y[m] | X[m] : \theta)$$

Equation 4.16

$P(X[i])$  only depends on  $\theta_x$  and  $P(Y[i] | X[i])$  only depends on  $\theta_{y|x}$ , Equation 4.16 can be simplified as follows:

$$\begin{aligned} L(D : \theta) &= \prod_m P(X[m] : \theta_x) P(Y[m] | X[m] : \theta_{y|x}) = \\ &= \prod_m P(X[m] : \theta_x) \prod_m P(Y[m] | X[m] : \theta_{y|x}) \end{aligned}$$

This way one can choose  $\theta_x$  to maximize  $\prod_m P(X[m] : \theta_x)$  and  $\theta_{y|x}$  to maximize  $\prod_m P(Y[m] | X[m] : \theta_{y|x})$ , independently. Note that the latter can be further decomposed as below:

$$\prod_m P(Y[m] | X[m] : \theta_{y|x}) = \prod_{m: X[m]=X0} P(Y[m] | X[m] : \theta_{y|x0}) \prod_{m: X[m]=X1} P(Y[m] | X[m] : \theta_{y|x1})$$

The final expression is:

$$L(D : \theta) = \prod_m P(X[m] : \theta_x) \prod_{m: X[m]=X0} P(Y[m] | X[m] : \theta_{y|x0}) \prod_{m: X[m]=X1} P(Y[m] | X[m] : \theta_{y|x1})$$

Equation 4.17

Since it is a product of positive expressions, it can be maximized for each parameter separately and we do not need to make a joint optimization through all parameters. To make the maximization easier, normally one maximizes the log of the likelihood function.

$$\begin{aligned} \frac{\partial \log \prod_m P(X[m]: \theta_x) = \log(\theta_{x1}^{M[X1]} \times (1 - \theta_{x1})^{M[X0]})}{\partial X} &= 0 \\ \Leftrightarrow \frac{M[X1] \times \log(\theta_{x1}) + M[X0] \times \log(1 - \theta_{x1})}{\partial X} &= 0 \\ \Rightarrow \hat{\theta}_{x1} &= \frac{M[X1]}{M[X1] + M[X0]}, \\ \Rightarrow \hat{\theta}_{x0} = 1 - \hat{\theta}_{x1} &= \frac{M[X0]}{M[X1] + M[X0]} \end{aligned}$$

Equation 4.18

Where  $M[X_i]$  are the counts of  $X = i$  (in this case  $i = 1$  or  $0$ )

The same way other parameters can be calculated:

$$\frac{\partial \log(\prod_{m: X[m]=X0} P(Y[m] | X[m]: \theta_{Y|X0}))}{\partial X} = 0 \Rightarrow \hat{\theta}_{Y|X0} = \frac{M[X0, Y1]}{M[X0]}$$

Note that this calculation is basically the same done to obtain Equation 4.18. So in a similar manner one will get the following results:

$$\hat{\theta}_{Y|X1} = \frac{M[X1, Y1]}{M[X1]}$$

Equation 4.19

$$\hat{\theta}_{Y0|X0} = \frac{M[X0, Y0]}{M[X0]}$$

Equation 4.20

$$\hat{\theta}_{Y1|X1} = \frac{M[X1, Y1]}{M[X1]}$$

Equation 4.21

Based on Equation 4.16 to Equation 4.21 it is possible to conclude that the problem of learning in the case of several variables that are related, i.e. BN can be reduced mainly to

the problem of learning one single variable. It is also possible to observe that the ML estimator is no more than the counts of the specific occurrence and dividing it by the number of all occurrences. Although very simple, this method has some shortcomings that will be presented in more detail in the next section. The derivation of the ML estimator for multinomial distributions can be done in a similar manner (Appendix F).

### *A.2 Maximum Likelihood Shortcomings*

This section will present an example of application of the Maximum Likelihood estimation applied to two different Bayesian Network, in order to illustrate the process of estimation, and as well as some of its shortcomings.

Consider three binomial variables A, B, C, two different BN (Figure 4.21) and a data set D, presented in Table 4.5.

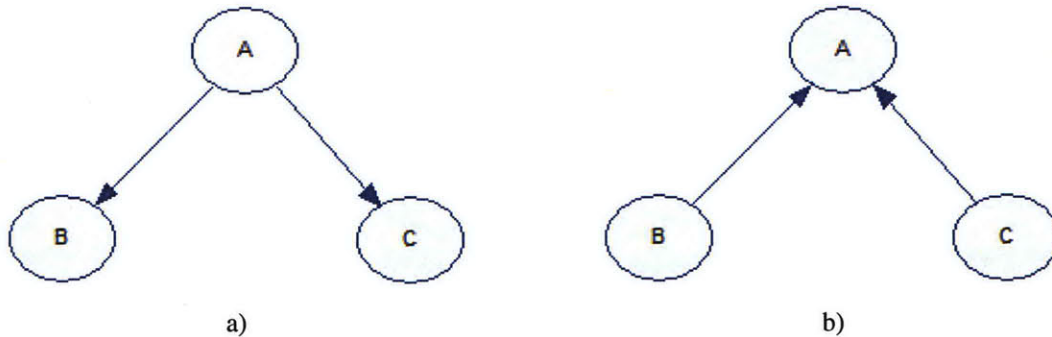


Figure 4.21 Two different configurations for BN with variables A, B, C

Table 4.5 Data set

A	B	C
0	1	1
0	1	1
1	0	0

For BN a) we need to estimate  $P(A)$ ,  $P(B|A)$  and  $P(C|A)$ , i.e. the tables associated with each node. For BN b) one needs to estimate  $P(B)$ ,  $P(C)$  and  $P(A|B, C)$ . For BN a), the probability table associated with node (variable) A is presented in Table 4.6.

Table 4.6 Probability of variable A in BN a)

P (A=0)	P (A=1)
$\theta_{A0}$	$\theta_{A1} = 1 - \theta_{A0}$

To calculate the probability of  $A = 0$ , one uses the results of maximum likelihood described previously, i.e. one counts the samples in the data set where  $A=0$ , and divides this by the total number of samples ( $A = 0$  or  $A = 1$ ). In this case the number of samples where  $A=0$  is 2. The total number of samples is 3 (applying Equation 4.15):

$$P(A = 0) = \theta_{A0} = \frac{M(A = 0)}{M(A = 0) + M(A = 1)} = 2/3$$

Equation 4.22

The same way, one can calculate the probability of  $A = 1$ :

$$P(A = 1) = \theta_{A1} = \frac{M(A = 1)}{M(A = 0) + M(A = 1)} = 1/3 = 1 - P(A = 0)$$

Equation 4.23

The conditional probability table (CPT),  $P(B|A)$  is presented in Table 4.7.

Table 4.7 Conditional Probability associated with variable B in BN a)

A	B=0	B=1
0	$P(B=0 A=0) = \theta_{B0 A0}$	$P(B=1 A=0) = \theta_{B1 A0}$
1	$P(B=0 A=1) = \theta_{B0 A1}$	$P(B=1 A=1) = \theta_{B1 A1}$

$$P(B = 1 | A = 0) = \theta_{B1|A0} = \frac{M[A = 0, B = 1]}{M[A = 0]} = 2/2 = 1$$

Equation 4.24

*Note: applying Equation 4.18.*

This is the probability of B having the value 1 given that A is 0. It will be equal to the number of samples from the data set that have  $A=0$  and  $B=1$ , simultaneously, divided by the number of samples where  $A=0$ . This is a conditional probability and it conditioned to

the “space” where A=0. So what we are doing here is to count the number of times we see B=1 in the world where A=0. The rest of the table can be calculated in similar way.

$$P(B = 1 | A = 1) = \frac{M[A = 1, B = 1]}{M[A = 1]} = 0/1 = 0$$

Equation 4.25

$$P(B = 0 | A = 0) = \frac{M[A = 0, B = 0]}{M[A = 0]} = 0/2 = 0$$

Equation 4.26

$$P(B = 0 | A = 1) = \frac{M[A = 1, B = 0]}{M[A = 1]} = 1/1 = 1$$

Equation 4.27

If we now look at the BN b) and try to estimate P (A| B, C), we realize that some table entries cannot be estimated. For example let’s look at  $P (A=1 | B=1, C=0)$  in Table 4.8.

Table 4.8 Conditional Probability associated with variable A in BN b)

B	C	A=0	A=1
0	0	$P (A=0   B=0, C=0) = \theta_{A0 B0,C0}$	$P (A=1   B=0, C=0) = \theta_{A1 B0,C0}$
0	1	$P (A=1   B=0, C=1) = \theta_{A1 B0,C1}$	$P (A=1   B=0, C=1) = \theta_{A1 B0,C1}$
1	0	$P (A=1   B=1, C=0) = \theta_{A1 B1,C0}$	$P (A=1   B=1, C=0) = \theta_{A1 B1,C0}$
1	1	$P (A=1   B=1, C=1) = \theta_{A0 B1,C1}$	$P (A=1   B=1, C=1) = \theta_{A1 B1,C1}$

In this case we want count the number of samples where A=1 in the space where B=1 and C=0. This is undefined since one does not have cases where this occurs:

$$P(A = 1 | B = 1, C = 1) = \theta_{A1|B1,C1} = \frac{M(A = 1, B = 1, C = 0)}{M(B = 1, C = 0)} = 0/0 = \text{undefined}$$

Equation 4.28

This is one of the major difficulties of Maximum Likelihood (ML). In some cases there may be not enough data in order to calculate all the parameters of the BN.



There are however other problems / shortcomings of ML. Namely, cases where the probabilities calculated are equal to zero, for example  $P(B=1|A=1)$ . In those cases we may have a problem. A probability equal to zero means that an event cannot occur. So whenever we run the BN for a specific query this event will never be a possibility. Can we say that an event cannot occur just because we do not have a sample? If the database is small and the event is rare it can occur that we don't have such example and however the event may indeed occur. Another issue is that ML does not consider any prior beliefs that one may have about the "world" that is being modeled. A method that avoids this problem, that enables one to include prior beliefs, is the Bayesian Estimation.

### ***A.3 Bayesian Estimation***

In the Bayesian view,  $\theta$  is the unknown value of a random variable  $\Theta$ , not a parameter like in ML.  $P(\Theta = \theta)$  is the prior probability distribution. If the parameter  $\theta$  can be any value in the interval  $[0, 1]$ , then  $P(\Theta = \theta)$  must be a continuous distribution between 0 and 1 and must integrate to 1. The beta distribution is a good candidate. This distribution is defined by two parameters  $\alpha, \beta$ , such that:

$$P(\theta) = \text{Beta}(\theta | \alpha, \beta) = \frac{\Gamma(\alpha + \beta)}{\Gamma(\alpha) \Gamma(\beta)} \theta^{\alpha-1} (1 - \theta)^{\beta-1}$$

Equation 4.29

where  $\alpha, \beta > 0$  are parameters of the beta distribution and  $\Gamma(\cdot)$  is the Gamma function.

Figure 4.22 shows how the beta distribution for different values of  $\alpha$  and  $\beta$ .

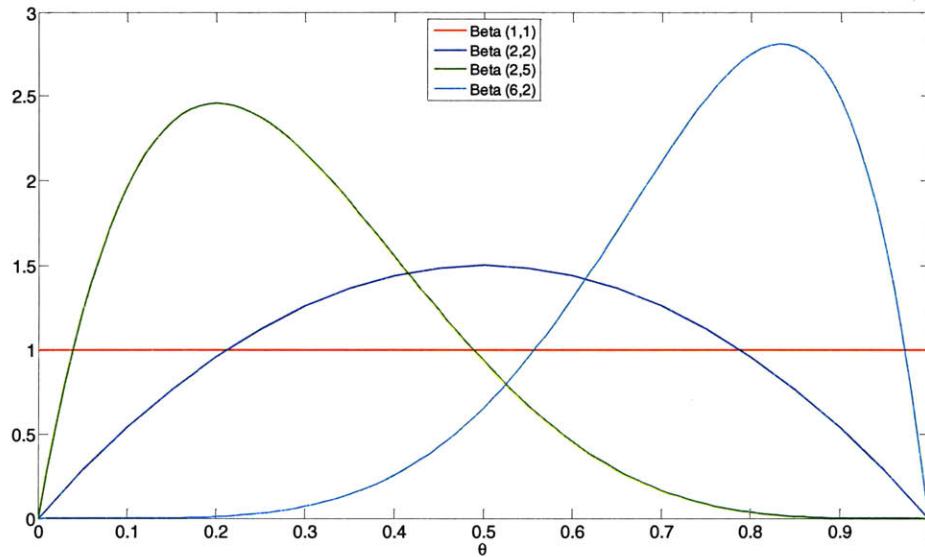


Figure 4.22 Beta distribution

The beta distribution is convenient for several reasons. If  $\Theta$  has a prior  $Beta(\alpha, \beta)$  then after a data point is observed the posterior distribution of  $\Theta$  is also a beta distribution. Imagine a random variable  $X$  that can take values 0 or 1. Suppose a data sample  $D$  is composed of only one observation,  $X=0$ .  $\Theta$  is a random variable that stands for the probability of  $X = 0$  and its distribution varies between 0 and 1. Now assume that this prior distribution of  $\Theta$  is a beta distribution with parameters  $\alpha$  and  $\beta$ ,  $Beta(\alpha, \beta)$ .

The distribution a posteriori of  $\Theta$ , after observing  $X=0$ , will be equal to (applying Bayes' rule):

$$P(\theta | X = 0) = \frac{P(X = 0 | \theta)P(\theta)}{P(X = 0)}$$

Equation 4.30

$P(X = 0 | \theta)$ , which is equal to  $\theta$ , stands for the probability of  $X = 0$  given the assumed model.  $P(\theta)$  is  $Beta(\alpha, \beta)$  distribution. Substituting  $P(\theta)$  and  $P(X = 0 | \theta)$ , in Equation 4.30:

$$P(\theta | X = 0) = \alpha \theta \text{Beta}(\alpha, \beta)(\theta) = \frac{\Gamma(\alpha + 1 + \beta)}{\Gamma(\alpha + 1)\Gamma(\beta)} \theta^\alpha (1 - \theta)^{\beta - 1} =$$

$$P(\theta | X = 0) = \frac{\Gamma(\alpha + 1 + \beta)}{\Gamma(\alpha + 1)\Gamma(\beta)} \theta^\alpha (1 - \theta)^{\beta - 1} = \text{Beta}(\alpha + 1, \beta)$$

Equation 4.31

The resulting probability distribution, i.e the posteriori distribution of  $P(\theta)$  is also a Beta distribution with parameters  $(\alpha + 1, \beta)$ . So after observing  $X = 0$  we have increased the parameter  $\alpha$  by one. If  $X = 1$  had been observed then the parameter  $\beta$  would have been increased by one (Remember that  $P(X = 1) = 1 - \theta$ ). Also the expectation of  $\Theta$  with respect to the Beta distribution has a simple form:

$$\int \theta \text{Beta}(\theta | \alpha, \beta) d\theta = \frac{\alpha}{\alpha + \beta}$$

Equation 4.32

The problem one is interested in is to know what is the probability of  $X = 0$  and/or  $X = 1$  given the available data. To illustrate this problem imagine one is flipping some kind of biased coin and that one has a certain amount of observations. What one wants to know now is the probability of getting heads or tails the next time the coin is tossed. This is a problem of Bayesian updating that can be represented in a Bayesian Network (Figure 4.23).

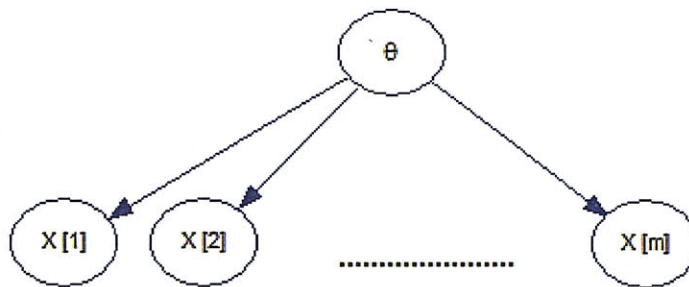


Figure 4.23 Bayesian Network model for estimating the parameter  $\theta$  given the observed data

One would like to estimate the probability that the next toss is heads, given what has been observed (given available data), i.e.  $P(X[m+1] | D)$ , where  $D = X[1], X[2], \dots, X[m]$ , are the available data.

To determine the probability that the next toss of the coin is heads, one averages over the possible values of  $\theta$  (using the expansion rule of probability):

$$P(X[m+1] | D) = \int_0^1 P(X[m+1] | \theta, D) P(\theta | D) \cdot d\theta$$

since the elements of  $D$  are independent given  $\theta$ :

$$P(X[m+1] | D) = \int_0^1 P(X[m+1] | \theta) P(\theta | D) \cdot d\theta$$

since the  $P(X[m+1] | \theta) = \theta$ , one will have:

$$P(X[m+1] | D) = \int_0^1 \theta P(\theta | D) \cdot d\theta \equiv E_{p(\theta|D)}(\theta)$$

Where  $E_{p(\theta|D)}(\theta)$  is the expectation of  $\theta$  with respect to the distribution  $P(\theta | D)$ .

Applying Equation 4.32 one will get:

$$P(X[m+1] | D) = \alpha' \int_0^1 \theta^{M_0} (1-\theta)^{M_1} \theta \cdot d\theta = P(X[m+1] | D) = \frac{M_0 + \alpha}{M_0 + M_1 + (\alpha + \beta)}$$

Equation 4.33

where  $M_0$  is the counts of  $X=0$  and  $M_1$  is the counts of  $X=1$ .

This is also called the Bayesian (or Laplace) correction. When using this correction, in the case  $M_0$  and  $M_1$  are equal to zero, i.e. if there are no observations the probability of the next toss given the available data (in this case none), and given a prior Beta (1,1) will be:

$$P(X | D) = \frac{M_0 + 1}{M_0 + M_1 + 2} = \frac{0 + 1}{0 + 0 + 2} = 0.5.$$

A prior of Beta (1, 1), i.e. uniform distribution, is called the “uninformed” prior, meaning that one believes that all values of  $\theta$  between 0 and 1 have the same probability. As seen before the Beta distribution family provides a great range of priors.

The parameters  $\alpha$  and  $\beta$  in the beta distribution can be seen has virtual counts. According to this idea, when the prior is equal to the uniform,  $\beta$  (1, 1), one is saying that our initial virtual count is one of each possible values. Basically one does not have strong beliefs and is saying the probabilities are  $P(X=0) = P(X=1) = 0.5$ . However it is possible that one has strong believes that the probabilities are  $P(X=0) = P(X=1) = 0.5$ , for example the probability that one get heads or tails when tossing a coin. In this case a probability distribution such as Beta (100, 100) is more adequate. In this case the “virtual counts” are 100 for each state, and what one is saying is that one has a strong belief that  $P(X=0) = P(X=1) = 0.5$  (because one “virtually” observed 100 tails and 100 heads). For Networks like the one in Figure 4.20, the Bayesian prior must cover all parameters  $\theta_1, \theta_2, \theta_3$ , i.e.  $P(X), P(Y|X=0), P(Y|X=1)$ , respectively. However  $P(\theta_1, \theta_2, \theta_3) = P(\theta_1) \times P(\theta_2) \times P(\theta_3)$ , since we have assumed that the parameters are independent from each other. Based on this assumption, each parameter can be represented by one random variable.

Applying the Bayesian correction to examples BN a) and BN b), presented in Figure 4.21, assuming a uniform prior one will get:

**BN a)**

$$P(A=0) = \frac{M(A=0)+1}{M(A=0)+M(A=1)+2} = 3/5$$

Equation 4.34

$$P(A=1) = \frac{M(A=1)+1}{M(A=0)+M(A=1)+2} = 2/5 = 1 - P(A=0)$$

Equation 4.35

(See examples BN a in Figure 4.21 and compare Equation 4.34 and Equation 4.35 with Equation 4.22 and Equation 4.23)

Table 4.9 P (B|A)

A	B=0	B=1
0	$P(B=0 A=0)$	$P(B=1 A=0)$
1	$P(B=0 A=1)$	$P(B=1 A=1)$

For the conditional probability table of P (B|A) presented in Table 4.9, one will get:

$$P(B = 1 | A = 0) = \frac{M(A = 0, B = 1) + 1}{M(A = 0) + 2} = 3/4$$

Equation 4.36

$$P(B = 1 | A = 1) = \frac{M(A = 1, B = 1) + 1}{M(A = 1) + 2} = 1/3$$

Equation 4.37

$$P(B = 0 | A = 0) = \frac{M(A = 0, B = 0) + 1}{M(A = 0) + 2} = 1/4 = 1 - P(B = 1 | A = 0)$$

Equation 4.38

$$P(B = 0 | A = 1) = \frac{M(A = 1, B = 0) + 1}{M(A = 1) + 2} = 2/3 = 1 - P(B = 1 | A = 1)$$

Equation 4.39

(Compare Equation 4.36 to Equation 4.39 to Equation 4.24 to Equation 4.27, respectively.)

The probabilities we obtain using Bayesian estimation are “smoother” than the ones obtained using the ML technique (i.e. Bayesian estimation combines the prior distributions with the available data whereas ML estimation only takes into consideration the available data. Bayesian estimation “smooths out” the estimation that would come out by only considering the data by combining it with prior distributions/ knowledge)



In the case of BN b) undefined probabilities is no longer the case.  $P(A=1|B=1, C=1)$  will be equal to  $\frac{1}{2}$ , based on the prior probability,

$$P(A=1|B=1, C=1) = \frac{M(A=1, B=1, C=1)+1}{M(B=1, C=1)+2} = \frac{0+1}{0+2} = \frac{1}{2}$$

Equation 4.40

(Compare Equation 4.40 to Equation 4.28)

To summarize, in this section two ways of “learning” parameters for a Bayesian Network with known structure and complete data were presented. ML counts the occurrences of different cases in the data set. Bayesian Estimation assumes a prior belief and updates this belief with counts from data. Note that when the data set is very large the results from Bayesian estimation will be approximately the same as the ones from ML.

### ***B. Structure Learning***

In recent years, AI researchers and statisticians have started to investigate methods for learning Bayesian Networks (Heckerman, 1997; Russel and Norvig, 2003). These methods range from Bayesian Methods, quasi-Bayesian Methods and non Bayesian methods. This section will focus on the Bayesian methods. The methods combine prior knowledge with data in order to learn a Bayesian Network. In order to use this method the user constructs a Bayesian Network that reflects his or her prior knowledge on the problem. This is called the prior network. The user will also need to assess her/his confidence on the prior network. Once the prior network has been determined, a *structure learning algorithm* will search for the “best” structure (including the respective conditional probability tables, which can be estimated using one of methods described in section A), i.e. the one that best fits the data.

Given a set of random variables the number of possible networks is well defined and finite. Unfortunately it grows exponentially with the number of variables. Although

*Structure Learning* in Bayesian Networks is still a topic of research, there are several algorithms that have been developed and can be applied (Heckerman, 1997; Finn, 2001, Russel and Norvig, 2003).

To specify a *structure learning algorithm* one must choose the following elements (the state space is known, i.e. the random variables are known):

- scoring function
- state transition operators
- search algorithm ( for example A\*, greedy hill-climbing, etc)

#### Scoring function (selection criterion)

The score of the network is used for model selection (i.e. some criterion is used to measure the degree to which a network structure fits the prior knowledge (if any) and the data. One of the most common criteria is the maximum likelihood (or log-likelihood). A penalty is normally introduced in order to account for overfitting (the most complex model is not always the most adequate). Figure 4.24 shows an example where using the most complex function is not the most adequate, i.e. one can use the higher polynomial curve to fit almost exactly the data points however this is clearly overfitting the data and will not fit correctly new data. In this case the 2<sup>nd</sup> order polynomial is the most adequate solution and not a more complex model.

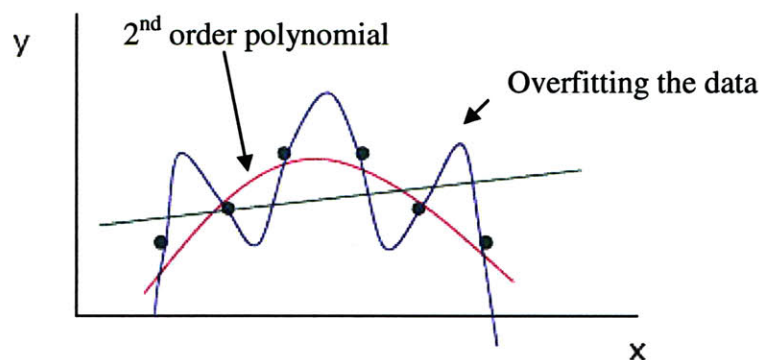


Figure 4.24 Example of overfitting

There are different possible scoring criteria. A good scoring criterion is the so-called Bayesian score.

When trying to find the best graph, the probability of a certain graph structure given the data is what one wants to calculate. This is given by Bayes' Rule.

$$P(G | D) = \frac{P(G, D)}{P(D)} = \frac{P(D | G) P(G)}{P(D)}$$

Since P (D) is just a normalizer and only depends on the data it can be ignored when comparing possible different graph structures. This way the numerator can be defined as the score for the graphs one wants to compare as follow:

$$S_G(G, D) = \text{Log}P(G, D) = \text{Log}P(D | G) + \text{Log}P(G) \quad ^7 \text{ where,}$$

Equation 4.41

$P(G)$  is the prior distribution on the graph structures,  $G$ , normally assumed to be a Dirichlet prior, and more specifically a uniform Dirichlet prior.

$P(D | G)$  is the marginal likelihood of the data given the structure which is equal to

$$P(D | G) = \int_{\theta_G} P(D | \theta_G, G) P(\theta_G | G) d\theta_G$$

The log marginal likelihood has the following interesting interpretation described by Dawid (1984). From the chain rule of probability,

$$P(D | G) = P(X[1])P(X[2] | X[1])...P(X[m] | X[1],...X[m-1])$$

Which looks like making successive predictions, i.e. approximately equal to the expected value of the  $P(X | G, D)$ .

---

<sup>7</sup> The logs are just used to simplify the math

Imagine we have a Dirichlet prior,  $P(\theta) \sim \text{Dirichlet}(\alpha_h, \alpha_t)$ ,  $\alpha_h + \alpha_t = \alpha$  and the data are  $D = \{H T T H T\}$

$$P(X[m] | X[1], \dots, X[m-1]) = \frac{M_h^m + \alpha_h}{m + \alpha}, \text{ where } M_h^m \text{ is the number of heads up to element } m$$

in our data sequence.

$$P(D | G) = \int_{\theta_G} P(D | \theta_G, G) P(\theta_G | G) d\theta_G$$

$$P(D | G) = \frac{\alpha_h}{\alpha} \frac{\alpha_t}{\alpha + 1} \frac{\alpha_t + 1}{\alpha + 2} \frac{\alpha_h + 1}{\alpha + 3} \frac{\alpha_t + 2}{\alpha + 4} = 0.017$$

For a  $P(\theta) \sim \text{Dirichlet}(\alpha_h, \alpha_t)$  and  $D = \{X[1] \dots X[M]\}$

$$P(D) = P(X[1], \dots, X[M]) = \frac{(\alpha_h \cdot (\alpha_h + 1) \dots (\alpha_h + M_h - 1)) (\alpha_t \cdot (\alpha_t + 1) \dots (\alpha_t + M_t - 1))}{\alpha \cdot (\alpha + 1) \dots (\alpha + M - 1)}$$

$$= \frac{\Gamma(\alpha)}{\Gamma(\alpha + M)} \frac{\Gamma(\alpha_h + M_h)}{\Gamma(\alpha_h)} \frac{\Gamma(\alpha_t + M_t)}{\Gamma(\alpha_t)}$$

Where  $\Gamma(x) = (x-1)!$  for  $x$  integer and  $\Gamma(x) = \int_0^\infty t^{x-1} e^{-t} dt = (z-1)\Gamma(z-1)$  for  $x$  real.

For a prior  $P(\theta) \sim \text{Dirichlet}(\alpha_1 \dots \alpha_k)$  and  $D = \{X[1] \dots X[M]\}$

$$P(D) = \frac{\Gamma(\sum_k \alpha_k)}{\Gamma(\sum_k (\alpha_k + M_k))} \frac{\Gamma(\alpha_h + M_h)}{\Gamma(\alpha_h)} \frac{\Gamma(\alpha_t + M_t)}{\Gamma(\alpha_t)} \prod_k \frac{\Gamma(\alpha_k + M_k)}{\Gamma(\alpha_k)}$$

Equation 4.42

One cannot assume that the data are independent because we do not know the parameters of the model that generated the data, because different network structures will entail different parameters. What one can say however is for a determined structure  $G$ , the data are independent given the parameters. This is the same case as the Bayesian parameter estimation described in Section 4.6.5. Figure 4.25 illustrates this independence between data given the structure  $G$  and the parameters  $\theta$  in the form of a Bayesian network.

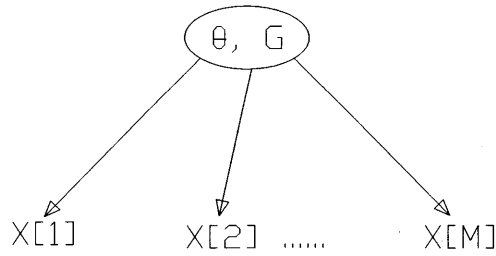


Figure 4.25 Bayesian Network describing the independence between data points given the structure and the parameters ( $G$  = BN structure;  $\theta$  = conditional probability table parameters)

As  $M$  goes to infinity (for Dirichlet priors) the log of margin likelihood can be approximated to the following equation:

$\log P(D|G) \approx \log P(D|\hat{\theta},G) - \frac{d}{2} \log M$ , where  $d$  is the number of parameters in  $G$ , and  $\hat{\theta}$  the estimator of  $\theta$ .

Equation 4.43

This approximation is called Bayes Information Criterion (BIC) and was first derived by Schwarz (1978). In particular; Schwarz shows that Equation 4.42 for curved exponential models can be approximated using Laplace's method for integrals, yielding Equation 4.43.

The BIC approximation is interesting in several respects. First, it does not depend on the prior. Consequently, we can use the approximation without assessing a prior. Second, the approximation is very intuitive. It contains a term that measures how well the model predicts the data,  $\log P(D|\hat{\theta},G)$  and a term that penalizes the complexity of the model,  $-\frac{d}{2} \log M$ .

### Priors

To compute the relative posterior probability of a network structure, we must assess the structure prior  $P(G)$  and the parameter priors  $P(\theta_G|G)$ , unless we are using large-sample approximations such as BIC.

It has been assumed previously that the prior distributions on the parameters are Dirichlet distributions. A special case is assuming a uninformative prior with  $(\alpha_1 \dots \alpha_k) = (1, \dots, 1)$ . This is called the K2 metric. However this metric can lead sometimes to inconsistent results (Heckerman, 94).

In order to avoid inconsistencies one can use the so-called BDe prior. In this metric the user assigns a prior sample size  $M'$  and a prior distribution  $p'$  to the whole space. Then  $\alpha_{x_j | Pa(x_j)} = M' p'(X_j | Pa(X_j))$ . A very common choice for  $p'$  is the uniform distribution over the whole space. This particular case of the BDe metric is called the BDeu.

### State transition operators

These are transition functions applied to the network structures to go between states (network structures) until reaching the final network structure, such as adding an arc, deleting an arc, or reversing the direction of an arc. They are basically used to transition from network to network during the search for the network with the best score.

For each state (each network structure), one takes the best guess regarding the parameters of that specific network structure given the data (for example using the maximum likelihood method) and determines the score of the network through a scoring function.

Figure 4.26 shows the typical transition operations (add, delete and reverse).



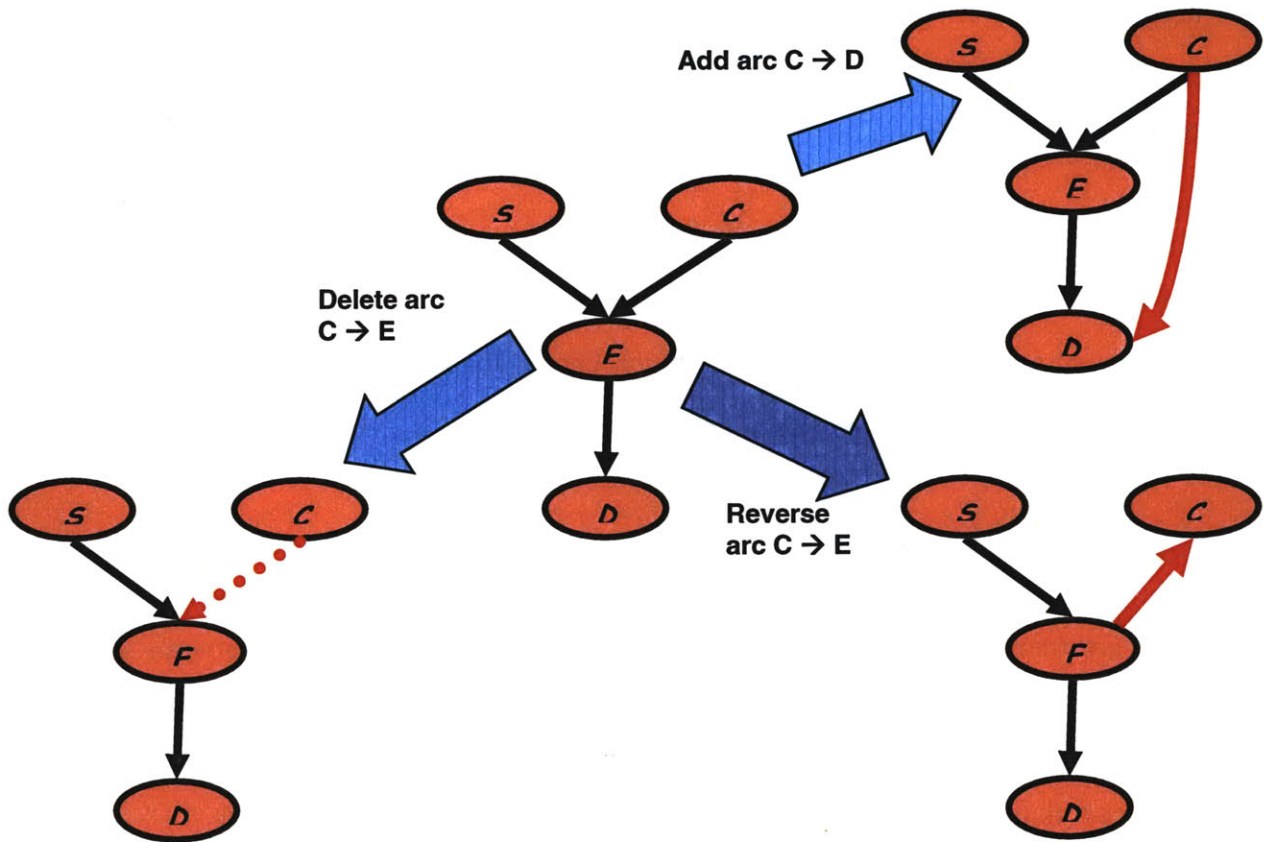


Figure 4.26 Typical transition operators (add, delete, reverse in blue)

### Search

Based on a defined scoring function that evaluates the “performance” of a certain Bayesian Network structure, the search is going to be reduced to a search for one or more structures that have high score. There are several search algorithms to perform the search.

The most common are:

- Greedy Hill Climbing, which consists of considering every legal move (transition between network structures) and takes the one that yields the highest score.
- Random Hill Climbing, which consists of considering moves (transition between network structures) drawn at random and takes the one that yields the highest score.

- Thick-Thin Greedy Search, which consists of greedily<sup>8</sup> add single arcs until reaching a local maximum and then Prune back edges which don't contribute to the score

These algorithms can be “stuck” in a local maximum and not return the optimal structure.

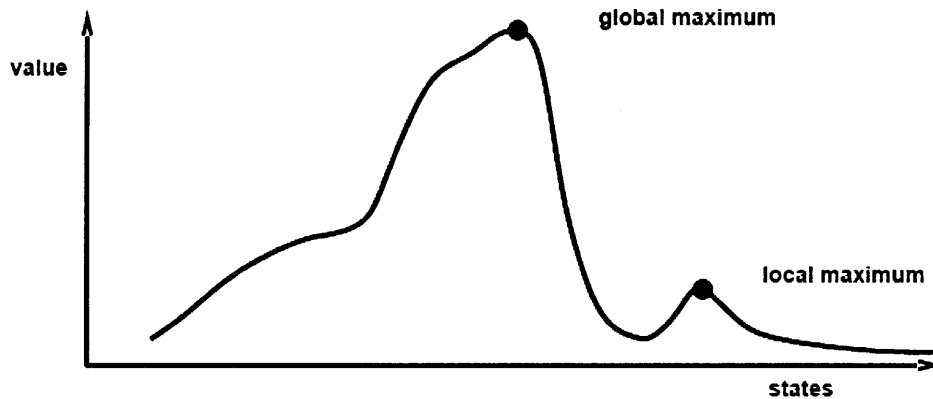


Figure 4.27 Local maximum versus global maximum

There are several ways one can do to avoid this situation, such as random re-starts and simulating annealing, which consists of allowing the algorithm some “bad” moves but gradually decrease their size and frequency, in order to escape local maximum.

## 4.7 Influence Diagrams

Bayesian networks can serve as a model of a part of the world, and the relations in the model reflect causal impact between events. However the reason we are building models is to use them when making decisions (i.e. the probabilities provided by the network are used to support some kind of decision making). Decision graphs or influence diagrams are an “extension” of Bayesian Networks. In addition to nodes for representing random variables, influence diagrams also provide node types for modeling alternatives and utilities. Besides chance nodes that denote random variables, and correspond to the only

<sup>8</sup> Consider all the possible addition of arcs and choose the one that yields the best score.

node type available in Bayesian networks, decision nodes are also modeled. A decision node indicates a decision facing the decision maker (similar to decision nodes in decision trees) and contains all alternatives available to the decision maker at that point. The third node type provided by these diagrams is the utility node. These nodes represent the utility function of the decision maker. In utility nodes, utilities are associated with each of the possible outcomes of the decision problem modeled by the influence diagram.

Directed links between nodes represent influences. Links between two chance nodes have the same semantics as in Bayesian networks. Other links in an influence diagram may also represent a temporal relation between the nodes involved. For example, a link from a decision node to a utility node not only indicates that the choice of action influences the utility, but also that the decision precedes the outcome in time.

Influence diagrams are useful in structuring a decision problem. While, for example, decision trees are more effective at presenting the details of a decision problem, influence diagrams more clearly show factors that influence a decision. Figure 4.28 illustrates a simplified scheme of an Influence Diagram. It is composed of two chance nodes (“Threat” and “Warning Device”), one decision node (“Decision”) and a utility node (“Consequence”). In this specific example, the chance node “Threat” can represent the occurrence or not of a natural threat (for example a tsunami or a hurricane). The “warning device” chance node represents the fact that a warning alarm maybe issued or not. The decision node represents the decision between evacuation a population or do not evacuate. The utility node (“consequences”) represents the consequences (expressed in utilities of the decision) in combination with the occurrence or not of the threat. The *warning device* issuing an alarm depends directly of the possibility of occurrence of the *threat*. The *decision* of evacuating or not evacuating the population will depend directly on the *warning device* issuing an alarm. Finally the consequences will depend on the decision taken and on whether or not the threat actually happens.

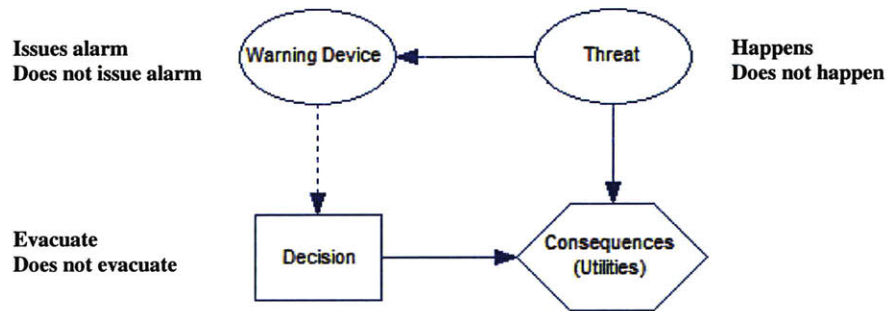


Figure 4.28 Influence Diagram

There are mainly four types of connections for structural influence in a decision graph. They are represented in Figure 4.29.

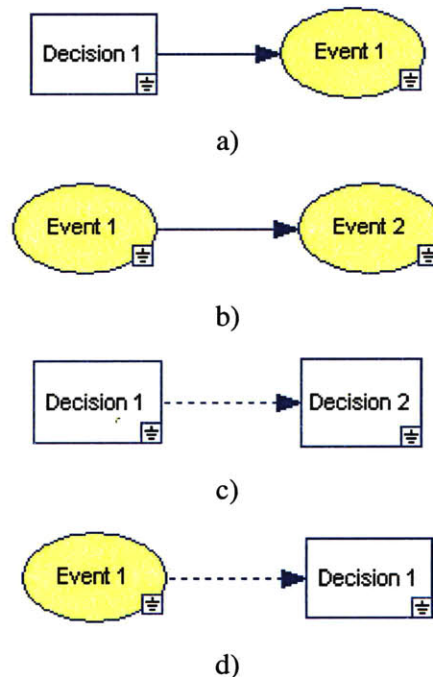


Figure 4.29 Influence Diagram connections

The first one (Figure 4.29a) is used when a Decision 1 affects the probabilities of event 1, i.e. Decision 1 is relevant for event 1. In Figure 4.29b the outcome of event 1 affects the probabilities of event 2, i.e. Event 1 is relevant for Event 2. This a typical Bayesian Network with no decision included. The type of connection in Figure 4.29c is used when Decision 1 occurs before Decision 2, i.e. Decisions 1 and 2 are sequential. Finally, Figure

4.29d represents a connection used when Decision 1 occurs after event 1. In this case the outcome of Event 1 is known when making Decision 1.

Besides the structural influences described in Figure 4.29, there are also value (utilities) influences such as the ones illustrated in Figure 4.30.

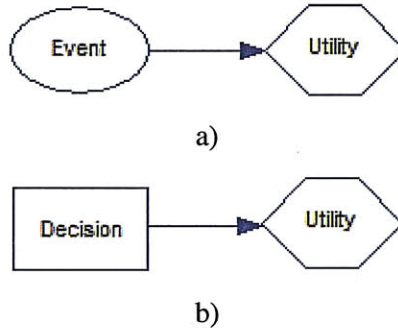


Figure 4.30 Value Influence

In Figure 4.30a) the value (or utility) depends on the (uncertain) event, for example a manufacturing cost depends on the (uncertain) availability of a certain input. In the second value influence (Figure 4.30b), a decision influences the value (or utility). For example a manager's decision influences the profit of a plant.

#### 4.7.1 Typical types of Influence diagrams

There are some typical situations that can be modeled through influence diagrams. The most simple of all is a one stage, non-strategic decision, which is represented in Figure 4.31. The utility will depend on the uncertainty outcome of an event and on the decision.

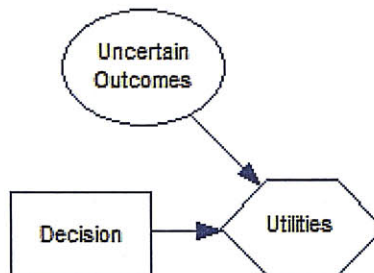


Figure 4.31 Simple one stage, non-strategic decision

The diagram of Figure 4.32 is similar to the simple one stage decision but includes the value of perfect information, which is the expected outcome with perfect information minus the expected outcome without perfect information. The value of perfect information is obtained through the link between the uncertain outcome and the decision. The table attached to the node decision reflects the fact that when the outcome is known with certainty, for example outcome equals 1, than the best decision to make is in this case Decision =1.

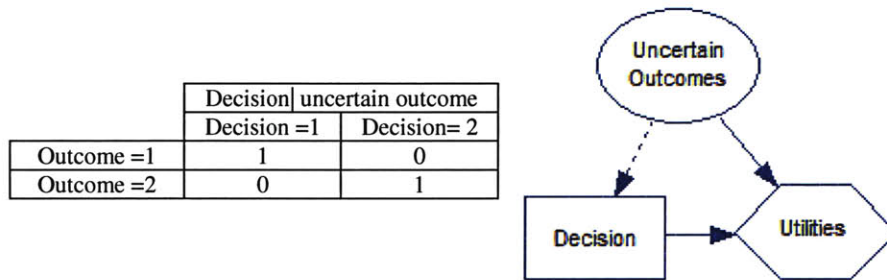


Figure 4.32 Simple one stage decision, plus value of perfect information

Figure 4.33 shows a simple one stage decision plus the value of Imperfect Information or Sample Information. This is defined by the price one would be willing to pay in order to gain information about the distribution from which the prediction has to be made. For example doing test marketing before launching a new product. The expected value of sample information is defined to be the difference between the expected value given the sample information and the expected value without that information. The arrow between uncertain outcome and test reflects the fact that the test results depend on the event. The conditional probability table attached to the node test reflects the fact the test is not perfect, i.e. it is the reliability of the test. The arrow between test and the decision reflects the fact that the results of the test are taken into consideration in the decision making process.



	P (test  uncertain outcome)	
	Test = 1	Test= 2
Outcome =1	0.8	0.2
Outcome =2	0.2	0.8

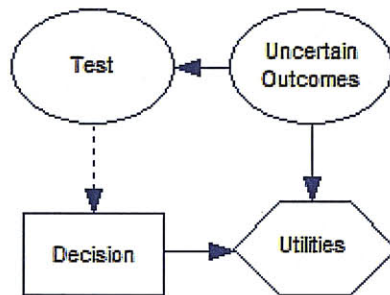


Figure 4.33 Simple one stage decision, plus value of imperfect information

The graph in Figure 4.34 shows a situation where the probabilities are a function of the alternative chosen, e.g. the probability that a threat (hazard) occurs depends on countermeasures taken.

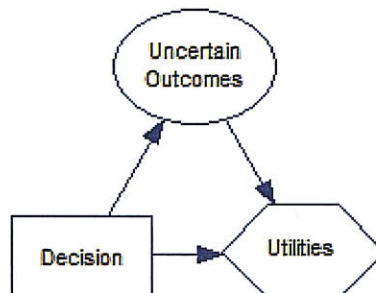


Figure 4.34 Event probabilities depend on the decision

Finally Figure 4.35 shows an example of a two staged decision situation, where the decisions are made sequentially. *Decision 1* is taken first. *Decision 2*, is influence by the results of *Decision 1* and an uncertain event, *Uncertainty 1*. The utilities associated with this specific decision problem depend on the results of both decisions, *Decision 1* and *Decision 2*, as well as on two uncertain events, *Uncertainty 1* and *Uncertainty 2*. An example of such a case could be: *Decision 1*: Choice of construction strategy for a tunnel, for example choice between NATM and TBM methods; *Decision 2*: Choice of pre-support method: None or fiberglass bolts.

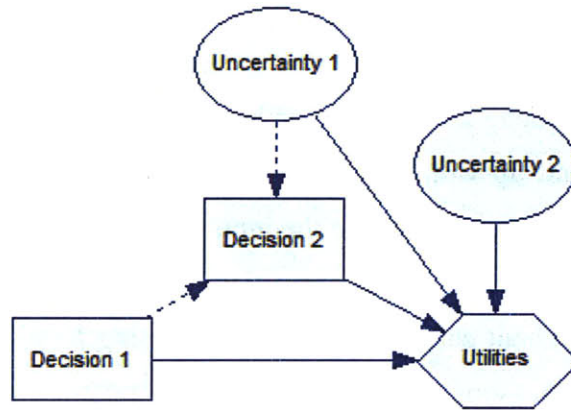


Figure 4.35 Two stage decision

### 4.7.2 Inference for Influence diagrams

The process of inference in an influence diagram consists of computing the expected utility associated with the different decisions or strategies. As in Bayesian networks there are two groups of algorithms that can be used to make inference in an influence diagram: exact and approximate. The most basic of way to solve an influence diagram is to unfold it into a decision tree and solve it. However if one wants to take advantage of the structure of an influence diagram and encoded conditional independences, one of the most common is the Variable Elimination algorithm for influence diagrams which has many similarities to the Variable Elimination technique described for Bayesian Networks. For more details reference is made to Jordan, M., 1998; Jensen, 2001.

## 4.8 Conclusions

There are a number of models available for data representation and decision making, which include rule based - systems, artificial neural networks, Fuzzy-rules, fault and event trees and decision trees. Among these, the Bayesian networks and Influence diagrams are considered to be the most suitable for the problem of accidents during tunnel construction. The main reasons for choosing BN representation over the others are as follows:

- They handle incomplete data sets without difficulty because they discover dependencies among all variables. When one of the inputs is not observed, most models will end up with an inaccurate prediction. That is because they do not calculate the correlation between the input variables. Bayesian networks suggest a natural way to encode these dependencies.
- One can learn about causal relationships by using Bayesian networks. There are two important reasons to learn about causal relationships. This is worthwhile when one would like to understand the problem domain, for instance, during exploratory data analysis. Additionally, in the presence of intervention, one can make predictions with the knowledge of causal relationships.
- Bayesian networks facilitate the combination of domain knowledge and data. Prior or domain knowledge is crucially important if one performs a real-world analysis; in particular, when data are inadequate or expensive. The encoding of causal prior knowledge is straightforward because Bayesian networks have causal semantics. Additionally, Bayesian networks encode the strength of causal relationships with probabilities. Therefore, prior knowledge and data can be put together with well-studied techniques from Bayesian statistics.
- Bayesian methods provide an efficient approach to avoid the over-fitting of data. Models can be “smoothed” in such a way that all available data can be used for training by using Bayesian approach.

In spite their potential to address inferential processes, there are however some limitations to Bayesian Networks:

- Depending on their size they may require initial knowledge of many probabilities. The results are very sensitive to the quality and extent of the prior knowledge, i.e. a Bayesian network is only as useful as this prior knowledge is reliable.
- Performing exact inference on a Bayesian network, as well as learning Bayesian networks from large amounts of data, can have a significant computational cost,

since they are a NP hard tasks<sup>9</sup>. Approximate algorithms can be used in these situations.

- The restriction of the Bayesian Network to be acyclic can be an issue when modeling problems where feedback loops are common features. There are however methods to deal with these situations as demonstrated in section 4.6.4.

Despite their limitations, from all methods, BN is the one with the ability to best represent problems in a complex domain of inherent probability and to provide project managers/ designers/ contractor with good understanding of the problem.

A comparison between the more classical tool for decision analysis, the decision tree, and the Bayesian networks (extended to influence diagrams) will be presented in the next chapter by means of an example, applied to tunneling, in order for a better understanding of similarities and differences between both techniques, as well as their advantages and disadvantages.

## 4.9 References

Ang, A. H-S., and W. H. Tang (1975). "Probability Concepts in Engineering Planning and Design", vol. 1, Basic Principles. New York, NY: John Wiley & Sons.

Baecher, G.B. (1972). "Site Exploration: A probabilistic approach". PhD Massachusetts Institute of Technology, Cambridge, MA.

Cowell., R. G., A. P. Dawid, S. L. Lauritzen, D. J. Spiegelhalter (2003) "Probabilistic Networks and Expert Systems", (Information Science and Statistics, 2003) .

Darlington, K (2000). "The essence of expert systems". Ed. Prentice Hall. 167 pages.

---

<sup>9</sup> NP hard (non-deterministic polynomial-time hard) problem informally that this problem is least as hard as the hardest problems in NP. For a NP hard problem it is not known any polynomial-time (this refers to a running time of an algorithm) algorithm solving the problem (exact solution). To try to solve this problems approximate algorithms are normally used.

Dempster, A.P. (1968). "A generalization of Bayesian inference". Journal of the Royal Statistical Society, Series B 30 205-247.

Eskesen, S.; Tengborg, P., Kampmann, J. and Veicherts, T. (2004) "Guidelines for tunnelling risk management": International Tunnelling Association, Working Group No. 2. Tunnelling and Underground Space Technology. Volume 19, Issue 3, May 2004, pages 217-237

Faber, M.H. (2005). "Risk and Safety in Civil", Surveying and Environmental Engineering. Lecture Notes. Swiss Federal Institute of Technology, ETHZ, Switzerland. 394p.

Jensen, F.V. (1996). "Introduction to Bayesian Networks". Taylor and Francis, London, UK, Springer-Verlag, New York, USA, 1996.

Jensen, F.V. (2001). "Bayesian Networks and Decision Graphs". Taylor and Francis, London, UK, Springer-Verlag, New York, USA, 2001

Jordan, M. (1998) "Learning in Graphical Models", (MIT Press 1998).

Heckerman, D. (1997). "A Tutorial on Learning with Bayesian Networks". Data Mining and Knowledge Discovery, 1:79-119, 1997.

Henrion, M.; Breese, J.; Horvitz, E. (1991). "Decision Analysis and Expert systems". AI Magazine Volume 12 Number 4

Howard, R.A., and J.E. Matheson (editors) (1984). "Readings on the Principles and Applications of Decision Analysis", 2 volumes, Menlo Park CA: Strategic Decisions Group.

Howard, R. A. (1966), "Decision Analysis: Applied Decision Theory," Proceedings of the 4th International Conference on Operational Research (1966) 55-77

Kjaerulff, U.; Madsen, A. (2008). "Bayesian Networks and Influence Diagrams. A Guide to Construction and Analysis". Springer Ed.

Melle, W. V.; Shortliffe, E. H.; Buchanan, B. G. (1981). "Rule-Based Expert Systems. The MYCIN Experiments of the Stanford Heuristic Programming Project". Technical Report Stanford School of Medicine. Published in 1981.

Mehrotra, K., Mohan, C. K. and Ranka, S. (1997) "Elements of Artificial Neural Networks". MIT Press, 344 pages.

Pearl, J., (1988) "Probabilistic Reasoning in Intelligent Systems: Networks of Plausible Inference", (San Mateo, CA: Morgan Kaufmann, 1988).

Russell, S. and Norvig, P. (2003) "Artificial Intelligence. A Modern Approach". Second Edition. Prentice Hall Series in Artificial Intelligence.

Shortliffe, E. H. (1976). "Computer based medical consultations: MYCIN", American Elsevier, 1976.

Silva, C. (2001). "Safety control in railway tunnels. Development of support methodologies and a knowledge based system" (in Portuguese). University of Porto, MSc Thesis, Porto, 267p.

Sonmez, H.; Gokceoglu, C. and Ulusay, R. (2003). "An application of fuzzy sets to the Geological Strength Index (GSI) system used in rock engineering". Engineering Applications of Artificial Intelligence. Volume 16, Issue 3, April 2003, Pages 251-269



Sousa, R.L.; Sousa, L.R.; Silva, C. (2007). "Maintenance of tunnels and the use of AI techniques". 11th ISRM Congress, Specialized Session S5 on Maintenance and Repair of Underground Structures in Rock Masses, Lisbon, 6p.

Suwansawat and Einstein (2006). "Artificial neural networks for predicting the maximum surface settlement caused by EPB shield tunneling". *Tunnelling and Underground Space Technology*. 21 (2) (2006), pp. 133–150

Suwansawat, S. (2002). "Earth pressure balance (EPB) shield tunneling in Bangkok: ground response and prediction of surface settlements using artificial neural networks". PhD Thesis. Massachusetts Institute of Technology. Dept. of Civil and Environmental Engineering.

Zadeh, L.A. (1965). "Fuzzy sets", *Information and Control* 8 (3): 338—353.

Zadeh, Lotfi (1999). "Fuzzy Sets as the Basis for a Theory of Possibility". *Fuzzy Sets and Systems* 1:3-28, 1978. (Reprinted in *Fuzzy Sets and Systems* 100 (Supplement): 9-34, 1999.

Von Neumann, J. and Morgenstern, O. (1944). "Theory of Games and Economic Behavior". Princeton University Press. 625pp.

#### 4.10 Appendix E – Example (adapted from Jensen, F. 1996)

Mary lives in Los Angeles. One morning when she leaves the house, she realizes that her grass is wet. Is it due to the rain (R) or has she forgotten to turn off the sprinkler (S)? Her belief in both events increases.

Next she notices that the grass of her neighbor, John is also wet. Now, she is almost certain that it has been raining. Figure 4.36 represents the network for this situation:

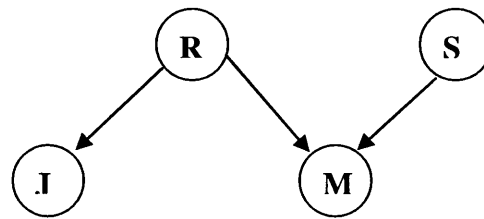


Figure 4.36 Bayesian Network for Grass wet example

R (Rain), S (Sprinkler), J (John's grass wet) and M (Mary's grass wet) are the variables. Yes and No are the states for each variable. J has R as parent. M has S and R as parents, i.e. Rain and Sprinkler are both causes for Mary's grass to be wet.

When Mary notices her own grass is wet, she is doing the reasoning in the opposite direction of the causal arrows. Her observation increases the certainty of both R and S. When Mary checks her neighbor grass, the observation that it is also wet increases the certainty of R drastically, i.e. the certainty that it has been raining or the  $P(R = \text{yes})$  increases after Mary's observation. The fact that the John's wet grass has been explained leads Mary to no longer have any reason to believe that the sprinkler has been on (this is called Explaining away). Hence the certainty that we had on the sprinkler being on ( $S = \text{yes}$ ) is reduced. This is an example of dependence changing with the information available. In the initial state when nothing is known R and S are independent. When we have the information on Mary's grass R and S become dependent.

In order for the network to be complete each variable with parents must have a conditional probability table. We should also have the prior certainties of Rain and Sprinkler. For this model one needs the prior probability of R and S. Lets assume all variables can only have two possible states yes or no and that their probability distribution is  $P(R) = (0.2, 0.8)$  and  $P(S) = (0.1, 0.9)$ , where for example the probability that it was raining is 0.2 ( $R = \text{yes}$ ) and the probability that the Sprinkler was on is 0.1 ( $S = \text{yes}$ ).  $P(J|R)$  and  $P(M|R, S)$  are in presented in table 4. These probabilities must be inputted in order for network to be completed. They can be subjective, or they can be extracted from databases, for example. Table 1 reads the following way:

$$P(J = \text{yes} | R = \text{yes}) = 1.0$$

$$P(J = \text{no} | R = \text{yes}) = 0$$

$$P(J = \text{yes} | R = \text{no}) = 0.2$$

$$P(J = \text{no} | R = \text{no}) = 0.8$$

Table 4.10 Conditional probabilities of the example.  $P(J|R)$

R	$P(J = \text{yes})$	$P(J = \text{no})$
yes	1	0
no	0.2	0.8

From table 1 it is possible to get the probability that john's grass is wet given that was not raining, i.e  $P(J=\text{yes} | R = \text{no}) = 0.2$ . This may implicitly reflect the fact that John might have forgot his sprinkler open during the night, for example.

Table 4.11 Conditional probabilities of the example.  $P(M|R, S)$

S	R	$P(M = \text{yes})$	$P(M = \text{no})$
yes	yes	1	0
yes	no	0.9	0.1
no	yes	1	0
no	no	0	1

From table 2 is possible to get the probability of Mary's grass being wet ( $M = \text{yes}$ ) given that the Sprinkler was ( $S = \text{yes}$ ) on and it was not raining ( $R = \text{no}$ ), i.e.  $P(M = \text{yes} | S = \text{yes}, R = \text{no}) = 0.9$ .

Now one needs to calculate the prior probabilities of  $M$  and  $J$ . For  $P(J)$  first calculate  $P(J, R)$  through  $P(J|R)P(R) = P(J, R)$  and then marginalize  $R$  out ( $P(J) = \sum P(J, R)$ ). The result is  $P(J) = (0.36, 0.64)$ . The result for  $P(J, R)$  is presented in table 3.

Table 4.12 Prior probability table for  $P(J, R)$

R =	P(J = yes)	P(J = no)	=	R =	P(J = yes)	P(J = no)
yes	$1 \times 0.2$	$0 \times 0.2$	=	yes	0.2	0
no	$0.2 \times 0.8$	$0.8 \times 0.8$	=	no	0.16	0.64
				P(J) =	0.36	0.64

For the calculation of  $P(M)$ , first one calculates  $P(M, R, S)$ . This calculation follows the same scheme has before. The product will be  $P(M, R, S) = P(M | R, S) P(R, S)$  and since  $R$  and  $S$  are independent  $P(M, R, S) = P(M | R, S) P(R) P(S)$ . After this one has to marginalize  $R$  and  $S$  in order to obtain  $P(M) = (0.272, 0.728)$ . The prior probability is for  $P(M, R, S)$  is shown in table 4.

Table 4.13 Prior probability table for  $P(M, R, S)$

S	R	P(M = yes)	P(M = no)
yes	yes	0.02	0
yes	no	0.072	0.008
no	yes	0.18	0
no	no	0	0.72
P(M) =		0.272	0.728

The evidence that the Mary's grass is wet can be used to update  $P(M, R, S)$  by annihilating all entries with  $M = \text{n}$  and normalize the table by dividing by the sum of the remaining entries ( $P(M = \text{yes})$ ), i.e. we know that the state of variable  $M$  is yes. The updated distributions of  $P^*(R)$  and  $P^*(S)$  are then calculated by marginalization of  $P^*(M, R, S)$ . The result is in table 5.

Table 4.14 Calculation of  $P^*(M, R, S) = P(M, R, S | M=y)$

S	R	P(M = yes)	P(M = no)		P(M = yes)	P(M = no)
yes	yes	0.02/ 0.272	0	=	0.074	0
yes	no	0.072/ 0.272	0	=	0.264	0
no	yes	0.18/ 0.272	0	=	0.662	0
no	no	0/ 0.272	0	=	0	0
		P (M) =			1	0

Note: if one marginalize S and R out of  $P^*(M, R, S)$   $P(M) = (1, 0)$  and this denotes the fact that state of M is known to be yes,  $P(M=yes) = 1$ .

From marginalization of  $P^*(M, R, S)$  one will get:

$$P^*(R = \text{yes}) = 0.074 + 0.662 = 0.736$$

(it is basically the summation of all possible cases where R =yes.)

$$P^*(S = \text{yes}) = 0.074 + 0.264 = 0.338.$$

The next step is to use  $P^*(R)$  to update  $P(J, R)$  through

$$P^*(J, R) = P(J | R)P^*(R) = P(J, R) \frac{P^*(R)}{P(R)}$$
, where  $P(R)$  is the prior probability of Rain and  $P^*(R)$  is the updated probability of Rain.

Table 4.15 Calculation of  $P^*(J, R)$

R =	P(J = yes)	P(J = no)		R =	P(J = yes)	P(J = no)
yes	0.2 * 0.736/0.2	0	=	yes	0.736	0
no	0.16 * 0.264/0.8	0.64 * 0.264/0.8	=	no	0.0528	0.2112
		P*(J) =			0.7888	0.2112

Note : remember that  $P(R) = (0.2, 0.8)$  and  $P^*(R) = (0.736, 0.264)$

After that one will use the evidence that John's grass is also wet ( $J = \text{yes}$ ) to update the distribution for  $(J, R)$  and get the new updated probability of Rain, i.e.,  $P^{**}(R = \text{yes}) = 0.933$ . Table 7 shows these calculations.

Table 4.16 Calculation of  $P^{**}(J, R) = P(J, R \mid J = \text{yes}, M = \text{yes})$

R =	P(J = yes)	P(J = no)		P(J = yes)	P(J = no)
yes	$0.736 / (0.736 + 0.0528)$	0	=	0.933	0
no	$0.0528 / (0.736 + 0.0528)$	0	=	0.067	0
$P^{**}(J) =$				1	0

Finally one will also want to calculate the probability of the sprinkler being on, given Mary's and John's grass being wet. First, one will calculate  $P^{**}(M, R, S)$  through,

$$P^{**}(M, R, S) = P(M, R, S) \frac{P^{**}(R)}{P^*(R)}, \text{ then by marginalizing one will get } P^{**}(S).$$

Table 4.17 Calculation of  $P^{**}(M, R, S) = P(M, R, S \mid M=\text{yes}, J=\text{yes}) = P(M, R, S \mid M=\text{yes})$

S	R	P(M = yes)	P(M = no)		P(M = yes)	P(M = no)
yes	yes	$0.074 * 0.933 / 0.736$	0	=	0.094	0
yes	no	$0.264 * 0.067 / 0.264$	0	=	0.067	0
no	yes	$0.662 * 0.933 / 0.736$	0	=	0.839	0
no	no	0	0	=	0	0

Note: remember that  $P^*(R) = (0.736, 0.264)$  and  $P^{**}(R) = (0.933, 0.067)$

Marginalizing one will get the probability for Sprinkler (S) to be on.

$$P^{**}(S = \text{yes}) = 0.094 + 0.067 = 0.161$$

This example intends to show how a Bayesian network works. The main idea of these networks is that not everything affects everything. What this model says is that Mary grass state is affected by the rain and the sprinkler but not by John's grass state. John's grass state is only affected by the rain. These are not all the relationships between variables. If I write a joint distribution on these four variables (Rain, Sprinkle, Mary and John) I can express every possible relationship between these variables, and I will have a



Joint probability table with  $2 \times 2 \times 2 \times 2 = 16$  entries. I will have to know  $16 - 1 = 15$  probabilities (minus 1 because the table must add up to one). In the case of the Bayesian network the tables I had to prescribe ( $P(R)$ ,  $P(S)$ ,  $P(M, R, S)$  and  $P(J, R)$ ) also had altogether 16 entries (this is a coincidence!) but the probabilities I have to prescribe are much less because each table is a distribution and they have to add up to one. So the number of probabilities I had to assign was only 8. What one did here was to simplify the model of the world and say that not everything depends on everything in order to have a more compact representation of the joint distribution of these variables and also a more efficient way of doing inference.

According to the Chain rule it is possible to represent the joint probability of  $R, S, J, M$  the following way:

$$P(R, S, J, M) = P(M | J, S, R) \times P(J | S, R) \times P(S | R) \times P(R)$$

Equation 4.44

But according to our model of the world,

$P(M | J, S, R) = P(M | S, R)$ , i.e.  $M$  just depends directly on  $S$  and  $R$

$P(J | S, R) = P(J | R)$ , i.e. according to our model the state of John's grass ( $J$ ) only depends on whether it has been raining ( $R$ ) or not (and not on Mary's Sprinkler ( $S$ ))

$P(S | R) = P(S)$ , i.e. according to our model the fact that the sprinkler was left on (or not) is independent from the fact that it was raining.

We can rewrite Equation 4.44 the following way:

$$P(R, S, J, M) = P(M | S, R) \times P(J | R) \times P(S) \times P(R)$$

Equation 4.45

It is therefore possible to generalize the Chain Rule to Bayesian Networks the following way:

In a Bayesian Network, for a variable  $A_i$  only its parents directly influence it, i.e. variable  $A_i$  is conditional independent from the all other variables except its parents.

Let BN be a Bayesian network over  $U = \{A_1, \dots, A_n\}$ . Then the joint probability distribution  $P(U)$  is the product of all conditional probabilities specified in BN:

$$P(U) = \prod_i^n P(A_i | pa(A_i))$$

Equation 4.46

Where  $pa(A_i)$  is the parent set of  $A_i$ .

## 4.11 Appendix F- Derivation of the ML estimator for a multinomial distribution – one variable

For the case of one variable X and k possible values, we will have:

$$P(X = x_i) = \theta_i, \text{ where } \theta_i \in [0, 1], \sum_{i=1}^k \theta_i = 1 \text{ and } i=1, \dots, k$$

Imagine we have a dataset D. D will be an array of  $M_1, M_2, \dots, M_k$ . where  $M_i$  is the number of times I observed the value i. For example in a die,  $k=6$ , the array D will have 6 components that correspond to the number of times I observed each side of the die.

$P(D: \theta)$  is the probability of our data D, when the model is  $\theta = \langle \theta_1, \theta_2, \dots, \theta_k \rangle$

By applying ML we are trying to find the set of parameters  $\theta_i$  such that if they will make the data as likely as possible.

$$\max_{\theta} P(D: \theta) = \prod_{i=1}^k \theta_i^{M_i}$$

(Proof: imagine my dataset is a sequence of sides of a die  $\langle 1, 3, 1, 3, 4, 1, 2, \dots \rangle$ , assuming that each one of the rolls of the die is independent, then:

$$P(D: \theta) = \theta_2 \theta_3 \theta_1 \theta_3 \theta_4 \theta_1 \theta_2 \dots = \theta_2^2 \theta_3^2 \theta_1^2 \theta_4 \dots, \text{ i.e } P(D: \theta) = \prod_{i=1}^k \theta_i^{M_i}$$

Taking logs on both sides of the equation, one will get:

$$\max_{\theta} \log P(D: \theta) = \sum M_i \log \theta_i$$

Maximizing  $\log P(D : \theta)$ ,

$$\frac{\partial (\log P(D : \theta))}{\partial \theta} = 0 \text{ and}$$

$$\sum_{i=1}^k \theta_i = 1 \Rightarrow \theta_k = 1 - \sum_{i=1}^{k-1} \theta_i$$

Substituting

$$\log P(D : \theta) = \sum_{i=1}^{k-1} M_i \log \theta_i + M_k \log(1 - \sum_{i=1}^{k-1} \theta_i)$$

And then

$$\frac{\partial (\log P(D : \theta))}{\partial \theta} = \frac{M_i}{\theta_i} - \frac{M_k}{\theta_k} = 0$$

Solving for  $\theta_i$ ,

$$\theta_i = \frac{M_i}{M_k} \theta_k$$

Equation 4.47

Based on the previous result (Equation 4.47):

$$\sum_{i=1}^{k-1} \theta_i = \sum_{i=1}^{k-1} \frac{M_i}{M_k} \theta_k = \theta_k \sum_{i=1}^{k-1} \frac{M_i}{M_k}$$

$$1 - \theta_k = \theta_k \sum_{i=1}^{k-1} \frac{M_i}{M_k}$$

$$\theta_k (1 + \sum_{i=1}^{k-1} \frac{M_i}{M_k}) = 1$$

$$\theta_k \left( 1 + \sum_{i=1}^{k-1} \frac{M_i}{M_k} \right) = 1$$

$$\theta_k \left( \frac{M_k}{M_k} + \frac{\sum_{i=1}^{k-1} M_i}{M_k} \right) = \theta_k \frac{\sum_{i=1}^k M_i}{M_k} = 1 \Leftrightarrow \theta_k = \frac{M_k}{\sum_{i=1}^k M_i}$$

Equation 4.48

Substituting  $\theta_k$  (from Equation 4.48) in Equation 4.47 one will get the following final result:

$$\theta_i = \frac{M_i}{\sum_{i=1}^k M_i}$$

## **CHAPTER 5 Risk Assessment and Mitigation**

In this chapter risk assessment and mitigation strategies are developed with the goal of avoiding the major problems described in Chapter 4. The focus will be on determining the “optimal” construction method for a given tunnel alignment. The developed methodology was divided into two parts: Design phase and Construction phase, emphasis being on the construction phase. In this chapter the basic principles of the methodology proposed are presented, and illustrated through a simple example. Basic concepts regarding risk and utility functions, necessary to the understanding of the methodology will be briefly discussed.

Risk assessment and management should be done during:

### **1. Design Phase**

During the design phase, information is available regarding geological, hydrological conditions, as well as regarding construction method costs and times. This information is used to determine, for the different possible alignments the “optimal” construction strategy for each alignment. Most existing tools, determine the “optimal” construction strategy in terms of costs and time. This is what the DAT (Decision Aids for Tunneling) do (See Einstein et al, 1978 and 1987). However, in the context of this study the main focus will be to determine the “optimal” construction strategy (or method) in terms of risk of an undesirable event for each given alignment.

### **2. Construction Phase**

Once an alignment and a construction strategy are chosen, the construction phase starts. During construction information becomes available regarding the geological conditions crossed by the tunnel, behavior of the excavation (e.g.



through deformation and stress measurements) as well as information on the construction. This information should and must be used to update the predictions made during the design phase. In the context of the developed methodology emphasis will be placed on updating the geological conditions for the part of tunnel that has not been excavated based on the geological conditions encountered during excavation. This will then be used to update the “optimal” construction strategy for the remaining unexcavated part of the tunnel.

### 3. Operation Phase

Risk management during operation will not be addressed in this work.

## 5.1 Risk Management

### 5.1.1 Definitions

#### 5.1.1.1 Risk

There are many definitions for risk (see Baecher 1981, Vanmarcke and Bohnenblust 1982). The simplest form to express risk is:

$$R = P[E] \times C$$

Equation 5.1

R is risk

P [E] is the hazard (i.e. the probability of an undesirable event E)

C is the consequence or loss

More generally, for an undesirable event E with different consequences, vulnerability levels are associated, and the risk can be defined as presented below (Einstein, 1997):

$$R = P[E] \times P[C | E] \times u[C]$$

Equation 5.2

R is the Risk

P [E] is the hazard (i.e. the probability of the event)

P [C|E] is vulnerability of event E

u [C] is the utility of consequences C

P [E], the **Hazard** and expresses the uncertainty of an undesirable event

P [C|E], the **Vulnerability** and translates the fact that if the undesirable event occurs the consequences are uncertain. The vulnerability is expressed by a conditional probability.

u [C], the **Utility** of the consequences, is very often expressed in monetary values. However utilities are extremely useful whenever other effects are associated with consequences such as environmental, social, etc.

More generally, for different failure modes,  $E_j$ , with which different consequences (discretized) and hence vulnerability levels are associated, expected risk can be defined as:

$$E[R] = \sum_j \sum_i P[E_j] \times P[C_i | E_j] \times C_i$$

Equation 5.3

$P[C_i | E_j]$  is the vulnerability to the failure mode j

$P[E_j]$  is the probability of failure mode j

Note that since consequences are continuous,  $C_i$  can refer to the average value of

consequences within a range, say  $C_i = \frac{c_i + c_{i+1}}{2}$ , in which case the vulnerability for failure

mode j is:

$$P[C_i | E_j] = P[c_i < C_i \leq c_{i+1} | E_j]$$

Equation 5.4

For one failure mode:

$$E[R] = P[E] \times \sum_i P[C_i | E] \times C_i$$

Equation 5.5

In the context of this chapter the definition of risk that will be used is as follows:

$$E[R] = \sum_j \sum_i P[E_j] \times P[u(C_i) | E_j] \times u(C_i)$$

Equation 5.6

$P[u(C_i) | E_j]$  is the vulnerability to the failure mode j

$P[E_j]$  is the probability of failure mode j

$u(C_i)$  is the utility of consequence i

### 5.1.1.2 Utility Function

In the planning stage of a project, construction managers assess construction options, and estimate project utility based on optimal options (those that maximize utility). One should start off by defining the objective(s). The objective(s) in the vast majority of engineering projects is to maximize utility. It is worth discussing utility and utility functions here in a little more depth.

Utility is defined as a true measure of value for the decision maker. Utility theory provides a framework whereby value can be measured, combined, and compared with respect to a decision maker. Utility functions are functions that describe the decision maker's relative preference between attributes (Bell, D. E., Raiffa, H., & Tversky, A., 1988). When cost or profit is considered the only attribute, the result is the simplest form of utility function, where utility is equated to cost or profit. This is what is most frequently done in practice. Multiattribute utility analyses (Keeney and Raiffa, 1976) though well-established in decision analysis science and management, has found limited use in practical engineering. This section will focus on methods to develop utility

functions based on one single attribute. For methods to develop simple multiattribute utility functions see Keeney and Raiffa, 1976 and a brief description is presented in Appendix G.

Determination of a Utility Function (one attribute)

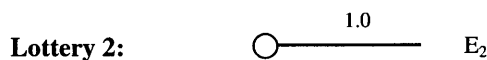
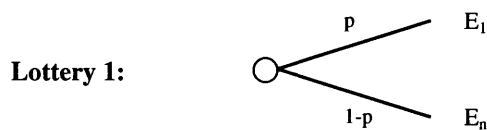
The utility function quantifies the order of preferences for a decision maker, allowing one to express these preferences numerically.

Suppose that there are n events ( $E_1, E_2, E_n$ ) to which utilities are to be assigned. The steps to determine the utility function values are the following (Ang and Tang, 1984):

**Step 1:** Arrange the events in decreasing order of preference:  $E_1 > E_2 > E_3$  (for example)

**Step 2:** Assign a utility 1 to the most preferred event and 0 to the least preferred event:  $u(E_1) = 1$  and  $u(E_n) = 0$

**Step 3:** To determine the utility of  $E_2$  relative to  $E_1$  and  $E_n$ , a method is to offer the decision maker the choice between the following lotteries:

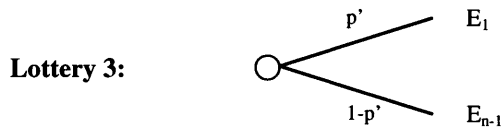


The value of p will be adjusted until the decision maker is indifferent between lottery 1 and lottery 2. An indirect way of obtaining the value of p is to use a probability wheel (see Spetzler & Staël von Hostein 1975). The utility of  $E_2$  will be equal to p, since:

$$\begin{aligned}
 u(\text{Lottery 2}) &= u(\text{Lottery 1}) \\
 u(E_2) &= pu(E_1) + (1 - p)u(E_n) \\
 u(E_2) &= p \times 1 + (1 - p) \times 0 \\
 u(E_2) &= p
 \end{aligned}$$

**Step 4:** Repeat step 3 (n-3) times with  $E_2$  replaced by  $E_3$  to  $E_{n-1}$ , to obtain the utility value of all n events.

**Step 5:** Cross check the values obtained in step 4 for consistency, by repeating step 3 using  $u(E_1)$  and  $u(E_{n-1})$ , as new reference points. Compare  $u'(E_2)$  with the previously obtained  $u(E_2)$



The utility of  $E_2$ ,  $u'(E_2)$  will be equal to:

$$u(\text{Lottery 4}) = u(\text{Lottery 3})$$

$$u'(E_2) = p'u(E_1) + (1 - p')u(E_{n-1})$$

$$u'(E_2) = p \times 1 + (1 - p')u(E_{n-1})$$

One must check that value of  $u'(E_2)$  is the same as the value of  $u(E_2)$  i.e. that the utility of  $E_2$ , is consistent, for this to happen:

$$u(E_2) = u'(E_2)$$

$$p = p \times 1 + (1 - p')u(E_{n-1})$$

**Step 6:** Repeat step 5 (n-4) times with  $E_2$  replaced each time by  $E_3$  to  $E_{n-2}$ , respectively.

If inconsistencies between the obtained utility values are found, the process must be repeated until the values agree satisfactorily.

## Common types of Utility Functions

The shape of the functions will depend on the decision maker's risk preference, i.e. risk neutral, risk averse, or risk prone. A representation of the shape of the utility functions for different risk preferences is shown in Figure 5.1.

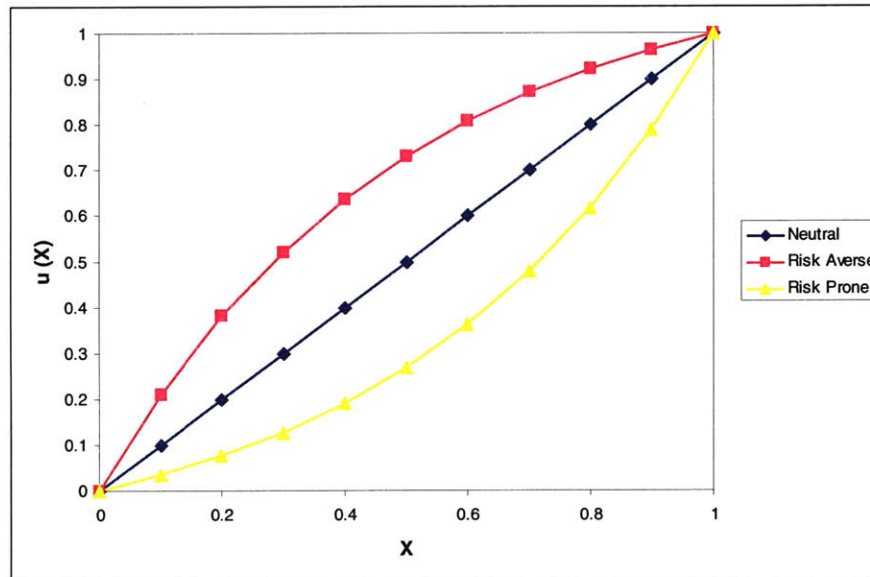


Figure 5.1 Marginal Utility function for different decision maker risk preference.

Several types of functions have been proposed for risk prone, and risk averse decision makers (Ang and Tang, 1976). Examples include logarithmic functions and exponential functions. These are expressed in general terms as, for example the exponential function:

$$u(x) = a + be^{-\gamma x}$$

Equation 5.7

where  $\gamma$  is a parameter that measures the degree of risk aversion or risk proneness.  $a$  and  $b$  are normalization constants. If the utility function is normalized so that  $u(0) = 0$  and  $u(1) = 1$  one will have:

$$u(x) = \frac{1}{1 - e^{-\gamma}} (1 - e^{-\gamma x})$$

Equation 5.8

For positive values, as  $|\gamma|$  increases the decision maker becomes more risk averse. For negative values of  $\gamma$ , as  $|\gamma|$  increases the more risk prone the decision maker becomes (Figure 5.2).

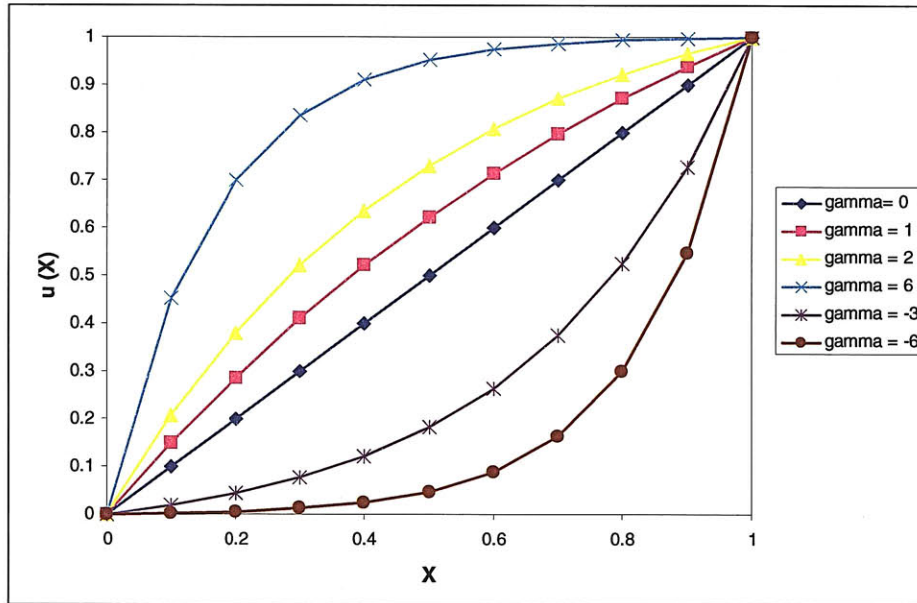


Figure 5.2 Exponential utility function

Consequences are often expressed in monetary units. In some cases monetary value may not be a consistent measure of utility, since the preference order and respective value of consequences may depend on the amount of money involved. The typical utility function for money is illustrated in Figure 5.3 for a risk averse decision maker. Although a decision maker maybe risk prone for positive values (i.e. gain or profit), but he/she is normally risk averse for negative values such as costs. The dotted line in Figure 5.3 shows the utility function for money for a decision maker with a risk neutral preference.



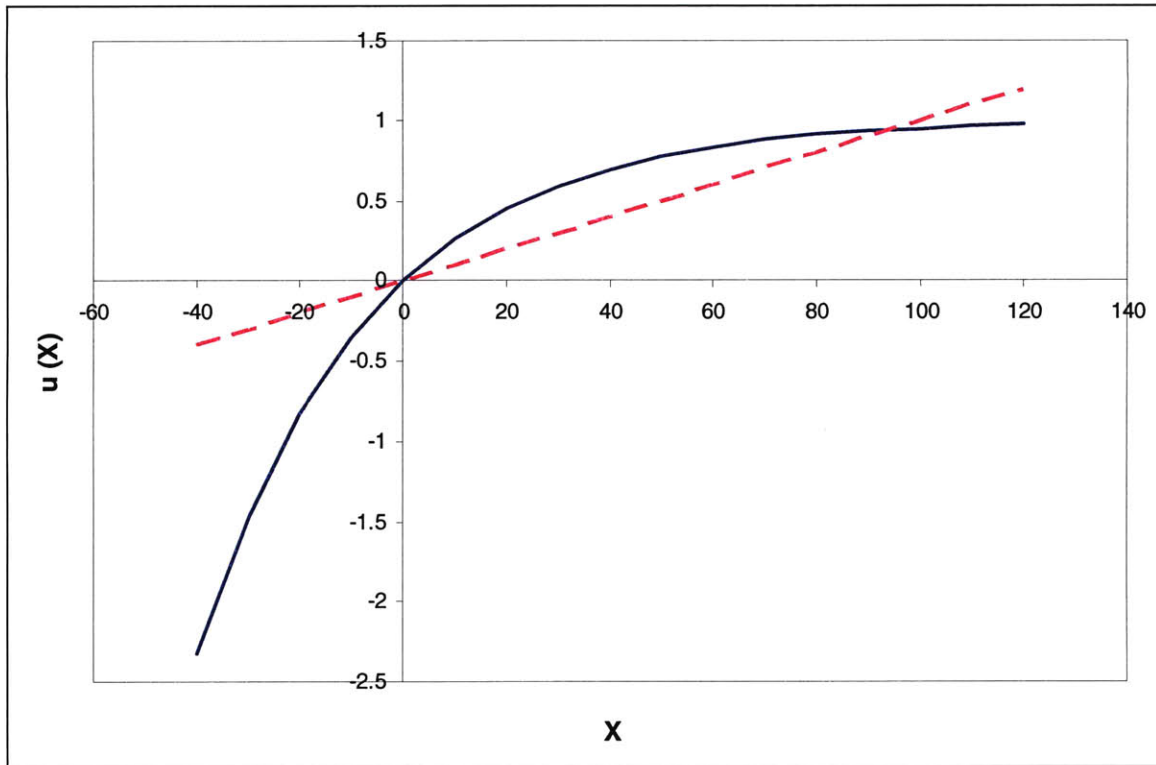


Figure 5.3 utility function for money ( $U(X) = -e^{-3X}$ )

### 5.1.2 “Classic” Risk Analysis techniques

Consider a simple example where an engineer is faced with the choice of two different construction strategies for a tunnel, as for example presented in Figure 5.4.

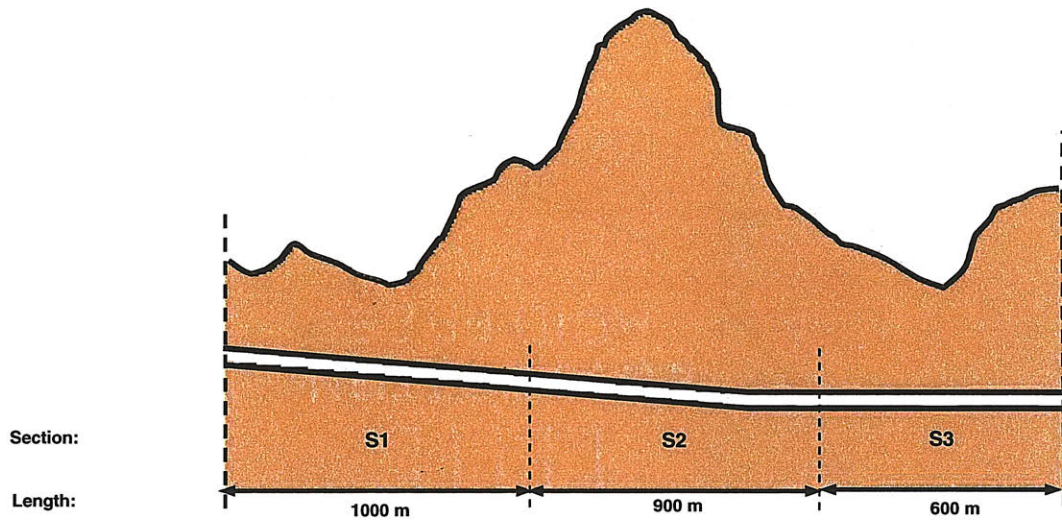


Figure 5.4 Topography and Tunnel Alignment (from Karam et al, 2007)

The tunnel is divided into sections, three in this example, which are assumed to be independent. In each section, different geologic states may be encountered and, consequently, different construction strategies might be used. For the purpose of this example only section 1 will be analyzed. The prior geological states (state variables) for tunnel section 1 are presented in Table 5.1. The construction strategies (decision variables) and associated costs for section 1 are shown in Table 5.2. The probability of failure given the construction strategy and the geological state, i.e. the vulnerabilities, are presented in Table 5.3. The consequences (utilities) associated with failure are presented in Table 5.4

Table 5.1 Prior geological states for section 1

Geological states	Probability
$G_1$	0.40
$G_2$	0.60

Table 5.2 Construction Strategies Costs

Construction strategy	$U = - \text{Cost}$
$CS_1$	-15
$CS_2$	-10

Table 5.3 Probability of Failure given construction strategy and geological state (vulnerability)

	CS <sub>1</sub>		CS <sub>2</sub>	
	G <sub>1</sub>	G <sub>2</sub>	G <sub>1</sub>	G <sub>2</sub>
Failure	0.01	0.001	0.1	0.005
No Failure	0.99	0.999	0.9	0.995

Table 5.4 Consequences of Failure (Utilities)

	CS <sub>1</sub>		CS <sub>2</sub>	
	G <sub>1</sub>	G <sub>2</sub>	G <sub>1</sub>	G <sub>2</sub>
Failure	-35	-25	-90	-70
No Failure	0	0	0	0

Note that construction strategies do not necessarily imply construction methods; strategies can refer to the same construction method, for example, EPBM with different modes of operation or NATM with different support types. Figure 5.5 show an example of different construction strategies. In this case the construction strategies refer to the same construction method, NATM, with different excavation sequences and supports.

In this example, the engineer is worried about failure of the face of the tunnel during construction. It is assumed that there is only one mode of failure.

The cost of constructing tunnel section 1 and associated risk is obtained by considering the section independently of others. A probabilistic model (decision tree) is constructed for each section. Figure 5.6 shows the decision tree for section 1 of the tunnel.

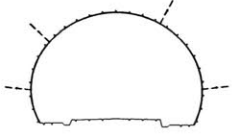
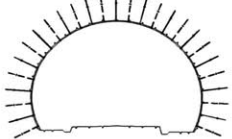
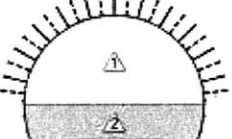
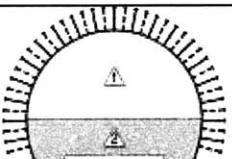
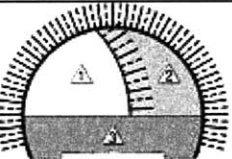
Construction Strategy	Description	
S1	Full face excavation with nominal support	
S2	Full face excavation with extensive support	
S3	Bench cut excavation with nominal support	
S4	Bench cut excavation with extensive support	
S5	Multi-Bench cut excavation	

Figure 5.5 Description of Construction Strategies (Min et al., 2003)

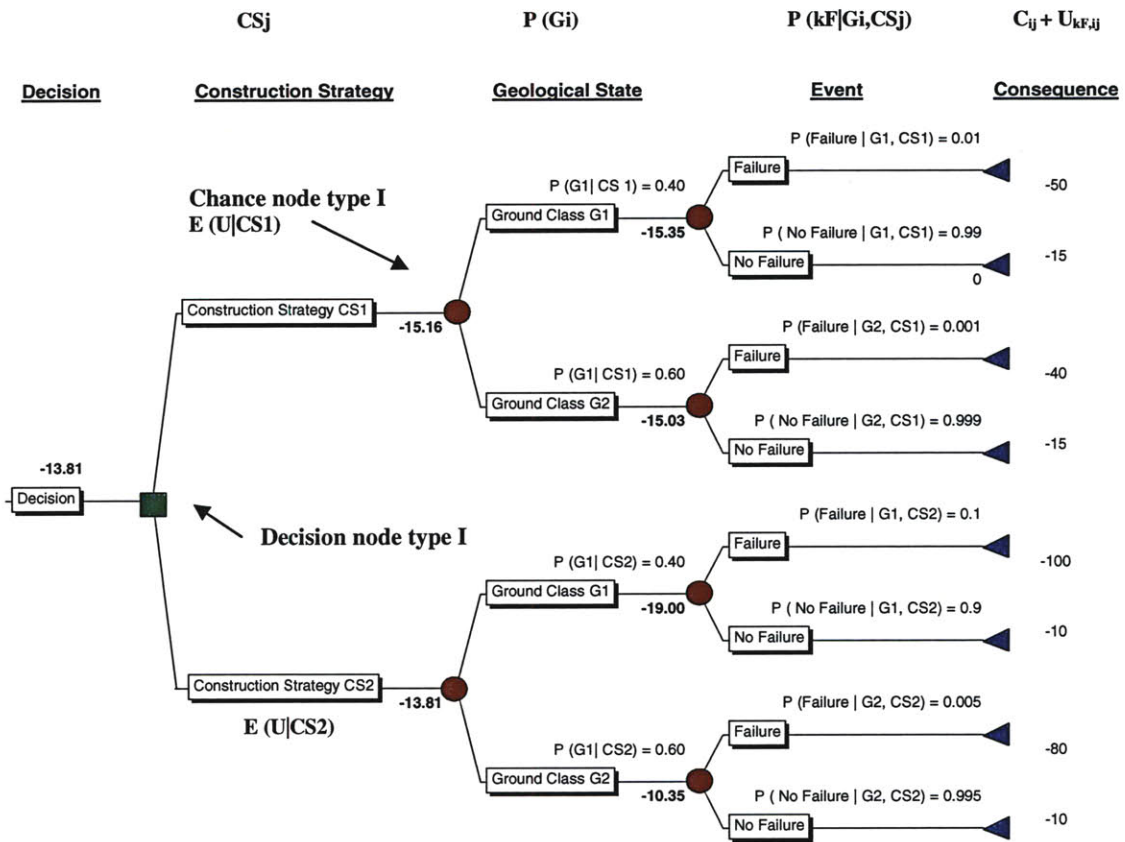


Figure 5.6 Probabilistic Model (Decision Tree) for Section 1

Chance nodes type I show the expected utilities for a given construction strategy, and are computed from:

$$E[U | CS_j] = \sum_{i=1}^n P(G_i) \left( \sum_{k=1}^m P(kF | G_i, CS_j) \times (U_{k,ij} + C_{ij}) \right)$$

Equation 5.9

where:

G<sub>i</sub> represents geologic state

n is the total number of geologic states

CS<sub>j</sub> is the construction strategy

P(G<sub>i</sub>) is the (prior) probability of geologic state i

m is the total number of failure modes (including no failure)

$P(kF | Gi, CSj)$  is probability of failure mode k, in geology i with construction strategy j. Note that in this specific case there are only two failure “modes” (k=1 Failure, k=2 No Failure).

$C_{ij}$  the cost of construction strategy j in geologic state Gi

$U_{k,ij}$  is the utility associated with Failure mode k, in geologic state Gi with construction strategy CSj

At the decision node type I, the maximum expected utility over all construction strategies is computed from:

$$\max_{j=1}^l \{E[U | CSj]\}$$

Equation 5.10

where:

j represents construction strategy

l is the total number of construction strategies

The expected utility of the tunnel section is:

$$E[U] = \max_{j=1}^l \left\{ \sum_{i=1}^n P(Gi) \left( \sum_{k=1}^m P(kF | Gi, CSj) \times (U_{k,ij} + C_{ij}) \right) \right\}$$

Equation 5.11

Decisions are made regarding the optimal construction strategy(ies) based on expected values of utility given the uncertain geology and possible failure mode. In the example above, the optimal construction strategy that leads to maximum utility is construction strategy 2, or CS2, and the maximum utility is -13.81.

### Sensitivity Analysis

Sensitivity analyses allow one to study how the variation of the input variables will change the output of a model. In the specific case of the tunnel decision model, this

means to observe how varying the costs of construction strategies, utilities associated with failure and prior probability distributions, will affect the expected value associated with both construction strategies, CS1 and CS2, and therefore the choice of the “optimal” construction strategy.

Figure 5.7 to Figure 5.10 show sensitivity analyses performed on the decision model of Figure 5.6 where expected utilities of both construction strategies, CS1 and CS2 are compared as the cost of Construction Strategy CS1 and Construction Strategy CS2, Consequences of Failure, Probability of failure in geological state G1 with Construction Strategy CS2 and (prior) probability of geological state are varied.

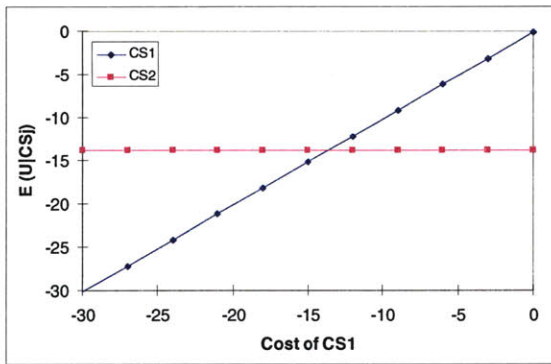


Figure 5.7 Sensitivity analysis – varying the cost of Construction Strategy CS1 (cost expressed in utilities)

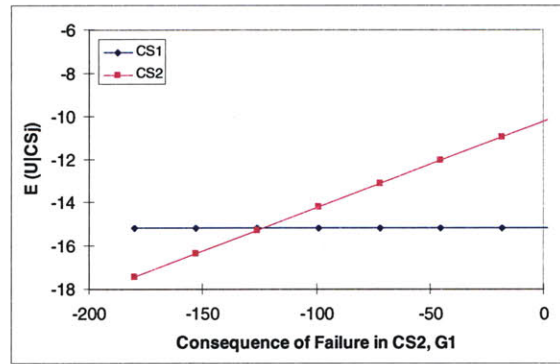


Figure 5.8 Sensitivity analysis – varying the Consequences of Failure using construction strategy CS2 in geology G1

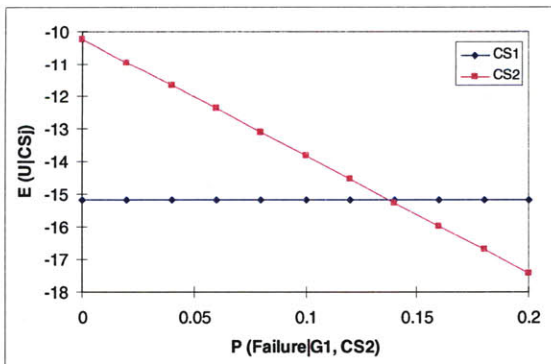


Figure 5.9 Sensitivity analysis – varying the Probability of failure in geological state G1 with Construction Strategy CS2

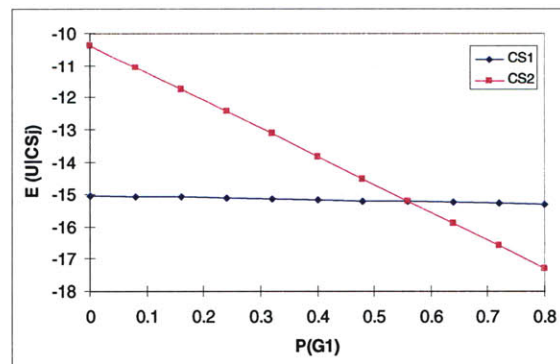


Figure 5.10 Sensitivity analysis – varying the (prior) Probability of geological state G1



By varying the cost of construction strategy CS1 in geology G1, one observes that for a cost of CS1 above 13.65 (monetary units), maintaining all the other variables the same, construction strategy CS2 becomes the “optimal” decision, i.e. the one with the highest expected utility associated (Figure 5.7).

If one varies the utility associated with consequences of failure with construction strategy CS2 (which includes also the cost of construction strategy CS2) in geology G1, as shown in Figure 5.8, it is noted that for utilities below about 133 (monetary units), construction strategy CS2 is the most attractive choice.

When varying the probability of failure in geology G1 with Construction Strategy CS2 the breakpoint between the two constructions strategies, CS1 and CS2, is about  $P(\text{Failure}|G1, \text{CS2}) = 0.138$ , i.e. for values of  $P(\text{Failure}|G1, \text{CS2})$  above 0.138, construction strategy CS1 is the “optimal” choice (see Figure 5.9).

Varying the (prior) probability of geological state has an effect on both the expected utility of construction strategy CS1 and construction strategy CS2. Figure 5.10 shows however that this effect is more pronounced in the case of the expected utility of construction strategy CS2. Also note that for values of  $P(G1)$  below 0.56 (and values of  $P(G2)$  above 0.44) construction strategy CS<sub>2</sub> has the highest utility.

Figure 5.11 shows the relative change of the base value<sup>1</sup> of utility of the cost variables, namely cost of CS1 (base value:-15) and CS2 (base value:-10), consequences of failure in G1 with CS1 (base value:-35) and CS2 (base value:-90) and consequences of failure in G2 with CS1 (base value:-25) and CS2 (base value:-70), and their effect on the expected utility calculated by Equation 5.11. One can observe that the cost of CS1 and the cost of CS2 are the variables that most influence the expected utility. Regarding the consequences of failure, only the “cost” of failure in G1 with CS2 has a significant influence on the expected utility. The change of consequences of failure in G2 (with construction strategy CS1 or CS2), and the consequence of failure in G1 with

---

<sup>1</sup> Base values refer to the values used originally in the model of Figure 5.6.

construction strategy CS1 have little effect on the maximum expected utility, for the considered range of percentage change in the base values (i.e. -100% and +100% of the base value).

The “breaks” in the different curves of Figure 5.11 correspond to values at which  $E(U|CS1) = E(U|CS2)$ . The break point for the utility of the cost of construction CS1 is around -9% of the base value of 15 (utility =-15), i.e. for a cost of CS1 of 13.7. This means that for a cost of CS1 lower than 13.7 (utility =-13.7) the optimal construction strategy is CS1 and for a cost above 13.7 the optimal construction strategy is CS2. The break point for the utility of the cost of construction CS2 is around 20% of the base value of 10 (utility =-10), i.e. cost of CS1 of 12 (utility =-12). For costs of CS2 up to 12, CS2 is still the “optimal” construction strategy and for costs higher than 12, CS1 will become the “optimal” construction strategy. The break point for the utility of consequences (“cost”) of failure in G1 with CS2 is around +37% of the base value (utility=-90), i.e. for a “cost” of failure in G1 with CS2, higher than 123 (utility=-123) the “optimal” construction strategy will be CS1, instead of CS2. The change of consequences of failure in G2 (with construction strategy CS1 or CS2), and the cost of failure in G1 with construction strategy CS1 (for the considered range of variation) have no effect on the “optimal” construction strategy, which will remain CS2, as shown in Figure 5.6.

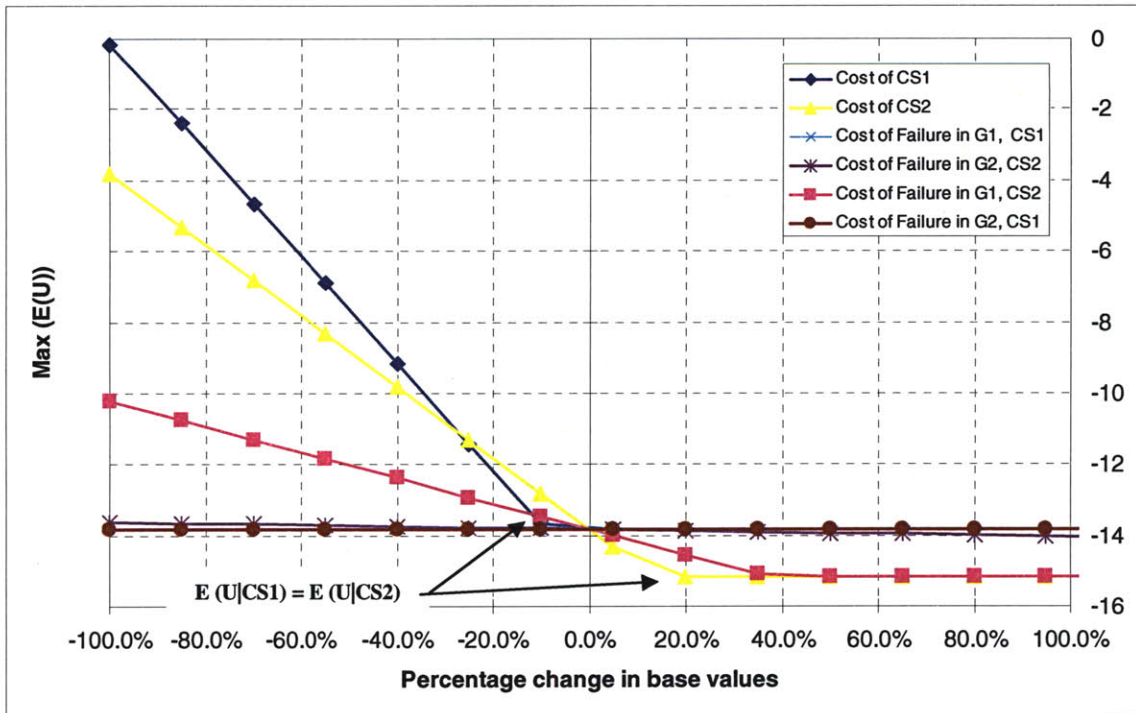


Figure 5.11 Sensitivity analysis – relative change of cost variables and their effect on the max of Expected Utility given the construction strategy (Equation 5.11)

Figure 5.12 shows the effect on the expected utility calculated with Equation 5.11 of the relative change of the base value of the probability of: G1 (base value: 0.4), failure in G1 with construction strategy CS1 (base value: 0.01) and CS2 (base value: 0.1), and failure in G2 with construction strategy CS1 (base value: 0.001) and CS2 (base value: 0.005). The probability of ground classes,  $P(G1)$ , and the probability of failure in G1 with CS2,  $P(\text{Failure}|G1, CS2)$  have the most influence on the expected utilities. For values of  $P(G1)$  up to around 0.56 (and  $P(G2) = 1 - 0.56 = 0.44$ ), the “optimal” construction strategy remains CS2, for  $P(G1) > 0.56$  the “optimal” construction strategy becomes CS1. For values of the  $P(\text{Failure}|G1, CS2)$  lower than 0.137 the “optimal” construction strategy remains CS2, for values above 0.137 the “optimal” construction strategy becomes CS1. The change in  $P(\text{Failure}|G1, CS1)$ ,  $P(\text{Failure}|G2, CS1)$  and  $P(\text{Failure}|G2, CS2)$ , have no effect on the “optimal” construction strategy, which will remain CS2, as shown in Figure 5.6.

The graphs of Figure 5.11 and Figure 5.12 show, which are the variables the model is most sensitive to, i.e. which are the variables that cause the most change to the model's output when varied. The variables that most influence the expected utilities are, for this model, the costs of the construction strategies CS1 and CS2.

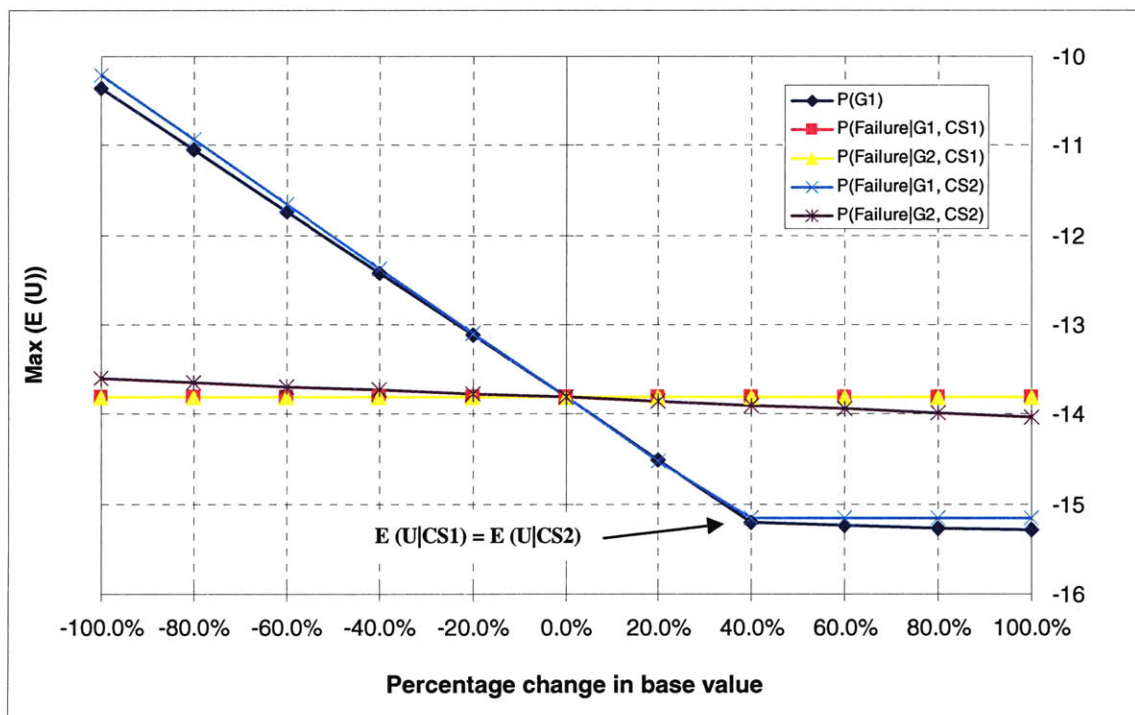


Figure 5.12 Sensitivity analysis – relative change of probabilities and their effect on the max of Expected Utility given the construction strategy (Equation 5.11)

Figure 5.13 shows a two-way analysis where both the cost of construction strategy CS1 and CS2 are varied and their effect on the maximum expected utility is studied. The red line corresponds to values of CS1 and CS2 that yield the same  $\text{Max}(E|U_{CSj})$ . The graph also indicates where  $E(U|CS1) > E(U|CS2)$  and  $E(U|CS1) < E(U|CS2)$ , i.e. where construction strategy CS1 is the “optimal construction” and where construction strategy CS2 is the “optimal construction”, respectively. Figure 5.14 shows the effect of the variation both the cost of construction strategy CS1 and CS2 on the choice for “optimal”

construction strategy. One can observe which is the "optimal" construction strategy for each combination of costs of the two possible strategies.

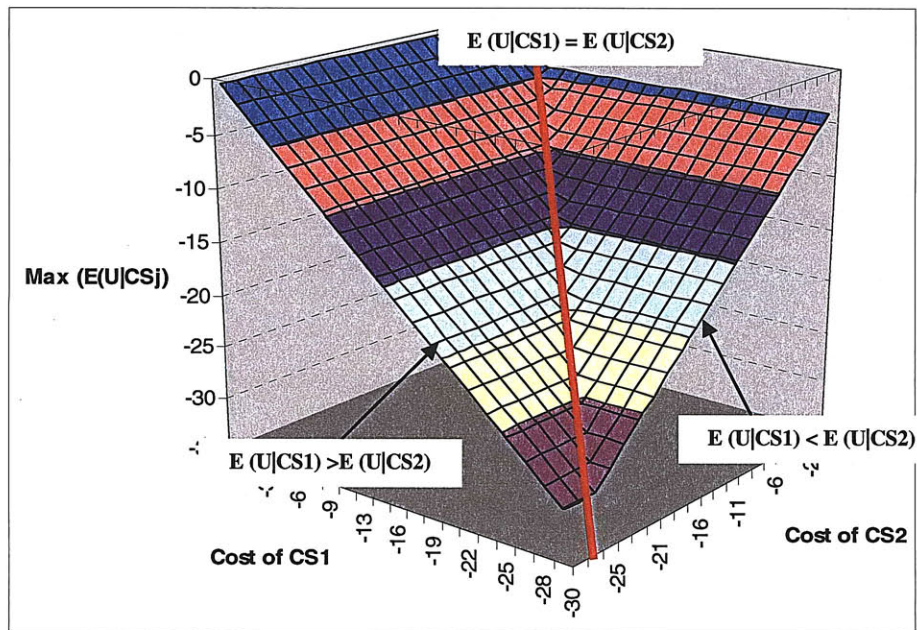


Figure 5.13 Sensitivity analysis – effect of varying cost of CS1 and CS2 on the max of the expected utility given construction strategy

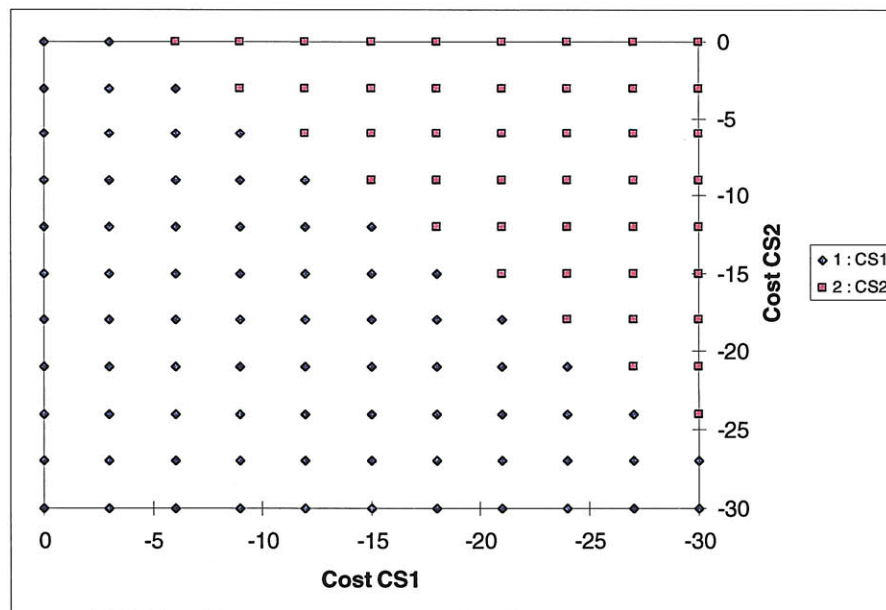


Figure 5.14 Sensitivity analysis – effect of varying cost of CS1 and CS2 on the "optimal" construction strategy



## The cost of changing (where relevant) construction strategies

The construction strategy with highest expected utility in a tunnel section, say  $x$ , may be different than for the construction strategy with highest expected utility in an adjacent section, say  $(x + 1)$ . Costs are incurred when changing (where relevant) construction strategies between adjacent sections. These costs will be referred to as switchover costs. There are several ways in which switchover costs can be incorporated into the analyses. For example, Einstein et al. (1987) use a dynamic programming approach to consider switchover costs when deciding on the optimal construction strategy. When using decision tree analyses (or a Bayesian Network), one inherently determines the most effective construction strategy in each tunnel section (since independence of sections is assumed). For example, Figure 5.6 shows that  $CS_2$  is the most effective construction strategy in section 1 of the tunnel shown in Figure 5.4. More generally, consider part of a tunnel as shown in Figure 5.15.

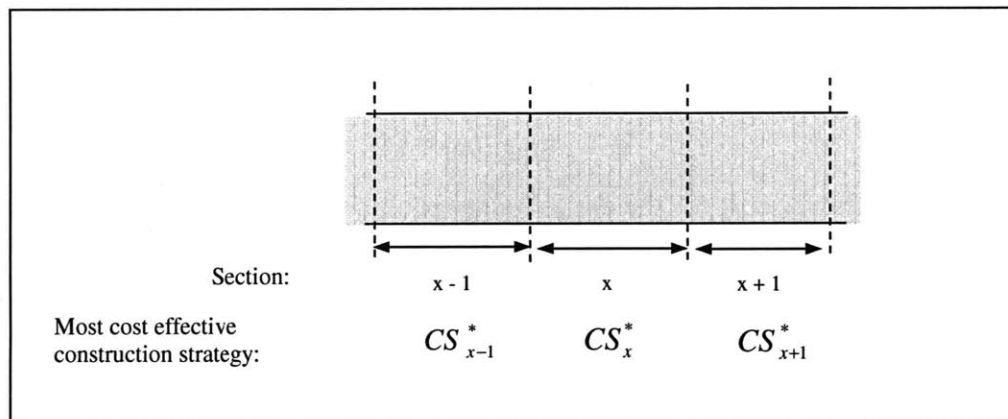


Figure 5.15 Illustration of Most Cost Effective Construction Strategies in Different Tunnel Sections

Let  $CS_x^*$  denote the most effective construction strategy in tunnel section  $x$ , and let  $C_{(x,x+1)}$  denote the cost of switchover from the most cost effective construction strategy in section  $x$  to the most effective construction strategy in section  $(x + 1)$ .  $CS_x^*$  is determined by decision tree analysis (or BN), and  $C_{(x,x+1)}$  is user-specified.  $C_{(x,x+1)}$  is zero if  $CS_x^*$  and  $CS_{x+1}^*$  are the same, and non-zero otherwise.

The switchover costs for the part of the tunnel in Figure 5.15. are therefore:

$$E[C_{switch}] = C_{(x-1,x)} + C_{(x,x+1)}$$

Equation 5.12

where:

$C_{(x-1,x)}$  is the switchover cost from  $CS_{x-1}^*$  to  $CS_x^*$  at the boundary between sections (x – 1) and x

$C_{(x,x+1)}$  is the switchover cost from  $CS_x^*$  to  $CS_{x+1}^*$  at the boundary between sections x and (x + 1)

if  $C_{(x-1,x)}$  and  $C_{(x,x+1)}$  are the same and  $C_{(x-1,x)} = C_{(x,x+1)} = C_{switch}$ , then Equation 5.12, will be written as:

$$E[C_{switch}] = 2 C_{switch}$$

Equation 5.13

The total switchover cost for the entire tunnel is obtained by summing up the switchover costs at all adjacent section boundaries as:

$$C_{switch}^{total} = \sum_{x=1}^{n-1} C_{(x,x+1)}$$

Equation 5.14

where:

n is the total number of sections (leading to n – 1 boundaries)

The total expected cost of the tunnel is given by the sum of the expected construction costs in each tunnel section, expressed in utilities, and the sum of the switchover costs between sections:



$$E[U^{total}] = \sum_{x=1}^n E[U^x] + C_{switch}^{total}$$

Equation 5.15

where:

$E[U^x]$  is the expected construction cost of section  $x$ , expressed in utilities.

$C_{switch}^{total}$  is the total switchover costs (see Equation 5.14)

$n$  is the total number of sections

### Information model phase

During the design phase of a tunnel it is often important to decide on an exploration scheme. Such tunnel exploration planning is also a process of decision making under uncertainty. The information (model) phase is related to the tunnel exploration problem in Table 5.5. In the information phase, one repeats the tunnel utility estimation as in the probabilistic phase but introduces the effects of (virtual) exploration into the analyses.

Table 5.5 Information Phase in Decision Analysis for Tunnel Exploration (after Einstein et al., 1978)

Step	Information (Model) Phase	Exploration for Tunnels
1	Information Model	Effect of exploration on expected construction utility; decision tree
2	Expected value of information (perfect and sample)	Expected value of exploration (perfect and imperfect)
3	Optimal information gathering scheme	Exploration method and configuration (geometry along tunnel)

The steps of for decision of the optimal exploration scheme are as follow (Karam et al, 2007)

### Step 1: Information Model

In step 1 of the information model, the characteristics of exploration (exploration strategies) are assigned. Exploration (exploration strategies) is characterized by its reliability defined as the probability that the exploration results indicate true conditions, and its cost. An information model, which is a decision tree, is used to determine the effects of exploration on expected costs.

### Step 2: Expected value of information (perfect and sample)

In step 2, the expected value of exploration (perfect and imperfect) is determined using the results of the information model (Step 1) and the probabilistic model in section 2.1.

### Step 3: Optimal information gathering scheme

In step 3, the expected value of exploration (perfect and imperfect) is used to determine the optimal information gathering scheme and to devise an optimal exploration plan for the tunnel.

To illustrate this, reconsider the tunnel with the alignment shown in Figure 5.4 with the same uncertain geology as expressed in Table 5.1, and the same utilities and probabilities of failure shown in Table 5.3 and Table 5.4, respectively. Let the characteristics of exploration (exploration reliability) be as shown in Table 5.6.

Table 5.6 Exploration Reliability Matrix

Exploration Indicates Geologic State given Reality	Reality	
	G <sub>1</sub>	G <sub>2</sub>
G <sub>1</sub>	0.6	0.1
G <sub>2</sub>	0.4	0.9

The total expected utility of constructing the tunnel has two main components, namely:

- (a) The expected utility of constructing each tunnel section (cost of construction and utility associated with failure)
- (b) The expected cost of exploration

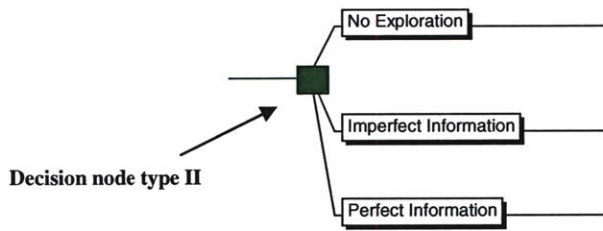


Figure 5.16 Information Decision Model for Section 1

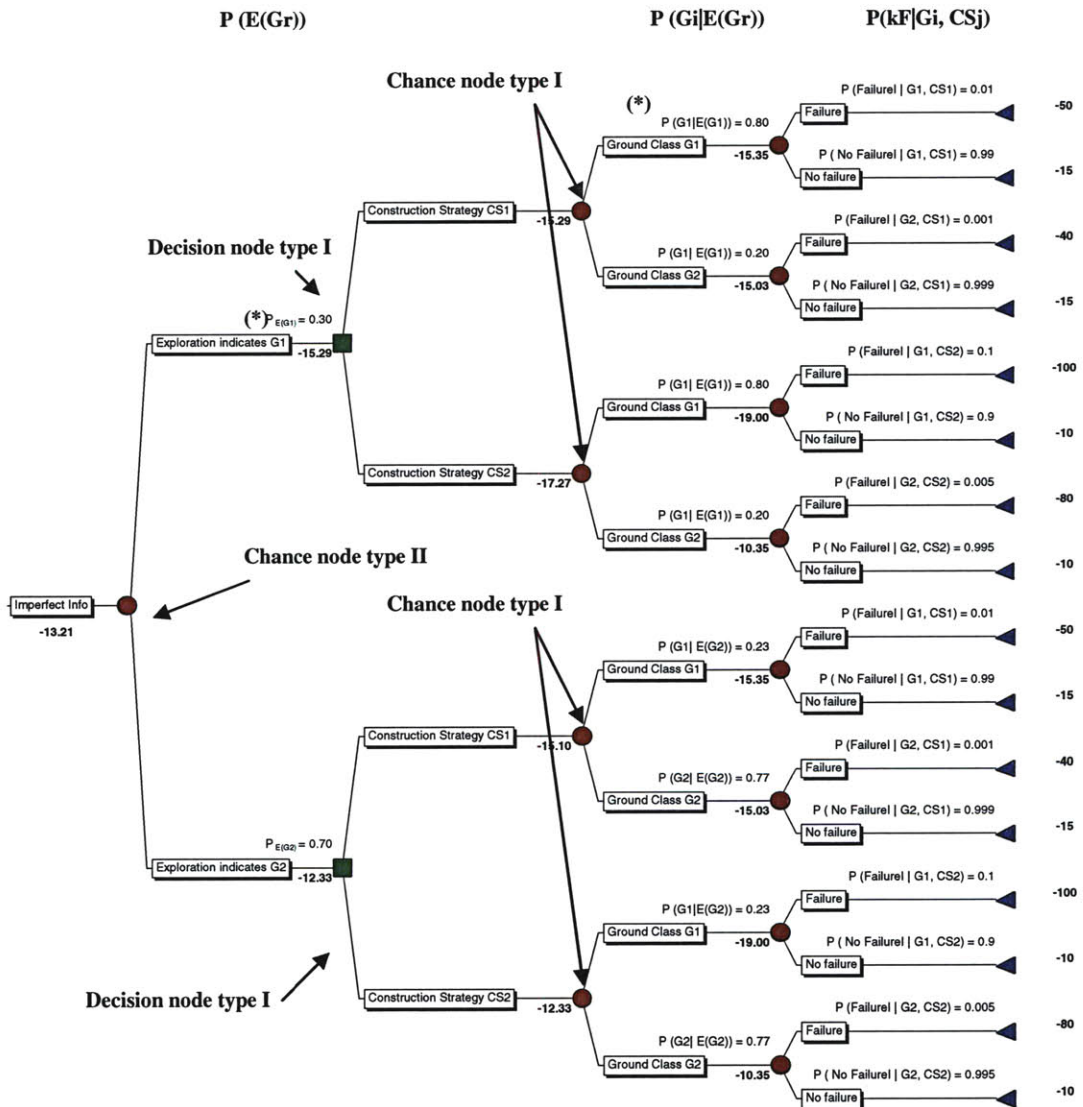


Figure 5.17 Information Sub-Model for Section 1 – Imperfect information  
 (\* For derivation of these probabilities see Equation 5.19 and Equation 5.20)

There are two types of chance nodes and two types of decision nodes in the information model.

Type I chance nodes show the expected utility for a given construction strategy and given exploration results in a certain geologic state. These are computed from:

$$E[U | CS_j \text{ and Exploration indicates } Gr] = \sum_{i=1}^n \left[ P(G_i | E(Gr)) \times \left( \sum_{k=1}^m P(kF | G_i, CS_j) (U_{k,ij} + C_{ij}) \right) \right]$$

Equation 5.16

where:

$i$  and  $r$  represent geologic states

$CS_j$  is the chosen construction strategy

$E(Gr)$  is the geologic state indicated by exploration

$P(G_i | E(Gr))$  is the (posterior) probability of geologic state  $G_i$  given that exploration indicates geologic state  $Gr$

$m$  is the total number of failure modes (including no failure)

$P(kF | G_i, CS_j)$  is probability of failure mode  $k$ , in geology  $i$  with construction strategy  $j$

$U_{k,ij}$  is the utility associated with Failure mode  $k$ , in geologic state  $G_i$  with construction strategy  $CS_j$

$C_{ji}$  is the cost of construction strategy  $j$  in geologic state  $G_i$

The posterior probability of geologic state  $G_i$  given that exploration indicates geologic state  $Gr$  is computed using Bayes' Rule as:

$$P(G_i | E(Gr)) = P(G_i) \frac{P(E(Gr) | G_i)}{P(E(Gr))}$$

Equation 5.17

where:

$P(E(Gr)|Gi)$  is the exploration reliability (from Table 5.6)

$P(E(Gr))$  is the probability that exploration indicates geologic state Gr, and is obtained from the Total Probability Rule as:

$$P(E(Gr)) = \sum_{i=1}^n P(E(Gr)|Gi)P(Gi)$$

Equation 5.18

since the geologic states  $G_i$  are mutually exclusive and collectively exhaustive.

In the example of Figure 5.17, for example, the probability that exploration indicates geologic state G1, was obtained applying Equation 5.18:

$$P(E(G1)) = P(E(G1)|G1)P(G1) + P(E(G1)|G2)P(G2) = 0.6 \times 0.4 + 0.1 \times 0.6 = 0.3$$

Equation 5.19

The posterior probability of geologic state G1 given that exploration indicates geologic state G1 is computed using Bayes' Rule as in Equation 5.17:

$$P(G1|E(G1)) = P(G1) \frac{P(E(G1)|G1)}{P(E(G1))} = 0.4 \frac{0.6}{0.3} = 0.8$$

Equation 5.20

At Type I decision nodes, the maximum expected utility over all construction strategies for a given exploration result is computed as:

$$\begin{aligned} & \max_{j=1}^l \{E[U | CSj, \text{Exploration indicates } Gr]\} = \\ & = \max_{j=1}^l \left\{ \sum_{i=1}^n P(Gi | E(Gr)) \left( \sum_{k=1}^m P(kF | Gi, CSj) (U_{k,ij} + C_{ij}) \right) \right\} \end{aligned}$$

Equation 5.21

The Type II chance node shows the expected utility of imperfect exploration, and is given by:

$$E[U_{\text{imperfect Exploration}}] = \sum_{r=1}^n \left\{ P(E(Gr)) \max_{j=1}^l \left\{ \sum_{i=1}^n P(Gi | E(Gr)) \left( \sum_{k=1}^m P(kF | Gi, CSj) (U_{k,ij} + C_{ij}) \right) \right\} \right\}$$

Equation 5.22

The Type II chance node can also give the expected utility of perfect exploration. This is obtained using the identity matrix as the exploration reliability matrix. When this is the case, the exploration reliability  $P(E(Gr) | Gi)$  has a value of one when  $r$  and  $i$  are the same, and is zero otherwise. Equation 5.22 becomes:

$$E[U_{\text{Perfect Exploration}}] = \sum_{r=1}^n \left\{ P(E(Gr)) \max_{j=1}^l \left( \sum_{k=1}^m P(kF | Gi, CSj) (U_{k,ij} + C_{ij}) \right) \right\}$$

Equation 5.23

At the Type II decision node (Figure 5.16), one can decide on whether to explore or not based on the costs of no exploration, perfect exploration, and imperfect exploration. The decision needs, however, to consider the cost of exploration, and this is shown next.

### The expected cost of exploration

The cost of exploration is cost that enters into the total cost of construction of the tunnel, expressed in utilities. If  $C_{\text{exp}}$  denotes the expected cost of exploration, then the expected utility of perfect exploration and imperfect exploration are given by:

$$E[U_{\text{Perfect Exploration}}] = \sum_{r=1}^n \left\{ P(E(Gr)) \max_{j=1}^l \left( \sum_{k=1}^m P(kF | Gi, CSj) (U_{k,ij} + C_{ij}) \right) \right\} + C_{\text{exp}}$$

Equation 5.24

And,

$$E[U_{\text{imperfect Exploration}}] = \sum_{r=1}^n \left\{ P(E(Gr)) \max_{j=1}^l \left\{ \sum_{i=1}^n P(Gi | E(Gr)) \left( \sum_{k=1}^m P(kF | Gi, CSj) (U_{k,ij} + C_{ij}) \right) \right\} \right\} + C_{\text{exp}}$$

Equation 5.25

The Expected Value of Sample Information (EVSI) is defined as:

$$EVSI = E[U_{\text{imperfect exploration}}] - E[U_{\text{noexploration}}]$$

Equation 5.26

Where

$E[U_{\text{imperfect exploration}}]$  is the expected value of imperfect exploration give by Equation 5.25.

$E[U_{\text{noexploration}}]$  is the expected value of no exploration give by Equation 5.10.

In the previous example the Expected Value of Sample Information (EVSI) is:

$$EVSI = E[U_{\text{imperfect exploration}}] - E[U_{\text{noexploration}}]$$

$$EVSI = -13.21 - (-13.81 + C_{\text{exp}})$$

$$EVSI = 0.6 + C_{\text{exp}}$$

This means that it is worth to explore as long as the cost of exploration is less than 0.6 (note that  $C_{\text{exp}}$  is a negative value).

### Sensitivity Analysis

As for the probabilistic model, sensitivity analysis can also be performed to assess the influence of the different variables on the expected utility of imperfect information. Figure 5.18 shows the effect of the (prior) probability of geological state G1 on the expected value of sample (or imperfect) information.



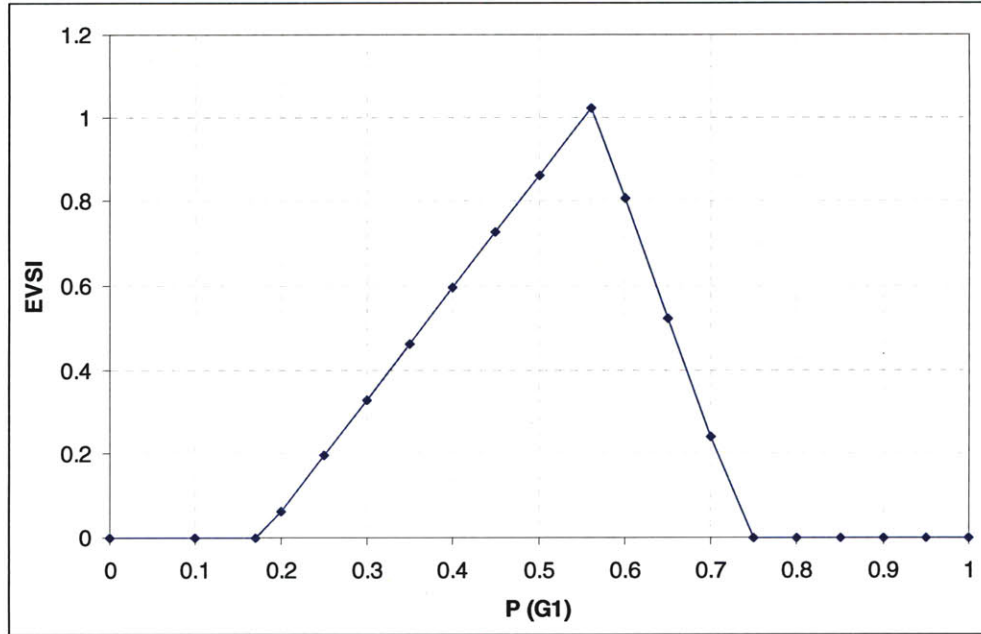


Figure 5.18 Effect of P (G1) on the expected value of sample information (EVSI)

Note that as the P (G<sub>1</sub>) increases, so does the EVSI, until P (G<sub>1</sub>) reaches 0.56, after which EVSI decreases with the increase of P (G<sub>1</sub>), until it becomes zero, when P (G<sub>1</sub>) reaches 0.75. It makes sense that when P (G<sub>1</sub>) is closer to 0 and 1, the EVSI is closer to zero, since in these cases the “certainty” of the geological state is higher, i.e. one is more certain that either state G<sub>1</sub> (in case of P (G<sub>1</sub>) close to 1) or state G<sub>2</sub> (in case of P (G<sub>1</sub>) close to 0) will occur. In these cases it is not as beneficial to explore as in the cases where one is less certain of the geology. The highest EVSI occurs at about P (G<sub>1</sub>) = 0.56. This has to do with the fact that for this value the expected value of both construction strategies is extremely close (see Figure 5.10), and therefore the value of getting information will be higher since it will set apart the two choices (CS1 and CS2) further.

### 5.1.3 Bayesian Networks and Influence Diagrams

The decision problem regarding the tunnel in Figure 5.4 can be modeled by the Bayesian Network (Influence diagram) in Figure 5.19 models the tunnel problem of Figure 5.4, for Section 1.

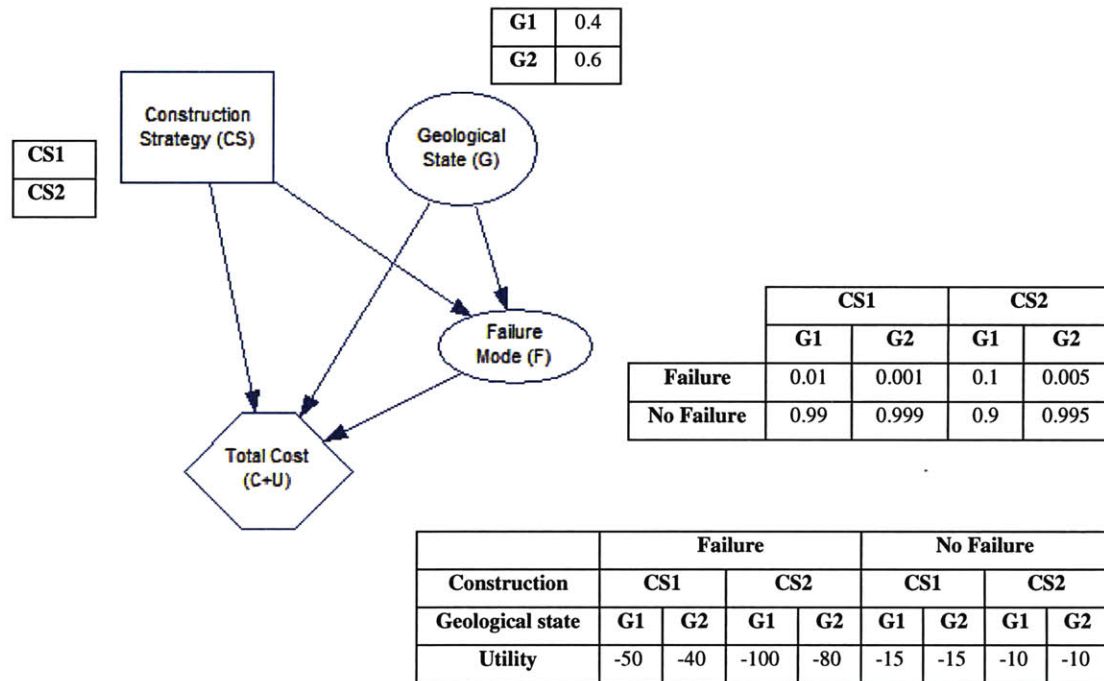


Figure 5.19 Bayesian Network for tunnel problem on Figure 5.4

The network consists of:

- Two chance nodes, *geological state* which represents the two possible geological states G1 and G2; and *Failure mode*, which represents the probability of failure. Attached to the geological state chance node is the prior probability table (same as the one in Table 5.1); and attached to the failure mode chance node is the conditional probability table, Probability of Failure given construction strategy and geological state, which is the same as the vulnerability presented in Table 5.3.
- One decision node, *Construction strategy*, which represents the two possible construction strategies.
- One utility node, “*Cost*” of failure which represents the sum of costs associated with the different construction strategies ( $C_{ij}$ ) and the utilities associated with failure ( $U_{k,ij}$ ). Attached to these nodes are the utilities associated with the consequences of failure (combination of Table 5.2 Table 5.4).

The arrows in Figure 5.19 represent the relationship and influence between variables. The Failure mode is influenced by the *geological state* and *construction strategy* used; the two arrows coming into this node reflect this. The “cost” of failure depends on the *failure mode*, the *construction strategy* and the *geological state*.

There are several algorithms to solve Influence Diagrams. The one used in this example is named *Policy Evaluation* (similar to variable elimination for Bayesian Networks). The *Policy Evaluation* algorithm solves the whole model, exploring all the possible combinations of decision nodes and observations. For all those combinations, it also calculates the posterior distributions of all those nodes in the network that are impacted by them. For more details see Chapter 4, Section 4.7.2.

The results after evaluating the influence diagram of Figure 5.19 are shown next in Figure 5.20.

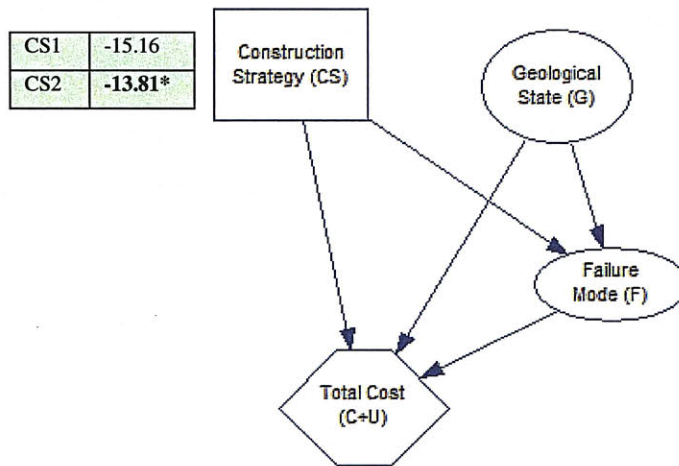


Figure 5.20 Results for influence diagram of Figure 5.19

(\* the same as decision node type I in Figure 5.6)

According to the model the “optimal” construction strategy based on the initial data is CS1 the same result was obtained with the decision tree. As in the decision tree sensitivity analyses can be conducted to assess the influence of the different variables on the “optimal” construction strategy. The results are the same as the ones presented in Figure 5.7 to Figure 5.10.

## Information model phase

The information model using Bayesian Networks / Influence Diagrams is presented in Figure 5.21.

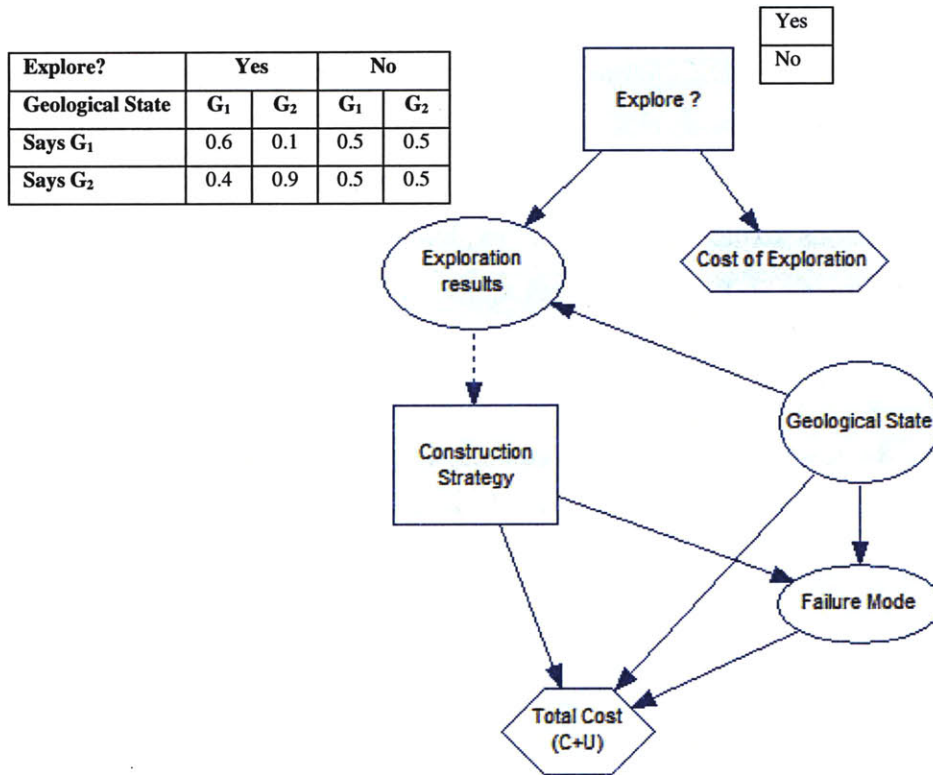


Figure 5.21 Information model

The information model contains three additional nodes:

- A decision node, *explore?*, which represents the option of exploring or not.
- A chance node, *exploration results*, with values “says G<sub>1</sub>” and “says G<sub>2</sub>”, which represent the outcome of the exploration.
- A utility node *cost of exploration*, which represents the cost associated with the exploration. In the model, the cost of exploration was not included in order to compare the results of the Bayesian network with the decision tree.

The *Exploration results* depend on the actual *geological state* and whether or not one explores (*explore?* decision node). The dashed arrow between the *exploration results* node and the *construction strategy* node denotes the fact that the construction strategy decision is posterior (in time) to the decision of *exploring*, and therefore to the *exploration results*. This is the same in the decision model represented in Figure 5.16 and Figure 5.17 by a tree. The node *Explore?* in Figure 5.21 corresponds to the decision node type II of Figure 5.16 and the node *Construction Strategy* to decision type node I in Figure 5.17. Attached to the exploration results node is the conditional probability table that represented the probability that the exploration indicates a Geologic State given the reality, for both decisions exploration and no exploration. This is the same as the exploration reliability matrix in the case of exploration (Table 5.6). The analysis of the information model yielded the following results, presented in Figure 5.22.

As one can observe the results are the same as calculated in Figure 5.17 with the decision tree. The Expected value of sample (or imperfect) information (Equation 5.26) will be as follows:

$$EVSI = E[U_{\text{imperfect exploration}}] - E[U_{\text{no exploration}}] = -13.21 - (-13.81) = 0.6 \text{ (monetary units)}$$

Note that the cost of exploration must be less than the EVSI in order to be worth it to explore.

Yes	-13.21
-----	--------



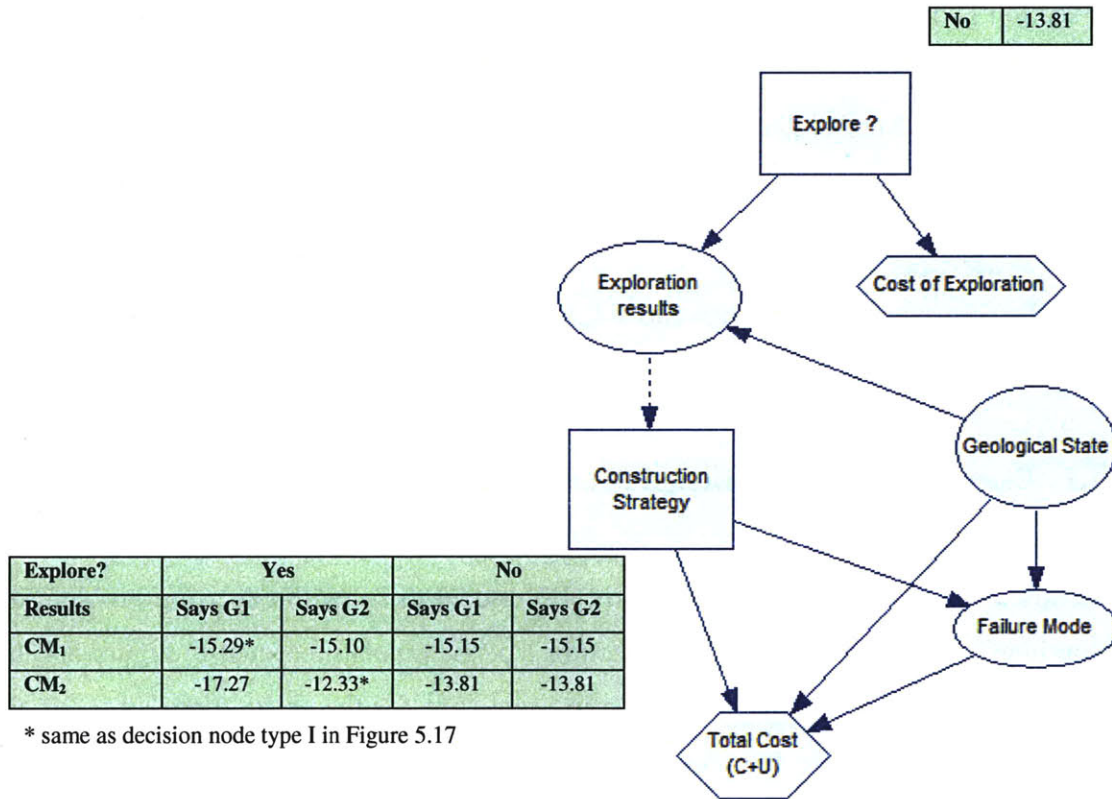


Figure 5.22 Information model results

## 5.2 Proposed Methodology for Decision Making during Design Phase and Construction Phase

In this section a methodology for risk assessment and decision making, using Bayesian networks, for tunnel projects during design phase and construction phase will be proposed.

### 5.2.1 Design Phase

During the design phase, the engineer will come up with the different strategies that he/she would like to evaluate. The engineer will then divide the tunnel alignment into different sections of more or less homogeneous conditions, similar to what is done in Figure 5.4.

Each section is then treated independently. For each section the following information is needed:

- Prior probability of geological states,  $P_{Gi}$
- Vulnerability, i.e. the probability of failure mode  $k$ , in geology  $i$  with construction strategy  $j$ ,  $P_{kFij}$
- The consequences of Failure mode  $k$ , expressed in utilities,  $U_{k,ij}$
- Cost of changing (where relevant) construction strategies,  $C_{switch}$ .

### 5.2.1.1 Example application (Design Phase)

In Section 5.1.3, Figure 5.19 represents the BN model to solve the decision problem of the “optimal” construction strategy for Section 1 of the tunnel presented in Figure 5.4. In order to determine the “optimal” construction sequence for the entire tunnel, i.e. for all three sections a model like the one presented on Figure 5.23 must be used. In order to complete the model the prior probability of the geological state for all sections, which are presented in Table 5.7, must be considered.

In this specific example the construction costs for each section are the ones presented in Table 5.8, and the vulnerability and cost of failure expressed in utilities, in Table 5.3 and Table 5.4, are the same for all sections. Finally consider that the cost of switching construction strategies is  $C_{switch} = 0$ . The goal of the analysis is to determine the optimal sequence of construction strategies for the tunnel presented in Figure 5.4, based on the available information.



Table 5.7 Geological state prior probability for each section

a) Section 1

b) Section 2

c) Section 3

Geological states	Probability
G <sub>1</sub>	0.40
G <sub>2</sub>	0.60

Geological states	Probability
G <sub>1</sub>	0.70
G <sub>2</sub>	0.30

Geological states	Probability
G <sub>1</sub>	0.10
G <sub>2</sub>	0.90

Table 5.8 Construction costs for each section (in utilities)

a) Section 1

b) Section 2

c) Section 3

Construction strategy	U = - Cost
CS <sub>1</sub>	-15
CS <sub>2</sub>	-10

Construction strategy	U = - Cost
CS <sub>1</sub>	-13.5
CS <sub>2</sub>	-9

Construction strategy	U = - Cost
CS <sub>1</sub>	-9
CS <sub>2</sub>	-6

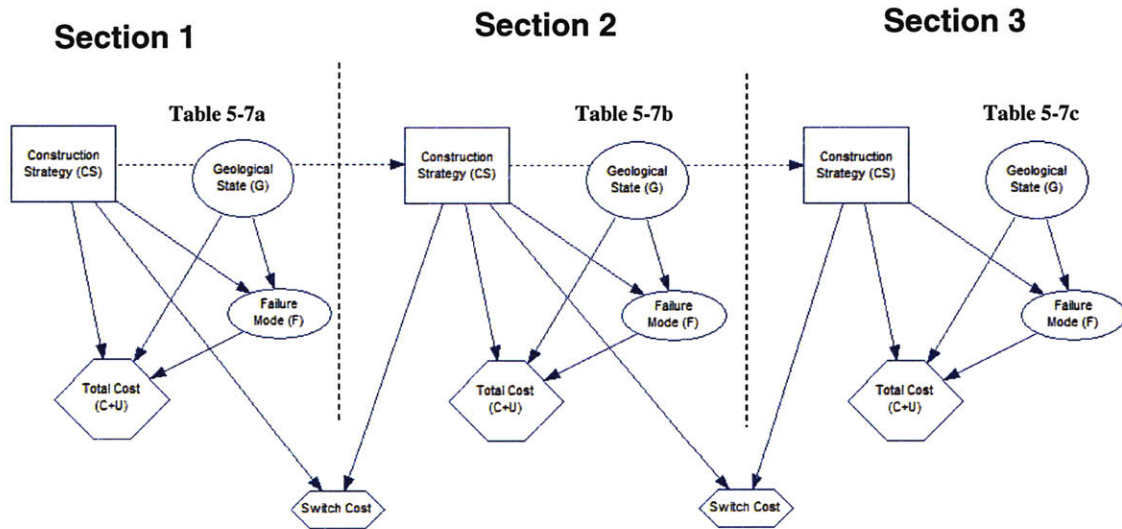


Figure 5.23 Influence diagram for Design phase

### Results

The Influence diagram for the design phase, presented in Figure 5.23, was solved using the *Policy Evaluation* algorithm. This algorithm computes the maximum expected utility for the whole tunnel and corresponding optimal construction strategy sequence. The total maximum expected utility for the tunnel is  $E(\text{Utility}) = -34.76$  and the corresponding

optimal construction strategy sequence is to use construction strategy CS2 in section 1 ( $E(U) = -13.81$ ), switch to construction strategy CS1 in section 2 ( $E(U) = -13.75$ ) and then switch back to construction strategy CS2 in section 3 ( $E(U) = -7.20$ ). A summary of the maximum expected utilities of the construction for each section, S1, S2 and S3 is presented in Figure 5.25. Since the Policy Evaluation algorithm only computes the maximum expected utility for the whole tunnel, in order to obtain the maximum utility at each section one needs to solve each Section individually without considering Switchover costs, as presented in Figure 5.24.

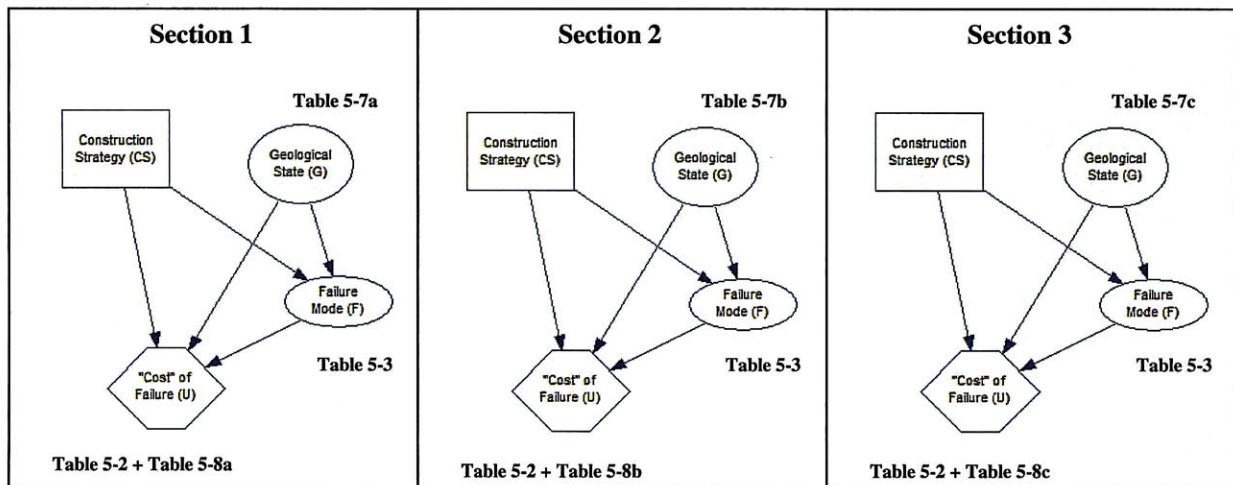


Figure 5.24 Influence diagrams used determined the max expected utility for each section

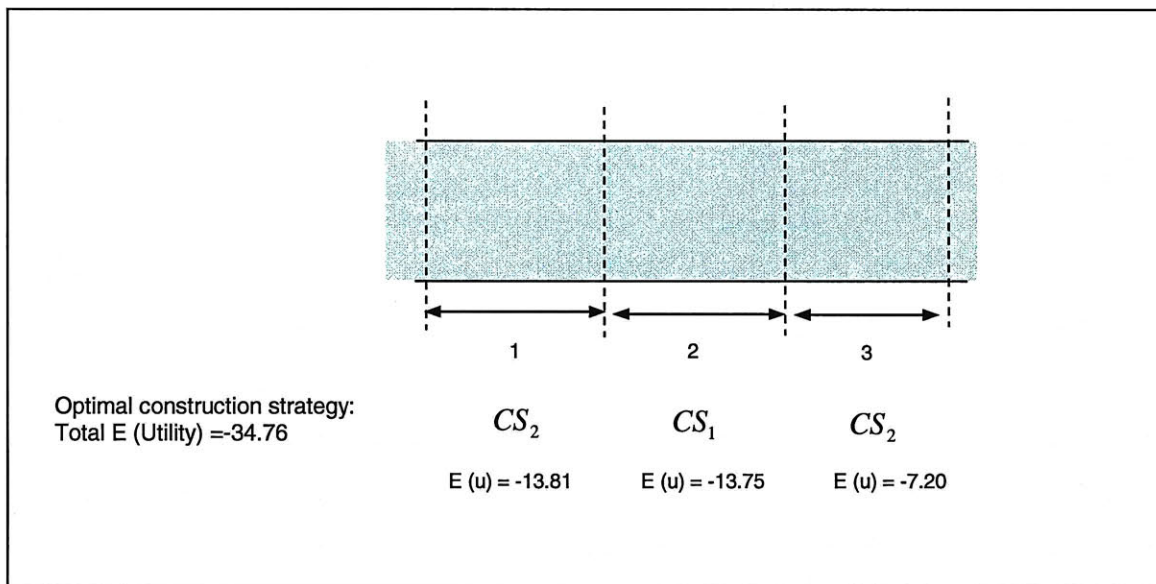


Figure 5.25 Optimal construction strategy for construction of tunnel presented in Figure 5.4

To determine the maximum switchover cost at which is no longer worth it to switch from construction strategy CS2 in Section 1 to construction strategy CS1 in Section 1, one must compare both options. Figure 5.26 shows two options for construction strategies for construction of tunnel presented in Figure 5.4: 1) Construction sequence presented in Figure 5.25 2) Construction sequence that consists on excavating the tunnel using construction strategy CS2 in all sections. Considering that there are costs associated with switching construction strategies (i.e. switchover costs are different from zero), then the maximum switchover cost possible for option 1 to be the optimal is (applying Equation 5.14 and Equation 5.15):

Option 1:

$$E(U^{total:option1}) = E(U^{section1}) + E(U^{section2}) + E(U^{section3}) + C_{switch}^{total} =$$

$$= -13.81 + (-13.75) + (-7.20) + 2C_{switch} = -34.76 + 2C_{switch}$$

Option 2:

$$E(U^{total:option2}) = E(U^{section1}) + E(U^{section2}) + E(U^{section3}) + C_{switch}^{total} =$$

$$= -13.81 + (-15.41) + (-7.20) = -36.42$$

So for switchover costs above  $C_{switch} = -0.83$ , option 1 is no longer the optimal construction sequence, as shown below

$$E(U^{total:option1}) < E(U^{total:option2})$$

$$-34.76 + 2C_{switch} < -36.42$$

$$|C_{switch}| > 0.83$$

If the switchover costs are  $C_{switch} = -0.83$  then option 1 and option 2 are both “optimal” since they have the same expected utility. This is shown in Figure 5.26.

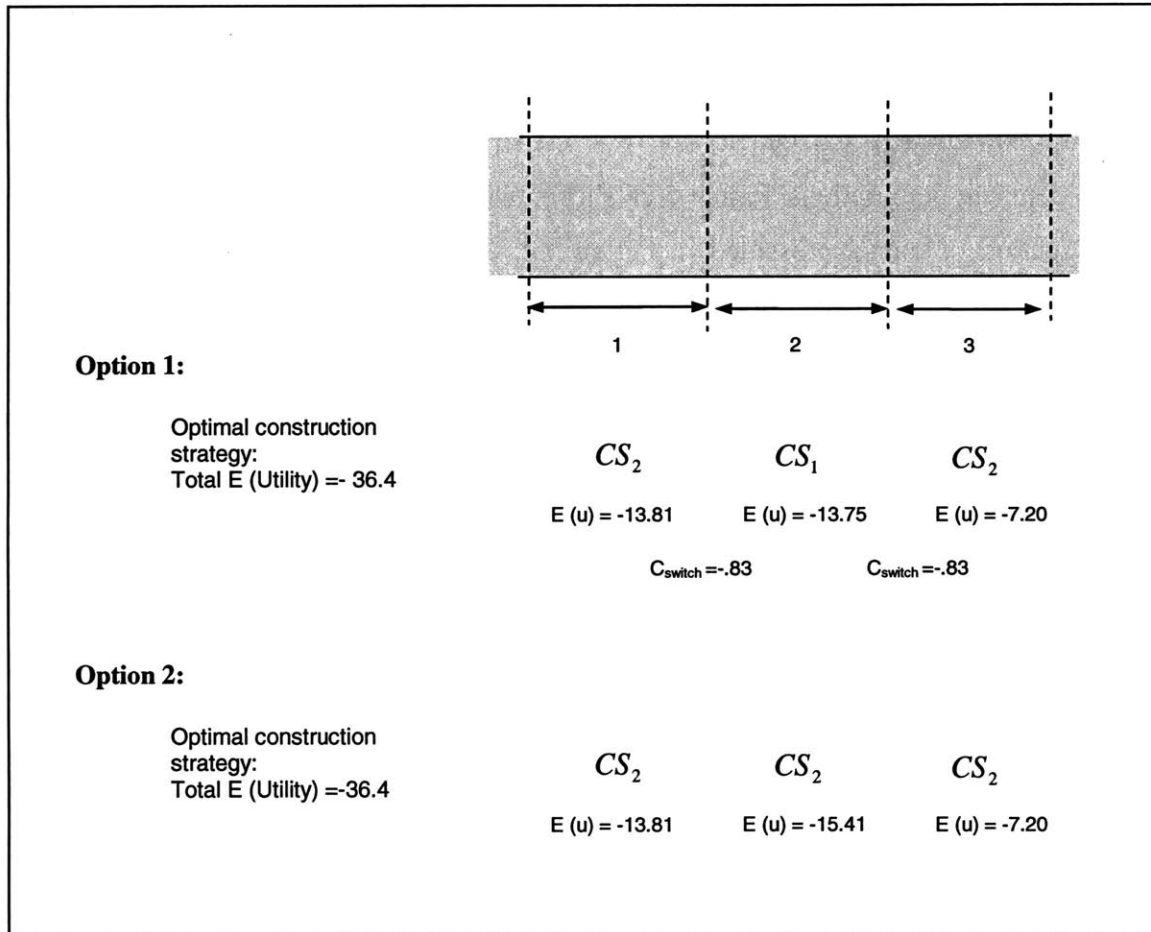


Figure 5.26 Optimal construction strategy for construction of tunnel presented in Figure 5.4, with (option 1) and without (option 2) considering switchover costs for the  $C_{switch} = -.83$  in option 1 (both options have the same total expected utility).

### 5.2.2 Tunnel construction Phase

When tunnel construction starts, new information is available as the excavation progresses. This information can and should be used to update the prior probability distribution of the geological states within each section. In tunnel construction the “state” of the ground invariably changes with respect to space. The transition from one state to another may generally depend on the prior states and can be translated into a transition model, i.e. a model that relates the ground state in space. In the context of the model used previously, where the variables are discrete the transition model will be a matrix correlating the ground type at different locations.

The proposed method consists of dividing each section into subsections as shown in Figure 5.27. Once the excavation progresses in section  $x$  and information is available regarding the geological state, data can be used to update the geological states in the remainder of the unexcavated section  $x$ . For this one needs a transition model, in this case, the probabilities of changing from one ground type to another ground type.

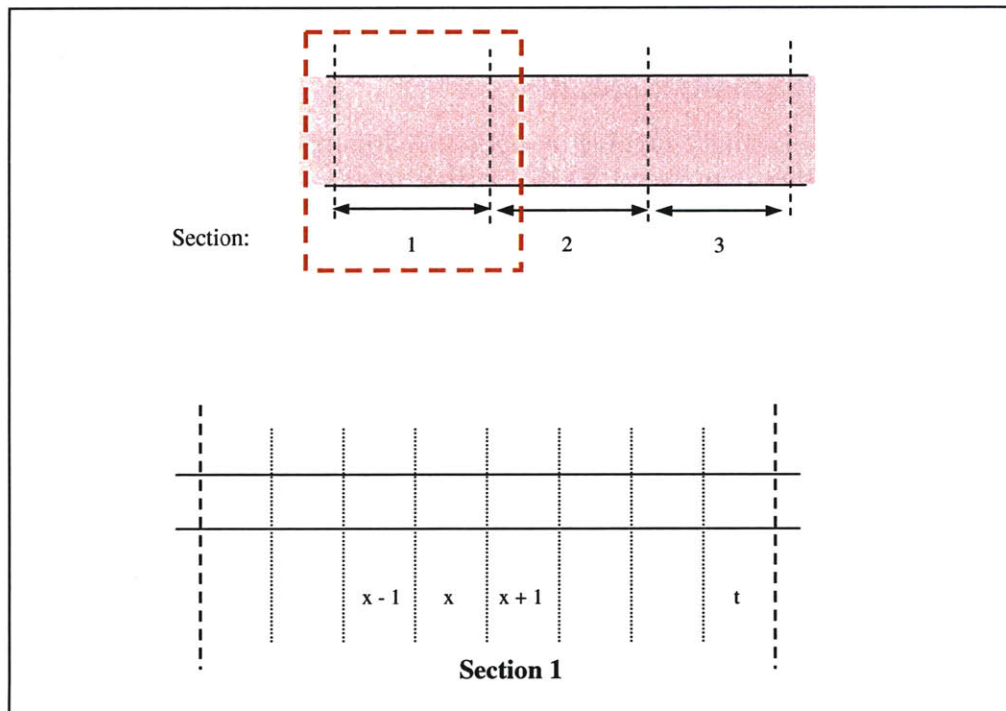


Figure 5.27 Division of Section 1 into subsections.

Dynamic Bayesian Networks are used to model problems where the state of the variables changes at each point in time, i.e. where the dynamic aspect of the problem is essential. A Dynamic Bayesian Network represents a “temporal” probability model by having state variables  $X_n$  replicated over time slices with the same conditional independences. However, in the specific case of tunnel construction one will have a sequence of lengths (within the same section) or tunnel sub-sections, instead of time slices. One then can assume that the excavation is a first order Markov process (i.e. that the conditions in the tunnel on slice  $n$ , only depend on the conditions of slice  $n-1$ , and so forth).

Once the state and evidence variables for a given problem are decided on, it is necessary to specify the dependencies between variables, as in a “static” Bayesian Networks. One choice is to order variables in their natural order (temporal or spatial in the case of a tunnel construction). One quickly runs into problems since the set of variables is unbounded, because it includes the state and evidence (observed) variables of every time slice. This creates two main problems (Murphy, 2002):

1. We might have to specify an unbounded number of conditional probability tables one for each variable in each slice
2. Each variable might involve an unbounded number of parents (variables that are above in the network hierarchy, i.e. that are causes to a variable)

The first problem can be solved by assuming that the changes in the world state are caused by a *stationary process*, i.e. the process of change is governed by laws that do not change over time (in the specific case of a tunnel, in space). In the example described before the conditional probability that a certain evidence (or observation that can be related with a certain geological state, such as penetration rate) will be present for all subsections  $x$ , and is for example  $P(P_x | G_x)$ , where  $P_x$  is variable penetration rate at slice  $x$  and  $G_x$  is the variable geological state at slice  $x$ . This means that given this assumption of stationarity it is only necessary to specify conditional distributions for a representative slice. This issue will be explained in more detail later, Chapter 6.

The second problem, i.e. handling the potential infinite number of parents, can be solved by making a *Markov assumption* that is that the current state depend only a finite history of previous states. In the present case we will assume a 1<sup>st</sup> order Markov process, in which the current state depends only on the previous state and not any of earlier states. This can be translate into

$$P(G_x | G_{0:x-1}) = P(G_x | G_{x-1})$$

Equation 5.27

So the transition model that describes how the state evolves over the representative slices depends only on the conditional distribution  $P(G_x | G_{x-1})$ .

### 5.2.2.1 Example application (Construction phase)

Continuing the example presented in Figure 5.4, imagine that construction started in Section 1 and new information regarding the geological states is available. It is possible to update the geological states for the remainder of Section 1 and reevaluate the decisions regarding the “optimal” construction strategy. For that one needs a transition (or correlation) model that relates the ground conditions between subsections.

#### Transition model (“correlation” model)

Imagine that the following transition model, presented in Table 5.9, which represents the probability of a geological state in subsection  $x$  of Section 1 of the tunnel given the geological state of the previous subsection  $x-1$ . In this case it is assumed that construction is a 1<sup>st</sup> order Markov process, in which the current state depends only on the previous state and not any on earlier states. This is not necessarily true in many cases and more complex transition models that take into consideration information of more than only the previous section can be used.

Table 5.9 transition model for section 1 of the tunnel in Figure 5.4

	$G_{1(x)}$	$G_{2(x)}$
$G_{1(x-1)}$	0.85	0.15
$G_{2(x-1)}$	0.10	0.90



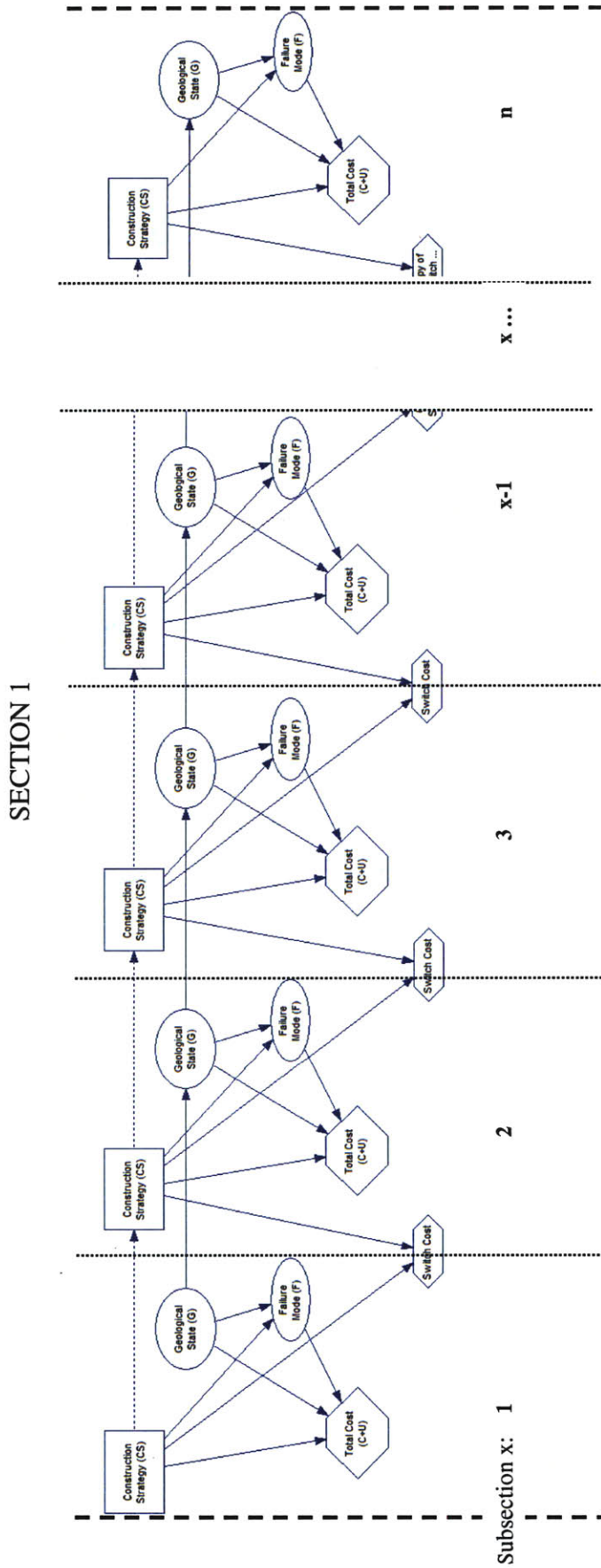


Figure 5.28 Subdivision of Section 1 of tunnel in Figure 5.4

## Construction

Figure 5.28 shows the subdivision of section 1 and how the Bayesian network would look like when applied to the construction stage. The transition model within the section is represented by the arrows between *geological state* variables in subsections  $x$  and  $x-1$  and so forth. Attached to these nodes is the transition model (Table 5.9).

### 5.2.3 Application Results

#### 5.2.3.1 Design Phase

Figure 5.29 to Figure 5.31 show the probability of the geological states, the expected utility, and the probability of failure, for the “optimal construction strategy”, for all three discretized sections of tunnel in Figure 5.4.

Figure 5.29 shows the (prior) probability of the geological states along the three sections. These plots are essentially the plots of Table 5.7 a, b and c on the discretized sections on the example tunnel. They correspond to flat lines because it was assumed that the prior probability geological states were constant along the sections. In Section 1 the prior probability geological states were constant along the sections. In Section 1 the prior probability of G1 is 0.4 and G2 is 0.6. In Section 2 the prior probability of G1 is 0.7 and G2 is 0.3. In section 3, the prior probability of G1 is 0.1 and G2 is 0.9.

Figure 5.30 shows the results of the influence diagram of Figure 5.23 (maximum expected utility), plotted along the discretized section, that were previously summarized in Figure 5.25. The maximum expected utility in section 1, section 2 and section 3 are -13.81; -13.75 and -7.20, respectively.

Figure 5.31 shows the overall probability of failure (with the “optimal strategy”) in each section given the “optimal” strategy. These results can be calculated by the following equation:

$$P(\text{Failure}) = \sum_{i=1}^n P(G_i)P(\text{Failure} | G_i, \text{Best CM}_j)$$

Equation 5.28

Where

$G_i$  represents geologic state

$n$  is the total number of geologic states

$P_{G_i}$  is the (prior) probability of geologic state  $i$

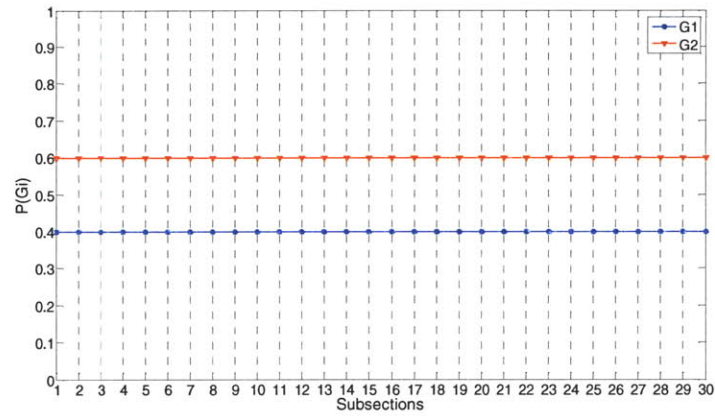
$B$  is the “optimal” construction strategy

$P_{kFij}$  is probability of failure mode  $k$ , in geology  $i$  with construction strategy  $j$ . Note that in this specific case there are only two failure “modes” ( $k=1$  Failure,  $k=2$  No Failure).

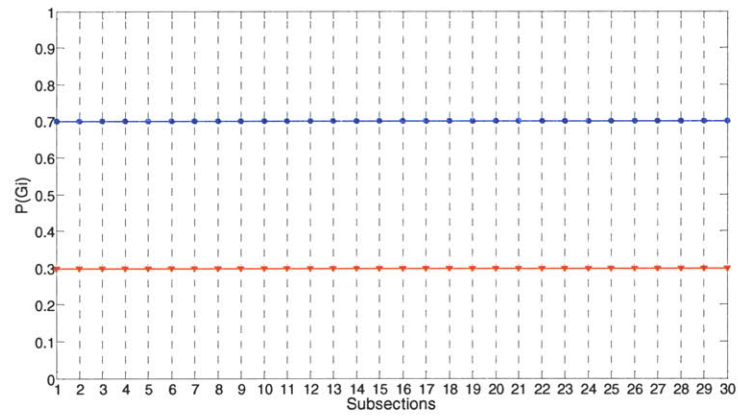
The probability of failure in section 1, with construction strategy CS2 (“optimal) is 0.043.

The probability of failure in section 2, with construction strategy CS1 (“optimal) is 0.0073. The probability of failure in section 3, with construction strategy CS2 (“optimal) is 0.015.

### Section 1



### Section 2



### Section 3

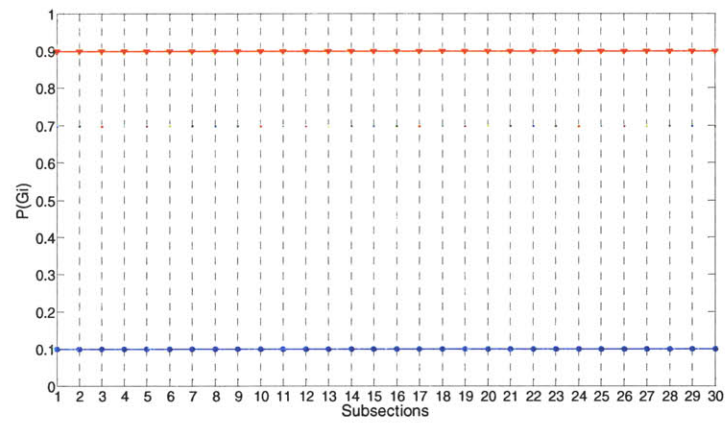


Figure 5.29 Probability of geological state for Section 1, 2 and 3

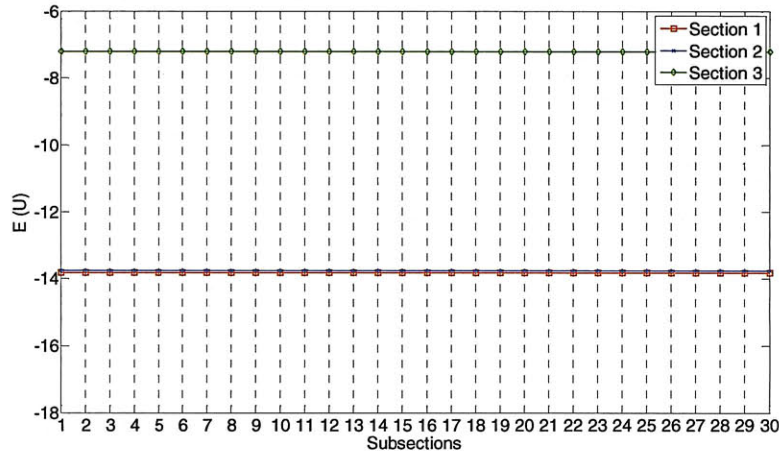


Figure 5.30 Expected utility for Sections 1, 2 and 3

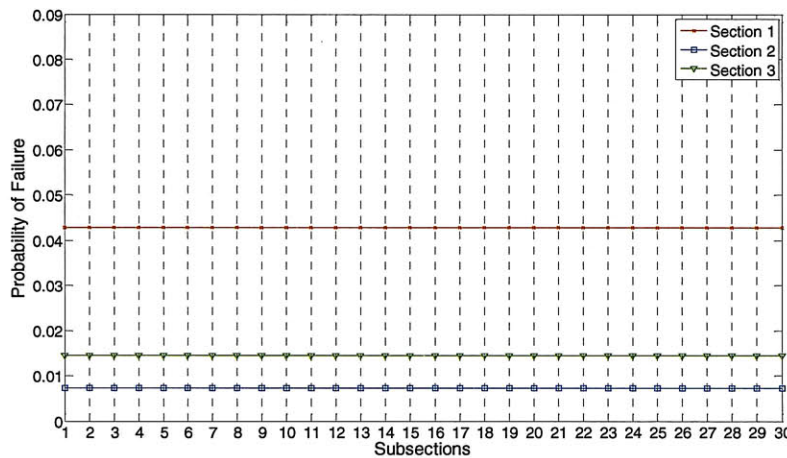


Figure 5.31 Probability of Failure for Sections 1, 2 and 3

### 5.2.3.2 Construction Phase

Imagine that construction started in Section 1, with construction strategy CS2 which is “optimal” construction strategy determined in the design phase (see Figure 5.25) and geology G2 is observed in the first 1m (length of a subsection).

Faced with this new information, one can update the geological states’ probability provided that a transition model is available. Using the transition model presented on Table 5.9 the geological states for the remaining unexcavated subsections are updated (from its prior state, presented in Figure 5.29), and presented in Figure 5.32 (only 30

subsections are presented). One can observe that the probability of G2 occurring is high for the next subsections, decreasing with distance until it reaches the design probability (of G2) at around subsection 15, in other words the “correlation” with the excavated subsection is high for the first meters and then eventually decreases until it reaches a point in space where the fact G2 was found in subsection 1 has no longer any influence on the updated geology, i.e. the updated probability of the geological state is equal the prior (or design) probability.

Once the geology has been updated for the remaining subsections along Section 1, the expected utilities and associated optimal construction strategy can also be updated. The updated utilities are presented in Figure 5.33. The updated “optimal” strategy for the remaining subsections is presented in Figure 5.34 (obtained by application of the model in Figure 5.28). Note that after updating the optimal construction strategy is still CS2.

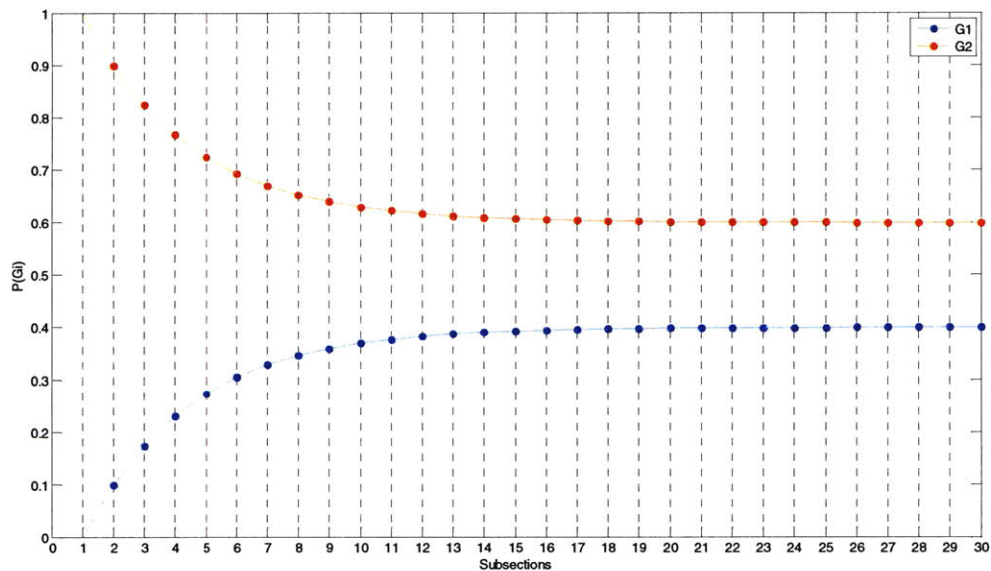


Figure 5.32 Updated Probability of geological state for Section 1, after excavation of subsection 1



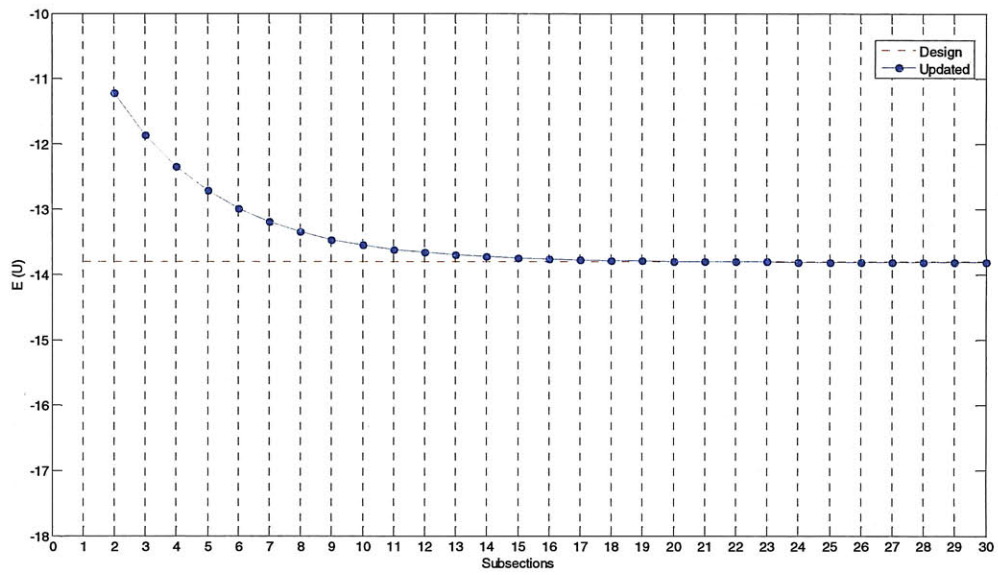


Figure 5.33 Updated Expected utility for Section 1, after excavation of subsection 1

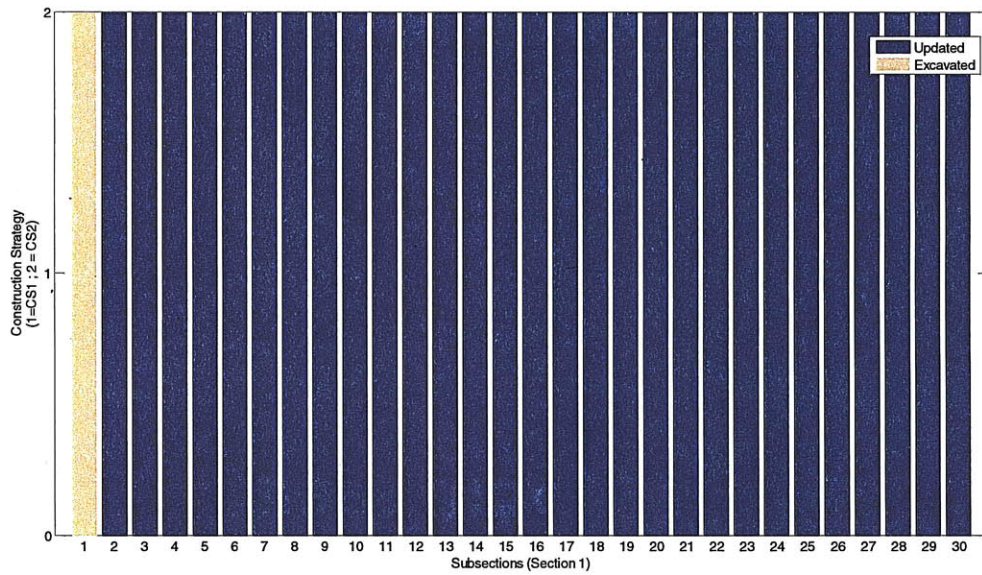


Figure 5.34 “Optimal” construction strategies for Section 1, after excavation of subsection 1



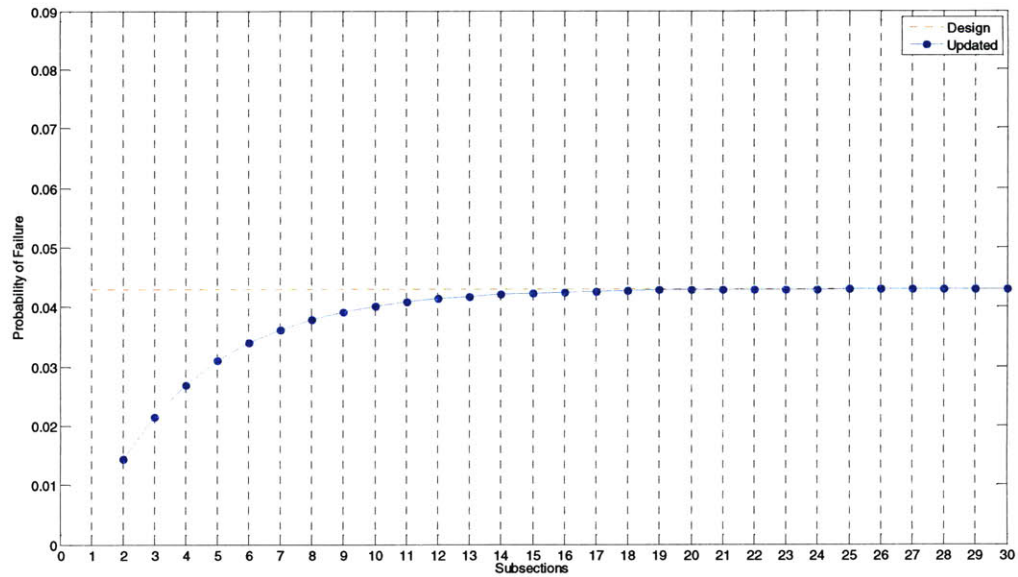


Figure 5.35 Updated Probability of Failure for Section 1, after excavation of subsection 1

- Excavation of subsection 2.

Imagine that another one linear meter is excavated with CS2 and again geology G2 is observed. The updated geological states for the remaining subsections are presented in Figure 5.36. With distance from subsection 2, where G2 was observed, the probability of G2 decreases and the probability of G1 increases until both become stationary for values corresponding to the design phase,  $P(G1)=0.4$  and  $P(G2)=0.6$ .

The updated expected utility for the remainder of section 1 is presented in Figure 5.37. Figure 5.38 and Figure 5.39 present the “optimal” construction strategy for the remaining sections (as well as the one used in the previous sections), and the updated probability of failure, respectively. The expected utility at subsection 3 is -11.2 and it decreases as the distance to subsection 3 increases until it reaches the stationary value of -13.81, the design value. The probability of failure, for the “optimal” construction strategy in subsection 3 is 0.15. This value increases with distance until it reaches the design value of 0.043.

Note the results are the same as the ones shown previously (after excavation of subsection 1), only moved one meter (one subsection). This is a result of the adopted transition model, which assumes that the geological state at section  $x$  only depends on the geological state at the previous section  $x-1$ .

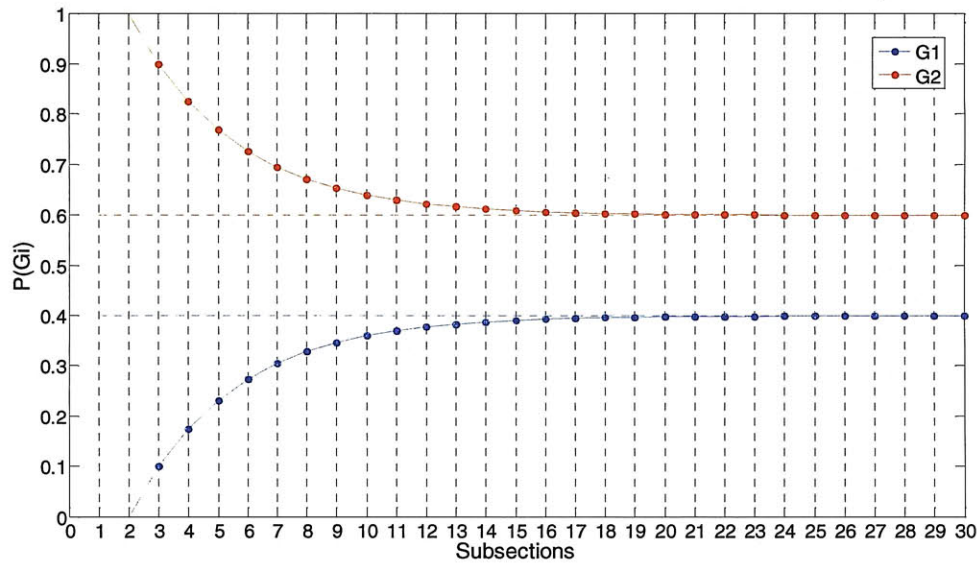


Figure 5.36 Updated Probability of geological state for Section 1, after excavation of subsection 2

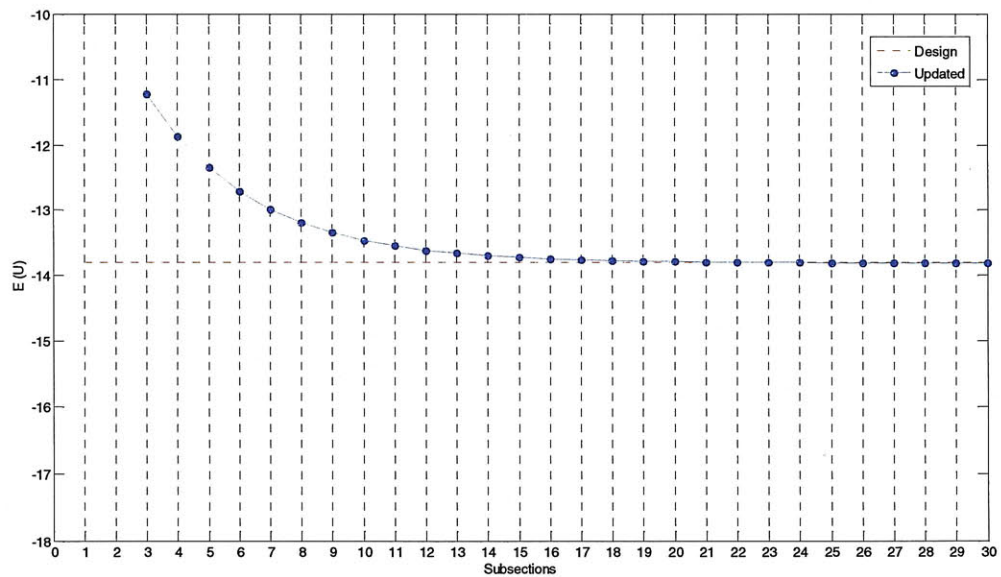


Figure 5.37 Updated Expected utility for Section 1, after excavation of subsection 2

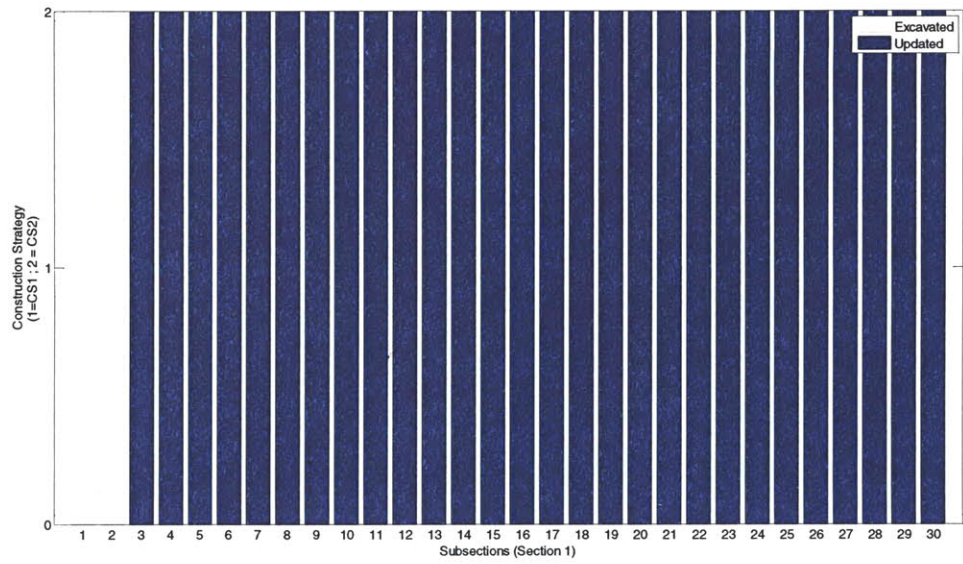


Figure 5.38 “Optimal” construction strategies for Section 1, after excavation of subsection 2

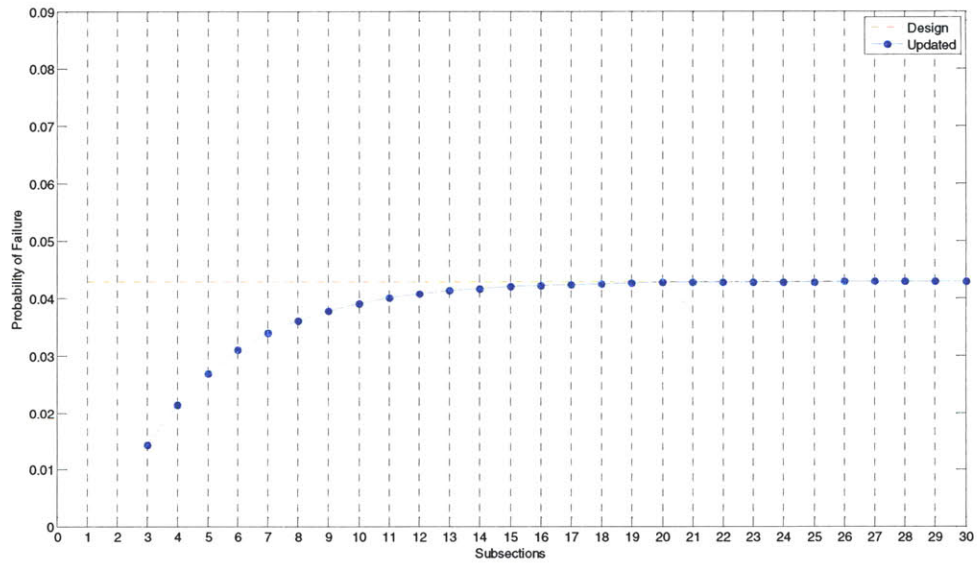


Figure 5.39 Updated Probability of Failure for Section 1, after excavation of subsection 2

- Excavation of subsection 3:

Observed Geology: G1

Now imagine that another one linear meter is excavated with CS2 and geology G<sub>1</sub> is encountered. The results of updating the geological states for the remaining subsections are presented in Figure 5.40. Once again, the influence of the observation of geology G1 at subsection 3 on the remaining subsections to be excavated decreases with distance and the probability distribution of the geological state tends to the prior probability distribution presented in Table 5.1, after several (around 15) subsections.

Due to the fact that a “worse” geology was found at subsection 3, the “optimal” construction strategy for the next 4 subsections will no longer be CS2, but CS1. The maximum expected utility given construction strategy,  $E(U | CS_j)$ , which is presented in Figure 5.41, shows precisely that. One can observe that  $E(U | CS1) > E(U | CS2)$  for the 4 not excavated subsections right after the subsection 3, which means that CS1 is the “optimal” construction strategy for the next 4 m. The updated “optimal” strategy for the remaining subsections is presented in Figure 5.42.

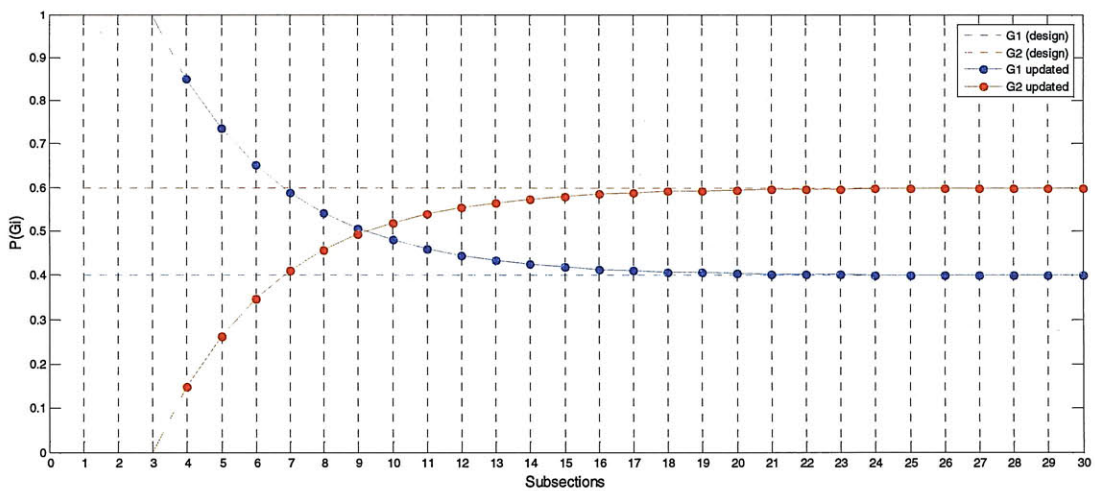


Figure 5.40 Updated Probability of geological state for Section 1, after excavation of subsection 3



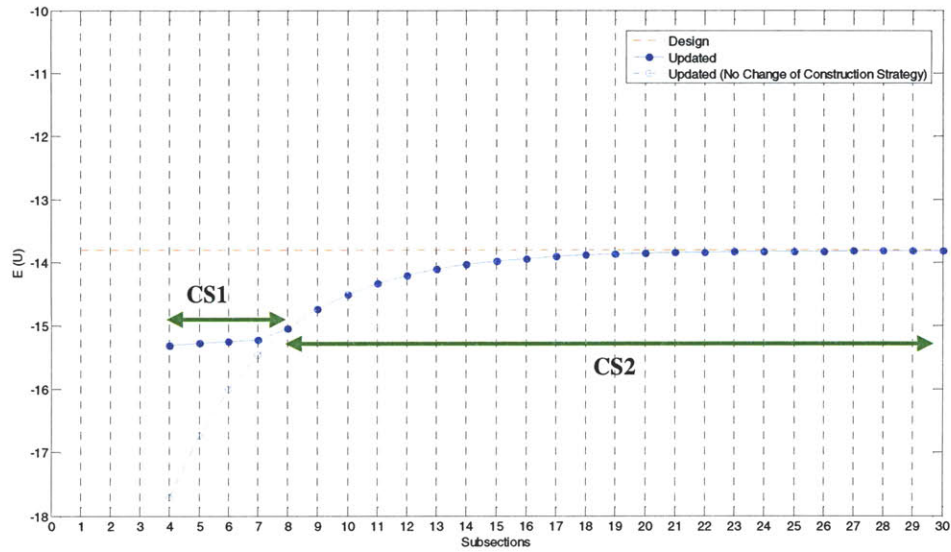


Figure 5.41 Updated Expected utility for Section 1, after excavation of subsection 3

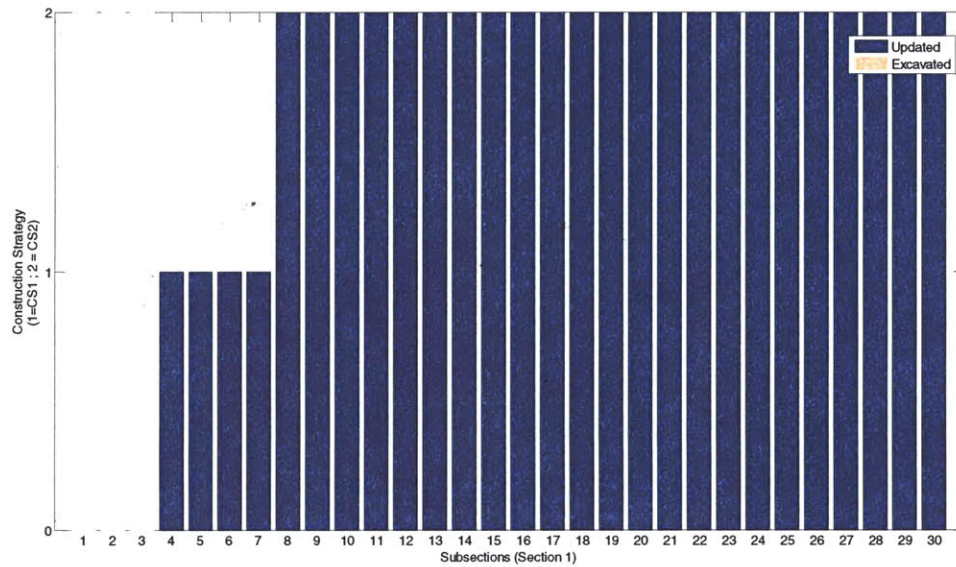


Figure 5.42 “Optimal” construction strategies for Section 1, after excavation of subsection 3

Figure 5.43 shows the updated probability of failure using the “optimal” strategies along section 1. The results show that for the next 4 subsections, i.e. for the next 4 linear meters, the optimal construction strategy is CS1 and no longer CS2, as previously (Figure 5.38). This has to do with the fact that the probability of failure with CS2 for the

encountered ground conditions is above a critical value (that is consequence of the utility function defined by the decision maker). Once the probability of failure is above that critical value (in this case 0.056), construction strategy CS2 is not the “optimal” one and strategy CS1 should be used, to reduce the probability of failure. The dotted line shows the probability of failure for section 1, using CS2, i.e. if it was decided not to change to CS1.

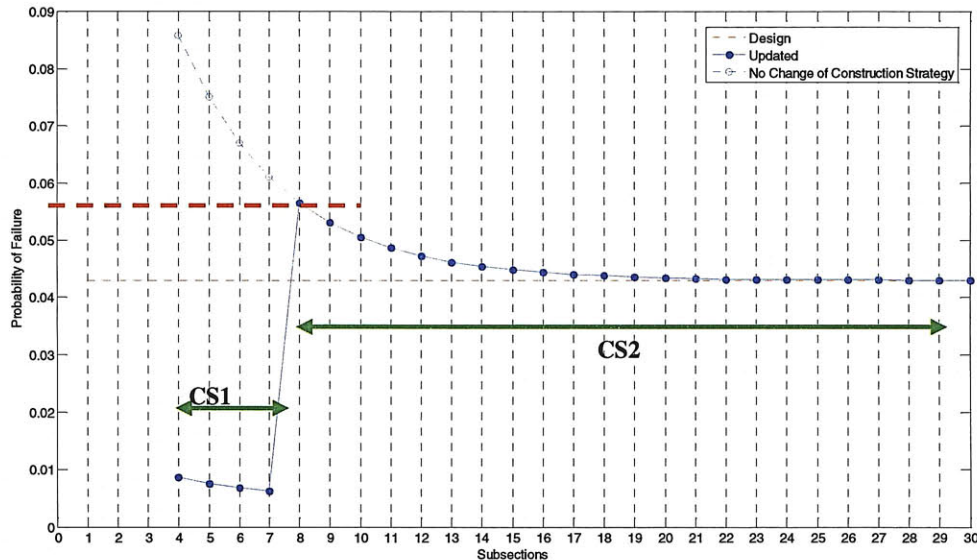


Figure 5.43 Updated Probability of Failure for Section 1, after excavation of subsection 3

### Switchover Costs

The previous results assume that there are no switchover costs between construction strategies. If switchover costs are considered, one will have different results. In order to consider switchover costs one can use for example, a dynamic programming approach when deciding on the optimal construction strategy (Kim, 1984 and Einstein et al., 1987).

When using influence diagram's there are some recent algorithms that can deal with this type of situation. One is the LIMID (Limited Memory Influence Diagrams), developed by Lauritzen and Nilsson, 2001 in an attempt to create an alternative to traditional IDs, which grows very complex when the number of variables included is increased. LIMIDs

do not have the “no forgetting” assumption included in IDs (Influence Diagrams) and thus only use the specified variables (the parents of the decision node) in the optimization of a given decision. The decision nodes are only influenced by their parents, and only variables that can be observed are used as parents for decision nodes. Based on the parental states, a strategy for the decision is given.

A LIMID finds an approximate optimal strategy (local optimum) through single policy updating (SPU). SPU can find locally optimal decision strategies. This means, that at a local maximum no single change of policy can increase the utility value. A general problem with such methods is that the complexity of the decision problem causes the required optimization calculations to become either impossible or at optimal very slow.

However, since one is interested mainly in checking whether or not the construction strategy being used is still the “optimal” (or the safest) for the geology encountered, and because considering all possible combinations for the rest of the tunnel is computationally time consuming, a simplification will be used. Instead of checking the whole tunnel, at every advance, switchover costs will be considered only in the first subsection, after the excavated one (i.e. if subsection 4 is excavated, only switchover costs between 4 and 5 will be considered in the updating). This simplification is reasonable because one is interested mainly in avoiding undesirable events to occur (such as heading failures etc) in the next subsection, by predicting and updating the geology as the excavation progresses, and one is looking for signs that would indicate that the stability of the tunnel could be in danger, i.e. an alarm criterion.

### **Transition (“Correlation”) Models**

Different transition models can be used during the updating of the geological state, in the construction phase. For example instead of just considering that the state of the geology only depends on the previous state, one can consider a second order Markov model, i.e. a model that correlates the ground in subsection x with the two previous subsections. Table 5.10 shows such model, which can be read the following way: for example, the probability of observing G1 in subsection x, given that G1 was observed at subsections x-



1 and x-2 is 0.90, i.e.  $P(G_x = G1 | G_{x-1} = G1, G_{x-2} = G1) = 0.90$ . On the other hand, if G1 is observed at subsection x-2 and then G2 is observed in subsection x-1, then the probability of observing G1 again in subsection x is, according to this model, low, only 0.18 ( $P(G_x = G1 | G_{x-1} = G2, G_{x-2} = G1)$ ). The rest of the entries in Table 5.10 can be read in a similar way.

Table 5.10 transition matrix (second order Markov model)

G <sub>x-2</sub>	G1		G2	
	G1	G2	G1	G2
G1	0.90	0.18	0.79	0.07
G2	0.10	0.82	0.21	0.93

Using the 2<sup>nd</sup> order transition model presented in Table 5.10 to update the probability for the geological states, after the excavation of the first two subsections, will yield the results presented in the graph of Figure 5.44. Plotted in the same graph are the results of updating with the 1<sup>st</sup> order Markov transition model of Table 5.9, also presented previously in Figure 5.36.

The second order Markov model (Table 5.10) produces higher “correlations” between subsections i.e. the effect of the new information (the geology found during the excavated subsections) is observed for almost 30 subsections, a longer distance than the 15 subsections affected by the first order Markov transition model (Table 5.9). This is mainly due to the fact that more of the past observations are considered in the updating process.

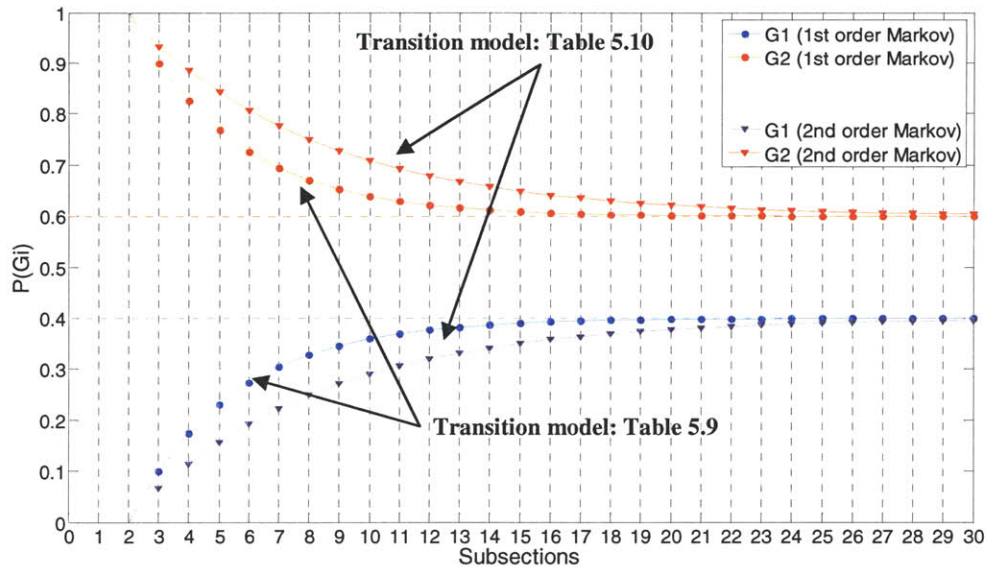


Figure 5.44 Geological states after excavation of subsections 1 and 2 (dotted lines are the design values)

Figure 5.45 shows the geological state updated probability after the excavation of subsection 3, using both the 1<sup>st</sup> order Markov model from Table 5.9 (results presented previously in Figure 5.40) and the 2<sup>nd</sup> order Markov model from Table 5.10. Again one can observe that the effect of the information obtained regarding the geology of the previously excavated section is observed for a longer distance when using the 2<sup>nd</sup> order Markov transition model.

The probability of geology G1, i.e.  $P(G1)$ , obtained for subsection 4 is lower when applying the 2<sup>nd</sup> Markov transition model, than when applying the 1<sup>st</sup> order Markov transition model. This has to do with the fact that 2<sup>nd</sup> Markov transition model considers the two last observations (G2 and G1), instead of only the last observation (G1) as the 1<sup>st</sup> order Markov does. Using the 2<sup>nd</sup> order Markov the probability that one finds G1 given that G2 and G1 were previously observed is 0.79 (see Table 5.10). Using the 1<sup>st</sup> order Markov model the probability that one finds G1 given that G2 and G1 were previously observed is equal to the probability that one finds G1 given that G1 was previously observed (since this model only takes into consideration the last observation), which is equal to 0.85 (see Table 5.9)

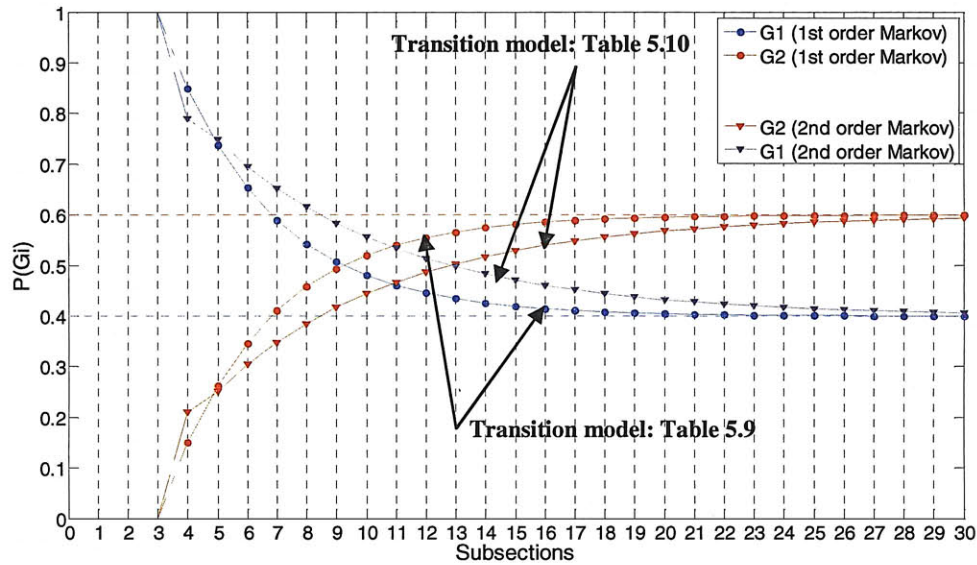


Figure 5.45 Geological states after excavation of subsections 1, 2 and 3

Using a different transition model will also have an effect on the (updated) maximum expected utility. Figure 5.46 show the updated maximum expected utility after excavation of subsection 3, where G1 was encountered, using both transition models. In both cases the “optimal” strategy for the next subsection is to switch from CS2 to CS1. However the difference between the results of the two models resides in the fact that for the 2nd order model CS1 is the “optimal” strategy for the next 6 subsections, instead of only for 4 subsections (results of 1<sup>st</sup> order Markov model).

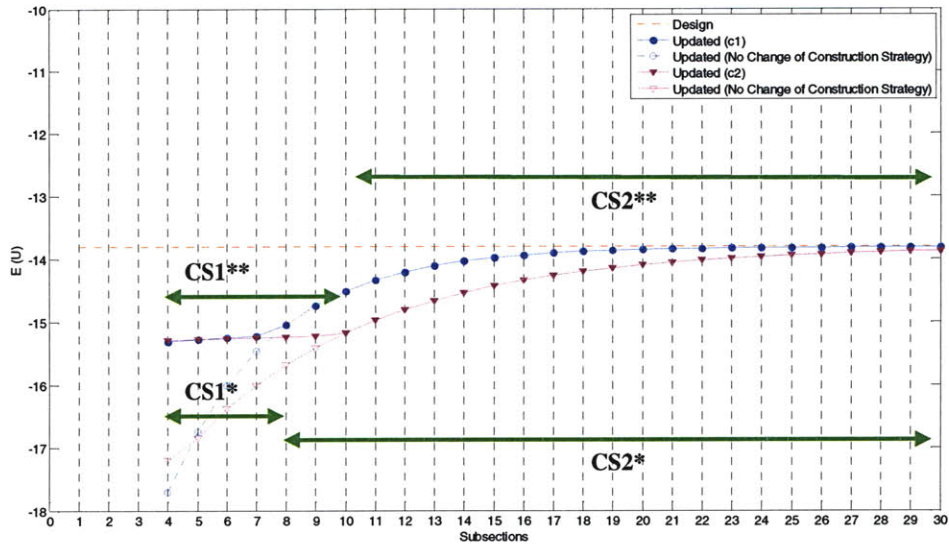


Figure 5.46 Updated Expected utility for Section 1, after excavation of subsection 3  
 (\*: 1<sup>st</sup> order Markov transition model; \*\*: 2<sup>nd</sup> order Markov transition model)

The transition (or correlation) models used should depend on the type of ground that is crossed. Correlation will depend on how homogenous, or heterogenous the ground is. Homogenous ground will have high correlation, whereas heterogenous ground will have low correlation. The model can be based on information available from other projects in the same formations, on subjective assesment from experts based on geological data available or a combination of both.

### Utility Function

In the developed methodology that was illustrated by example of Figure 5.4 the consequences were expressed in monetary terms. However there are situations where monetary value is not a consistent measure of utility, since the preference of the decision maker may depend on the magnitude of the amount of money involved or the severity of the consequences, such is in the cases of collapses. In the case of costs associated with failure a more adequate family of utility functions are risk averse ones, such as the ones presented in Equation 5.29, for example.

$$U_c(C) = 200(1 - e^{-\gamma C})$$

Equation 5.29

Figure 5.47 shows a plot of the utility function in Equation 5.29 for different values of  $\gamma$ , which represent the risk averseness of the decision maker. The lower the value  $\gamma$  the more risk averse, the decision maker. Figure 5.48 shows the results of the Expected Utility given the construction strategy for Section 1 of the tunnel in Figure 5.4, for different utility functions. One can observe that for  $\gamma$  values lower than -0.7 the “optimal” construction strategy in Section 1 becomes CS1. This reflects a utility function that associates very low utility (higher costs) with situations of failure.

The choice of utility function will also affect the construction phase update results. Figure 5.49 shows the updated maximum expected utility after excavation of subsection 3. The utility function was the one presented in Equation 5.29, with a  $\gamma$  of -0.6. If one compares the results of Figure 5.49 with the ones of Figure 5.41 where a linear utility function was used and no switchover cost, one can observe that for a more risk averse utility function (Figure 5.49) once G1 is encountered the updated “optimal” construction strategy until subsection 14 is CS1, compared with 4 subsections when using a linear utility function. This is expected because a more risk averse utility function associates much lower utilities with situations that are undesirable to the decision maker (such as collapses) than a linear utility function. This way CS2 will correspond to the optimal construction strategy for much lower  $P(G1)$ , in the risk averse utility function than in the linear one.

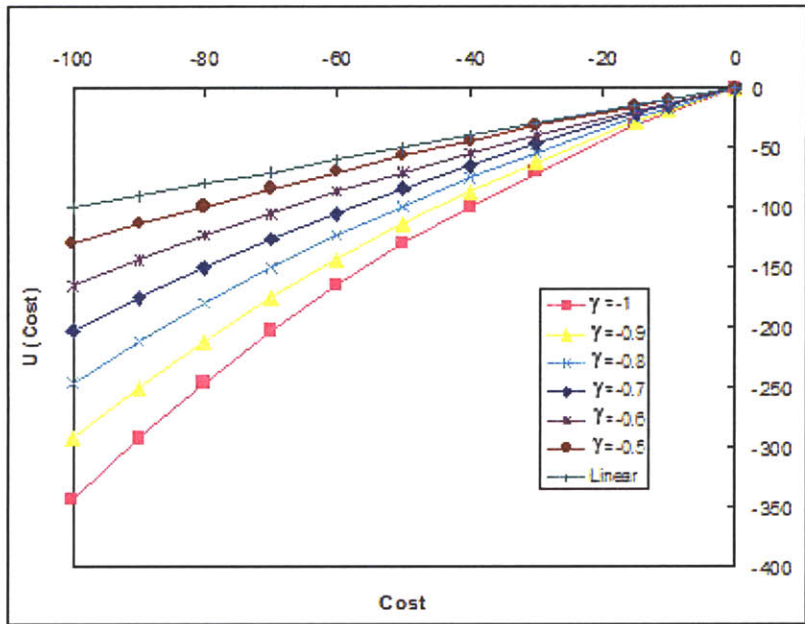


Figure 5.47 Utility function plot

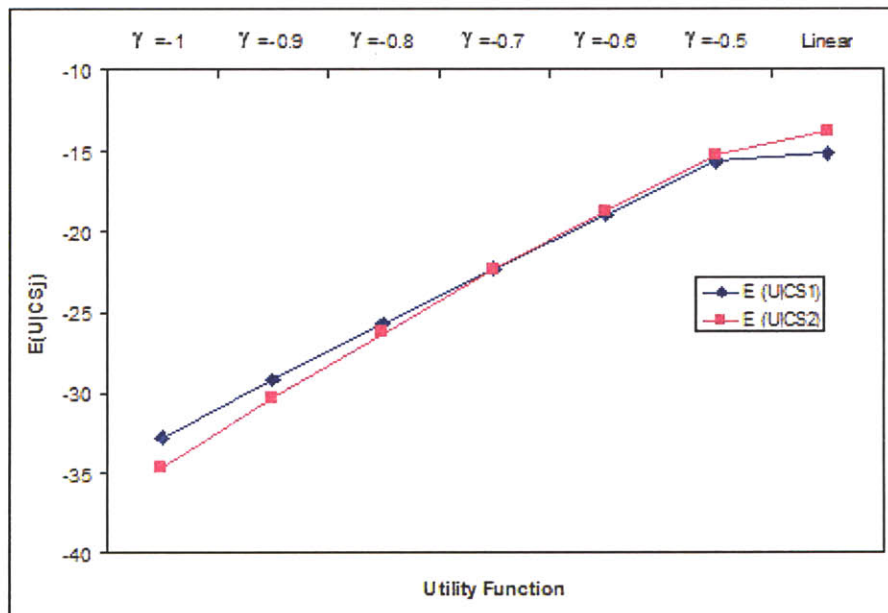


Figure 5.48 Expected Utility given Construction Strategy



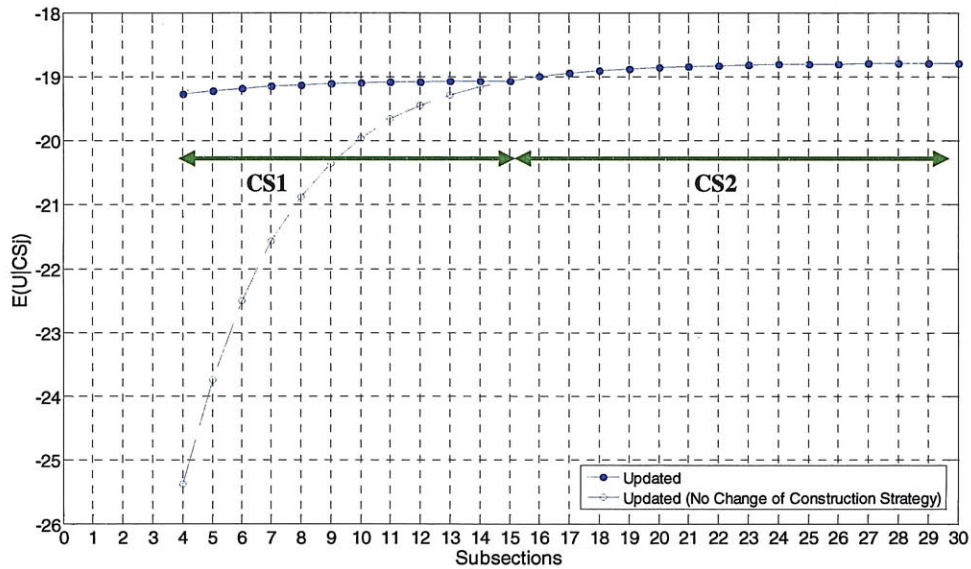


Figure 5.49 Updated Expected utility for Section 1, after excavation of subsection 3, with utility function presented in Figure 5.47

### 5.3 Conclusions

In this chapter a methodology to systematically incorporate risk of undesirable events during tunnel design and construction was presented. The methodology is divided into two parts: 1) Determination of the “optimal” construction strategy (regarding risk of undesirable events), in the design stage; 2) Updating and control of excavation during the construction phase.

An abstract example was presented to illustrate the basic principles. Bayesian Networks, with their extension to influence diagrams, were used to model the problem. A comparison (during the design phase) between the Bayesian Networks and the more classical decision analysis method was made. The agreement was generally very good.

The main focus on the developed methodology was on updating and controlling the excavation during construction phase. As the excavation starts information becomes available regarding the geological state and behavior of the excavation (monitoring). The



methodology presented here takes only into consideration information on geological states, since it is assumed that the “failure” of the tunnel depends mainly on the ground (geological state) and the construction strategy. Once the information on the geological state is available, the geology of the remainder of the tunnel is updated by means of a transition model (or correlation model). Then the “optimal” construction strategy is also updated for the remainder of the unexcavated part of the tunnel.

## 5.4 References

Baecher, (1981). "Risk Screening for Civil Facilities", Massachusetts Institute of Technology, Dept.of Civil Eng. CER-81-9. 20 p.

Bell, D. E., Raiffa, H., & Tversky, A. (Eds.). (1988). "Decision making: Descriptive, normative, and prescriptive interactions". New York: Cambridge University Press, ISBN: 0521368510. (Richard Gonzalez, Psychology Department)

Einstein, H.H. (1997). "Landslide Risk: Systematic Approaches to Assessment and Management". In: Cruden, A. and Fell, R. (editors). Landslide Risk Assessment. Balkema, Rotterdam. pp 25-50.

Einstein, H. H.; Descoudres, J; Dudt, J.P.; Halabe,V. (1991). Decision Aids in tunnelling. Monograph.

Einstein, H.H; Salazar, G.F; Kim, Y.W and Ioannou, P.G. (1987). "Computer Based Decision Support Systems for Underground Construction". Proceedings, of Rapid Excavation And Tunneling Conference; Vol. 2, pp. 1287-1308.

Einstein, H.H. Labreche, D.A., Markow, M.J., and Baecher, G.B. (1978). "Decision Analysis Applied to Rock Tunnel Exploration". Engineering Geology, Vol. 12, pp 143-161.

Eskesen, S. D., Tengborg, P., Kampmann, J., Veicherts, T. (2004). "Guidelines for tunneling risk management". International Tunnelling Association, Working Group No. 2. Tunnelling and Underground Space Tecnology 19 (2004) pp 217-237.

Karam, K.; Karam, J.; Einstein, H. (2007). "Decision Analysis Applied to Tunnel Exploration Planning. I: Principles and Case Study". Journal of Construction Engineering and Management. Volume 133, Issue 5, pp. 344-353

Keeney, R.L., Raiffa, H. (1976). "Decisions with multiple objectives", John Wiley & Sons

Min, S.Y., Einstein, H.H., Lee, J.S., and Kim, T.K. 2003. „Application of decision aids for tunneling (DAT) to a drill & blast tunnel” J. of Civil Eng., KSCE, Vol. 7, pp.619-628.

Murphy, K. (2002). "Dynamic bayesian networks". Representation, inference and learning, 2002.

Spetzler, C., and Staël von Hostein, C.-A. (1975). "Probability encoding in decision analysis". Management Science 22:340–358.

Vanmarcke, E.H.; Bohnenblust, H. (1982). "Methodology for Integrated Risk Assessment for Dams". MIT Research Report R-82-11.

## 5.5 Appendix G - Multiattribute utility functions

Appendix G shows some basic concepts and initial work on multiattribute utility function. This is a complex subject and requires further detailed research.

### Mutual Utility Independence of Attributes

When mutual utility independence is assumed, say between two attributes,  $x$  and  $y$ , the multiattribute utility function is of the linear form (Keeney and Raiffa, 1976):

$$U_{xy}(x, y) = k_x U_x(x) + k_y U_y(y) + k_{xy} U_x(x) U_y(y)$$

Equation 5.30

where  $k_x$ ,  $k_y$ , and  $k_{xy} = 1 - k_x - k_y$  are constants, and  $U_x(x)$ , and  $U_y(y)$  are the marginal utility functions of attributes  $x$  and  $y$  respectively.

Note that when  $k_x = k_y = 1$ , then the multiattribute utility function is the sum of the marginal utility functions.

In the following, steps to determine the multiattribute utility function are described.

#### *STEP 1: SELECTION OF ATTRIBUTES*

In this step, the decision maker selects attributes. Attributes in engineering projects can be, for example, those for cost/profit (cost overrun/cost underrun), time to completion (time delay/time underrun), quality, safety, and environmental amongst others.

#### *STEP 2: DETERMINATION OF MARGINAL UTILITY FUNCTIONS*

In this step, the marginal utility function of each attribute is determined. Consider an attribute,  $x$ , for example.  $C$  is within a range, such that  $C \in [C_{\min}, C_{\max}]$ , where  $C_{\min}$ , and

$C_{\max}$  are the specified minimum and maximum values of cost, and are determined subjectively. The marginal utility function for cost,  $U_c(c)$ , is then a function that is normalized such that:  $U_c(C_{\min}) = 1$ , and  $U_c(C_{\max}) = 0$ .

The shape of the functions will depend on the decision maker's risk preference, i.e. risk neutral, risk averse, or risk prone. A representation of the shape of the marginal utility functions for different risk preferences is shown in Figure 5.50.

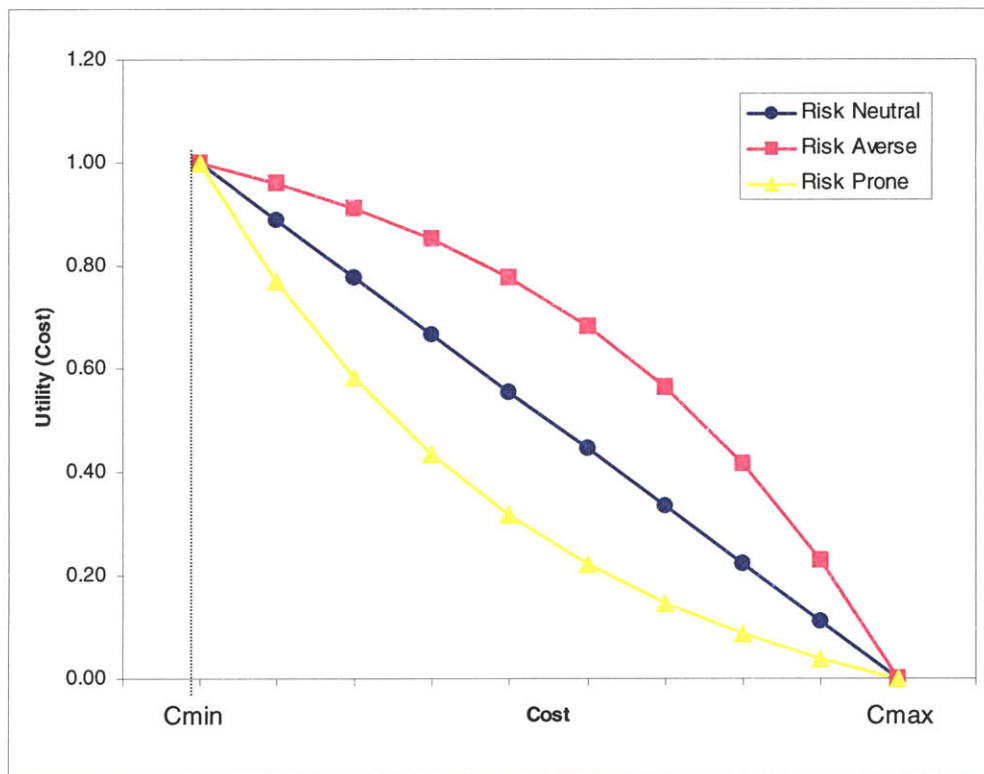


Figure 5.50 Marginal Utility function for different decision maker risk preference.

Risk neutral decision makers have a utility function that is a straight line, and can be expressed analytically as:

$$U_c(C) = \begin{cases} 1; C \leq C_{\min} \\ \frac{C_{\max} - C}{C_{\max} - C_{\min}}; C_{\min} \leq C \leq C_{\max} \\ 0; C \geq C_{\max} \end{cases}$$

Equation 5.31

Several types of functions have been proposed for risk prone, and risk averse decision makers (references). Examples include logarithmic functions and exponential functions. These are expressed in general terms as, for example the exponential function:

$$U_c(C) = \begin{cases} 1; C \leq C_{\min} \\ 1 - e^{-\gamma \left( \frac{C_{\max} - C}{C_{\max} - C_{\min}} \right)}; C_{\min} \leq C \leq C_{\max} \\ 0; C \geq C_{\max} \end{cases}$$

Equation 5.32

where  $\gamma$  is a constant that describes the degree of risk averseness of the decision maker (see Figure 5.51 and Figure 5.52).

Similar utility functions can be derived for other attributes, such as time, or any other chosen attribute.

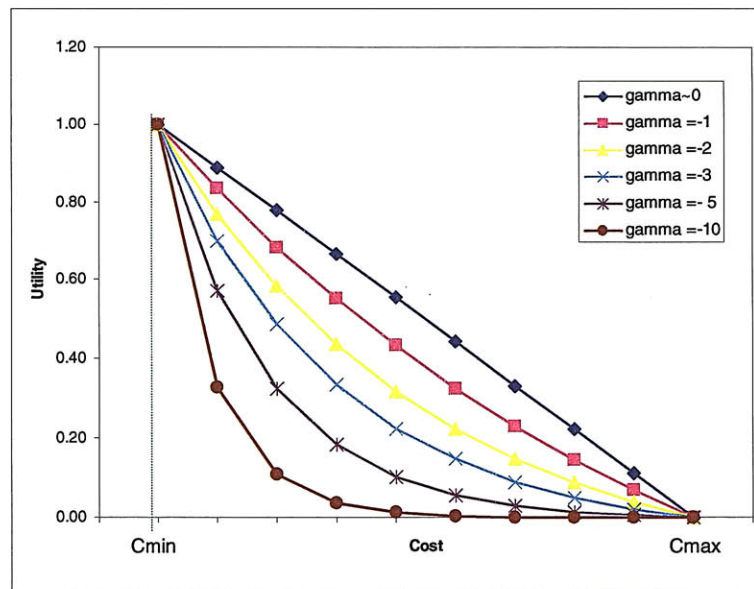


Figure 5.51 Exponential utility function plot (risk prone)

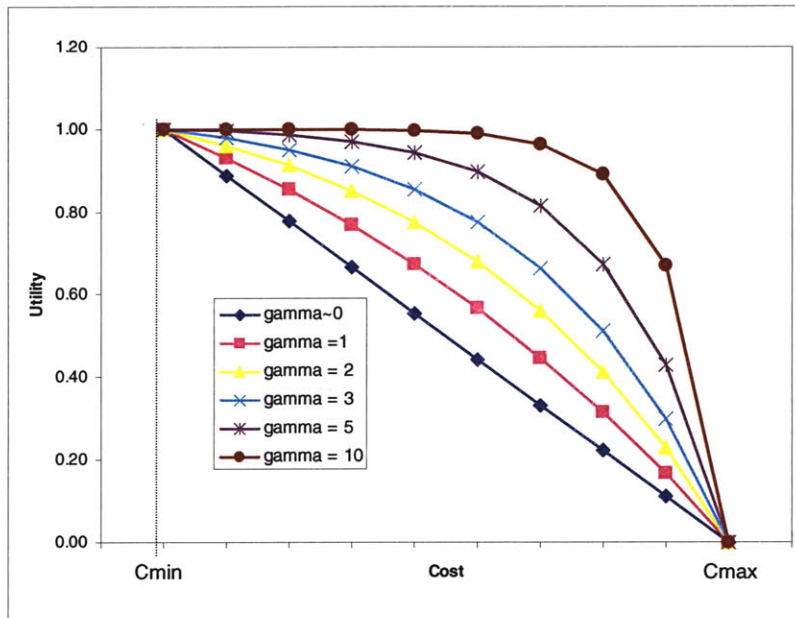


Figure 5.52 Exponential utility function plot (risk averse)

### STEP 3: DETERMINATION OF WEIGHTS

In this step, the weights of the different attributes are determined. In tunnel projects the most common attributes considered are costs and time. If one considers a situation where cost and times are the two parameters of interest, in this step,  $k_C$  for cost and  $k_T$  for time will be determined (see Equation 5.33). This is achieved using classic von Neumann and Morgenstern (1949) probabilistic indifference assessment to a binary lottery that provides the most preferred and least preferred options. A simple example is provided next:

Suppose that the project manager is indifferent between the following choices:

- (a) A lottery with probability  $p_1$  of minimum cost, and minimum time, ( $C_{min}$ ,  $T_{min}$ ) and  $(1-p_1)$  of maximum cost, and maximum time ( $C_{max}$ ,  $T_{max}$ ) (Lottery 1 in Figure 5.53) versus a sure option (Lottery 2 in Figure 5.53) of minimum cost, and maximum time ( $C_{min}, T_{max}$ ). Figure 5.53 illustrates the process of the determination  $k_C$ .



- (b) A lottery with probability  $p_2$  of minimum cost, and minimum time, ( $C_{min}, T_{min}$ ) (Lottery 1 in Figure 5.54) and  $(1-p_2)$  of maximum cost, and maximum time ( $C_{max}, T_{max}$ ) versus a sure option (Lottery 2 in Figure 5.54) of maximum cost, and minimum time ( $C_{max}, T_{min}$ ). Figure 5.54 illustrates the process of the determination  $k_T$ .

The probabilities  $p_1$  and  $p_2$  in these lotteries are changed until the *point of indifference* is obtained. At this point, the weights  $k_C$  and  $k_T$  are given by:  $k_C = p_1$  and  $k_T = p_2$ .

The weight  $k_C$  measures how much one is willing to give up on attribute cost, to gain a specific amount on attribute time. The weight  $k_T$ , measures how much one is willing to give up on attribute time, to gain a specific amount on attribute cost.

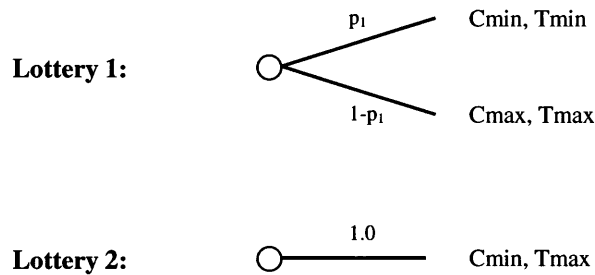


Figure 5.53 Determination of weight  $k_C$  for cost

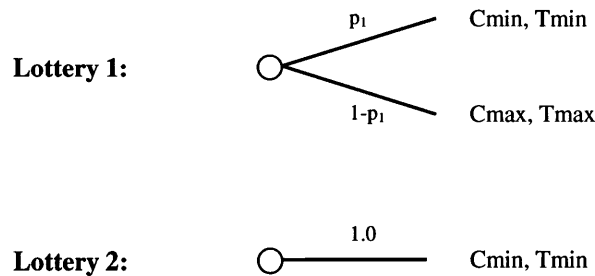


Figure 5.54 Determination of weight  $k_T$  for cost

#### *STEP 4: DETERMINATION OF MULTIATTRIBUTE UTILITY FUNCTION*

In the final step, the decision maker's multiattribute utility function is expressed as:

$$U_{ct}(c, t) = k_c U_c(c) + k_t U_t(t) + k_{ct} U_c(c) U_t(t)$$

Equation 5.33

Figure 5.55 shows examples of utility functions for decision makers with different risk preferences:

#### **Mutual Utility Dependence of Attributes**

In many practical decision problems the attributes are not utility independent. For example an utility function for money may change with another attribute such as wealth. It is, in these cases, necessary to incorporate dependence between attributes when constructing a multiattribute utility function.

Several methods have been developed by which dependence between the utility of different attributes can be included in constructing utility functions, namely Kirkwood (1976), Bell (1979), Keeney (1981), Farquhar and Fishburn (1982), and Abbas and Howard (2005). Abbas and Howard (2005) propose an analogy between a class of multiattribute utility functions, namely attribute dominance utility functions, and joint cumulative probability distributions, and use this analogy to construct multiattribute utility functions.

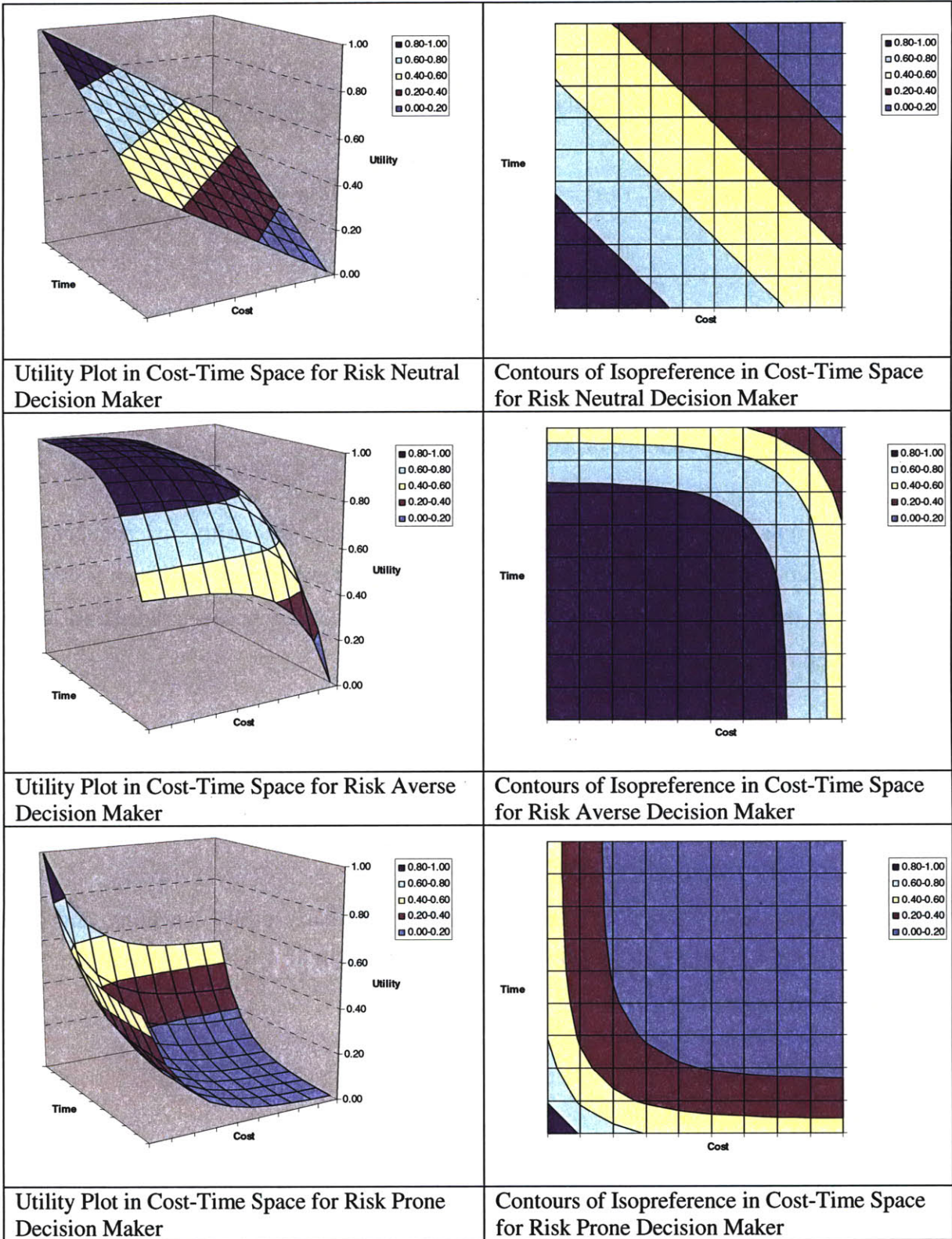


Figure 5.55 Utility Functions for decision makers with different risk preferences

Consider two attributes,  $x$  and  $y$ , such that  $x \in [x_{\min}, x_{\max}]$ , and  $y \in [y_{\min}, y_{\max}]$  where  $[x_{\min}, y_{\min}]$  is the least preferred consequence, and  $[x_{\max}, y_{\max}]$  is the most preferred consequence. Assuming mutual preferential independence, attribute dominance utility functions are then defined such that:

$$U_{xy}(x_{\min}, y_{\min}) = U_{xy}(x_{\min}, y) = U_{xy}(x, y_{\min}) = 0, \quad \text{and} \quad U_{xy}(x_{\max}, y_{\max}) = 1 \quad \text{for all} \\ x \in [x_{\min}, x_{\max}], \text{ and } y \in [y_{\min}, y_{\max}].$$

For attribute dominance utility functions, the marginal utility function of an attribute, say  $x$ , can be expressed as (see Figure 5.56):

$$U_x(x) = U_{xy}(x, y_{\max})$$

And a so-called conditional utility function, say for attribute  $y$  given  $x$ , expressed as:

$$U_{y|x}(y) = \frac{U_{xy}(x, y)}{U_x(x)} = \frac{U_{xy}(x, y)}{U_{xy}(x, y_{\max})}, \quad x \neq x_{\min}$$

Equation 5.34

The denominator,  $U_{xy}(x, y_{\max})$ , serves as a normalizing expression, such that  $U_{y|x}(y_{\min}) = 0$  and  $U_{y|x}(y_{\max}) = 1$  when  $x \neq x_{\min}$ .

Re-arranging Equation 5.34, the multiattribute utility function of the two attributes,  $x$  and  $y$ , can be expressed as:

$$U_{xy}(x, y) = U_{y|x}(y)U_x(x) = U_{x|y}(x)U_y(y)$$

Equation 5.35

Equation 5.35 provides an appealing method to construct multiattribute utility functions in many engineering problems, particularly since it is convenient, sometimes, to express conditional utility rather than marginal utility. This is so, since many other attributes of engineering projects, such as time to completion (time delay), translate, in one way or another and to a certain extent to cost/profit.

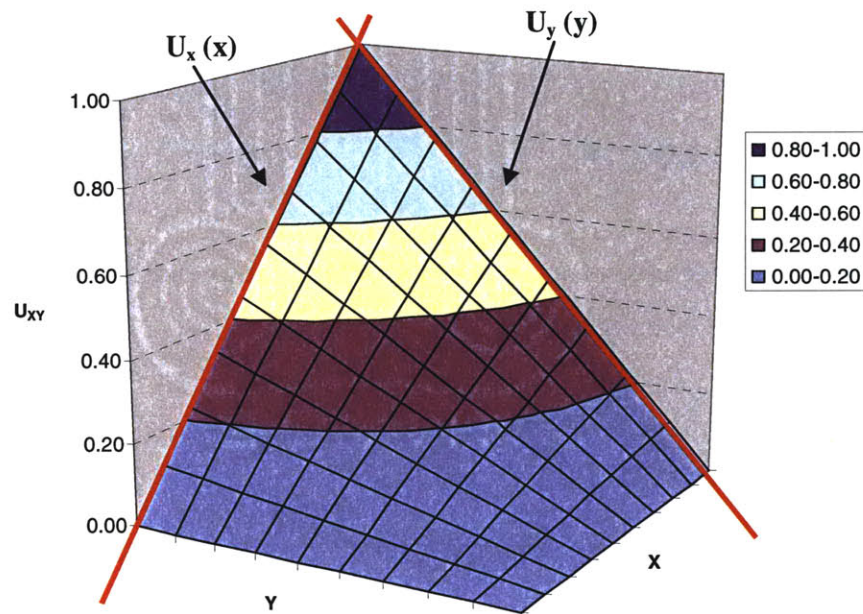


Figure 5.56 Multiattribute utility function

For example, it may be easier to define the utility of a time attribute at any given cost, because the shorter the time in which the project or a task is completed, the greater the utility. This function is easier to define than a marginal utility function for time. Moreover, since time essentially translates to cost, e.g. long delays, and penalties, it is reasonable to assume and construct multiattribute utility functions this way. The shape of this conditional utility function will again depend on the decision maker's risk preference. If one assumes a risk neutral attitude for time then the conditional utility function is as shown in Figure 5.57.



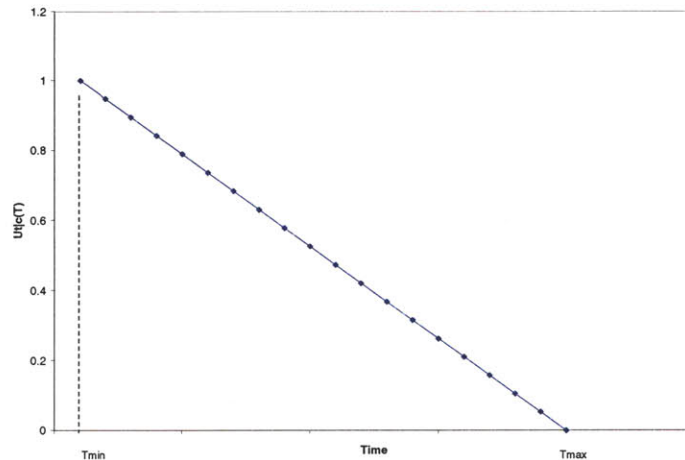


Figure 5.57 risk neutral conditional utility function

Figure 5.58 compares the multiattribute utility functions for risk neutral, risk prone, and risk averse with respect to cost decision maker's attitude and risk neutral conditional utility as in Figure 5.55.

Note that there is a difference, and an important one between the utility functions in Figure 5.55 and Figure 5.58, namely that utility is zero when either of the attributes is zero in utility dominance attribute functions (Figure 5.58) while both attributes need to be zero in utility independent attributes (Figure 5.55)

It is worth noting here that constructing multiattribute utility functions is in itself a process of decision making under uncertainty.

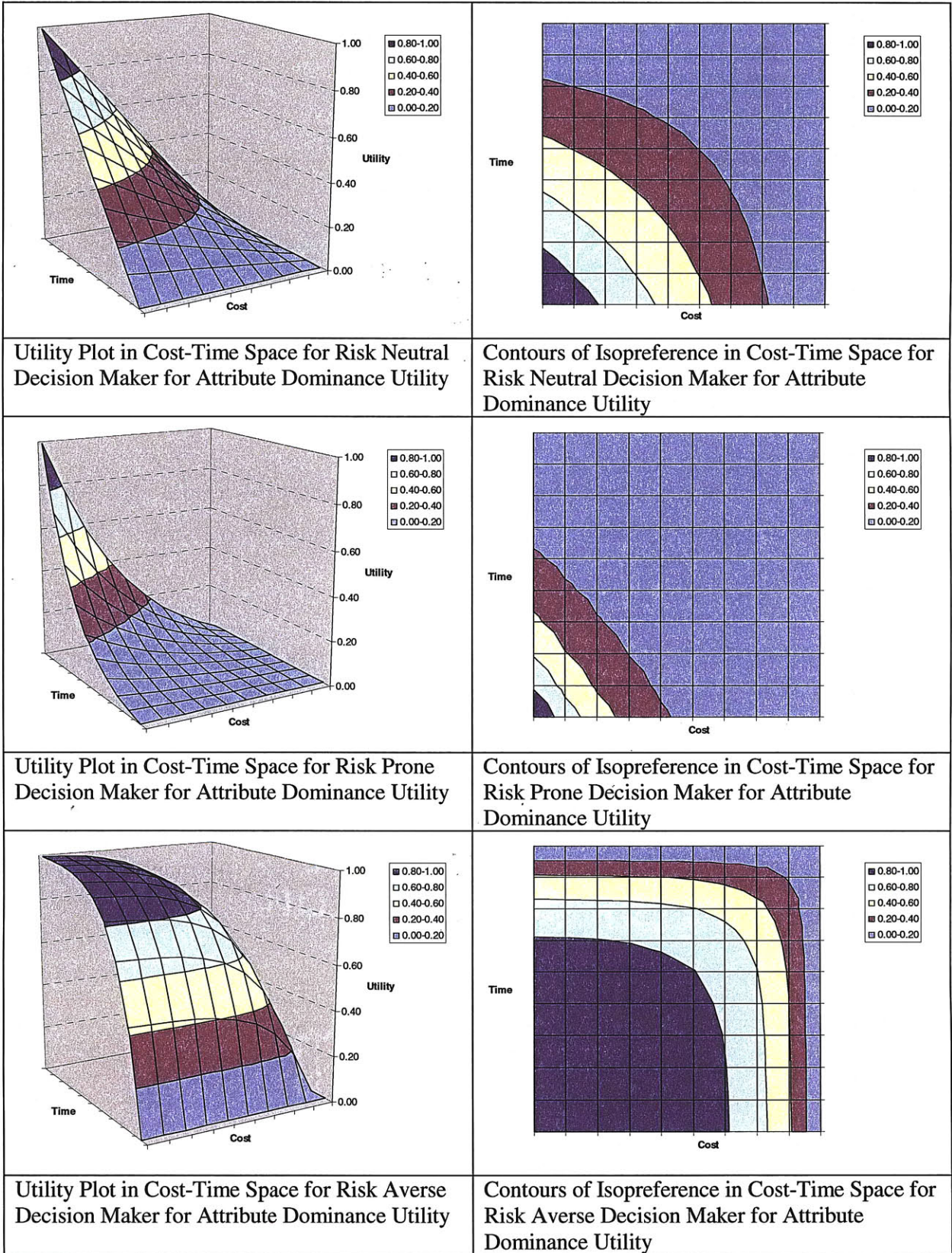


Figure 5.58 Utility Functions for decision makers with different risk preferences (Attribute dominance utility)



## **CHAPTER 6 Porto Metro Case study**

In this chapter the Porto Light Metro, where three collapses occurred between 2000 and 2001 will be presented. The Project will be described as well as the collapses that occurred. The author had access to the accident report written by the Porto Accident Commission and to New Guidelines for Tunnelling Works produced by the designer, both done after the accidents occurred. These reports discuss the different possible scenarios and possible causes for the collapses. The results of these two reports will be summarized and analyzed. Finally construction data obtained from the Owner will be used to apply and further develop the methodology presented in Chapter 5. The results will be presented and analyzed.

This application is based on the data that were made available by the Porto Metro Owner. Its goal was to apply the methodology developed in Chapter 5 to a real case. The analyses of the data do not intend to substitute the official Porto accident report results, nor attribute any guilt to any of the parts.

### **6.1 The Project**

The first phase of Porto Light Metro Project consists of 4 lines, with an overall length of about 70 km. These lines will connect Porto, the main city of Northern Portugal, with 6 other Municipalities of the Porto Metropolitan Area, with a population of about 1.2 million. The Porto Project was the largest light metro project awarded in one single contract.

The Project has two lines (Line C and Line S) that include tunnels that run beneath the centre of the city. The Line C tunnel is 2.3km long and the Line S tunnel is 3.7 km long. The average overburden thickness ranges from 15-30m, with the minimum value of 3-4m occurring in the final section of the Line C tunnel. The tunnels were excavated by earth

pressure balance shields (EPB-shields), which were capable of both closed and open mode excavation in mixed face conditions. Tunneling started with the Line C, from Campanhã to Trindade, in June 2000 with an 8.7m diameter Herrenknecht TBM. The driving stopped in December 2000 as a consequence of a major incident after about 470m. Work resumed in September 2001 and the Line C tunnel was completed in October 2002. In June 2002 a second 8.9 m diameter Herrenknecht EPB machine began a 2.7 km long Line S tunnel, from Salgueiros to São Bento, which was completed in October 2003. After Line C tunnel completion, the first TBM was disassembled and reassembled to restart in February 2003 on the remaining 1.0 km of Line S, which was completed in November 2003.

Figure 1 shows the Metro Porto network and the tunnel locations.



Figure 6.1 Porto Metro Network. The tunnels are Line C from Campanhã to Trindade (green) and Line S from Salgueiros to São Bento (purple).

### 6.1.1 The geology

The main formation crossed by the Porto metro tunnels is the Granitic Formation (Porto Granite). Figure 2 shows the distribution of this formation within the city of Porto. It is a deeply weathered formation, especially in faults and joints, resulting in a very irregular profile. Alteration grades range from residual soil (W6) to fresh granite (W1); As a result of the highly variable weathering grade, there are large variations in density, permeability and geo-mechanical parameters. Figure 3 shows the appearance of the granite and its degrees of weathering in a core recovered from a site investigation borehole in the tunnel alignment. In this figure one can observe that the weathered granite in the left box is at a depth of about 24m under the sound granite of the right box. This type of profile is not uncommon below the city of Porto.

The hydrology / water flow is a function of the granite-weathering grade. In the less weathered granite (W2-W3) the flow can be associated with water carrying fractures, while in the more weathered ground it can be associated with that of a porous medium. This combination results in a very variable rock/soil mass permeability following the alteration patterns. The interfaces between the different formations are generally diffused and impossible to predict precisely.

Four principal sets of discontinuities exist along the Line C tunnel alignment: i) two subvertical oriented NW-SE and SW-NE and ii) two inclined between 50 to 70 degrees oriented N-S. The Line C tunnel is aligned approximately E-W.

A particular feature associated with the local conditions of the Porto area is the frequent occurrence of wells connected by drainage galleries that, in the past, ensured the population's water supply. These wells are not well charted.

The water table is located between 10 m-25 m above the tunnel crown and 20% of the tunnels' length has very low overburden.

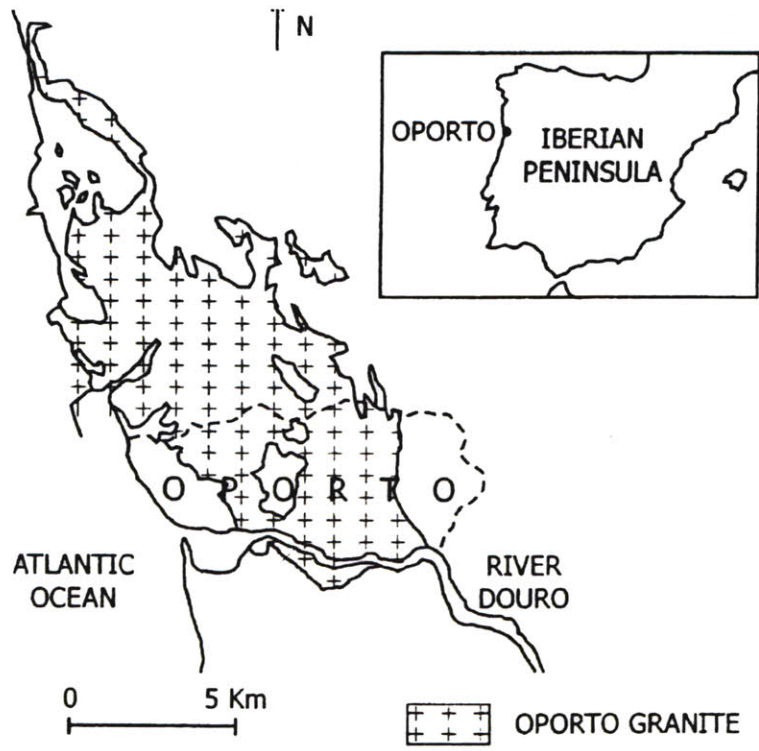


Figure 6.2 Distribution of the Granite formation within the city of Porto



Figure 6.3 Appearance of the different degrees of weathering of the granite formation in a core recovered from a site investigation borehole in the Line C tunnel alignment.

The designer considered seven geomechanical groups of homogeneous conditions in terms of weathering. The design geomechanical groups and associated conditions are presented in Table 6.1.

Table 6.1 Geomechanical groups and associated conditions

Geomechanical groups	Weathering degree (W) of intact rock	Fracturing degree (f) <sup>(1)</sup>	Correlation [%] W-f	Discontinuity Condition <sup>(2)</sup>	GSI
g1	W1	f1-f2	80-85	d1-d2	68-85
g2	W2	f1-f2	80-85	d1-d2	45-65
g3	W3	f1-f2	70-75	d1-d2	30-45
g4	W4	f1-f2	65-70	d1-d2	15-30
g5	W5	(f5)	90-95	(d5)	(<20)
g6	W6	n.a.	-	n.a.	n.a.
g7 <sup>(3)</sup>	n.a.	n.a.	-	n.a.	n.a.

Notes: <sup>(1)</sup> based on ISRM (1981) to which classes correspond the following (in cm) discontinuity spacing ranges: f1:>200, f2:60-200, f3:20-60, f4:6-20, f5<6; <sup>(2)</sup>classes of surface conditions for “GSI-Based geomechanical groups “; <sup>(3)</sup>g7 correspond to man made material and alluvial soils.

Idealized weathered profiles based on classification by the Geological Society of London, 1995, and the recommendations of ISRM are presented in Figure 6.3.

Figure 6.5 shows the layout of the line C tunnel and Figure 6.6 shows the geological conditions along the Line C tunnel.



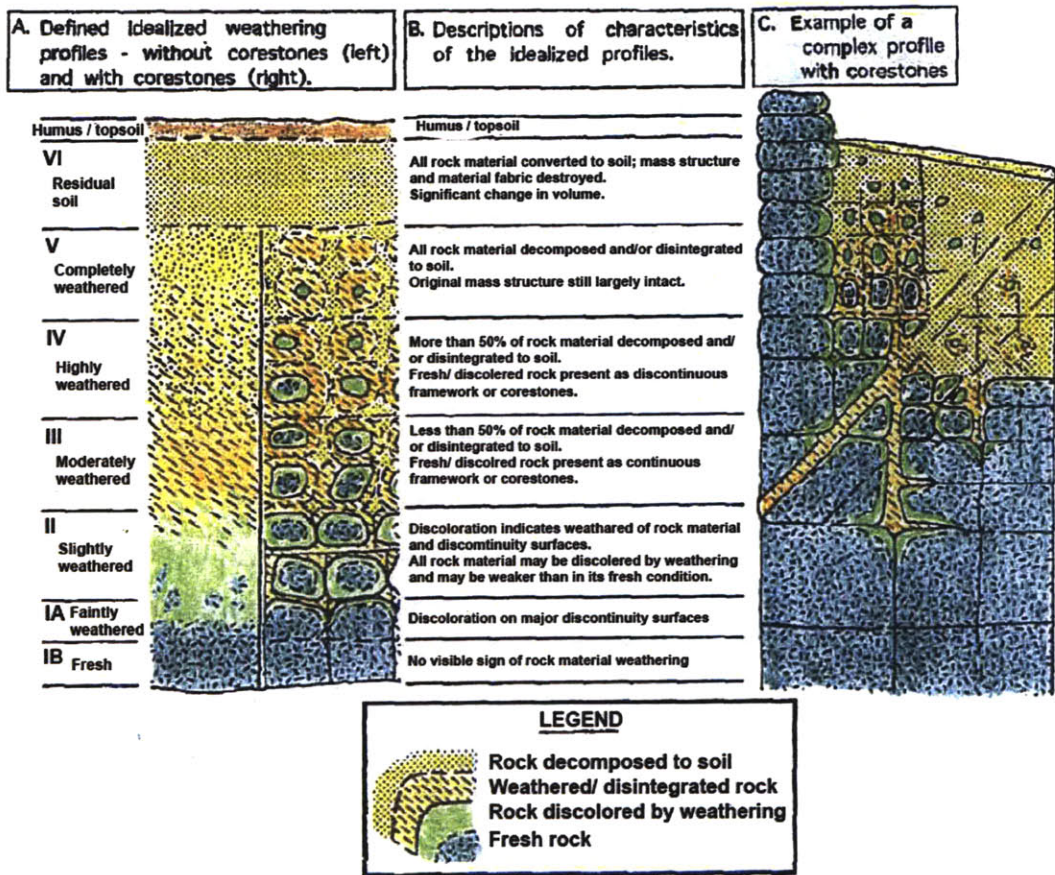


Figure 6.4 Idealized weathered profiles based on classification by Geological Society of London, 1995, and the recommendations of ISRM



Figure 6.5 Line C Tunnel layout



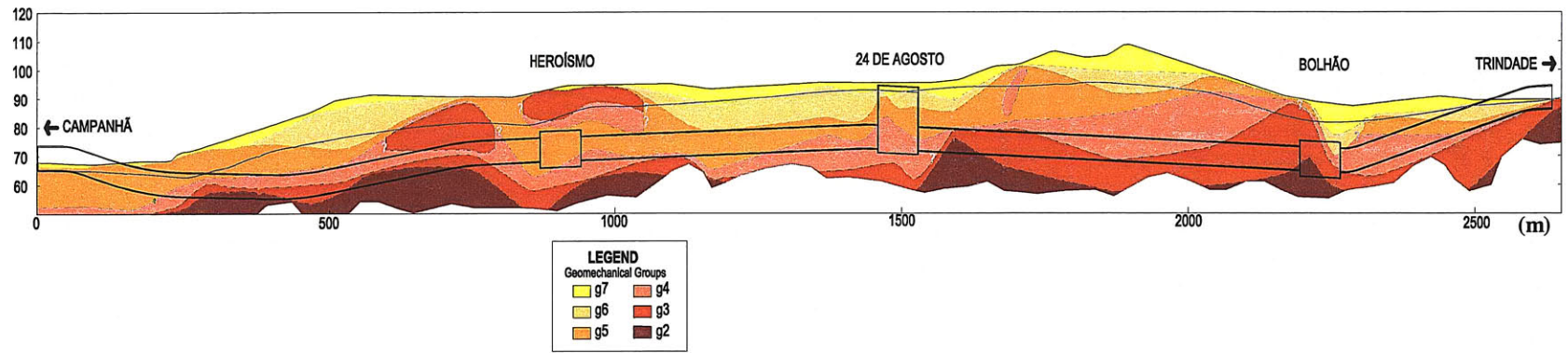


Figure 6.6 Longitudinal Campanhã to Trindade section

## 6.1.2 Construction method

Line C was excavated by an 8.7 m Herrenknecht Earth Pressure Balance Machine. This machine can advance in different modes (open, closed, semi-closed) as will be described below.

As the machine advances a segmented tunnel lining is put in place inside the shield. The lining comprises six segments and a key. Dowel connectors are used in the radial joints while guidance rods are used in the longitudinal joints. Behind the shield grout is injected to seal the annular gap between the lining and the ground (Figure 6.7). The head of the TBM is located approximately 6 m from the ring. The width of each ring is 1.4 m. This means that when the machine excavates the distance of a ring, the ring being mounted in that cycle corresponds to about four rings before. The ring being injected in the same cycle will be located two rings before the one being mounted.

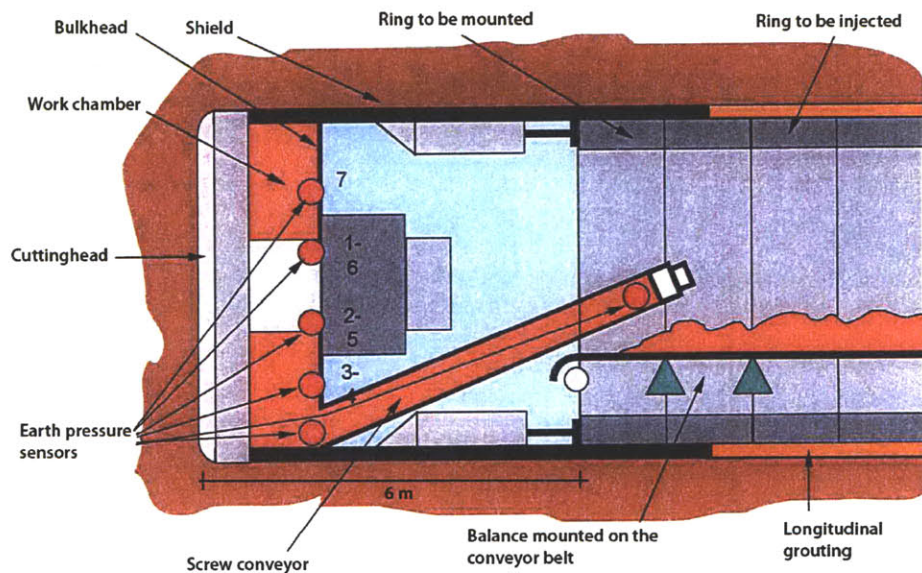


Figure 6.7 EPBM machine scheme

This specific machine adapts to different excavation conditions by changing the support system at the face. The machine can operate in three different modes (Figure 6.8): Open mode, Closed mode and Semi-Closed. In the Closed Mode the work chamber is

completely filled with excavated pressurized material. The Semi-closed Mode corresponds to a situation where the work chamber is only partially filled with muck and compressed air is used to support the empty part of the chamber to prevent local instability of the face. This method allows the machine to achieve a higher rate of advance, less tool wear and savings on conditioning additives and therefore is an attractive mode to the contractor in more stable, cohesive ground. Finally operation of the machine without any active face support is called Open Mode (Babendererde et al., 2005)

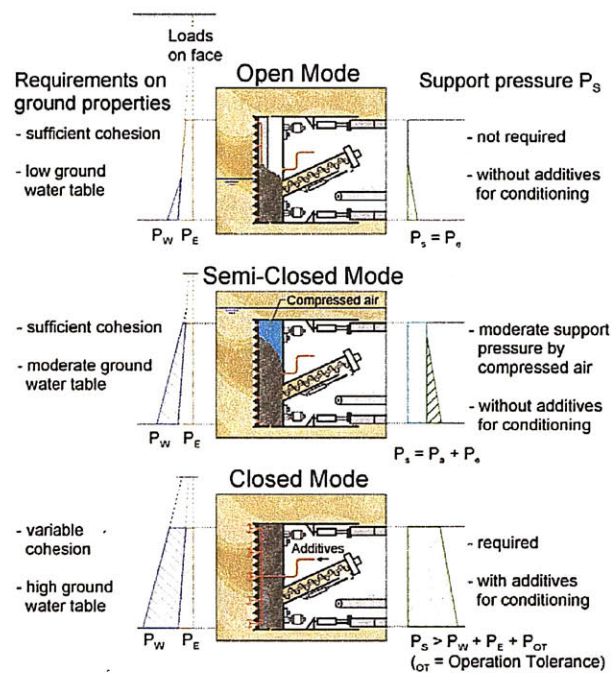


Figure 6.8 EPBM Operation modes (Babendererde et al., 2005)

The face pressure is controlled by balancing the advance of the cutting wheel (or cutting head) and the discharge of the screw conveyor, which is controlled by the rotation of the screw conveyor. The material discharged by the screw conveyor is weighted. The advance of the cutting wheel and rotation of the screw conveyor are controlled by the machine operator (Transmetro, 2000b).

The determination of the operating mode for driving the tunnel of Line C was based on two main criteria: i) assurance of the stability of the face and ii) assurance that the

deformations and distortions of the buildings at the surface are admissible. Based on these two criteria the sequence for the Operation Mode of the machine, presented in Table 6.2 was obtained (Transmetro, 2000a).

Table 6.2 Mode of Operation of the Porto Metro EPBM Machine along Line C tunnel (from Transmetro, 2000)

Section	Operation Mode	Section length [m]	Pressure at face [kPa]
0+150 - 0+530	CLOSED	380	65
0+530 - 0+800	OPEN	270	---
0+800 - 0+840	CLOSED	40	180
0+840 - 1+030	OPEN / CLOSED	190	70
1+030 - 1+460	CLOSED	430	285
1+460 - 1+530	<i>Estação 42 de Agosto (cut &amp; cover, about 70m)</i>		
1+530 - 1+600	CLOSED	70	280
1+600 - 1+750	OPEN	150	---
1+750 - 1+950	OPEN / CLOSED	200	100-160-100
1+950 - 2+230	OPEN	280	---
2+230 - 2+480	CLOSED	250	105

In reality, at the time of the accident, as pointed out by the official Accident Investigation Commission the machine had been operating in semi-closed mode with an active face pressure of 65 kPa in the section 0+530 - 0+800 and not in the Open Mode as determined in the design.

### 6.1.3 The accidents

Three accidents occurred during the excavation of the first 300m of line C tunnel. Not a lot of information was made available to the author regarding the first two accidents. The

main focus of this chapter will be on the third accident, since it was the one with most serious consequences and the one for which the most information is available.

- 1) First incident, 30 of September 2000 (during this day the rings 123 to 126 were excavated, station 0+326.69 to 0+330.90)

The EPBM had advanced 120m from the beginning of construction when it intercepted a former well resulting in the discharge of its water. The overburden in this area was 12m. The ground collapsed below two buildings causing damages to the structures. The settlement at the surface was about 2.5m, within an area of approximately 40m<sup>2</sup>.

The tenants were evacuated. The commercial activities were interrupted for 2 months. The work restarted 6 weeks later.

Figure 6.10 shows a detail of the accident zone.

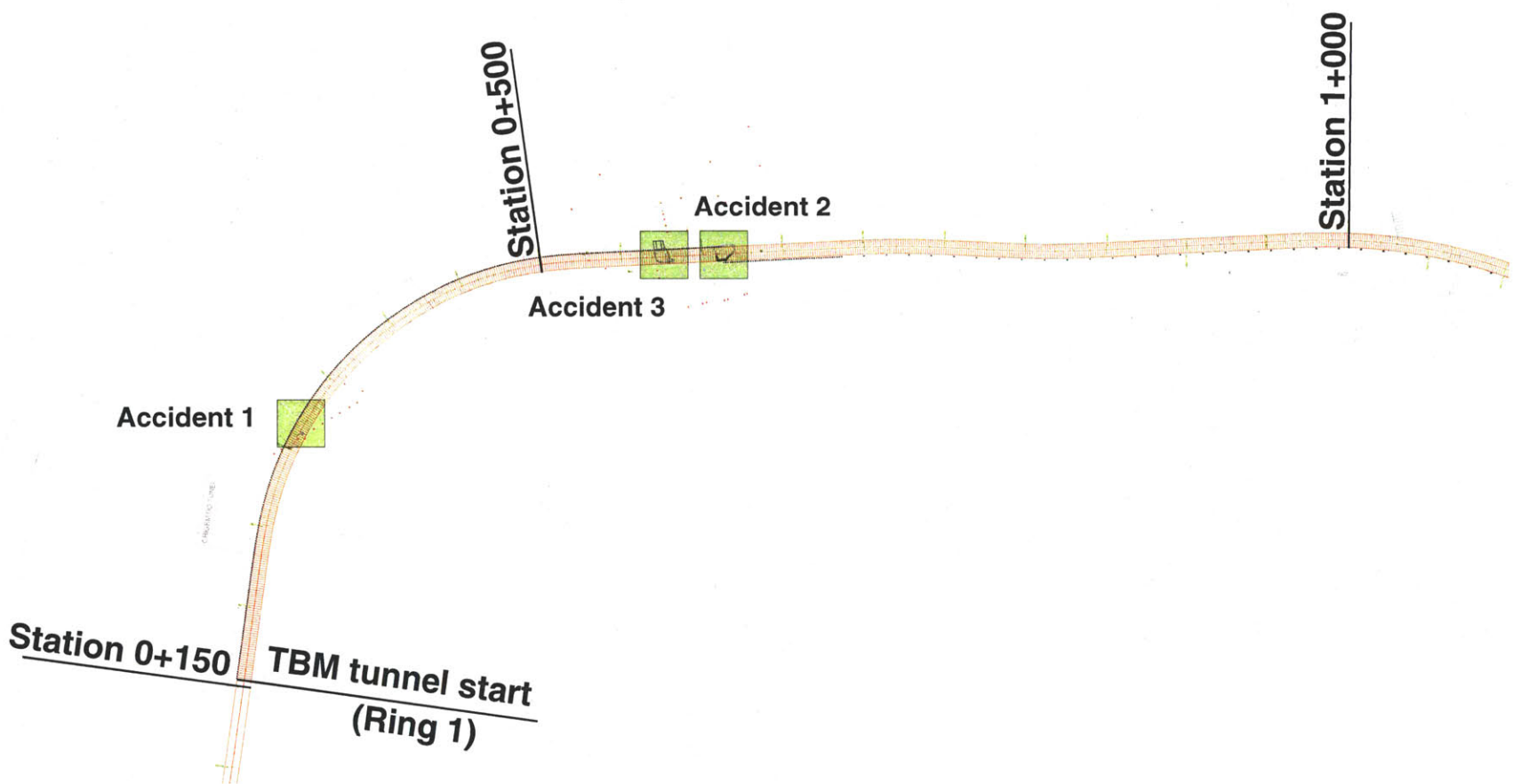


Figure 6.9 Line C and location of the accidents





Figure 6.10 Zone of Accident 1 (building 44)

2) Second accident, 22 December 2000

After the passage of the TBM cracks were encountered in the walls of a building followed by 250m<sup>3</sup> of subsidence of the back gardens (over-excitation during installation of rings 318, station 0+606.51, and 327, station 0+619.15). The tunnel depth was about 26m. This accident is located a couple of meters just before the TBM stopped (see Figure 6.11).

3) Third incident, 12 January 2001

The accident occurred under houses 182 and 183, under approximately rings number 297 to 301 (station 0+570.99 to station 0+576.60). A building fell into the 8mx8mx6m crater resulting in the death of a person. The overburden was of about 25m.

The TBM had passed under these houses on the 16 to 18<sup>th</sup> of December 2000, and it was stopped 50 m ahead since 28 December (Figure 6.11). This stoppage was due excessive settlement at the surface and to fill a cavity of around 15 m<sup>3</sup> due to over-excitation. In the period between 28 December 2000 and 12 January 2001 (when the accident occurred)



consolidation works from the tunnel and the surface were executed. In addition the ground below Building n.183 was injected through 5 inclined, lateral boreholes from the surface. These injection holes had been decided upon after it was realized that the machine had over-excavated when driving underneath this building (Geodata, 2001). The consolidation works underneath building n. 183 were concluded on 29 December 2000.

Figure 6.11 shows the location of the 3<sup>rd</sup> incident (and 2<sup>nd</sup> accident)

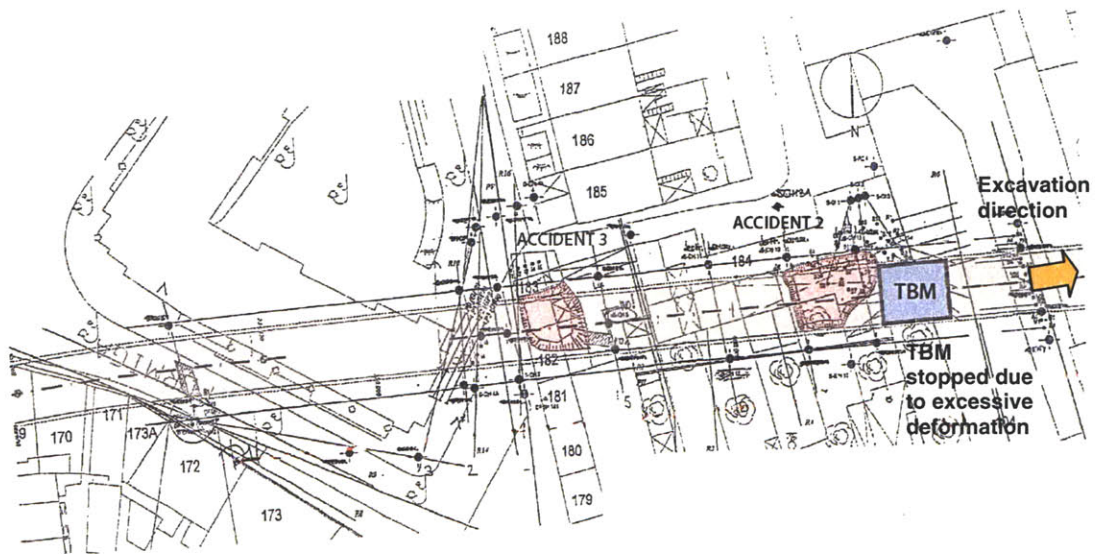


Figure 6.11 Location of the 2<sup>nd</sup> incident and 3<sup>rd</sup> accident

The time elapsed between the passage of the TBM under building n.183 and the actual collapse was about 25-28 days. The monitoring was not able to alert of the imminent accident. The instrumentation in the accident zone was only composed of surface deformation measurements (Figure 6.12), and the settlement registered at the building before the accident was less than 10mm and showing signs of stabilization.

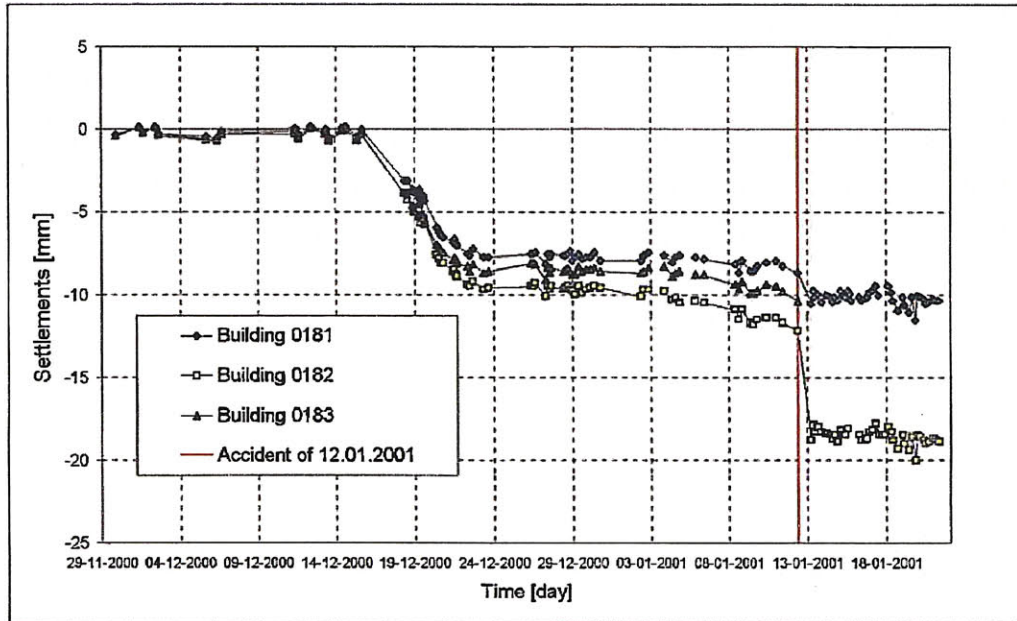


Figure 6.12 Monitoring results (vertical deformations at surface) for buildings 181, 182, 183. The warning value is 28mm.

The walls of the crater were sub-vertical and it could be observed that W5 granite was predominant in the area.

#### 6.1.4 Reported possible causes of Accident 3

The author had access to the official Accident Investigation report, as well as the report made by the designer for the owner regarding the last accident (accident 3).

The Accident Investigation Committee's preliminary report contains the following recommendations and conclusions (Comissão de Inquerito, 2001):

- The geological conditions throughout the tunnel alignment are extremely complex and heterogeneous.

- According to the monitoring data, the mechanical behavior of this geological formation is apparently characterized by an initial rigid behavior followed by a sudden loss of strength.
- Being a design-build contract it was observed that the attitude and coordination between the different teams (TBM, supervision, designer, etc) was inadequate for the timely resolution of geotechnical problems that would emerge during construction. There was also not a good control of the construction and a prompt analysis of anomalous situations that occurred and were reported during construction.
- The commission finds it difficult to understand why the geological and geotechnical model was not defined and controlled during construction by the designer.
- The surveying ahead of the face, which was required in the design, but was never done, should have been performed and would have helped with the detection of weathered zones and other geological features ahead of the face. The design determined that boreholes were to be placed every 30 m if operating in open mode; and 50-60 m if operating in closed mode. The surveying ahead of the face as it was required by design was not done during the driving of the tunnel up to the last collapse.
- The fact that the real geology did not match the design but no action was taken to adapt the excavation (mode of operation, rate of excavation, face pressure) to the found geology.
- A lot of emphasis was given to the monitoring at the surface (deformations) and not much attention was given to automatically recorded data by the machine (extracted weight, advance rate, injected grout, face pressure, etc)
- There were no established methodologies and procedures to control the excavation at the face that would have allowed one to anticipate problems.

The preliminary causes determined by the commission for the 12 January 2001 accident (3<sup>rd</sup> and last accident) were due to an incorrect execution of the tunnel excavation, due inadequate operation of the TBM machine, specifically the face pressure:

- Deficient design, which did not include continuous analysis of the crossed geology and adjustment to the excavation to the encountered conditions.
- Insufficient geological characterization of the ground due to the lack of boreholes from the surface and the lack of boreholes from the machine's face that were required in the design but were never done.
- Non prompt analysis of the monitoring results
- Deficient supervision of the work and communication between the different teams.

The analysis of the accident that led to these possible causes was made before the site investigations that will be detailed later in this chapter. However the lack of continuous and prompt analysis of monitoring data, including the machine recorded parameters and the inability of adapting the excavation and operation mode of the TBM to the actual conditions seem to be causes for the collapse

The committee made some recommendations for the re-starting of the excavation works:

- More experienced and adequate crew for the type of work.
- Complete revision of the design, focusing on the geological-geotechnical characterization of the ground, including the execution of boreholes at the face of the tunnel and from the surface.
- Implementation of procedures to better control the TBM excavation
- Continuous and prompt attention to all aspects of monitoring (at surface and from TBM)
- Systematic and prompt analysis of registered anomalies, including the ones of the already excavated sections.
- Better interaction and communication between involved parties, designer, contractor and owner and between specialists (such as geotechnical engineer, geologist, monitoring engineers, TBM operators)

A site investigation was performed after the accident (3<sup>rd</sup> accident) of 12 January 2001 in order to assess the causes of the accident as well as to support future decisions regarding the progress of the excavation. The investigation included (Geodata, 2001):

- Boreholes with in-situ testing (SPT and permeability) and recovery of samples
- Installation of monitoring instrumentation (piezometers and inclino-extensometers) in some boreholes
- Geophysical survey including resistivity profiling and cross-hole seismic testing and georadar survey.
- Laboratory test (physical and mechanical properties)

Figure 6.13 shows the location of investigation points and chronology their installation.

Besides the investigation the designer also conducted detailed analysis of the data collected by the TBM during excavation in order to better understand the performance of the TBM and its interaction with the ground.

Some of the main results of the site investigation according to Geodata (2001) are the following:

- The ground at the crown of the tunnel was mainly composed of W5, a worse than the predicted scenario. This is in agreement with what was observed at the exposed part of the face of the tunnel at chainage 0+577 m and the analysis of the muck recovered with prevalent sandy granulometry and presence of W5 fragments.
- High variability of SPT values, even within the same weathering degree in particular within W5.
- The possibility of preferential channels of water circulation (due to the existence of old galleries and channels), accentuated by the existence of strongly weathered granite horizons along major discontinuities.

- The laboratory tests on the samples recovered at tunnel level, in the boreholes in the zone of the accident (in particular from S-CH5, S-CH8, S-CH16 and SPZ1) show very low values of dry unit weight, between 12-15.1kN/m<sup>3</sup>, while the dry density assumed in the design was of 15.8-19.8kN/m<sup>3</sup>. The designer believes that these samples correspond to leached granite. The leaching of the granite caused by the rainfall regime as well as an old well construction technique, which caused intense bleeding of fine materials around the well. Laboratory testing and in situ pumping testing seem to confirm the existence of low density W5 horizons near these old wells. Figure 6.14 shows a schematic of a typical old well.



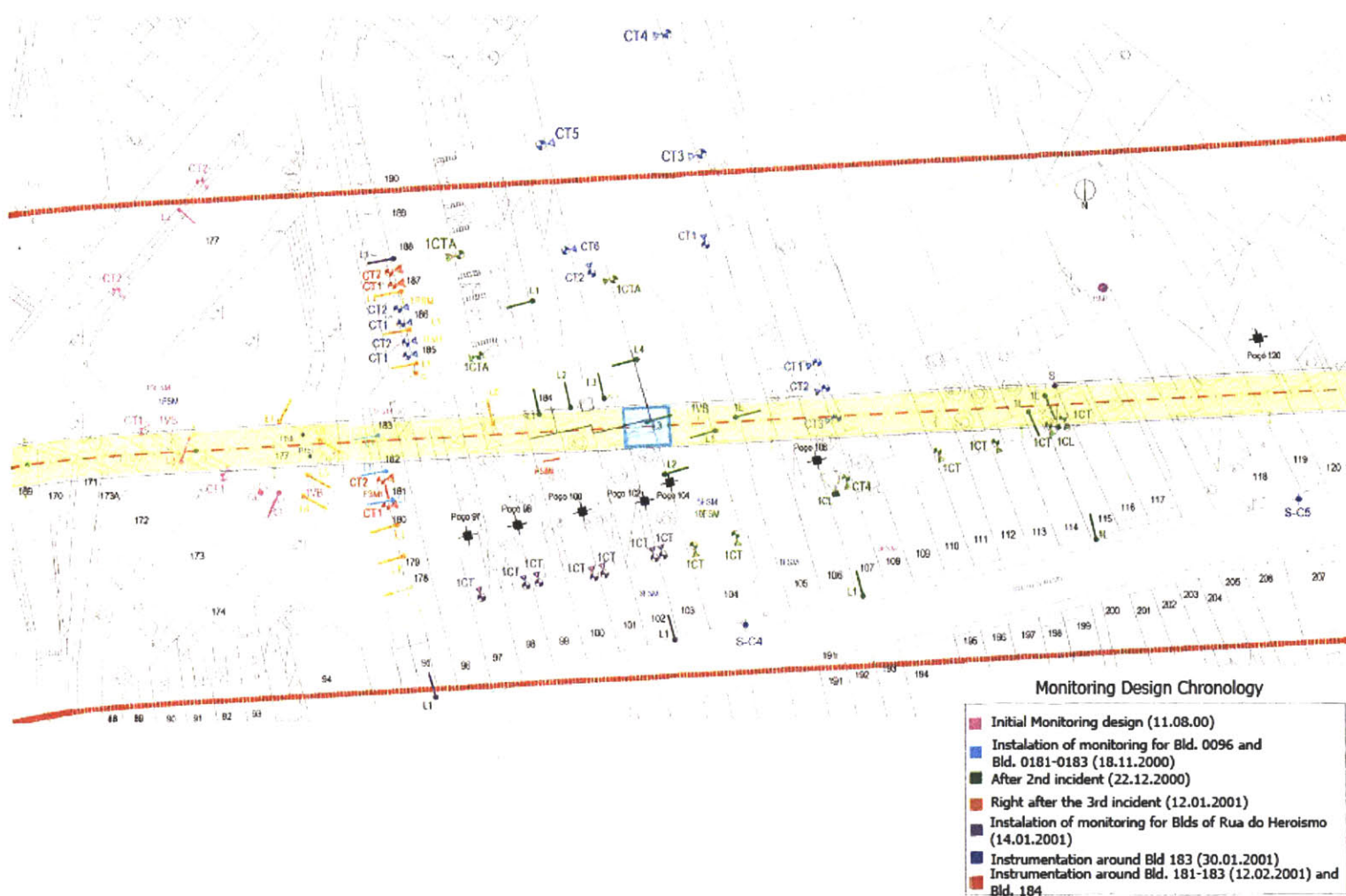


Figure 6.13 Location of investigation points and chronology their installation

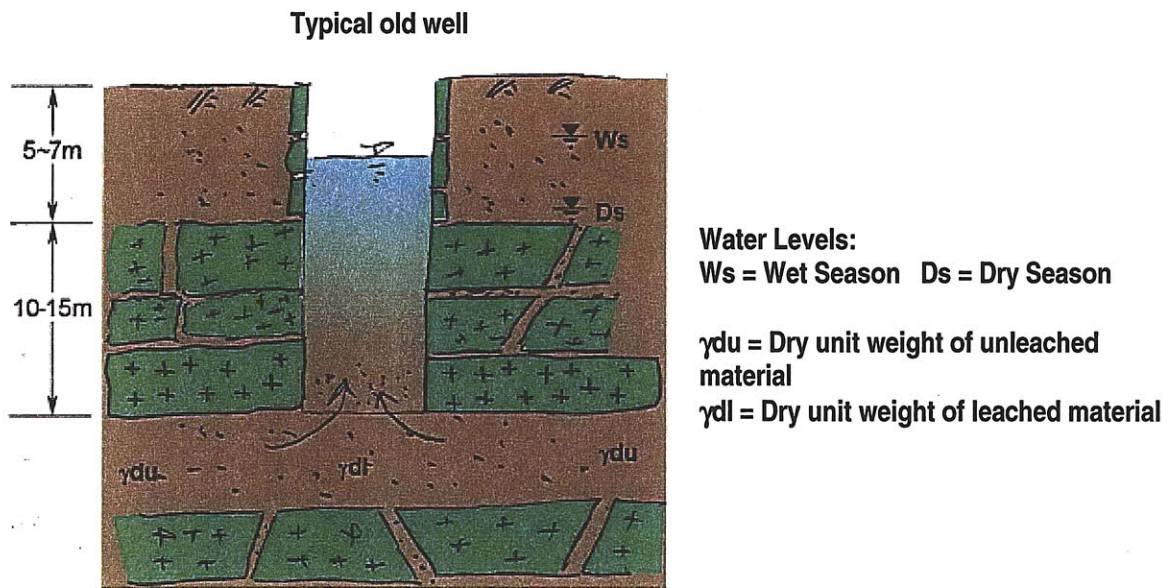
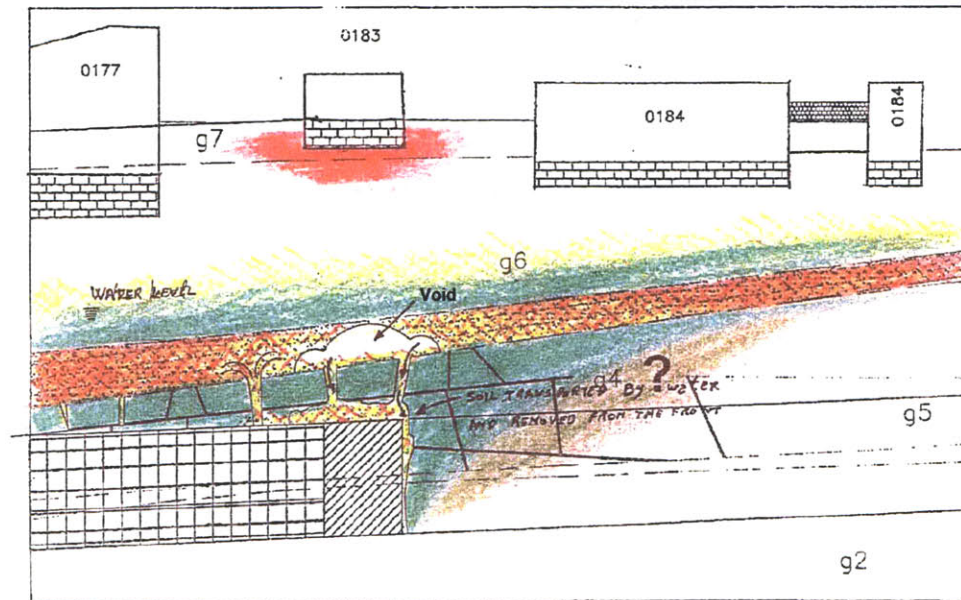


Figure 6.14 Typical old well (Geodata, 2001)

Based on the results of the site investigation and analysis of TBM recorded data Geodata came up with three different possible mechanisms for the ground collapse at building n.183:

### **Hypothesis 1**

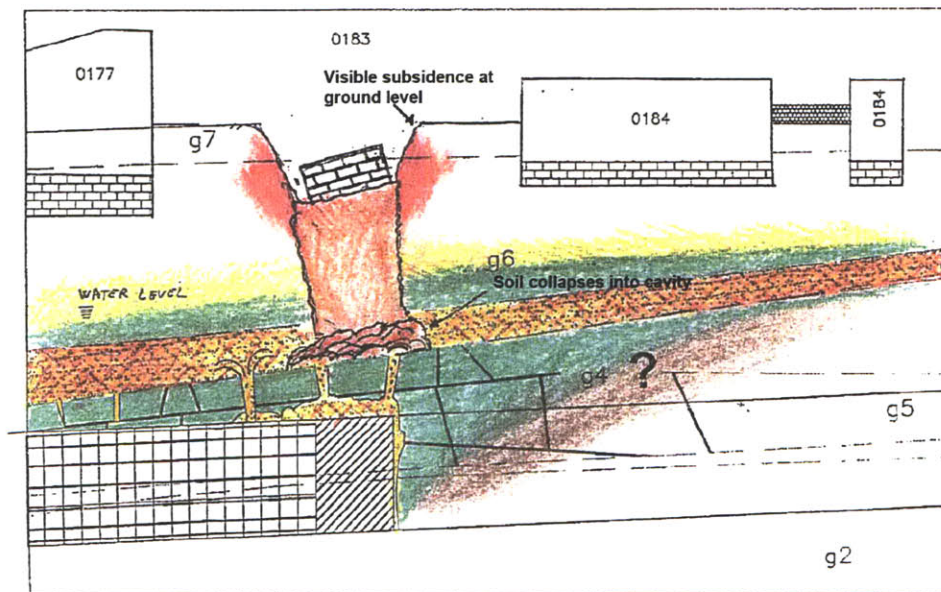
The first scenario contemplated the existence of voids located somewhere near the tunnel, not necessarily distributed symmetrically with respect to the cross section. According to this hypothesis the void would have progressively slowly moved upwards to the failure of the ground arch assisted by groundwater inflow. The final sudden collapse occurred due to the brittle failure of the thin arch under building n. 183. In this scenario the originally predicted G4 layer did not exist. Figure 6.15 illustrates the failure mechanism of hypothesis 1.



Station (m): 550,0

600 0

a) Existing void



Station (m): 550,0

600,0

b) sudden collapse

Figure 6.15 Failure mechanism – hypothesis 1 (adapted from Geodata, 2001)

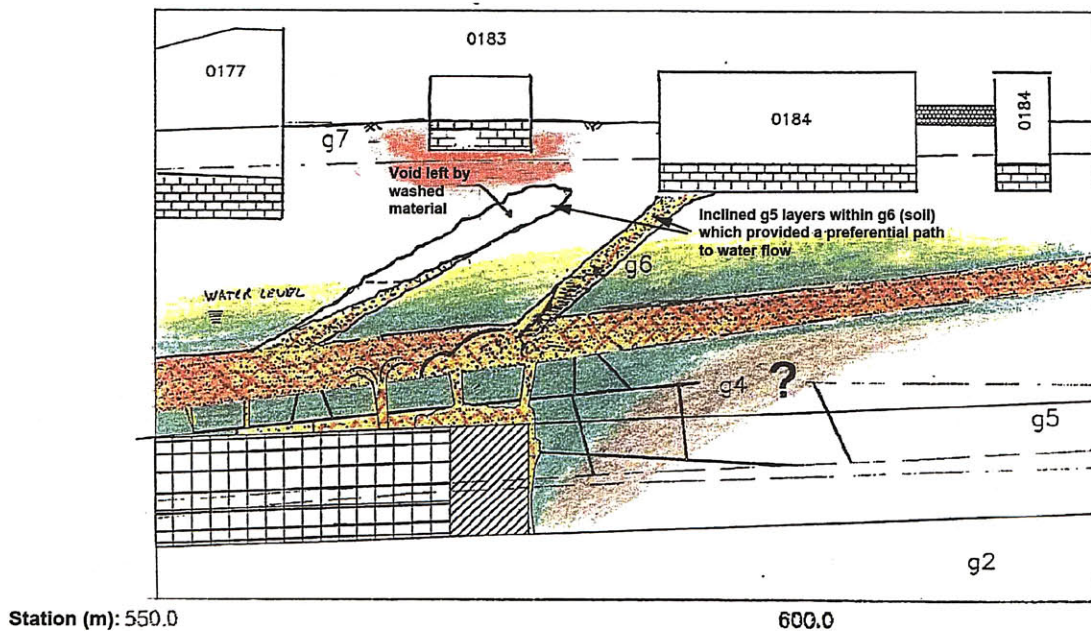
## Hypothesis 2



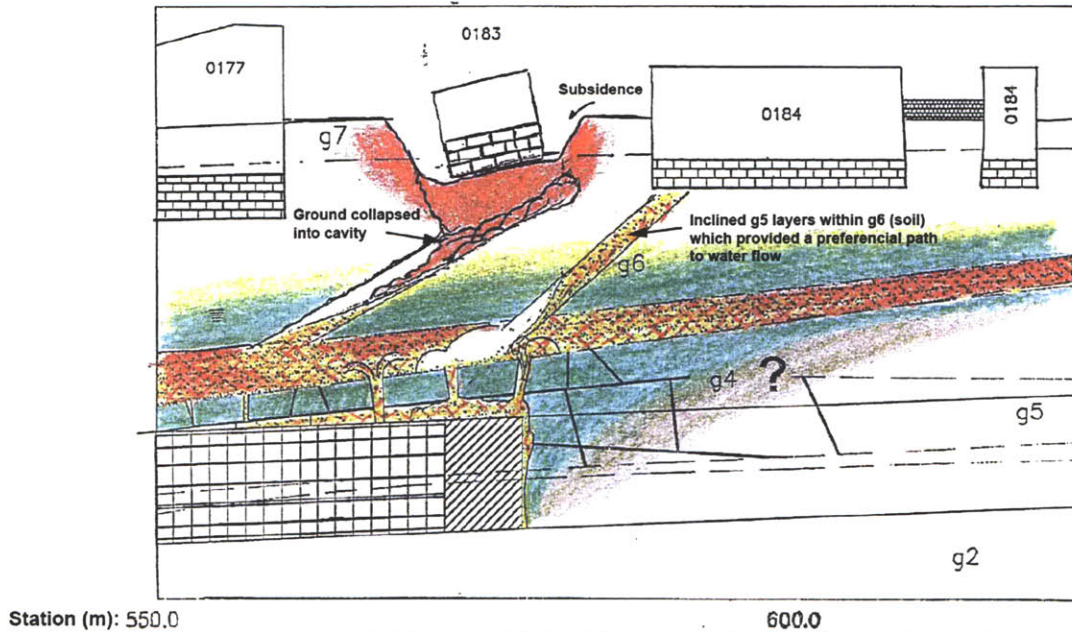
In this hypothesis the over excavation caused an irregular void around the tunnel which partially emptied an adjacent inclined g5 layer (see Figure 6.16), asymmetric in cross-section. This void slowly progressed upwards after the passage of the TBM influenced by:

- The continuous heavy rain that occurred the month of December
- Complex underground and “minas” network in the area
- Alteration of the ground water regime due to both tunnel excavation and injection works executed nearly one month before the collapse.

Again the final sudden collapse occurred due to the brittle failure of the thin inclined slab under building n. 183. Figure 6.16 illustrates the failure mechanism of hypothesis 2.



a) Progressive void



**b) Sudden collapse**

Figure 6.16 Failure mechanism – hypothesis 2 (adapted from Geodata, 2001)

**Hypothesis 3**

In this scenario the g5 layer was confined by a g4 layer, and therefore the over excavation induced void was also limited to progress upwards (Figure 6.17). As the TBM advanced other similar voids due face instabilities were created. These voids, limited vertically by the g4 layer, were aggravated probably by the water flow above the tunnel, in the longitudinal direction. This caused the possible effects:

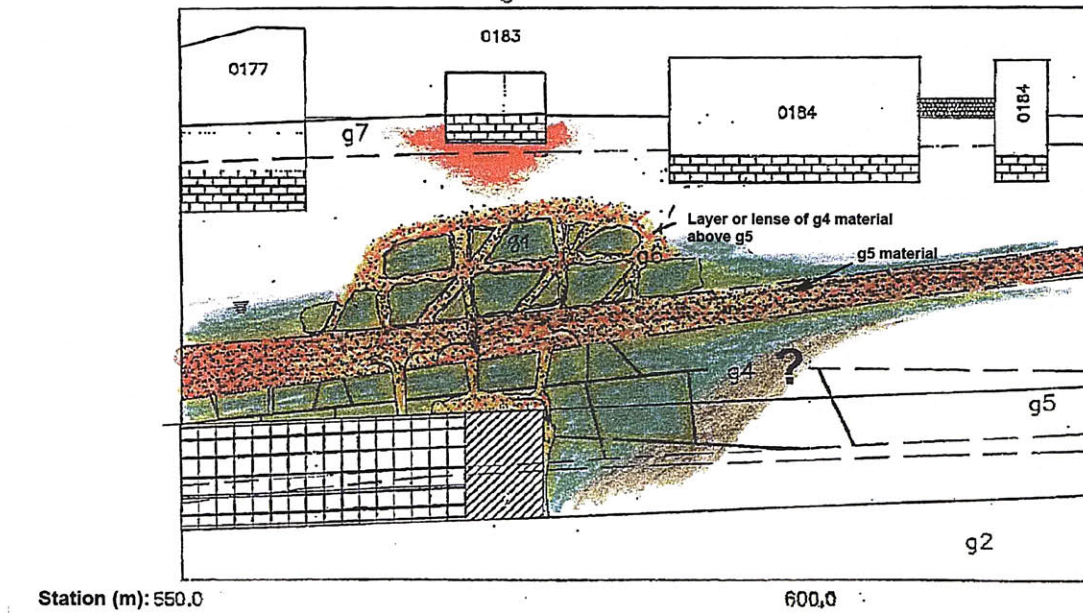
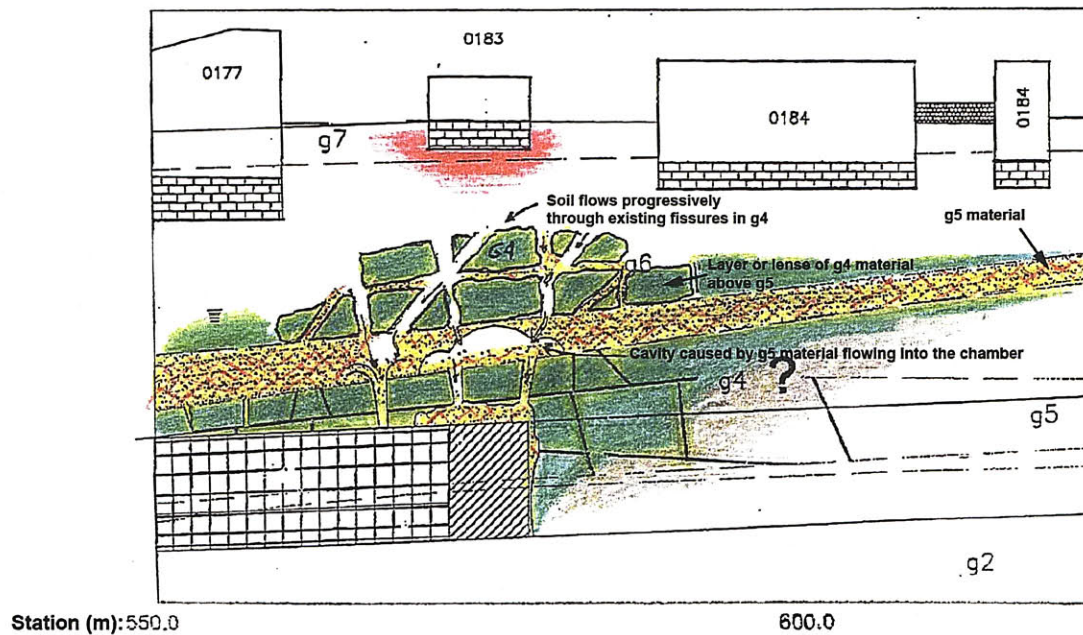


Figure 6.17 Geological scenario for Hypothesis 3 (adapted from Geodata, 2001)

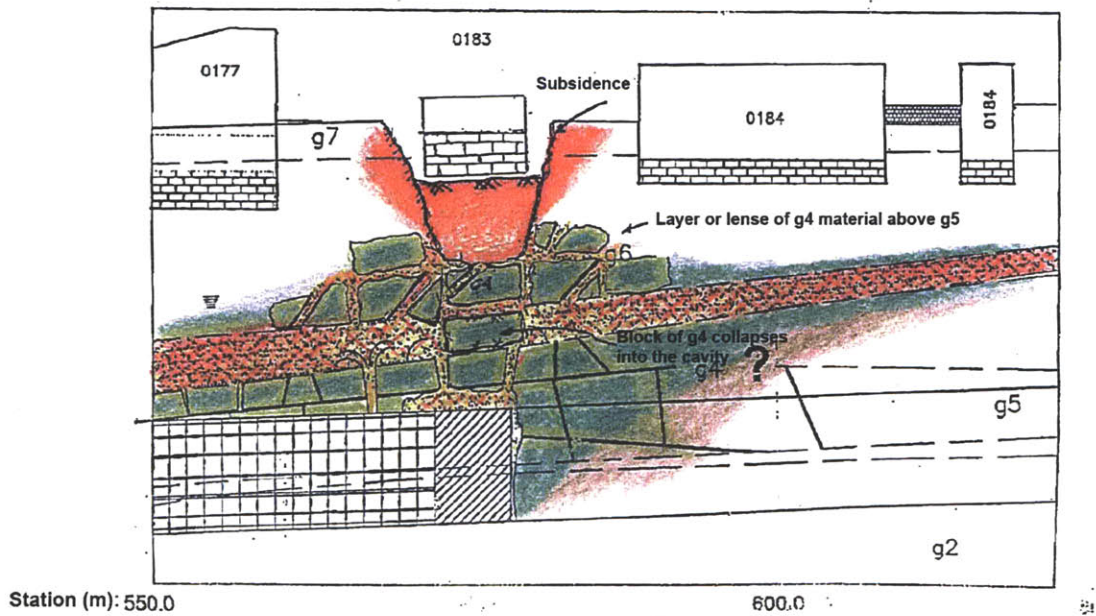
*Hypothesis 3a*

Progressive upward enlargement of the initial over extraction induced void(s), emptying the sub-vertical fractures in g4, which lead to the final and sudden collapse. This mechanism is illustrated in Figure 6.18.



a) progressive void





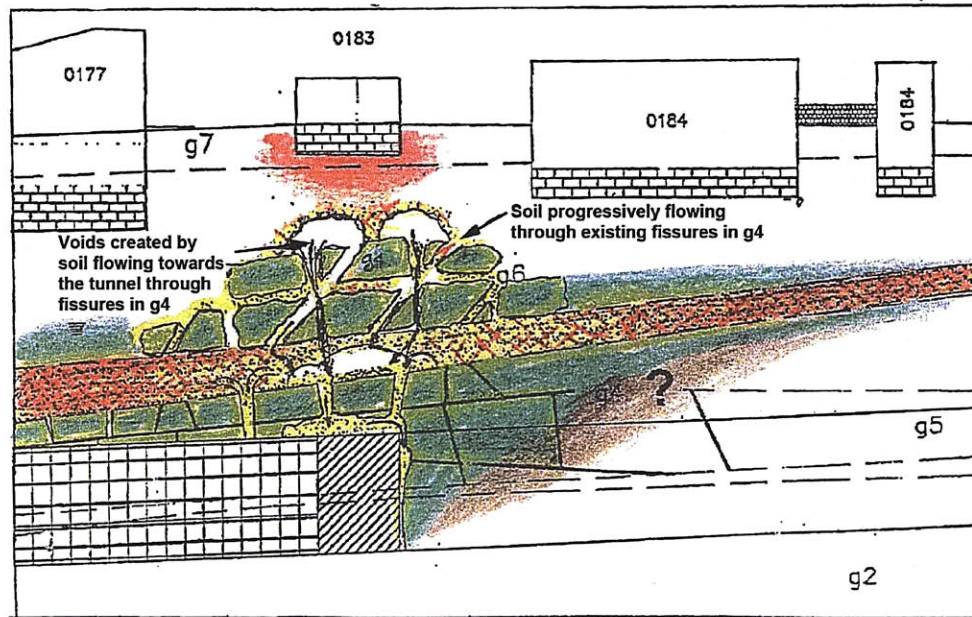
**b) sudden collapse**

Figure 6.18 Failure mechanism – hypothesis 3a (adapted from Geodata, 2001)

*Hypothesis 3b*

Creation of a new void(s) in the g5/g6 layer overlying the g4 lense, though the migration of material through the g4 fractures, assisted by downward flow of water from the surface in the long periods of heavy rain, leading to the final and sudden collapse.

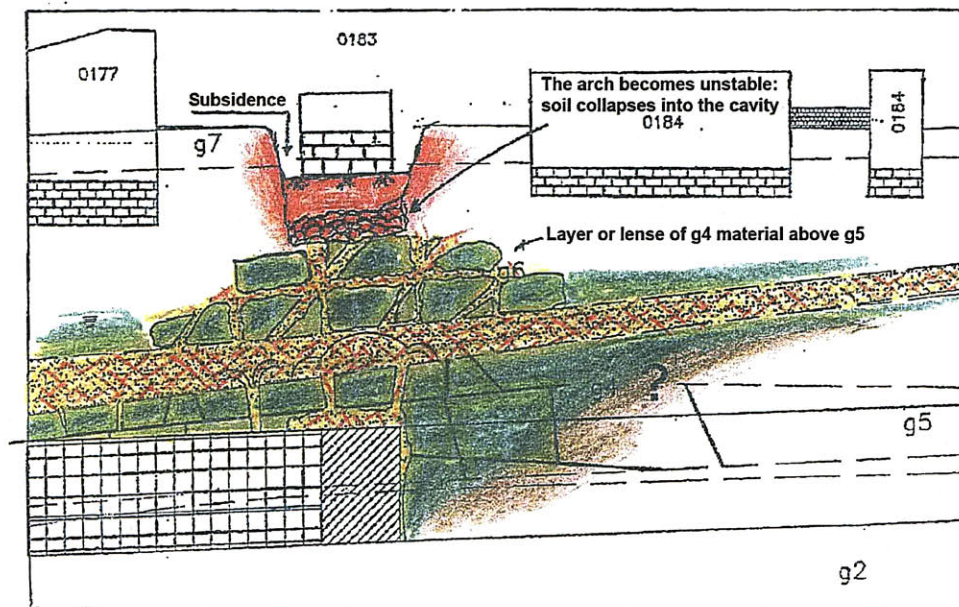




Station: 550.0

600.0

**a) progressive void**



Section (m): 550.0

600.0

**b) sudden collapse**

Figure 6.19 Failure mechanism – hypothesis 3b (adapted from Geodata, 2001)



Figure 6.20 Location of boreholes where leached granite samples were obtained (Geodata, 2001)

The panel of experts that was in charge of the executive review of the construction behavior up to the occurrence of the accidents, described different geological models than those described by Geodata (2001), at the face and immediately above the EPBM (Babendererde et al, 2004)

1. Fresh or slightly weathered Granite with no weathered material in the discontinuities;
2. Fresh or slightly weathered Granite but with very weathered material (filled or in situ) in substantial fractures; these fractures may communicate with overlaying parts of completely weathered granite;
3. Very weathered or completely weathered granite, W5 (almost granular soil with little or no cohesion);
4. Very weathered or completely weathered granite with blocks of the rock core;
5. Mixed conditions with both sound mass and completely weathered granite at the face.

For all 5 cases the water table is above the tunnel crown. According to the panel the machine should operate in Open Mode only in the first situation, and only if there was strong indication that this situation would persist for a considerable length of tunnel. Due to the heterogeneous nature and high variability of the ground mass, the panel considered that it is too risky to drive in Open Mode. Besides that, the deficiency of face support pressure can be compensated for by the addition of an Active Support System, proposed by Dr Siegmund Babendererde (panel member) that will be described in more detail in the Supplementary measures section

### **6.1.5 Supplementary measures**

After the third and fatal collapse, the construction was stopped for nine months and it was subjected to the Portuguese Government's Commission of Inquiry Investigation. In addition to the Commission's report, a panel of experts was assembled to perform an

executive review, providing constructive criticism and making recommendations on changes to be made to the EPBMs. Major changes and improvements were made to the construction process in order to ensure the safe completion of the tunnel excavation.

The two major proposals related to the machine operation itself (Babendererde, 2005):

- i) the EPBM required to operate only in Closed Mode
- ii) Installation of an Active Face Support System in the EPBM

The Active Face Support System, designed to compensate for deficiencies of the face support pressure, is composed of a container filled with pressurized bentonite slurry linked to a regulated compressed air reservoir. The way this system works is if the support pressure in the work chamber drops below a predetermined level the Active Face Support System automatically injects pressurized bentonite slurry until the pressure level loss in the work chamber is compensated, resulting in an operation similar to that of a Slurry-TBM (Babendererde, S, 2004). Figure 6.21 presents the additional slurry injection system (Active Face Support System) connected to the crown area of the work chamber.

A situation that can cause a drop in the face support pressure corresponds to the one presented in Figure 6.22, in which the lower part of the cross-section is composed of fresh granite and the upper part is in residual soil. In this situation the thrust of the machine is consumed by the cutter forces required to excavate the fresh granite and there is not enough “force” to generate the required pressure in the upper part of the work chamber, resulting in an imbalance between the soil and water pressure in the weathered granite and the pressure generated in the work chamber in the upper part of the work chamber. If this difference is too large, the face will collapse inwards into the working chamber and this will result in progressive over-excavation ahead and above the face (Babendererde, 2004). The additional pressure generated by the active support system will compensate for this deficiency.



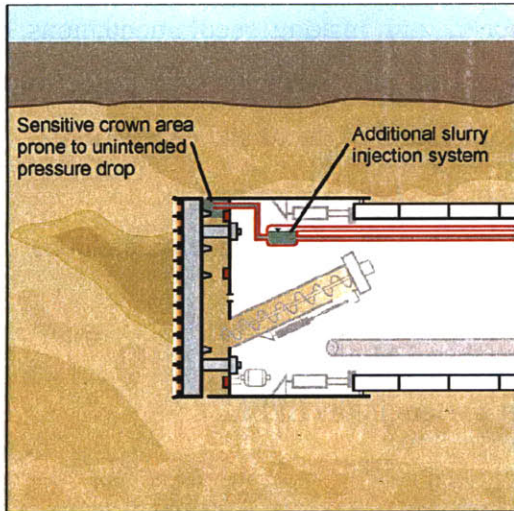


Figure 6.21 Additional Face Support System (Babendererde, 2005)

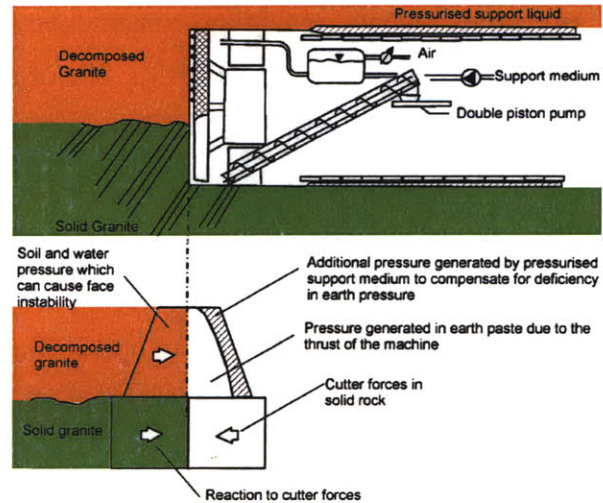


Figure 6.22 Illustration of Active Support System for overcoming the support pressure deficiency in mixed face conditions for Porto Metro (Babendererde, 2004)

There were other modifications to the EPBM that consisted of (Guglielmetti,V, 2003):

- Installation of an Emergency Double Piston Pump to help control the support pressure oscillations. When the muck is too liquid emergency situations can occur, because in such cases muck flow maybe too difficult to regulate, making it difficult to control the oscillations of pressures inside the chamber. This Pump, connected to the screw conveyer, will be activated to extract the muck whenever it is too liquid, allowing it to avoid these situations.
- Installation of a second belt scale in order to cross check the results of the first one.

Besides the modifications to the EPB machine, before re-starting tunneling, Plans for Advance of TBM (PATs) were produced for each section, so that all parameters and design issues related to tunnelling were addressed prior to the actual excavation of that section. For each TBM parameter, the PAT defined an operational range and counter-

measures to be applied if the attention/ alarm limits were exceeded. Three automatic alarms were set up (Guglielmetti,V, 2003):

- An alarm for going over the extracted weight upper limit, which immediately stops the EPB machine
- An alarm for going below the face pressure lower limit, which activates the Active Support System.
- An alarm for going below the lower limit of the muck apparent density, which activates a red light to alert the operator.

Finally, following the recommendations of the official Accident Commission's report, the roles of the contractor and construction manager were re-organized and new design and resident engineer responsibilities were introduced (Figure 6.23).

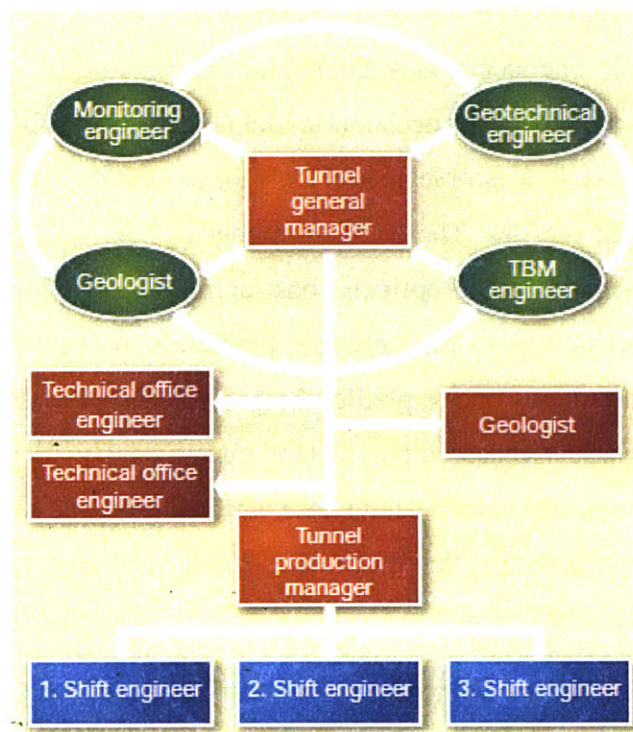


Figure 6.23 TBM follow up team organizational chart (T&TI, 2003)

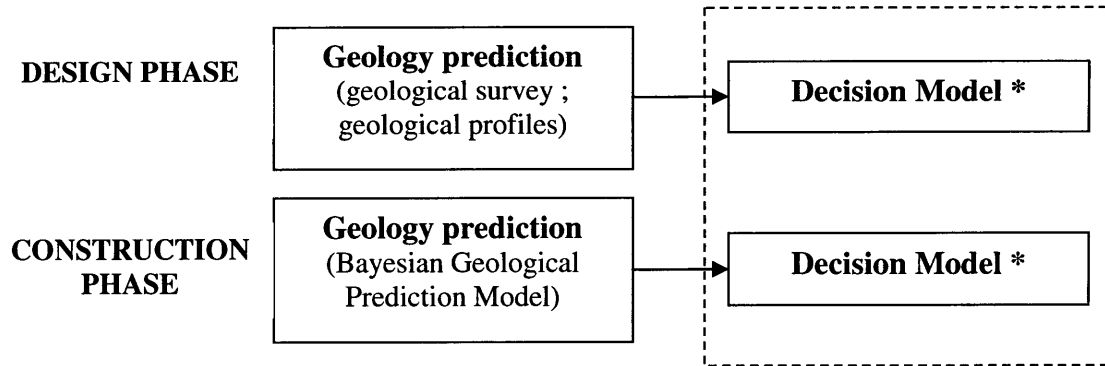
The TBM-follow up team consisted of specialists from both the contractor and the designer. The main scope of this team was to continuously interpret the excavation behavior (T&TI, 2003).

The introduction of additional measures such as the Active Face Support System, the Emergency Double Piston Pump, and the Plans for Advance of TBM (PATs) among others proved to be a very effective and led to the safe completion of the tunnel of Line C and the excavation of the tunnel of Line S.

## **6.2 Application of Risk Analysis Methodology**

Based on the analysis of Porto metro case study, the decision support framework for determining the “optimal” (minimum risk) construction method for a given tunnel alignment, presented in Chapter 5 was further developed for the specific case of the Porto metro line C tunnel. The decision support framework consists of three models: two geologic prediction models and a decision model (Figure 6.24). During the design phase the geology prediction is a simple model only based on the results of the geological survey and geological profiles. The decision model is a Bayesian network based model that allows one to decide on the optimal construction strategy for a given the geology. During the construction phase the geologic prediction model is a Bayesian network prediction model that allows one to predict the geology ahead of a tunnel machine based on observations of various machine parameters, during construction. The decision model is the same as the one used in the design phase which allows one to decide on the optimal construction strategy for the predicted geology. When combined the models allow one to asses risks during tunnel construction.





\* The decision model in the design and construction phases is the same.

Figure 6.24 decision support framework for the design and construction phase

## 6.2.1 Design Phase

In the design phase the geology is predicted based on the results of a survey and geological profiles. This information is then used in the Bayesian Decision Model, which will now be described.

### 6.2.1.1 Bayesian Decision model

In order to build the Bayesian Decision model for the specific problem, it is necessary to determine which factors are important for the stability of the tunnel. This was based on information made available to the author by the Porto Metro. The data gathered consisted of:

- Design geological and geotechnical profiles.
- Plans for Advance of TBM (PATs) 3 to 6, corresponding to Section to 0+907 to Section 2+450. These documents were produced so that all parameters and design issues related to tunneling were addressed prior to the actual excavation of that section (Transmetro, 2002a; 2002b; 2002c and 2002d)
- Estimated (after excavation) geological condition at TBM face from Section 0+635 to section 2+450, from contractor/ designer.

- Logs of the TBM containing the automatically recorded data.

#### A) Important Variables for tunnel stability

The list the most important and influential variables (ground and surface conditions) for the line C tunnel stability are:

- Weathering degree (W1 to W6)
- Distribution of weathering degree at the face.
- Permeability
- Water (Piezometric) level
- Overburden
- Geomechanical parameters (Uniaxial compressive strength, “permeability”, in soil: cohesion and friction angle)
- Building vulnerability (geometry layout, position in reference to the tunnel and structural characteristics)

The parameters to observe and control are:

- Extracted volume
- Penetration rate
- Earth pressure
- Torque
- Volume of injected grout
- Muck density
- Piezometric levels
- Deformations (surface and deep)

Figure 6.25 shows the influence diagram for the Porto Metro Line C tunnel. The governing factor for the determination of the ground classes is the weathering degree. It is important to have information not only on the weathering degree but also on its

distribution at the face. Mixed faces are the ones that normally cause the most difficulties for the stability of the face.

The piezometric level is also of great importance due to effect it has on the stability of the face during excavation. In case the water level is above the crown of the tunnel the permeability of the ground is of great interest. It is important to know if the permeability is low or high and what is the permeability of the ground.

The overburden has also an effect on the stability. At shallow overburden the ground is normally weaker and if the tunnel is very close to the surface an arching effect may not occur naturally. In these cases treatment of the ground maybe required

External factors, such the existence of structures at the surface and in the ground are also very important parameters to be considered. They affect not only the probability of failure but the extent of the damage, inside the tunnel and at the surface, in case failure occurs. In the next section these factors will be discussed further.

Also during construction observations are made, through monitoring. These observations can tell something about the ground conditions as well as the behavior of the excavation and therefore failure.

All these parameters affect tunnel stability. In an urban environment as for the Porto metro this produces the risk scenarios such as: collapse up to the surface and damage at the surface due to ground settlements.

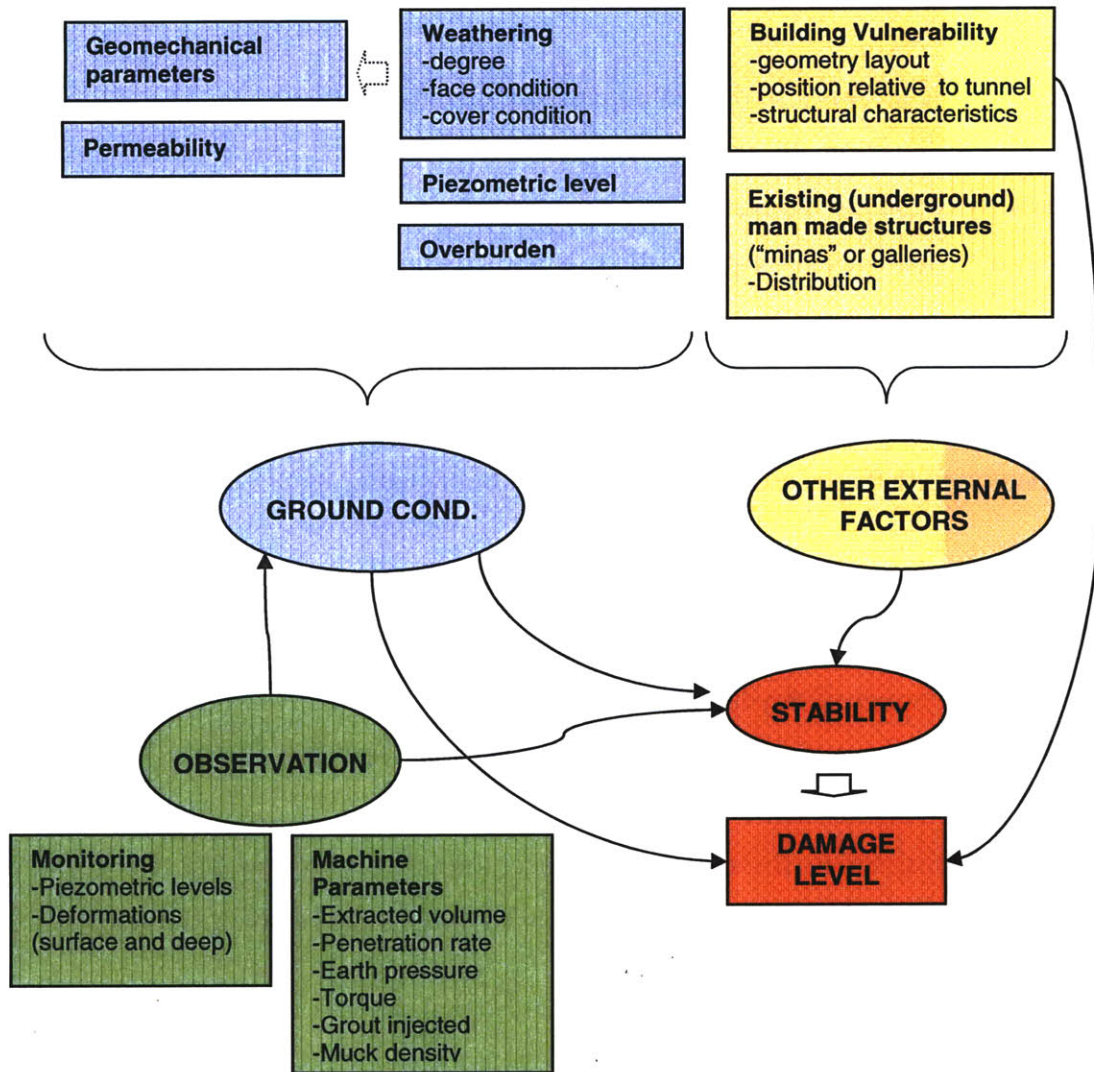


Figure 6.25 Influence diagram for Porto Metro Line C tunnel

B) Ground class definition

A very important part of the development and application of the methodology to this real case is to define ground classes and determine which variables are most important.

The influence diagram of Figure 6.25 shows the variables that were considered by the author to be the most influential for the stability of the excavation. The variables used for the definition of the ground classes and their values are:

- **Weathering grades (W): W1, W2, W3, W4, W5, W6**

Weathering was a governing factor in the geomechanical properties of the granitic rock mass. In the Porto Metro case, all weathering grades (W1 to W6, as established in the engineering geological classification according to the scheme proposed by the Geological Society of London, 1995, and the recommendations of ISRM) can be encountered:

- W1: fresh granite
- W2: slightly weathered
- W3: moderately weathered
- W4: highly weathered
- W5: completely weathered - saprolite
- W6: decomposed rock - residual soil

According to ISRM recommendations, geological materials with uniaxial compressive strength ( $C_0$ ) greater than 1MPa (which correspond to granites with weathering degree from W1-W4) are considered to be “rock”, while geological materials with uniaxial compressive strength ( $C_0$ ) lower than 1MPa (i.e. saprolite W5 and residual soil W6) are considered to be soil.

- **Overburden (O): O1, O2, O3**

The overburden in tunnel C varies from about 4 m to 30 m. The overburden influences the structural behavior of the tunnel, and therefore the probability of

failure. It also influences the type of failure. The smaller the overburden the more probable is that the failure reaches the surface. The possible states for overburden are:

O1 – overburden <10 m

O2 – overburden 10-20 m

O3 – overburden 20-30 m

- **Piezometric level (H) : H1, H2**

As stated before, the piezometric level has an important effect on the stability of the face and is a crucial factor in the determination of the effective pressure to apply at the face.

H1 – piezometric level < 10m

H2 – piezometric level 10-100m

- **Face condition**

1 – Soil-like material (W5, W6)

2 – Mixed Conditions

3 – Discontinuous rock Mass (W1-W4)

- **Cover condition**

1 – Soil-like material (W5, W6)

2 – Mixed Conditions

3 – Discontinuous rock Mass (W1-W4)

Based on the project information, mainly the geological interpretative profiles (Transmetro drawing TM DS-0123-01 A04), six ground classes were determined (Table 6.3). Figure 6.26 illustrates the different classes.



**Table 6.3 Ground Classes**

Cover Condition	Face Condition		
	Soil	Mixed	Rock
Soil	GC1	GC2	GC3a <sup>(1)</sup>
Mixed	GC3	GC4	GC5
Rock	GC5a <sup>(1)</sup>	GC4a	GC6

(1) Did not find evidence of this type of class along the line

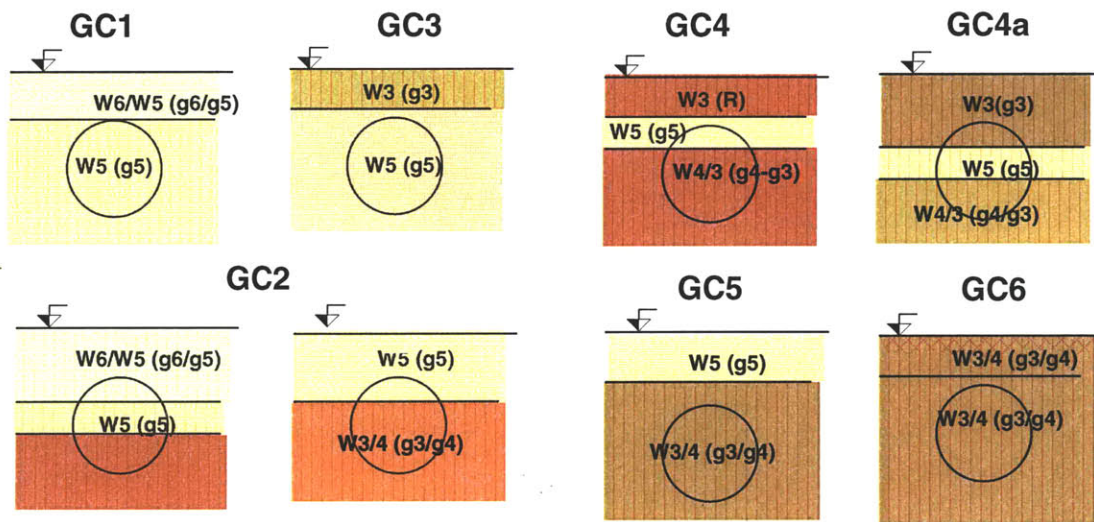


Figure 6.26 Geological ground class

(note: in ( ) are the geomechanical groups used by the designer that were described in section 6.1.1)

For simplifying purposes only the face conditions will be considered in the definition of ground classes (Figure 6.26), i.e. Soil (GC1, GC3), Mixed (GC2, GC4, GC4a) and Rock (GC5, GC6). Another reason for this is the fact that there is only information regarding the face conditions (from the face mapping) and little regarding the cover conditions, since it is only possible to know it for sure through the few boreholes made.

### C) Bayesian Network / Influence Diagram Model

Based on the influence diagram presented on Figure 6.25, a Bayesian network model (extended influence diagram) was built in order to support a decision process during construction. The decision model for Line C tunnel of the Porto Metro is presented in Figure 6.27. The idea behind the model was to support the decision of the optimal construction strategy for the tunnel. In this specific case, it seems that one of the major issues was what would be the optimal mode for the EPBM to operate in given geological conditions. For this reason the construction strategies to be considered in the model of Figure 6.27 will be: CS1) EPBM with operation in open mode and CS2) EPBM with operation in closed mode.

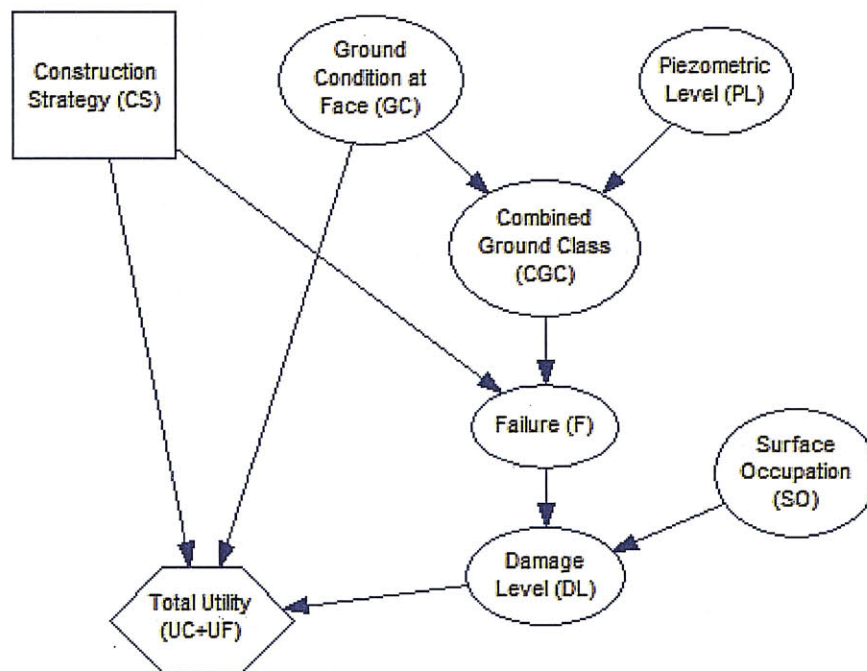


Figure 6.27 Decision Model for Line C tunnel

The Bayesian network extended to a decision graph contains 6 chance nodes, 1 decision node and two utility nodes.

The Decision node, *Construction Strategy (CS)*, represents the two possible Construction Strategies, 1- Open Mode and 2- Closed Mode.

The chance node *Ground condition at the face (GC)* represents the different possible geological states that can be found in the sections at the face:

- 1- Soil (GC1, GC3);
- 2- Mixed (GC2, GC4, GC5) and
- 3- Rock (GC6).

The chance node *Piezometric Level (PL)* represents the possible piezometric levels:

- 1 – piezometric level < 10m
- 2 – piezometric level >10m.

The chance node *Combined ground class (CGC)* represents the combination between face condition and piezometric level. The possible values are:

- 1-Soil with low piezometric level,
- 2- Soil with high piezometric level,
- 3-Mixed with low piezometric level,
- 4- Mixed with high piezometric level
- 5- Rock

The chance node *Failure (F)* represents probability of failure of the face occurring given the combined geological and hydrological conditions, and the construction strategy used.

The possible values are:

- 1- Failure
- 2- No Failure

The chance node *Surface Occupation (SO)* represents the occupation degree at the surface. The possible values are:

- 1- Low,
- 2-Medium;
- 3- High.

The chance node *Damage Level (DL)* represents the vulnerability, i.e. the fact that if the failure occurs the consequences are uncertain. The possible values are:

- 1- No damage;
- 2- Level 1 damage. This damage level corresponds to the situation of the first and second accident that occurred at the Line C tunnel, i.e. damages at the surface to buildings and other structures due to excessive deformation, including partial collapse of a building.
- 3- Level 2 damage. This damage level corresponds to scenario of collapse to the surface causing total collapse of at least a building and damage to buildings and other structures at the surface. This is the situation of the 3rd collapse that occurred in the Line C tunnel.

Note that in the model used the Damage Level also depends on the surface occupation.

The utility node *Total Utility* consists of the cost of Construction (UC) and Cost of Failure (UF), which represent the costs associated with the construction and a possible failure, respectively.

### **Sections Analyzed**

The risks assessment methodology described in Chapter 5 and the model will be applied to a portion of about 320 m of the Line C tunnel of the Porto Metro, where the accidents occurred. The design geological profile of that stretch of the line is presented in Figure 6.28. The sections were defined based on the overburden. In section 1 the overburden varies from 10-20 m (O2) and in Section 2 it varies from 20-30 m (O3). Figure 6.28 shows the location of the three incidents that occurred during the initial phase of the construction of Porto Metro Line C.

For the purposes of this application the ground will be divided as previously mentioned into Soil or Rock. Geomechanical design groups (conditions) g5, g6 and g7 refer to material with a soil-like behavior, and geomechanical design groups (conditions) g1 to g4 represent material with rock like behavior (geomechanical design groups are described in section 6.1.1). Also indicated in Figure 6.28 are the location and simplified results of survey boreholes.

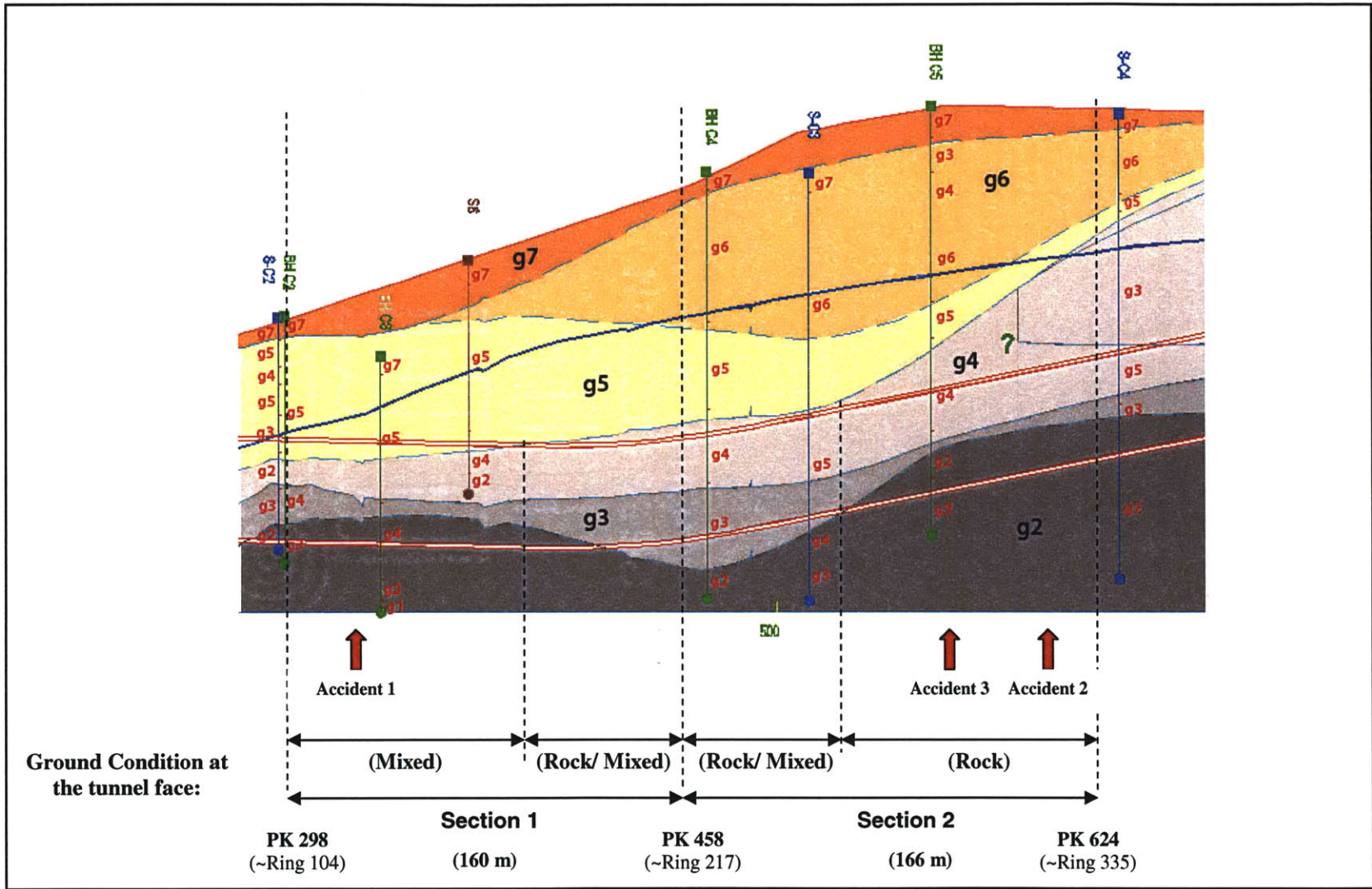


Figure 6.28 Geological longitudinal profile for Line C tunnel (from PK 298 to PK 624)



## Conditional and prior probability tables

The prior probability and conditional probability tables, as well as utilities, attached to each node of the influence diagram presented on Figure 6.25 are presented below:

- **Ground condition at tunnel face (GC)**

Table 6.4 and Table 6.5 show the prior probability of Ground condition at tunnel face in Section 1 and Section 2, respectively. The geological state prior probabilities were determined subjectively based on the design geological longitudinal profiles as well as the results of boreholes presented in Figure 6.28.

Table 6.4 Prior Probability of Ground Condition at tunnel face (Section 1)

GC	P (GC)
Soil (G1)	0.10
Mixed (G2)	0.85
Rock (G3)	0.05

Table 6.5 Prior Probability of Ground Condition at tunnel face (Section 2)

GC	P (GC)
Soil (1)	0.30
Mixed (2)	0.55
Rock (3)	0.15

Despite the fact that the design geological profile show that the tunnel face in section 2 will be mostly located in mixed and rock, the boreholes SC-3 and SC-4 show the occurrence of g5 (soil like material) at the tunnel depth. For this reason the probability of occurrence of soil at tunnel face in section 2,  $P(G1) = 0.30$ , is higher than in section 1,  $P(G1) = 0.10$ .

- **Piezometric level (PL)**

Table 6.6 presents the prior probability table for the piezometric level, P (PL). The piezometric level prior probabilities were also determined subjectively, based on results of the boreholes and what is known regarding the rainfall in winter around the Porto area.

Table 6.6 Prior Probability of piezometric level (Section 1 and Section2)

PL	P (PL)
Low	0.10
High	0.90

- **Combined ground classes (CGC)**

Table 6.7 shows the probability of CGC. This was considered, for simplification reasons, to be a deterministic variable that just combines geological state and hydrological state.

Table 6.7 Probability of GC (Section 1 and Section2)

FC=	PL =	P(CGC FC, PL)				
		Soil low (1)	Soil high (2)	Mixed low (3)	Mixed high (4)	Rock (5)
Soil (1)	Low (1)	1	0	0	0	0
Mixed (2)	Low (1)	0	0	1	0	0
Rock (3)	Low (1)	0	0	0	0	1
Soil (1)	High (2)	0	1	0	0	0
Mixed (2)	High (2)	0	0	0	1	0
Rock (3)	High (2)	0	0	0	0	1

- **Probability of Failure given CGC (Combined Ground Class) and CS (construction Strategy)**

The occurrence failure depends on the geological and hydrological conditions as well as the construction strategy employed. Table 6.8 shows the conditional probability table P (Failure|CGC, CS), attached to the variable Failure (F). The probability of failure distribution was also determined subjectively.

Note that the probability of failure could have been determined based on mechanical models for face stability with EPBM, such as the method of Jancsecz and Steiner (J&S, 1994), the method of Leca & Dormieux (L&D, 1990 or the method of Anagnostou and Kovari (A&K, 1996). If one has an expression for the factor of safety, depending on several variables, such as friction angle,  $\phi$ , cohesion,  $c'$ , among others, and their

respective probability distributions, it is possible to determine the probability of failure as being equal to probability that the factor of being below 1.

Table 6.8 Probability of Failure given CGC and construction strategy (Section 1 and Section 2)

P(Failure  CGC, CS)	Soil low		Soil high		Mixed low		Mixed high		Rock	
	CS1	CS2	CS1	CS2	CS1	CS2	CS1	CS2	CS1	CS2
Failure (1)	0.2	0.01	0.3	0.02	0.15	0.01	0.25	0.1	0.01	0.005
No Failure (2)	0.8	0.99	0.7	0.98	0.85	0.99	0.75	0.9	0.99	0.995

- **Probability of Damage Level given SO (Surface Occupation) and Failure,  $P(DL|SO, F)$**

Table 6.9 Probability of Damage Level given SO and Failure, (Section 1 and Section 2)

Failure	SO (Surface Occupation)	P (DL  Failure, SO)		
		No Damage (1)	Level 1 (2)	Level 2 (3)
Failure (1)	High (1)	0.02	0.18	0.8
No Failure (2)	High (1)	1	0	0
Failure (1)	Medium (2)	0.05	0.4	0.55
No Failure (2)	Medium (2)	1	0	0
Failure (1)	High (3)	0.1	0.5	0.4
No Failure (2)	High (3)	1	0	0

### Utility Functions

The utility function used was equal to “-cost”. The costs (expressed in utilities) of construction are presented in euro per section (each section is about 160 m), in Table 6.10.

- **Construction Costs (Utilities)**

Table 6.10 Construction costs (Section 1 and Section 2)

CS	Open (CS1)	Closed (CS2)	Open (CS1)	Closed (CS2)	Open (CS1)	Closed (CS2)
GC	Soil (1)	Soil (1)	Mixed (2)	Mixed (2)	Rock (3)	Rock (3)
UC	-1	-9	-1	-9	-1	-8

The utilities associated with consequences of failure and respective damage levels, presented in Table 6.11, were determined based on similar collapse cases from the database of accidents.

- **Failure “Costs” (Utilities)**

Table 6.11 Failure “costs” (Section 1 and Section 2)

CS	Open (CS1)	Closed (CS2)	Open (CS1)	Closed (CS2)	Open (CS1)	Closed (CS2)	Open (CS1)	Closed (CS2)	Open (CS1)	Closed (CS2)
GC	Soil (1)	Soil (1)	Mixed (2)	Mixed (2)	Rock (3)	Rock (3)	Soil (1)	Soil (1)	Mixed (2)	Mixed (2)
DL	No Damage (1)	No Damage (1)	No Damage (1)	No Damage (1)	No Damage (1)	No Damage (1)	Level 1 (2)	Level 1 (2)	Level 1 (2)	Level 1 (2)
UF	0	0	0	0	0	0	-50	-50	-10	-40

CS	Open (CS1)	Closed (CS2)	Open (CS1)	Closed (CS2)	Open (CS1)	Closed (CS2)	Open (CS1)	Closed (CS2)
GC	Rock (3)	Rock (3)	Soil (1)	Soil (1)	Mixed (2)	Mixed (2)	Rock (3)	Rock (3)
DL	Level 1 (2)	Level 1 (2)	Level 2 (3)	Level 2 (3)	Level 2 (3)	Level 2 (3)	Level 2 (3)	Level 2 (3)
UF	-15	-5	-100	-70	-80	-50	-50	-10

## D) Application of Bayesian Decision Model

Using the data (probability and utility functions) presented in the previous section, the results show that the optimal Construction Strategy is to both sections drive in closed mode. Figure 6.29 shows the results of solving the decision model in Figure 6.27 in terms of expected utilities and optimal construction strategy for sections 1 and 2. The decision model is solved by the algorithm *decision policy*, described in Chapter 5.

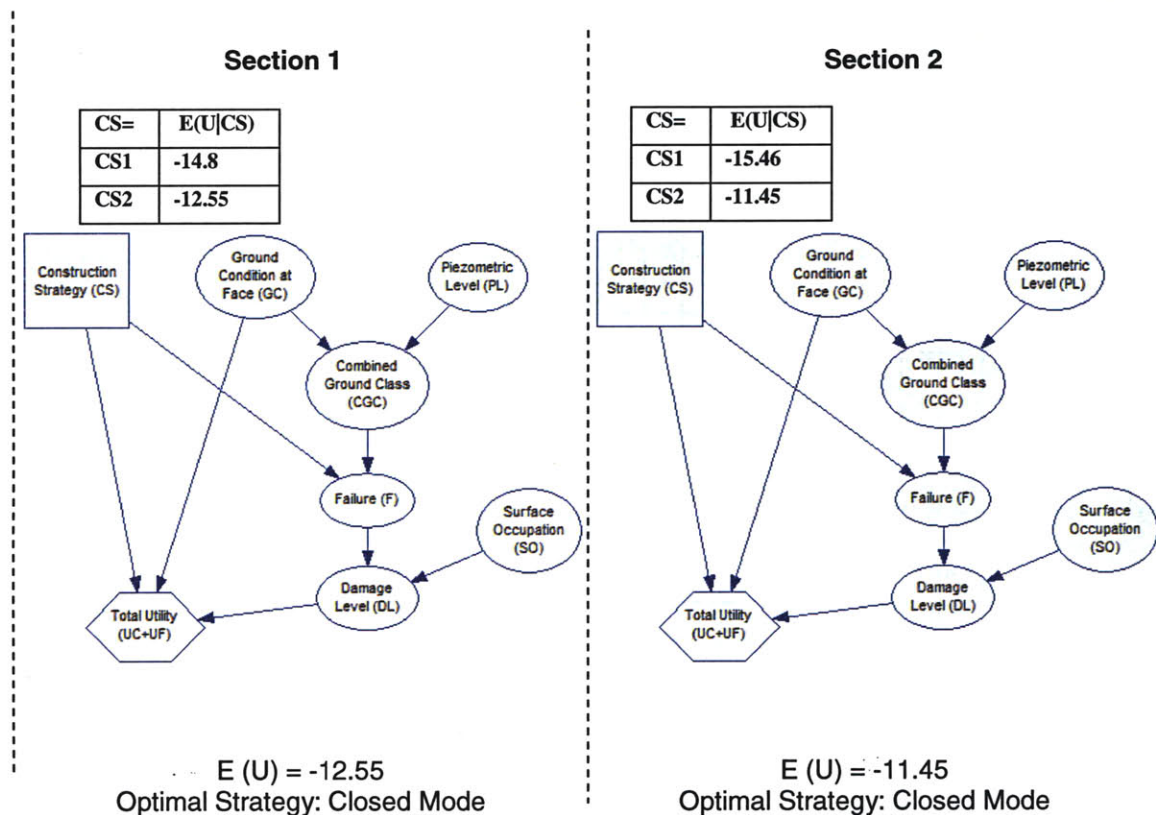


Figure 6.29 Design Results – Optimal Construction strategy

In the design phase a decision is made on the “optimal” construction strategy for the tunnel, in this case tunnel sections. Once the construction starts, with the “optimal” construction, information is available (regarding geology, machine parameters, deformations etc) and should be use to update the geological conditions ahead of the tunnel face and adapt the construction strategy to the found geology. This will be done in the next sections.



## **6.2.2 Construction Phase – Bayesian Prediction Model**

In this section, a Bayesian Model that predicts the geology ahead of a TBM face is developed. The model makes use of information that becomes available during construction to update the geologic predictions ahead of the machine. The ultimate aim of the model is to act a decision aid for assessing and mitigating risk. If one knows the geology ahead of the machine, then one can prepare for any risks, and chose optimal construction methods as was described in the previous section.

Prior to developing the model, it is necessary to chose parameters that are important in distinguishing between geologies. These are the parameters that the model will be based on, and that are observed during construction. This section is organized as follows. An extensive analysis of the data from the Porto Metro case is performed in order to find which parameters are important in distinguishing between geologies. The inter-relationships are also analyzed. The important parameters, and the important inter-relationships are then retained in the model, and the structure of the model is based on these. Once the structure of the model is chosen, the model is applied to the Porto Metro Case. A portion of the dataset is used to ‘learn’ the model. The model is then used to predict the geologies ahead of the EPB machine. The results are then compared to the actual geologies encountered.

### **6.2.2.1 TBM Data**

The TBM registers automatically every 10 seconds several operation related parameters. The ones looked at in this study are presented below:

- Weight of excavated material (ton).  
The extracted material is weighted by scales located in the conveyor belt.
  
- Penetration rate (mm/rev):

- The rate at which the machine penetrates the ground, measured in mm per revolution
- Torque of the cutting wheel (MNm)  
Twist force applied to the cutting wheel.
- Total Thrust (KN)  
Corresponds to the total force applied by the thrust cylinders (or jacks) required to push the shield forward. The last segmental lining ring built inside the shield tail serves as abutment for the thrust cylinders.
- Cutting wheel Force (KN)  
Force that is transmitted onto the cutting wheel.
- Grout volume (m<sup>3</sup>)  
This is the volume of grout injected in the annular gap between the lining and the ground.
- Earth pressure (bar).  
Earth pressure inside the chamber, measured by means earth pressure sensors located inside the work chamber. The earth pressure is controlled through regulating the rotation of the screw conveyor.
- Advance rate (mm/min).  
The rate at which the machine penetrates the ground, measured in mm per minute

Figure 6.30 shows a schematic of the EPBM used during the construction of the Porto Metro Line C. The head of the TBM is located approximately 6 m from the ring. The width of each ring is 1.4 m. According to these dimensions (width of the rings elements, distance of ring to head of the TBM), when the machine excavates the distance of a ring, the ring being mounted in that cycle corresponds to about four rings before, i.e. for example, in the cycle in which ring 200 is being installed, the machine will be excavating the section that will be part of ring n. 204 and of part of ring n. 205. The ring being injected in the same cycle will be ring n. 198.

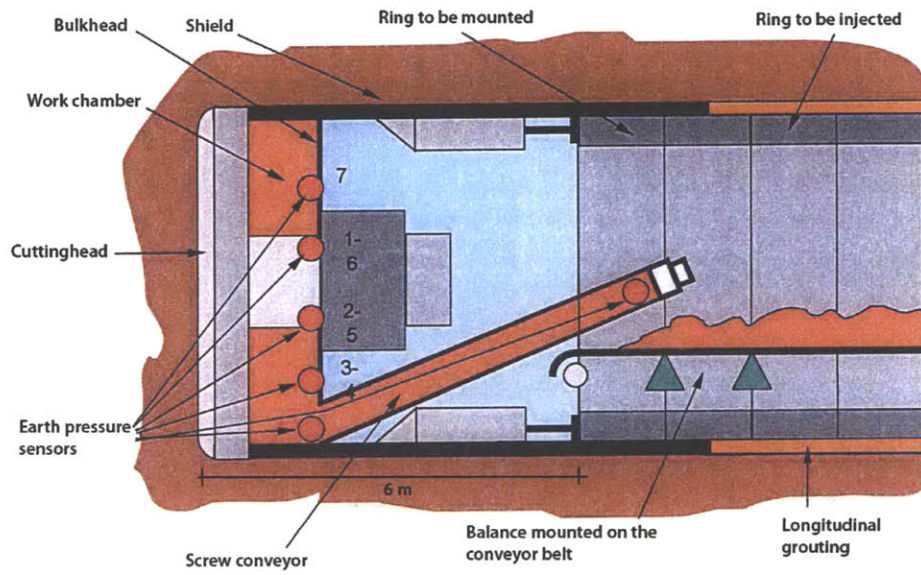


Figure 6.30 TBM machine scheme

Besides the data available from the TBM, for this application the author had access to the following information:

- Mapping of the face
- Monitoring results, consisting mostly of deformations at the surface.
- Topographic and design geological profiles.

The analysis of accident reports and construction data suggests that the data automatically recorded by the TBM was not considered and was not used to infer and update the behavior of the excavation, and consequently adjust it.

### 6.2.2.2 Data Analysis

The Bayesian Model that is developed in this section predicts geologies ahead of the tunnel using information that is obtained during construction. To develop the model, it is first important to determine how to distinguish between geologies. In this section, the dataset that was obtained for the Porto Metro case is analyzed to determine which

parameters were relevant when distinguishing between ground conditions. A single parameter analysis is first done. A two-parameter analysis follows in order to determine which inter-relationships between these parameters are important in distinguishing geologies.

### **A. Single Parameter analysis**

In order to determine, which parameters are important in distinguishing geologies, a single parameter analysis is first performed. This consists of finding the mean values, standard deviations, and relative frequency of the parameters from the dataset that is observed for the Porto Metro case. The relative frequencies for the different geologies are then compared. If there is a significant difference then the parameter is good at distinguishing between the geologies, and if the differences are not great, then the parameter is not good at distinguishing between the geologies.

#### **Cutting Wheel Force (CF)**

Table 6.12 shows the mean value, standard deviation and coefficient of variation of the variable Cutting Wheel Force (CF), for each ground condition (G1, G2 and G3) separately. The mean value of CF is low in soil (G1), 7581 kN and high in rock (G3), 11088 kN. The standard deviation is the highest in soil, and least in rock. Figure 6.31 presents the relative frequencies of the Cutting Wheel Force for the different ground classes. Since Bayesian Models are based on discrete variables, CF was discretized into five bins as presented in Table 6.13. Figure 6.32 shows the relative frequency of the discretized variable Cutting Wheel Force (CF), with the contribution of the different ground conditions (G1, G2 and G3). One can observe if CF is high (i.e.  $CF > 10200$  kN) one is more likely in Rock, and if CF is low ( $CF < 7100$  kN) one is more likely in soil. It can be concluded that Cutting Wheel Force (CF) is an important parameter in distinguishing between ground conditions, since one can see a clear difference between the CF distribution of relative frequencies in Soil (G1) and in Rock (G3). Mixed (G2) is

more difficult to distinguish. This is due to the fact Mixed (G2) can vary from a face that contains as much as 90% Soil to one that contains as much as 90% Rock.

The cutting wheel force, CF is therefore retained in the Bayesian Model.

Table 6.12 Mean Value (in kN), Standard Deviation (in kN) and Coefficient of Variation for Cutting Wheel Force

<b>All ground conditions:</b>	
Mean Value	9519
Standard Deviation	2597
Coefficient of Variation	0.273
<b>In G1:</b>	
Mean Value	7581
Standard Deviation	2241
Coefficient of Variation	0.296
<b>In G2:</b>	
Mean Value	9053
Standard Deviation	2329
Coefficient of Variation	0.257
<b>In G3:</b>	
Mean Value	11088
Standard Deviation	2087
Coefficient of Variation	0.188

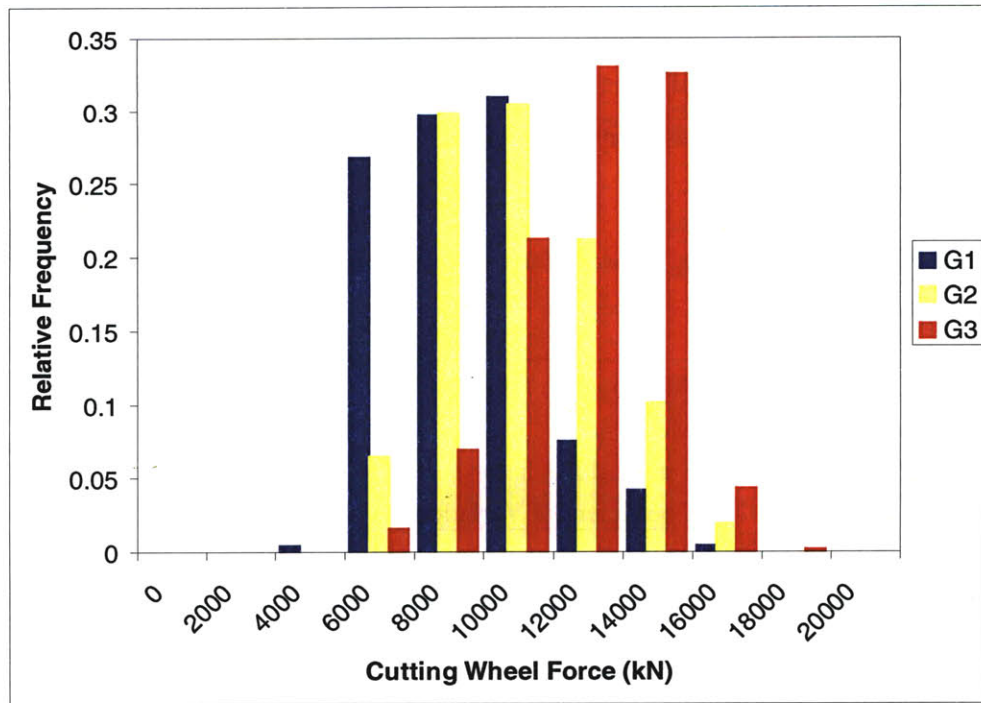


Figure 6.31 Relative Frequency of Cutting Wheel Force in Ground conditions G1, G2, G3

Table 6.13 Discretization of the variable Cutting Wheel Force (CF)

Bin	Range (kN)
1	CF < 7100
2	7100 < CF > 10200
3	10200 < CF > 12600
4	12600 < CF > 14000
5	CF > 14000



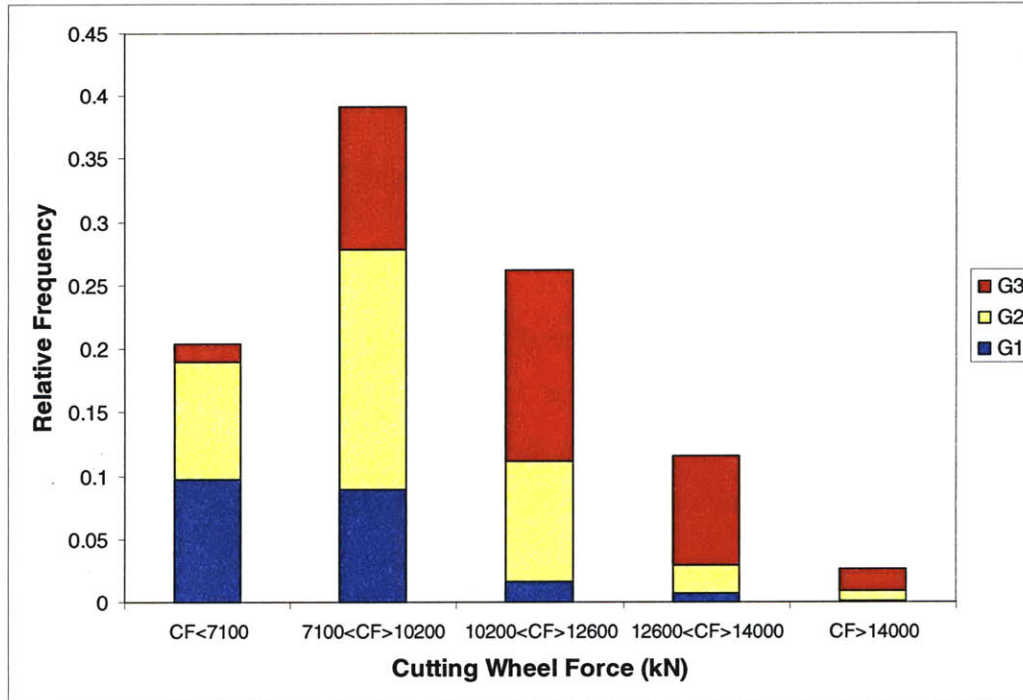


Figure 6.32 Relative Frequency of the discretized variable Cutting Wheel Force showing the contribution of ground conditions G1, G2, G3

### Penetration rate (P)

Table 6.14 shows the mean value, standard deviation and coefficient of variation of the variable Penetration (P), for each ground condition (G1, G2 and G3) separately. The mean value of Penetration (P) is high in soil (G1), 8.87 mm/rev and low in rock (G3), 4.86 mm/rev. The standard deviation is the highest in soil, and lowest in rock. This makes sense due to the excavation method used, EPB. In soil (G1) the face must be fully pressurized and the earth pressure to balance the face fluctuates more due to the changing soil conditions (not to forget that Porto Granite is a highly heterogeneous weathered formation) and the existence of boulders.

Figure 6.33 presents the relative frequencies of the Penetration rate (P) for the different ground classes. Since Bayesian Models are based on discrete variables, P is again discretized into five bins as presented in Table 6-15. Figure 6.34 shows the relative

frequency of the discretized variable Penetration rate (P), with the contribution of the different ground conditions (G1, G2 and G3). One can observe that if P is low ( $P < 5.3$  rpm) one is more likely in rock (G3) and if P is high-medium ( $P > 9.5$  rpm) is more than in soil (G1). For values of P between 5.3rpm and 9.5rpm one is more likely to be crossing Mixed (G2).

It can be concluded that Penetration rate (P) is an important parameter in distinguishing between ground conditions, since one can see a clear difference between the P distribution of relative frequencies in Soil (G1). Mixed (G2) and Rock (G3). The Penetration, P is therefore retained in the Bayesian Model.

Table 6.14 Mean Value (in mm/rev), Standard Deviation (in mm/rev) and Coefficient of Variation for Penetration rate (P)

<b>All ground conditions:</b>	
Mean Value	6.50
Standard Deviation	2.835
Coefficient of Variation	0.436
<b>In G1:</b>	
Mean Value	8.87
Standard Deviation	3.217
Coefficient of Variation	0.363
<b>In G2:</b>	
Mean Value	6.81
Standard Deviation	2.221
Coefficient of Variation	0.326
<b>In G3:</b>	
Mean Value	4.86
Standard Deviation	2.047
Coefficient of Variation	0.421

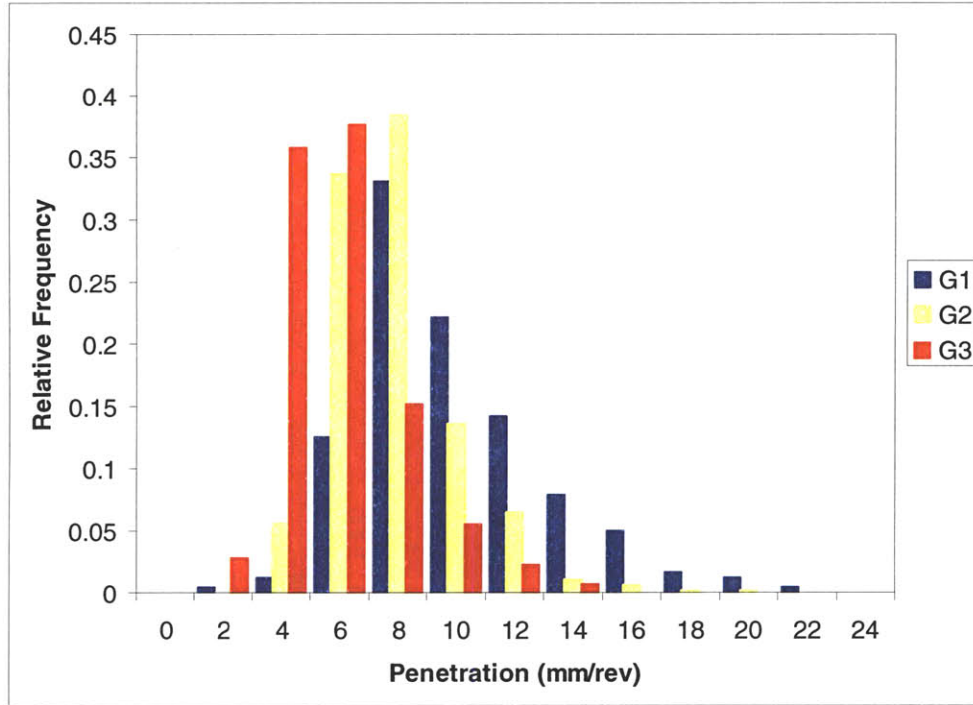


Figure 6.33 Relative Frequency of Penetration rate in ground conditions G1, G2, G3

Table 6.15 Discretization of the variable Penetration rate (P)

Bin	Range (mm/rev)
1	$P < 5.3$
2	$5.3 < P < 9.5$
3	$9.5 < P < 13.4$
4	$13.4 < P < 16.4$
5	$P > 16.4$

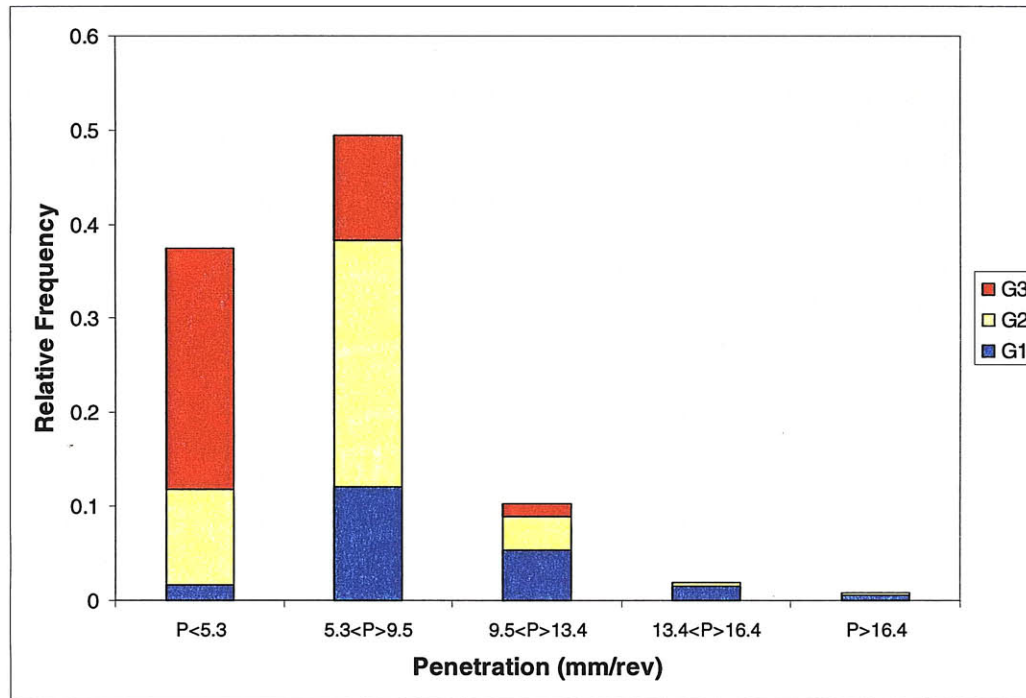


Figure 6.34 Relative Frequency of discretized variable Penetration rate showing contribution of ground conditions G1, G2, G3

### Torque of the Cutting Wheel (TO)

Table 6.16 shows the mean value, standard deviation and coefficient of variation of TO in all ground conditions and for each ground condition (G1, G2 and G3) separately. Figure 6.35 presents the relative frequencies of the Torque of the Cutting Wheel (TO) for the different ground classes. The mean value of Torque is almost the same in Soil (6.85 MNm) and Mixed (6.92 MNm) and slightly lower in Rock (6.24 MNm). The spread or standard deviation is also almost the same for all geological conditions, slightly higher in Rock (1.415 MNm) and slightly lower in Mixed (1.302MNm).

Torque was also discretized into five bins as presented in Table 6.17. Figure 6.36 shows the probability distribution of the discretized variable Torque of the Cutting Wheel (TO), with the contribution of the different ground conditions (G1, G2 and G3). It is very difficult to determine the ground condition based on the value of Torque, since the relative frequency distribution is almost the same in soil, rock and mixed.

The reason for this is that the torque is applied by the operator and therefore it is difficult to predict where one is tunneling just based on values of Torque alone. The Torque is nevertheless retained in the Bayesian Model, because it will be shown later that the inter-relationship between Torque and other parameters such as penetration rate and cutting wheel force is extremely important.

Table 6.16 Mean Value (in MNm), Standard Deviation (in MNm) and Coefficient of Variation for Torque of the Cutting Wheel (TO)

<b>All ground conditions:</b>	
Mean Value	6.65
Standard Deviation	1.332
Coefficient of Variation	0.200
<b>In G1 (Soil):</b>	
Mean Value	6.85
Standard Deviation	1.302
Coefficient of Variation	0.190
<b>In G2 (Mixed):</b>	
Mean Value	6.92
Standard Deviation	1.164
Coefficient of Variation	0.168
<b>In G3 (Rock):</b>	
Mean Value	6.24
Standard Deviation	1.415
Coefficient of Variation	0.227

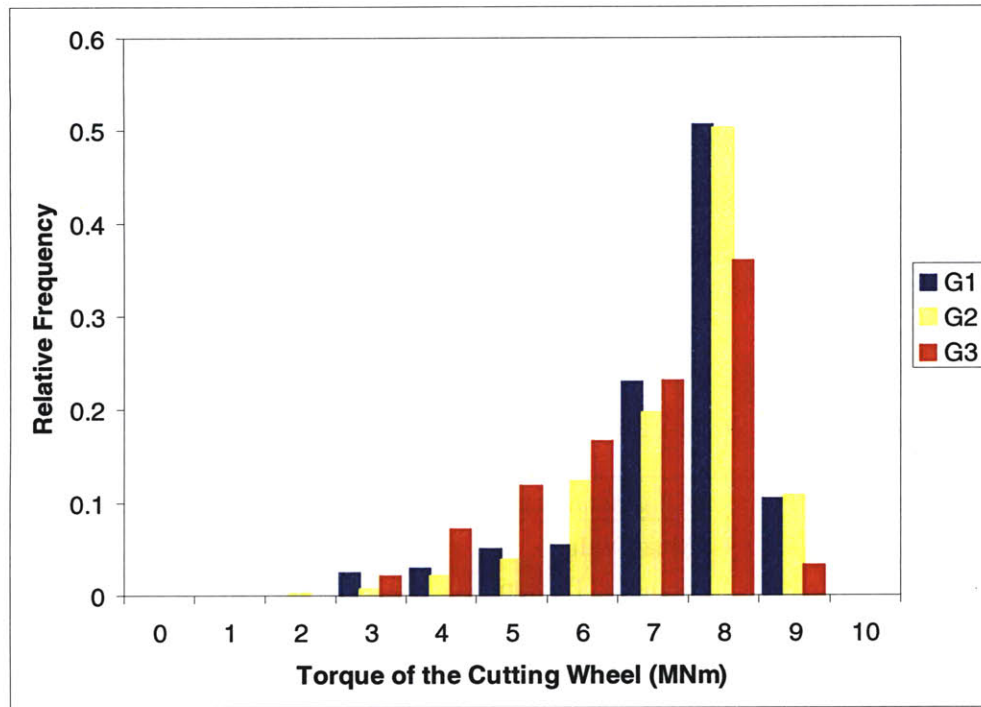


Figure 6.35 Relative Frequency of Torque of the Cutting Wheel in ground conditions G1, G2, G3

Table 6.17 Discretization of the variable Torque of the Cutting Wheel (TO)

Bin	Range (MNm)
1	$TO < 3.65$
2	$3.65 < TO > 5$
3	$5 < TO > 6$
4	$6 < TO > 7.3$
5	$TO > 7.3$



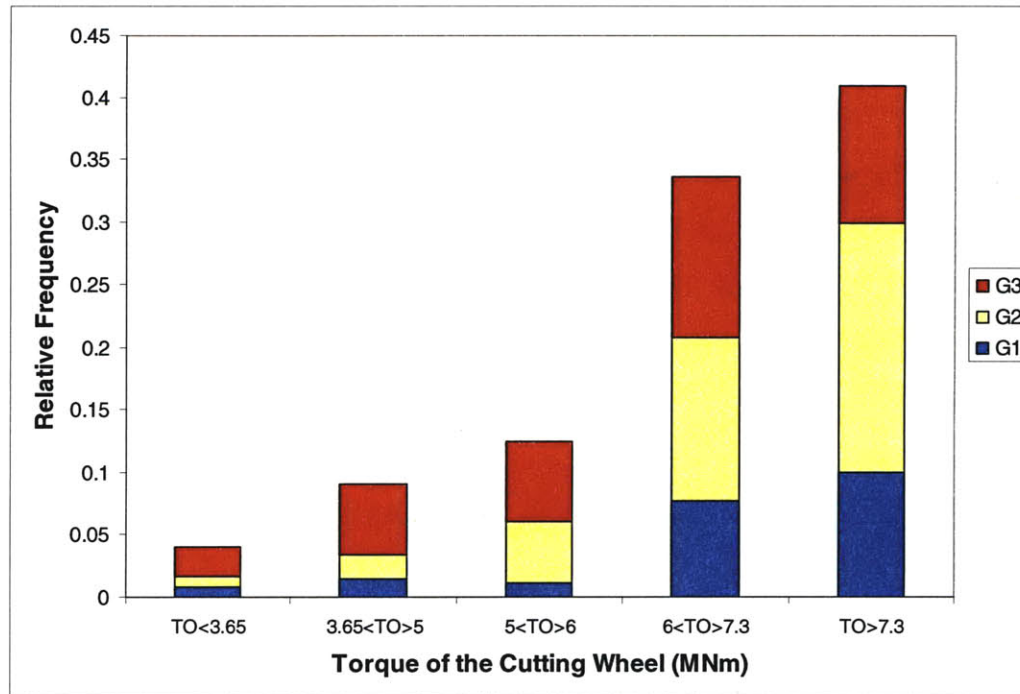


Figure 6.36 Relative Frequency of discretized variable Torque of Cutting Wheel showing contribution of ground conditions G1, G2, G3

### Torque / Cutting Wheel Force (TOC)

Table 6.18 shows its mean value, standard deviation and coefficient of variation in all ground conditions and for each ground condition (G1, G2 and G3) separately. The mean value of TOC is much higher in soil (0.96 m) than in rock (0.58 m) while the mean values of TOC in soil and mixed (0.81) are much closer. The standard deviation is highest in soil (0.273 m), and lowest in rock (0.169 m). Figure 6.37 presents the relative frequencies of the parameter Torque/Cutting Wheel Force (TOC) for the different ground classes.

TOC was discretized into five bins as presented in Table 6.19. Figure 6.38 shows the probability distribution of the discretized variable TOC, with the contribution of the different ground conditions (G1, G2 and G3). The relative frequencies are different for rock (G3) and soil (G1). The relative frequencies show that if TOC is low then there is a high probability that one is excavating through G3 (rock). So for a given value of Torque

(TO), for high values of Cutting Wheel Force (CF) one is probably driving through rock (G3) and for low values of CF one is probably going through G1(soil) or G2 (mixed).

It can be concluded that TOC is an important parameter in distinguishing between ground conditions, since a distinct difference in the relative frequencies of TOC for Soil (G1) and Rock (G3) can be observed. The relative frequency distribution of G2 (mixed) is much closer, in this case, to the one of G1 (soil) than that of G3 (rock). The parameter TOC is therefore retained in the Bayesian Model.

Table 6.18 Mean Value (in m), Standard Deviation (in m) and Coefficient of Variation for Torque / Cutting Wheel Force (TOC)

<b>All ground conditions:</b>	
Mean Value	0.75
Standard Deviation	0.263
Coefficient of Variation	0.349
<b>In G1:</b>	
Mean Value	0.96
Standard Deviation	0.273
Coefficient of Variation	0.284
<b>In G2:</b>	
Mean Value	0.81
Standard Deviation	0.228
Coefficient of Variation	0.282
<b>In G3:</b>	
Mean Value	0.58
Standard Deviation	0.169
Coefficient of Variation	0.291

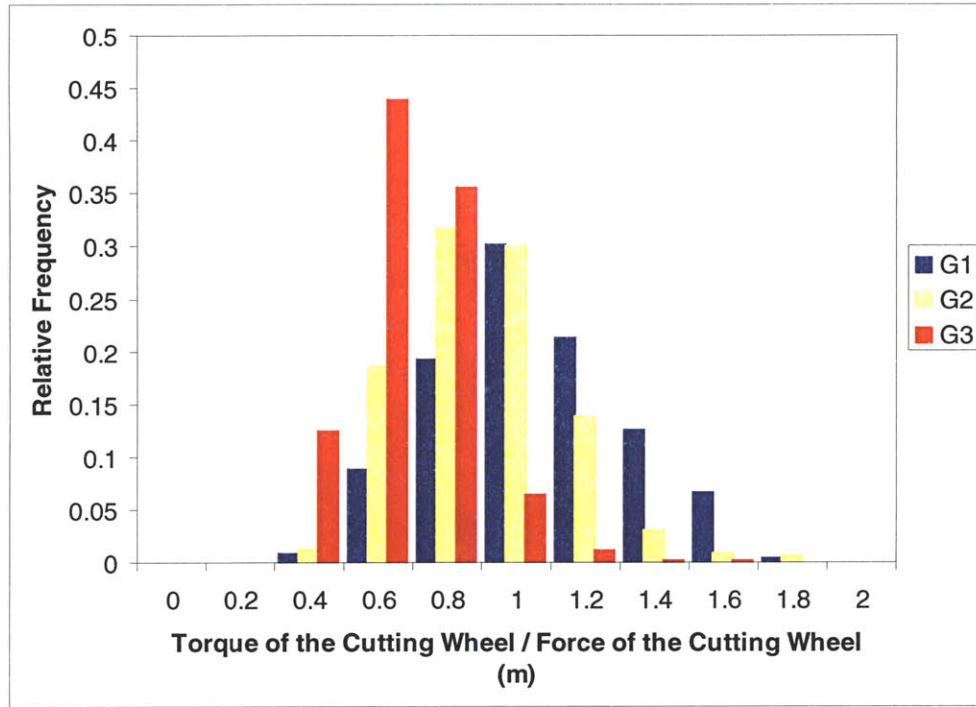


Figure 6.37 Relative Frequency of Torque/Force of the Cutting Wheel in ground conditions G1, G2, G3

Table 6.19 Discretization of the variable Torque / Cutting Wheel Force (TOC)

Bin	Range
1	TOC < 0.6
2	0.6 < TOC > 0.825
3	0.825 < TOC > 1.05
4	1.05 < TOC > 1.4
5	TOC > 1.4

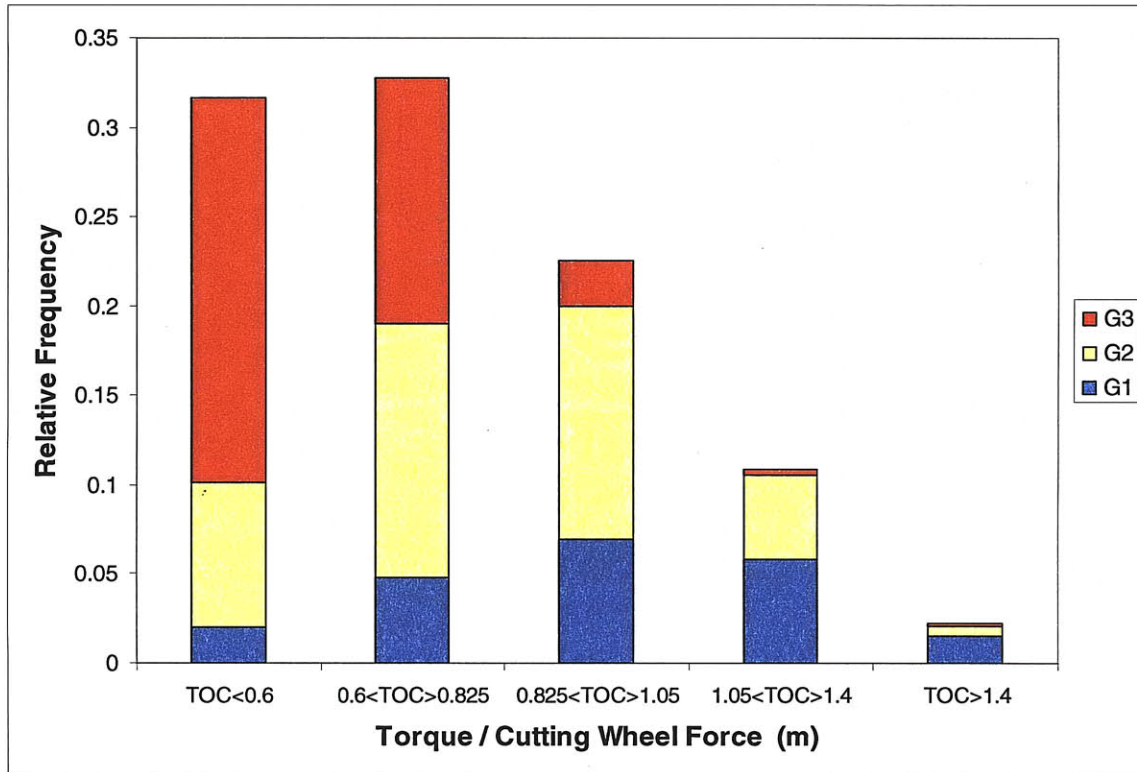


Figure 6.38 Relative Frequency of discretized variable TOC showing contribution of ground conditions G1, G2, G3

### Total Thrust Force

The total thrust is a force applied by the thrust cylinders against the last installed ring of lining in order to make the TBM advance through the ground. This force can be controlled by the operator.

Table 6.20 contains the mean value, standard deviation and coefficient of variation of the Total Thrust Force (TT) in all ground conditions and for each ground condition (G1, G2 and G3) separately. The mean value of TT is the highest in rock (33613 kN) and lowest in soil (31188 kN). The mean value of TT in mixed (31664 kN) is very close to that of TT in soil. The standard deviation of TT is the highest in rock (6516 kN) and lowest in mixed (5188 kN). Figure 6.39 shows the relative frequency of the Total Thrust Force in ground conditions G1, G2 and G3.

The range of Total Thrust and its relative frequency are relatively similar in soil, mixed and rock. It can, therefore, be concluded that TT is not an important parameter when distinguishing between ground classes. For this reason this parameter will not be retained to the Bayesian model. The model will include the Cutting Wheel Force instead. This force is a fraction of the Total Thrust, since part of this force is lost by friction between the surrounding ground and the TBM shield.

Table 6.20 Mean Value (in kN), Standard Deviation (in kN) and Coefficient of Variation for Total Thrust Force (TT)

All ground conditions:	
Mean Value	32307
Standard Deviation	5975
Coefficient of Variation	0.185
In G1:	
Mean Value	31188
Standard Deviation	5968
Coefficient of Variation	0.191
In G2:	
Mean Value	31664
Standard Deviation	5188
Coefficient of Variation	0.164
In G3:	
Mean Value	33613
Standard Deviation	6516
Coefficient of Variation	0.194

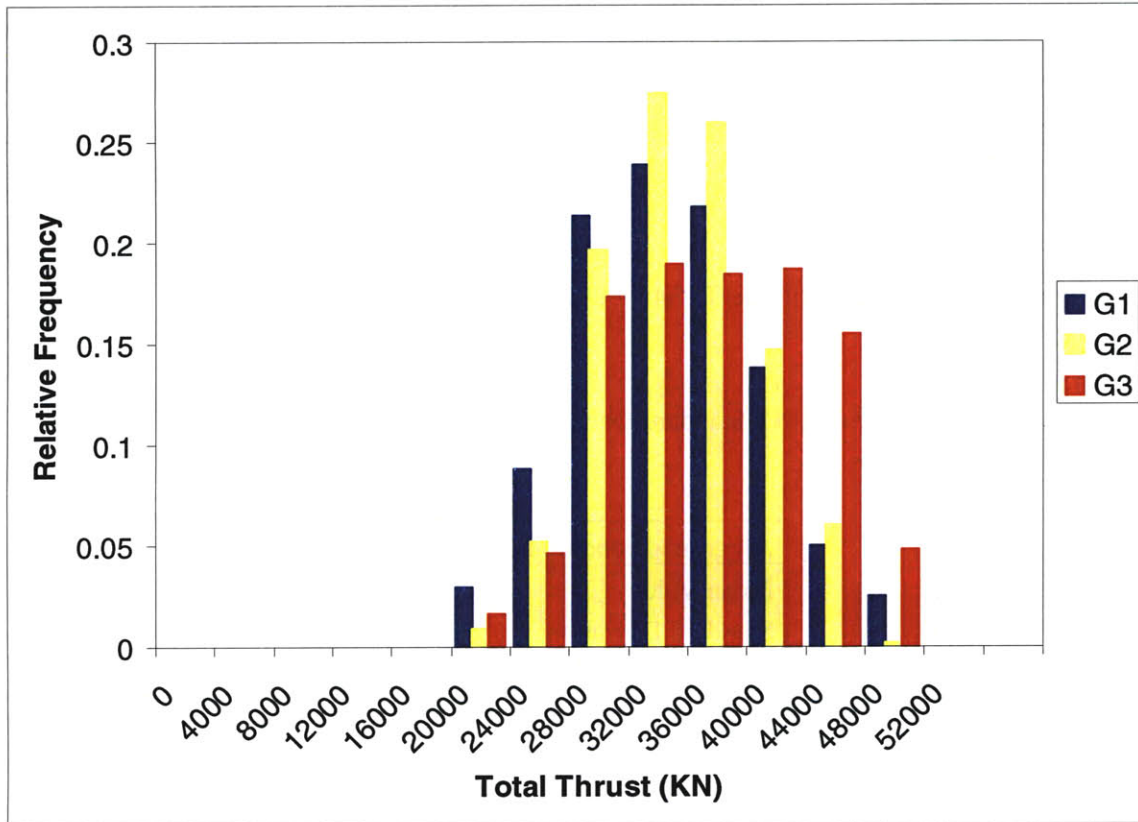


Figure 6.39 Relative Frequency Total Thrust Force in ground conditions G1, G2, G3

### Cutting Wheel Force / Total Thrust Force (COTT)

Table 6.21 presents the mean value, standard deviation and coefficient of variation of COTT in all ground conditions and for each ground condition (G1, G2 and G3) separately. The mean value of COTT is the lowest in soil (0.246) and the highest in rock (0.344). The standard deviation of COTT is highest in rock and lowest in soil. However the coefficient of variance is the same in soil, mixed and rock.

Figure 6.40 presents the relative frequencies of the Cutting wheel force / Total Thrust (COTT) for the different ground classes. Cutting Wheel Force/Total Thrust (COTT) was discretized into five bins as presented in Table 6.20. Figure 6.41 shows the relative frequencies of the discretized variable COTT with the contribution of ground conditions G1, G2, G3. For lower values of COTT, one is more likely driving through soil (G1) than rock through (G3). For higher values of COTT it is more likely that one is either



excavating through rock (G3) or mixed ground (G2). So for a given Total Thrust, if the Cutting Wheel Force is low, one is probably driving through soil (G1). This difference may be explained by the fact that the friction around the shield is higher in soil (G1), since it is a more deformable ground and therefore the pressure around the shield is higher, causing more friction than in a less deformable ground such as rock (G3). From the results one can conclude that COTT is an important parameter in distinguishing soil (G1) from rock (G3) and mixed (G2), since the relative frequencies are quite different. However distinguishing between rock (G3) and mixed (G2) is more difficult because the relative frequencies are not as different (Figure 6.40).

Table 6.21 Mean Value, Standard Deviation and Coefficient of Variation for Cutting Wheel Force / Total Thrust Force (COTT)

Mean Value	0.301
Standard Deviation	0.0913
Coefficient of Variation	0.303
In G1:	
Mean Value	0.246
Standard Deviation	0.0695
Coefficient of Variation	0.282
In G2:	
Mean Value	0.291
Standard Deviation	0.0820
Coefficient of Variation	0.282
In G3:	
Mean Value	0.344
Standard Deviation	0.0975
Coefficient of Variation	0.283

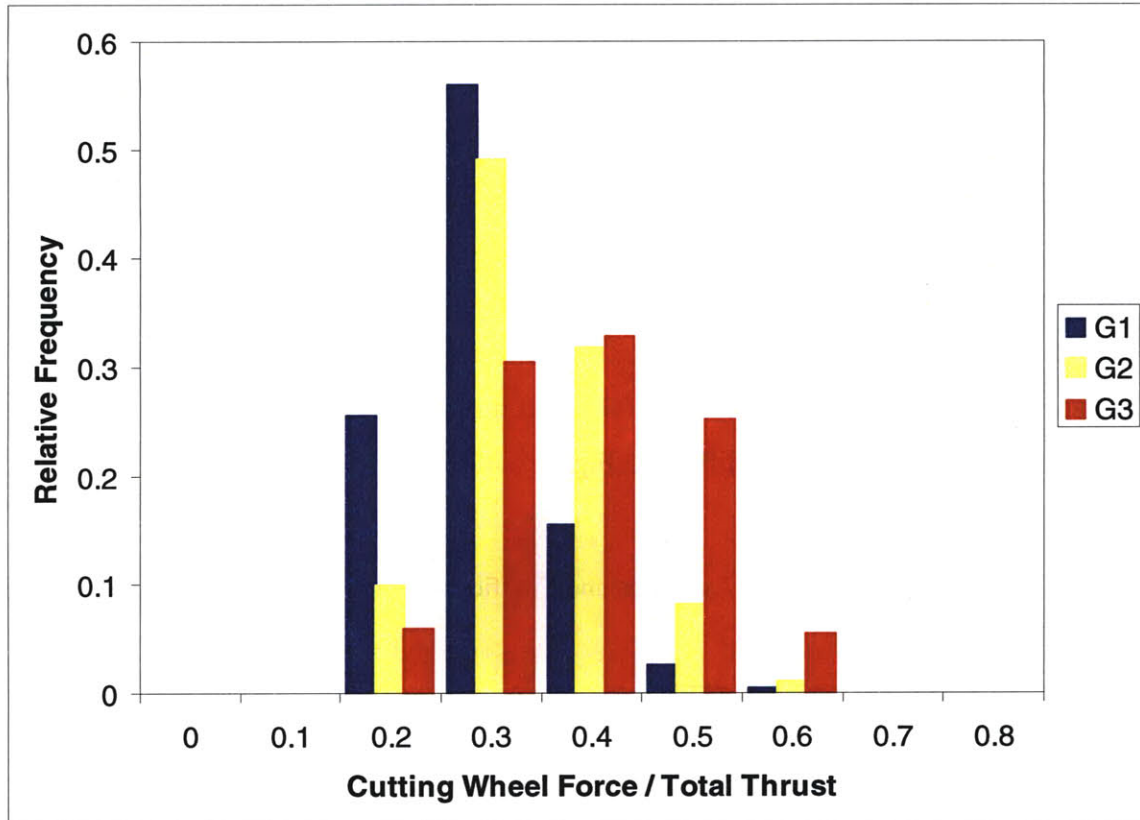


Figure 6.40 Relative Frequency Cutting Wheel Force / Total Thrust in ground conditions G1, G2, G3

Table 6.22 Discretization of the variable Cutting Wheel Force/Total Thrust (COTT)

Bin	Range
1	$COTT < 0.25$
2	$0.25 < COTT < 0.35$
3	$0.35 < COTT < 0.45$
4	$0.45 < COTT < 0.5$
5	$COTT > 0.5$

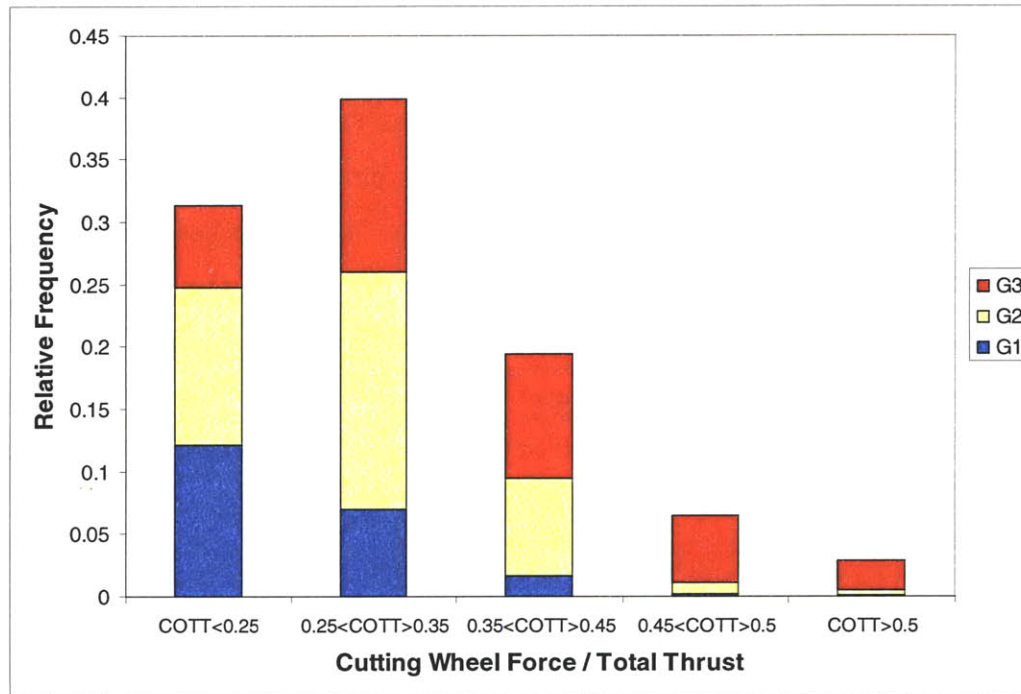


Figure 6.41 Relative Frequency of discretized variable COTT showing contribution of ground conditions G1, G2, G3

## B. Two Parameter analysis

The tunneling process is influenced not only by specific parameters, but also by the inter-relationship between them. In this section, a two parameter analysis is performed on the dataset from the Porto Metro to determine which relationships between parameters are important in distinguishing between ground classes. The joint relative frequencies of both parameters for the different geologies are compared. If there is a significant difference in the joint relative frequencies for the different ground classes, then the relationship between the parameters is good at distinguishing between the geologies, and if the differences are not great, then the relationship between the parameters is not good at distinguishing between the geologies. Where there is a significant difference, both parameters are retained in the Bayesian Model, as well as the relationship between them, which is considered in the model.

## Penetration rate (P) and Cutting Wheel Force (CF)

Figure 6.42 shows a scatter plot of the Cutting Wheel Force (CF) versus Penetration (P) for the data from the Porto Metro. The scatter plot shows that considering both Penetration and Cutting Wheel Force is important to distinguish between soil (G1) and rock (G3), since there is a clear difference between rock and soil values. In rock (G3) high values of Cutting Wheel Force (CF) are needed to penetrate the ground even at low penetration rates. In soil (G1) low values of CF will translate into high Penetration (P). The plot shows that there is a lower limit of CF for which the machine is able to penetrate the ground. This limit is about 4000 KN (for softer materials).

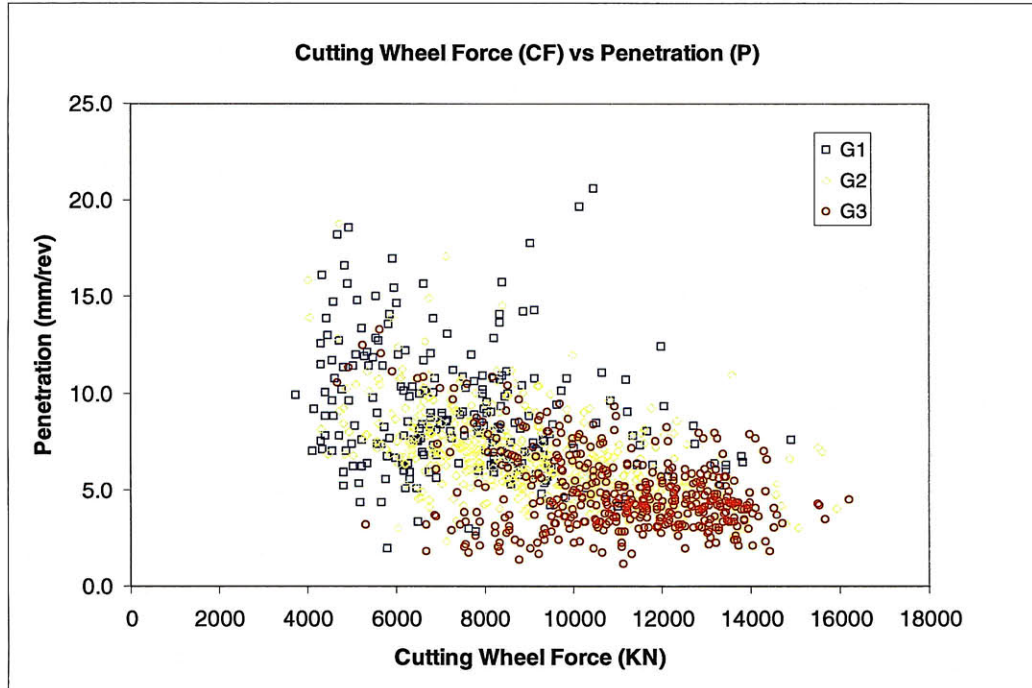


Figure 6.42 Penetration rate (P) versus Cutting Wheel Force (CF), in G1, G2, G3

Table 6.23 presents the correlation coefficients between P and CF for the different ground conditions. There is a negative correlation between penetration and cutting wheel force. This means that in softer materials one needs less cutting wheel force (CF) to get the same penetration (P).

Table 6.23 Correlation coefficient between Penetration rate and Cutting Wheel Force in G1, G2 and G3

Ground Condition	Correlation coefficient
G1	-0.2479
G2	-0.529
G3	-0.3468

Figure 6.43 shows the joint relative frequency of cutting wheel force (CF) and penetration rate (P) discretized according to tables Table 6.13 and Table 6.15, respectively. Figure 6.44, Figure 6.45 and Figure 6.46 show the joint distribution of penetration rate (P) and cutting wheel force (CF) for ground conditions G1, G2 and G3, respectively.

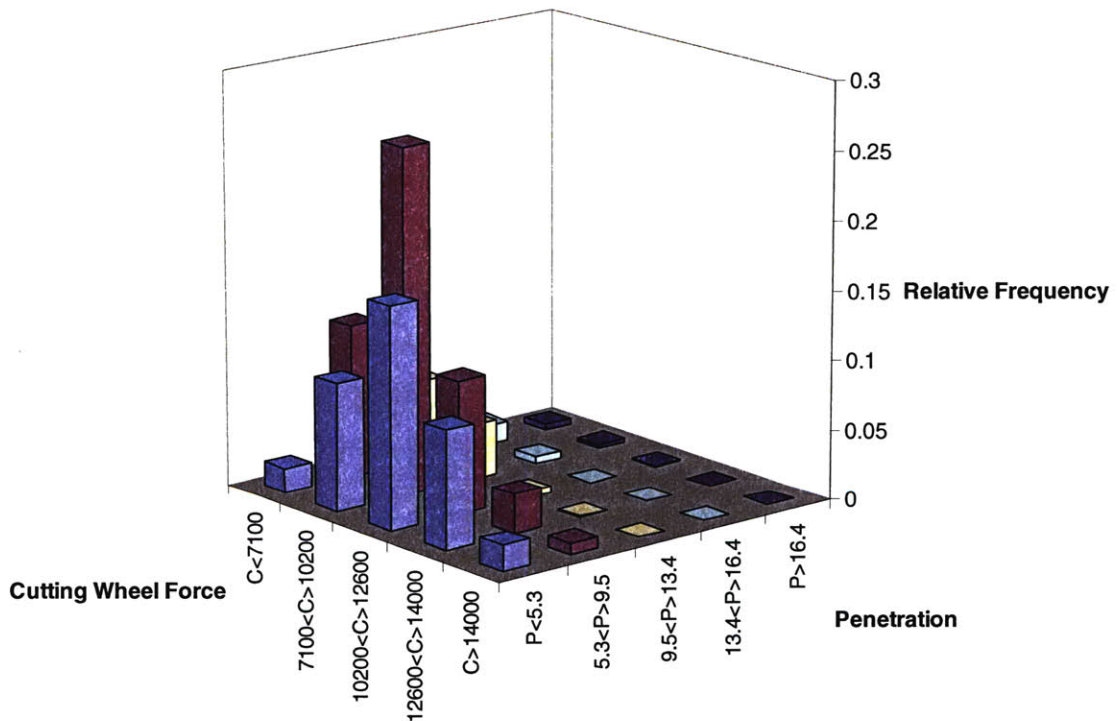


Figure 6.43 Joint relative frequency of penetration rate (P) and cutting wheel force (CF) for all ground conditions (G1, G2 and G3)

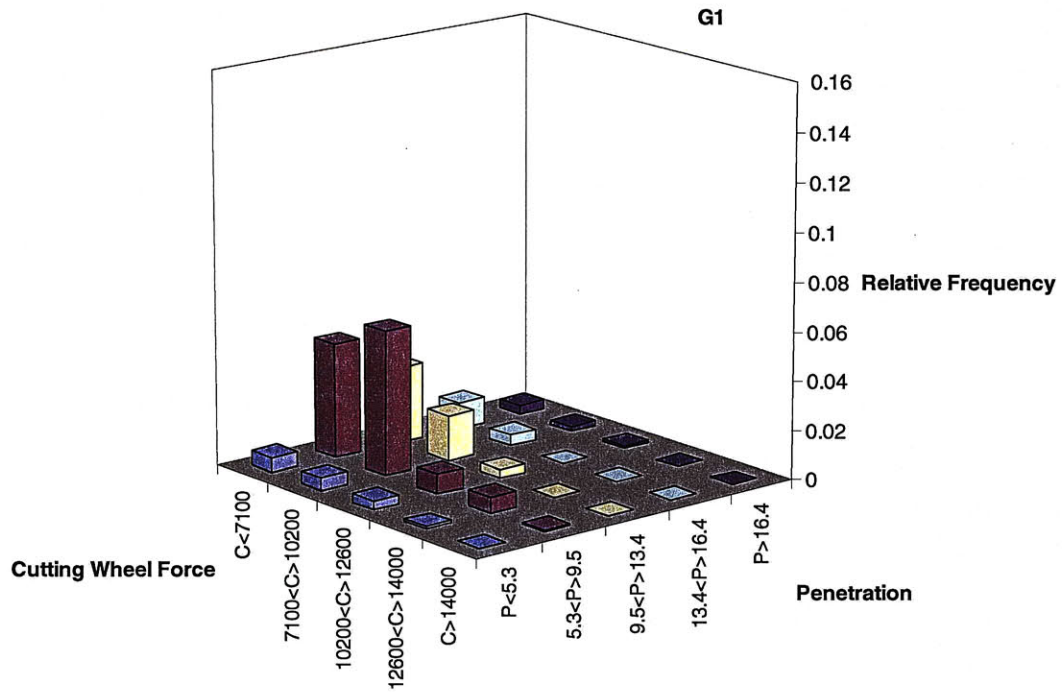


Figure 6.44 Joint relative frequency of penetration rate (P) and cutting wheel force (CF), in G1 (soil)

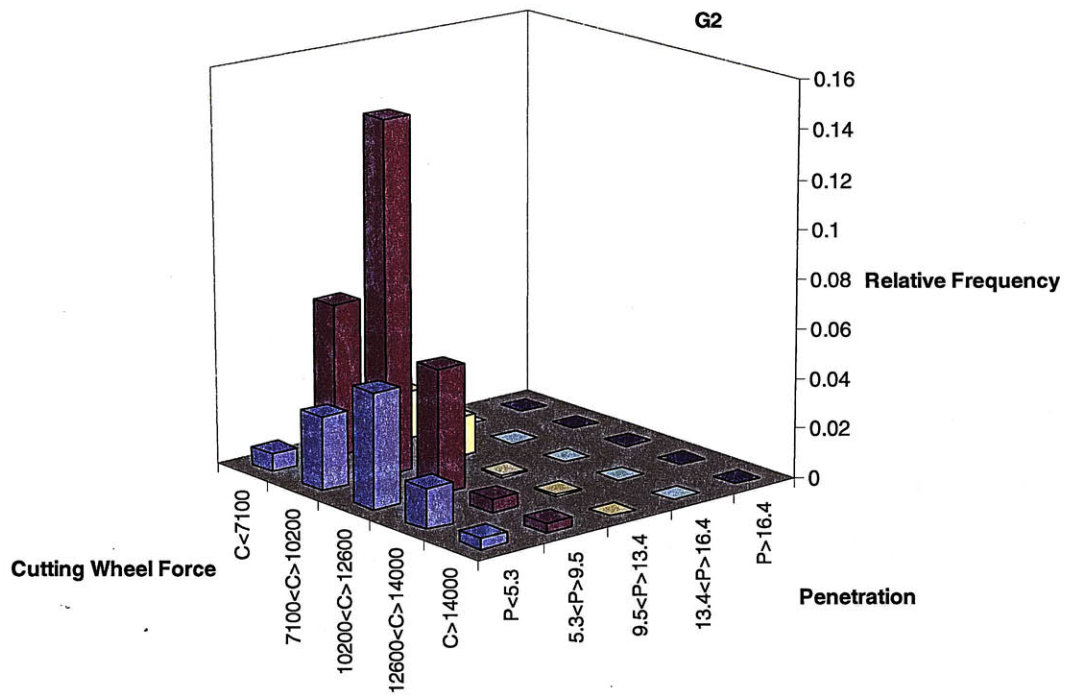


Figure 6.45 Joint relative frequency of penetration rate (P) and cutting wheel force (CF), in G2 (mixed)



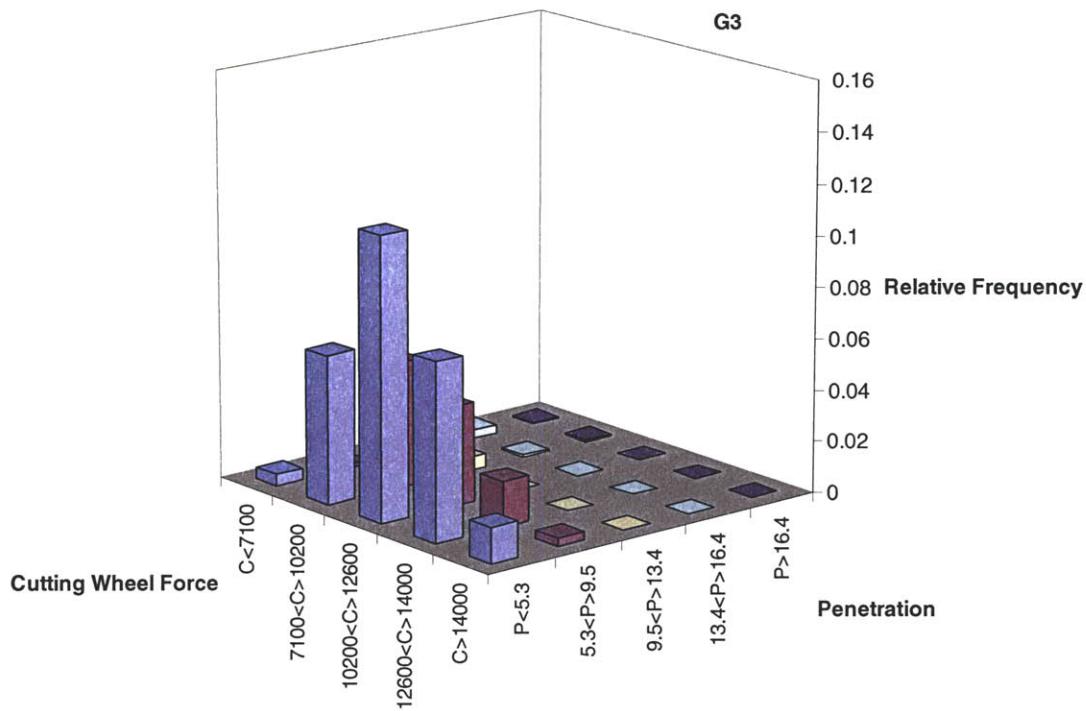


Figure 6.46 Joint relative frequency of penetration rate(P) and Cutting wheel force (CF), in G3 (rock)

The joint relative frequencies are different for the possible ground conditions. They show that for values of low penetration (below 5.3 mm/rev) and high cutting wheel force (above 10200 kN) it is more likely that the machine is crossing rock (G3). For higher values of penetration (between 5.3 and 16.4 m/rpm) and lower values of cutting wheel force (below 12000 kN) the probability of being in soil (G1) is high. For mixed conditions (G2) the relative frequencies are mostly concentrated in the range of CF below 12600 kN and in the range of penetration between 5.3mm/rev and 13.4 mm/rev.

From the results in this section, it can be concluded that considering cutting wheel force (CF), and penetration rate (P) together is important in distinguishing between ground conditions. The relationship between these two parameters is important, and therefore, both parameters, as well the relationship between them are retained in the Bayesian Model.

### Penetration rate (P) and Torque of the Cutting Wheel (TO)

Figure 6.47 shows penetration rate (P) versus torque of the cutting wheel (TO) scatter plot of the data. In Table 6.24 are the correlation coefficients between P and TO in G1, G2 and G3. Penetration and torque are strongly correlated in rock (G3) but uncorrelated in soil (G1) and mixed (G3). This can also be observed in the scatter plot. This means that for rock (G3), for a constant value of the cutting wheel force (CF) when the torque is increased (TO) the penetration also increases (P). The plot also shows that it seems that there is limit for applied torque around 9 MNm.

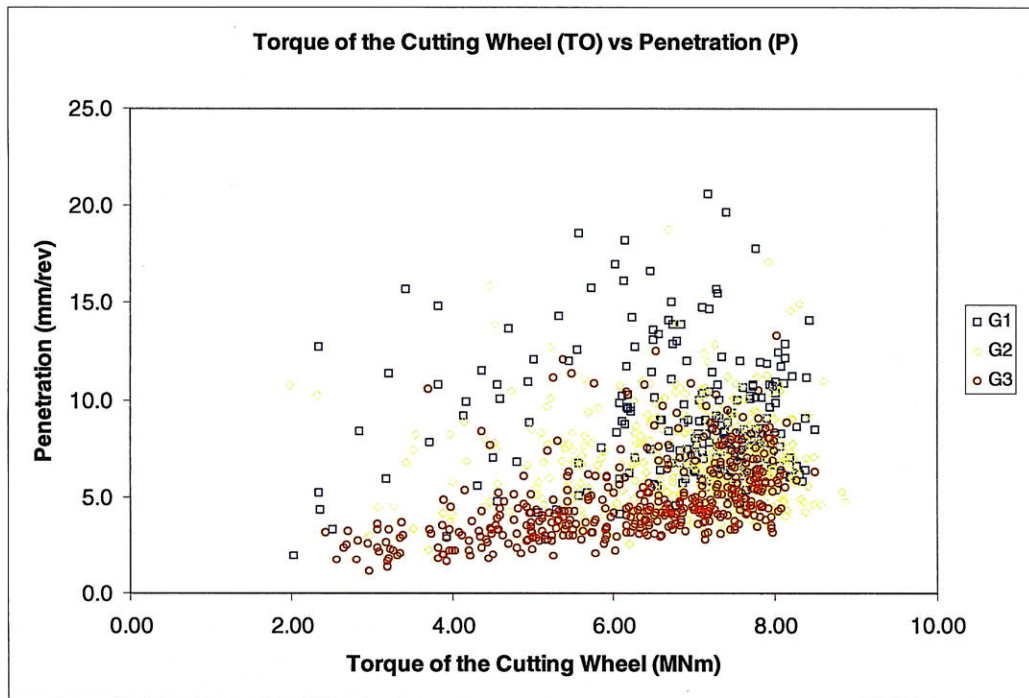


Figure 6.47 Penetration rate (P) versus Torque of the Cutting Wheel (TO), in G1, G2, G3

Table 6.24 Correlation coefficient between P and TO in G1, G2 and G3

Ground Condition	Correlation coefficient
G1	-0.025
G2	0.052
G3	0.496

Figure 6.48 shows the joint relative frequency of penetration rate (P) and torque of the cutting wheel (TO), discretized according as presented in Table 6.15 and Table 6.17, respectively. Figure 6.49, Figure 6.50 and Figure 6.51 show the joint relative frequency of penetration (P) and torque of the cutting wheel (TO) in ground condition G1, G2, G3, respectively. The joint relative frequency of P and TO is concentrated at the upper end of the diagonal in Figure 6.48, which means that there is little (in some cases none) data for high values of penetration and low torque. The joint relative frequency of P and TO in soil (Figure 6.49) show a concentration of data around the high penetration values (i.e. above 5.3mm/rev) and high torque values (i.e. above 6MNm). The joint relative frequency of P and TO in mixed conditions is close to that of the soil, although shifted to the left, i.e to lower values of penetration than those observed in soil. The range of torque values observed in mixed conditions is greater than in soil, since lower values of torque than in soil are observed. In rock, the joint relative frequency of P and TO shows that the data are mostly concentrated around low values of penetration and almost all values of torque.

Based on the results, one can conclude that considering penetration rate (P) and torque of the cutting wheel (CF) together is important in distinguishing between ground conditions. The relationship between these two parameters is important, and therefore, both parameters, as well the relationship between them are retained in the Bayesian Model.

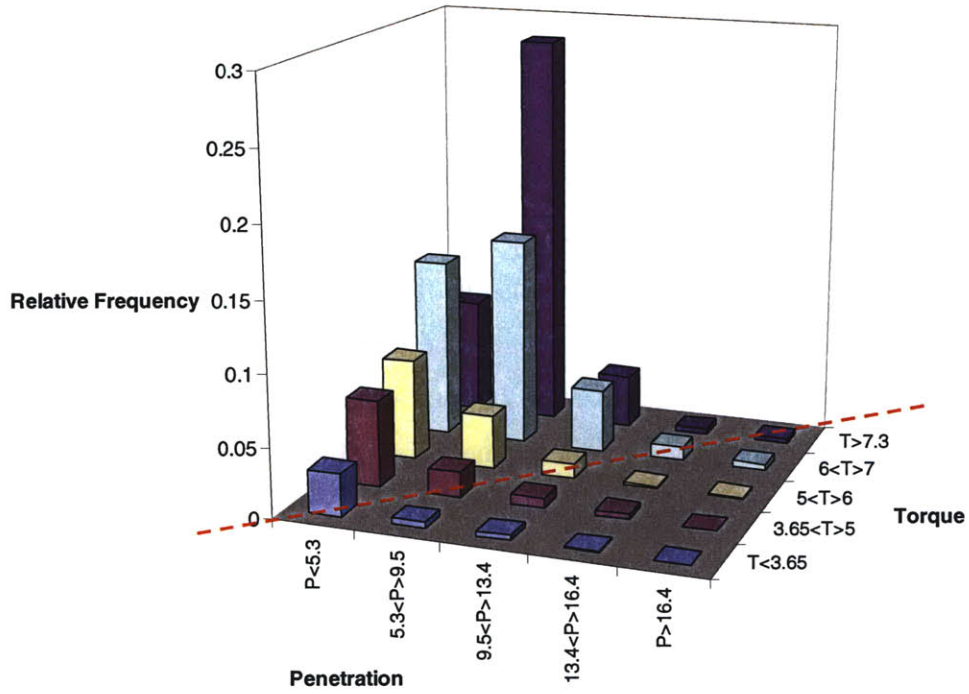


Figure 6.48 Joint relative frequency of penetration (P) and torque of the cutting wheel (TO) for all ground conditions (G1, G2 and G3)

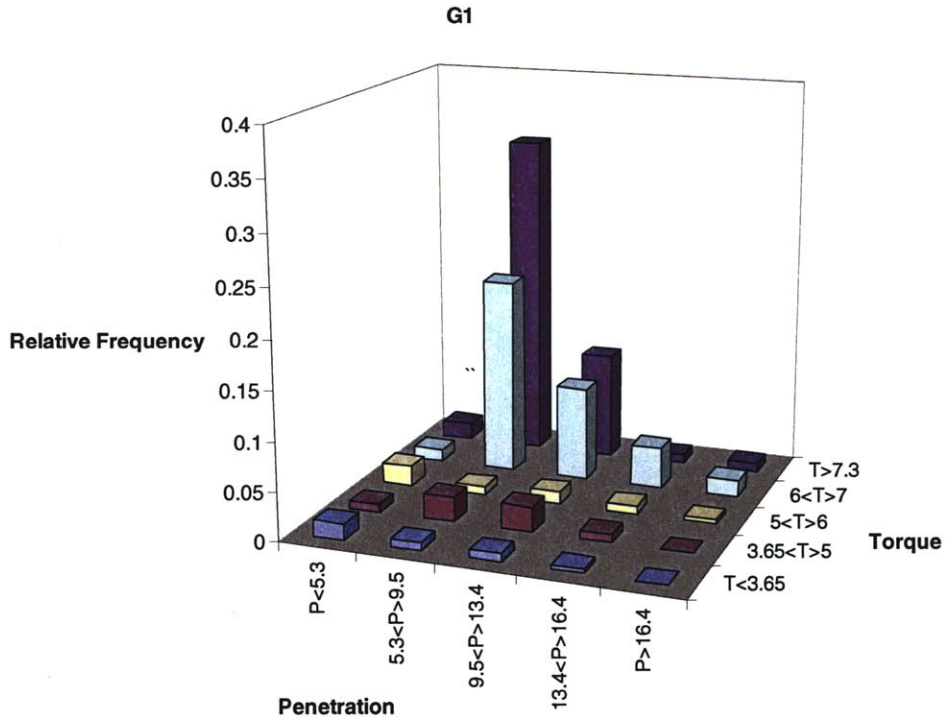


Figure 6.49 Joint relative frequency of penetration (P) and torque of the cutting wheel (TO), in G1

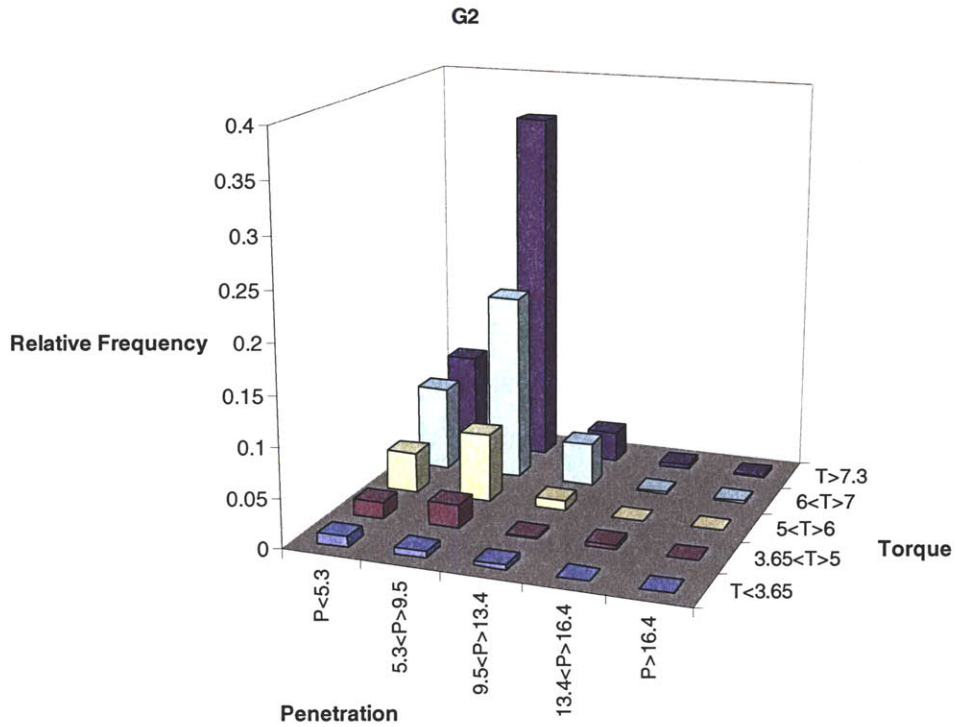


Figure 6.50 Joint relative frequency of penetration (P) and torque of the cutting wheel (TO), in G2 (mixed)

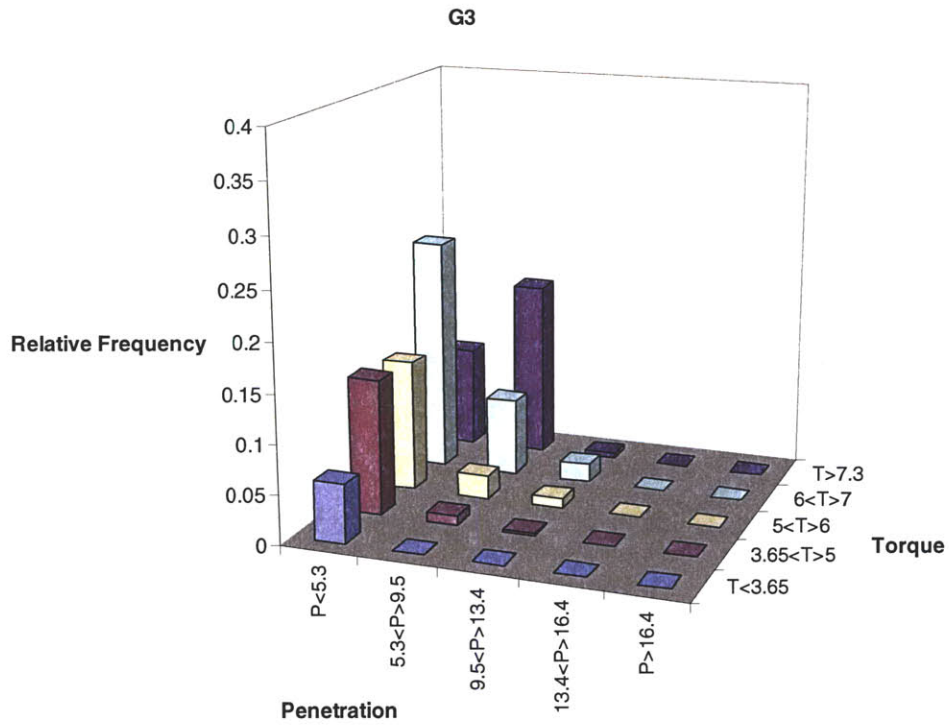


Figure 6.51 Joint relative frequency of penetration (P) and torque of the cutting wheel (TO), in G3 (rock)



## Cutting Wheel Force (CF) and Torque of the Cutting Wheel (TO)

Figure 6.52 shows cutting wheel force (CF) versus torque of the cutting wheel (TO) scatter plot of the data. In Table 6.25 are the correlation coefficients between CF and TO in G1, G2 and G3.

One can observe a clear difference between values of CF and TO in G1 (soil) and G3 (rock). Note that both of these parameters are directly or indirectly controlled by the operator (CF indirectly through the total thrust). The correlation between variables is thus induced by the operation of the machine. The maximum torque of around 9 MNm, observed previously in Figure 6.47 can be observed also in Figure 6.52. It is also interesting to observe that the operating torque and cutting wheel force must be above 2 MNm and 4000 KN respectively, for the machine to penetrate through the softer materials, i.e. soil.

The CF-TO scatter plot shows that for constant values of torque, if the cutting wheel force is high one is more likely to be in rock (G3) and if the cutting wheel force is low one is more likely to be in soil (G1).

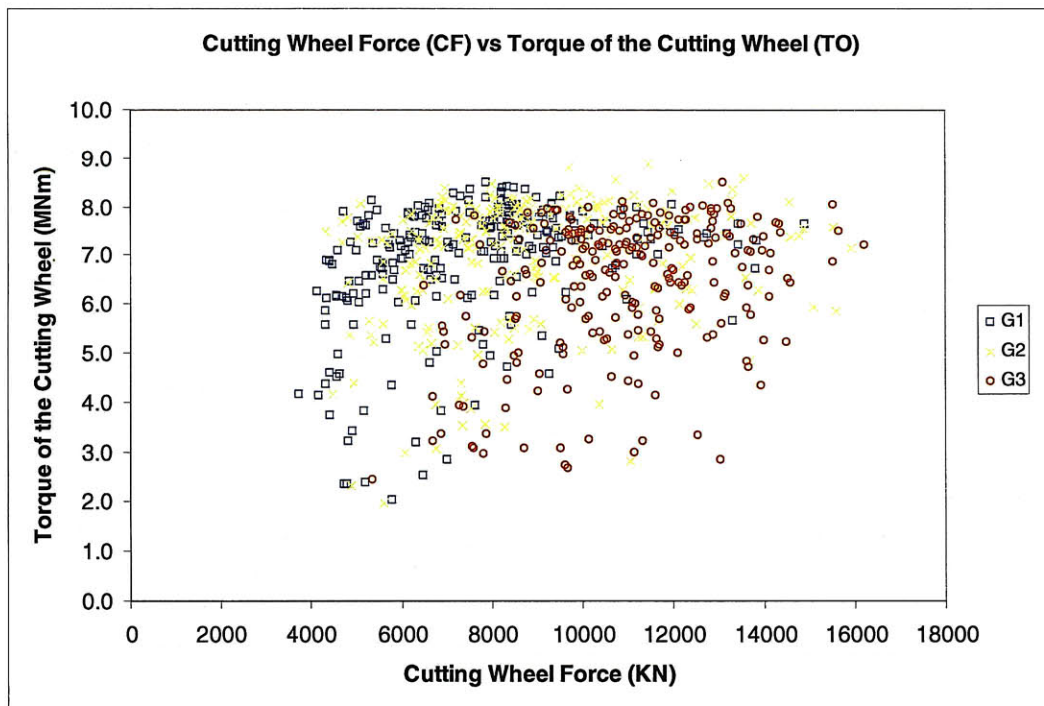


Figure 6.52 Cutting Wheel Force (CF) versus Torque of the Cutting Wheel (TO), in G1, G2, G3



Table 6.25 Correlation coefficient between cutting wheel force (CF) and Torque of the cutting wheel (TO) in G1, G2 and G3

Ground Condition	Correlation coefficient
G1	0.362
G2	0.219
G3	0.176

The correlation coefficient between CF and TO is the highest in soil (0.362) and the lowest in rock (0.176). For all ground conditions the correlation coefficient between CF and TO is positive. This means that when the torque increases the cutting wheel force also increases, more precisely if a value of torque is above its mean, then the value of the cutting wheel force is also above its mean.

Figure 6.53 shows the joint relative frequencies of the discretized variables cutting wheel force (CF) and torque (TO). The discretizations for cutting wheel force (CF) and for torque (TO) are presented in Table 6.13 and Table 6.17, respectively. For all ground conditions it is more likely to have values of TO in higher ranges (above 5 or 6MNm), while cutting wheel force values (CF) are more likely to be below 14000 KN.

Figure 6.54, Figure 6.55 and Figure 6.56 show the joint relative frequencies of the discretized variables cutting wheel force (CF) and torque (TO) for ground conditions, G1 (soil), G2 (mixed) and G3 (rock), respectively. The joint relative frequencies of CF and TO data in soil (Figure 6.54) are higher for values of CF below 10200 KN and values of TO above 6 MNm. Thus if the values of TO are high and of CF are low, then the probability that the machine is driving through soil (G1) is high. The joint relative frequencies of CF and TO data in mixed conditions (Figure 6.55) are similar to those for soil conditions. The main difference is that in the case of mixed conditions the most frequent values of CF and TO are more spread than in soil conditions. In mixed conditions the most frequent values of CF are in the range 0 to 12600 KN and the most frequent values of TO are above 5 MNm. The joint relative frequencies of CF and TO data in rock (Figure 6.56) are higher for high values of cutting wheel force (10200 to

14000 KN) and high values of torque (above 6 MN). Thus if the values of TO are high and of CF are high the probability that the machine is driving through rock (G3) is high.

Based on the results, one can conclude that considering torque of the cutting wheel (CF) and torque of the cutting wheel (TO) together is important in distinguishing between ground conditions. The relationship between these two parameters is important, and therefore, both parameters, as well the relationship between them are retained in the Bayesian Model.

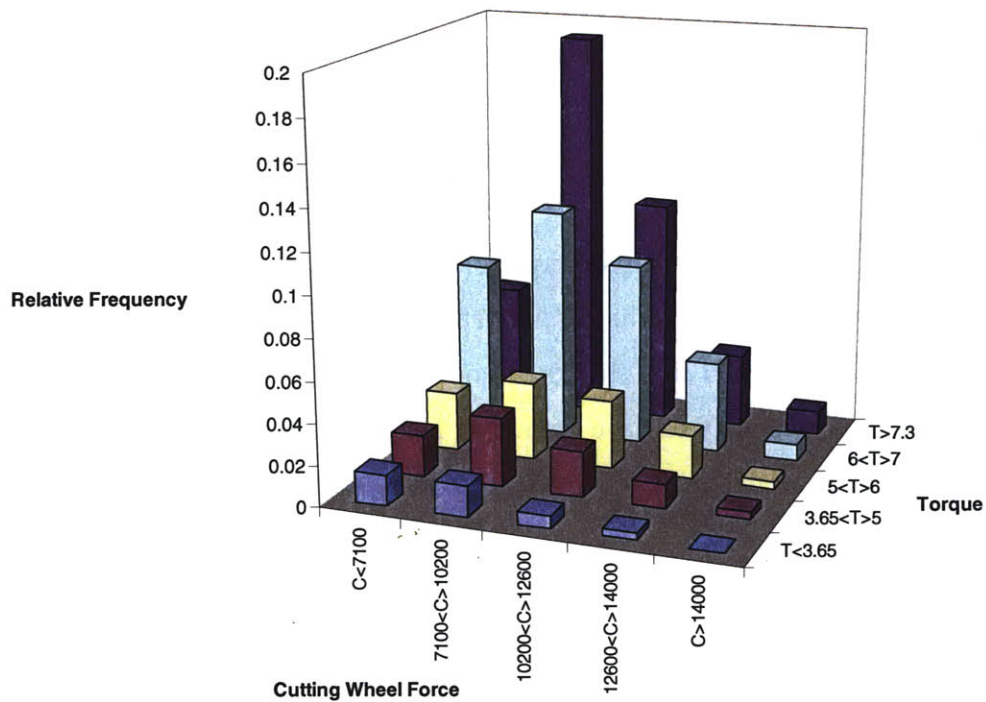


Figure 6.53 Joint relative frequency of cutting wheel force (CF) and torque of the cutting wheel (TO) for all ground conditions (G1, G2 and G3)

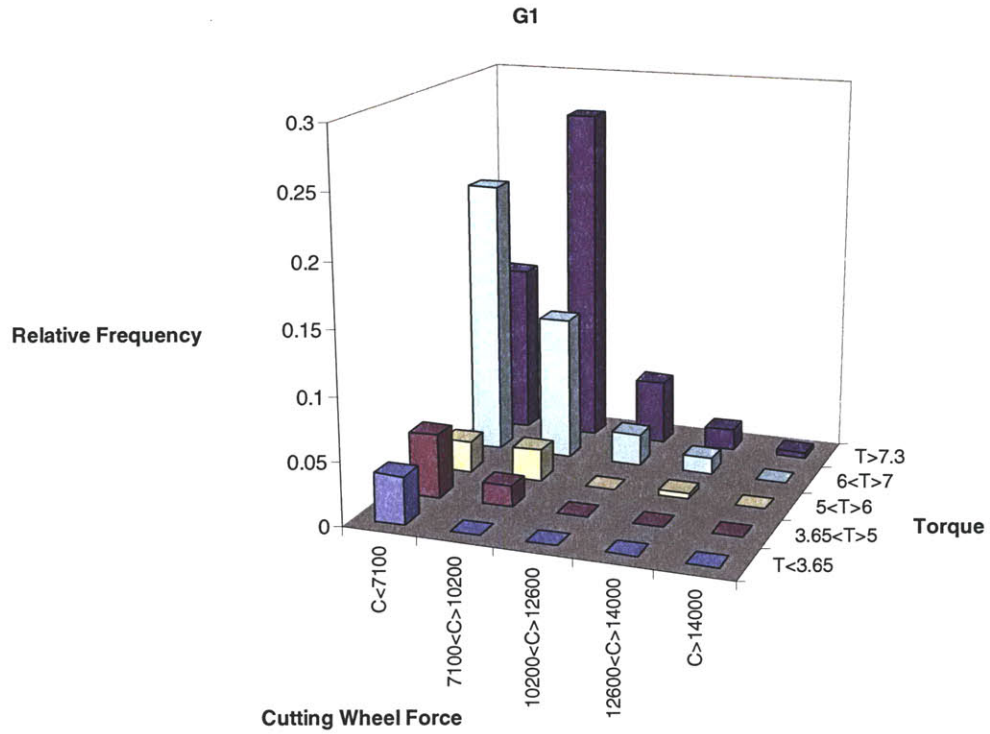


Figure 6.54 Joint relative frequency of cutting wheel force (CF) and torque of the cutting wheel (TO), in G1 (soil)

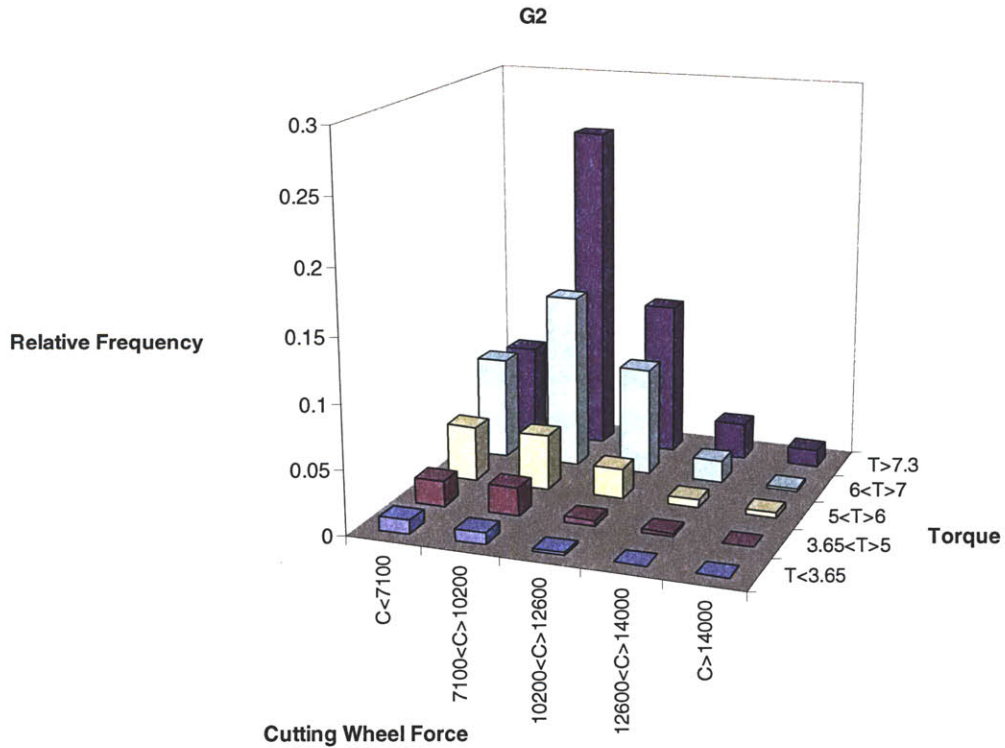


Figure 6.55 Joint relative frequency of cutting wheel force (CF) and torque of the cutting wheel (TO), in G2 (mixed)

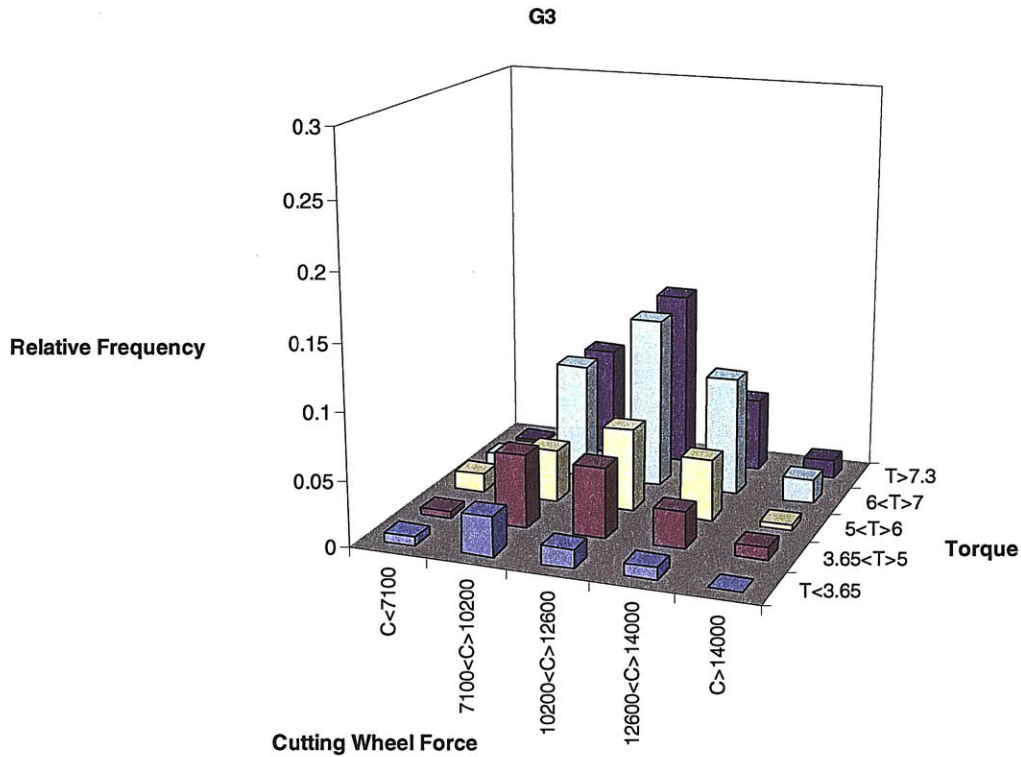


Figure 6.56 Joint relative frequency of cutting wheel force (CF) and torque of the cutting wheel (TO), in G3 (rock)

### Penetration (P) and Torque of the Cutting Wheel / Cutting Wheel Force (TOC)

Figure 6.57 shows a scatter plot of the torque / cutting wheel force (TOC) versus penetration (P) data. In Table 6.26 the correlation coefficients between TOC and P in each ground condition are presented. There is a high correlation between TOC and P in rock (G3). In soil (G1) this correlation is small. This can also be seen in the scatter plot of Figure 6.57, which also indicates that the relationship between TOC and P is very important in distinguishing between ground conditions. At low TOC and low penetration (P) the ground conditions are most likely rock (G3). For rock conditions, the distribution of TOC-P values is very concentrated, with a small scatter. At high TOC and high penetrations the ground conditions are most likely soil (G1). The distribution of TOC-P values for soil (G1) is much more scattered than that of rock (G3) and mixed (G2).

It seems that there is a lower limit of the ratio torque over cutting force of about 0.20, and an upper limit of about 1.67, for which there is also no data points.

In order to better visualize these limits, the cutting wheel force / torque versus penetration (P) scatter plot of the data is presented in Figure 6.58. In this plot is easier to visualize that there are no data points for cutting force / torque below 0.6. It seems that for relationships of CF/TO below 0.6 (i.e.  $TOC > 1.67$ ) the machine is not able to penetrate the soil ground conditions. This shows that for a given torque there is likely a minimal of cutting force necessary to penetrate even soft materials. Also there are no data for values of CF/TO above 5 (i.e.  $TOC < 0.2$ ). It is also possible to observe an upper boundary of penetration in both Figure 6.57 and Figure 6.58 (approximately 20 mm/rev). This can be explained by the fact that for a fixed cutting wheel force increasing the torque won't have much effect on the penetration or because the torque as reached the operational safe limit.

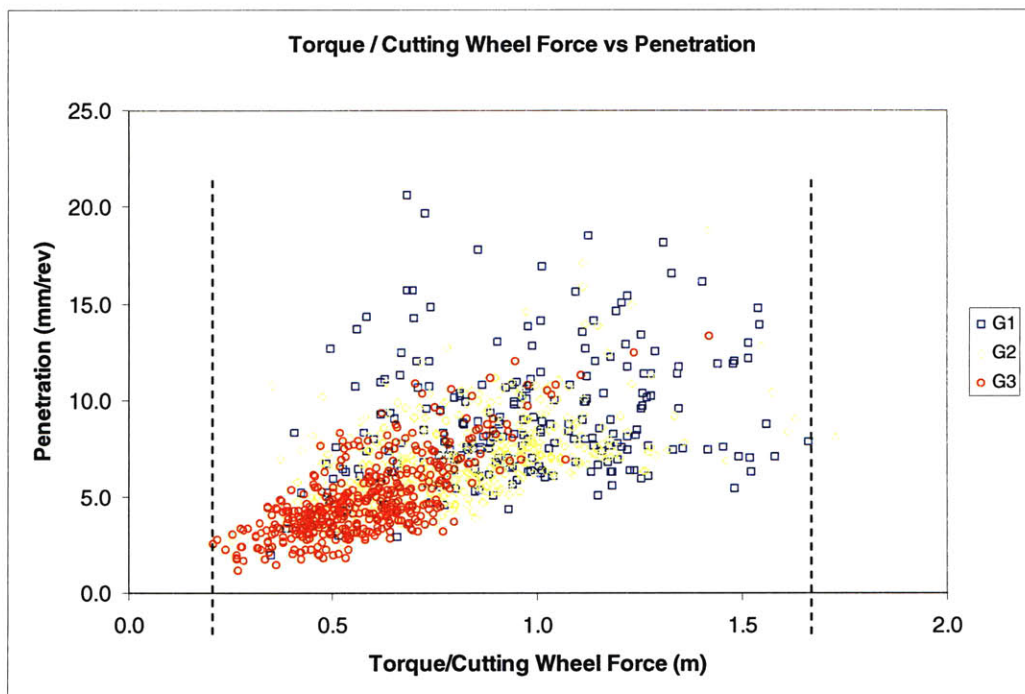


Figure 6.57 Torque / Cutting Wheel Force (TOC) versus Penetration (P), in G1, G2, G3



Table 6.26 Correlation coefficient between Torque / Cutting Wheel Force (TOC) and Penetration (P), in G1, G2 and G3

Ground Condition	Correlation coefficient
G1	0.247
G2	0.537
G3	0.733

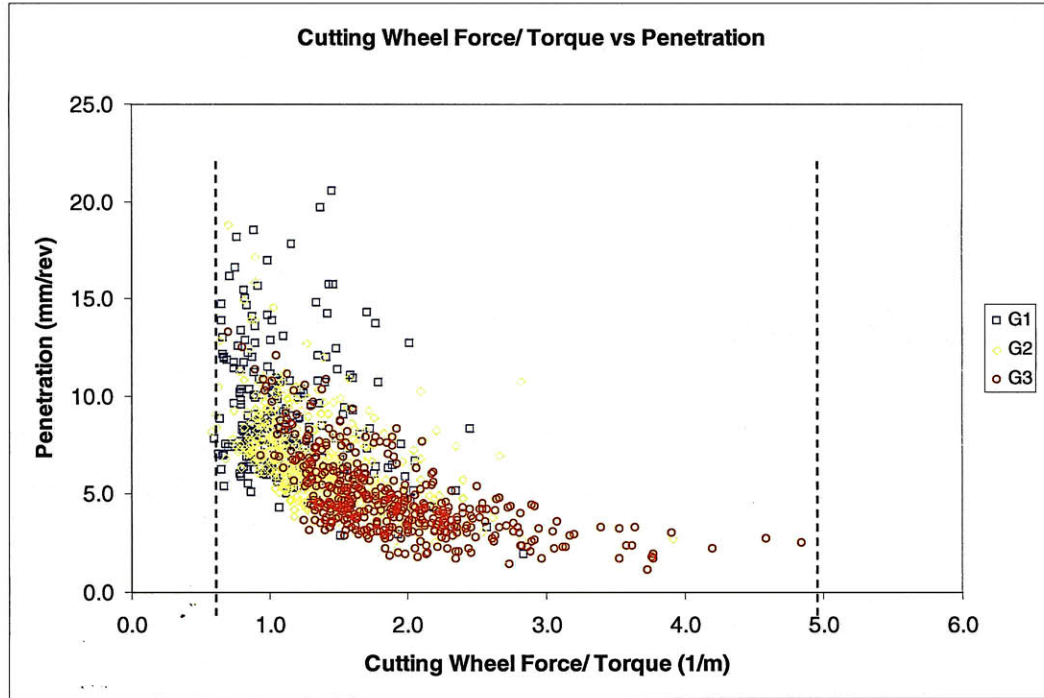


Figure 6.58 Cutting Wheel Force / Torque (COT) versus Penetration (P), in G1, G2, G3

Figure 6.59 shows the joint relative frequencies of penetration (P) and torque of the cutting wheel / cutting wheel force (TOC), discretized as in Table 6.15 and Table 6.19, respectively. It is possible to observe the importance of rock on the joint distribution (low values of penetration and TOC), by comparing Figure 6.60, Figure 6.61 and Figure 6.62, which show the joint relative frequency of the discretized variables penetration (P) and torque of the cutting wheel / cutting wheel force (TOC) for ground conditions, G1, G2 and G3, respectively. The joint relative frequency of penetration (P) and TOC in G1 (Figure 6.60) is higher for high values of penetration ( $P > 5.3$  mm/rev) and high values of cutting force over torque ( $0.6 < \text{TOC} < 1.4$ ). This means that for higher P and high TOC it is likely that one is driving through soil (G1). The joint relative frequency of penetration (P)



and TOC in G2 (Figure 6.61) is similar to that of G1, but shifted towards lower values of TOC and lower values of P, than those that occur in G1. The joint relative frequency of penetration (P) and TOC in G3 (Figure 6.62) shows is highly concentrated in lower values of penetration ( $P < 5.3$  KN) and low valued of torque over cutting wheel force ( $TOC < 0.825$ ). This means that if one has low P and low TOC it is much more likely one is in rock (G3) is then in soil (G1) .

Based on the results, one can conclude that considering penetration (P) and torque of the cutting wheel over cutting wheel force (TOC) together is important in distinguishing between ground conditions. The relationship between these two parameters is important, and therefore, both parameters, as well the relationship between them are retained in the Bayesian Model.

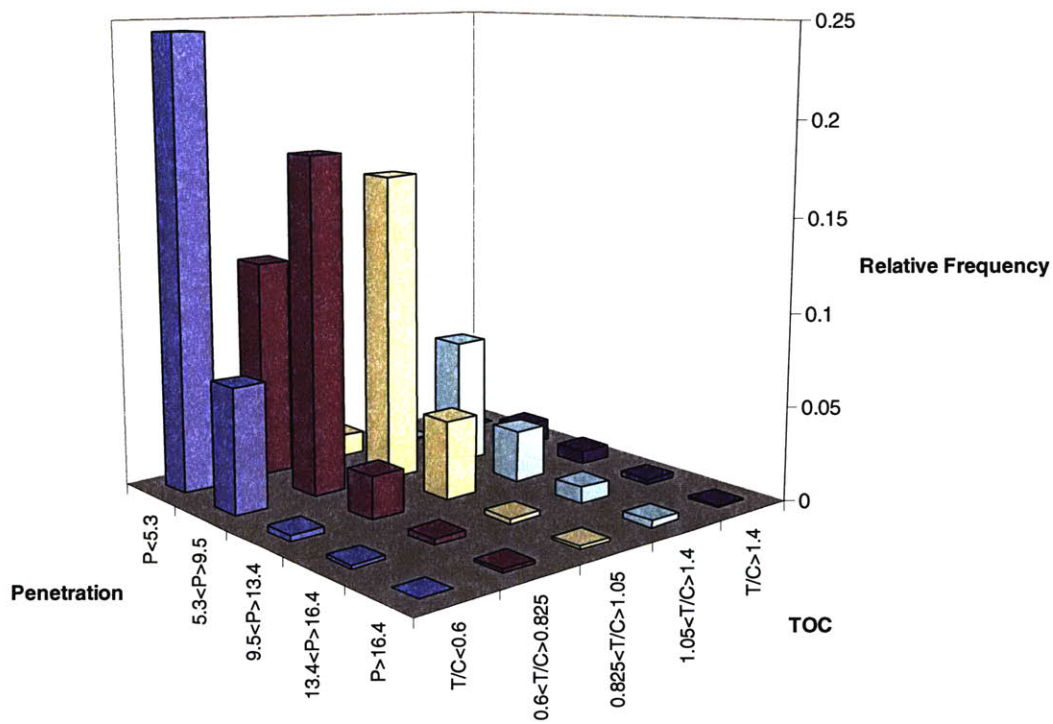


Figure 6.59 Joint relative frequency of penetration (P) and torque of the cutting wheel / cutting wheel force (TOC) for all ground conditions (G1, G2 and G3)

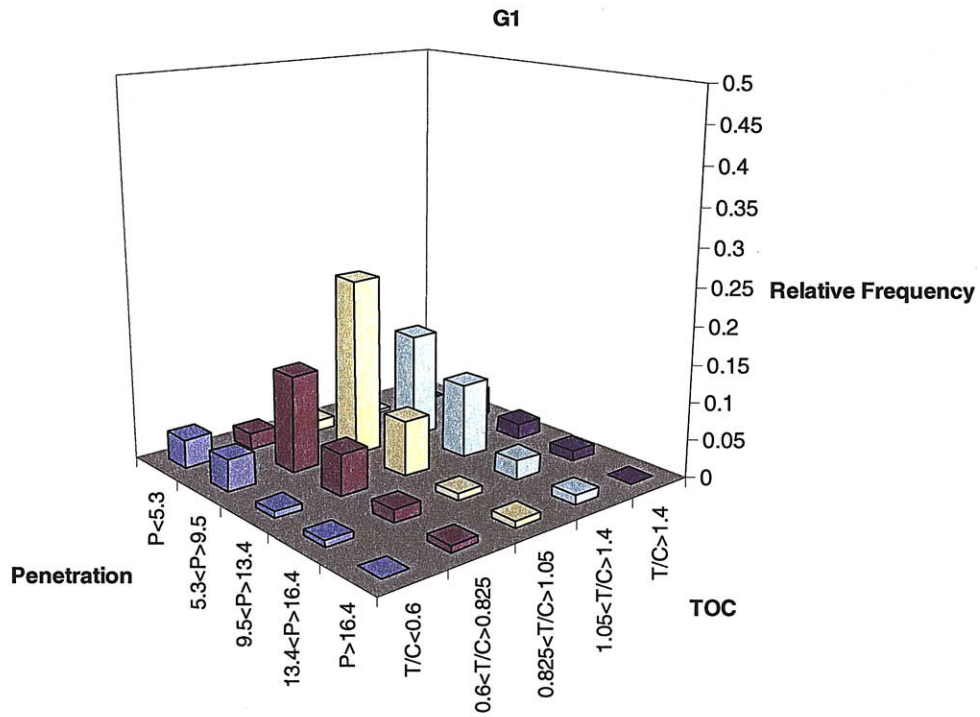


Figure 6.60 Joint relative frequency of penetration (P) and torque of the cutting wheel / cutting wheel force (TOC) in G1 (soil)

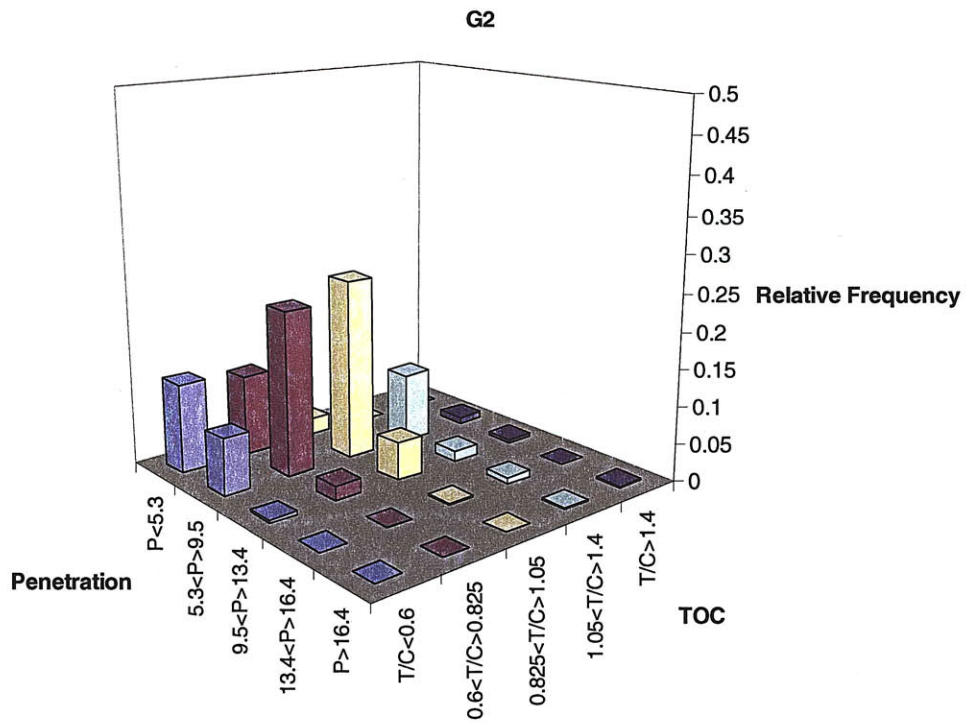


Figure 6.61 Joint relative frequency of penetration (P) and torque of the cutting wheel / cutting wheel force (TOC) in G2 (mixed)

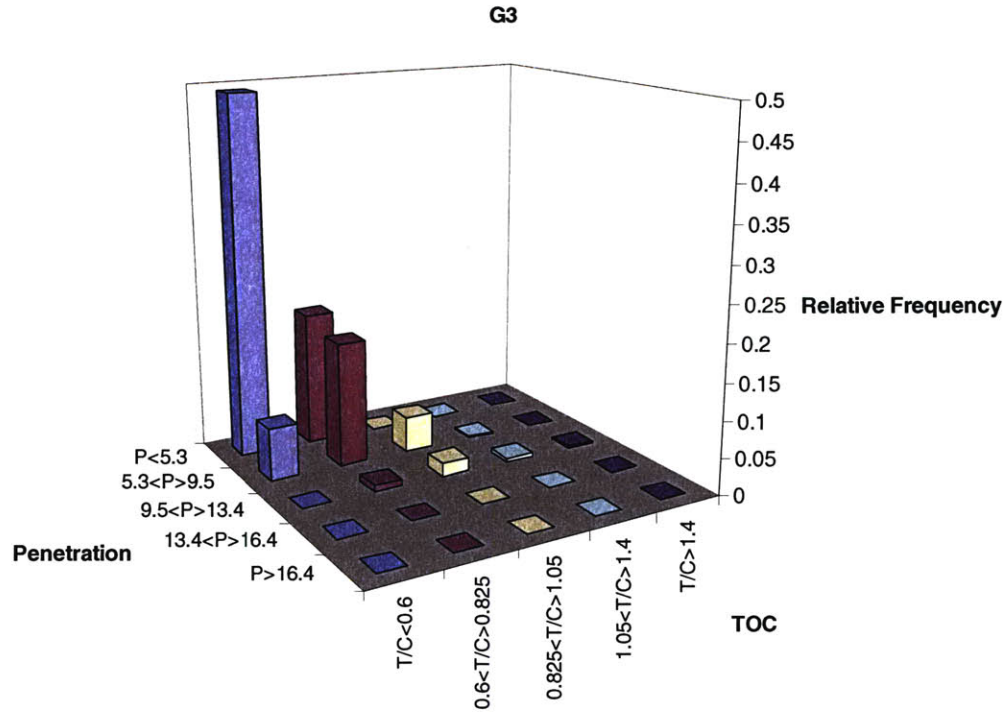


Figure 6.62 Joint relative frequency of penetration (P) and torque of the cutting wheel / cutting wheel force (TOC) in G3 (rock)

### Penetration (P) and Cutting Wheel Force/ Total Thrust Force (COTT)

Figure 6.63 shows a scatter plot of the cutting wheel force over total thrust (COTT) versus penetration (P) data. In Table 6.26 the correlation coefficients between COTT and P in each ground condition are presented. The highest correlation coefficient is in G2 (-0.318) and is negative. The smallest correlation coefficient is in G3 (-0.062) and is also negative. The correlation coefficient in G1 (soil) is positive and equal to 0.163.

The scatter plot in Figure 6.63 of COTT and P show that in G1 the data is most frequent for high values of penetration and low valued of COTT. The distribution of the data in G2 is similar to G1, but shifted toward lower values of penetration and slightly higher values of COTT than those encountered in G1. In G3, the frequencies are the highest for low values of penetration and higher values of COTT than in G1 and G2. Thus if one has high penetration and low cutting wheel force over total thrust, one is more likely to be

going through G1. On the other hand if the penetration is low and cutting wheel force over total thrust is high, one is more likely to the going through G3.

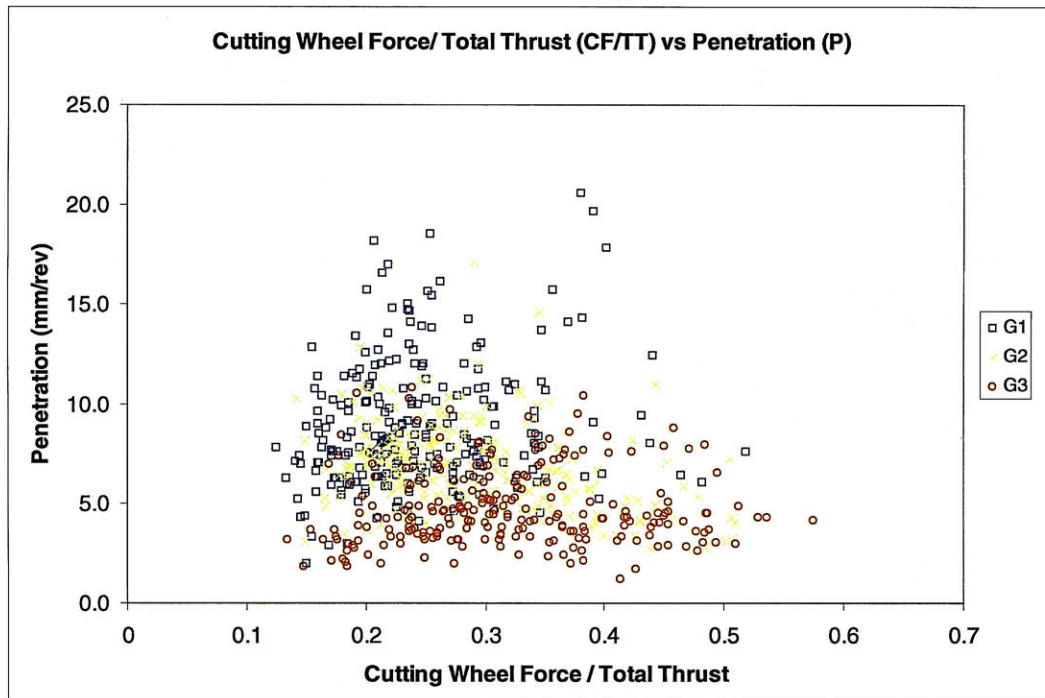


Figure 6.63 Penetration (P) versus Cutting Wheel Force / Total Thrust Force (COTT), in G1, G2, G3

Table 6.27 Correlation coefficient between Penetration (P) and Cutting Wheel Force/ Total Thrust (COTT) in G1, G2 and G3

Ground Condition	Correlation coefficient
G1	0.163
G2	-0.318
G3	-0.062

Figure 6.64 shows the joint relative frequency of the penetration (P) and cutting wheel force/ total thrust (COTT), discretized as in Table 6.15 and Table 6.22, respectively.

Figure 6.65, Figure 6.66 and Figure 6.67 show the joint relative frequency of the discretized variables penetration (P) and cutting wheel force/ total thrust (COTT), for ground conditions, G1, G2 and G3, respectively. The joint relative frequency of



penetration (P) and cutting wheel force/ total thrust (COTT), in G1 is the highest for high values of penetration ( $P > 5.3 \text{ mm/rev}$ ) and low values of COTT ( $< 0.35$ ). The joint relative frequency of penetration (P) and cutting wheel force/ total thrust (COTT), in G2 is the similar to that of G1, although shifted towards lower values of penetration (between 0 and  $13.4 \text{ mm/rev}$ ) and higher values of COTT (between 0 and 0.5). The joint relative frequency of penetration (P) and cutting wheel force/ total thrust (COTT), in G3 is the highest for low values of penetration (below  $5.3 \text{ mm/rev}$ ) and higher values of COTT than in G2 and G3.

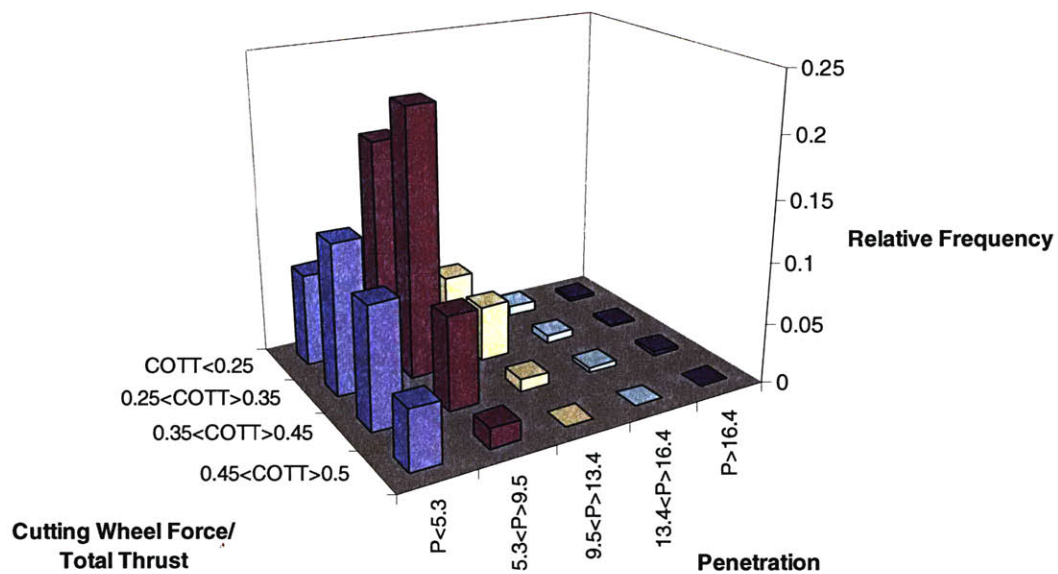


Figure 6.64 Joint relative frequency of cutting wheel force/ total thrust (COTT) and penetration rate (P) for all ground conditions (G1, G2 and G3)

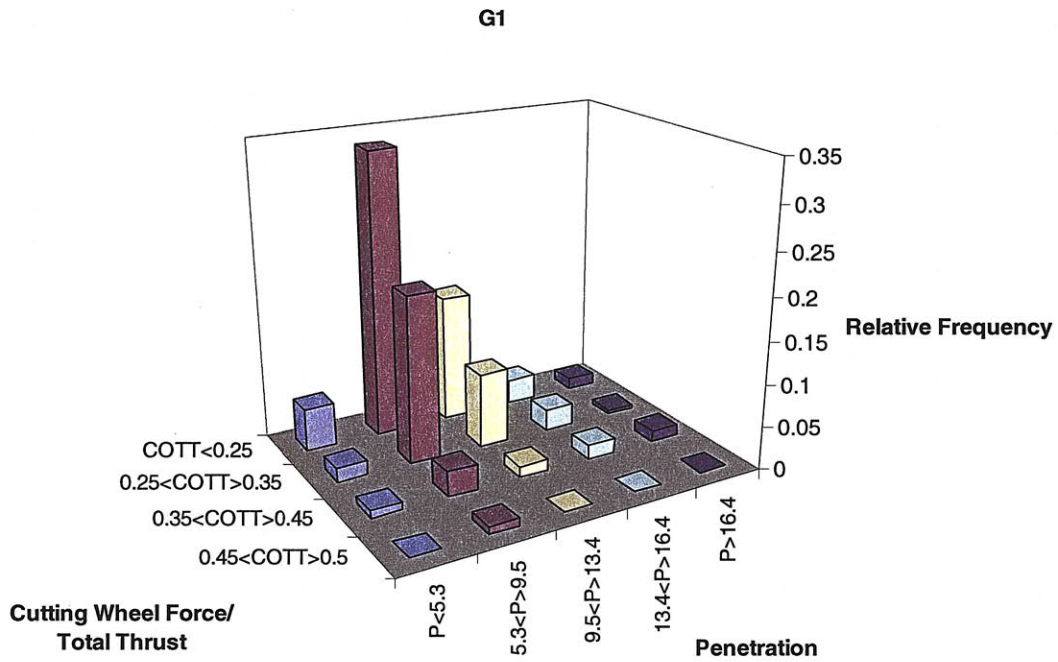


Figure 6.65 Joint relative frequency of cutting wheel force/ total thrust (COTT) and penetration (P), in G1 (Soil)

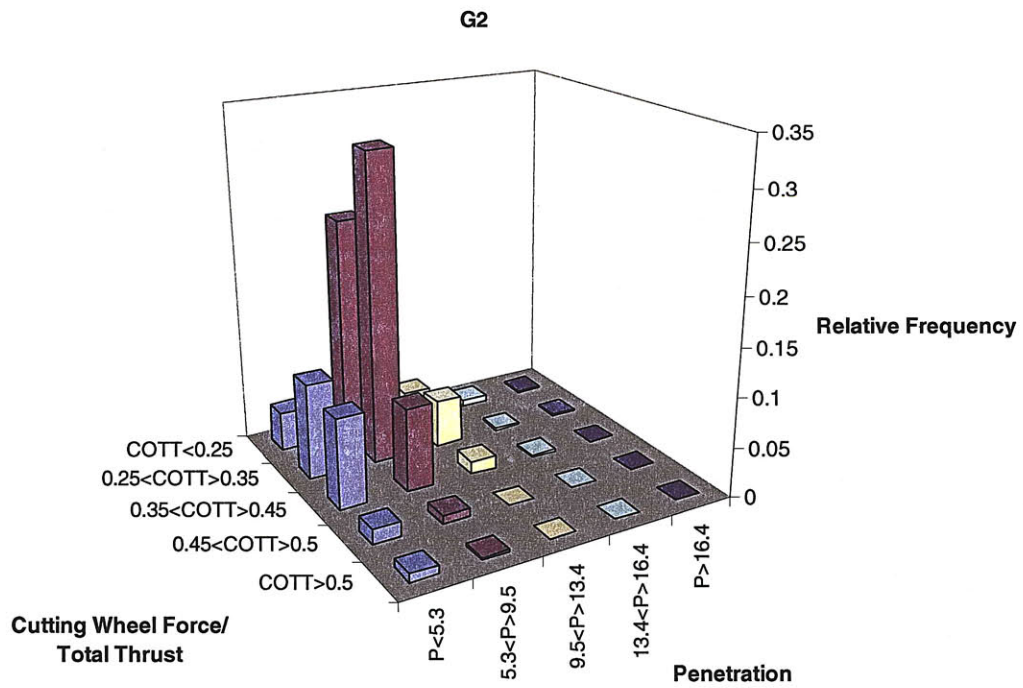


Figure 6.66 Joint relative frequency of cutting wheel force/ total thrust (COTT) and penetration (P), in G2 (mixed)



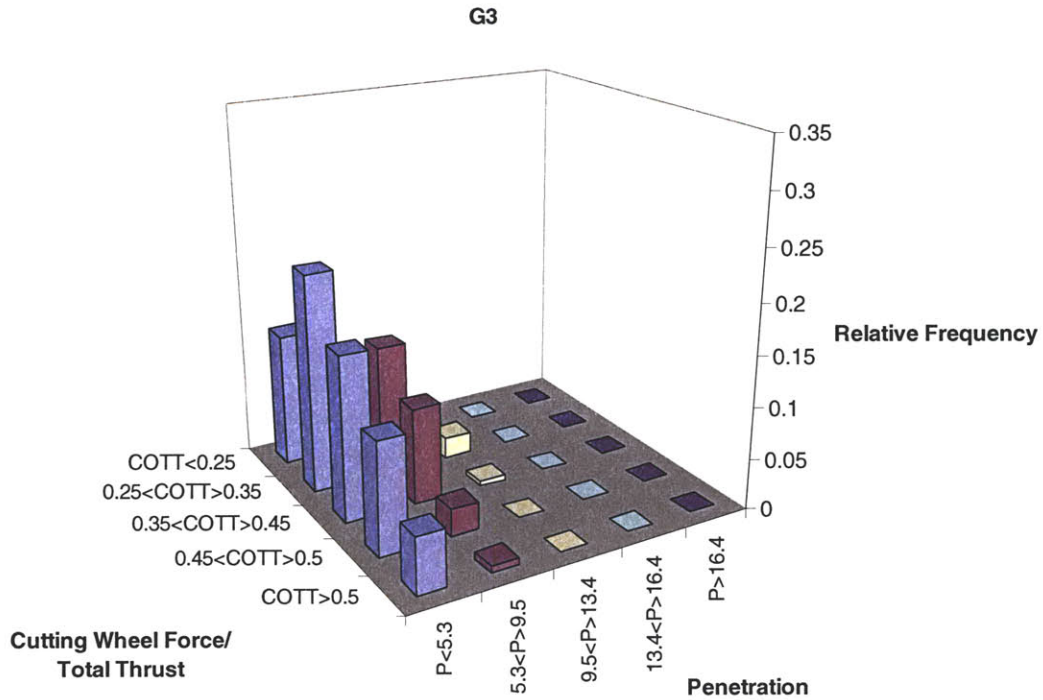


Figure 6.67 Joint relative frequency of cutting wheel force/ total thrust (COTT) and penetration (P), in G3 (rock)

### C. More than two parameter analysis

It is difficult to visualize and draw conclusions from 3D scatter plots of the data. For this reason sensitivity analysis will be performed on the models in order to determine the important relationships between more than two variables.

As an example consider the scatter plot of the cutting force (CF) – torque (TO) – penetration (P) data shown in Figure 6.68. It is quite difficult to visualize and draw conclusions regarding the importance of the relationship between the three variables. For this reason sensitivity analyses will be performed on the predictor model in order to assess the importance of relationships between three or more variables. This is will done in section 6.2.2.3.

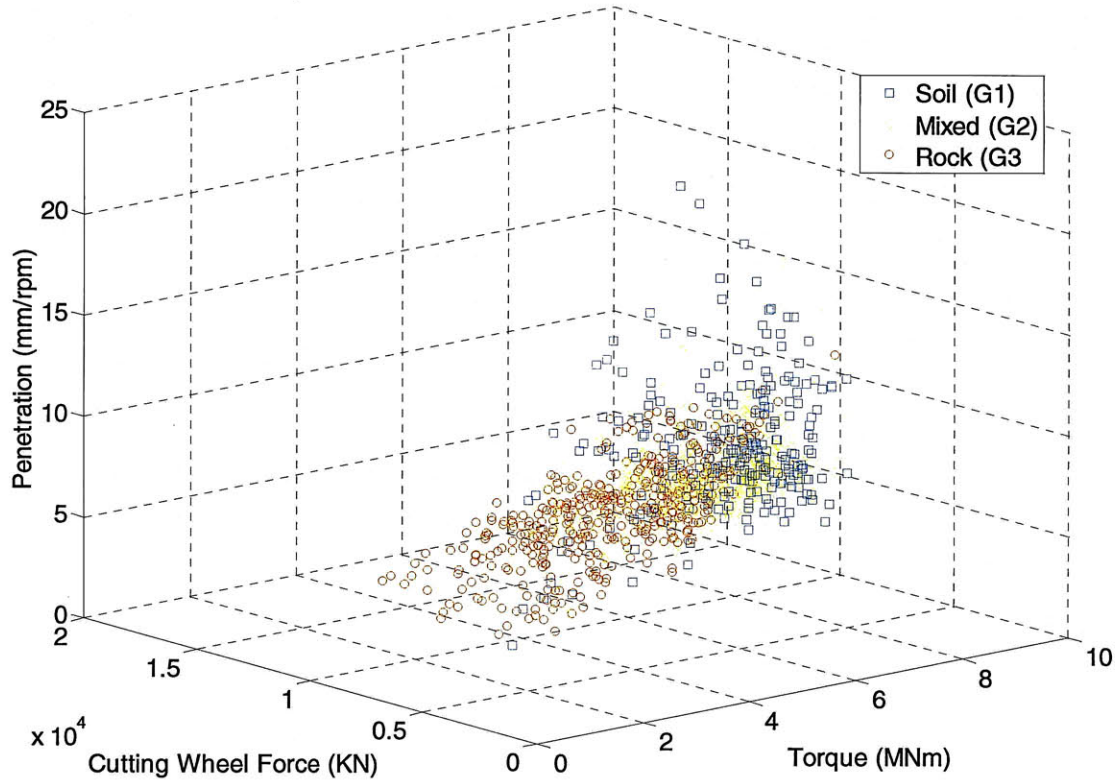


Figure 6.68 Scatter plot of CF, TO and P of the data

Summary of the results:

The results of the analysis of the data for single parameters, and two parameters show that:

- Penetration (P), Cutting Wheel Force (CF), Torque / Cutting Force (TOC) and Cutting Force / Total Thrust (COTT) are important parameters when distinguishing between the effects on tunneling of different ground conditions. These parameters are retained for the geological prediction Bayesian modeling in the next section.
- Torque (TO) and Total Thrust (TT), when used on their own, are not an important parameters when distinguishing between the effects on tunneling of different ground conditions. TT will not be considered for the geological prediction Bayesian modeling in the next section. CF, which will be included in the

geological prediction model, reflects not only the variation of TT but also the type of ground that the TBM is going through since part of the TT is lost in friction around the TBM shield, when transmitted to the cutting wheel.

- The relationships between Torque (TO) and Penetration (P), Cutting Wheel Force (CF) and Penetration (P); Torque / Cutting Force (TOC) and Penetration (P); and Cutting Wheel Force / Total Thrust (COTT) and Penetration (P) are important when distinguishing between the effects on tunneling of different ground conditions. These parameters and the relationships between them are retained for the Bayesian Modeling in the next section.
- The relationship between Torque (TO) and Cutting Force (CF) is also important to distinguish between the effects on tunneling of G1, G2 and G3. Despite the fact that this relation is induced by the operator, the relationship between Torque (TO) and Cutting Wheel Force (CF) is considered in the Bayesian Modeling in the next section.

### **6.2.2.3 Bayesian Model for Prediction of Ground Conditions**

In this section, a Bayesian Model for predicting ground conditions is developed. The aim of the model is to predict ground conditions ahead of the tunneling machine, given information on the machine performance parameters that have been observed. The model is 'learned' from data that are obtained by observations during the construction process. The model is then used to predict geological conditions ahead.

This is the first stage in the proposed risk assessment and mitigation procedure proposed in this chapter. The second step is a decision making problem whereby decisions are made regarding the optimal construction strategies given the predicted geologic conditions. This way, risk can be assessed, and minimized by choosing the optimal construction method.

The model is based on parameters that are important in the tunneling process. Since the model aims to distinguish between parameters, the parameters and interrelationships

between them that are best suited at distinguishing between ground classes are used in the model. These parameters and inter-relationships have been identified in the previous section.

Different models, with different parameters, and various configurations can be constructed given the results of the previous section. This can be considered as a model sensitivity analysis. In this section, several models are developed. These models are 'learned' from observations using the Porto Metro dataset, and used to make predictions on geologic conditions. Since the actual conditions are known, the results of the models are compared to reality and to one another. The model that performs best is then proposed as a model/model structure to be used.

#### A) Bayesian Model Structure

This section provides a description on the development of the various structures of the Bayesian prediction Model.

The machine parameters used in the modeling were the following:

- Penetration (P)
- Cutting Wheel Force (CF)
- Torque of the Cutting Wheel (TO)
- Torque / Cutting Wheel Force (TOC)
- Cutting Wheel Force / Total Thrust (COTT)

The general configuration of the model is as shown in Figure 6.69. The model is a dynamic Bayesian network (in this specific case a Markov chain), which consists of a structure that is replicated for each ring. Each ring's model structure contains a node GC representing the possible ground conditions, G1, G2 and G3, and several nodes X1, X2...Xn representing different machine parameters, for that specific ring. Attached to each node is a conditional probability distribution. Between the rings' structures, there is

a spatial transition probability table, which relates the ground condition in space, i.e. it contains the probability that geological state  $y$  occurs at ring  $r$ , given that geological state  $z$  occurred at ring  $r-1$ . All models are first order Markov chains. This means that the probability of geological state  $y$  occurring at ring  $r$ , only depends on the geological state that occurred at ring  $r-1$ . These tables are attached to the GC nodes for each ring. At ring 1 the node GC has a prior probability table, which reflects the prior probability of the geological states.

All conditional probability tables were estimated from the available data, using a Bayesian estimator, with uniform priors, using the existing learning algorithms as described in Chapter 4, Section 4.6.5.

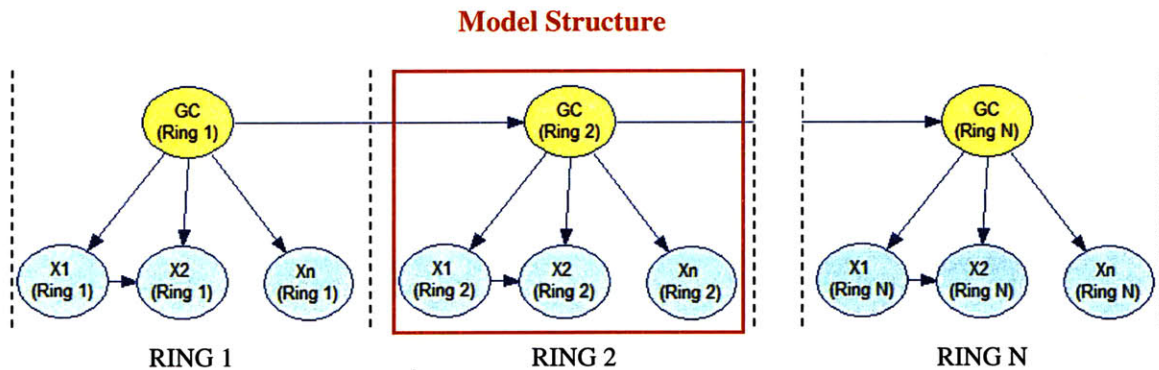


Figure 6.69 General configuration for the geological prediction Bayesian model

The transition matrix was “learned” from the data. The results are shown in Table 6.28.

Table 6.28 Geological transition matrix

		GC(r-1)		
		G1	G2	G3
GC(r)	G1	0.956	0.027	0.000
	G2	0.044	0.958	0.059
	G3	0.000	0.015	0.941

## **Training data set**

As previously described, all prior and conditional probabilities of the geological prediction Bayesian model, were estimated (parameter estimation) from the available data. Two different sets (training sets) of data were used for parameter estimation. This made it possible to determine the sensibility of the predictor model to different training sets. The training data sets used to estimate the parameters of the geological prediction model were the following:

### Training set A

This data set consists of 720 rings which correspond to about 1 km of tunnel, selected randomly. The data used consisted of an equal distribution of soil, mixed, and rock data corresponding, i.e. 1/3 of soil (G1), to 1/3 of mixed (G2) and 1/3 of rock (G3). The rings used and the data are presented in Appendix H.

### Training set B

This data set consists of 720 rings which correspond to around 1 km of tunnel, selected randomly. The data used correspond to 34% of soil (G1), 22% of mixed (G2), and 44% of rock (G3). The rings used and the data is presented in Appendix H

The “real” geological states along the tunnel, which were used in the learning, are the ones determined by the contractor/designer, based on face surveys. At the face survey locations the geological states are known. Between face surveys the geological states were estimated by the contractor/designer. It was assumed that the geology would vary linearly between face surveys.

## **Discretization**



As previously mentioned in Section 6.2.2.2, the machine parameter variables were discretized into 5 bins. Table 6.29 is a summary of the discretization of all machine parameters used in the geological prediction model. The variables were discretized using a discretization algorithm, based on hierarchical cluster analysis. The way the algorithm works is described in Figure 6.70. This algorithm organizes the data in different clusters (the number of clusters is defined by the user). It starts by N number of bins (or clusters), where N is equal to the total data points. Then it iteratively starts combining the bins (or clusters) whose mean has the smallest separation until it reaches the desired number of bins.

Table 6.29 Discretization of the machine parameter variables

a) Cutting Wheel Force (CF)

Bin	Range (kN)
1	CF < 7100
2	7100 < CF > 10200
3	10200 < CF > 12600
4	12600 < CF > 14000
5	CF > 14000

b) Penetration (P)

Bin	Range (mm/rev)
1	P < 5.3
2	5.3 < P > 9.5
3	9.5 < P > 13.4
4	13.4 < P > 16.4
5	P > 16.4

c) Torque (TO)

Bin	Range (MNm)
1	TO < 3.65
2	3.65 < TO > 5
3	5 < TO > 6
4	6 < TO > 7.3
5	TO > 7.3

d) Torque / Cutting wheel force (TOC)

Bin	Range
1	TOC < 0.6
2	0.6 < TOC > 0.825
3	0.825 < TOC > 1.05
4	1.05 < TOC > 1.4
5	TOC > 1.4

e) Cutting wheel force / Total thrust (COTT)

Bin	Range
1	COTT < 0.25
2	0.25 < COTT > 0.35
3	0.35 < COTT > 0.45
4	0.45 < COTT > 0.5
5	COTT > 0.5

Input: N=# of records, K=# of desired bins.

1. Let k denote the running number of bins, initialized to k=N (each record starts in its own cluster).
2. If k=K quit, else set k=k-1 by combining the two bins whose mean value has the smallest separation.
3. Repeat 2.

Figure 6.70 Hierarchical discretization algorithm

In order to assess the influence of the variable discretization, i.e. of the bin choice, on the model accuracy a different discretization was tested. This discretization consisted on uniform width bins, i.e. same length bins (Table 6.30).

Table 6.30 Discretization of the machine parameter variables (uniform width)

a) Cutting Wheel Force (CF)		b) Penetration (P)		c) Torque (TO)	
Bin	Range (kN)	Bin	Range (mm/rev)	Bin	Range (MNm)
1	CF < 6252	1	P < 5.05	1	TO < 3.37
2	6252 < CF > 8734	2	5.05 < P > 8.93	2	3.37 < TO > 4.75
3	8734 < CF > 11235	3	8.93 < P > 12.80	3	4.75 < TO > 6.12
4	11235 < CF > 13733	4	12.80 < P > 16.78	4	6.12 < TO > 7.5
5	CF > 13733	5	P > 16.78	5	TO > 7.5
d) Torque / Cutting wheel force (TOC)		e) Cutting wheel force / Total thrust (COTT)			
Bin	Range	Bin	Range		
1	TOC < 0.52	1	COTT < 0.22		
2	0.52 < TOC > 0.815	2	0.22 < COTT > 0.305		
3	0.815 < TOC > 1.13	3	0.305 < COTT > 0.395		
4	1.13 < TOC > 1.43	4	0.395 < COTT > 0.488		
5	TOC > 1.43	5	COTT > 0.488		

The discretization with uniform bin width was used in combination with training data set A. As a consequence there will be three training data sets: A, B and A1:

A: Training data set A with Hierarchical discretization of continuous variables

B: Training data set B with Hierarchical discretization of continuous variables

A1: Training data set A with uniform bin width discretization of continuous variables

### **Model structure determination**

This section shows the results of the application of the different structure geological prediction model (Figure 6.69) to the tunnel C line. The application of the prediction model started at ring 336, station 0+631 (after the accidents) and ended at ring 1611, station 2+418. Figure 6.71 illustrates the application of the geological prediction model (with a general structure) for two steps: 1) Tunnel face at ring 1 with no available face survey and 2) Tunnel face at ring 2 and face survey is available.

Step 1: The TBM is driving through ring 1. The information regarding the machine parameters (e.g. penetration, cutting wheel force) is entered in the model and used as evidence to update (predict) the probability distribution for the geological state at ring 1 and all the rings ahead at the tunnel face (e.g. rings 2 to n). Note that the inference is done in the opposite sense of the arrows between geological conditions and machine parameters (arrow in bold).

Step 2: The TBM advances to ring 2. The machine is stopped and a face survey is made available. The information regarding the machine parameters and the “real” geological state is entered in the model and used to update (predict) the geological state ahead of the TBM face. Note since the geological state at this ring is known, the information regarding the machine parameters is superfluous and not needed. This is because the geological state at ring 3 only depends on the geological state at ring 2.

The process is then replicated for the next rings as the TBM advances, until it reaches the end of the tunnel. Every time a survey of the face was made, and that information was available for the author, it was entered in the model.

Table 6.31 shows the results of the application of the geological prediction model of Figure 6.69, with different structures. The results are presented in form of percentage of correctly determined geological states (G1, G2 and G3). The updated geological state at ring x (given the evidence, e.g. the machine parameters) was obtained as described previously for Figure 6.71. The results will be in the form of, for example at ring x,  $P(G=G1|parameters) = 0.3$ ,  $P(G=G2|parameters) = 0.2$ ,  $P(G=G3|parameters) = 0.5$ . The geological state with highest probability associated, in this case G3, will be compared with the “actual” geological state. If they match it will be considered that the geological state was predicted accurately.

Table 6.31 contains the model number, the respective structure, and the percentage of correctly predicted geological states (overall and per geological state). For each structure the conditional probability tables were estimated based on different training sets: A, B and A1, previously described. The first column, Model number contains the model number. The second column illustrates the structure referent to each model number. The third column says, which training data set is used to train the model. The fourth column contains the overall performance of the model, i.e. the percentage of correctly predicted geological states. The fifth, sixth and seventh column contain the performance of the models in each of the ground classes, G1, G2 and G3, respectively, i.e. the percentage of accurately predicted geological states G1 G2 and G3, respectively, by each model.

Step 1: Tunnel face at ring 1



\* inference direction

Step 2: Tunnel face at ring 2 (with face survey)

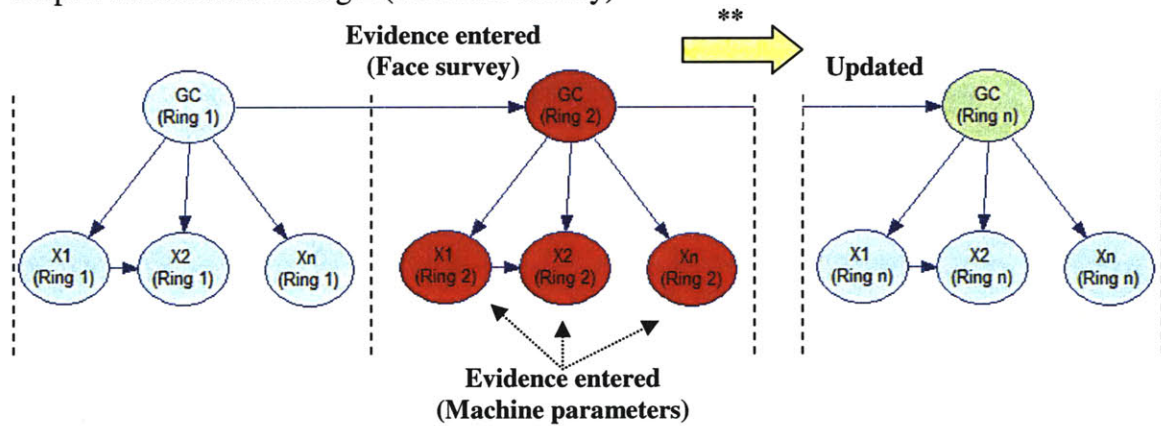


Figure 6.71 Illustration of the application of the geological prediction model (\*\* if GC is known, it is not necessary to enter evidence on the machine parameters to update geological conditions ahead of the face, since the model assumes that geological condition at ring 3 only depends on the geology at ring 2)

The models' structure start with simple one parameter structures (models 1 to 4). In these cases the geological states are predicted by using only one machine parameter. Then structures with two parameters are used (models 6 to 17). In these cases the models use two parameters to predict the geological states. The parameters may or not be inter-related. For example in the case of model 6, the structure contains as variables, machine parameters CF and P, and assumes they are conditionally independent given the variable

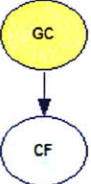
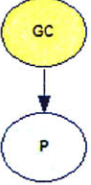
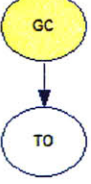
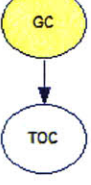
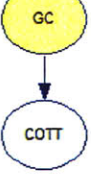
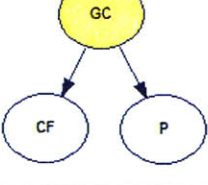
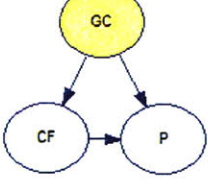
GC (geological condition). Model 7 considers the same to machine parameters CF and P, and assumes that they are not conditionally independent given the variable GC, by considering an arrow between them, i.e. by considering their inter-relationship.

More complex models of four variables (GC and three machine parameters) are then considered (Models 18 to 30). Within the four variable models, one will have simpler models such as model 18 or 19 where only one (model 19) or none (model 18) inter-relationship between machine parameters is considered; and more complex models such as 22 and 23 where two (model 22) or all (model 23) relationships are considered among the machine parameters variables.

Finally model 31 is a fully learned model, i.e. both the structure and the parameters of the network were learned based on the training data sets. The algorithm used for the learning of model 31 was the “greedy thick thinning” with a uniform prior. The basic principles of learning algorithms can be found in Chapter 4, section 4.6.52. For detailed information on the greedy thick thinning algorithm please refer to Heckerman, 1997.



Table 6.31 Model structure results

Model Number	Structure	Set/ Bins	Overall accuracy	Soil (G1)	Mixed (G2)	Rock (G3)
1		A:	62.7%	52%	59%	76%
		B:	63.2%	57%	54%	79%
		A1:	63.3%	50%	59%	78%
2		A:	63.4%	70%	53%	72%
		B:	63.9%	72%	54%	71%
		A1:	66.4%	72%	59%	72%
3		A:	61.2%	54%	68%	58%
		B:	61.1%	66%	64%	54%
		A1:	59.6%	56%	66%	55%
4		A:	61.4%	46%	52%	85%
		B:	62.5%	58%	48%	84%
		A1:	63.4%	47%	55%	86%
5		A:	55.5%	65%	56%	48%
		B:	55.2%	69%	57%	43%
		A1:	56.3%	55%	62%	50%
6		A:	64.0%	66%	53%	76%
		B:	66.0%	75%	53%	76%
		A1:	66.0%	75%	53%	76%
7		A:	66.0%	71%	53%	78%
		B:	66.2%	74%	50%	80%
		A1:	66.2%	74%	50%	80%

Model	Structure	Set/ Bins	Overall accuracy	Soil (G1)	Mixed (G2)	Rock (G3)
8		A:	64.1%	53%	60%	77%
		B:	64.6%	60%	54%	80%
		A1:	63.8%	52%	60%	77%
9		A:	63.5%	52%	57%	80%
		B:	64.5%	72%	49%	80%
		A1:	64.9%	52%	57%	84%
10		A:	66.9%	73%	59%	72%
		B:	66.9%	77%	58%	70%
		A1:	67.6%	73%	61%	72%
11		A:	69.4%	74%	63%	74%
		B:	69.1%	79%	62%	71%
		A1:	68.8%	78%	61%	72%
12		A:	61.7%	51%	50%	84%
		B:	60.5%	60%	41%	85%
		A1:	62.8%	50%	52%	86%
13		A:	62.8%	48%	55%	83%
		B:	62.1%	61%	44%	85%
		A1:	64.7%	49%	57%	86%

Model	Structure	Set/ Bins	Overall accuracy	Soil (G1)	Mixed (G2)	Rock (G3)
14	<pre> graph TD   GC((GC)) --&gt; P((P))   GC --&gt; TOC((TOC)) </pre>	A:	65.5%	68%	53%	79%
		B:	65.8%	72%	52%	79%
		A1:	68.4%	69%	59%	79%
15	<pre> graph TD   GC((GC)) --&gt; P((P))   GC --&gt; TOC((TOC))   TOC --&gt; P </pre>	A:	67.0%	66%	56%	82%
		B:	65.5%	69%	50%	82%
		A1:	68.6%	67%	60%	81%
16	<pre> graph TD   GC((GC)) --&gt; P((P))   GC --&gt; COTT((COTT)) </pre>	A:	62.1%	78%	48%	68%
		B:	61.7%	81%	45%	68%
		A1:	66.4%	61%	64%	73%
17	<pre> graph TD   GC((GC)) --&gt; P((P))   GC --&gt; COTT((COTT))   COTT --&gt; P </pre>	A:	64.8%	72%	53%	74%
		B:	64.3%	78%	49%	74%
		A1:	66.9%	59%	64%	76%
18	<pre> graph TD   GC((GC)) --&gt; CF((CF))   GC --&gt; P((P))   GC --&gt; TO((TO)) </pre>	A:	65.5%	66%	57%	76%
		B:	67.3%	76%	56%	76%
		A1:	65.9%	68%	57%	75%
19	<pre> graph TD   GC((GC)) --&gt; CF((CF))   GC --&gt; P((P))   GC --&gt; TO((TO))   TO --&gt; P </pre>	A:	67.6%	70%	59%	77%
		B:	68.4%	77%	56%	78%
		A1:	68.0%	69%	60%	77%

Model	Structure	Set/ Bins	Overall accuracy	Soil (G1)	Mixed (G2)	Rock (G3)
20	<pre> graph TD   GC((GC)) --&gt; CF((CF))   GC --&gt; P((P))   GC --&gt; TO((TO))   CF --&gt; P </pre>	A:	69.6%	73%	60%	80%
		B:	68.8%	78%	54%	80%
		A1:	68.5%	63%	60%	82%
21	<pre> graph TD   GC((GC)) --&gt; CF((CF))   GC --&gt; P((P))   GC --&gt; TO((TO))   CF --&gt; TO   P --&gt; TO </pre>	A:	66.1%	69%	56%	77%
		B:	66.8%	79%	51%	77%
		A1:	66.9%	66%	58%	78%
22	<pre> graph TD   GC((GC)) --&gt; CF((CF))   GC --&gt; P((P))   GC --&gt; TO((TO))   CF --&gt; P   TO --&gt; P </pre>	A:	71.9%	73%	63%	82%
		B:	69.3%	77%	54%	82%
		A1:	71%	64%	64%	84%
23	<pre> graph TD   GC((GC)) --&gt; CF((CF))   GC --&gt; P((P))   GC --&gt; TO((TO))   CF --&gt; P   P --&gt; TO   TO --&gt; P </pre>	A:	71.6%	79%	59%	82%
		B:	67.4%	79%	48%	83%
		A1:	70.5%	61%	64%	86%
24	<pre> graph TD   GC((GC)) --&gt; CF((CF))   GC --&gt; P((P))   GC --&gt; TOC((TOC))   CF --&gt; P </pre>	A:	63.2%	63%	48%	82%
		B:	64.0%	72%	45%	82%
		A1:	64.7%	62%	51%	84%
25	<pre> graph TD   GC((GC)) --&gt; CF((CF))   GC --&gt; P((P))   GC --&gt; TOC((TOC))   TOC --&gt; P </pre>	A:	64.1%	63%	49%	83%
		B:	63.6%	72%	42%	84%
		A1:	64.8%	60%	52%	85%



Model	Structure	Set/ Bins	Overall accuracy	Soil (G1)	Mixed (G2)	Rock (G3)
26	<pre> graph TD   GC((GC)) --&gt; CF((CF))   GC --&gt; P((P))   GC --&gt; TOC((TOC))   CF --&gt; P </pre>	A:	65.3%	66%	51%	83%
		B:	66.0%	75%	46%	84%
		A1:	66.7%	60%	54%	87%
27	<pre> graph TD   GC((GC)) --&gt; CF((CF))   GC --&gt; P((P))   GC --&gt; TOC((TOC))   CF --&gt; TOC </pre>	A:	65.6%	70%	52%	80%
		B:	65.9%	74%	50%	80%
		A1:	67%	65%	58%	80%
28	<pre> graph TD   GC((GC)) --&gt; CF((CF))   GC --&gt; P((P))   GC --&gt; TOC((TOC))   TOC --&gt; P </pre>	A:	65.3%	63%	52%	84%
		B:	64.5%	73%	50%	85%
		A1:	66.4%	57%	55%	87%
29	<pre> graph TD   GC((GC)) --&gt; CF((CF))   GC --&gt; P((P))   GC --&gt; TOC((TOC))   CF --&gt; P   CF --&gt; TOC   TOC --&gt; P </pre>	A:	67.6%	71%	55%	81%
		B:	64.8%	74%	45%	82%
		A1:	69.3%	65%	60%	84%
30	<pre> graph TD   GC((GC)) --&gt; CF((CF))   GC --&gt; P((P))   GC --&gt; TOC((TOC))   CF --&gt; P   CF --&gt; TOC   TOC --&gt; P </pre>	A:	69.4%	73%	57%	83%
		B:	65.1%	76%	43%	85%
		A1:	70.6%	61%	63%	87%
31	<pre> graph TD   GC((GC)) --&gt; COTT((COTT))   GC --&gt; CF((CF))   GC --&gt; TOC((TOC))   GC --&gt; TO((TO))   GC --&gt; P((P))   COTT --&gt; CF   TOC --&gt; TO   TOC --&gt; P </pre>	A:	68.4%	71%	55%	83%
		B:	59.8%	63%	40%	82%
		A1:	70.1%	68%	59%	85%

## **Results of the Model Sensitivity Analysis:**

In this section, the results of the sensitivity analysis on the model structure are discussed, and the “best” performing model is chosen. The “best” model will be defined as the one that predicts correctly the highest percentage of all ground conditions. However, because the geological conditions crossed range from hard rock to soil, it is also important to evaluate how the models perform in each geological condition.

Table 6.32 , Table 6.33 and Table 6.34 show the best models in predicting the overall geology, in predicting soil (G1) and in predicting rock (G3), respectively for training set A. Table 6.35, Table 6.36 and Table 6.37, show the best models in predicting the overall geology, in predicting soil (G1) and in predicting rock(G3), respectively for training set B. Since it was determined that the discretization based of uniform width bins (training set A1) did not perform as well as the one based on hierarchical clustering (training set A), the results of training set A1 will not be further analyzed

The results of Table 6.32 and Table 6.35 show that the best overall model for set A, B was structure 22. This structure contains the variables, CF, P and TO (Figure 6.72), and considers arrows between CF (cutting force) and P (penetration), and TO (torque) and P (penetration). This model makes sense mechanically since Penetration (P) depends not only on the cutting wheel force (CF) but also on the torque (TO) that is applied. Although it was shown previously that torque (TO) on its own was not a good predictor of ground conditions, its presence and relation to the other machine parameters (CF and P) is definitely important, as also shown before in the scatter plots of Figure 6.47 and Figure 6.52.



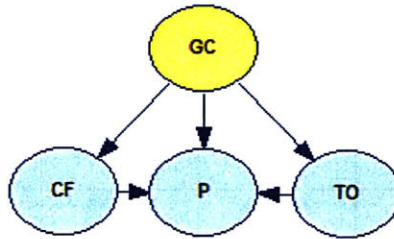


Figure 6.72 best structure for geological prediction model

Since one is trying to use one model to predict both soil (G1) and rock (G3) it is important to assess how well the different models predict soil and rock. The results presented in Table 6.33 and Table 6.36 show that models containing the variables CF, TO and P and models containing the variables P and COTT, are the ones that perform the best in soil (G1), and that the inter-relationships between CF and P; TO and P and CF and TO are important. When predicting rock (G3), the results presented in Table 6.34 and Table 6.37 show that TOC is an extremely important variable. In fact a simple model like model 4 with only TOC as machine variable performs quite well (the best for data set B and within the best 5 for data set A). This can be seen in the plots of Figure 6.37, Figure 6.38 and Figure 6.57, which show how important TOC is (alone and in combination with P) in identifying rock (G3). Because the relative frequency of TOC in G1 and in G2 are more scattered and overlap more, this variable does not perform as well when identifying soil (G1).

Table 6.32 Five best overall models – Set A.

	Model 22	Model 23	Model 20	Model 30	Model 11
Overall	<b>71.9%</b> (best)	71.6% (-0.3%)	69.6% (-2.3%)	69.4% (-2.5%)	69.4% (-2.5%)
G1	72.8% (-6.6%)	<b>79.3%</b> (best)	73.1% (-6.2%)	72.8% (-6.6%)	74.5% (-4.8%)
G2	63.1% (-4.6%)	59.1% (-8.6%)	59.5% (-8.2%)	56.5% (-11.2%)	62.9% (-4.8%)
G3	82.1% (-2.5%)	81.6% (-3.0%)	79.7% (-5.0%)	82.9% (-1.7%)	73.7% (-10.9%)

Note: in ( ) is the difference in performance between the specific model and the best model.

Table 6.33 Best models in predicting G1 (Soil) – Set A

	Model 23	Model 16	Model 11	Model 10	Model 20
Overall	71.6% (-0.3%)	62.1% (-9.8%)	69.4% (-2.5%)	66.9% (-4.9%)	69.6% (-2.3%)
G1	<b>79.3%</b> <b>(best)</b>	77.9% (-1.4%)	74.5% (-4.8%)	73.4% (-5.9%)	73.1% (-6.2%)
G2	59.1% (-8.6%)	47.9% (19.8%)	62.9% (-4.8%)	58.9% (-8.8%)	59.5% (-8.2%)
G3	81.6% (-3.0%)	68.2% (-16.4%)	73.7% (-10.9%)	72.2% (-12.4%)	79.7% (-5.0%)

Note: in ( ) is the difference in performance between the specific model and the best model.

Table 6.34 Best models in predicting G3 (Rock) – Set A

	Model 4	Model 12	Model 28	Model 26	Model 25
Overall	61.4% (-10.5%)	61.7% (-10.2%)	65.3% (-6.6%)	65.3% (-6.6%)	64.1% (-7.8%)
G1	46.2% (-33.1%)	51.0% (-28.3%)	62.8% (-16.6%)	65.9% (-13.4%)	63.1% (-16.2%)
G2	51.5% (-16.2%)	49.9% (-17.8%)	51.9% (-15.8%)	50.5% (-17.2%)	49.3% (-18.4%)
G3	<b>84.6%</b> <b>(best)</b>	83.9% (-0.7%)	83.6% (-1.0%)	83.1% (-1.5%)	83.1% (-1.5%)

Note: in ( ) is the difference in performance between the specific model and the best model.

Table 6.35 Five best overall models – Set B

	Model 22	Model 11	Model 20	Model 19	Model 23
Overall	<b>69.3%</b> <b>(best)</b>	69.1% (-0.2%)	68.8% (-0.5%)	68.4% (-0.9%)	67.4% (-1.8%)
G1	77.2% (-3.4%)	79.3% (-1.4%)	78.3% (-2.4%)	76.9% (-3.8%)	79.0% (-1.7%)
G2	54.1% (-9.6%)	61.5% (-2.2%)	53.9% (-9.8%)	55.7% (-8.0%)	48.3% (-15.4%)
G3	82.4% (-2.7%)	71.2% (-13.9%)	80.4% (-4.7%)	77.9% (-7.2%)	82.9% (-2.2%)

Note: in ( ) is the difference in performance between the specific model and the best model.

Table 6.36 Best models in predicting G1 (soil) – Set B

	Model 16	Model 11	Model 21	Model 23	Model 20
Overall	61.7% (-7.6%)	69.1% (-0.2%)	66.8% (-2.5%)	67.4% (-1.8%)	68.8% (-0.5%)
G1	<b>80.7%</b> <b>(best)</b>	79.3% (-1.4%)	79.0% (-1.7%)	79.0% (-1.7%)	78.3% (-2.4%)
G2	45.3% (-18.4%)	61.5% (-2.2%)	51.1% (-12.6%)	48.3% (-15.4%)	53.9% (-9.8%)
G3	68.2% (0.0%)	71.2% (-13.9%)	77.4% (-7.7%)	82.9% (-2.2%)	80.4% (-4.7%)

Note: in ( ) is the difference in performance between the specific model and the best model.

Table 6.37 Best models in predicting G3 (rock) – Set B

	Model 28	Model 30	Model 12	Model 13	Model 4
Overall	64.5% (-4.8%)	65.1% (-4.2%)	60.5% (-8.8%)	62.1% (-7.2%)	62.5% (-6.8%)
G1	72.8% (-7.9%)	75.5% (-5.2%)	60.3% (-20.3%)	60.7% (-20.0%)	57.6% (-23.1%)
G2	43.1% (-20.6%)	42.9% (-20.8%)	40.9% (-22.8%)	44.5% (-19.2%)	47.7% (-16.0%)
G3	<b>85.1%</b> <b>(best)</b>	<b>85.1%</b> <b>(best)</b>	84.9% (-0.2%)	84.9% (-0.2%)	84.4% (-0.7%)

Note: in ( ) is the difference in performance between the specific model and the best model.

The models were rated according to their performance, which was measured by the percentage of correctly predicted geological states. It is important to also check, in the cases where the model does not accurately predict the geological state, which state is predicted. For that the confusion matrices are presented in Table 6.38 and Table 6.39, for training data set A and B, respectively. Each row of the matrix represents the predicted geological states, while each column represents the actual geological states. One benefit of a confusion matrix is that it is easy to see if the model is confusing two geological states. For training data set A (Table 6.38 ) geological state G1 is mistaken as G2 (mixed) in 25.5% of the rings and in very few cases, 1.7%, as G3 (rock). Geological state G3 (rock) is mistaken as G2(mixed) in 13.9% of the cases and in 4% of the cases as G1 (soil). Geological state G2 is mistaken as G1 (soil) in 14.2% of the cases and as G3 (rock) in 22.6% of the cases.

Table 6.38 Confusion matrix for model 22 (training set A)

		Reality		
		G1	G2	G3
Predicted	G1	72.8%	14.2%	4.0%
	G2	25.5%	63.1%	13.9%
	G3	1.7%	22.6%	82.1%

For training data set B (Table 6.39) geological state G1 is mistaken as G2 (mixed) in 20.3% of the rings and in 2.4% of the cases, as G3 (rock). Geological state G3 (rock) is mistaken as G2(mixed) in 10.9% of the cases and in 6.7% of the cases as G1 (soil). Geological state G2 is mistaken as G1 (soil) in 22.8% of the cases and as G3 (rock) in 23% of the cases. The percentage of rings that are G1 (soil) and are mistaken as G3 (rock) and vice versa are small (i.e. 1.7% (set A); 2.4% (set B); and 4% (set A); and 6.7% (set B), respectively). The majority of the cases where G1 (soil) and G3 (rock) were not predicted accurately, the model confused them with G2 (mixed). This is mostly due to the fact that a ring is considered to be in G2 (mixed) if it crosses soil and rock. This includes a wide range of possibilities that can e.g. consist of as much as 90% G1 (soil) and 10% G3(rock), (which can be confused with a ring in G1), to as little as 10% G1(soil) and 90% G3 (rock), (which can be confused with a ring in G3).

Table 6.39 Confusion matrix for model 22 (training set B)

		Reality		
		G1	G2	G3
Predicted	G1	77.2%	22.8%	6.7%
	G2	20.4%	54.1%	10.9%
	G3	2.4%	23.0%	82.4%

**Other Considerations:**

This section will discuss in more details other considerations regarding the results of Table 6.31, namely how different training sets, different discretizations of the machine parameter variables and transition models affect the geological prediction model results.

Effect of Training Set

The effect of the training set, more specifically of the ratio of G1/G2/G3 data points, used in the learning process of the probability tables of the models, can be observed when comparing the performance of each model on data set A and data set B. The greatest

difference can be observed when predicting G1 and G2. The same structures perform better, in average 7%, when predicting G1. In one case, Model 9, this value goes up to 20%. In the case of G2 the models learned with data set B performed worse in average 5%. The probability distributions of machine parameters, as previously seen, are more spread (higher standard deviation) in soil than in rock. Also The probability distributions in soil and mixed then to overlap more that those of mixed and rock. For this reason the models will have a greater tendency to mistake soil (G1) for mixed (G2) and vice verse, than rock for mixed. When the models are trained with a ratio G1/G2 that is higher they yield probability distributions that will enable to better identify G1, at the expense of not doing such a great job identifying G2.

When predicting G3 the models where less sensitive to the training sets. This can be explained by the fact that the probability distributions of the machine parameters have lower standard deviation in G3 than the other two geological conditions. So the distributions are less spread and also they overlap less with those in ground conditions G1 and G2.

### Effect of Discretization

The effect of discretization can be observed by comparing the results of the geological prediction model for data set A and A1, in Table 6.31 . Overall the models trained using the discretization in Table 6.29 performed slightly better than the ones using a uniform width discretization. This is probably due to the fact that the discretization based on the hierarchical clustering better captures the boundaries between the geological conditions (G1, G2, G3) distributions making then easier to distinguish.

### Transition Matrix

A sensitivity analysis to consider the effect of the transition matrix between geological states was done with the best model, structure 22, in data set B. The transition matrices used are presented in Table 6.40. Transition matrix A was learned from the results of



model 22 in data set B. Transition matrices B, C and D were arbitrarily determined with the goal of portraying different situations of ground conditions, ranging from more homogenous ground (matrix B) to highly heterogeneous ground (low spatial correlation) (matrix D)

Table 6.40 Transition matrices used in sensitivity analysis for model 22

a) Transition matrix A

		GC(r-1)		
		G1	G2	G3
GC(r)	G1	0.92	0.07	0.000
	G2	0.07	0.88	0.06
	G3	0.01	0.05	0.94

b) Transition matrix B

		GC(r-1)		
		G1	G2	G3
GC(r)	G1	0.85	0.10	0.03
	G2	0.10	0.85	0.07
	G3	0.05	0.05	0.90

c) Transition matrix C

		GC(r-1)		
		G1	G2	G3
GC(r)	G1	0.75	0.15	0.05
	G2	0.15	0.70	0.15
	G3	0.05	0.15	0.75

c) Transition matrix D

		GC(r-1)		
		G1	G2	G3
GC(r)	G1	0.34	0.33	0.33
	G2	0.33	0.34	0.33
	G3	0.33	0.33	0.34

Table 6.41 Results of sensitivity analysis (for the effect of geological transition matrices) on model 22, data set B.

Transition matrix	Overall	Soil (G1)	Mixed (G2)	Rock (G3)
Learned from data	69.3%	77%	54%	82%
A	66.2%	77%	45%	85%
B	66.7%	74%	46%	86%
C	64.3%	73%	42%	85%
D:	55.9%	72%	24%	84%

The results in Table 6.41 show how sensitive the model is to the geological transition matrices. These matrices are used to update the geological condition at ring  $r$ , once ring  $r-1$  has been excavated and its geology has been determined (either by actually seeing it, or by inferring the geology, given the observed machine parameters). Once the machine moves to ring  $r$ , and machine parameters are observed, the geology at ring  $r$  will be updated again in light of the new information. So basically the sensitivity on the transition matrix, determines how sensitive each model structure is to a geological condition prior. The model is quite sensitive to the geological prior when determining mixed conditions. However it is not so sensitive when distinguishing soil conditions and rock conditions, even when a “flat” transition matrix ( $D$ ), which reflects a very heterogeneous ground, where there is little correlation between the ground conditions at one ring and the ground conditions at the next one. Overall the performance of the model decreases as the transition matrix gets closer to a “flat” one, i.e. all probabilities are equal, mainly due to the decrease in performance when identifying mixed conditions (G2).

### **6.2.3 Combined Risk Assessment Model**

In this section, a risk assessment, and mitigation model is proposed by combining the Bayesian prediction model presented in section 6.2.2, and the decision model presented in section 6.2.1.1. The Bayesian prediction model allows one to predict the geologies ahead of the machine based on the parameters that are observed during construction. The decision model allows one to choose amongst several construction strategies, the best or optimal strategy for a given geology. When combined, a model that allows one to predict geology, and optimal construction strategy ahead of the tunnel machine is developed. By doing so, risk can be assessed, and mitigated by selecting construction strategies that minimize risk. Regions of high risk can be anticipated, and measures taken to minimize the risk. In this section, the combined prediction -decision model is presented. The model is then used on the Porto Metro case to illustrate it, and its capabilities.

The steps in the combined risk assessment model are as follows:

Step 1: Prediction of Geology that the tunnel is passing through using model of Figure 6.73. This is done based on relationships between observable parameters and geology as described in Section 6.2.2.

Step 2: Prediction of Geology ahead of tunnel using model of Figure 6.73. This is done based on the prediction of the geology that the tunnel is passed (predicted in step 1) and on the transition matrix proposed in Table 6.28.

The details of Step 1 and Step 2 were previously described in section 6.2.2.3.

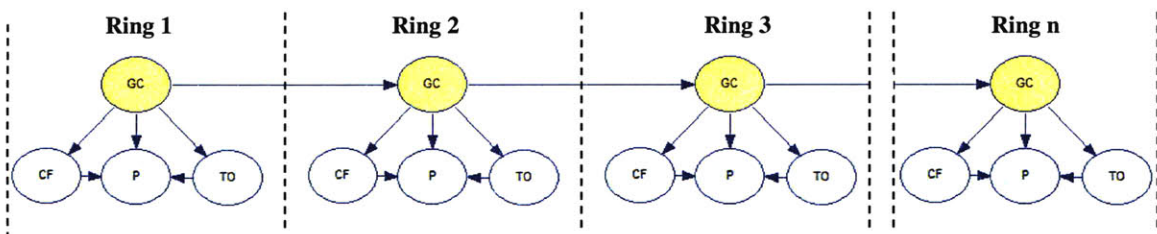


Figure 6.73 Geological prediction Bayesian model (same model as the one of Figure 6.69, with structure 22)

Step 3: Choosing the optimal construction strategy ahead of the face. This is done with the Bayesian decision model that was described in Section 6.2.1.1, and is presented in Figure 6.74. The prior probability tables for the Ground condition at the face (GC), in red in the figure, are obtained from the Geological prediction Bayesian model in Figure 6.73.

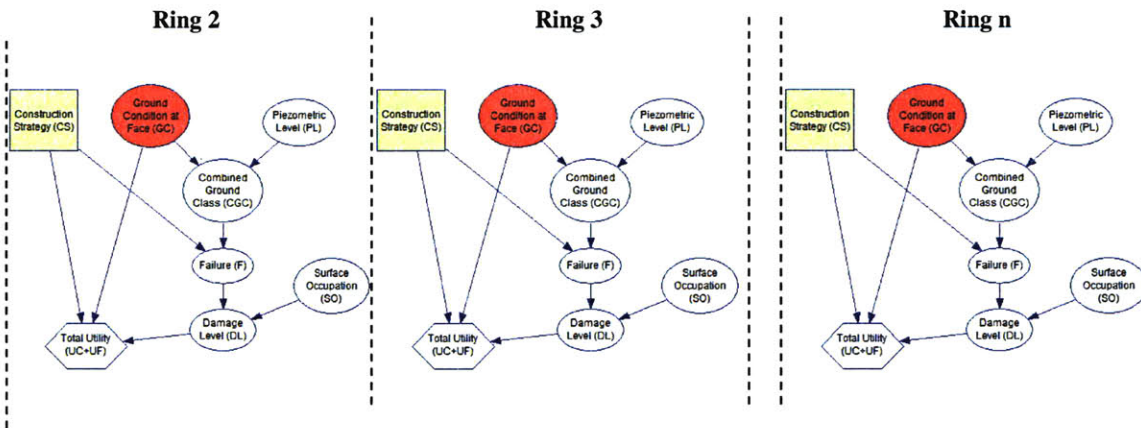


Figure 6.74 Bayesian decision model

Suppose that the tunnel started the excavation at ring 1, with a construction strategy defined by design (e.g. CS2). At ring 1 machine parameters are observed. These are used to predict the geology that the tunnel (to be more precise to update the prior probability of the geology) is passing through and to update the geology ahead of the tunnel face as shown in Figure 6.75 (step 1 and step 2).

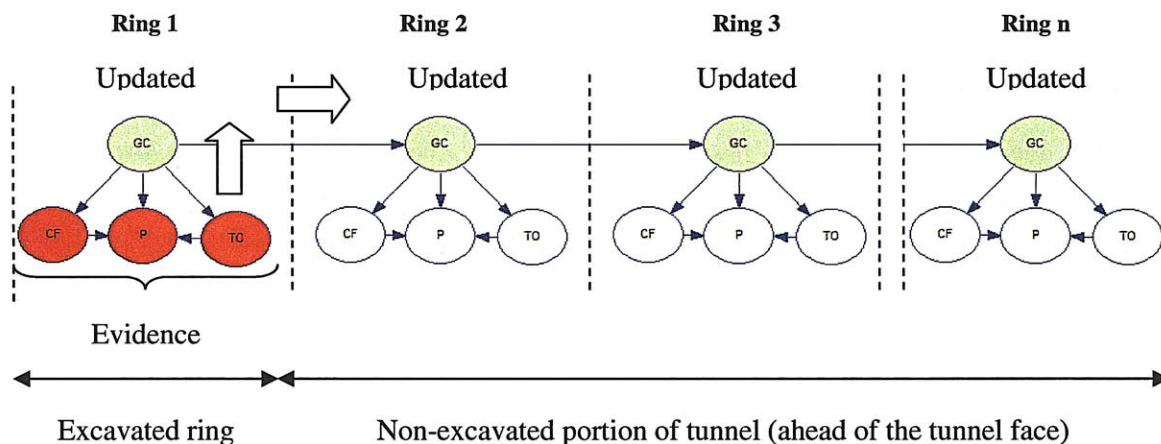


Figure 6.75 illustration of step 1 and 2 for tunnel at ring 1

(Bold arrows illustrate the transmission of information, direction of updating, nodes in red are evidence entered in the model and the nodes in green are the updated nodes)

The results of updating are used to choose optimal construction strategy ahead of the face, in this case at ring 3 to n (step 3) using the Bayesian decision model, as in illustrated in Figure 6.76.

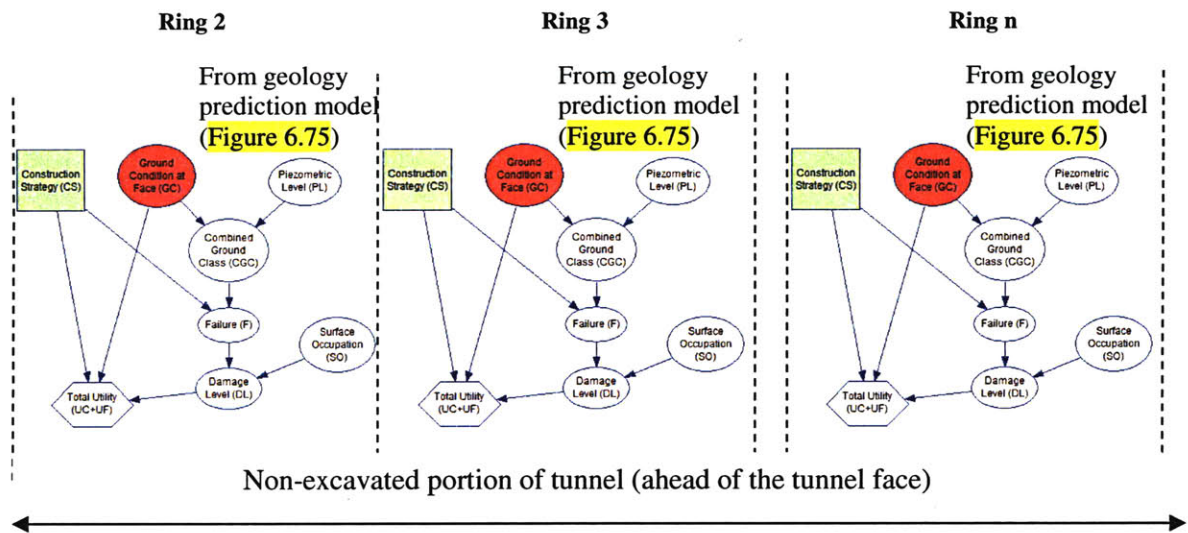


Figure 6.76 Bayesian decision model (nodes in red are the updated geological states obtained from Figure 6.75, in green is the updated “optimal” decision)

This process is repeated as the tunnel face excavates ring 2 and the tunnel face reaches ring 3, and so on, until it reaches the end of the tunnel.

The combined risk assessment model was applied to section 1 and section 2, which were previously defined in 6.2.1 and are again presented in Figure 6.77. Figure 6.78 to Figure 6.81 show the results of updating the geological conditions at the ring being excavated and ahead of the face given the information obtained (machine parameters or mapping of the face) in the area of accident 3 (corresponding to area of installation of ring 292/3 to 298/9) . One can observe that the probability of softer geological conditions (G1) increases as one approaches 297-8, i.e. as one enter the center of the collapse area. Note that when one refers to ring 297, this refers to the installation of ring 297, which means that the machine just excavated the section where 301 will be installed.



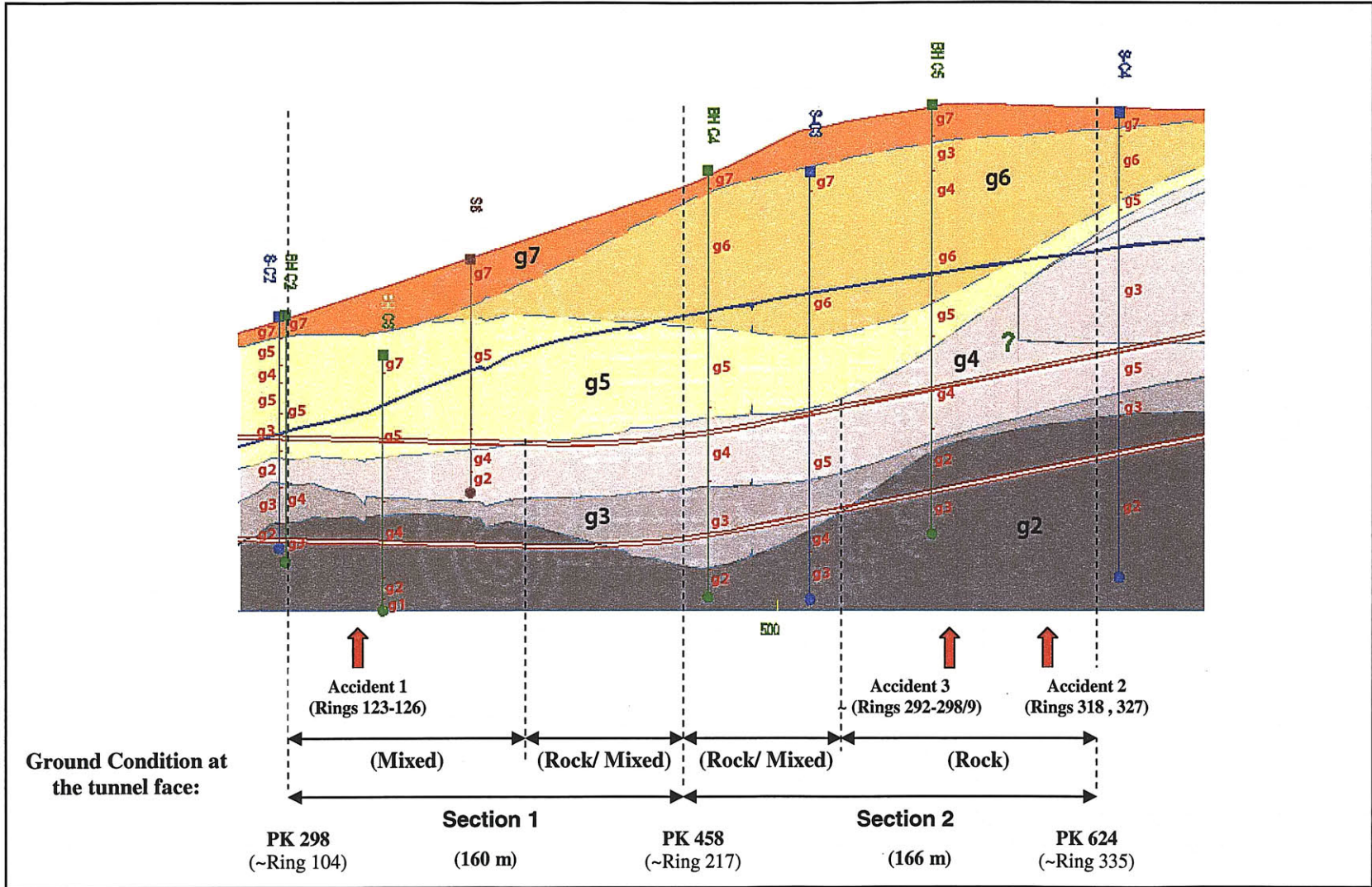


Figure 6.77 Geological longitudinal profile for Line C tunnel (from PK 298 to PK 624)



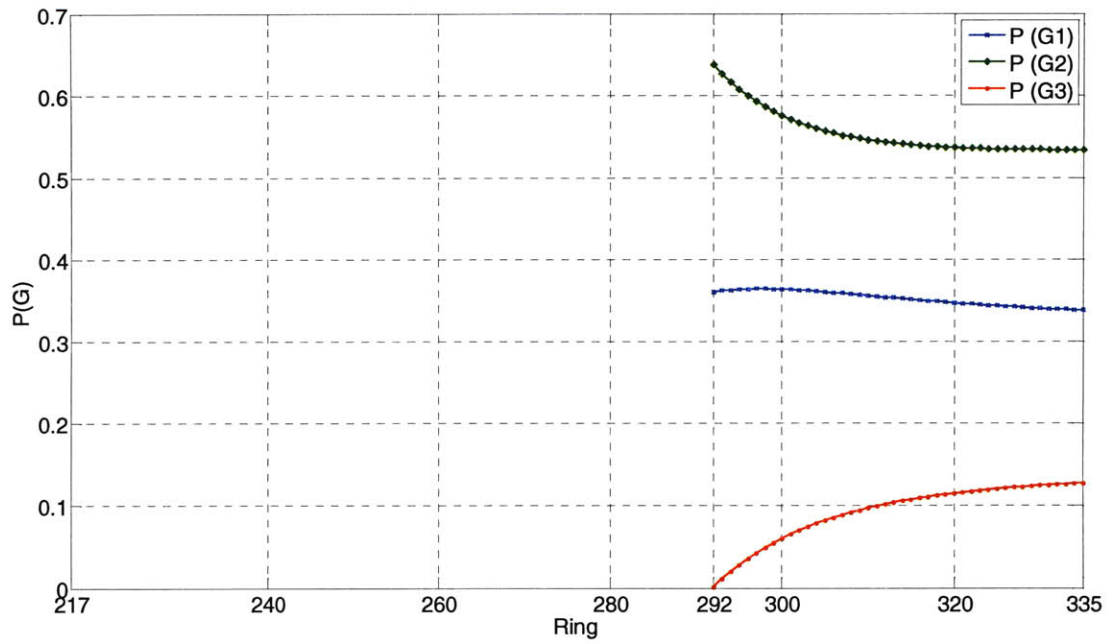


Figure 6.78 Geology updating after excavating ring 292 (accident zone 3)

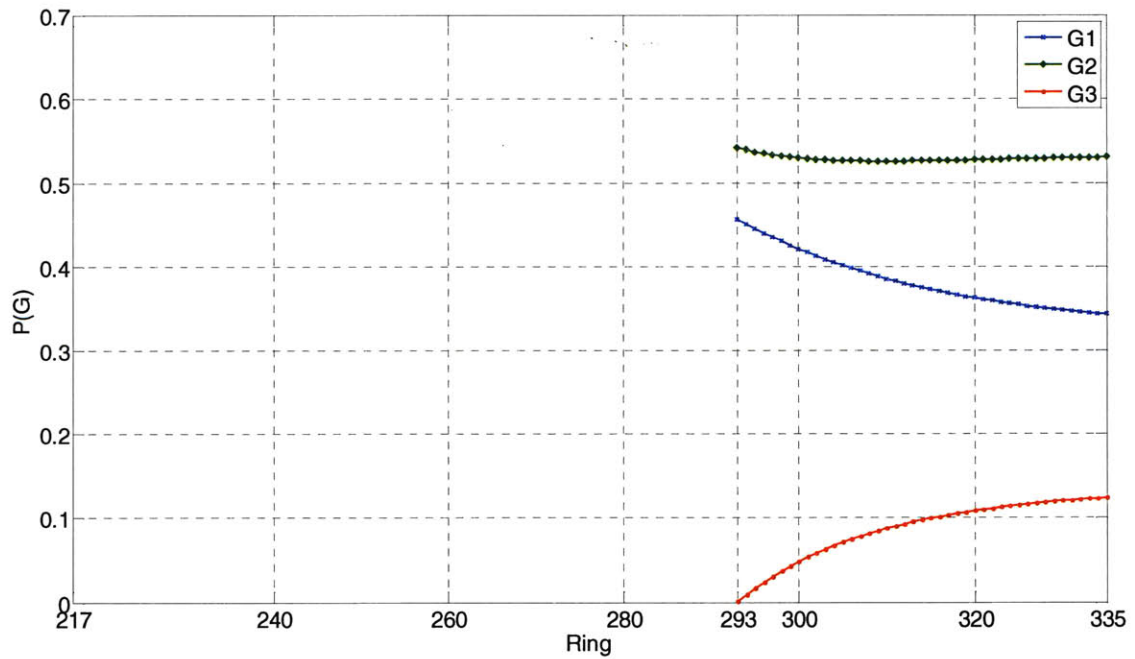


Figure 6.79 Geology updating after excavating ring 293 (accident zone 3)

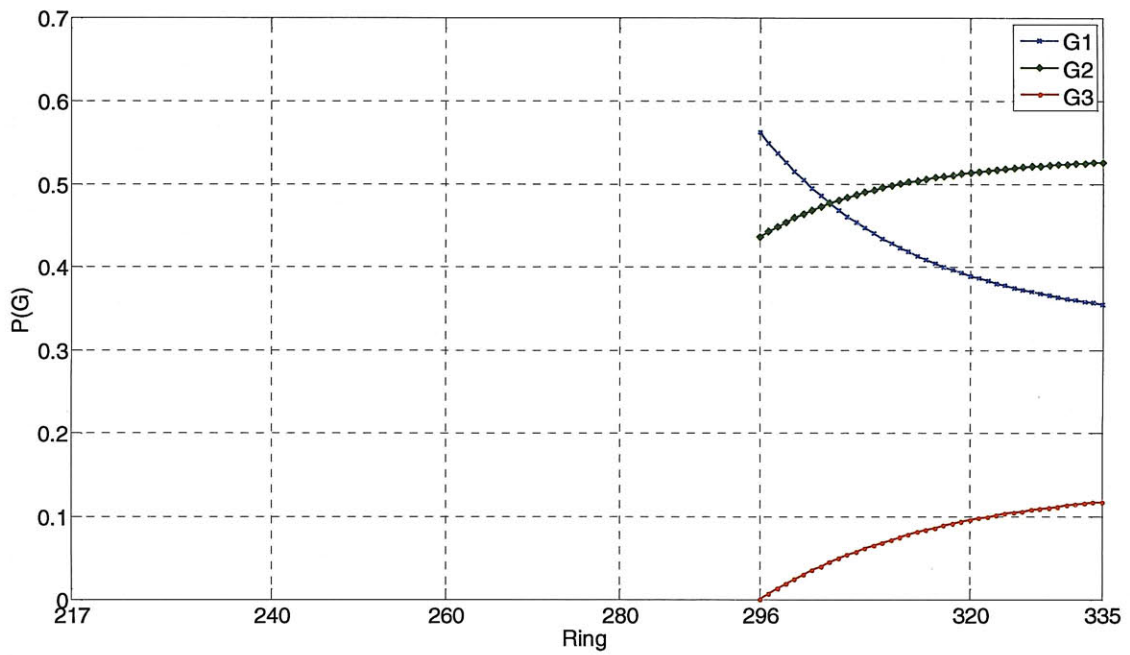


Figure 6.80 Geology updating after excavating ring 296 (accident zone 3)

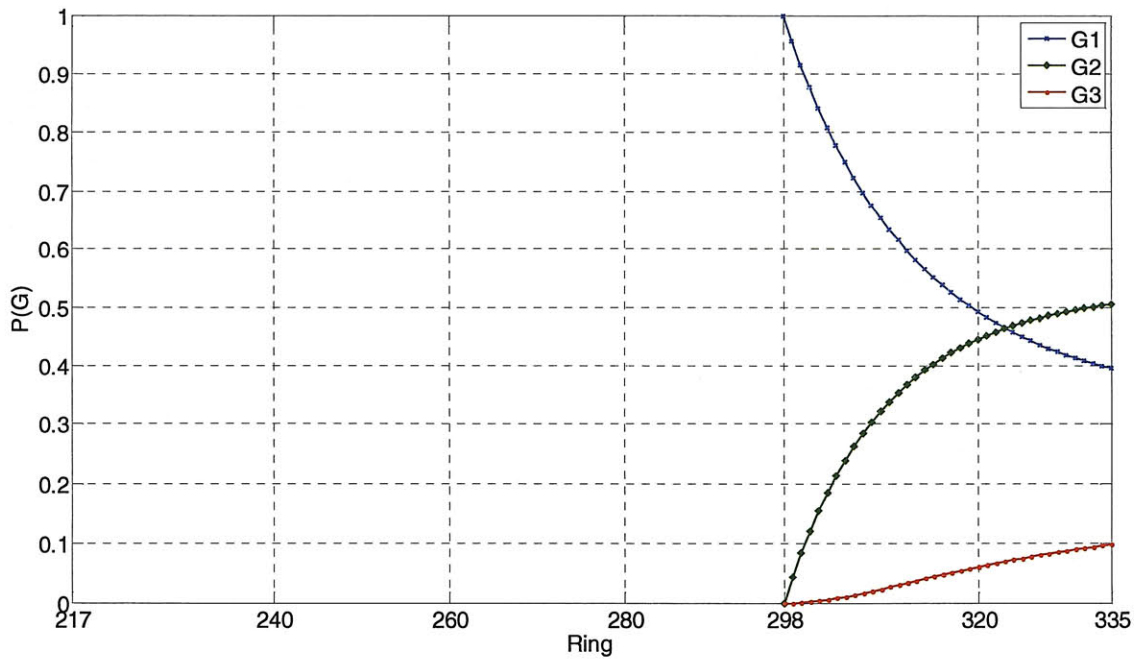


Figure 6.81 Geology updating after excavating ring 298 (accident zone 3)

Figure 6.82 to Figure 6.85 show the updated maximum utility predicted for the rings 292, 293, 296 and 298 (zone of accident 3) based on the results of the geological prediction model (step 3), using the Bayesian decision model of Figure 6.76. The optimal construction method, associated with maximum utilities in the zone of accident 3 is to use the EPBM in closed mode (CS2).

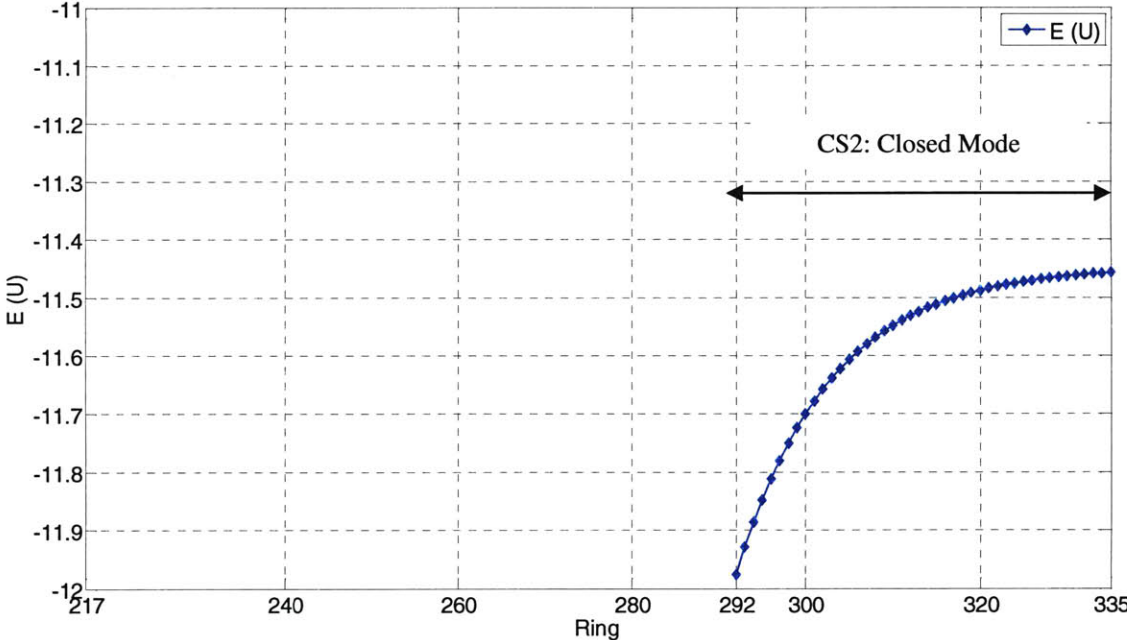


Figure 6.82 Expected utility updating after excavating ring 292 (accident zone 3)

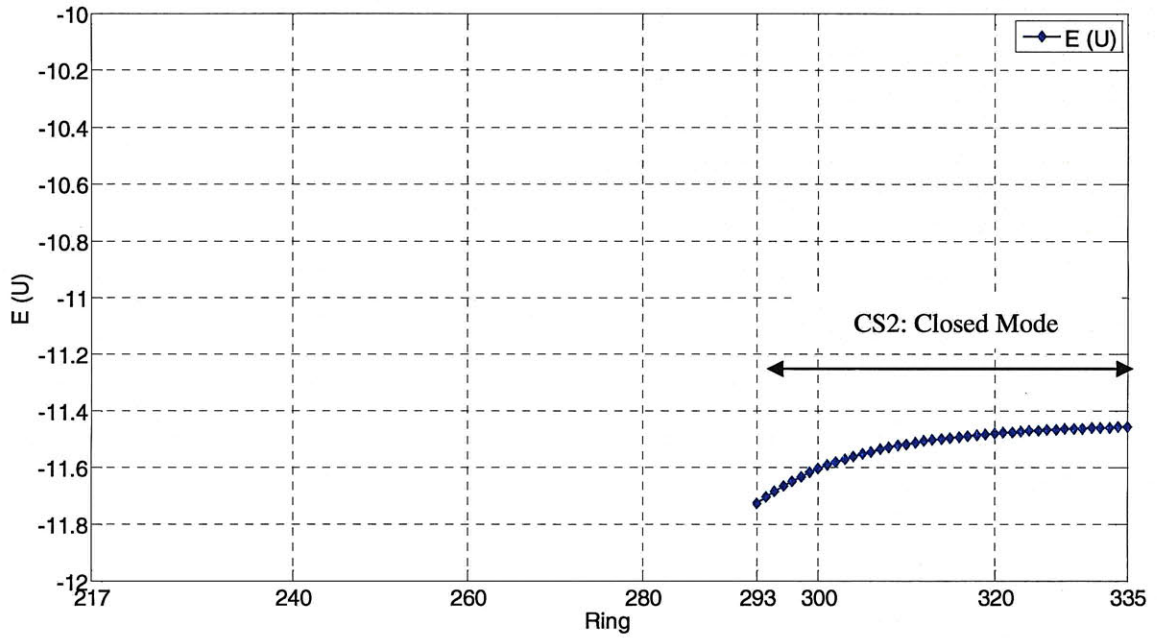


Figure 6.83 Expected utility updating after excavating ring 293 (accident zone 3)

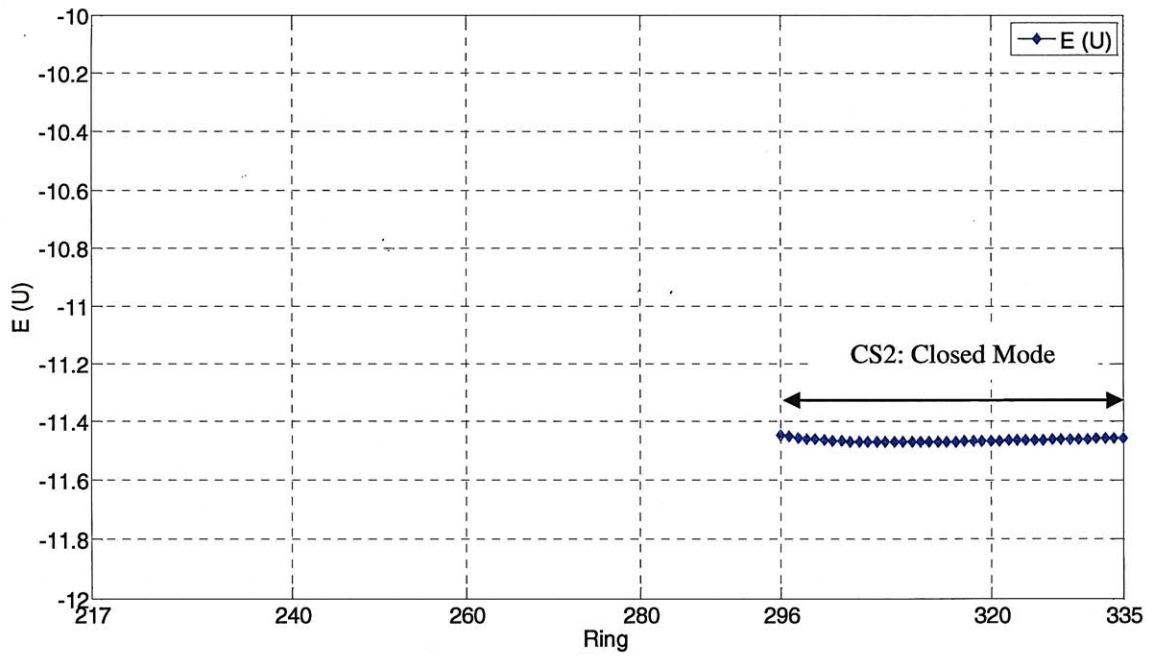


Figure 6.84 Expected utility updating after excavating ring 296 (accident zone 3)

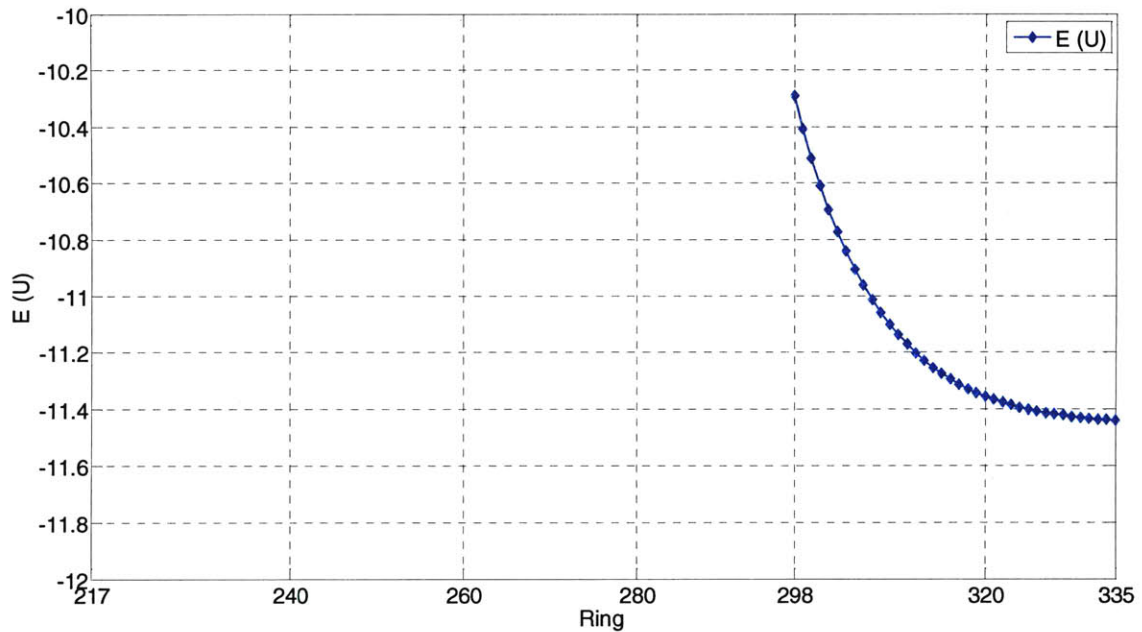


Figure 6.85 Expected utility updating after excavating ring 298 (accident zone 3)

Figure 6.86, Figure 6.87 and Figure 6.88 show the results of updating the probability of failure given the construction strategy, ahead of the tunnel face in the zone of accident 3 (corresponding to approximately the area of installation of ring 292/3 to 298/9). The probability of failure using construction strategy CS1, i.e. open mode is between 0.25 and 0.30, while the probability of failure using construction strategy CS2, which is the “optimal” strategy, closed mode, is about 0.05.

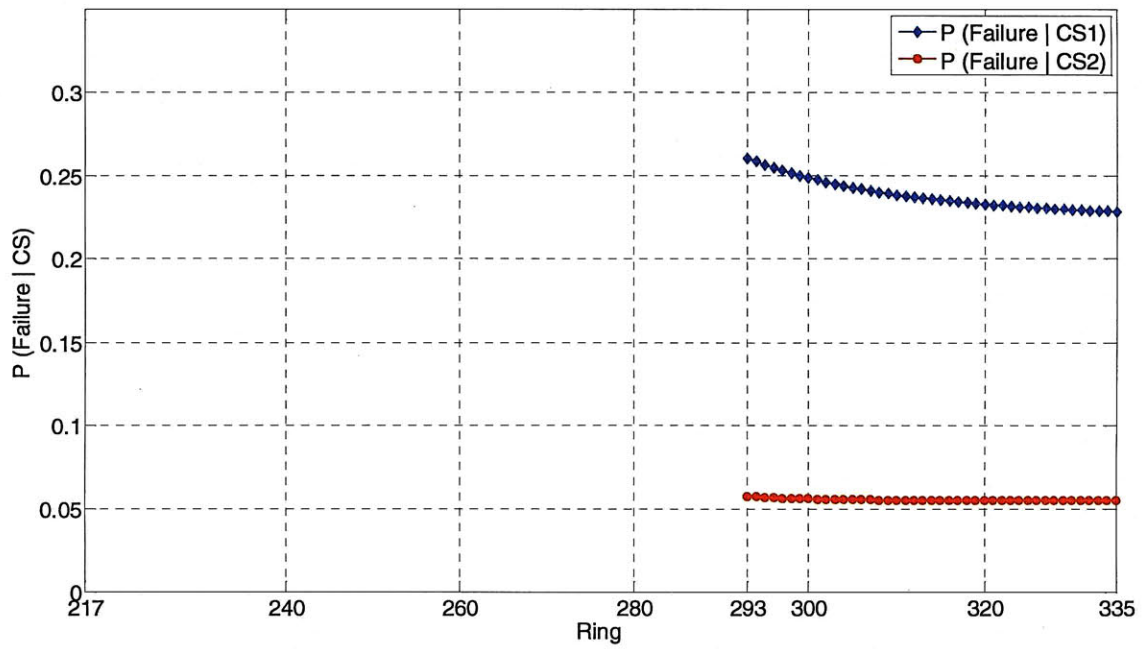


Figure 6.86 probability failure updating after excavating ring 293 (accident zone 3)

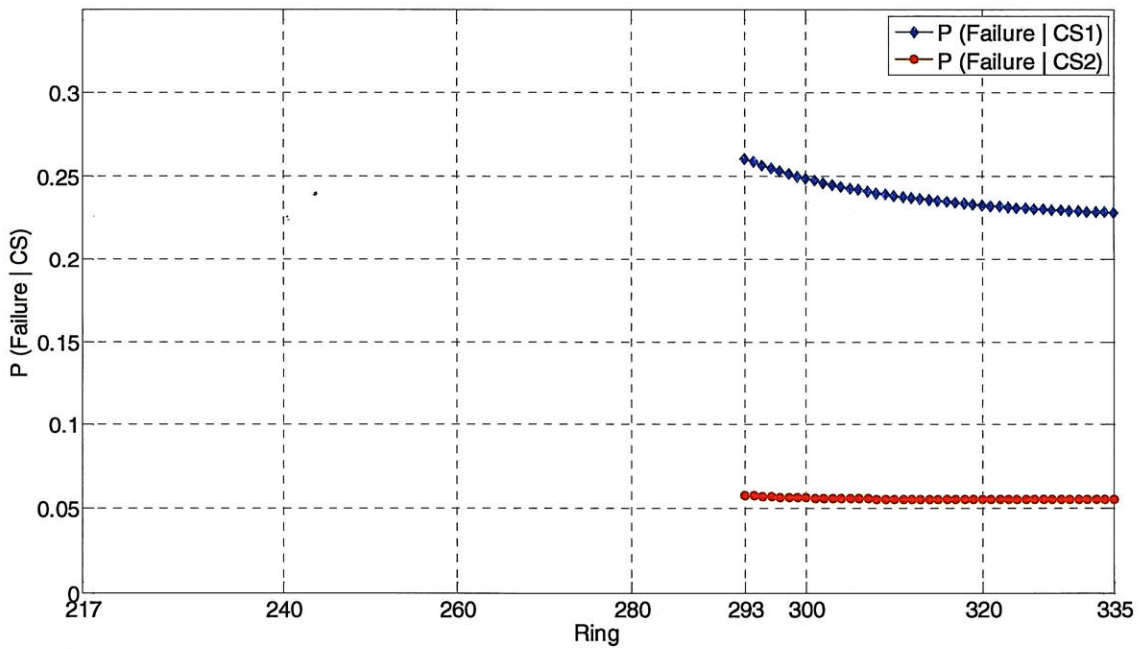


Figure 6.87 probability failure updating after excavating ring 296 (accident zone 3)



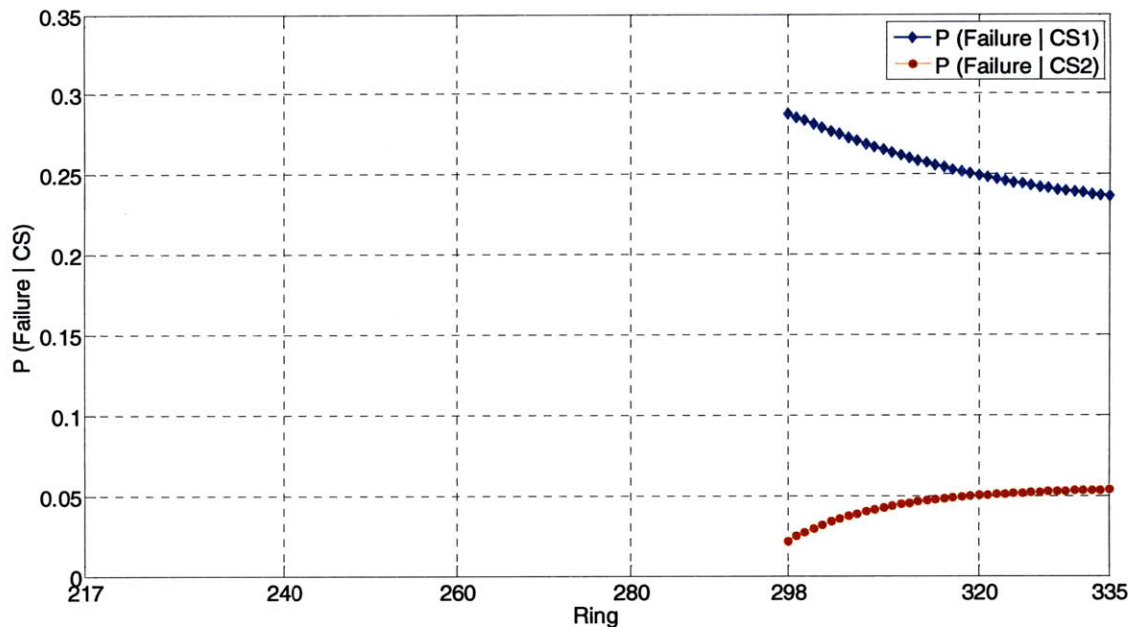


Figure 6.88 probability failure updating after excavating ring 298 (accident zone 3)

Figure 6.89 and Figure 6.90, shows summaries of the results of applying the combined risk assessment model to sections 1 and 2 (steps 1 to 3), respectively. First they show the prediction of Geology that the tunnel passed through (step 1). They also show the optimal construction strategy for one ring ahead of the face (in blue in Figure 6.89 and Figure 6.90), which consists of the results of step 3 (base on step 1 and 2).

Regarding the geological prediction, the model predicts that in section 1 (Figure 6.89) TBM went mostly through mixed and rock conditions up to ring 197, where it entered a more soft formation (G1), until ring 216. In section 2, Figure 6.90, the model predicts that machine went through mostly rock (G3) and mixed (G2) until the zone of accident 3, where the TBM entered a zone of soil (G1) that lasted until the zone of accident 2 (ring 318). From there until ring 335, where the machine stopped is an area of higher probability of mixed (G2), but with considerable probability of soil (G1). These results seem to be in good agreement with what the accident report suggests, and with the survey results done in the area of collapse 3, after the works stopped. Figure 6.91 show the post accident survey results and geology predicted by model 22 (set B). It is possible to see

that there is a good agreement between predicted geology and the results of the post accident borehole results.

Regarding the risk assessment and choice of optimal construction strategy ahead of the face, the results of Figure 6.89 show that the best construction strategy is CS2, use of the TBM in closed mode, in almost all of section 1 (where soil and mixed is predicted). This includes the zone where accident 1 occurred. In section 2, the results presented in Figure 6.90, show that the optimal construction strategy to be CS2 (EPBM in closed mode) in the zone between ring 217 to ring 234; ring 244 to ring 253; ring 283 to ring 335 (zone of accident 2 and 3). This correspond to zones where soil (G1) and mixed (G2) were predicted. The optimal construction strategy is CS1 (EPBM in open mode) in the zones where rock was predicted, from ring 235 to ring 243; ring 254 to ring 257; ring 259 to ring 260 and form ring 263 to ring 282.

In Appendix I is the results of applying the geological prediction model to the tunnel from ring 336 (station 0+631) to ring 1611 (station 2+418) are presented.

Additional background information is provided in Appendix J. Figure 6.95, Figure 6.96 and Figure 6.97 show the data regarding extracted weight, injected grout and machine parameters along section 1. (Figure 6.95 shows the design geological profile and the extracted weight for section 1, Figure 6.96 shows the volume of injected grouted per ring and the total thrust and cutting wheel force for section 1 and Figure 6.97 shows the torque of the cutting wheel and penetration rate along this section). Figure 6.98, Figure 6.99, Figure 6.100 show the data regarding extracted weight, injected grout and machine parameters along section 2. (Figure 6.98 shows the design geological profile and the extracted weight for section 1, Figure 6.99 shows the volume Figure 6.100 shows the torque of the cutting wheel and penetration rate along section.)

## Alarm Criteria

It is important to know or have a good indication about the geology that the machine is going through; however this is not enough when trying to avoid accidents. It is crucial to have some sort of alarm system that allows one to act promptly when the excavation is not behaving according to what is expected.

For closed mode TBM operation, the most important parameters to control during the excavation are the support pressure and the weight of the extracted material. In order to ensure the stability of the face at every moment the support pressure, given by the earth pressure inside the EPBM chamber, must be in balance with or higher than the earth pressure and the water pressure. There are various models to predict the necessary support pressure. The one used in the design of Porto Metro line C tunnel, after the last accident occurred, was limit equilibrium method by Anagnostou and Kovari (Anagnostou and Kovari, 1996). The support pressure should be increased by a factor of safety but should not reach the passive earth pressure in order not create heave at the surface. In low overburden if the support pressure exceeds this limit it could lead to not only to heave but to other problems such as blow-outs. However if the support pressure lies below a set value, there is the danger of loss of stability and collapse of the face. For these reasons it is important to use an appropriate model to predict the support pressure and have a tight control of pressures during construction. After the collapses several supplementary measures were put in place to ensure that the support pressures were adequate during construction (see Section 6.1.5), and therefore this issue will not be addressed.

The control of the weight of the excavated material is also extremely important, due to the possibility of overexcavation as may seem to have occurred in accidents 2 and 3 at the Porto metro. If the extracted weight (or volume) is above the theoretical, the machine may be overexcavating. If the extracted weight is below the theoretical then one is probably in a different formation than expected, a less dense one, assuming that the measuring of the weights is being done accurately. When analyzing the extracted weight data in the accident areas it seems that not only the weight of the extracted material was

significantly higher than the theoretical one, but also that there was a sudden increase in the rate of change of the weight extracted material from one ring to another, right before the zone of the accidents 2 and 3. For this reason I believe that not only the total weight of the extracted material should be controlled but also the rate at which it changes from one ring to another. The control of the extracted weight or volumes was not done correctly prior to the accidents.

Based on these observations, the author suggests the following alarm criteria:

- Lower and upper limit on total extracted weight per ring
- Lower and upper limit on rate of change of extracted weight

The limits will be based on the reference unit weight values for different design formations (Table 6.42). Note that g5, g6 and g7 correspond to soil like material, and g1, g2, g3 and g4 to rock. It was assumed that the geological conditions at the face only range from g1 to g5, since g6 (residual soil) and g7 (fill) are located above tunnel level.

Table 6.42 Reference unit weight values (kN/m<sup>3</sup>)

UNIT	min	med	max
g7	18	19	20
g6	18	19	20
g5*	13.3	15.35	17.4
g5	19	20	21
g4	22	23	24
g3	23	24	25
g2	25	26	27
g1	25	26	27

\* leached granite

The total weight per ring was determined by multiplying the unit weight by the volume of a ring section, which is about 81 m<sup>3</sup>. In soil the lower limit corresponds to a ring composed all of g5 unit (minimum unit weight) and the upper limit of a ring composed of only g5 (maximum unit weight). So the lower and upper limit for soil is:

$$\text{lower limit}(G1) = \min g5 \times V_{ring} = 19 \times 81 = 1539 \text{KN} \approx 154 \text{ton}$$

where

$\min g5$  is the minimum unit weight value for g5 given by Table 6.42

$V_{ring}$  is the volume of a ring section, equal to  $81 \text{m}^3$

$$\text{upper limit}(G1) = \max g5 \times V_{ring} = 21 \times 81 = 1701 \text{KN} \approx 170 \text{ton}$$

where

$\max g5$  is the maximum unit weight value for g5 given by Table 6.42

$V_{ring}$  is the volume of a ring section, equal to  $81 \text{m}^3$

In rock the lower limit corresponds to a ring composed all of g4 unit and the upper limit a ring composed of only g1. So the lower and upper limit for rock is:

$$\text{lower limit}(G3) = \min g4 \times V_{ring} = 22 \times 81 = 1782 \text{KN} \approx 178 \text{ton}$$

where

$\min g4$  is the minimum unit weight value for g4 given by Table 6.42

$V_{ring}$  is the volume of a ring section, equal to  $81 \text{m}^3$

$$\text{upper limit}(G3) = \max g1 \times V_{ring} = 27 \times 81 = 2187 \text{KN} \approx 219 \text{ton}$$

where

$\max g1$  is the maximum unit weight value for g1 given by Table 6.42

$V_{ring}$  is the volume of a ring section, equal to  $81 \text{m}^3$

In mixed the lower limit corresponds to a ring composed all of 90% of g5 unit and 10% of g4, the upper limit corresponds to a ring composed of 10% g5 and 90% of g1/2. So the lower and upper limit for mixed is:

$$\text{lower limit}(G2) = (0.9 \times \min g5 + 0.1 \times \min g4) \times V_{ring} = (0.9 \times 19 + 0.1 \times 22) \times 81 = 1563 \text{KN}$$

$\approx 156 \text{ton}$

where

*min g5* is the minimum unit weight value for g5 given by Table 6.42

*min g4* is the minimum unit weight value for g4 given by Table 6.42

$V_{ring}$  is the volume of a ring section, equal to 81 m<sup>3</sup>

$$upper\ limit(G2) = (0.1 \times max\ g5 + 0.1 \times max\ g1) \times V_{ring} = (0.9 \times 21 + 0.1 \times 27) \times 81 = 2138\ KN$$

$\approx 214\ ton$

where

*max g5* is the maximum unit weight value for g5 given by Table 6.42

*max g4* is the maximum unit weight value for g4 given by Table 6.42

$V_{ring}$  is the volume of a ring section, equal to 81m<sup>3</sup>

The weights calculated above are summarized in Table 6.43.

Table 6.43 total weight values per ring (ton)

GC	Lower limit	medium	Upper limit
Soil	154	162	170
Mixed	156	185	214
Rock	178	198	219

The actual extracted weights (reduced by the weight of injected foam and water, which were recorded by the EPB machine) during the excavation of section 1 and 2 were compared to the “expected” limits. One does not with certainty in which geological condition the ring is located, but one has an estimated probability distribution through the application of model 22. The expected limits were calculated as follows:

$$E(\text{lower limit}) = P(G1) * \text{lower limit}(G1) + P(G2) * \text{lower limit}(G2) + P(G2) * \text{lower limit}(G1)$$

$$E(\text{upper limit}) = P(G1) * \text{upper limit}(G1) + P(G2) * \text{upper limit}(G2) + P(G2) * \text{upper limit}(G1)$$

The rate of change of the actual extracted weight was computed as follows:



$$\Delta W = W_{ring\ r} - W_{ring\ r-1},$$

where

$W_{ring\ r}$  is the extracted material's weight at ring r

$W_{ring\ r-1}$  is the extracted material's weight at ring r-1

The results of these comparisons are shown in Figure 6.92 and Figure 6.93 for section 1 and section 2, respectively. One can see that there seems to be a consistent overexcavation of material in the zones of accident 2 and 3. The values range from 50 to 80 tons. Also between the location of the accident 2 and accident 3 there seems to be a consistent "underexcavation". This can only be explained, assuming that the extracted measured weights are accurate, by the fact that there is a material in this area that is much lighter than the assumed G1. This theory is supported by the results of the post accident survey that shows the existence of a leached granite in this area (Section 6.1.4), with a much lower unit weight value of in average 15KN/m<sup>3</sup> (see g5\* in Table 6.43)

Figure 6.92 and Figure 6.93 contain also the rate of change of extracted weight from one ring to the next one. It is interesting to observe that from ring 249 to 250, rings 289-290 and 290-291 (right before accident 3 location), ring 317 to 318 and 326 to 327 (accident 2 location), the rate of change of extremely high ranging from 60 to 170 tons. On average, if one changes from a ring composed only of soil (G1) to one composed one of rock (G3), the change rate should be in absolute values, 36 ton (average value:  $|W_{rock} - W_{soil}| = 198 - 162 = 36$  ton from Table 6.43), which is much lower than what was observed in the indicated areas. This sudden increase seems to confirm the theory that there was overexcavation in the areas of accident 2 and 3. Therefore it is important that limits are set not only for the total extracted weights in each ring but also for the rate in which these weights change. If these changes are above (in absolute values) a certain limit this may indicate overexcavation or sudden change of ground conditions.

Section 1 (rings 105-216)

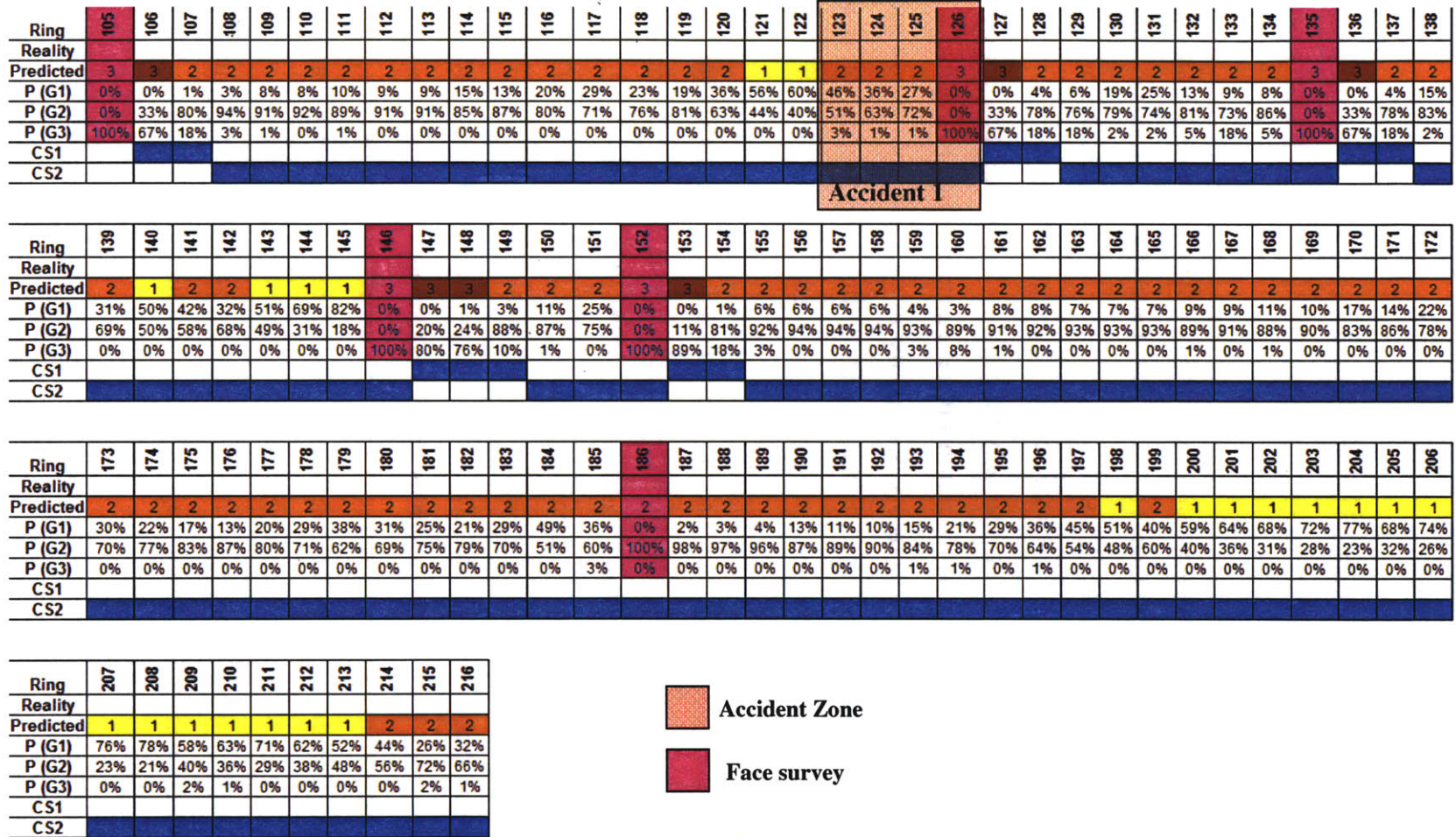


Figure 6.89 Prediction of geological conditions along section 1 (using model 22). Note that for this section there is no detailed information regarding the encountered geology except at face survey points.



Section 2 (rings 217-335)

Ring	217	218	219	220	221	222	223	224	225	226	227	228	229	230	231	232	233	234	235	236	237	238	239	240	241	242	243	244	245	246	247	248	249	250		
Reality																																				
Predicted	2	2	2	2	2	2	2	2	2	2	2	2	2	2	2	2	2	2	2	3	3	3	3	3	3	2	2	2	2	2	2	2	2	2		
P (G1)	39%	32%	26%	33%	42%	35%	28%	35%	41%	34%	28%	34%	19%	15%	8%	5%	3%	2%	2%	1%	1%	0%	0%	1%	3%	6%	11%	21%	18%	15%	11%	3%	7%	4%		
P (G2)	60%	68%	74%	67%	58%	65%	71%	65%	58%	66%	72%	65%	78%	84%	87%	86%	79%	70%	58%	46%	34%	0%	11%	27%	45%	61%	70%	77%	82%	85%	88%	87%	91%	90%		
P (G3)	1%	0%	0%	1%	0%	0%	0%	1%	1%	0%	0%	1%	3%	1%	4%	10%	18%	28%	40%	53%	65%	100%	89%	73%	52%	33%	19%	3%	0%	0%	0%	10%	2%	6%		
CS1																																				
CS2																																				

Ring	251	252	253	254	255	256	257	258	259	260	261	262	263	264	265	266	267	268	269	270	271	272	273	274	275	276	277	278	279	280	281	282	283	284		
Reality																																				
Predicted	2	2	2	2	3	2	2	2	2	2	2	3	3	3	3	3	3	3	3	3	3	3	3	3	3	3	3	3	3	3	2	2	2			
P (G1)	4%	4%	1%	1%	1%	3%	8%	4%	2%	4%	14%	0%	0%	0%	0%	0%	0%	0%	0%	0%	0%	0%	0%	0%	0%	0%	0%	0%	0%	0%	2%	3%	8%			
P (G2)	77%	90%	67%	54%	42%	59%	71%	62%	51%	92%	86%	0%	3%	5%	2%	5%	31%	23%	17%	13%	11%	10%	3%	2%	4%	6%	7%	3%	2%	14%	11%	81%	96%	91%		
P (G3)	19%	6%	32%	44%	57%	37%	22%	34%	47%	3%	1%	100%	97%	95%	98%	95%	69%	77%	83%	87%	89%	90%	97%	98%	96%	94%	93%	97%	98%	86%	89%	18%	1%	0%		
CS1																																				
CS2																																				

Accident 3

Ring	285	286	287	288	289	290	291	292	293	294	295	296	297	298	299	300	301	302	303	304	305	306	307	308	309	310	311	312	313	314	315	316	317	318		
Reality																																				
Predicted	2	2	2	2	2	2	2	2	2	2	2	1	1	1	1	1	2	2	2	2	2	1	1	2	2	2	2	2	1	1	1	1	1	2		
P (G1)	13%	19%	24%	31%	25%	21%	27%	36%	46%	38%	47%	56%	100%	100%	83%	65%	43%	34%	25%	34%	44%	50%	56%	44%	36%	30%	39%	49%	57%	65%	79%	70%	61%	24%		
P (G2)	86%	80%	75%	68%	74%	79%	73%	64%	54%	62%	53%	44%	0%	0%	17%	34%	54%	65%	74%	65%	56%	50%	44%	56%	64%	70%	61%	51%	42%	35%	21%	30%	39%	70%		
P (G3)	1%	1%	1%	1%	0%	0%	1%	0%	0%	0%	0%	0%	0%	0%	0%	1%	3%	1%	1%	0%	0%	0%	1%	0%	0%	0%	0%	0%	0%	0%	0%	0%	0%	0%	6%	
CS1																																				
CS2																																				

Ring	319	320	321	322	323	324	325	326	327	328	329	330	331	332	333	334	335
Reality																	
Predicted	2	2	2	2	2	2	2	2	2	2	2	2	2	2	2	2	2
P (G1)	15%	26%	36%	29%	24%	33%	43%	35%	26%	7%	2%	5%	9%	15%	9%	2%	5%
P (G2)	64%	71%	64%	70%	76%	67%	57%	65%	74%	83%	80%	85%	85%	82%	71%	65%	76%
P (G3)	21%	3%	0%	0%	0%	0%	0%	0%	0%	10%	18%	10%	6%	3%	20%	33%	19%
CS1																	
CS2																	

 Accident Zone  
 Face survey

Accident 2

Figure 6.90 Prediction of geological conditions along section 2 (using model 22). Note that for this section there is no detailed information regarding the encountered geology except at face survey points.

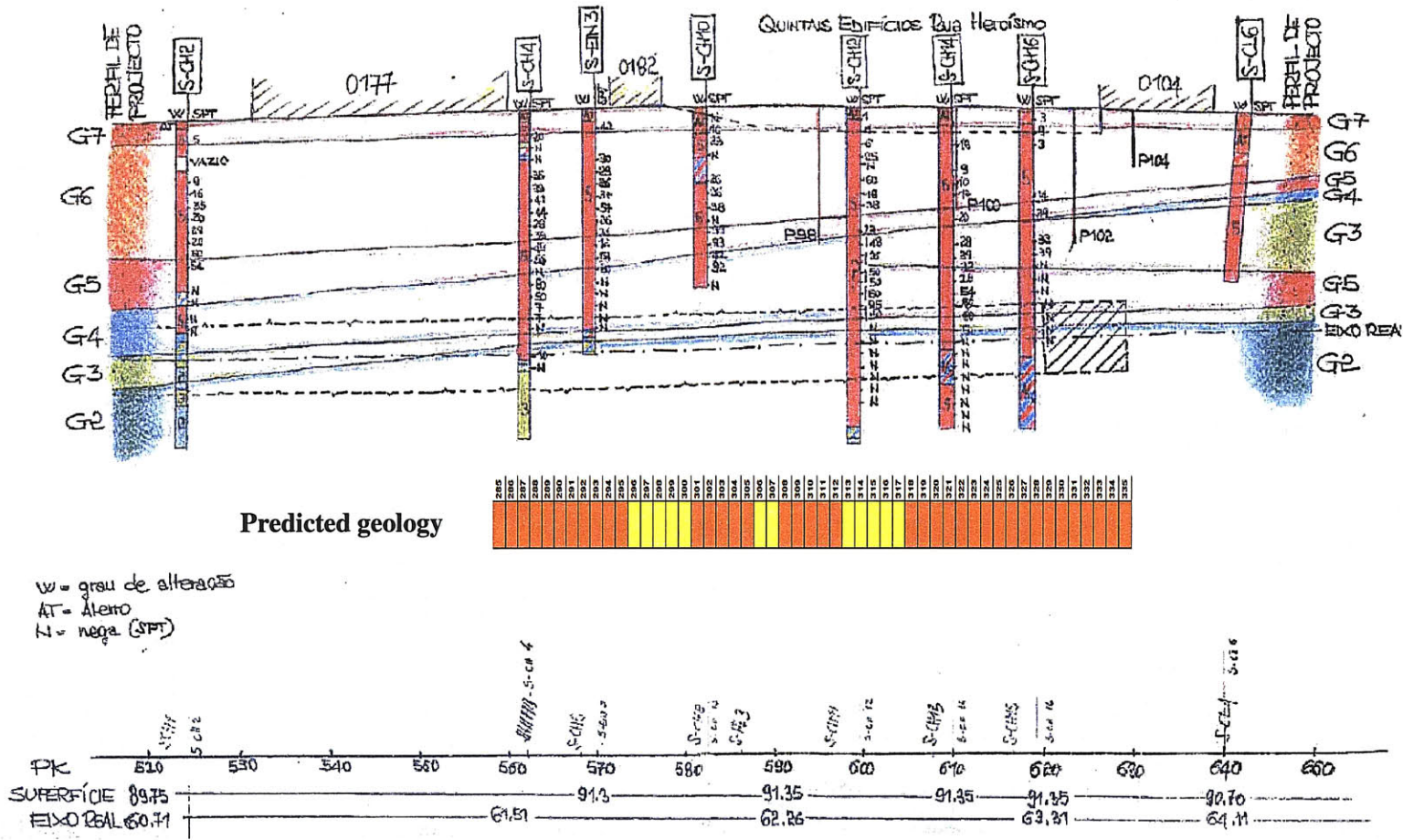


Figure 6.91 Post accident survey results and predicted geology

(Note that for the actually encountered geology red correspond to soil like and blue and green correspond to rock like material)



### Accident 1

Ring	105	106	107	108	109	110	111	112	113	114	115	116	117	118	119	120	121	122	123	124	125	126	127	128	129	130	131	132	133	134	135	136	137	138
Predicted	3	2	2	2	2	2	2	2	2	2	2	2	2	2	2	2	1	1	2	2	2	3	2	2	2	2	2	2	2	2	3	2	2	2
P (G1)	0%	0%	1%	3%	8%	8%	10%	9%	9%	15%	13%	20%	29%	23%	19%	36%	56%	60%	46%	36%	27%	0%	0%	4%	6%	19%	25%	13%	9%	8%	0%	0%	4%	15%
P (G2)	0%	33%	80%	94%	91%	92%	89%	91%	91%	85%	87%	80%	71%	76%	81%	63%	44%	40%	51%	63%	72%	0%	33%	78%	76%	79%	74%	81%	73%	86%	0%	33%	78%	83%
P (G3)	100%	67%	18%	3%	1%	0%	1%	0%	0%	0%	0%	0%	0%	0%	0%	0%	0%	3%	1%	1%	100%	67%	18%	18%	2%	2%	5%	18%	5%	100%	67%	18%	2%	
Measured W	206	245	247	247	247	232	?	234	186	128	210	171	167	168	136	166	167	151	231	120	153	240	87	63	?	102	65	87	87	85	?	78	107	81
Lower Limit (ton)	178	171	160	157	156	156	156	156	156	156	156	156	156	156	156	155	155	155	156	156	156	178	171	160	160	156	156	157	160	157	178	171	160	157
Upper Limit (ton)	219	217	214	213	210	210	210	210	210	207	208	205	201	204	205	198	189	188	194	198	202	219	217	213	212	206	203	208	211	211	219	217	213	208
Alarm (ton)		28	33	34	37	22		25		-28	2				-20			-4	37	36	3	21	-84	-97		-55	-91	-70	-73	-72		-93	-53	-76
Delta W		40	2.2	-0.6	0.1	-15			-49	-58	83	-39.2	-4.07	1.02	-32	30	1.2	-16	80	-111	33	87.1	-153	-24			-37	22	-0	-2.1			29	-26

Ring	139	140	141	142	143	144	145	146	147	148	149	150	151	152	153	154	155	156	157	158	159	160	161	162	163	164	165	166	167	168	169	170	171	172
Predicted	2	1	2	2	1	1	1	3	2	2	2	2	2	3	2	2	2	2	2	2	2	2	2	2	2	2	2	2	2	2	2	2	2	2
P (G1)	31%	50%	42%	32%	51%	69%	82%	0%	0%	1%	3%	11%	25%	0%	0%	1%	6%	6%	6%	6%	4%	3%	8%	8%	7%	7%	7%	9%	9%	11%	10%	17%	14%	22%
P (G2)	69%	50%	58%	68%	49%	31%	18%	0%	20%	24%	88%	87%	75%	0%	11%	81%	92%	94%	94%	94%	93%	89%	91%	92%	93%	93%	93%	89%	91%	88%	90%	83%	86%	78%
P (G3)	0%	0%	0%	0%	0%	0%	0%	100%	80%	76%	10%	1%	0%	100%	89%	18%	3%	0%	0%	0%	3%	8%	1%	0%	0%	0%	1%	0%	1%	0%	0%	0%	0%	0%
Measured W	93.7	112	174	139	212	189	122	115	176	199	162	220	146	97.1	189	160	176	159	158	161	174	184	84	163	175	161	164	167	202	?	180	164	170	150
Lower Limit (ton)	156	155	155	156	155	155	154	178	174	173	158	156	156	178	176	160	157	156	156	156	157	158	156	156	156	156	156	156	156	156	156	156	156	156
Upper Limit (ton)	200	192	196	200	192	184	178	219	218	217	213	209	203	219	218	214	212	211	211	211	212	213	210	211	211	211	211	210	210	209	210	207	208	204
Alarm (ton)	-62	-43		-17	21	6	-33	-63		61	23	-37	11	-10	-81								-72											-5
Delta W	13	18	63	-36	73	-23	-68	-7	61	23	-37	58	-74	-49	92	-29	16	-17	-1	4	13	10	-99	79	12	-14	3	3	35	-202	180	-16	6	-20

Ring	173	174	175	176	177	178	179	180	181	182	183	184	185	186	187	188	189	190	191	192	193	194	195	196	197	198	199	200	201	202	203	204	205	206
Predicted	2	2	2	2	2	2	2	2	2	2	2	2	2	2	2	2	2	2	2	2	2	2	2	2	2	1	2	1	1	1	1	1	1	1
P (G1)	30%	22%	17%	13%	20%	29%	38%	31%	25%	21%	29%	49%	36%	0%	2%	3%	4%	13%	11%	10%	15%	21%	29%	36%	45%	51%	40%	59%	64%	68%	72%	77%	68%	74%
P (G2)	70%	77%	83%	87%	80%	71%	62%	69%	75%	79%	70%	51%	60%	100%	98%	97%	96%	87%	89%	90%	84%	78%	70%	64%	54%	48%	60%	40%	36%	31%	28%	23%	32%	26%
P (G3)	0%	0%	0%	0%	0%	0%	0%	0%	0%	0%	0%	0%	3%	0%	0%	0%	0%	0%	0%	1%	1%	0%	1%	0%	0%	0%	0%	0%	0%	0%	0%	0%	0%	0%
Measured W	167	136	170	159	169	154	197	171	162	176	154	122	?	166	139	166	195	195	179	172	210	188	180	193	172	200	140	176	187	189	175	193	175	189
Lower Limit (ton)	156	156	156	156	156	156	155	156	156	156	156	155	156	156	156	156	156	156	156	156	156	156	156	155	155	155	155	155	155	155	155	155	155	155
Upper Limit (ton)	201	204	207	208	205	201	197	200	203	205	201	193	198	214	213	212	212	208	209	209	207	205	201	198	194	191	196	188	186	184	182	180	184	181
Alarm (ton)		-20				-2					-2	-33			-17						3					9	-15		1	5		12		7
Delta W	16	-31	34	-11	10	-15	43	-26	-10	14	-22	-32			-27	27	29	0	-16	-7	38	-22	-8	13	-20	28	-60	36	11	2	-14	17	-17	13

Ring	207	208	209	210	211	212	213	214	215	216
Predicted	1	1	1	1	1	1	1	2	2	2
P (G1)	76%	78%	58%	63%	71%	62%	52%	44%	26%	32%
P (G2)	23%	21%	40%	36%	29%	38%	48%	56%	72%	66%
P (G3)	0%	0%	2%	1%	0%	0%	0%	0%	2%	1%
Measured W	200	184	151	192	195	177	150	139	163	222
Lower Limit (ton)	155	154	155	155	155	155	155	155	156	156
Upper Limit (ton)	180	180	188	186	183	187	191	195	203	200
Alarm (ton)	19	4	-5	6	12		-5	-17		22
Delta W	11	-16	-33	41	3	-18	-27	-12	24	59

 Accident Zone  
 Face survey

Figure 6.92 Alarm criteria for extracted weight limits and rate (section 1)



Ring	217	218	219	220	221	222	223	224	225	226	227	228	229	230	231	232	233	234	235	236	237	238	239	240	241	242	243	244	245	246	247	248	249	250	
Predicted	2	2	2	2	2	2	2	2	2	2	2	2	2	2	2	2	2	2	2	3	3	3	3	3	3	2	2	2	2	2	2	2	2	2	
P (G1)	39%	32%	26%	33%	42%	35%	28%	35%	41%	34%	28%	34%	19%	15%	8%	5%	3%	2%	2%	1%	1%	0%	0%	1%	3%	6%	11%	21%	18%	15%	11%	3%	7%	4%	
P (G2)	60%	68%	74%	67%	58%	65%	71%	65%	58%	66%	72%	65%	78%	84%	87%	86%	79%	70%	58%	46%	34%	0%	11%	27%	45%	61%	70%	77%	82%	85%	88%	87%	91%	90%	
P (G3)	1%	0%	0%	1%	0%	0%	0%	1%	1%	0%	0%	1%	3%	1%	4%	10%	18%	28%	40%	53%	65%	100%	89%	73%	52%	33%	19%	3%	0%	0%	0%	10%	2%	6%	
Measured W	184	180	172	168	189	173	171	166	187	203	133	195	164	191	178	186	151	218	187	186	201	130	197	169	172	180	164	181	164	186	199	206	119	229	
Lower Limit (ton)	156	156	156	156	155	155	156	156	155	156	156	156	157	156	157	158	160	162	165	168	171	178	176	172	168	163	160	156	156	156	156	159	157	158	
Upper Limit (ton)	197	200	202	200	195	199	201	199	196	199	202	199	206	207	211	212	213	214	215	216	217	219	218	217	215	213	210	205	206	207	209	213	211	212	
Alarm (ton)										4	-23						-9	3				-48		-3										-38	17
Delta W	-38	-4	-7	-4	21	-16	-2	-6	21	16	-70	63	-31	27	-13	9	-35	66	-31	-1	15	-71	67	-27	2	9	-17	17	-17	22	13	7	-87	110	

Ring	251	252	253	254	255	256	257	258	259	260	261	262	263	264	265	266	267	268	269	270	271	272	273	274	275	276	277	278	279	280	281	282	283	284
Predicted	2	2	2	2	3	2	2	2	2	2	2	3	3	3	3	3	3	3	3	3	3	3	3	3	3	3	3	3	3	3	2	2	2	2
P (G1)	4%	4%	1%	1%	1%	3%	8%	4%	2%	4%	14%	0%	0%	0%	0%	0%	0%	0%	0%	0%	0%	0%	0%	0%	0%	0%	0%	0%	0%	0%	2%	3%	8%	
P (G2)	77%	90%	67%	54%	42%	59%	71%	62%	51%	92%	86%	0%	3%	5%	2%	5%	31%	23%	17%	13%	11%	10%	3%	2%	4%	6%	7%	3%	2%	14%	11%	81%	96%	91%
P (G3)	19%	6%	32%	44%	57%	37%	22%	34%	47%	3%	1%	100%	97%	95%	98%	95%	69%	77%	83%	87%	89%	90%	97%	98%	96%	94%	93%	97%	98%	86%	89%	18%	1%	0%
Measured W	237	226	224	194	205	204	166	170	186	208	186	200	175	158	190	161	242	120	187	186	216	171	158	151	178	171	162	186	189	180	205	184	179	161
Lower Limit (ton)	160	157	163	166	169	164	161	164	167	157	156	178	177	177	178	177	171	173	174	175	176	176	177	178	177	177	177	178	178	175	176	160	156	156
Upper Limit (ton)	213	212	215	216	216	214	212	214	215	212	208	219	219	218	219	218	217	217	218	218	218	218	219	219	218	218	218	219	219	218	214	212	210	
Alarm (ton)	24	14	9			11	-1	-38		4	16	22	-21	14	-3	-19	-16	25	-53			-5	-19	-26		-6	-15							
Delta W	8	-11	-2	-30															67	-1	30	-46	-12	-7	26	-7	-9	24	3	-9	25	-20	-5	-18

Ring	285	286	287	288	289	290	291	292	293	294	295	296	297	298	299	300	301	302	303	304	305	306	307	308	309	310	311	312	313	314	315	316	317	318	
Predicted	2	2	2	2	2	2	2	2	2	2	2	1	1	1	1	1	2	2	2	2	2	1	1	2	2	2	2	2	1	1	1	1	1	1	2
P (G1)	13%	19%	24%	31%	25%	21%	27%	36%	46%	38%	47%	56%	100%	100%	83%	65%	43%	34%	25%	34%	44%	50%	56%	44%	36%	30%	39%	49%	57%	65%	79%	70%	61%	24%	
P (G2)	86%	80%	75%	68%	74%	79%	73%	64%	54%	62%	53%	44%	0%	0%	17%	34%	54%	65%	74%	65%	56%	50%	44%	56%	64%	70%	61%	51%	42%	35%	21%	30%	39%	70%	
P (G3)	1%	1%	1%	1%	0%	0%	1%	0%	0%	0%	0%	0%	0%	0%	0%	1%	3%	1%	1%	0%	0%	0%	1%	0%	0%	0%	0%	0%	0%	0%	0%	0%	0%	0%	6%
Measured W	157	175	165	167	167	108	231	213	240	213	221	246	248	237	140	102	85	107	124	118	108	113	107	115	114	126	108	99	108	90	109	138	120	252	
Lower Limit (ton)	156	156	156	156	156	156	156	155	155	155	155	155	154	154	154	155	156	156	156	156	155	155	155	155	155	156	155	155	155	155	154	155	155	157	
Upper Limit (ton)	208	206	203	200	203	205	202	198	194	197	193	189	170	170	177	186	195	199	203	199	195	192	190	195	198	201	197	193	189	185	179	183	187	204	
Alarm (ton)	-1				-48	29	15	47	15	28	57	78	67		-14	-53	-71	-48	-32	-38	-48	-42	-48	-40	-41	-30	-47	-56	-47	-64	-45	-17	-35	48	
Delta W	-4	18	-10	2	0	-60	123	-18	-28	-28	8	25	2	-11	-97	-38	-17	23	17	-7	-10	6	-6	9	-1	11	-18	-9	8	-17	19	29	-18	132	

Ring	319	320	321	322	323	324	325	326	327	328	329	330	331	332	333	334	335
Predicted	2	2	2	2	2	2	2	2	2	2	2	2	2	2	2	2	2
P (G1)	15%	26%	36%	29%	24%	33%	43%	35%	26%	7%	2%	5%	9%	15%	9%	2%	5%
P (G2)	64%	71%	64%	70%	76%	67%	57%	65%	74%	83%	80%	85%	85%	82%	71%	65%	76%
P (G3)	21%	3%	0%	0%	0%	0%	0%	0%	0%	10%	18%	10%	6%	3%	20%	33%	19%
Measured W	89.1	89	93	83	83	108	96	114	284	127	88	79.8	83.9	84.7	104	88	88
Lower Limit (ton)	160	156	156	156	156	156	155	155	156	158	160	158	157	157	160	163	160
Upper Limit (ton)	208	203	198	201	203	199	195	198	202	211	214	212	210	208	211	215	213
Alarm (ton)	-71	-67	-63	-73	-72	-48	-59	-41	82	-32	-72	-79	-73	-72	-56	-75	-72
Delta W	-163	0	4	-10	0	25	-12	18	-170	-158	-39	-8	4	1	20	-16	0

 Accident Zone  
 Face survey

Figure 6.93 Alarm criteria for extracted weight limits and rate (section 2)

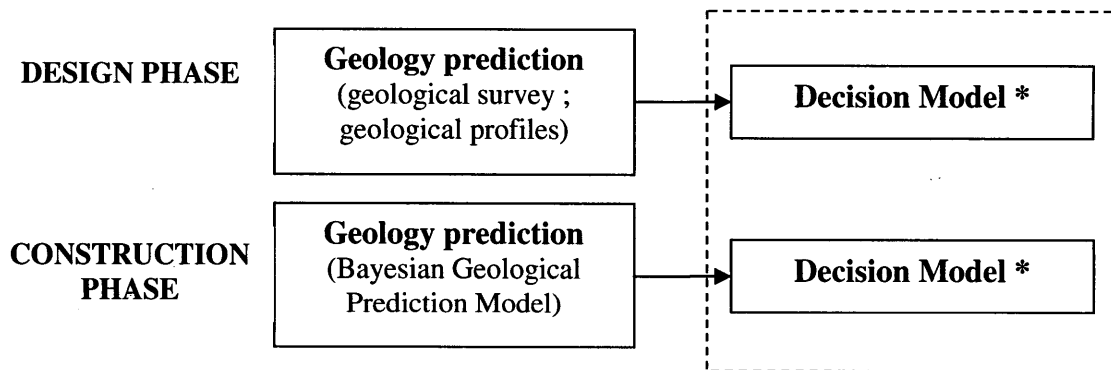


### **6.3 Summary and Conclusions of Porto Metro Case Study**

In this chapter the project of Porto Light Metro, where three collapses occurred between 2000 and 2001 Line C tunnel was summarized. The three collapses were described and their possible causes as identified by the Porto Accident Commission and the designer were presented and analyzed. The main formation crossed by the Line C tunnel is the Granitic Formation, which is deeply weathered with alteration grades that range from residual soil to fresh granite in a very irregular profile. The construction method used was an Earth Pressure Balance Machine (EPBM), which can be adapted to different excavation conditions by changing the support system at the face (open mode – no support of the face; closed mode – total support of the face and semi-closed mode- face partially supported by earth pressure).

The first accident in the Line C tunnel occurred on 30 September 2000 when the EPBM intercepted a former well resulting in the discharge of its water and collapse of the ground, causing damages to two buildings located at the surface. The second accident occurred, on 22 December 2000, when cracks and 250m<sup>3</sup> subsidence were noticed in the back garden of a building. This occurred right after the EPBM had passed through this location. The EPBM was stopped in order for consolidation works from the tunnel and the surface to take place. While the EPBM was stopped at the location of accident 2, another collapse (accident 3) occurred 50 m back in the already constructed part of the tunnel in January 2001. The collapse reached the surface and caused a building to fall into the crater resulting in the death of a person. The analysis of the accident commission report and available data given to the author by Porto Metro, indicate that the two last accidents were mainly caused by overexcavation of the EPBM due to wrong operation of the machine. The fact that the real geology did not match the design assumptions and no action was taken to adapt the excavation (mode of operation, rate of excavation, face pressure) to the actual geology, combined with fact that no or little attention was given to the automatically recorded data regarding the machine operation (extracted weight, penetration etc) led to an inadequate operation of the machine for the encountered geologies.

Based on the analysis of this case study, the decision support framework for determining the “optimal” (minimum risk) construction method for a given tunnel alignment, presented in Chapter 5 was further developed for the specific case of the Porto metro line C tunnel. The decision support framework consists of three models, two geology prediction model and a decision model (Figure 6.96). During the design phase the geology prediction is a simple model only based on the results of the geological survey and geological profiles. The decision model is a Bayesian network based model that allows one to decide on the optimal construction strategy for a given the geology. During the construction phase the geologic prediction model is a Bayesian network prediction model that allows one to predict the geology ahead of a tunnel machine based on observations of various machine parameters, during construction. The decision model is the same as the one used in the design phase, which allows one to decide on the optimal construction strategy for the predicted geology. When combined the models allow one to asses risks during tunnel construction.



\* The decision model in the design and construction phases is the same.

Figure 6.94 decision support framework for the design and construction phase

The emphasis of this research is on the construction phase where the decision model is used in combination with the (Bayesian) geological prediction model. The geological prediction model allows one to predict the geology crossed and ahead of the tunnel face, and based on this, it is possible to decide on the optimal construction strategy for the “updated” geologies.

## Design Phase

During the design phase a decision is made on the “optimal” construction strategy for the tunnel, regarding the stability of the face. This is done through application of the decision model developed specifically for the Porto Metro case using the information provided by the geological model consisting of geological profiles. The decision model was built based on information made available to the author. The construction strategies considered in the model were: 1) EPBM with operation in open mode and 2) EPBM with operation in closed mode. The variables found to be important for face stability, and this influences the decision on the “optimal” construction strategy, were the ground conditions at the face, the piezometric level, the occupation at the surface and underground man made existing structures. Due to the lack of information on underground man-made existing structures this factor was dropped from the model. The model considered that the failure of the face was dependent on the combination of the construction strategy used, the ground conditions at the face and the hydrological conditions (piezometric level). In the model different damage levels were considered in order to portray different scenarios. There was a scenario where no damage occurred (no failure). Another scenario corresponded to damages at the surface due to excessive deformation, including partial collapse of a building (Level 1 damage). This corresponded to a damage level equivalent to what had occurred in accident 2. A third scenario consisted of a collapse of the tunnel reaching the surface, causing the collapse of at least a building and causing damage to others (Level 2 damage). This corresponds to a damage level equivalent to that of accident 3. Finally, the model considers the utilities, which represented the costs associated with the different construction methods and consequences of failure.

The decision model was applied during the design phase for 320 m of Line C tunnel (from station 0+301 to station 0+630), where the accidents occurred. The design information (geological longitudinal profile, construction costs), and accident database information (for the consequences of collapses in similar circumstances) was used in the decision model to determine the “optimal” construction strategy”. The results show that the “optimal” construction strategy would have been to use the EPBM in closed mode.

This coincides in part with the Porto metro design, which determined that the EPBM should operate in closed mode (fully pressurized face) from station 0+150 to 0+530 (Table 6.2). However from station 0+530 to 0+630 (section 2, where accident 2 and 3 occurred) the actual design prescribed that the EPBM should operate in the open mode (without face support). The fact that Porto metro design prescribed the open mode in this area has to do with the fact that the geological profile for this area predicted that the tunnel would mainly go through rock (Figure 6.28). However, looking at these profiles and the borehole information (Figure 6.28), this study considered that the tunnel might probably go through mixed conditions, with some probability of occurrence of soil at the tunnel level. This was captured by the prior probability table for section 2 presented in Table 6.7. Based on this it was determined in this study that the EPBM should operate in closed mode (fully pressurized face) in section 2.

Once the construction starts, with the “optimal” construction, information on the actual conditions (regarding geology, machine parameters, deformations etc) becomes available and should be used to update the geological conditions ahead of the tunnel face and adapt the construction strategy to the found geology. This was done in the construction phase through the application of the Bayesian Network based geologic prediction model in combination with the decision model.

### Construction Phase

For the construction strategy the geological prediction model based on a Bayesian Network for predicting ground conditions was developed. The aim of the Bayesian geological prediction model was to predict the ground conditions ahead of the EPBM during construction, given information on observed machine performance parameters. The model is ‘learned’ from data that are obtained by observations during the construction process. The model is then used to predict geologic conditions ahead.

The geological conditions in the Porto metro line C tunnel were simplified to soil (G1), mixed (G2) and rock (G3). The machine parameter data corresponding to the section of

the tunnel from ring 336, station 0+631, to ring 1611, station 2+418 (i.e. the section beyond the location where the machine was stopped due to the last collapse) were analyzed. Emphasis was placed on choosing the machine parameters that best distinguish between geological conditions. For this a single parameter analysis is first done. This consists of determining the mean values, standard deviations and relative frequencies of the parameters. The relative frequencies for different geologies are compared. If there are significant differences then the parameter is considered to be good at distinguishing between geologies. A two-parameter analysis followed in order to determine which inter-relationships between these parameters are important in distinguishing geologies. This consists of finding the relative frequency of two parameters at time, for different geological conditions. The joint relative frequencies of two parameters for different geologies are compared. If there is a significant difference between joint relative frequencies for different geological conditions then the relationship between the two parameters is important when distinguishing between geologies; consequently the parameters and inter-relationship was retained in the model. Finally, because it is difficult to visualize the importance of relationships between more than two variables, sensitivity analyses are done on the structure of the prediction model. Several different structures were tested and the one that most accurately predicted the ground conditions was chosen. The results of the data analysis show that:

- Penetration rate (P) and cutting wheel force (CF) are important parameters when distinguishing between ground condition, while torque of the cutting wheel (TO) and Total Thrust (TT) are less important. Although torque (TO) by itself is not important to distinguish between ground conditions, the relation between torque, cutting wheel force and penetration is extremely important (see below)
- The ratio between some machine parameters was considered as one variable and found out to be important when distinguishing between geologies. This is the case for torque of the cutting wheel over the cutting wheel force (COT). This ratio is important in all geologies but it becomes more important as the geological conditions are closer to rock conditions. Another parameter ratio that proved to be important when identifying ground conditions is the cutting wheel force over

total thrust (COTT). The total thrust is the force that is applied by the thrust cylinders (or jacks). Only a portion of this force will reach the cutting wheel, the remainder is needed to overcome the friction of the ground around the shield. In soil COTT is lower than in rock since a larger portion of the total thrust is lost by friction around the shield, due to the fact that soil formations are more deformable than rock.

- It is difficult to create a model that performs well when predicting geologies so extreme as rock and soil. The best model overall is not the best model identifying soil, nor the best model identifying rock.
- Mixed conditions (G2) were extremely difficult to predict. This was expected, and has to do with how mixed conditions were defined. Mixed conditions ranged from 10% soil with 90% rock (i.e. almost all rock), to 10% rock and 90% soil (i.e. almost all soil).
- The model that performed the best overall contained the parameters penetration rate (P), cutting wheel force (CF), and torque of cutting wheel (TO), and considered the inter-relationship between torque and penetration; and the inter-relationship between cutting wheel force and penetration, i.e. the model contained an arrow between the variables P and TO and an arrow between CF and P (Figure 6.72). Note that despite the fact that TO is not an important variable on its own when distinguishing geologies, the relationship between TO and P, as well as the relationship between TO and CF are important, and therefore TO must be considered in the model.
- The models that performed the best in soil (G1), contain the variables CF, P and TO (in combination and inter-related with CF and P) or COTT. The models that perform the best in rock (G3), contained the variables CF, P and TOC.

Once the best structure for the Bayesian geological prediction model was determined based on the Porto metro data, a risk assessment, and mitigation model is proposed by combining the Bayesian geological prediction model presented in section 6.2.2, and decision model presented in section 6.2.1.1. The Bayesian prediction model allows one to predict the geologies ahead of the machine based on the parameters that are observed



during construction. The decision model allows one to choose the best or optimal strategy for a given geology amongst several construction strategies. When combined, a model that allows one to predict geology, and optimal construction strategy ahead of the tunnel machine is obtained. By doing so, risk can be assessed, and mitigated by selecting construction strategies that minimize risk. Regions of high risk can be anticipated, and measures taken to minimize the risk. This model was used for the Porto Metro Line C tunnel.

The results show that the model can predict changes in geology and suggests changes in construction strategy. This is most visible in the zone of accident 2 and 3, where the model accurately predicts the change in geology and occurrence of soil (as shown in Figure 6.91). The “optimal” construction strategy determined by the combined risk assessment model is EPBM in closed mode, i.e. with a fully pressurized face, in the areas where accident 2 and 3 occurred, and not what was actually used during construction, EPBM in open/semi closed mode. This difference is due to the fact that during the actual construction there was not an efficient system to predict changes in geologies and therefore adapt the construction strategy.

Thus the combined risk assessment model proved to work in predicting changes in geologies (through geological prediction model), namely in the areas of accident 2 and 3, and adapting construction strategy based on the predicted geological states ahead of the face. This is done through a decision model that allows one to chose amongst several construction strategies, the best or optimal strategy for a given geology.

### Alarm Criteria

Alarm criteria were developed to use in combination with the risk assessment model, with the goal to act as an alarm system that allows one to act promptly when the excavation is not behaving according to what is expected, and thus try to avoid major problems and accidents.

The focus was to develop an alarm criterion based on the total weight of the extracted material and its rate of change, since controlling the extracted weight is one of the most important tasks in the operation of the EPB machine.

The author suggests the following alarm criteria:

- Lower and upper limit on total extracted weight per ring
- Lower and upper limit on rate of change of extracted weight

The goal of these criteria is to issue an alarm whenever the measured value of the weight is above or below the theoretical limit or drastic changes in the weight of the extracted weight occur. Both of these situations may indicate that the machine is overexcavating (if extracted weight (or volume) is above the theoretical), or the machine entered a different geological formation.

When analyzing the extracted weight data in the Porto metro accident areas it seems that not only the weight of the extracted material was higher than the theoretical one, indicating that the machine was overexcavating and producing a probable cause for the accidents but also that there was a sudden increase in the rate of the weight extracted material, right before the zone of the accidents 2 and 3.

Finally, the author would like to mention that results analyses of the data do not intend to substitute the official Porto accident report results, nor attribute any guilt to any of the parties.

## **6.4 References**

Anagnostou G. and Kovari K., 1996: "Face stability conditions with Earth-Pressure-Balanced Shields". *Tunneling and Underground Space Technology*, Vol.11, No.2, pp 165-173;

Babendererde,S.; Hoek, E.; Marinos, P.G.; Cardoso, A.S. (2005). “EPB-TBM Face Support Control in the Metro do Porto Project, Portugal”. Proceedings 2005 Rapid Excavation & Tunneling Conference, Seattle

Babendererde, S, Hoek, E., Marinos, P. and Cardoso, A.S. (2004). “Characterization of Granite and the Underground Construction in Metro do Porto, Portugal.” Proc. International Conference on Site Characterization, Porto, Portugal, 19-22 September, 2004

Guglielmetti,V.; Grasso, P.; Gaj, F., Giacomini, G. (2003). “Mechanized tunneling in urban environment: control of ground response and face stability when excavating with EPB Machine”. (re)Claiming the underground space Saveur (Ed.)

Geodata (2001). New Guidelines for tunneling works. April 2001.

Transmetro (2000a). “Escolha do método de escavação com o uso da herrenknecht EPB-shield”. Technical report.

Transmetro (2000b). “Operação da tuneladora (TBM operation)”. Technical report.

Transmetro (2002a). Tunnel Line C - PAT n.03. Section between pk 0+906.7 and 1+125 (in Portuguese). Technical report.

Transmetro (2002b). “Tunnel Line C - PAT n.04. Section between pk 1+125 and pk 1+480.25” (in Portuguese). Technical report.

Transmetro (2002c). “Tunnel Line C - PAT n.05. Section between pk 1+480,25 and pk 2+160,52” (in Portuguese). Technical report.

Transmetro (2002d). “Tunnel Line C PAT n.06. Section between pk 2+160,52 and pk 2+450,68” (in Portuguese). Technical report.

T&TI, (2003). "Experience on Porto – EPB follow-up" Tunnels and Tunnelling, December 2003.

## 6.5 Appendix H – Training Data set A and B

### Training Data set A

RING	GC	CF	P	TO	TOC	TT	COTT
336	2	4880	10.26	2.33	0.48	34363	0.14
337	2	6677	10.65	6.84	1.02	29952	0.22
338	2	8205	8.18	5.64	0.69	26556	0.31
339	2	11326	7.77	5.34	0.47	31308	0.36
344	2	5611	10.79	1.99	0.35	26108	0.21
345	2	7858	8.25	3.56	0.45	30588	0.26
346	2	8850	8.34	5.48	0.62	31441	0.28
347	2	7820	5.87	6.27	0.80	33942	0.23
348	2	8927	9.40	5.69	0.64	33958	0.26
349	2	10912	6.70	6.28	0.58	35359	0.31
350	2	11043	7.40	6.50	0.59	35914	0.31
351	2	9991	12.00	7.18	0.72	33963	0.29
352	2	6752	4.50	3.08	0.46	33621	0.20
353	2	10250	9.00	8.00	0.78	30567	0.34
354	2	10547	6.50	7.01	0.66	33241	0.32
355	2	12134	4.44	6.00	0.49	33794	0.36
356	3	16230	4.50	7.21	0.44	33413	0.49
357	3	10753	3.15	5.73	0.53	27921	0.39
358	3	10766	4.34	6.85	0.64	24673	0.44
359	3	11618	4.50	6.34	0.55	26094	0.45
360	3	11722	3.06	5.16	0.44	32746	0.36
361	3	14591	3.65	6.44	0.44	29873	0.49
362	3	13653	3.31	5.91	0.43	32888	0.42
363	3	13733	4.37	7.08	0.52	30506	0.45
364	3	13171	4.49	6.21	0.47	27060	0.49
365	3	11235	3.80	5.78	0.51	29353	0.38
366	3	11953	3.56	6.45	0.54	31129	0.38
367	3	12859	3.81	7.89	0.61	29289	0.44
368	3	11163	2.79	4.96	0.44	25088	0.44
369	3	12928	3.04	6.44	0.50	26781	0.48
370	3	15526	4.27	8.04	0.52	28935	0.54
371	2	11470	4.50	7.95	0.69	25122	0.46
372	2	9450	4.44	7.55	0.80	23953	0.39
373	2	8504	5.35	5.52	0.65	23054	0.37
374	2	12293	4.10	6.31	0.51	28582	0.43
375	2	12194	4.06	6.78	0.56	31104	0.39
376	2	11628	3.88	6.32	0.54	29903	0.39
377	2	12523	3.38	5.62	0.45	31324	0.40
378	2	12381	4.38	6.96	0.56	29701	0.42
379	2	13612	4.29	6.54	0.48	31157	0.44
380	2	13885	4.16	6.29	0.45	32273	0.43
381	2	14581	4.80	8.11	0.56	32101	0.45
382	2	11623	8.15	6.34	0.55	27375	0.42
383	2	10505	5.13	8.10	0.77	24563	0.43

384	2	10519	5.27	7.75	0.74	25095	0.42
385	2	7896	7.18	6.27	0.79	25879	0.31
386	2	8043	5.24	7.23	0.90	27174	0.30
387	2	7675	5.13	7.16	0.93	27277	0.28
388	2	6565	4.64	5.44	0.83	29183	0.22
389	2	6486	5.16	5.07	0.78	32410	0.20
390	1	5793	5.53	4.33	0.75	36455	0.16
391	1	6906	5.60	6.51	0.94	38236	0.18
392	1	6770	5.96	6.90	1.02	36539	0.19
393	1	4811	5.21	2.35	0.49	33463	0.14
394	1	6226	5.06	5.58	0.90	32023	0.19
395	1	6468	5.08	7.44	1.15	28479	0.23
397	1	6314	5.56	7.48	1.18	26688	0.24
398	1	6865	7.32	7.96	1.16	26978	0.25
399	1	6402	7.62	7.30	1.14	26563	0.24
400	1	5760	8.25	7.16	1.24	26475	0.22
401	1	5087	8.30	6.04	1.19	27448	0.19
402	1	5162	5.38	7.65	1.48	28611	0.18
403	1	5047	6.24	7.69	1.52	28915	0.17
404	1	5236	7.56	7.62	1.46	29650	0.18
405	1	5681	7.39	7.57	1.33	30931	0.18
406	1	6175	6.03	7.86	1.27	32207	0.19
407	1	6300	6.35	7.80	1.24	33612	0.19
408	1	6196	6.26	7.03	1.13	35274	0.18
409	1	5681	4.32	5.29	0.93	38054	0.15
410	1	5243	6.24	6.21	1.18	39399	0.13
411	1	6012	6.62	6.91	1.15	37731	0.16
412	1	6154	6.25	7.26	1.18	34284	0.18
413	1	6476	7.58	7.81	1.21	37446	0.17
414	1	6535	8.17	7.99	1.22	39483	0.17
415	1	6271	8.50	7.82	1.25	38817	0.16
416	1	6370	10.36	8.01	1.26	38901	0.16
417	1	5723	11.39	7.23	1.26	35608	0.16
418	1	6861	10.07	7.71	1.12	34194	0.20
419	1	7510	10.82	8.13	1.08	36952	0.20
420	1	6520	7.49	6.72	1.03	34929	0.19
421	2	6221	5.28	5.97	0.96	37305	0.17
422	2	6605	4.88	5.50	0.83	39604	0.17
423	2	7040	5.33	6.12	0.87	39226	0.18
424	2	7351	3.42	3.52	0.48	40131	0.18
425	2	8398	5.49	5.69	0.68	37910	0.22
426	2	11139	5.79	8.25	0.74	33520	0.33
427	2	10350	4.72	8.04	0.78	30278	0.34
428	2	10944	4.87	8.09	0.74	30805	0.36
429	2	10033	4.33	7.97	0.79	29597	0.34
430	2	9660	5.28	7.96	0.82	27712	0.35
431	2	11982	4.92	8.33	0.69	27014	0.44
432	2	13725	4.14	7.67	0.56	29978	0.46
433	2	13291	4.52	7.80	0.59	31647	0.42
434	2	13149	5.85	7.42	0.56	28200	0.47



435	2	13306	4.32	8.15	0.61	26283	0.51
436	2	11241	3.39	5.35	0.48	26425	0.43
437	2	15936	4.03	7.16	0.45	31196	0.51
438	2	15095	3.06	5.94	0.39	30086	0.50
439	2	14795	3.22	7.43	0.50	29114	0.51
440	2	11071	2.74	2.82	0.25	25248	0.44
441	2	13707	2.75	4.85	0.35	28255	0.49
442	2	12413	3.44	6.29	0.51	30291	0.41
443	2	7530	4.18	3.89	0.52	21768	0.35
444	2	9262	5.52	7.96	0.86	24664	0.38
445	2	9082	4.69	7.92	0.87	25440	0.36
446	2	9644	4.36	7.51	0.78	26002	0.37
447	2	11766	4.87	7.69	0.65	28172	0.42
448	2	10368	3.78	3.97	0.38	26734	0.39
449	2	11663	3.94	5.65	0.48	29745	0.39
450	3	12304	4.59	7.72	0.63	27097	0.45
451	3	11752	4.46	7.86	0.67	26063	0.45
452	3	11060	4.57	7.71	0.70	26452	0.42
453	3	9067	5.20	4.58	0.51	28469	0.32
454	3	11631	4.21	7.67	0.66	29128	0.40
455	3	12861	3.97	7.96	0.62	28800	0.45
456	3	11574	3.84	6.85	0.59	27755	0.42
457	3	10977	8.80	7.21	0.66	23941	0.46
458	3	14394	6.55	7.47	0.52	29061	0.50
459	3	13795	3.96	7.34	0.53	30400	0.45
460	3	12985	3.36	7.97	0.61	29651	0.44
461	3	11104	2.84	7.15	0.64	35412	0.31
462	3	10481	1.95	5.27	0.50	38136	0.27
463	3	13142	4.44	6.16	0.47	34361	0.38
464	3	11988	3.57	6.72	0.56	32160	0.37
465	2	8069	4.36	5.43	0.67	27820	0.29
466	2	9004	5.29	6.68	0.74	27400	0.33
467	2	8871	4.76	7.70	0.87	27834	0.32
468	2	9741	5.71	8.28	0.85	25129	0.39
469	2	10111	5.58	7.75	0.77	29954	0.34
470	2	8323	6.50	7.56	0.91	33400	0.25
471	2	8004	7.08	8.48	1.06	29829	0.27
472	2	7881	6.47	7.49	0.95	29713	0.27
473	2	6658	6.00	5.20	0.78	32500	0.20
474	2	7655	6.08	7.96	1.04	33078	0.23
475	2	8615	6.87	7.96	0.92	32162	0.27
476	2	8867	5.56	7.54	0.85	35449	0.25
477	2	9986	5.50	5.05	0.51	35257	0.28
478	2	10190	6.20	8.28	0.81	31957	0.32
479	2	9550	5.96	8.25	0.86	27731	0.34
480	2	8672	6.40	7.97	0.92	24695	0.35
481	2	8499	6.76	8.20	0.96	23953	0.35
482	2	8786	6.71	8.14	0.93	24289	0.36
483	2	6466	7.81	6.29	0.97	25282	0.26
484	2	8182	9.43	7.18	0.88	29029	0.28

485	2	12343	8.63	7.74	0.63	33412	0.37
486	2	14877	6.65	7.56	0.51	37629	0.40
487	2	8983	6.07	6.90	0.77	30727	0.29
488	2	8043	9.44	7.75	0.96	27067	0.30
489	2	7708	9.39	7.79	1.01	28794	0.27
490	2	4826	8.43	7.79	1.61	23940	0.20
491	2	8469	7.02	7.79	0.92	26669	0.32
498	2	7127	17.14	7.93	1.11	24455	0.29
499	2	13593	10.95	8.60	0.63	30706	0.44
500	2	15527	7.23	7.60	0.49	30681	0.51
501	2	14614	5.33	7.38	0.50	30546	0.48
502	2	7378	5.75	4.01	0.54	25409	0.29
503	2	6931	8.64	7.55	1.09	24489	0.28
504	2	5570	7.45	7.34	1.32	25171	0.22
505	2	5048	6.81	7.39	1.46	25087	0.20
506	2	6886	7.09	8.10	1.18	26258	0.26
507	2	7775	6.17	7.73	0.99	26854	0.29
508	2	7577	5.97	7.33	0.97	27997	0.27
509	2	6946	6.12	7.57	1.09	27009	0.26
510	2	6407	8.51	6.61	1.03	26269	0.24
511	2	6827	7.21	7.80	1.14	29127	0.23
512	2	6788	6.29	7.34	1.08	31165	0.22
513	2	6199	6.34	7.81	1.26	33208	0.19
514	2	6233	6.35	7.88	1.26	33839	0.18
515	2	6906	7.29	8.21	1.19	32594	0.21
516	2	7148	6.68	8.03	1.12	31547	0.23
517	2	6974	7.02	8.14	1.17	29419	0.24
518	2	6935	6.30	7.19	1.04	30405	0.23
519	2	6980	7.04	8.40	1.20	33108	0.21
520	2	6396	7.09	7.39	1.16	31772	0.20
521	2	6983	7.25	7.94	1.14	30352	0.23
522	2	7076	7.54	7.90	1.12	34652	0.20
523	2	6709	7.79	7.78	1.16	32218	0.21
524	2	4492	6.90	4.18	0.93	24188	0.19
525	2	4945	8.01	4.41	0.89	21653	0.23
526	2	8405	14.61	8.20	0.98	24332	0.35
527	2	6371	7.56	7.31	1.15	21377	0.30
528	2	5613	8.44	6.86	1.22	21398	0.26
529	1	6869	13.86	6.74	0.98	26810	0.26
530	1	7180	13.06	6.50	0.91	24192	0.30
531	1	8353	14.12	8.42	1.01	22545	0.37
532	1	9059	17.81	7.77	0.86	22550	0.40
533	1	6793	8.00	7.61	1.12	19853	0.34
535	1	6785	12.04	5.02	0.74	23947	0.28
536	1	11681	8.03	7.02	0.60	26651	0.44
537	1	11239	9.06	7.32	0.65	28713	0.39
538	1	6786	8.99	6.58	0.97	26570	0.26
539	1	10473	20.58	7.18	0.69	27504	0.38
540	1	10166	19.66	7.41	0.73	26007	0.39
541	1	8353	13.69	4.70	0.56	24002	0.35

542	1	9131	14.30	5.34	0.58	23918	0.38
543	1	6313	9.82	6.08	0.96	20536	0.31
544	1	4317	7.53	5.86	1.36	21125	0.20
545	1	3742	9.92	4.17	1.12	20803	0.18
546	1	4941	18.54	5.57	1.13	19436	0.25
547	1	8398	15.72	5.74	0.68	23538	0.36
548	1	11989	12.44	8.05	0.67	27170	0.44
549	1	14928	7.58	7.63	0.51	28788	0.52
550	1	13453	6.04	7.64	0.57	27940	0.48
551	1	13196	6.38	7.45	0.56	28425	0.46
552	1	7460	8.88	6.11	0.82	24165	0.31
553	1	6614	6.92	7.92	1.20	25675	0.26
554	1	6923	6.78	7.58	1.10	29961	0.23
555	1	5820	6.75	6.83	1.17	29664	0.20
556	1	5359	6.36	6.59	1.23	27071	0.20
557	1	4835	5.90	6.07	1.26	25883	0.19
558	1	4565	7.00	4.51	0.99	28462	0.16
559	1	4878	7.03	7.28	1.49	30303	0.16
560	1	4741	7.83	7.89	1.66	29045	0.16
561	1	4415	8.82	6.89	1.56	29308	0.15
562	1	4129	6.97	6.28	1.52	28326	0.15
563	1	4361	7.07	6.89	1.58	30902	0.14
564	2	4331	8.18	7.49	1.73	29035	0.15
565	2	5121	10.48	8.07	1.58	28355	0.18
566	2	4812	9.25	6.43	1.34	24802	0.19
567	2	5328	7.87	5.36	1.01	26307	0.20
568	2	5284	7.67	5.65	1.07	24766	0.21
569	2	4871	6.86	5.37	1.10	26209	0.19
570	2	5595	7.50	6.53	1.17	28572	0.20
571	2	5400	10.12	5.22	0.97	28454	0.19
572	2	6233	9.22	7.50	1.20	29617	0.21
573	2	6015	8.69	6.29	1.04	26523	0.23
574	2	6525	8.88	7.17	1.10	24915	0.26
575	2	6107	7.80	6.71	1.10	24521	0.25
576	2	6628	8.68	7.68	1.16	24734	0.27
577	2	6421	8.24	7.12	1.11	23924	0.27
578	2	6806	7.97	8.01	1.18	26755	0.25
579	2	7490	10.35	7.16	0.96	27739	0.27
580	2	8103	7.21	8.19	1.01	26333	0.31
581	2	8553	6.80	8.01	0.94	24415	0.35
582	2	8705	6.57	7.84	0.90	24230	0.36
583	2	10009	6.45	7.54	0.75	27134	0.37
584	2	11239	6.04	8.04	0.72	28450	0.40
585	2	10464	5.83	7.67	0.73	28901	0.36
586	2	8867	5.19	7.85	0.89	29277	0.30
587	2	9369	4.38	6.55	0.70	30795	0.30
588	2	7312	4.58	4.41	0.60	30862	0.24
589	2	10100	5.68	7.42	0.73	36692	0.28
590	2	9749	5.25	7.44	0.76	36295	0.27
591	2	8364	4.03	5.29	0.63	34780	0.24

592	2	9107	4.34	5.59	0.61	32974	0.28
593	2	8515	5.38	7.36	0.86	32677	0.26
594	2	6355	8.33	6.28	0.99	28769	0.22
595	2	5785	7.17	7.45	1.29	28304	0.20
596	2	5693	7.36	7.25	1.27	28449	0.20
597	2	6041	7.54	7.74	1.28	26390	0.23
598	2	7586	6.99	7.85	1.04	28736	0.26
599	2	7689	8.62	6.84	0.89	28106	0.27
600	2	7447	7.14	7.71	1.04	29208	0.25
601	2	6328	7.09	6.87	1.09	30043	0.21
602	2	6821	6.86	7.23	1.06	30874	0.22
603	2	6204	6.74	6.83	1.10	33574	0.18
604	2	6073	6.37	6.19	1.02	34179	0.18
605	2	6103	6.72	6.10	1.00	36518	0.17
606	1	5548	12.88	6.75	1.22	35531	0.16
607	1	7236	8.02	7.91	1.09	33898	0.21
608	1	6585	7.65	7.75	1.18	31242	0.21
609	1	6905	8.10	7.84	1.14	31980	0.22
610	1	6196	7.82	7.42	1.20	31589	0.20
611	1	5593	7.40	6.83	1.22	32536	0.17
612	1	5863	7.67	7.45	1.27	33982	0.17
613	1	5012	7.39	7.11	1.42	34526	0.15
614	1	4415	7.81	3.73	0.84	35256	0.13
615	1	5595	8.97	6.61	1.18	34945	0.16
616	1	4651	10.73	4.57	0.98	29532	0.16
617	1	5387	11.40	7.24	1.34	29445	0.18
618	1	4579	9.61	6.16	1.35	28532	0.16
619	1	4791	10.21	6.12	1.28	27637	0.17
620	1	5944	16.97	6.03	1.01	27048	0.22
621	1	6119	10.35	7.11	1.16	29086	0.21
622	1	6179	10.13	7.84	1.27	30636	0.20
623	1	4604	8.78	4.97	1.08	27443	0.17
624	1	4166	9.18	4.14	0.99	24410	0.17
625	1	4585	11.73	6.17	1.35	23459	0.20
626	1	5477	9.74	6.89	1.26	24839	0.22
627	1	4950	9.59	6.22	1.26	26601	0.19
628	1	5295	11.91	7.83	1.48	25416	0.21
629	1	5360	12.17	8.14	1.52	24353	0.22
630	1	5101	12.01	7.57	1.48	23873	0.21
631	1	4917	15.71	3.43	0.70	24339	0.20
632	1	6645	15.67	7.27	1.09	26308	0.25
633	1	7317	11.23	8.23	1.12	29215	0.25
634	2	7789	7.53	7.62	0.98	32828	0.24
635	2	8952	5.76	6.75	0.75	39423	0.23
636	2	6064	3.06	2.98	0.49	40653	0.15
637	3	9585	3.29	5.12	0.53	43222	0.22
638	3	9950	2.96	6.04	0.61	43347	0.23
639	3	8713	2.37	3.09	0.35	43047	0.20
640	3	13879	3.45	7.79	0.56	44321	0.31
641	3	11120	2.26	6.03	0.54	44433	0.25

642	3	12541	3.14	7.33	0.58	41654	0.30
643	3	12347	5.04	6.57	0.53	31742	0.39
644	3	10986	3.62	7.55	0.69	33402	0.33
645	3	10890	4.00	7.83	0.72	36193	0.30
646	2	12784	4.62	8.48	0.66	38399	0.33
647	2	10733	4.62	8.57	0.80	34997	0.31
648	2	11459	4.74	8.87	0.77	36003	0.32
649	2	11897	4.84	7.61	0.64	34458	0.35
650	2	12479	3.65	7.77	0.62	39724	0.31
651	2	11247	3.19	5.92	0.53	40902	0.27
652	2	13317	4.74	8.37	0.63	40086	0.33
653	2	10585	4.04	8.14	0.77	42218	0.25
654	2	9924	4.27	8.39	0.85	42406	0.23
655	2	8964	5.89	6.59	0.74	41213	0.22
656	2	9723	5.27	8.83	0.91	39097	0.25
657	2	8933	3.91	7.59	0.85	41925	0.21
658	2	8996	3.65	6.79	0.75	44742	0.20
659	1	9849	4.55	7.65	0.78	41790	0.24
660	1	9020	8.82	7.42	0.82	35400	0.25
661	1	9740	5.39	7.80	0.80	32873	0.30
662	1	9531	6.06	8.21	0.86	27713	0.34
663	1	8566	6.56	8.06	0.94	34154	0.25
664	1	8763	5.81	8.35	0.95	40398	0.22
665	1	7869	6.03	8.19	1.04	40746	0.19
666	1	8511	6.45	7.96	0.93	38941	0.22
667	1	9214	7.12	7.03	0.76	38241	0.24
668	1	8374	6.94	7.91	0.94	37026	0.23
669	1	9321	6.77	7.82	0.84	39330	0.24
670	1	9169	5.81	7.15	0.78	41767	0.22
671	1	9504	4.22	5.08	0.53	45225	0.21
672	1	11000	4.09	6.08	0.55	44789	0.25
673	1	9287	4.77	4.57	0.49	40988	0.23
674	1	8296	7.44	6.92	0.83	40016	0.21
675	1	7164	8.57	8.27	1.15	38086	0.19
676	1	7535	9.04	8.38	1.11	34269	0.22
677	1	7890	8.42	8.50	1.08	32657	0.24
678	2	7986	7.97	7.91	0.99	33413	0.24
679	2	8036	7.86	7.95	0.99	35397	0.23
680	2	8150	8.07	8.03	0.99	36777	0.22
681	2	7373	7.48	7.33	0.99	37282	0.20
682	2	7324	8.46	7.82	1.07	36832	0.20
683	2	7578	8.32	6.88	0.91	33638	0.23
684	2	6394	6.80	5.14	0.80	33936	0.19
685	2	7494	10.73	8.07	1.08	37456	0.20
686	2	7462	10.61	7.15	0.96	36256	0.21
687	2	6541	10.85	6.46	0.99	33186	0.20
688	2	8273	11.21	7.43	0.90	32719	0.25
689	2	9228	10.38	7.94	0.86	32944	0.28
690	2	9885	9.15	6.91	0.70	33226	0.30
691	2	9017	9.13	6.55	0.73	30484	0.30

692	2	8493	9.92	6.60	0.78	28163	0.30
693	2	7279	9.39	7.42	1.02	24975	0.29
694	2	8285	10.69	7.60	0.92	25192	0.33
695	2	8711	10.52	7.11	0.82	26433	0.33
696	2	8889	10.02	7.63	0.86	25102	0.35
697	2	8527	9.88	7.09	0.83	24804	0.34
698	1	8355	10.69	7.73	0.93	26041	0.32
699	1	8512	11.12	8.40	0.99	26797	0.32
700	1	8213	10.78	7.73	0.94	27283	0.30
701	1	7791	10.61	7.61	0.98	27265	0.29
702	1	8226	12.85	8.14	0.99	28044	0.29
703	1	7963	10.20	7.71	0.97	26640	0.30
704	1	8413	10.93	8.02	0.95	25873	0.33
705	1	8472	9.83	8.02	0.95	27616	0.31
706	1	8252	8.03	7.39	0.90	28023	0.29
707	1	8088	7.77	7.19	0.89	27422	0.29
708	1	7871	7.98	7.71	0.98	27232	0.29
709	1	7547	7.77	7.87	1.04	27866	0.27
710	1	8599	7.46	7.61	0.89	32995	0.26
711	1	8478	6.78	7.66	0.90	31067	0.27
712	1	8606	5.30	7.31	0.85	30825	0.28
713	1	8569	5.58	6.55	0.76	31383	0.27
714	1	8447	6.72	5.58	0.66	32415	0.26
715	1	8909	6.90	7.12	0.80	29943	0.30
716	1	7708	12.01	5.45	0.71	31883	0.24
717	1	11209	10.69	7.98	0.71	31872	0.35
718	1	9252	6.99	7.46	0.81	29242	0.32
719	2	9301	7.92	7.83	0.84	30462	0.31
720	2	9504	8.06	7.96	0.84	31431	0.30
721	2	9897	7.71	8.10	0.82	33166	0.30
723	2	8861	6.21	8.16	0.92	34617	0.26
724	2	10352	5.44	8.00	0.77	34420	0.30
725	2	9401	6.90	6.56	0.70	32478	0.29
726	2	6763	9.81	6.53	0.97	30149	0.22
727	2	7317	9.35	7.47	1.02	29520	0.25
728	2	8177	6.14	7.88	0.96	27487	0.30
729	1	8211	6.17	8.31	1.01	27721	0.30
730	1	8254	6.36	8.38	1.02	28674	0.29
731	1	8227	6.56	8.27	1.01	30100	0.27
732	1	8899	14.24	6.24	0.70	31015	0.29
733	1	8384	9.34	7.45	0.89	30687	0.27
734	1	8358	8.13	7.67	0.92	27648	0.30
735	1	8331	8.24	8.09	0.97	29244	0.28
736	1	8078	8.96	6.94	0.86	30022	0.27
737	1	10548	8.47	7.63	0.72	31103	0.34
738	1	10680	11.07	6.72	0.63	30756	0.35
739	1	9001	7.01	8.18	0.91	30415	0.30
740	1	7582	10.25	6.18	0.81	30211	0.25
741	1	9327	7.56	8.07	0.87	32096	0.29
742	1	8825	6.16	7.79	0.88	32336	0.27



743	1	8153	6.26	7.99	0.98	33146	0.25
744	1	8234	6.73	7.59	0.92	33321	0.25
745	1	7038	8.81	7.27	1.03	34993	0.20
746	2	6928	7.72	8.23	1.19	34485	0.20
747	2	7981	7.04	8.24	1.03	32348	0.25
748	2	8637	5.80	7.73	0.90	35794	0.24
749	2	8621	5.53	7.58	0.88	37259	0.23
750	2	8647	11.20	7.78	0.90	35186	0.25
751	2	7621	6.67	5.52	0.72	33323	0.23
752	2	7679	8.50	4.98	0.65	32570	0.24
753	2	8481	7.82	5.73	0.68	30726	0.28
754	2	9243	6.12	7.95	0.86	28202	0.33
755	2	8506	5.63	7.99	0.94	27629	0.31
756	2	8330	7.05	6.59	0.79	30057	0.28
757	2	11783	9.25	6.85	0.58	34658	0.34
758	2	11372	5.14	7.27	0.64	30776	0.37
759	2	10830	5.31	7.49	0.69	36073	0.30
766	2	13466	5.73	5.60	0.42	32410	0.42
767	2	13339	6.62	6.94	0.52	32294	0.41
768	1	13329	5.19	5.67	0.43	33705	0.40
769	1	11201	4.51	7.01	0.63	32297	0.35
770	1	10269	4.71	7.63	0.74	33399	0.31
771	1	9351	5.31	8.04	0.86	33688	0.28
772	1	6637	6.79	4.81	0.72	31739	0.21
773	1	9112	7.43	7.87	0.86	32141	0.28
774	1	8400	6.99	7.82	0.93	30306	0.28
775	1	8009	8.32	7.57	0.95	31894	0.25
776	1	8700	8.43	7.77	0.89	30722	0.28
777	1	9360	7.55	7.77	0.83	30797	0.30
778	1	10039	7.13	7.90	0.79	33391	0.30
792	2	6377	7.40	5.88	0.92	39023	0.16
793	2	6412	7.49	5.40	0.84	38802	0.17
794	2	7969	7.54	4.55	0.57	36747	0.22
795	2	9862	7.11	7.71	0.78	36473	0.27
796	2	9201	6.84	7.42	0.81	34872	0.26
797	2	9174	9.06	8.23	0.90	38546	0.24
798	2	10395	9.27	8.42	0.81	40329	0.26
799	2	13083	7.86	7.97	0.61	41543	0.31
800	3	14302	7.03	7.66	0.54	41203	0.35
801	3	12270	5.68	6.44	0.52	37046	0.33
802	3	12928	5.30	7.84	0.61	36280	0.36
803	3	12903	5.85	7.70	0.60	35327	0.37
804	3	12686	5.84	8.03	0.63	38765	0.33
805	3	13115	6.29	8.50	0.65	39109	0.34
806	3	11681	5.16	6.33	0.54	38389	0.30
807	3	12551	6.07	7.43	0.59	38530	0.33
808	3	11528	5.12	7.35	0.64	37455	0.31
809	3	10749	4.73	7.14	0.66	39253	0.27
810	3	11719	4.65	7.57	0.65	37914	0.31
811	2	10443	4.90	6.26	0.60	37895	0.28

812	2	10953	5.45	7.98	0.73	36624	0.30
813	2	10239	4.65	7.40	0.72	34428	0.30
814	2	7991	4.27	4.70	0.59	34974	0.23
815	2	9942	4.13	5.89	0.59	38431	0.26
816	2	7146	2.32	3.71	0.52	39346	0.18
817	3	9565	4.31	7.06	0.74	42134	0.23
818	3	6695	3.15	4.10	0.61	37762	0.18
819	3	8575	3.71	5.76	0.67	32585	0.26
820	3	10234	4.55	7.08	0.69	38540	0.27
821	3	9814	4.64	7.43	0.76	42102	0.23
822	3	9104	4.29	6.44	0.71	43106	0.21
823	3	7828	3.86	4.77	0.61	40324	0.19
824	3	7277	2.92	3.94	0.54	39033	0.19
825	3	7562	3.83	5.32	0.70	37611	0.20
826	3	6919	3.65	5.53	0.80	39677	0.17
827	3	5345	3.18	2.43	0.45	39952	0.13
829	3	6931	6.04	5.43	0.78	36822	0.19
830	3	7763	8.43	7.23	0.93	43144	0.18
831	3	7616	10.51	7.81	1.03	39390	0.19
832	3	8237	6.93	6.68	0.81	39930	0.21
833	3	10914	6.13	8.11	0.74	39787	0.27
834	3	10223	4.62	7.55	0.74	38457	0.27
835	3	9782	6.03	5.92	0.61	32676	0.30
836	3	12042	5.49	7.42	0.62	40227	0.30
837	3	12185	5.16	7.30	0.60	39909	0.31
838	3	10555	3.43	5.30	0.50	43254	0.24
839	3	11660	4.82	5.87	0.50	40712	0.29
840	3	13683	4.09	7.11	0.52	40438	0.34
841	3	11930	3.13	6.52	0.55	42942	0.28
842	3	12398	3.17	7.98	0.64	44847	0.28
843	3	9624	3.24	2.73	0.28	37523	0.26
844	3	12809	4.68	7.23	0.56	38228	0.34
845	3	13506	4.11	7.66	0.57	40845	0.33
846	3	11915	3.09	7.14	0.60	43714	0.27
847	3	11243	4.24	4.37	0.39	41638	0.27
848	3	14353	4.93	7.63	0.53	35210	0.41
849	3	13286	5.27	7.97	0.60	40905	0.32
850	3	11339	4.47	7.84	0.69	40018	0.28
851	3	9993	4.85	7.53	0.75	42184	0.24
852	3	10464	6.00	6.15	0.59	41867	0.25
853	3	13391	6.89	7.03	0.52	38740	0.35
854	3	14531	4.08	6.52	0.45	34405	0.42
855	3	11659	4.13	5.28	0.45	34062	0.34
856	3	12314	4.44	7.93	0.64	34084	0.36
905	2	6069	12.43	7.13	1.17	27028	0.22
906	1	6054	12.02	6.92	1.14	24301	0.25
907	1	5860	14.11	6.69	1.14	24565	0.24
908	1	6026	14.65	7.19	1.19	25494	0.24
909	1	5978	15.43	7.30	1.22	23349	0.26
910	1	5484	11.88	7.92	1.44	22167	0.25

911	1	6627	11.74	8.08	1.22	22499	0.29
913	1	4739	12.70	2.35	0.50	19761	0.24
914	1	9654	9.38	6.22	0.64	22369	0.43
915	1	4361	16.14	6.13	1.41	16612	0.26
916	1	4435	13.90	6.85	1.55	17932	0.25
917	1	4489	12.97	6.80	1.52	18940	0.24
918	1	4612	14.75	7.11	1.54	19593	0.24
919	1	4319	12.57	5.56	1.29	21527	0.20
931	3	10408	7.26	7.51	0.72	28670	0.36
932	3	10250	7.61	6.56	0.64	24212	0.42
933	3	9666	7.41	6.10	0.63	26396	0.37
934	3	10465	8.35	7.28	0.70	25978	0.40
935	3	9995	7.35	7.47	0.75	26574	0.38
936	3	9247	8.59	7.95	0.86	24933	0.37
937	3	8798	8.53	7.89	0.90	25646	0.34
938	3	8552	10.37	6.16	0.72	22331	0.38
939	3	9711	9.45	7.42	0.76	25678	0.38
940	3	7392	4.84	3.89	0.53	35869	0.21
941	3	10655	7.64	7.52	0.71	31109	0.34
942	3	11342	7.14	6.97	0.61	31624	0.36
960	3	6521	10.78	6.39	0.98	27196	0.24
964	3	8523	9.11	7.61	0.89	35009	0.24
965	3	8625	6.78	7.33	0.85	35836	0.24
966	3	9720	8.30	7.52	0.77	37001	0.26
967	3	10710	7.45	7.59	0.71	35083	0.31
968	3	8748	6.66	6.70	0.77	33294	0.26
969	3	10937	9.34	6.80	0.62	32414	0.34
970	3	12137	8.21	7.72	0.64	34179	0.36
971	3	11253	6.30	5.45	0.48	38676	0.29
972	3	12850	7.92	7.56	0.59	37431	0.34
973	3	12966	7.64	7.35	0.57	33848	0.38
974	3	12148	7.49	6.43	0.53	30098	0.40
975	3	13212	7.92	7.46	0.56	27297	0.48
976	3	13266	7.69	7.37	0.56	28126	0.47
977	3	14011	7.89	7.38	0.53	31093	0.45
978	3	14137	7.67	6.69	0.47	38506	0.37
979	3	9537	3.62	3.09	0.32	39813	0.24
1006	3	9988	7.68	7.32	0.73	32550	0.31
1007	3	9434	8.05	7.94	0.84	31839	0.30
1008	3	9476	8.02	7.92	0.84	32227	0.29
1009	3	9124	7.21	7.87	0.86	34852	0.26
1010	3	10176	6.87	7.54	0.74	34626	0.29
1011	3	10360	6.35	7.21	0.70	34103	0.30
1012	3	11696	4.96	5.69	0.49	39275	0.30
1013	3	13232	6.07	8.06	0.61	37497	0.35
1014	3	12280	4.87	7.22	0.59	38862	0.32
1015	3	11691	4.06	7.42	0.63	40416	0.29
1016	3	7322	10.26	6.18	0.84	30981	0.24
1017	3	9744	6.42	7.79	0.80	29184	0.33
1018	3	11464	6.38	7.83	0.68	35008	0.33

1019	3	10600	6.19	7.25	0.68	37448	0.28
1020	3	8787	9.67	6.62	0.75	32396	0.27
1021	3	10145	7.84	7.99	0.79	29127	0.35
1022	3	9931	6.79	7.46	0.75	33237	0.30
1023	3	9643	6.82	7.46	0.77	36819	0.26
1024	1	8866	6.38	7.55	0.85	39085	0.23
1025	1	8235	5.95	7.08	0.86	34926	0.24
1026	1	7436	6.32	7.34	0.99	34711	0.21
1027	1	8041	7.04	7.73	0.96	37763	0.21
1028	1	6311	5.89	3.18	0.50	36714	0.17
1029	1	8198	7.42	6.47	0.79	37614	0.22
1030	1	7838	8.27	7.06	0.90	35241	0.22
1031	1	7989	9.16	7.28	0.91	33823	0.24
1032	1	7977	9.96	7.55	0.95	33332	0.24
1033	1	7779	8.91	7.08	0.91	33626	0.23
1034	1	7158	8.51	7.23	1.01	31344	0.23
1035	1	6610	8.36	6.68	1.01	30767	0.21
1036	1	6542	9.95	7.31	1.12	30835	0.21
1037	1	4832	11.33	3.23	0.67	25032	0.19
1038	1	5619	12.69	6.28	1.12	26596	0.21
1039	1	5061	11.39	6.48	1.28	24511	0.21
1040	1	5228	13.39	6.57	1.26	27214	0.19
1041	1	4411	10.02	4.60	1.04	23726	0.19
1042	1	4327	11.49	4.37	1.01	22774	0.19
1043	1	4694	18.18	6.16	1.31	22591	0.21
1044	1	4872	16.59	6.47	1.33	22676	0.21
1045	1	5570	15.03	6.73	1.21	23657	0.24
1046	1	5156	14.81	3.83	0.74	23184	0.22
1047	1	5829	13.55	6.49	1.11	26657	0.22
1048	1	6228	12.21	7.35	1.18	27581	0.23
1049	1	6661	10.11	6.51	0.98	27884	0.24
1050	1	6792	8.77	6.16	0.91	30133	0.23
1051	1	7057	8.96	7.15	1.01	30613	0.23
1052	1	7279	7.62	7.04	0.97	32412	0.22
1075	3	7231	6.95	7.74	1.07	42737	0.17
1076	3	6966	7.39	5.19	0.74	39260	0.18
1077	3	9175	6.74	7.65	0.83	39042	0.24
1078	3	9233	5.87	7.10	0.77	38791	0.24
1079	3	8438	4.49	6.46	0.77	43102	0.20
1080	3	7458	3.16	5.76	0.77	45348	0.16
1081	3	6876	3.68	3.37	0.49	44413	0.15
1082	3	8513	2.74	4.94	0.58	44530	0.19
1083	3	8575	3.09	4.80	0.56	44195	0.19
1084	3	6698	1.79	3.22	0.48	45110	0.15
1085	3	7807	2.57	2.97	0.38	42141	0.19
1086	3	9044	1.96	4.23	0.47	42497	0.21
1087	3	8361	1.83	4.46	0.53	45158	0.19
1088	3	7600	3.33	3.08	0.41	43254	0.18
1089	3	10404	4.27	7.20	0.69	43414	0.24
1101	3	12268	4.41	7.74	0.63	40274	0.30

1102	3	11184	5.21	6.02	0.54	37518	0.30
1103	3	10982	4.32	7.26	0.66	26208	0.42
1104	3	9133	3.70	6.84	0.75	27445	0.33
1105	3	9788	5.40	7.72	0.79	31587	0.31
1106	3	8945	5.67	7.55	0.84	37757	0.24
1107	3	8402	6.31	7.67	0.91	40208	0.21
1108	3	8531	6.11	5.70	0.67	34815	0.25
1109	3	9315	5.61	7.30	0.78	32170	0.29
1110	3	9778	4.13	7.31	0.75	34169	0.29
1111	3	10723	4.59	7.86	0.73	41757	0.26
1112	3	10094	4.87	5.70	0.56	41198	0.25
1113	3	11412	4.27	7.17	0.63	35677	0.32
1114	3	11211	3.77	7.15	0.64	35611	0.31
1115	3	11929	4.65	7.83	0.66	40960	0.29
1116	3	10147	5.07	5.74	0.57	38737	0.26
1117	3	10839	3.78	7.20	0.66	35831	0.30
1118	3	9906	3.28	6.90	0.70	30367	0.33
1119	3	10306	5.19	6.89	0.67	34088	0.30
1120	3	10083	3.19	7.17	0.71	32317	0.31
1121	3	10016	3.69	7.13	0.71	35145	0.28
1122	3	11203	4.08	7.76	0.69	39118	0.29
1123	3	9680	3.72	4.26	0.44	40160	0.24
1124	3	10518	3.44	6.69	0.64	40449	0.26
1125	3	10005	3.96	6.34	0.63	36850	0.27
1126	3	11316	4.74	7.01	0.62	40394	0.28
1127	3	10634	4.88	6.63	0.62	38153	0.28
1128	3	10088	6.87	6.57	0.65	33370	0.30
1129	3	11053	5.14	7.10	0.64	34260	0.32
1130	3	10747	4.74	6.82	0.63	38527	0.28
1131	3	10730	3.77	6.56	0.61	45212	0.24
1132	3	7580	2.20	3.10	0.41	41897	0.18
1133	3	10401	4.77	5.44	0.52	40696	0.26
1134	3	12022	4.42	6.70	0.56	39160	0.31
1135	3	10542	3.19	6.23	0.59	42233	0.25
1136	3	10974	3.52	6.17	0.56	44217	0.25
1137	3	9537	2.85	5.20	0.54	44293	0.22
1138	3	9597	4.19	4.99	0.52	44003	0.22
1139	3	11963	3.31	7.46	0.62	35395	0.34
1140	3	11106	2.80	5.91	0.53	39391	0.28
1141	3	10253	3.31	5.40	0.53	41303	0.25
1143	3	11911	3.07	6.61	0.55	28985	0.41
1144	3	11226	4.10	7.37	0.66	31623	0.36
1145	3	10786	4.22	7.08	0.66	27092	0.40
1146	3	12205	3.81	6.39	0.52	33407	0.37
1147	3	10646	3.32	4.50	0.42	40804	0.26
1148	3	13532	3.36	6.75	0.50	43247	0.31
1149	3	14185	3.61	7.05	0.50	37904	0.37
1150	3	15676	3.50	7.51	0.48	32356	0.48
1151	3	14525	3.06	5.24	0.36	33971	0.43
1152	3	13642	2.39	4.82	0.35	41487	0.33

1153	3	13732	2.08	5.79	0.42	35875	0.38
1154	3	11342	1.69	3.21	0.28	26569	0.43
1155	3	11141	1.17	2.98	0.27	26917	0.41
1156	3	9688	2.36	2.67	0.28	26412	0.37
1157	3	11035	4.29	5.36	0.49	30640	0.36
1158	3	11691	3.89	5.13	0.44	31953	0.37
1159	3	12108	3.21	5.00	0.41	31951	0.38
1171	3	13680	2.61	4.71	0.34	28576	0.48
1172	3	11616	3.02	4.13	0.36	32697	0.36
1173	3	14123	4.08	6.16	0.44	30246	0.47
1174	3	13990	4.30	7.09	0.51	26432	0.53
1175	3	12889	5.04	6.87	0.53	28429	0.45
1176	3	13661	5.47	6.37	0.47	30483	0.45
1177	3	12783	4.28	5.33	0.42	30636	0.42
1178	3	12906	3.99	5.38	0.42	29182	0.44
1179	3	12674	4.19	6.01	0.47	30209	0.42
1180	3	10615	3.32	3.97	0.37	33487	0.32
1181	3	11395	3.66	5.66	0.50	38699	0.29
1182	3	11602	2.70	4.43	0.38	41356	0.28
1183	3	13450	4.39	4.60	0.34	28373	0.47
1184	3	13940	4.03	6.64	0.48	30933	0.45
1185	3	13198	4.76	6.57	0.50	30321	0.44
1186	3	12587	4.49	4.93	0.39	35643	0.35
1187	3	12938	4.04	4.59	0.35	40608	0.32
1188	3	12195	3.38	4.48	0.37	35719	0.34
1189	3	13863	3.40	5.93	0.43	33390	0.42
1190	3	11999	2.74	5.25	0.44	34520	0.35
1191	3	9246	1.69	3.93	0.43	41651	0.22
1192	3	9325	2.66	3.19	0.34	40511	0.23
1193	3	13884	3.97	6.23	0.45	32411	0.43
1194	3	12322	3.06	5.50	0.45	34970	0.35
1195	3	8794	1.41	3.21	0.36	43338	0.20
1196	3	10703	2.89	3.36	0.31	40967	0.26
1197	3	13935	4.18	6.67	0.48	32583	0.43
1198	3	12693	4.10	6.72	0.53	37541	0.34
1199	3	9191	2.24	4.01	0.44	44057	0.21
1221	3	9750	7.96	7.59	0.78	36256	0.27
1222	3	8889	8.28	8.01	0.90	35816	0.25
1223	3	9262	8.80	8.16	0.88	36779	0.25
1224	1	9740	10.14	7.77	0.80	37546	0.26
1225	1	8149	9.00	7.91	0.97	33567	0.24
1226	1	8550	9.95	7.07	0.83	34979	0.24
1227	1	9140	10.79	7.94	0.87	34446	0.27
1228	1	8845	10.37	7.19	0.81	31903	0.28
1229	1	9858	10.75	7.29	0.74	33422	0.29
1230	1	6883	10.73	3.83	0.56	29576	0.23
1231	1	10856	9.62	7.94	0.73	31717	0.34
1232	1	12059	9.30	7.48	0.62	35251	0.34
1233	1	12720	8.33	7.36	0.58	36890	0.34
1234	1	12772	7.36	7.45	0.58	38328	0.33



1235	1	13820	6.69	6.73	0.49	40628	0.34
1236	1	11510	7.31	7.34	0.64	39228	0.29
1237	1	7020	8.36	2.86	0.41	33731	0.21
1238	1	11366	7.80	7.63	0.67	32887	0.35
1239	1	13850	6.44	7.29	0.53	34798	0.40
1240	1	13463	6.29	7.21	0.54	35034	0.38
1241	1	11470	6.28	7.47	0.65	32657	0.35
1242	1	11809	6.27	7.63	0.65	36124	0.33
1243	1	12159	5.74	7.52	0.62	37074	0.33
1244	1	5803	1.97	2.04	0.35	38614	0.15
1245	1	7643	2.94	3.94	0.52	41231	0.19
1246	1	10757	4.59	6.78	0.63	39179	0.27
1278	1	5196	4.31	2.37	0.46	35545	0.15
1279	1	8075	9.53	6.18	0.77	37296	0.22
1280	1	9557	8.39	7.38	0.77	38115	0.25
1281	1	8219	7.46	6.93	0.84	37865	0.22
1282	1	9489	7.84	7.36	0.78	39687	0.24
1283	1	9207	7.12	7.51	0.82	40420	0.23
1284	1	7964	10.94	4.94	0.62	39013	0.20
1285	1	8811	8.14	7.66	0.87	41145	0.21
1286	1	8775	6.35	7.00	0.80	41675	0.21
1287	1	9448	6.34	7.56	0.80	45034	0.21
1288	1	9435	5.71	6.86	0.73	47171	0.20
1289	1	9384	5.50	7.16	0.76	46931	0.20
1290	1	6493	3.30	2.52	0.39	41685	0.16
1291	1	7813	2.85	5.16	0.66	46024	0.17

## Training Data Set B

RING	GC	CF	P	TO	TOC	TT	COTT
336	2	4880	10.26	2.33	0.48	34363	0.14
337	2	6677	10.65	6.84	1.02	29952	0.22
338	2	8205	8.18	5.64	0.69	26556	0.31
339	2	11326	7.77	5.34	0.47	31308	0.36
340	2	15607	6.99	5.85	0.37	34508	0.45
341	2	7250	9.69	5.18	0.71	27719	0.26
342	2	7318	8.92	4.15	0.57	28722	0.25
343	2	6756	8.23	3.97	0.59	26186	0.26
344	2	5611	10.79	1.99	0.35	26108	0.21
345	2	7858	8.25	3.56	0.45	30588	0.26
346	2	8850	8.34	5.48	0.62	31441	0.28
347	2	7820	5.87	6.27	0.80	33942	0.23
348	2	8927	9.40	5.69	0.64	33958	0.26
349	2	10912	6.70	6.28	0.58	35359	0.31
350	2	11043	7.40	6.50	0.59	35914	0.31
351	2	9991	12.00	7.18	0.72	33963	0.29
352	2	6752	4.50	3.08	0.46	33621	0.20
353	2	10250	9.00	8.00	0.78	30567	0.34
354	2	10547	6.50	7.01	0.66	33241	0.32
355	2	12134	4.44	6.00	0.49	33794	0.36
356	3	16230	4.50	7.21	0.44	33413	0.49
357	3	10753	3.15	5.73	0.53	27921	0.39
358	3	10766	4.34	6.85	0.64	24673	0.44
359	3	11618	4.50	6.34	0.55	26094	0.45
360	3	11722	3.06	5.16	0.44	32746	0.36
361	3	14591	3.65	6.44	0.44	29873	0.49
362	3	13653	3.31	5.91	0.43	32888	0.42
363	3	13733	4.37	7.08	0.52	30506	0.45
364	3	13171	4.49	6.21	0.47	27060	0.49
365	3	11235	3.80	5.78	0.51	29353	0.38
366	3	11953	3.56	6.45	0.54	31129	0.38
367	3	12859	3.81	7.89	0.61	29289	0.44
368	3	11163	2.79	4.96	0.44	25088	0.44
369	3	12928	3.04	6.44	0.50	26781	0.48
370	3	15526	4.27	8.04	0.52	28935	0.54
371	2	11470	4.50	7.95	0.69	25122	0.46
372	2	9450	4.44	7.55	0.80	23953	0.39
373	2	8504	5.35	5.52	0.65	23054	0.37
374	2	12293	4.10	6.31	0.51	28582	0.43
375	2	12194	4.06	6.78	0.56	31104	0.39
376	2	11628	3.88	6.32	0.54	29903	0.39
377	2	12523	3.38	5.62	0.45	31324	0.40
378	2	12381	4.38	6.96	0.56	29701	0.42
379	2	13612	4.29	6.54	0.48	31157	0.44
380	2	13885	4.16	6.29	0.45	32273	0.43
381	2	14581	4.80	8.11	0.56	32101	0.45
382	2	11623	8.15	6.34	0.55	27375	0.42

383	2	10505	5.13	8.10	0.77	24563	0.43
384	2	10519	5.27	7.75	0.74	25095	0.42
385	2	7896	7.18	6.27	0.79	25879	0.31
386	2	8043	5.24	7.23	0.90	27174	0.30
387	2	7675	5.13	7.16	0.93	27277	0.28
388	2	6565	4.64	5.44	0.83	29183	0.22
389	2	6486	5.16	5.07	0.78	32410	0.20
390	1	5793	5.53	4.33	0.75	36455	0.16
391	1	6906	5.60	6.51	0.94	38236	0.18
392	1	6770	5.96	6.90	1.02	36539	0.19
393	1	4811	5.21	2.35	0.49	33463	0.14
394	1	6226	5.06	5.58	0.90	32023	0.19
395	1	6468	5.08	7.44	1.15	28479	0.23
397	1	6314	5.56	7.48	1.18	26688	0.24
398	1	6865	7.32	7.96	1.16	26978	0.25
399	1	6402	7.62	7.30	1.14	26563	0.24
400	1	5760	8.25	7.16	1.24	26475	0.22
401	1	5087	8.30	6.04	1.19	27448	0.19
402	1	5162	5.38	7.65	1.48	28611	0.18
403	1	5047	6.24	7.69	1.52	28915	0.17
404	1	5236	7.56	7.62	1.46	29650	0.18
405	1	5681	7.39	7.57	1.33	30931	0.18
406	1	6175	6.03	7.86	1.27	32207	0.19
407	1	6300	6.35	7.80	1.24	33612	0.19
408	1	6196	6.26	7.03	1.13	35274	0.18
409	1	5681	4.32	5.29	0.93	38054	0.15
410	1	5243	6.24	6.21	1.18	39399	0.13
411	1	6012	6.62	6.91	1.15	37731	0.16
412	1	6154	6.25	7.26	1.18	34284	0.18
413	1	6476	7.58	7.81	1.21	37446	0.17
414	1	6535	8.17	7.99	1.22	39483	0.17
415	1	6271	8.50	7.82	1.25	38817	0.16
416	1	6370	10.36	8.01	1.26	38901	0.16
417	1	5723	11.39	7.23	1.26	35608	0.16
418	1	6861	10.07	7.71	1.12	34194	0.20
419	1	7510	10.82	8.13	1.08	36952	0.20
420	1	6520	7.49	6.72	1.03	34929	0.19
421	2	6221	5.28	5.97	0.96	37305	0.17
422	2	6605	4.88	5.50	0.83	39604	0.17
423	2	7040	5.33	6.12	0.87	39226	0.18
424	2	7351	3.42	3.52	0.48	40131	0.18
425	2	8398	5.49	5.69	0.68	37910	0.22
426	2	11139	5.79	8.25	0.74	33520	0.33
427	2	10350	4.72	8.04	0.78	30278	0.34
428	2	10944	4.87	8.09	0.74	30805	0.36
429	2	10033	4.33	7.97	0.79	29597	0.34
430	2	9660	5.28	7.96	0.82	27712	0.35
431	2	11982	4.92	8.33	0.69	27014	0.44
432	2	13725	4.14	7.67	0.56	29978	0.46
433	2	13291	4.52	7.80	0.59	31647	0.42

434	2	13149	5.85	7.42	0.56	28200	0.47
435	2	13306	4.32	8.15	0.61	26283	0.51
436	2	11241	3.39	5.35	0.48	26425	0.43
437	2	15936	4.03	7.16	0.45	31196	0.51
438	2	15095	3.06	5.94	0.39	30086	0.50
439	2	14795	3.22	7.43	0.50	29114	0.51
440	2	11071	2.74	2.82	0.25	25248	0.44
441	2	13707	2.75	4.85	0.35	28255	0.49
442	2	12413	3.44	6.29	0.51	30291	0.41
443	2	7530	4.18	3.89	0.52	21768	0.35
444	2	9262	5.52	7.96	0.86	24664	0.38
445	2	9082	4.69	7.92	0.87	25440	0.36
446	2	9644	4.36	7.51	0.78	26002	0.37
447	2	11766	4.87	7.69	0.65	28172	0.42
448	2	10368	3.78	3.97	0.38	26734	0.39
449	2	11663	3.94	5.65	0.48	29745	0.39
450	3	12304	4.59	7.72	0.63	27097	0.45
451	3	11752	4.46	7.86	0.67	26063	0.45
452	3	11060	4.57	7.71	0.70	26452	0.42
453	3	9067	5.20	4.58	0.51	28469	0.32
454	3	11631	4.21	7.67	0.66	29128	0.40
455	3	12861	3.97	7.96	0.62	28800	0.45
456	3	11574	3.84	6.85	0.59	27755	0.42
457	3	10977	8.80	7.21	0.66	23941	0.46
458	3	14394	6.55	7.47	0.52	29061	0.50
459	3	13795	3.96	7.34	0.53	30400	0.45
460	3	12985	3.36	7.97	0.61	29651	0.44
461	3	11104	2.84	7.15	0.64	35412	0.31
462	3	10481	1.95	5.27	0.50	38136	0.27
463	3	13142	4.44	6.16	0.47	34361	0.38
464	3	11988	3.57	6.72	0.56	32160	0.37
465	2	8069	4.36	5.43	0.67	27820	0.29
466	2	9004	5.29	6.68	0.74	27400	0.33
467	2	8871	4.76	7.70	0.87	27834	0.32
468	2	9741	5.71	8.28	0.85	25129	0.39
469	2	10111	5.58	7.75	0.77	29954	0.34
470	2	8323	6.50	7.56	0.91	33400	0.25
471	2	8004	7.08	8.48	1.06	29829	0.27
472	2	7881	6.47	7.49	0.95	29713	0.27
473	2	6658	6.00	5.20	0.78	32500	0.20
474	2	7655	6.08	7.96	1.04	33078	0.23
475	2	8615	6.87	7.96	0.92	32162	0.27
476	2	8867	5.56	7.54	0.85	35449	0.25
477	2	9986	5.50	5.05	0.51	35257	0.28
478	2	10190	6.20	8.28	0.81	31957	0.32
479	2	9550	5.96	8.25	0.86	27731	0.34
480	2	8672	6.40	7.97	0.92	24695	0.35
481	2	8499	6.76	8.20	0.96	23953	0.35
482	2	8786	6.71	8.14	0.93	24289	0.36
483	2	6466	7.81	6.29	0.97	25282	0.26

484	2	8182	9.43	7.18	0.88	29029	0.28
485	2	12343	8.63	7.74	0.63	33412	0.37
486	2	14877	6.65	7.56	0.51	37629	0.40
487	2	8983	6.07	6.90	0.77	30727	0.29
488	2	8043	9.44	7.75	0.96	27067	0.30
489	2	7708	9.39	7.79	1.01	28794	0.27
505	2	5048	6.81	7.39	1.46	25087	0.20
506	2	6886	7.09	8.10	1.18	26258	0.26
507	2	7775	6.17	7.73	0.99	26854	0.29
508	2	7577	5.97	7.33	0.97	27997	0.27
509	2	6946	6.12	7.57	1.09	27009	0.26
510	2	6407	8.51	6.61	1.03	26269	0.24
511	2	6827	7.21	7.80	1.14	29127	0.23
512	2	6788	6.29	7.34	1.08	31165	0.22
513	2	6199	6.34	7.81	1.26	33208	0.19
514	2	6233	6.35	7.88	1.26	33839	0.18
515	2	6906	7.29	8.21	1.19	32594	0.21
516	2	7148	6.68	8.03	1.12	31547	0.23
517	2	6974	7.02	8.14	1.17	29419	0.24
518	2	6935	6.30	7.19	1.04	30405	0.23
519	2	6980	7.04	8.40	1.20	33108	0.21
520	2	6396	7.09	7.39	1.16	31772	0.20
521	2	6983	7.25	7.94	1.14	30352	0.23
522	2	7076	7.54	7.90	1.12	34652	0.20
523	2	6709	7.79	7.78	1.16	32218	0.21
524	2	4492	6.90	4.18	0.93	24188	0.19
525	2	4945	8.01	4.41	0.89	21653	0.23
526	2	8405	14.61	8.20	0.98	24332	0.35
527	2	6371	7.56	7.31	1.15	21377	0.30
528	2	5613	8.44	6.86	1.22	21398	0.26
529	1	6869	13.86	6.74	0.98	26810	0.26
530	1	7180	13.06	6.50	0.91	24192	0.30
531	1	8353	14.12	8.42	1.01	22545	0.37
532	1	9059	17.81	7.77	0.86	22550	0.40
533	1	6793	8.00	7.61	1.12	19853	0.34
535	1	6785	12.04	5.02	0.74	23947	0.28
536	1	11681	8.03	7.02	0.60	26651	0.44
537	1	11239	9.06	7.32	0.65	28713	0.39
538	1	6786	8.99	6.58	0.97	26570	0.26
539	1	10473	20.58	7.18	0.69	27504	0.38
540	1	10166	19.66	7.41	0.73	26007	0.39
541	1	8353	13.69	4.70	0.56	24002	0.35
542	1	9131	14.30	5.34	0.58	23918	0.38
543	1	6313	9.82	6.08	0.96	20536	0.31
544	1	4317	7.53	5.86	1.36	21125	0.20
545	1	3742	9.92	4.17	1.12	20803	0.18
546	1	4941	18.54	5.57	1.13	19436	0.25
547	1	8398	15.72	5.74	0.68	23538	0.36
548	1	11989	12.44	8.05	0.67	27170	0.44
549	1	14928	7.58	7.63	0.51	28788	0.52

550	1	13453	6.04	7.64	0.57	27940	0.48
551	1	13196	6.38	7.45	0.56	28425	0.46
552	1	7460	8.88	6.11	0.82	24165	0.31
553	1	6614	6.92	7.92	1.20	25675	0.26
554	1	6923	6.78	7.58	1.10	29961	0.23
555	1	5820	6.75	6.83	1.17	29664	0.20
556	1	5359	6.36	6.59	1.23	27071	0.20
557	1	4835	5.90	6.07	1.26	25883	0.19
558	1	4565	7.00	4.51	0.99	28462	0.16
559	1	4878	7.03	7.28	1.49	30303	0.16
560	1	4741	7.83	7.89	1.66	29045	0.16
561	1	4415	8.82	6.89	1.56	29308	0.15
562	1	4129	6.97	6.28	1.52	28326	0.15
563	1	4361	7.07	6.89	1.58	30902	0.14
564	2	4331	8.18	7.49	1.73	29035	0.15
565	2	5121	10.48	8.07	1.58	28355	0.18
566	2	4812	9.25	6.43	1.34	24802	0.19
567	2	5328	7.87	5.36	1.01	26307	0.20
568	2	5284	7.67	5.65	1.07	24766	0.21
569	2	4871	6.86	5.37	1.10	26209	0.19
570	2	5595	7.50	6.53	1.17	28572	0.20
571	2	5400	10.12	5.22	0.97	28454	0.19
572	2	6233	9.22	7.50	1.20	29617	0.21
573	2	6015	8.69	6.29	1.04	26523	0.23
574	2	6525	8.88	7.17	1.10	24915	0.26
575	2	6107	7.80	6.71	1.10	24521	0.25
576	2	6628	8.68	7.68	1.16	24734	0.27
577	2	6421	8.24	7.12	1.11	23924	0.27
578	2	6806	7.97	8.01	1.18	26755	0.25
579	2	7490	10.35	7.16	0.96	27739	0.27
580	2	8103	7.21	8.19	1.01	26333	0.31
581	2	8553	6.80	8.01	0.94	24415	0.35
582	2	8705	6.57	7.84	0.90	24230	0.36
583	2	10009	6.45	7.54	0.75	27134	0.37
584	2	11239	6.04	8.04	0.72	28450	0.40
585	2	10464	5.83	7.67	0.73	28901	0.36
586	2	8867	5.19	7.85	0.89	29277	0.30
587	2	9369	4.38	6.55	0.70	30795	0.30
588	2	7312	4.58	4.41	0.60	30862	0.24
589	2	10100	5.68	7.42	0.73	36692	0.28
590	2	9749	5.25	7.44	0.76	36295	0.27
591	2	8364	4.03	5.29	0.63	34780	0.24
592	2	9107	4.34	5.59	0.61	32974	0.28
593	2	8515	5.38	7.36	0.86	32677	0.26
594	2	6355	8.33	6.28	0.99	28769	0.22
595	2	5785	7.17	7.45	1.29	28304	0.20
596	2	5693	7.36	7.25	1.27	28449	0.20
597	2	6041	7.54	7.74	1.28	26390	0.23
598	2	7586	6.99	7.85	1.04	28736	0.26
599	2	7689	8.62	6.84	0.89	28106	0.27



600	2	7447	7.14	7.71	1.04	29208	0.25
601	2	6328	7.09	6.87	1.09	30043	0.21
602	2	6821	6.86	7.23	1.06	30874	0.22
603	2	6204	6.74	6.83	1.10	33574	0.18
604	2	6073	6.37	6.19	1.02	34179	0.18
605	2	6103	6.72	6.10	1.00	36518	0.17
606	1	5548	12.88	6.75	1.22	35531	0.16
607	1	7236	8.02	7.91	1.09	33898	0.21
608	1	6585	7.65	7.75	1.18	31242	0.21
609	1	6905	8.10	7.84	1.14	31980	0.22
610	1	6196	7.82	7.42	1.20	31589	0.20
611	1	5593	7.40	6.83	1.22	32536	0.17
612	1	5863	7.67	7.45	1.27	33982	0.17
613	1	5012	7.39	7.11	1.42	34526	0.15
614	1	4415	7.81	3.73	0.84	35256	0.13
615	1	5595	8.97	6.61	1.18	34945	0.16
616	1	4651	10.73	4.57	0.98	29532	0.16
617	1	5387	11.40	7.24	1.34	29445	0.18
618	1	4579	9.61	6.16	1.35	28532	0.16
619	1	4791	10.21	6.12	1.28	27637	0.17
620	1	5944	16.97	6.03	1.01	27048	0.22
621	1	6119	10.35	7.11	1.16	29086	0.21
622	1	6179	10.13	7.84	1.27	30636	0.20
623	1	4604	8.78	4.97	1.08	27443	0.17
624	1	4166	9.18	4.14	0.99	24410	0.17
625	1	4585	11.73	6.17	1.35	23459	0.20
626	1	5477	9.74	6.89	1.26	24839	0.22
627	1	4950	9.59	6.22	1.26	26601	0.19
628	1	5295	11.91	7.83	1.48	25416	0.21
629	1	5360	12.17	8.14	1.52	24353	0.22
630	1	5101	12.01	7.57	1.48	23873	0.21
631	1	4917	15.71	3.43	0.70	24339	0.20
632	1	6645	15.67	7.27	1.09	26308	0.25
633	1	7317	11.23	8.23	1.12	29215	0.25
634	2	7789	7.53	7.62	0.98	32828	0.24
635	2	8952	5.76	6.75	0.75	39423	0.23
636	2	6064	3.06	2.98	0.49	40653	0.15
637	3	9585	3.29	5.12	0.53	43222	0.22
638	3	9950	2.96	6.04	0.61	43347	0.23
639	3	8713	2.37	3.09	0.35	43047	0.20
640	3	13879	3.45	7.79	0.56	44321	0.31
641	3	11120	2.26	6.03	0.54	44433	0.25
642	3	12541	3.14	7.33	0.58	41654	0.30
643	3	12347	5.04	6.57	0.53	31742	0.39
644	3	10986	3.62	7.55	0.69	33402	0.33
645	3	10890	4.00	7.83	0.72	36193	0.30
659	1	9849	4.55	7.65	0.78	41790	0.24
660	1	9020	8.82	7.42	0.82	35400	0.25
661	1	9740	5.39	7.80	0.80	32873	0.30
662	1	9531	6.06	8.21	0.86	27713	0.34

663	1	8566	6.56	8.06	0.94	34154	0.25
664	1	8763	5.81	8.35	0.95	40398	0.22
665	1	7869	6.03	8.19	1.04	40746	0.19
666	1	8511	6.45	7.96	0.93	38941	0.22
667	1	9214	7.12	7.03	0.76	38241	0.24
668	1	8374	6.94	7.91	0.94	37026	0.23
669	1	9321	6.77	7.82	0.84	39330	0.24
670	1	9169	5.81	7.15	0.78	41767	0.22
671	1	9504	4.22	5.08	0.53	45225	0.21
672	1	11000	4.09	6.08	0.55	44789	0.25
673	1	9287	4.77	4.57	0.49	40988	0.23
674	1	8296	7.44	6.92	0.83	40016	0.21
675	1	7164	8.57	8.27	1.15	38086	0.19
676	1	7535	9.04	8.38	1.11	34269	0.22
677	1	7890	8.42	8.50	1.08	32657	0.24
698	1	8355	10.69	7.73	0.93	26041	0.32
699	1	8512	11.12	8.40	0.99	26797	0.32
700	1	8213	10.78	7.73	0.94	27283	0.30
701	1	7791	10.61	7.61	0.98	27265	0.29
702	1	8226	12.85	8.14	0.99	28044	0.29
703	1	7963	10.20	7.71	0.97	26640	0.30
704	1	8413	10.93	8.02	0.95	25873	0.33
705	1	8472	9.83	8.02	0.95	27616	0.31
706	1	8252	8.03	7.39	0.90	28023	0.29
707	1	8088	7.77	7.19	0.89	27422	0.29
708	1	7871	7.98	7.71	0.98	27232	0.29
709	1	7547	7.77	7.87	1.04	27866	0.27
710	1	8599	7.46	7.61	0.89	32995	0.26
711	1	8478	6.78	7.66	0.90	31067	0.27
712	1	8606	5.30	7.31	0.85	30825	0.28
713	1	8569	5.58	6.55	0.76	31383	0.27
714	1	8447	6.72	5.58	0.66	32415	0.26
715	1	8909	6.90	7.12	0.80	29943	0.30
716	1	7708	12.01	5.45	0.71	31883	0.24
717	1	11209	10.69	7.98	0.71	31872	0.35
718	1	9252	6.99	7.46	0.81	29242	0.32
729	1	8211	6.17	8.31	1.01	27721	0.30
730	1	8254	6.36	8.38	1.02	28674	0.29
731	1	8227	6.56	8.27	1.01	30100	0.27
732	1	8899	14.24	6.24	0.70	31015	0.29
733	1	8384	9.34	7.45	0.89	30687	0.27
734	1	8358	8.13	7.67	0.92	27648	0.30
735	1	8331	8.24	8.09	0.97	29244	0.28
736	1	8078	8.96	6.94	0.86	30022	0.27
737	1	10548	8.47	7.63	0.72	31103	0.34
738	1	10680	11.07	6.72	0.63	30756	0.35
739	1	9001	7.01	8.18	0.91	30415	0.30
740	1	7582	10.25	6.18	0.81	30211	0.25
741	1	9327	7.56	8.07	0.87	32096	0.29
742	1	8825	6.16	7.79	0.88	32336	0.27

743	1	8153	6.26	7.99	0.98	33146	0.25
744	1	8234	6.73	7.59	0.92	33321	0.25
745	1	7038	8.81	7.27	1.03	34993	0.20
768	1	13329	5.19	5.67	0.43	33705	0.40
769	1	11201	4.51	7.01	0.63	32297	0.35
770	1	10269	4.71	7.63	0.74	33399	0.31
771	1	9351	5.31	8.04	0.86	33688	0.28
772	1	6637	6.79	4.81	0.72	31739	0.21
773	1	9112	7.43	7.87	0.86	32141	0.28
774	1	8400	6.99	7.82	0.93	30306	0.28
775	1	8009	8.32	7.57	0.95	31894	0.25
776	1	8700	8.43	7.77	0.89	30722	0.28
777	1	9360	7.55	7.77	0.83	30797	0.30
778	1	10039	7.13	7.90	0.79	33391	0.30
800	3	14302	7.03	7.66	0.54	41203	0.35
801	3	12270	5.68	6.44	0.52	37046	0.33
802	3	12928	5.30	7.84	0.61	36280	0.36
803	3	12903	5.85	7.70	0.60	35327	0.37
804	3	12686	5.84	8.03	0.63	38765	0.33
805	3	13115	6.29	8.50	0.65	39109	0.34
806	3	11681	5.16	6.33	0.54	38389	0.30
807	3	12551	6.07	7.43	0.59	38530	0.33
808	3	11528	5.12	7.35	0.64	37455	0.31
809	3	10749	4.73	7.14	0.66	39253	0.27
810	3	11719	4.65	7.57	0.65	37914	0.31
817	3	9565	4.31	7.06	0.74	42134	0.23
818	3	6695	3.15	4.10	0.61	37762	0.18
819	3	8575	3.71	5.76	0.67	32585	0.26
820	3	10234	4.55	7.08	0.69	38540	0.27
821	3	9814	4.64	7.43	0.76	42102	0.23
822	3	9104	4.29	6.44	0.71	43106	0.21
823	3	7828	3.86	4.77	0.61	40324	0.19
824	3	7277	2.92	3.94	0.54	39033	0.19
825	3	7562	3.83	5.32	0.70	37611	0.20
826	3	6919	3.65	5.53	0.80	39677	0.17
827	3	5345	3.18	2.43	0.45	39952	0.13
829	3	6931	6.04	5.43	0.78	36822	0.19
830	3	7763	8.43	7.23	0.93	43144	0.18
831	3	7616	10.51	7.81	1.03	39390	0.19
848	3	14353	4.93	7.63	0.53	35210	0.41
849	3	13286	5.27	7.97	0.60	40905	0.32
850	3	11339	4.47	7.84	0.69	40018	0.28
851	3	9993	4.85	7.53	0.75	42184	0.24
852	3	10464	6.00	6.15	0.59	41867	0.25
853	3	13391	6.89	7.03	0.52	38740	0.35
854	3	14531	4.08	6.52	0.45	34405	0.42
855	3	11659	4.13	5.28	0.45	34062	0.34
856	3	12314	4.44	7.93	0.64	34084	0.36
906	1	6054	12.02	6.92	1.14	24301	0.25
907	1	5860	14.11	6.69	1.14	24565	0.24

908	1	6026	14.65	7.19	1.19	25494	0.24
909	1	5978	15.43	7.30	1.22	23349	0.26
910	1	5484	11.88	7.92	1.44	22167	0.25
911	1	6627	11.74	8.08	1.22	22499	0.29
913	1	4739	12.70	2.35	0.50	19761	0.24
914	1	9654	9.38	6.22	0.64	22369	0.43
915	1	4361	16.14	6.13	1.41	16612	0.26
916	1	4435	13.90	6.85	1.55	17932	0.25
917	1	4489	12.97	6.80	1.52	18940	0.24
918	1	4612	14.75	7.11	1.54	19593	0.24
919	1	4319	12.57	5.56	1.29	21527	0.20
931	3	10408	7.26	7.51	0.72	28670	0.36
932	3	10250	7.61	6.56	0.64	24212	0.42
933	3	9666	7.41	6.10	0.63	26396	0.37
934	3	10465	8.35	7.28	0.70	25978	0.40
935	3	9995	7.35	7.47	0.75	26574	0.38
936	3	9247	8.59	7.95	0.86	24933	0.37
937	3	8798	8.53	7.89	0.90	25646	0.34
938	3	8552	10.37	6.16	0.72	22331	0.38
939	3	9711	9.45	7.42	0.76	25678	0.38
940	3	7392	4.84	3.89	0.53	35869	0.21
941	3	10655	7.64	7.52	0.71	31109	0.34
942	3	11342	7.14	6.97	0.61	31624	0.36
960	3	6521	10.78	6.39	0.98	27196	0.24
964	3	8523	9.11	7.61	0.89	35009	0.24
965	3	8625	6.78	7.33	0.85	35836	0.24
966	3	9720	8.30	7.52	0.77	37001	0.26
967	3	10710	7.45	7.59	0.71	35083	0.31
968	3	8748	6.66	6.70	0.77	33294	0.26
969	3	10937	9.34	6.80	0.62	32414	0.34
970	3	12137	8.21	7.72	0.64	34179	0.36
971	3	11253	6.30	5.45	0.48	38676	0.29
972	3	12850	7.92	7.56	0.59	37431	0.34
973	3	12966	7.64	7.35	0.57	33848	0.38
974	3	12148	7.49	6.43	0.53	30098	0.40
975	3	13212	7.92	7.46	0.56	27297	0.48
976	3	13266	7.69	7.37	0.56	28126	0.47
977	3	14011	7.89	7.38	0.53	31093	0.45
978	3	14137	7.67	6.69	0.47	38506	0.37
979	3	9537	3.62	3.09	0.32	39813	0.24
1006	3	9988	7.68	7.32	0.73	32550	0.31
1007	3	9434	8.05	7.94	0.84	31839	0.30
1008	3	9476	8.02	7.92	0.84	32227	0.29
1009	3	9124	7.21	7.87	0.86	34852	0.26
1010	3	10176	6.87	7.54	0.74	34626	0.29
1011	3	10360	6.35	7.21	0.70	34103	0.30
1012	3	11696	4.96	5.69	0.49	39275	0.30
1013	3	13232	6.07	8.06	0.61	37497	0.35
1014	3	12280	4.87	7.22	0.59	38862	0.32
1015	3	11691	4.06	7.42	0.63	40416	0.29

1016	3	7322	10.26	6.18	0.84	30981	0.24
1017	3	9744	6.42	7.79	0.80	29184	0.33
1018	3	11464	6.38	7.83	0.68	35008	0.33
1019	3	10600	6.19	7.25	0.68	37448	0.28
1020	3	8787	9.67	6.62	0.75	32396	0.27
1021	3	10145	7.84	7.99	0.79	29127	0.35
1022	3	9931	6.79	7.46	0.75	33237	0.30
1023	3	9643	6.82	7.46	0.77	36819	0.26
1024	1	8866	6.38	7.55	0.85	39085	0.23
1025	1	8235	5.95	7.08	0.86	34926	0.24
1026	1	7436	6.32	7.34	0.99	34711	0.21
1027	1	8041	7.04	7.73	0.96	37763	0.21
1028	1	6311	5.89	3.18	0.50	36714	0.17
1029	1	8198	7.42	6.47	0.79	37614	0.22
1030	1	7838	8.27	7.06	0.90	35241	0.22
1031	1	7989	9.16	7.28	0.91	33823	0.24
1032	1	7977	9.96	7.55	0.95	33332	0.24
1033	1	7779	8.91	7.08	0.91	33626	0.23
1034	1	7158	8.51	7.23	1.01	31344	0.23
1035	1	6610	8.36	6.68	1.01	30767	0.21
1036	1	6542	9.95	7.31	1.12	30835	0.21
1037	1	4832	11.33	3.23	0.67	25032	0.19
1038	1	5619	12.69	6.28	1.12	26596	0.21
1039	1	5061	11.39	6.48	1.28	24511	0.21
1040	1	5228	13.39	6.57	1.26	27214	0.19
1041	1	4411	10.02	4.60	1.04	23726	0.19
1042	1	4327	11.49	4.37	1.01	22774	0.19
1043	1	4694	18.18	6.16	1.31	22591	0.21
1044	1	4872	16.59	6.47	1.33	22676	0.21
1045	1	5570	15.03	6.73	1.21	23657	0.24
1046	1	5156	14.81	3.83	0.74	23184	0.22
1047	1	5829	13.55	6.49	1.11	26657	0.22
1048	1	6228	12.21	7.35	1.18	27581	0.23
1049	1	6661	10.11	6.51	0.98	27884	0.24
1050	1	6792	8.77	6.16	0.91	30133	0.23
1051	1	7057	8.96	7.15	1.01	30613	0.23
1052	1	7279	7.62	7.04	0.97	32412	0.22
1075	3	7231	6.95	7.74	1.07	42737	0.17
1076	3	6966	7.39	5.19	0.74	39260	0.18
1077	3	9175	6.74	7.65	0.83	39042	0.24
1078	3	9233	5.87	7.10	0.77	38791	0.24
1079	3	8438	4.49	6.46	0.77	43102	0.20
1080	3	7458	3.16	5.76	0.77	45348	0.16
1081	3	6876	3.68	3.37	0.49	44413	0.15
1082	3	8513	2.74	4.94	0.58	44530	0.19
1083	3	8575	3.09	4.80	0.56	44195	0.19
1084	3	6698	1.79	3.22	0.48	45110	0.15
1085	3	7807	2.57	2.97	0.38	42141	0.19
1086	3	9044	1.96	4.23	0.47	42497	0.21
1087	3	8361	1.83	4.46	0.53	45158	0.19

1088	3	7600	3.33	3.08	0.41	43254	0.18
1089	3	10404	4.27	7.20	0.69	43414	0.24
1090	3	10190	4.17	6.60	0.65	42920	0.24
1091	3	9839	3.64	6.34	0.64	44574	0.22
1092	3	8585	2.89	5.00	0.58	45332	0.19
1093	3	7891	2.11	3.36	0.43	45777	0.17
1094	3	10825	3.31	7.50	0.69	46993	0.23
1095	3	8325	2.02	3.88	0.47	45151	0.18
1096	3	10934	3.56	7.97	0.73	46124	0.24
1097	3	7862	5.34	5.43	0.69	39793	0.20
1098	3	9825	3.62	6.78	0.69	38573	0.25
1099	3	9970	3.51	6.82	0.68	38226	0.26
1100	3	11572	4.44	8.09	0.70	36222	0.32
1101	3	12268	4.41	7.74	0.63	40274	0.30
1102	3	11184	5.21	6.02	0.54	37518	0.30
1103	3	10982	4.32	7.26	0.66	26208	0.42
1104	3	9133	3.70	6.84	0.75	27445	0.33
1105	3	9788	5.40	7.72	0.79	31587	0.31
1106	3	8945	5.67	7.55	0.84	37757	0.24
1107	3	8402	6.31	7.67	0.91	40208	0.21
1108	3	8531	6.11	5.70	0.67	34815	0.25
1109	3	9315	5.61	7.30	0.78	32170	0.29
1110	3	9778	4.13	7.31	0.75	34169	0.29
1111	3	10723	4.59	7.86	0.73	41757	0.26
1112	3	10094	4.87	5.70	0.56	41198	0.25
1113	3	11412	4.27	7.17	0.63	35677	0.32
1114	3	11211	3.77	7.15	0.64	35611	0.31
1115	3	11929	4.65	7.83	0.66	40960	0.29
1116	3	10147	5.07	5.74	0.57	38737	0.26
1117	3	10839	3.78	7.20	0.66	35831	0.30
1118	3	9906	3.28	6.90	0.70	30367	0.33
1119	3	10306	5.19	6.89	0.67	34088	0.30
1120	3	10083	3.19	7.17	0.71	32317	0.31
1121	3	10016	3.69	7.13	0.71	35145	0.28
1122	3	11203	4.08	7.76	0.69	39118	0.29
1123	3	9680	3.72	4.26	0.44	40160	0.24
1124	3	10518	3.44	6.69	0.64	40449	0.26
1125	3	10005	3.96	6.34	0.63	36850	0.27
1126	3	11316	4.74	7.01	0.62	40394	0.28
1127	3	10634	4.88	6.63	0.62	38153	0.28
1128	3	10088	6.87	6.57	0.65	33370	0.30
1129	3	11053	5.14	7.10	0.64	34260	0.32
1130	3	10747	4.74	6.82	0.63	38527	0.28
1131	3	10730	3.77	6.56	0.61	45212	0.24
1132	3	7580	2.20	3.10	0.41	41897	0.18
1133	3	10401	4.77	5.44	0.52	40696	0.26
1134	3	12022	4.42	6.70	0.56	39160	0.31
1135	3	10542	3.19	6.23	0.59	42233	0.25
1136	3	10974	3.52	6.17	0.56	44217	0.25
1137	3	9537	2.85	5.20	0.54	44293	0.22



1138	3	9597	4.19	4.99	0.52	44003	0.22
1139	3	11963	3.31	7.46	0.62	35395	0.34
1140	3	11106	2.80	5.91	0.53	39391	0.28
1141	3	10253	3.31	5.40	0.53	41303	0.25
1143	3	11911	3.07	6.61	0.55	28985	0.41
1144	3	11226	4.10	7.37	0.66	31623	0.36
1145	3	10786	4.22	7.08	0.66	27092	0.40
1146	3	12205	3.81	6.39	0.52	33407	0.37
1147	3	10646	3.32	4.50	0.42	40804	0.26
1148	3	13532	3.36	6.75	0.50	43247	0.31
1149	3	14185	3.61	7.05	0.50	37904	0.37
1150	3	15676	3.50	7.51	0.48	32356	0.48
1151	3	14525	3.06	5.24	0.36	33971	0.43
1152	3	13642	2.39	4.82	0.35	41487	0.33
1153	3	13732	2.08	5.79	0.42	35875	0.38
1154	3	11342	1.69	3.21	0.28	26569	0.43
1155	3	11141	1.17	2.98	0.27	26917	0.41
1156	3	9688	2.36	2.67	0.28	26412	0.37
1157	3	11035	4.29	5.36	0.49	30640	0.36
1158	3	11691	3.89	5.13	0.44	31953	0.37
1159	3	12108	3.21	5.00	0.41	31951	0.38
1160	3	10144	2.31	3.24	0.32	28656	0.35
1161	3	12368	2.57	5.89	0.48	32342	0.38
1162	3	11523	3.55	5.42	0.47	24170	0.48
1163	3	11037	2.81	4.42	0.40	23546	0.47
1164	3	12403	3.01	5.93	0.48	25112	0.49
1165	3	13075	2.85	5.61	0.43	28822	0.45
1166	3	14016	4.82	5.26	0.37	27345	0.51
1167	3	15550	4.17	6.87	0.44	27031	0.58
1168	3	12548	1.94	3.32	0.26	33730	0.37
1169	3	13052	2.75	2.84	0.22	34834	0.37
1170	3	13965	2.95	4.35	0.31	27390	0.51
1171	3	13680	2.61	4.71	0.34	28576	0.48
1172	3	11616	3.02	4.13	0.36	32697	0.36
1173	3	14123	4.08	6.16	0.44	30246	0.47
1174	3	13990	4.30	7.09	0.51	26432	0.53
1175	3	12889	5.04	6.87	0.53	28429	0.45
1176	3	13661	5.47	6.37	0.47	30483	0.45
1177	3	12783	4.28	5.33	0.42	30636	0.42
1178	3	12906	3.99	5.38	0.42	29182	0.44
1179	3	12674	4.19	6.01	0.47	30209	0.42
1180	3	10615	3.32	3.97	0.37	33487	0.32
1181	3	11395	3.66	5.66	0.50	38699	0.29
1182	3	11602	2.70	4.43	0.38	41356	0.28
1183	3	13450	4.39	4.60	0.34	28373	0.47
1184	3	13940	4.03	6.64	0.48	30933	0.45
1185	3	13198	4.76	6.57	0.50	30321	0.44
1186	3	12587	4.49	4.93	0.39	35643	0.35
1187	3	12938	4.04	4.59	0.35	40608	0.32
1188	3	12195	3.38	4.48	0.37	35719	0.34

1189	3	13863	3.40	5.93	0.43	33390	0.42
1190	3	11999	2.74	5.25	0.44	34520	0.35
1191	3	9246	1.69	3.93	0.43	41651	0.22
1192	3	9325	2.66	3.19	0.34	40511	0.23
1193	3	13884	3.97	6.23	0.45	32411	0.43
1194	3	12322	3.06	5.50	0.45	34970	0.35
1195	3	8794	1.41	3.21	0.36	43338	0.20
1196	3	10703	2.89	3.36	0.31	40967	0.26
1197	3	13935	4.18	6.67	0.48	32583	0.43
1198	3	12693	4.10	6.72	0.53	37541	0.34
1199	3	9191	2.24	4.01	0.44	44057	0.21
1200	3	9370	2.39	4.38	0.47	45300	0.21
1201	3	11917	3.99	5.98	0.50	41300	0.29
1202	3	10298	3.33	4.58	0.44	41961	0.25
1203	3	7651	1.70	2.58	0.34	36283	0.21
1204	3	9386	2.73	5.09	0.54	35999	0.26
1205	3	8823	2.26	3.97	0.45	38626	0.23
1206	3	9357	2.99	5.01	0.54	39863	0.23
1207	3	8243	2.73	4.21	0.51	40707	0.20
1208	3	7571	2.04	3.91	0.52	40962	0.18
1209	3	7906	3.31	4.57	0.58	42614	0.19
1210	3	11873	7.50	7.77	0.65	31729	0.37
1211	3	13034	5.80	7.80	0.60	31772	0.41
1212	3	8336	2.23	4.05	0.49	38290	0.22
1213	3	8465	3.55	3.89	0.46	42003	0.20
1214	3	12033	5.34	7.79	0.65	38059	0.32
1215	3	11164	5.16	7.47	0.67	33344	0.33
1216	3	9483	4.43	5.91	0.62	34961	0.27
1217	3	9278	4.41	7.03	0.76	38999	0.24
1218	3	10292	6.14	7.32	0.71	38629	0.27
1219	3	8768	6.46	6.67	0.76	36573	0.24
1220	3	9901	8.66	6.52	0.66	36056	0.27
1221	3	9750	7.96	7.59	0.78	36256	0.27
1222	3	8889	8.28	8.01	0.90	35816	0.25
1223	3	9262	8.80	8.16	0.88	36779	0.25
1224	1	9740	10.14	7.77	0.80	37546	0.26
1225	1	8149	9.00	7.91	0.97	33567	0.24
1226	1	8550	9.95	7.07	0.83	34979	0.24
1227	1	9140	10.79	7.94	0.87	34446	0.27
1228	1	8845	10.37	7.19	0.81	31903	0.28
1229	1	9858	10.75	7.29	0.74	33422	0.29
1230	1	6883	10.73	3.83	0.56	29576	0.23
1231	1	10856	9.62	7.94	0.73	31717	0.34
1232	1	12059	9.30	7.48	0.62	35251	0.34
1233	1	12720	8.33	7.36	0.58	36890	0.34
1234	1	12772	7.36	7.45	0.58	38328	0.33
1235	1	13820	6.69	6.73	0.49	40628	0.34
1236	1	11510	7.31	7.34	0.64	39228	0.29
1237	1	7020	8.36	2.86	0.41	33731	0.21
1238	1	11366	7.80	7.63	0.67	32887	0.35

1239	1	13850	6.44	7.29	0.53	34798	0.40
1240	1	13463	6.29	7.21	0.54	35034	0.38
1241	1	11470	6.28	7.47	0.65	32657	0.35
1242	1	11809	6.27	7.63	0.65	36124	0.33
1243	1	12159	5.74	7.52	0.62	37074	0.33
1244	1	5803	1.97	2.04	0.35	38614	0.15
1245	1	7643	2.94	3.94	0.52	41231	0.19
1246	1	10757	4.59	6.78	0.63	39179	0.27
1278	1	5196	4.31	2.37	0.46	35545	0.15
1279	1	8075	9.53	6.18	0.77	37296	0.22
1280	1	9557	8.39	7.38	0.77	38115	0.25
1281	1	8219	7.46	6.93	0.84	37865	0.22
1282	1	9489	7.84	7.36	0.78	39687	0.24
1283	1	9207	7.12	7.51	0.82	40420	0.23
1284	1	7964	10.94	4.94	0.62	39013	0.20
1285	1	8811	8.14	7.66	0.87	41145	0.21
1286	1	8775	6.35	7.00	0.80	41675	0.21
1287	1	9448	6.34	7.56	0.80	45034	0.21
1288	1	9435	5.71	6.86	0.73	47171	0.20
1289	1	9384	5.50	7.16	0.76	46931	0.20
1290	1	6493	3.30	2.52	0.39	41685	0.16
1291	1	7813	2.85	5.16	0.66	46024	0.17
1292	3	9122	5.54	7.11	0.78	41690	0.22
1293	3	10043	5.00	7.02	0.70	39267	0.26
1294	3	9989	6.52	6.07	0.61	39405	0.25
1295	3	9849	5.17	6.44	0.65	42263	0.23
1296	3	8245	3.08	3.75	0.45	40862	0.20
1297	3	11434	4.21	6.65	0.58	41761	0.27
1298	3	10433	5.36	4.17	0.40	42340	0.25
1299	3	13123	3.48	5.93	0.45	38049	0.34
1300	3	12167	3.29	4.34	0.36	41082	0.30
1301	3	10678	1.72	2.82	0.26	42086	0.25
1302	3	10984	3.32	3.23	0.29	34737	0.32
1303	3	11308	3.49	4.98	0.44	27677	0.41
1304	3	11674	3.58	4.55	0.39	31797	0.37
1305	3	12376	3.67	5.24	0.42	34790	0.36
1306	3	11575	4.48	3.99	0.34	29130	0.40
1307	3	12530	4.29	5.45	0.44	27239	0.46
1308	3	13319	4.14	6.78	0.51	28376	0.47
1309	3	13552	4.23	5.53	0.41	28317	0.48
1310	3	13416	3.79	5.31	0.40	29886	0.45
1311	3	12996	6.10	5.92	0.46	26871	0.48
1312	3	13466	5.23	6.43	0.48	26450	0.51
1313	3	13641	4.25	5.40	0.40	28185	0.48
1314	3	13525	4.34	7.01	0.52	30015	0.45
1315	3	11541	3.66	4.98	0.43	37007	0.31
1316	3	10701	6.05	4.90	0.46	32460	0.33
1317	3	11636	5.30	6.42	0.55	24945	0.47
1318	3	12184	6.00	7.52	0.62	29774	0.41
1319	3	12266	6.18	7.81	0.64	33546	0.37

1320	3	11651	5.44	7.75	0.67	32804	0.36
1321	3	12985	4.13	7.16	0.55	41047	0.32
1322	3	11234	3.90	4.56	0.41	39544	0.28
1323	3	13220	3.64	6.28	0.47	36021	0.37
1324	3	13452	3.81	6.42	0.48	36788	0.37
1325	3	14051	3.76	6.40	0.46	36159	0.39
1326	3	13921	3.96	6.76	0.49	34412	0.40
1327	3	12283	4.76	4.64	0.38	32681	0.38
1328	3	12998	4.67	7.07	0.54	31304	0.42
1329	3	12720	5.35	7.81	0.61	33530	0.38
1330	3	12225	5.24	7.60	0.62	37326	0.33
1331	3	12707	4.74	6.83	0.54	38751	0.33
1332	3	11992	5.68	7.90	0.66	35042	0.34
1333	3	8392	8.36	4.37	0.52	30031	0.28
1334	3	13222	4.61	6.67	0.50	30948	0.43
1335	3	13494	3.39	6.34	0.47	30592	0.44
1336	3	12865	3.11	6.33	0.49	30090	0.43
1337	3	12276	4.21	6.53	0.53	29033	0.42
1338	3	13307	5.60	6.08	0.46	26532	0.50
1339	3	13431	5.68	7.78	0.58	28481	0.47
1340	3	13513	4.95	6.98	0.52	27039	0.50
1341	3	13342	4.24	6.25	0.47	25840	0.52
1342	3	12579	4.70	6.83	0.54	22719	0.55
1343	3	12888	5.49	6.48	0.50	23154	0.56

## **6.6 Appendix I – Geological Prediction Model Results for Rings 336 to 1611**





Ring	472	473	474	475	476	477	478	479	480	481	482	483	484	485	486	487	488	489	490	491	492	493	494	495	496	497	498	499	500	501	502	503	504	505	
Reality	2	2	2	2	2	2	2	2	2	2	2	2	2	2	2	2	2	2	2	2	2	2	2	2	2	2	2	2	2	2	2	2	2	2	2
Predicted	2	2	2	2	2	2	2	2	2	2	2	2	2	2	2	2	2	2	2	2	2	2	2	2	2	2	2	2	2	2	2	2	2	2	
P (G1)	13%	4%	7%	9%	12%	2%	5%	8%	10%	13%	0%	3%	12%	9%	3%	12%	15%	17%	17%	19%	21%	23%	8%	9%	10%	47%	62%	53%	22%	7%	6%	8%	9%	10%	
P (G2)	85%	95%	92%	89%	87%	97%	94%	91%	88%	86%	100%	97%	87%	88%	92%	83%	82%	81%	83%	80%	78%	76%	92%	91%	90%	53%	37%	45%	75%	88%	90%	92%	91%	90%	
P (G3)	1%	0%	1%	1%	1%	1%	1%	1%	1%	1%	0%	0%	1%	3%	5%	5%	3%	2%	0%	0%	1%	1%	0%	0%	0%	0%	0%	0%	1%	3%	5%	4%	0%	0%	

Ring	506	507	508	509	510	511	512	513	514	515	516	517	518	519	520	521	522	523	524	525	526	527	528	529	530	531	532	533	534	535	536	537	538	539
Reality	2	2	2	2	2	2	2	2	2	2	2	2	2	2	2	2	2	2	2	2	2	2	2	2	2	2	2	2	2	2	2	2	2	2
Predicted	2	2	2	2	2	2	2	2	2	2	2	2	2	2	2	2	2	2	2	2	2	2	2	2	2	2	2	2	2	2	2	2	2	2
P (G1)	11%	14%	16%	0%	3%	5%	7%	8%	9%	11%	13%	14%	16%	16%	16%	17%	17%	0%	4%	9%	7%	9%	11%	55%	68%	56%	70%	100%	96%	91%	70%	57%	68%	
P (G2)	89%	86%	83%	100%	97%	95%	93%	91%	89%	86%	84%	84%	84%	84%	84%	83%	83%	100%	96%	91%	92%	91%	89%	44%	31%	44%	30%	4%	9%	30%	41%	43%	31%	
P (G3)	0%	1%	1%	0%	0%	0%	0%	0%	0%	1%	0%	0%	0%	0%	0%	0%	0%	0%	0%	0%	0%	0%	0%	0%	0%	0%	0%	0%	1%	2%	0%	0%	0%	

Ring	540	541	542	543	544	545	546	547	548	549	550	551	552	553	554	555	556	557	558	559	560	561	562	563	564	565	566	567	568	569	570	571	572	573	
Reality	1	1	1	1	1	1	1	1	1	1	1	1	1	1	1	1	1	1	1	1	1	1	1	1	1	1	1	1	1	1	1	1	1		
Predicted	1	1	1	1	1	1	1	1	1	1	1	1	1	1	1	1	1	1	1	1	1	1	1	1	1	1	1	1	1	1	1	1	1		
P (G1)	79%	89%	90%	98%	78%	94%	92%	93%	93%	67%	76%	75%	87%	86%	81%	79%	76%	100%	97%	93%	88%	85%	82%	79%	75%	93%	90%	61%	27%	9%	0%	3%	5%	7%	
P (G2)	21%	11%	9%	2%	22%	6%	8%	8%	7%	32%	21%	13%	8%	14%	19%	21%	24%	0%	3%	7%	12%	15%	18%	21%	25%	7%	10%	39%	73%	91%	100%	97%	95%	93%	
P (G3)	0%	0%	0%	0%	0%	0%	0%	0%	0%	1%	3%	12%	5%	0%	0%	0%	0%	0%	0%	0%	0%	0%	0%	0%	0%	0%	0%	0%	0%	0%	0%	0%	0%	0%	0%

Ring	574	575	576	577	578	579	580	581	582	583	584	585	586	587	588	589	590	591	592	593	594	595	596	597	598	599	600	601	602	603	604	605	606	607		
Reality	2	2	2	2	2	2	2	2	2	2	2	2	2	2	2	2	2	2	2	2	2	2	2	2	2	2	2	2	2	2	2	2	2			
Predicted	2	2	2	2	2	2	2	2	2	2	2	2	2	2	2	2	2	2	2	2	2	2	2	2	2	2	2	2	2	2	2	2	2			
P (G1)	10%	12%	13%	15%	15%	28%	29%	31%	32%	33%	25%	18%	5%	0%	3%	6%	2%	2%	2%	2%	2%	4%	7%	9%	11%	12%	0%	6%	6%	11%	14%	16%	18%	20%	63%	62%
P (G2)	90%	88%	87%	85%	84%	72%	70%	68%	67%	66%	72%	77%	93%	100%	90%	90%	97%	92%	84%	87%	93%	91%	89%	88%	100%	93%	90%	89%	86%	84%	82%	80%	37%	38%		
P (G3)	0%	0%	0%	0%	0%	1%	1%	1%	1%	1%	3%	5%	2%	0%	7%	4%	2%	6%	14%	8%	0%	0%	0%	0%	0%	0%	1%	1%	0%	0%	0%	0%	0%	0%	0%	

Ring	608	609	610	611	612	613	614	615	616	617	618	619	620	621	622	623	624	625	626	627	628	629	630	631	632	633	634	635	636	637	638	639	640	641
Reality	1	1	1	1	1	1	1	1	1	1	1	1	1	1	1	1	1	1	1	1	1	1	1	1	1	1	1	1	1	1	1	1	1	
Predicted	1	1	1	1	1	1	1	1	1	1	1	1	1	1	1	1	1	1	1	1	1	1	1	1	1	1	1	1	1	1	1	1	1	
P (G1)	58%	55%	51%	51%	48%	100%	97%	100%	99%	99%	99%	100%	98%	99%	99%	100%	97%	99%	99%	99%	99%	99%	99%	96%	96%	95%	77%	31%	20%	20%	4%	1%		
P (G2)	42%	45%	49%	49%	52%	0%	3%	0%	1%	1%	1%	0%	2%	1%	1%	0%	3%	1%	1%	1%	1%	1%	1%	1%	4%	1%	5%	4%	7%	22%	65%	65%	33%	
P (G3)	0%	0%	0%	0%	0%	0%	0%	0%	0%	0%	0%	0%	0%	0%	0%	0%	0%	0%	0%	0%	0%	0%	0%	0%	0%	0%	0%	0%	0%	1%	4%	14%	29%	65%







Ring	846	847	848	849	850	851	852	853	854	855	856	857	858	859	860	861	862	863	864	865	866	867	868	869	870	871	872	873	874	875	876	877	878	879
Reality	2	2	2	2	2	2	2	2	2	2	2	2	2	2	2	2	2	2	2	2	2	2	2	2	2	2	2	2	2	2	2	2	2	2
Predicted	3	3	3	3	3	3	3	3	3	3	3	3	3	3	3	3	3	3	3	3	3	3	3	3	3	3	3	3	3	3	3	3	3	
P (G1)	0%	0%	0%	0%	0%	0%	0%	0%	0%	0%	0%	0%	0%	0%	0%	0%	0%	0%	0%	0%	0%	0%	0%	0%	0%	0%	0%	0%	0%	0%	0%	0%	0%	
P (G2)	7%	8%	3%	4%	2%	4%	16%	11%	4%	28%	20%	6%	3%	4%	65%	89%	85%	97%	87%	87%	42%	25%	36%	77%	93%	90%	71%	38%	14%	2%	2%	5%	4%	
P (G3)	93%	92%	97%	96%	98%	96%	84%	89%	96%	72%	80%	94%	97%	96%	96%	35%	8%	9%	1%	2%	2%	1%	2%	10%	4%	6%	27%	62%	86%	98%	95%	96%	99%	

Ring	846	847	848	849	850	851	852	853	854	855	856	857	858	859	860	861	862	863	864	865	866	867	868	869	870	871	872	873	874	875	876	877	878	879
Reality	3	3	3	3	3	3	3	3	3	3	3	3	3	3	3	3	3	3	3	3	3	3	3	3	3	3	3	3	3	3	3	3	3	
Predicted	3	3	3	3	3	3	3	3	3	3	3	3	3	3	3	3	3	3	3	3	3	3	3	3	3	3	3	3	3	3	3	3	3	
P (G1)	0%	0%	0%	0%	0%	0%	0%	1%	0%	0%	0%	0%	0%	0%	0%	0%	2%	4%	14%	17%	19%	38%	59%	59%	59%	66%	65%	63%	62%	50%	50%	70%	83%	
P (G2)	2%	1%	9%	8%	8%	35%	23%	5%	4%	2%	5%	3%	7%	33%	24%	30%	84%	88%	79%	79%	78%	60%	39%	40%	41%	34%	35%	36%	37%	38%	49%	29%	16%	
P (G3)	98%	99%	91%	92%	92%	63%	77%	93%	96%	98%	95%	97%	93%	66%	76%	68%	14%	8%	7%	4%	3%	3%	2%	1%	1%	1%	0%	0%	0%	1%	2%	1%	1%	

Ring	880	881	882	883	884	885	886	887	888	889	890	891	892	893	894	895	896	897	898	899	900	901	902	903	904	905	906	907	908	909	910	911	912	913
Reality	2	2	2	2	2	2	2	2	2	2	2	2	2	2	2	2	2	2	2	2	2	2	2	2	2	2	2	2	2	2	2	2	2	
Predicted	1	1	1	1	1	1	1	1	1	1	1	1	1	1	1	1	1	1	1	1	1	1	1	1	1	1	1	1	1	1	1	1	1	
P (G1)	90%	68%	55%	43%	11%	9%	7%	19%	38%	40%	41%	42%	63%	79%	50%	51%	50%	50%	86%	90%	86%	97%	99%	95%	90%	86%	97%	99%	99%	95%	98%	99%	87%	
P (G2)	9%	30%	41%	50%	85%	85%	84%	73%	56%	57%	57%	57%	36%	20%	45%	46%	50%	49%	50%	14%	3%	1%	5%	10%	14%	3%	1%	1%	1%	1%	5%	2%	1%	
P (G3)	0%	2%	4%	7%	4%	6%	9%	8%	6%	3%	2%	1%	1%	1%	4%	3%	0%	0%	0%	0%	0%	0%	0%	0%	0%	0%	0%	0%	0%	0%	0%	0%	0%	

Ring	914	915	916	917	918	919	920	921	922	923	924	925	926	927	928	929	930	931	932	933	934	935	936	937	938	939	940	941	942	943	944	945	946	947
Reality	1	1	1	1	1	1	1	1	1	1	1	1	1	1	1	1	1	1	1	1	1	1	1	1	1	1	1	1	1	1	1	1	1	
Predicted	1	1	1	1	1	1	1	1	1	1	1	1	1	1	1	1	1	1	1	1	1	1	1	1	1	1	1	1	1	1	1	1	1	
P (G1)	93%	98%	99%	99%	99%	95%	94%	94%	96%	99%	99%	99%	99%	97%	99%	95%	96%	88%	64%	80%	51%	52%	53%	53%	53%	66%	66%	66%	66%	66%	66%	66%	66%	
P (G2)	7%	2%	1%	1%	1%	5%	6%	6%	4%	1%	1%	1%	1%	3%	1%	5%	4%	12%	34%	19%	44%	45%	45%	46%	32%	34%	29%	40%	54%	42%	51%	35%		
P (G3)	0%	0%	0%	0%	0%	0%	0%	0%	0%	0%	0%	0%	0%	0%	0%	0%	0%	0%	2%	1%	5%	3%	2%	1%	1%	1%	1%	5%	8%	23%	29%	55%	48%	65%

Ring	948	949	950	951	952	953	954	955	956	957	958	959	960	961	962	963	964	965	966	967	968	969	970	971	972	973	974	975	976	977	978	979	980	981
Reality	2	2	2	2	2	2	2	2	2	2	2	2	2	2	2	2	2	2	2	2	2	2	2	2	2	2	2	2	2	2	2	2	2	
Predicted	3	3	3	3	3	3	3	3	3	3	3	3	3	3	3	3	3	3	3	3	3	3	3	3	3	3	3	3	3	3	3	3	3	
P (G1)	0%	0%	1%	3%	5%	37%	76%	94%	89%	85%	95%	97%	99%	95%	90%	87%	84%	81%	79%	67%	82%	54%	42%	10%	14%	10%	14%	10%	2%	1%	0%	0%	0%	
P (G2)	22%	21%	21%	31%	48%	57%	22%	6%	11%	14%	2%	3%	1%	5%	9%	13%	16%	19%	21%	32%	18%	42%	52%	62%	52%	19%	14%	4%	2%	7%	9%	5%	8%	
P (G3)	76%	76%	79%	67%	47%	7%	0%	0%	0%	0%	0%	0%	0%	0%	0%	0%	0%	0%	0%	1%	1%	4%	6%	8%	34%	71%	64%	95%	86%	93%	91%	95%	95%	91%













Ring	Reality	1492	1493	1494	1495	1496	1497	1498	1499	1500	1501	1502	1503	1504	1505	1506	1507	1508	1509	1510	1511	1512	1513	1514	1515	1516	1517	1518	1519	1520	1521	1522	1523	1524	1525	
Predicted	1	1	2	2	2	2	2	2	2	2	2	2	2	2	2	2	2	2	1	1	1	1	1	1	1	1	1	1	1	1	1	1	1	1	1	
P (G1)	54%	68%	46%	27%	43%	37%	53%	32%	32%	18%	31%	20%	11%	22%	37%	24%	39%	55%	69%	86%	83%	80%	77%	78%	90%	95%	89%	81%	74%	67%	61%	59%	80%	77%	85%	
P (G2)	45%	31%	53%	72%	56%	62%	46%	66%	81%	67%	78%	87%	62%	74%	60%	44%	30%	14%	17%	20%	23%	20%	23%	22%	10%	5%	11%	19%	25%	32%	39%	41%	19%	22%	15%	
P (G3)	1%	0%	1%	1%	1%	1%	1%	1%	1%	1%	1%	2%	2%	2%	1%	2%	1%	1%	1%	0%	0%	0%	0%	0%	0%	0%	0%	0%	0%	0%	0%	0%	0%	0%	0%	0%

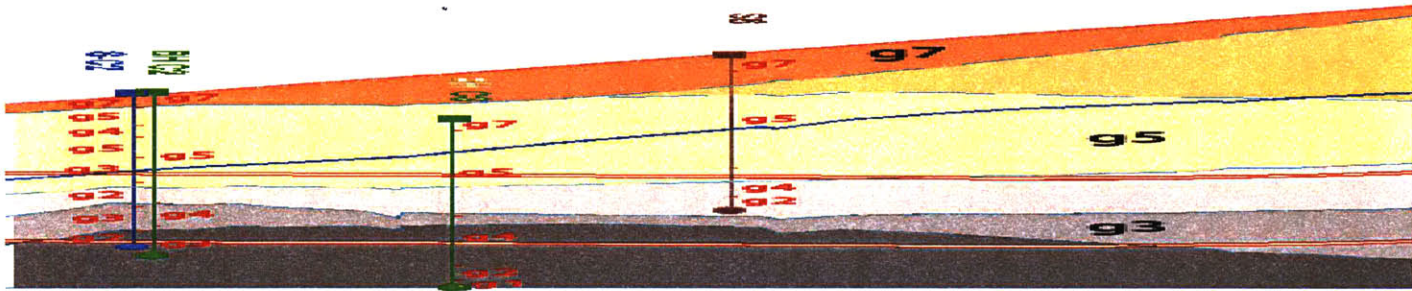
Ring	Reality	1526	1527	1528	1529	1530	1531	1532	1533	1534	1535	1536	1537	1538	1539	1540	1541	1542	1543	1544	1545	1546	1547	1548	1549	1550	1551	1552	1553	1554	1555	1556	1557	1558	1559		
Predicted	1	1	1	1	1	1	1	1	1	1	1	1	1	1	1	1	2	2	2	2	2	2	2	2	3	3	3	2	2	2	2	2	2	2	2	1	1
P (G1)	78%	71%	63%	61%	74%	83%	68%	61%	61%	82%	79%	71%	87%	94%	96%	97%	98%	96%	97%	91%	93%	87%	80%	87%	0%	3%	0%	4%	2%	2%	2%	2%	2%	2%	2%	1%	1%
P (G2)	22%	29%	36%	38%	25%	17%	31%	38%	38%	18%	21%	28%	13%	6%	4%	3%	2%	4%	3%	9%	7%	13%	20%	13%	0%	10%	39%	56%	72%	60%	36%	60%	33%	30%	0%	0%	
P (G3)	0%	0%	0%	1%	1%	0%	1%	0%	0%	0%	0%	0%	0%	0%	0%	0%	0%	0%	0%	0%	0%	0%	0%	0%	100%	90%	61%	43%	33%	15%	6%	2%	0%	0%	0%	0%	

Ring	Reality	1560	1561	1562	1563	1564	1565	1566	1567	1568	1569	1570	1571	1572	1573	1574	1575	1576	1577	1578	1579	1580	1581	1582	1583	1584	1585	1586	1587	1588	1589	1590	1591	1592	1593	
Predicted	1	1	1	1	1	1	1	1	1	1	2	2	2	2	2	2	2	2	2	2	2	1	1	1	1	1	1	1	1	1	1	1	1	1	1	1
P (G1)	95%	100%	94%	87%	80%	86%	80%	73%	75%	100%	0%	1%	2%	6%	10%	9%	10%	10%	10%	100%	100%	94%	87%	79%	72%	55%	34%	47%	45%	57%	100%	100%	90%	78%	79%	
P (G2)	5%	0%	6%	13%	14%	20%	27%	25%	25%	0%	100%	97%	96%	94%	90%	91%	90%	90%	90%	90%	0%	6%	13%	21%	28%	44%	65%	52%	53%	41%	0%	0%	10%	22%	21%	
P (G3)	0%	0%	0%	0%	0%	0%	0%	0%	0%	0%	0%	1%	2%	0%	0%	0%	0%	1%	1%	1%	0%	0%	0%	0%	0%	0%	1%	1%	2%	2%	0%	0%	0%	0%	0%	0%

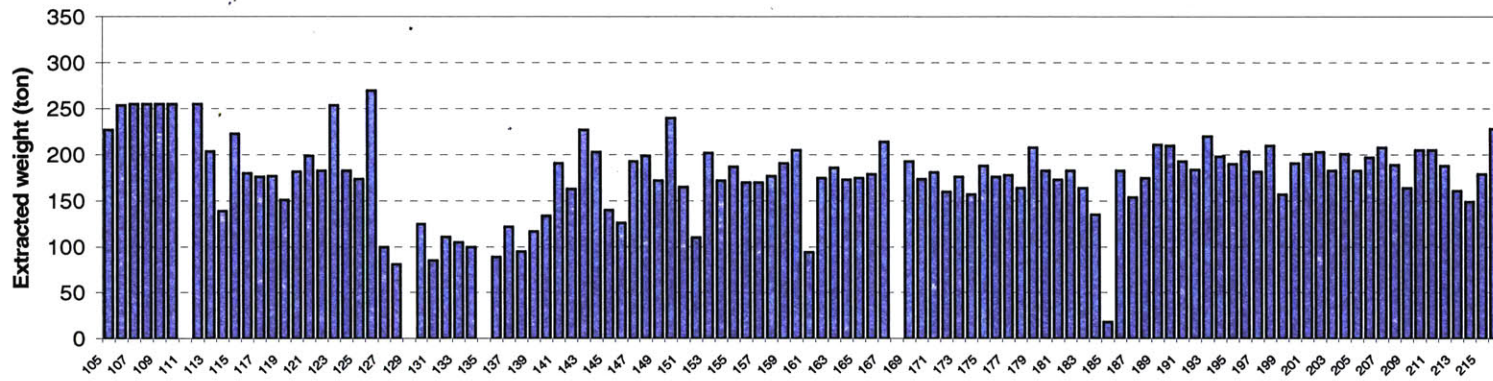
Ring	Reality	1594	1595	1596	1597	1598	1599	1600	1601	1602	1603	1604	1605	1606	1607	1608	1609	1610	1611
Predicted	1	1	1	1	1	1	1	1	1	1	1	1	1	1	1	1	3	3	3
P (G1)	80%	100%	94%	94%	95%	92%	91%	89%	89%	100%	98%	100%	95%	97%	84%	76%	67%	45%	0%
P (G2)	20%	0%	6%	6%	5%	8%	9%	11%	11%	0%	2%	0%	5%	3%	16%	24%	32%	54%	0%
P (G3)	0%	0%	0%	0%	0%	0%	0%	0%	0%	0%	0%	0%	0%	0%	0%	0%	1%	1%	100%

## **6.7 Appendix J – Machine Parameters Plots (Section 1 and 2)**





a)



b)

Figure 6.95 Section 1: a) design geological longitudinal profile ; b) Extracted weight (measured by the EPBM scales) per ring

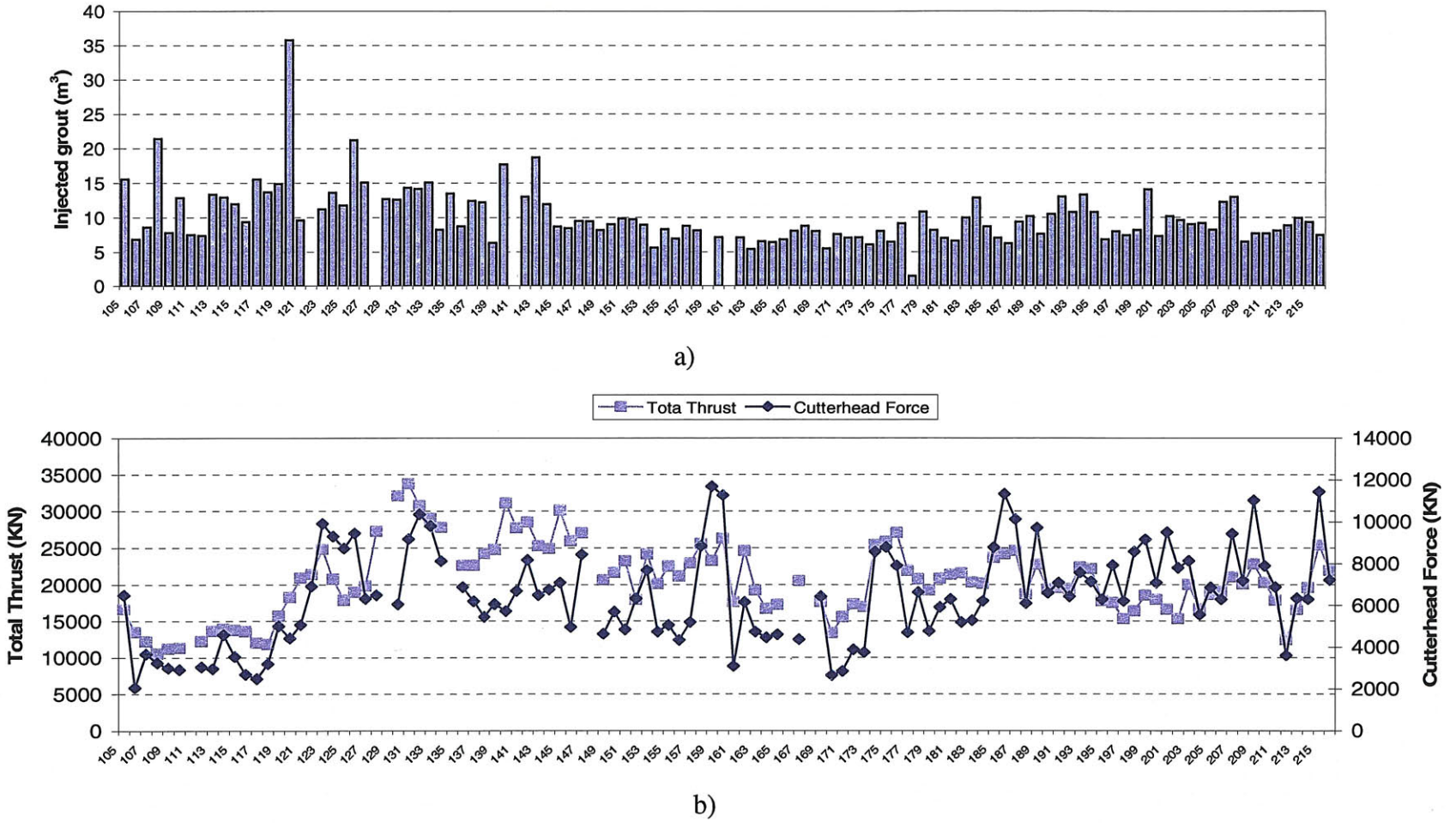
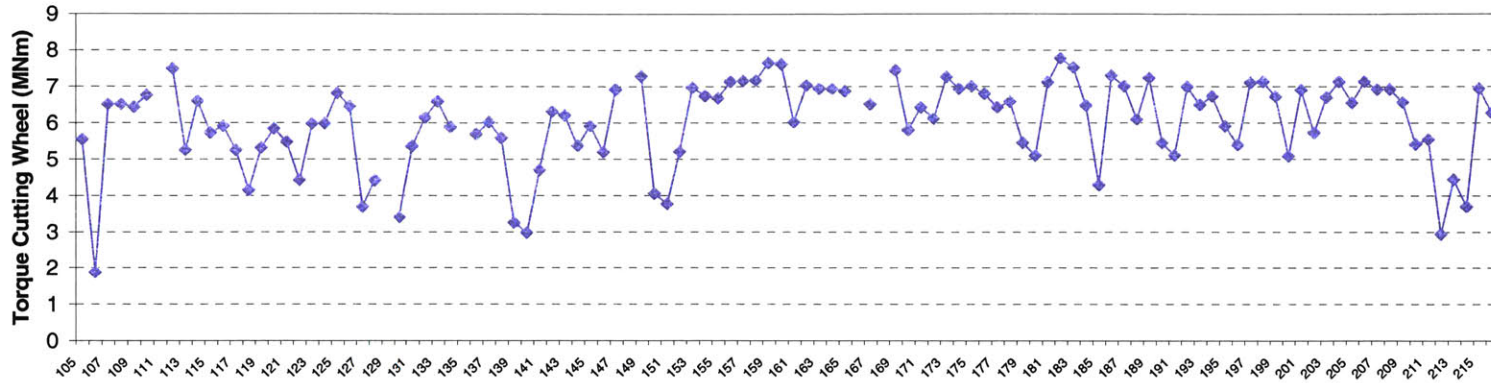
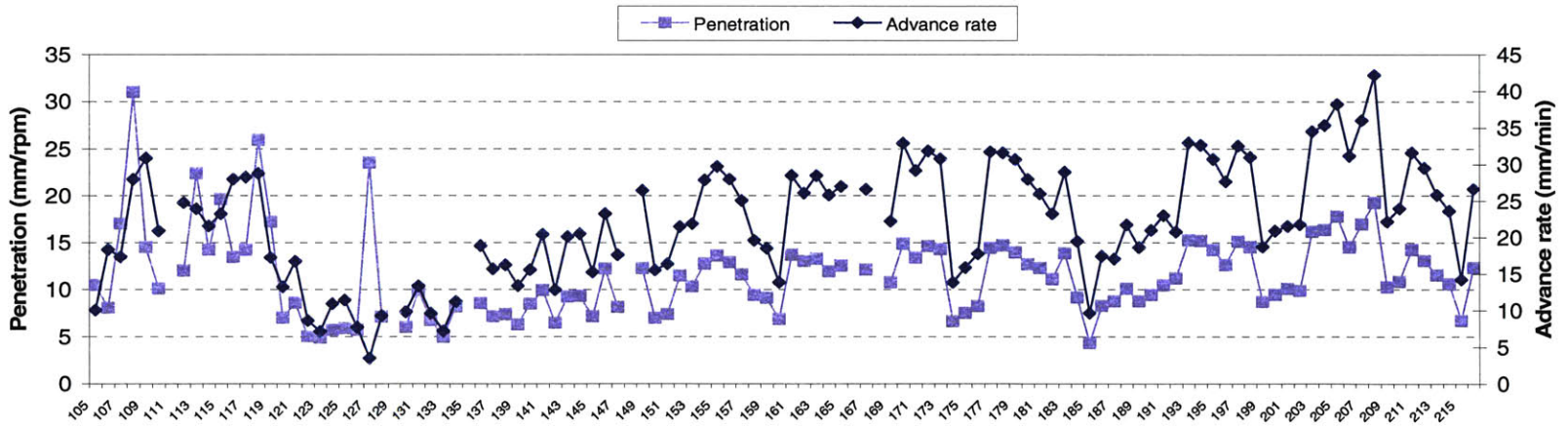


Figure 6.96 Section 1 a) Injected grout per ring in Section 1; b) Total thrust and cutting wheel force per ring



a)

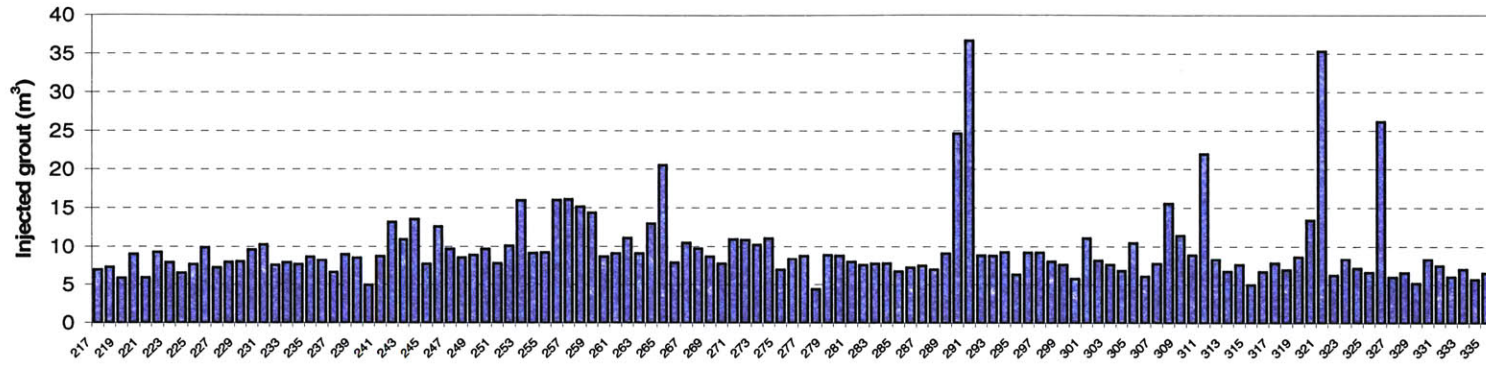


b)

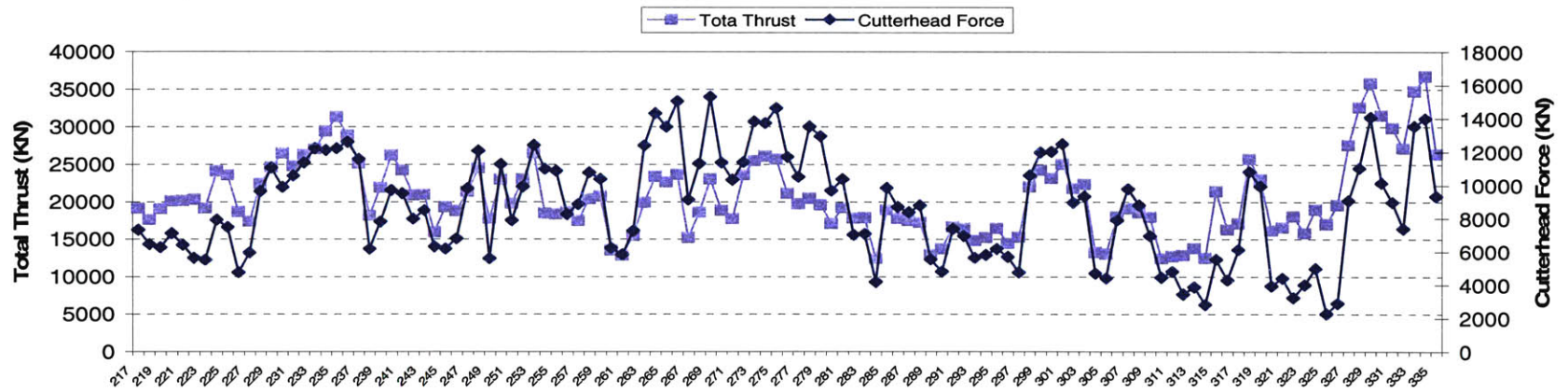
Figure 6.97 Section 1: a) torque of the cutting wheel; b) penetration and advance rate





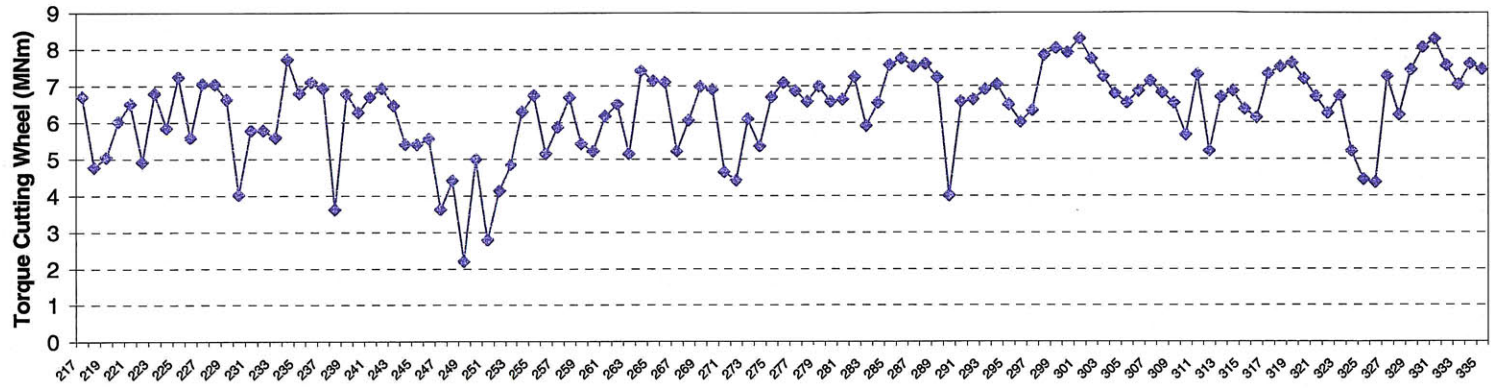


a)

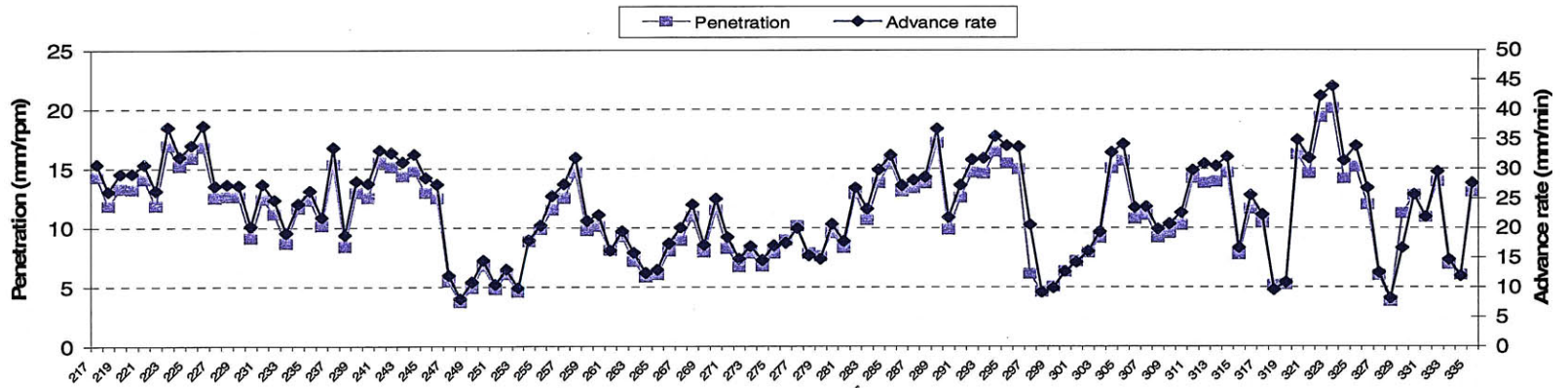


b)

Figure 6.99 Section 2: a) Injected grout per ring in Section 1; b) Total thrust and cutting wheel force per ring



a)



b)

Figure 6.100 Section 1: a) torque of the cutting wheel; b) penetration and advance rate

## CHAPTER 7 Conclusions and Recommendations

### 7.1 Conclusions

There is an intrinsic risk associated with tunnel construction because of the limited *a priori* knowledge of the existing subsurface conditions. Although the majority of tunnel construction projects have been completed safely there have been several incidents in various tunneling projects that have resulted in delays, cost overruns, and in a few cases more significant consequences such as injury, and loss of life. It is therefore important to systematically assess and manage the risks associated with tunnel construction.

This study has first tried to improve on existing knowledge regarding the conditions surrounding accidents. A database of accidents was assembled and studied to better understand the importance of various parameters in the occurrence of accidents.

Two Bayesian based models were then combined to assess risks during tunnel construction. The first model allows one to predict the geology ahead of a tunnel machine based on observations of various machine parameters. The second model allows one to decide on the best construction strategy for a given geology. When combined, the resulting model allows one to predict geology, and choose the best construction strategy ahead of a tunnel machine, thereby minimizing risk.

#### Accident Database

There are not enough and reliable data regarding the conditions under which accidents can occur during tunnel construction. For this reason a database of accidents that occurred during tunnel construction was created. The database contains 204 cases all around the world with different construction methods and different types of accidents. The accident cases were obtained from the technical literature, newspapers and correspondence with experts in the tunneling domain. The data were stored in a database that is the most comprehensive database to date. The database contains exhaustive (as





- **Consequences:** Undesirable events always have consequences on the tunneling process, but many times they can also have consequences on the surface as well (people, traffic) and on other subsurface structures (other existing tunnels, utilities). These consequences can be catastrophic, especially in the case of daylight collapses in urban areas where consequences are typically heavy financial loss, and possible loss of life. In the past decade there have been a number of great consequences involving tunnels in urban areas, which in some cases amount to about US\$ 100M. The delays associated with accidents were on average 6 months. In 7 cases the delays reported were over 12 months.
- **Mitigation and Remedial Measures:** The remedial methods used to overcome an accident and the mitigation measures used to ensure safe completion of tunnel excavation are very specific to each situation. However it was possible to identify some methods that were commonly used, in many of these situations. For collapses or daylight collapses, the mitigation and remedial measures ranged from filling the tunnel with material (concrete, rock, sand bags and even water) for immediate stabilization to prevent further propagation of the collapse; to bypass tunnels (used also in combination with grouting from inside the bypass tunnel) or to a change in construction method or even alignment changes in the most severe cases. For rock falls the most common measure was to fill in the ensuing cavity(ies) with concrete, and use rock bolts and shotcrete to advance the tunnel. For water inflow the most common mitigation and remedial measure was to drain (in advance and from the surface) and / or grout. In rockburst situations the use of special bolts and destress blasting were the most common measures. When excessive deformations occurred the most common mitigation and remedial measures were to re-mine the deformed section, use yielding support elements, modify the shape / dimensions of the cross section, and modify and reinforce the lining, such as a reinforced invert or a deformable invert (in swelling cases).

The analysis of the database led to a better understanding of the main causes and consequences of accidents, and allowed one to compile a list of main factors, and their

interactions that affect tunnel construction. For each undesirable event, it was possible to identify different scenarios, in which these events are most likely to occur.

Influence diagrams, containing parameters (ground, construction, observations) identified in these scenarios, were built with this information.

The knowledge gained from the analysis of the database, and the analysis of the data (a good amount was available) from the Porto Metro in Portugal, were then used to develop the risk assessment methodology that was presented in this work.

### Risk Assessment Methodology

A decision support framework for determining the “optimal” (minimum risk) construction method for a given tunnel alignment was developed. The support system consists of two models: a geologic prediction model, and a construction strategy decision model. Both models are based on the Bayesian Network technique, and when combined allow one to determine the ‘optimal’ construction strategies during tunnel construction by including information from the excavated tunnel sections.

Bayesian networks were considered to be the most suitable model structures for the problem of accidents during tunnel construction, compared to other techniques due to:

- 1) Their ability of encoding dependencies among variables;
- 2) Facilitating the combination of domain knowledge and data, through well-studied techniques from Bayesian statistics. Prior or domain knowledge is crucially important if one performs a real-world analysis; in particular, when data are inadequate or expensive to observe. The encoding of causal prior knowledge is straightforward because Bayesian networks have causal semantics.
- 3) Their ability to learn causal relationships, which is important when one would like to understand the problem domain.

- 4) Providing an efficient approach to avoid the over-fitting of data. Models can be “smoothed” in such a way that all available data can be used for training by using the Bayesian approach.

In order to develop a geological prediction model, a study was performed on the data available from the Porto Metro to determine the parameters that allow one to most easily distinguish between different ground conditions. The Porto Metro case provided a good opportunity to do this because of the considerable amount of data available on different geological formations. The study allowed one to determine important parameters, which were retained for modeling, and less important parameters, which were dropped.

The geological conditions in the Porto metro tunnel, which consisted of granite with different degrees of weathering, were simplified into soil (G1), mixed (G2) and rock (G3). One-parameter and two-parameter analyses were performed on the Porto Metro data. The one-parameter analyses allowed one to determine the important parameters, and the two-parameter analyses allowed one to determine which interrelationships between the parameters are important. The results can be summarized as follows:

- Penetration rate (P) and cutting wheel force (CF) are important parameters when distinguishing between ground condition, while torque of the cutting wheel (TO) and Total Thrust (TT) are less important. Although torque (TO) by itself is not important to distinguish between ground conditions, the relation between torque, cutting wheel force and penetration is extremely important (see below)
- The ratio between torque of the cutting wheel (TO) and the cutting wheel force (COT) is important to distinguish between ground conditions. This ratio is important in all geologies but it becomes relatively more important in rock conditions. This is due to the fact that torque becomes a more significant parameter when driving through rock.
- The ratio of cutting wheel force to the total thrust (COTT) is important to distinguish between ground conditions. The total thrust is the force that is applied by the thrust cylinders (or jacks). Only a portion of this force will reach the

cutting wheel. Portions of the cutting wheel force are lost to friction between the ground around the shield, as well as to support pressure necessary to maintain the face stable. In soil conditions, COTT is lower than in rock conditions since a larger portion of the total thrust is lost by friction around the shield. This is because soil formations are more deformable than rock and the normal force on the shield will be greater and consequently so will the friction. The support pressure necessary to maintain the face stable is also greater in soil-like formations than in rock.

From the results discussed above, penetration rate (P), cutting wheel force (CF), torque of cutting wheel (TO)<sup>1</sup>, the ratio between torque and cutting wheel force (TOC) and the relation between cutting wheel force and total thrust (COTT) were retained for the modeling studies. The relationships between torque (TO) and penetration (P); cutting wheel force (CF) and penetration (P); TOC and penetration (P) and COTT and penetration (P) were also retained.

Various model configurations or model structures can be produced given the parameters (and the relationships between them). In order to determine, which structure produces the best model, a sensitivity analysis was performed on different model structures by considering various combinations of the important parameters and various relationships between these parameters. The aim of the model is to predict ground conditions ahead of the tunneling machine given information from the machine performance parameters. The model is first 'learned' from data (three different data sets were used) that are obtained by observations during the construction process. The model is then used to predict geological conditions ahead. The data from the tunnel C line of the Porto Metro were used to assess the various model configurations.

The results of the sensitivity analysis are summarized below:

---

<sup>1</sup> TO is retained in the models because, although it is not important to distinguish between classes by itself, it is extremely important when combined with other machine parameters such as P and CF.

- Different model structures performed differently in rock (G3) and soil (G1). This is to be expected, since the parameters are of differing importance in soil, and in rock.
- The models that performed the best in soil (G1), contain the variables CF, P and TO or COTT; with the relationships between CF and P; between TO and P; and between CF and TO being most important.
- The models that perform the best in rock (G3), contained the variables CF, P and TOC; with the relationships between CF and P; TOC and P being most important.
- Mixed conditions (G2) were difficult to predict. This was expected, and has to do with how mixed conditions were defined. Mixed conditions ranged from 10% soil with 90% rock (i.e. almost all rock), to 10% rock and 90% soil (i.e. almost all soil).
- The model that performed the best overall contained the parameters penetration rate (P), cutting wheel force (CF), and torque of cutting wheel (TO); it considers the inter-relation between torque and penetration and between cutting wheel force and penetration. Recall again that the best overall model is neither the best model identifying soil only, nor the best model identifying rock only. This has to do with the fact that the importance of some parameters of the construction process, and the relationships among them, depends on whether the tunnel is being driven through rock or through soil. However the best overall model does quite well when identifying both rock and soil.

The best overall model was applied as a geological prediction model to the Porto Metro. The model was first applied from ring 336, station 0+631 (after the accidents) to ring 1611, station 2+418, i.e. in a section beyond the one where the accidents occurred. The results of the geologic prediction model showed good agreement with the observed geological conditions, particularly in identifying soil (G1) and rock (G3). In the case of soil, 77.2% of the rings sections that consisted of soil were correctly identified, 20.4% were misclassified as mixed and 2.4% as rock. In the case of rock, 82.4% of the ring sections that consisted of rock were correctly identified, while 10.9% were misclassified as mixed and 6.7% as soil.



The best overall model was then used to predict the geological conditions for the first 320 m of the Line C of the Porto Metro, where the accidents occurred. Information on geologic conditions was available where the last accident occurred, because a post accident survey was made. The geological prediction model was also combined with the Bayesian decision model to determine optimal construction strategies ahead of the tunneling, in this section. The results of the prediction model showed that the model can predict changes in geology and consequently change the construction strategy to minimize risk. This was most visible in the zone of accidents 2 and 3, where the model accurately predicts the change in geology and occurrence of a soil formation. This was confirmed by the post accident survey boreholes. The results of the decision model showed that in the area of accidents 2 and 3, the “optimal” construction strategy is to use the EPBM with a fully pressurized face instead of the EPBM with the open (or semi-closed) mode as was actually used during construction.

The overall contributions of this work can be summarized as:

- (a) Creation of a comprehensive database of accidents during tunnel construction, and a better understanding of the parameters, which are important in risk assessment regarding tunnel stability. The database is available to decision makers in the domain (owners, contractors, designers) and can serve as basis for the building of risk assessment models for tunneling projects.
- (b) Development of a risk assessment methodology based on a combined geological prediction and decision model tool, to identify optimal construction strategies during construction. This allows one to predict changes in geology and consequently adapt the construction method to these changes, thereby minimizing the risk.

## 7.2 Recommendations for future work

Despite recent efforts and advances in the field of tunneling comprehensive risk assessment still remains a challenge. This is due to the complexity of the problem, the many factors that affect it, and the associated incomplete understanding of the mechanisms involved.

This study has advanced the knowledge of conditions under which accidents occurred, and presented a systematic methodology to assess risk during tunnel construction. There are various areas that require future research, some of which are presented below:

### Database

- (a) Publication and enrichment of the database. The database can be made available on the internet, for example through the international tunneling society (or other similar societies). There are two main benefits of doing so. First, the data will be available to designers, consultants and construction engineers worldwide. Second, the possibility of adding new cases and expanding the database. This should probably be done under the supervision of a moderator, to avoid false and erroneous entries.
- (b) Expansion of the database of accidents for other types of construction methods such as the cut and cover.

### Risk Assessment methodology

- (c) Use of continuous random variables. A limitation of the decision framework system presented in this study is the use of discretized continuous variables for the machine parameters (penetration (P), cutting wheel force (CF), torque of the cutting wheel (TO), which are actually continuous. This is a disadvantage related to the use of Bayesian based systems that have been for the most part developed and used with discrete, or discretized continuous variables. A suggestion for

future work is to assume that the machine parameter variables follow continuous distributions, and train the models assuming continuous distributions. More specifically, these are Gaussian distributions since new techniques that allow one to combine discrete variables and Gaussian variables have recently become available for Bayesian Networks.

- (d) Refining the geological prediction and decision models, specifically:
- Refine the definition of ground classes. Use of more detailed ground classes based on geomechanical parameters of the ground such as compressive strength, jointing spacing (for rock) and cohesion and friction angle (soil)
  - Consider other observed variables such as deformations inside the tunnel and at the surface, in predicting geology and assessing risk.
- (e) Utility functions. In this study, simple utility functions were used to decide between construction strategies. This was done to illustrate the model in a clear way. Different types of utility functions should be used when applying the model to different projects. Utility functions that reflect the decision maker's attitude towards risk should be used, particularly risk averse utility functions. Furthermore, single variable utility functions were used. Multi-attribute utility functions can be developed and used in the future. These utility functions consider different attributes for engineering projects, other than cost, such as cost/profit (cost overrun/cost underrun), time to completion (time delay/time underrun), quality, safety, and environmental issues amongst others.
- (f) Application of the risk assessment methodology to other tunnels with different ground conditions and different construction methods. This study has applied the risk assessment methodology to the Porto Metro since a large amount of data was available. The risk assessment methodology can be applied to similar projects, where data are available. It would also be interesting to compare the results of several of these studies, in particular with regard to the structure of models that perform best in predicting geology.
- (g) The Porto Metro dataset is valuable, and the author would like to once again extend the thanks to Porto Metro for allowing the use of this dataset. The dataset

itself was essential to this study, but can also be useful in other studies. For example, the dataset can be used to study and create models that predict penetration rates based on observed, and predicted geologies. These models can or can not be based on Bayesian methods.

- (h) The Bayesian techniques used to build the geological prediction model in this study can also be used to create a TBM performance prediction model. It would be interesting to develop such a model, and compare its results with those obtained by applying several existing and established TBM performance models for rock TBMs.

## REFERENCES

AFTES (2000). “New recommendations on Choosing mechanized tunneling techniques”. French Tunnelling and Underground Engineering Association.

(url: [http://www.rocsience.com/hoek/pdf/Practical\\_Rock\\_Engineering.pdf](http://www.rocsience.com/hoek/pdf/Practical_Rock_Engineering.pdf))

AlpTransit-Tagung (2004). “Fauchtagung für Untertagbau“. D 0202. Band 3. 17 Juni 2004 in Interlaken.

American Society of Mechanical Engineers International (1997). “National Historic Mechanical Engineering Landmark – San Francisco Bay Area Rapid Transit System”.

Anagnostou G. and Kovari K., 1996: “Face stability conditions with Earth-Pressure-Balanced Shields”. Tunneling and Underground Space Technology, Vol.11, No.2, pp 165-173;

Ang, A. H-S., and W. H. Tang (1975). “Probability Concepts in Engineering Planning and Design”, vol. 1, Basic Principles. New York, NY: John Wiley & Sons.

Apostol, T. (2004). “The Tunnel of Samos”. Engineering & Science No.1 2004

Appleton, J. (1998) “Acidente nas Obras da Estação Olivais Sul do Metropolitano de Lisboa” (in Portuguese). Parecer n.º 241/PI. Conselho Superior das Obras Públicas.

Assis, A. (2001). “Métodos construtivos aplicados a túneis urbanos” (In Portuguese). Curso sobre Túneis em Meios Urbanos, SPG, Coimbra.

Ayaydin, N., (2001) “Istanbul Metro collapse investigations”, World Tunnelling.

Babendererde, S.; Hoek, E.; Marinos, P.G.; Cardoso, A.S. (2005). “EPB-TBM Face Support Control in the Metro do Porto Project, Portugal”. Proceedings 2005 Rapid Excavation & Tunneling Conference, Seattle.

Babendererde, S, Hoek, E., Marinos, P. and Cardoso, A.S. (2004). "Characterization of Granite and the Underground Construction in Metro do Porto, Portugal." Proc. International Conference on Site Characterization, Porto, Portugal, 19-22 September, 2004

Babendererde, S.; Hoek, E.; Marinos, P.; Silva Cardoso, A. (2004). "Geological risk in the use of TBMs in heterogeneous rock masses - The case of "Metro do Porto" and the measures adopted". Presented at the Course on Geotechnical Risks in Rock Tunnels, University of Aveiro, Portugal, 16-17 April, 2004.

Baecher, G.B. (1981). "Risk Screening for Civil Facilities", Massachusetts Institute of Technology, Dept.of Civil Eng. CER-81-9. 20 p.

Baecher, G.B. (1972). "Site Exploration: A probabilistic approach". PhD Massachusetts Institute of Technology, Cambridge, MA.

Barla, M. (2008). "Numerical Simulation of the swelling behaviour around tunnels based on triaxial tests". Tunnelling and Underground 23 (2008) 508-521.

Barla G. (2000). "Lessons learnt from the excavation of a large diameter TBM tunnel in complex hydrogeological conditions". GeoEng 2000, International Conference on Geotechnical & Geological Engineering, Melbourne, Australia, 19-24 November 2000.

Barla G. and Pelizza S. (2000), "TBM tunneling in difficult ground conditions", GeoEng 2000, International Conference on Geotechnical & Geological Engineering, Melbourne, Australia, 19-24 November 2000.

Barton, N. (2008). "Summary of the main factors that caused the uniquely sudden collapse at Pinheiros". Presentation.

Barton, N. (2006). "Fault Zones and TBM. Geotechnical risk in rock tunnels", ed. Matos; Sousa; Kleberger and Pinto, Taylor and Francis, pp. 75-118

Bell, D. E., Raiffa, H., & Tversky, A. (Eds.). (1988). "Decision making: Descriptive,



normative, and prescriptive interactions”. New York: Cambridge University Press, ISBN: 0521368510. (Richard Gonzalez, Psychology Department)

Broch, E. And Nilsen, B. (1977) “Comparison of Calculated, Measured and Observed Stresses at the Ortfjell Open Pit (Norway)”. Norwegian Hard Rock Tunneling. Norway Tunneling Society. url: <http://www.tunnel.no/article.php?id=113&p=>

Brown, D.A. (2004). Hull wastewater flow transfer tunnel: recovery of tunnel collapse by ground freezing. Geotechnical Engineering 157 Issue GE2. April 2004. pp. 77-83

Chienbergtunnel (N2 Umfahrung Sissach). 9 pages , private correspondence.

Clayton, C. (2008). “The Heathrow Tunnel Collapse”. Advanced Course on Risk Management in Civil Engineering LNEC Lisbon November 17-22 2008.

Cowell., R. G., A. P. Dawid, S. L. Lauritzen, D. J. Spiegelhalter (2003) “Probabilistic Networks and Expert Systems”, (Information Science and Statistics, 2003) .

Dalgıç, S (2002). “Tunneling in squeezing rock, the Bolu tunnel, Anatolian Motorway, Turkey”. Engineering Geology 67 (2002) 73–96.

Darlington, K (2000). “The essence of expert systems”. Ed. Prentice Hall. 167 pages.

Dempster, A.P. (1968). “A generalization of Bayesian inference”. Journal of the Royal Statistical Society, Series B 30 205-247.

Discovery Channel (2003), “Extreme Engineering”: Transatlantic Tunnel. DVD.

Einstein, H.H. (2007). “Transalpine Tunnels in Switzerland“. MIT MEng Presentation.

Einstein, H.H. (2000). “Tunnels in, Opalinus Clayshale“. A Review of Case Histories and

Einstein, H.H. (1997). “Landslide Risk: Systematic Approaches to Assessment and

Management". In: Cruden, A. and Fell, R. (editors). *Landslide Risk Assessment*. Balkema, Rotterdam. pp 25-50.

Einstein, H. H. (1996). "Tunnelling in Difficult Ground - Swelling Behaviour and Identification of Swelling Rocks". *Rock Mech. Rock Engineering*. (1996) 29 (3), 113-124

Einstein, H. H.; Descoudres, J; Dudt, J.P.; Halabe, V. (1991). *Decision Aids in tunnelling*. Monograph.

Einstein, H.H; Salazar, G.F; Kim, Y.W and Ioannou, P.G. (1987). "Computer Based Decision Support Systems for Underground Construction". *Proceedings, of Rapid Excavation And Tunneling Conference; Vol. 2*, pp. 1287-1308.

Einstein, H.H. Labreche, D.A., Markow, M.J., and Baecher, G.B. (1978). "Decision Analysis Applied to Rock Tunnel Exploration". *Engineering Geology*, Vol. 12, pp 143-161.

*Engineering News Record* (1989). "L.A. tunnelers overcome gassy soil". *ENR* 1989 222 (23), pg. 38-43

Eskesen, S. D., Tengborg, P., Kampmann, J., Veicherts, T. (2004). "Guidelines for tunneling risk management". *International Tunnelling Association, Working Group No. 2. Tunnelling and Underground Space Tecnology* 19 (2004) pp 217-237.

Faber, M.H. (2005). "Risk and Safety in Civil", *Surveying and Environmental Engineering. Lecture Notes*. Swiss Federal Institute of Technology, ETHZ, Switzerland. 394p.

Forrest, M. (2006). "Porto pressure". *Materials World* July 2006 pp 31-33.

Friedrichsen G (1998). "Wos für ein Einbruch". *Der Spiegel* Nr 19, Spiegel-Verlag, Hamburg.

Fukushima, H. (2002). “Examples of the tunnel portal collapse excavated in highly weathered granite”.

Galera J.M. and Pescador S. (2005), “Métodos geofísicos no destructivos para predecir el terreno por delante de las tuneladoras”, IV UN-ITA Workshop on “Gibraltar Strait crossing”, Madrid (in Spanish).

Geodata (2001). New Guidelines for tunneling works. April 2001.

Ghasemi, H.; Cooper, J.; Imbsen, R.; Piskin, H, Imal, F. and Tiras, A. (2000). “The November 1999 Duzce Earthquake: Post Earthquake Investigation of the Structures on the TEM (Trans-European Motorway)”. Publication No. FHWA-RD 00-146. 26 pages

Gradori, R. et al. (1995). “Evinos-Mornos tunnel – Greece construction of a 30 km long hydraulic tunnel in less than three years under the most adverse geological conditions”. 1995 RETC Proceedings.

Grantz, W (1997). “Steel-Shell Immersed tunnels - Forty years of experience”. Tunnelling and Underground Space Technology, Vol. 12, No. 1, pp. 23-31, 1997.

Grasso et al. (2003) “Experience on Porto – EPB follow up”. Tunnel and Tunnelling International, Dec 2003.

Grimstad, E. and Bhasin, R. (1999) “Rock support in hard rock tunnels under high stress”. Norwegian Geotechnical Institute.

Grose, J. W. and Benton, L. (2005). “Hull wastewater flow transfer tunnel: tunnel collapse and causation investigation. Geotechnical Engineering 158 Issue GE4”. October 2005. pp. 179-185.

Guglielmetti,V.; Grasso, P.; Gaj, F., Giacomini, G. (2003). “Mechanized tunneling in urban environment: control of ground response and face stability when excavating with EPB Machine”. (re)Claiming the underground space Saveur (Ed.)

Hashimoto, K. and Tanabe, Y. (1986). "Construction of the Seikan Undersea Tunnel--II. Execution of the Most Difficult Sections". *Tunnelling and Underground Space Technology*, Vol. 1, No. 3/4, pp. 373-379, 1986.

Health Safety of New Austrian (2006). "The risk to third parties from bored tunnelling in soft ground". HSE Books, 78 pages.

Health & Safety Executive (2000). "The collapse of NATM tunnels at Heathrow Airport – a report on the investigation", by the Health & Safety Executive, Sudbury, Suffolk, HSE Books.

Health Safety of New Austrian (1996), "Tunnelling Method (NATM) tunnels". A review of sprayed concrete lined tunnels with particular reference to London Clay. HSE Books, 1996.

Heckerman, D. (1997). "A Tutorial on Learning with Bayesian Networks". *Data Mining and Knowledge Discovery*, 1:79-119, 1997.

Henrion, M.; Breese, J.; Horvitz, E. (1991). "Decision Analysis and Expert systems". *AI Magazine* Volume 12 Number 4

Herrenknecht, M., Rehm, U. (2003a). "Earth Pressure Balanced Shield Technology". *Soft Ground and Hard Rock Mechanical Tunneling Technology Seminar*, held on March 28, 2003 at Colorado School of Mines campus.

Herrenknecht, M., Rehm, U. (2003b). "Mixshield Technology". *Soft Ground and Hard Rock Mechanical Tunneling Technology Seminar*, held on March 28, 2003 at Colorado School of Mines campus.

Hoek, E. (2007). "Practical rock engineering. Graduate courses notes in rock engineering at the University of Toronto".

Hoek, E. (2001). "Big Tunnels in Bad Rock". *ASCE Journal of Geotechnical and Geoenvironmental Engineering* Vol. 127, No. 9. September 2001, pages 726-740.

Horgan, D.; Madsen, D. (2008). "Crossing the Bosphorus and beyond". BTS meeting report.

Howard, R. A. (1966), "Decision Analysis: Applied Decision Theory," Proceedings of the 4th International Conference on Operational Research (1966) 55-77

Howard, R.A., and J.E. Matheson (editors) (1984). "Readings on the Principles and Applications of Decision Analysis", 2 volumes, Menlo Park CA: Strategic Decisions Group.

Ingerslev, L. (2005). "Considerations and strategies behind the design and construction requirements of the Istanbul Strait immersed tunnel". Tunnelling and Underground Space Technology, 20, pp. 604–608.

Ingerslev, L. (2004). "Immersed and floating tunnels across Lake Zurich". Tunnelling and Underground Space Technology, 19, pp. 477–478

Inokuma, A. et al. (1994). "Studies on the present state and the mechanism of trouble occurrence in tunnel in Japan 1994". ITA Conference (Cairo) Tunnelling Ground Conditions pages 283-246, Balkema.

International Tunnelling Association (2000). "Recommendations and Guidelines for Tunnel Boring Machines (TBMs)" Working Group N°14 - Mechanized Tunnelling -. Tribune Hors Série Mai 2001 - ISSN1267-8422. 34 pages.

Japan Society of Civil Engineers (1996). "Japanese standard for shield tunneling". The third edition.

Jensen, F.V. (2001). "Bayesian Networks and Decision Graphs". Taylor and Francis, London, UK, Springer-Verlag, New York, USA, 2001

Jensen, F.V. (1996). "Introduction to Bayesian Networks". Taylor and Francis, London, UK, Springer-Verlag, New York, USA, 1996.

- Jordan, M. (1998) "Learning in Graphical Models", (MIT Press 1998).
- Kaiser, P. (1999). "Lessons learned for deep tunnelling from rockbursts in Mining". GEAT'99 Switzerland.
- Karam, K.; Karam, J.; Einstein, H. (2007). "Decision Analysis Applied to Tunnel Exploration Planning. I: Principles and Case Study". Journal of Construction Engineering and Management. Volume 133, Issue 5, pp. 344-353
- Keeney, R.L., Raiffa, H. (1976). "Decisions with multiple objectives", John Wiley & Sons
- Khoury, G. (2003). "Passive fire protection in tunnels". Concrete: Feb 2003. Vol. 37, Iss. 2; pg. 31, 6 pgs
- Kirkland, C. J. (1986). "The proposed design of the English Channel tunnel". Tunnelling and Underground Space Technology, Vol. 1, No. 3/4, pp. 271-282.
- Kjaerulff, U.; Madsen, A. (2008). "Bayesian Networks and Influence Diagrams. A Guide to Construction and Analysis". Springer Ed.
- Knights, M. (2006). "Are we managing the risks in tunnelling?". International Seminar on Tunnels and Underground Works. Lisbon 2006.
- Kolymbas, D. (2005). "Tunnelling and Tunnel Mechanics". A Rational Approach to Tunnelling. Ed. Springer. 437 pages.
- Kovári (2001). "The Control of Ground Response - Milestones up to the 1960s". AITES - ITA 2001 World Tunnel Congress, Milano. 26 pp.
- Kovári, K. & Ramoni, M. (2006): "Urban tunnelling in soft ground using TBMs"; Tunnelling and trenchless technology in the 21st century; International conference and exhibition on tunnelling and trenchless technology, Subang Jaya – Selangor Darul Ehsan; 17-31; The Institution of Engineers, Malaysia.



Kovari, K. and Descoedres, F. (2001). "Tunnelling Switzerland". Swiss Tunnelling Society, Bertelsmann Fachzeitschriften GmbH, Gütersloh/Germany.

Kovari, K. and Staus, J. (1996). "Basic Considerations on Tunnelling in Squeezing". *Ground. Rock Mechanics and Rock Engineering*, 29 (4), pp. 203-210.

Landrin et al. (2006). "ALOP/DSU coverage for tunneling risks?". The international Association of Engineering Insurers. 39th Annual Conference, Boston, 2006.

Lee, S.M., Park B.S., Lee, S.W. (2004). "Analysis of Rockbursts that have occurred in a waterway Tunnel in Korea". *Int. J. Rock Mech. Min. Sci.* Vol. 41, No. 3, SINOROCK 2004 Symposium.

Leichnetz, W. (1990). "Analysis of Collapses on Tunnel Construction Sites on the New Lines of the German Federal Railway". *Tunnelling and Underground Space Technology*, Vol. 5, No. 3, pp. 199-203

Longo, S. (2006). "Análise e Gestão do Risco Geotécnico de Tuneis" (In Portuguese). 309 pp. Instituto Superior Técnico da Universidade Técnica de Lisboa. PhD Thesis.

Lovat, R. (2006). "TBM Design Considerations: Selection of Earth Pressure Balance or Slurry Pressure Balance Tunnel Boring Machines". *International Symposium on Utilization of Underground Space In Urban Areas*. Sharm El Sheikh, Egypt, November 2006

Lykke, S.; Belkaya, H. (2005). "Marmaray project: The project and its management". *Tunnelling and Underground Space Technology*, Vol. 1, No. 20, pp. 600-603.

McNichol, Dan. (2000) "The Big Dig". Silver Lining Books, Inc. pp. 239

Mehrotra, K., Mohan, C. K. and Ranka, S. (1997) "Elements of Artificial Neural Networks". MIT Press, 344 pages.

Melle, W. V.; Shortliffe, E. H.; Buchanan, B. G. (1981). "Rule-Based Expert Systems.

The MYCIN Experiments of the Stanford Heuristic Programming Project”. Technical Report Stanford School of Medicine. Published in 1981.

Min, S.Y., Einstein, H.H., Lee, J.S., and Kim, T.K. 2003. “Application of decision aids for tunneling (DAT) to a drill & blast tunnel” J. of Civil Eng., KSCE, Vol. 7, pp.619-628.

Moe, G. (1997). “Design philosophy of floating bridges with emphasis on ways to ensure long life”. Journal of Marine Science and Technology, 2:182-189.

Müller, L., Fecker, E. (1978). Grundgedanken und Grundsätze der "Neuen Österreichischen Tunnelbauweise", Felsmechanik Kolloquium Karlsruhe, Trans Tech Publ., Claustal.

Munich Re Group (2004). “Underground transportation systems. Chances and risks from the reinsurer’s point of view”. 69pp.

Murphy, K. (2002). “Dynamic bayesian networks”. Representation, inference and learning, 2002.

Ortlepp, W. D. (2001).“The behaviour of tunnels at great depth under large static and dynamic pressures”. Tunnelling and Underground Space Technology 16 - 2001. pp 41-48

Ortlepp, W. D. and Stacey, T. R. (1994) “Rockburst Mechanisms in Tunnels and Shafts”. Tunnelling and Underground Space Technology, Vol. 9, No. 1, pp. 59-65, 1994

Pearl, J., (1988) “Probabilistic Reasoning in Intelligent Systems: Networks of Plausible Inference”, (San Mateo, CA: Morgan Kaufmann, 1988).

Pelizza, S. (1999a). “Scavo Meccanizzato delle Gallerie” (in Italian). Gallerie e Grandi Opere Sotteranee. 59: 48.

Pelizza, S. (1999b). “TBM Bored Long Rock Tunnels”. ITA 25th Anniversary Commemorative Book, ITA 60pp.

Pelizza, S. and Peila, D. (2005). “TBM Tunnelling In Rock: Ground Probing and

Treatments”. World Long Tunnels, 2005.

Rabcewicz L. (1965). “The New Austrian Tunnelling Method”, Part one, Part Three, Water Power, January 1965, 19-24.

Rocha, M. (1977). “Some Problems related to the rock mechanics of low strength material” (in Portuguese). Journal Geotecnia, no.18, pp. 3-27.

Russell, S. and Norvig, P. (2003) “Artificial Intelligence. A Modern Approach”. Second Edition. Prentice Hall Series in Artificial Intelligence.

Saveur, J.; Grantz, W. (1993). “Structural design of immersed tunnels”. Tunnelling and Underground Space Technology, Vol. 8, No. 2, pp. 123-139.

Schultz, C.; Kochen, R. (2005). “Túneis imersos para travessias subaquáticas” (in Portuguese). Principais aspectos geotécnicos e construtivos. Revista Engenharia, 569, pp. 95-98.

SchweizerBauJournal. Tunnelbau. 3/2004.

Seidenfuss, T. (2006). “Collapses in Tunnelling”. Master Thesis, University of Stuttgart, EPFL and ITA.

Shortliffe, E. H. (1976). “Computer based medical consultations: MYCIN”, American Elsevier, 1976.

Silva, C. (2001). “Safety control in railway tunnels. Development of support methodologies and a knowledge based system” (in Portuguese). University of Porto, MSc Thesis, Porto, 267p.

Sonmez, H.; Gokceoglu, C. and Ulusay, R. (2003). “An application of fuzzy sets to the Geological Strength Index (GSI) system used in rock engineering”. Engineering Applications of Artificial Intelligence. Volume 16, Issue 3, April 2003, Pages 251-269

Sousa, L.R. (2002). “Innovative aspects in the design and construction of underground

structures” (in Portuguese). 7th Portuguese Geotechnical Congress, Porto, pp. 1313-1373.

Sousa, L.R. (2006). “Big Dig the major road project in USA” (in Portuguese). *Journal Engenharia e Vida*, no. 26 July/August, Lisbon.

Sousa, L.R. (2006). “Learning with accidents and damage associated to underground works”. *Geotechnical Risk in Rock Tunnels*. Ed(s) Campos e Matos, A; Sousa, L.R.; Kleberger, J. Pinto, P., Francis & Taylor, 199p.

Sousa, R.L.; Sousa, L.R.; Silva, C. (2007). “Maintenance of tunnels and the use of AI techniques”. 11th ISRM Congress, Specialized Session S5 on Maintenance and Repair of Underground Structures in Rock Masses, Lisbon, 6p.

Spetzler, C., and Staël von Hostein, C.-A. (1975). “Probability encoding in decision analysis”. *Management Science* 22:340–358.

Stack, B. (1982). “Handbook of Mining and Tunnelling Machinery”. John Wiley and Sons Ltd, 772 pp.

Stallmann, M. (2005) “Verbrüche im Tunnelbau Ursachen und Sanierung”. Diplomarbeit. Fachhochschule Hochschule Für Stuttgart Technik Stuttgart University Of Applied Sciences. 122 pages.

Suwansawat and Einstein (2006). “Artificial neural networks for predicting the maximum surface settlement caused by EPB shield tunneling”. *Tunnelling and Underground Space Technology*. 21 (2) (2006), pp. 133–150

Suwansawat, S. (2002). “Earth pressure balance (EPB) shield tunneling in Bangkok: ground response and prediction of surface settlements using artificial neural networks”. PhD Thesis. Massachusetts Institute of Technology. Dept. of Civil and Environmental Engineering.

T&TI, (2003). “Experience on Porto – EPB follow-up” *Tunnels and Tunnelling*, December 2003.

Toan, Nguyen Duc (2006). "TBM and Lining Essential Interfaces". Postgraduate master course in Tunnelling and Tunnel Boring Machines, V Edition 2005-06, Politecnico di Torino, Italia.

Transmetro (2000a). "Escolha do método de escavação com o uso da herrenknecht EPB-shield". Technical report.

Transmetro (2000b). "Operação da tuneladora (TBM operation)". Technical report.

Transmetro (2001). "Face mapping for Line C of the Porto Metro".

Transmetro (2002a). Tunnel Line C - PAT n.03. Section between pk 0+906.7 and 1+125 (in Portuguese). Technical report.

Transmetro (2002b). "Tunnel Line C - PAT n.04. Section between pk 1+125 and pk 1+480.25" (in Portuguese). Technical report.

Transmetro (2002c). "Tunnel Line C - PAT n.05. Section between pk 1+480,25 and pk 2+160,52" (in Portuguese). Technical report.

Transmetro (2002d). "Tunnel Line C PAT n.06. Section between pk 2+160,52 and pk 2+450,68" (in Portuguese). Technical report.

Tunnelling and Underground Space Technology, Vol. 15, No. 1, pp. 13-29, 2000. "New Developments".

Tunnels and Tunnelling International, August 2003

Tunnels and Tunnelling International, July 2003.

Tunnels and Tunnelling International, October 2003. "Learning from the Laerdal tunnel".

Tunnels and Tunnelling International, September 1999. "Laerdal collapse halts progress".

Tunnels and Tunnelling International, September 1999. "The world's longest road

tunnel”.

Tunnels and Tunnelling International. August 2000. “Heathrow collapse was organizational”.

Tunnels and Tunnelling International. October 2000. “When Hull freezes over”. pp. 16-17.

United States Department of Transportation (1993). “Charles River Crossing - Central Artery / tunnel project, Boston, Massachusetts Supplemental environmental impact statement” report by US Department of Transportation, Federal Highway Administration and Massachusetts Highway Department.

Vanmarcke, E.H.; Bohnenblust, H. (1982). “Methodology for Integrated Risk Assessment for Dams”. MIT Research Report R-82-11.

Vlasov, S.N. et al. (2001). “Accidents in Transportation and Subway Tunnels. Construction to Operation”. Russian Tunnelling Association. Elex-KM Publ. Ltd. Pagg.200. ISBN 5-93815-002-7.

Von Neumann, J. and Morgenstern, O. (1944). “Theory of Games and Economic Behavior”. Princeton University Press. 625pp.

Wallis, S. (1991) “Non-shielded TBM holds squeezing clay in check”. Tunnels and Tunnelling International. January 1991. pp. 50-52

Wallis, S. (1995). “NATM challenge at Montemor tunnel”. Tunnels and Tunnelling International, Dec 1995, pp. 32-34.

Wannick, H.(2006). “The Code of Practice for Risk Management of Tunnel Works Future Tunnelling Insurance from the Insurers” Point of View (Presentation). ITA Conference Seoul, April 25, 2006

Weber, J. (1987). “Limits of shotcrete construction methods in urban railway tunneling”.



Tunnel 3/87. pp. 116-124.

Wittke, W. et al. (2002) New Austrian Tunnelling Method (NATM), “Stability Analysis and Design”. Geotechnical Engineering in Research and Practice WBI Print 6. Editor WBI Professor Dr.-Ing. W. Wittke, Beratende Ingenieure für Grundbau Und Felsbau GmbH, Aachen,Germany, 424 pages.

Wittke, W. et al. (2002). “New Austrian Tunnelling Method (NATM), Stability Analysis and Design”. Geotechnical Engineering in Research and Practice WBI Print 6. Editor WBI Professor Dr.-Ing. W. Wittke, Beratende Ingenieure für Grundbau Und Felsbau GmbH, Aachen,Germany, 424 pages.

Wittke, W. et al. (2007), “Stability Analysis and Design for Mechanized Tunneling”. Geotechnical Engineering in Research and Practice WBI Print 6. Editor WBI Professor Dr.-Ing. W. Wittke, Beratende Ingenieure für Grundbau Und Felsbau GmbH, Aachen,Germany, 563 pages.

Wittke, W. et al. (2007). “Stability Analysis and Design for Mechanized Tunneling”. Geotechnical Engineering in Research and Practice WBI Print 6. Editor WBI Professor Dr.-Ing. W. Wittke, Beratende Ingenieure für Grundbau Und Felsbau GmbH, Aachen,Germany, 563 pages.

Yoshimitsu Maru and Takashi Maeda (1986). “Construction of the Seikan General Scheme of Execution Undersea Tunnel—I”. Tunnelling and Underground Space Technology, Vol. 1, No. 3/4, pp. 357-371, 1986.

Zadeh, L.A. (1965). “Fuzzy sets”, Information and Control 8 (3): 338—353.

Zadeh, Lotfi (1999). “Fuzzy Sets as the Basis for a Theory of Possibility”. Fuzzy Sets and Systems 1:3-28, 1978. (Reprinted in Fuzzy Sets and Systems 100 (Supplement): 9-34, 1999.

## **Internet references**

Herrenknecht url :[www.herrenknecht.com](http://www.herrenknecht.com)

<http://www.stuttgart21.de> (in german)

Norwegian Public Roads Administration (2006) <http://www.vegvesen.no>

"Archimedes Bridge". Ponte di Archimede International S.p.A.

"First Archimedes bridge prototype to be realized in southern China". People's Daily Online (April 18, 2007).